(12) INTERNATIONAL APPLICATION PUBLISHED UNDER THE PATENT COOPERATION TREATY (PCT)

(19) World Intellectual Property Organization
International Bureau

(43) International Publication Date
7 November 2013 (07.11.2013)

WIPO | PCT

(10) International Publication Number
WO 2013/166464 A1

(51) International Patent Classification:
G08B 13/18 (2006.01)

(21) International Application Number:
PCT/US2013/039580

(22) International Filing Date:
3 May 2013 (03.05.2013)

(25) Filing Language: English

(26) Publication Language: English

(30) Priority Data:
13/464,648 4 May 2012 (04.05.2012) US

(71) Applicant: **REARDEN, LLC** [US/US]; 355 Bryant Street, Suite 110, San Francisco, California 94017 (US).

(72) Inventors: **FORENZA, Antonio**; 355 Bryant Street, Suite 110, San Francisco, California 94107 (US). **PERLMAN, Stephen G.**; 355 Bryant Street, Suite 110, San Francisco, California 94107 (US).

(74) Agents: **VINCENT, Lester J.** et al.; Blakely, Sokoloff, Taylor & Zafman LLP, 1279 Oakmead Parkway, Sunnyvale, California 94085 (US).

(81) Designated States *(unless otherwise indicated, for every kind of national protection available)*: AE, AG, AL, AM, AO, AT, AU, AZ, BA, BB, BG, BH, BN, BR, BW, BY, BZ, CA, CH, CL, CN, CO, CR, CU, CZ, DE, DK, DM, DO, DZ, EC, EE, EG, ES, FI, GB, GD, GE, GH, GM, GT, HN, HR, HU, ID, IL, IN, IS, JP, KE, KG, KM, KN, KP, KR, KZ, LA, LC, LK, LR, LS, LT, LU, LY, MA, MD, ME, MG, MK, MN, MW, MX, MY, MZ, NA, NG, NI, NO, NZ, OM, PA, PE, PG, PH, PL, PT, QA, RO, RS, RU, RW, SC, SD, SE, SG, SK, SL, SM, ST, SV, SY, TH, TJ, TM, TN, TR, TT, TZ, UA, UG, US, UZ, VC, VN, ZA, ZM, ZW.

(84) Designated States *(unless otherwise indicated, for every kind of regional protection available)*: ARIPO (BW, GH, GM, KE, LR, LS, MW, MZ, NA, RW, SD, SL, SZ, TZ, UG, ZM, ZW), Eurasian (AM, AZ, BY, KG, KZ, RU, TJ, TM), European (AL, AT, BE, BG, CH, CY, CZ, DE, DK, EE, ES, FI, FR, GB, GR, HR, HU, IE, IS, IT, LT, LU, LV, MC, MK, MT, NL, NO, PL, PT, RO, RS, SE, SI, SK, SM, TR), OAPI (BF, BJ, CF, CG, CI, CM, GA, GN, GQ, GW, ML, MR, NE, SN, TD, TG).

Published:

— *with international search report (Art. 21(3))*

(54) Title: SYSTEM AND METHODS FOR COPING WITH DOPPLER EFFECTS IN DISTRIBUTED-INPUT DISTRIBUTED-OUTPUT WIRELESS SYSTEMS

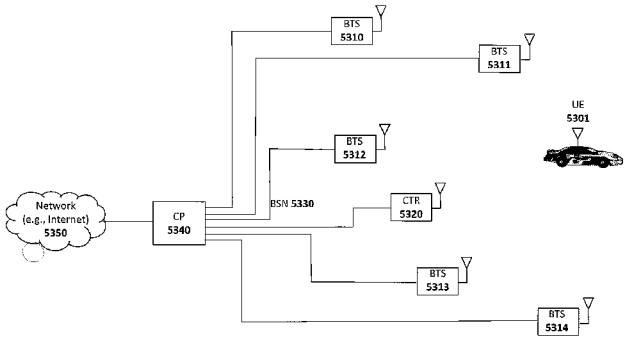

Fig. 53

(57) Abstract: A system and methods are described which compensate for the adverse effect of Doppler on the performance of DIDO systems. One embodiment of such a system employs different selection algorithms to adaptively adjust the active BTSs to different UEs based by tracking the changing channel conditions. Another embodiment utilizes channel prediction to estimate the future CSI or DIDO precoding weights, thereby eliminating errors due to outdated CSI.

WO 2013/166464 A1

SYSTEM AND METHODS FOR COPING WITH DOPPLER EFFECTS IN DISTRIBUTED-INPUT DISTRIBUTED-OUTPUT WIRELESS SYSTEMS

RELATED APPLICATIONS

[0001] This application is a continuation-in-part of the following co-pending U.S. Patent Applications:

[0002] U.S. Application Serial No. 12/917,257, filed November 1, 2010, entitled "Systems And Methods To Coordinate Transmissions In Distributed Wireless Systems Via User Clustering"; U.S. Application Serial No. 12/802,988, filed June 16, 2010, entitled "Interference Management, Handoff, Power Control And Link Adaptation In Distributed-Input Distributed-Output (DIDO) Communication Systems"; U.S. Application Serial No. 12/802,976, filed June 16, 2010, entitled "System And Method For Adjusting DIDO Interference Cancellation Based On Signal Strength Measurements", now U.S. Issued Patent 8,170,081, Issued on May 1, 2012; U.S. Application Serial No. 12/802,974, filed June 16, 2010, entitled "System And Method For Managing Inter-Cluster Handoff Of Clients Which Traverse Multiple DIDO Clusters"; U.S. Application Serial No. 12/802,989, filed June 16, 2010, entitled "System And Method For Managing Handoff Of A Client Between Different Distributed-Input-Distributed-Output (DIDO) Networks Based On Detected Velocity Of The Client"; U.S. Application Serial No. 12/802,958, filed June 16, 2010, entitled "System And Method For Power Control And Antenna Grouping In A Distributed-Input-Distributed-Output (DIDO) Network"; U.S. Application Serial No. 12/802,975, filed June 16, 2010, entitled "System And Method For Link adaptation In DIDO Multicarrier Systems"; U.S. Application Serial No. 12/802,938, filed June 16, 2010, entitled "System And Method For DIDO Precoding Interpolation In Multicarrier Systems"; U.S. Application Serial No. 12/630,627, filed December 3, 2009, entitled "System and Method For Distributed Antenna Wireless Communications"; U.S. Application Serial No. 12/143,503, filed June 20, 2008 entitled "System and Method For Distributed Input-Distributed Output Wireless Communications", now U.S. Issued Patent 8,160,121, Issued on April 17, 2009; U.S. Application Serial No. 11/894,394, filed August 20, 2007 entitled, "System and Method for Distributed Input Distributed Output Wireless Communications", now U.S. Issued Patent 7,599,420, Issued on October 6, 2009; U.S. Application Serial No. 11/894,362, filed August 20, 2007 entitled, "System and method for Distributed Input-Distributed Wireless Communications", now U.S. Issued Patent, 7,633,994, Issued on December 15, 2009; U.S. Application Serial No. 11/894,540, filed August 20, 2007 entitled "System and Method For Distributed Input-Distributed Output Wireless Communications", now U.S. Issued Patent No. 7,636,381, Issued on December 22, 2009; U.S. Application Serial No. 11/256,478, filed October 21, 2005 entitled "System and Method For Spatial-Multiplexed Tropospheric Scatter Communications", now U.S.

Issued Patent 7,711,030, Issued on May 4, 2010; U.S. Application Serial No. 10/817,731, filed April 2, 2004 entitled "System and Method For Enhancing Near Vertical Incidence Skywave ("NVIS") Communication Using Space-Time Coding", now U.S. Issued Patent No. 7,885,354, Issued on February 28, 2011.

BACKGROUND

[0003] Prior art multi-user wireless systems may include only a single base station or several base stations.

[0004] A single WiFi base station (e.g., utilizing 2.4 GHz 802.11b, g or n protocols) attached to a broadband wired Internet connection in an area where there are no other WiFi access points (e.g. a WiFi access point attached to DSL within a rural home) is an example of a relatively simple multi-user wireless system that is a single base station that is shared by one or more users that are within its transmission range. If a user is in the same room as the wireless access point, the user will typically experience a high-speed link with few transmission disruptions (e.g. there may be packet loss from 2.4GHz interferers, like microwave ovens, but not from spectrum sharing with other WiFi devices), If a user is a medium distance away or with a few obstructions in the path between the user and WiFi access point, the user will likely experience a medium-speed link. If a user is approaching the edge of the range of the WiFi access point, the user will likely experience a low-speed link, and may be subject to periodic drop-outs if changes to the channel result in the signal SNR dropping below usable levels. And, finally, if the user is beyond the range of the WiFi base station, the user will have no link at all.

[0005] When multiple users access the WiFi base station simultaneously, then the available data throughput is shared among them. Different users will typically place different throughput demands on a WiFi base station at a given time, but at times when the aggregate throughput demands exceed the available throughput from the WiFi base station to the users, then some or all users will receive less data throughput than they are seeking. In an extreme situation where a WiFi access point is shared among a very large number of users, throughput to each user can slow down to a crawl, and worse, data throughput to each user may arrive in short bursts separated by long periods of no data throughput at all, during which time other users are served. This "choppy" data delivery may impair certain applications, like media streaming.

[0006] Adding additional WiFi base stations in situations with a large number of users will only help up to a point. Within the 2.4GHz ISM band in the U.S., there are 3 non-interfering channels that can be used for WiFi, and if 3 WiFi base stations in the same coverage area are configured to each use a different non-interfering channel, then the aggregate throughput of the coverage area among multiple users will be increased up to a factor of 3. But, beyond that,

adding more WiFi base stations in the same coverage area will not increase aggregate throughput, since they will start sharing the same available spectrum among them, effectually utilizing time-division multiplexed access (TDMA) by "taking turns" using the spectrum. This situation is often seen in coverage areas with high population density, such as within multi-dwelling units. For example, a user in a large apartment building with a WiFi adapter may well experience very poor throughput due to dozens of other interfering WiFi networks (e.g. in other apartments) serving other users that are in the same coverage area, even if the user's access point is in the same room as the client device accessing the base station. Although the link quality is likely good in that situation, the user would be receiving interference from neighbor WiFi adapters operating in the same frequency band, reducing the effective throughput to the user.

[0007] Current multiuser wireless systems, including both unlicensed spectrum, such as WiFi, and licensed spectrum, suffer from several limitations. These include coverage area, downlink (DL) data rate and uplink (UL) data rate. Key goals of next generation wireless systems, such as WiMAX and LTE, are to improve coverage area and DL and UL data rate via multiple-input multiple-output (MIMO) technology. MIMO employs multiple antennas at transmit and receive sides of wireless links to improve link quality (resulting in wider coverage) or data rate (by creating multiple non-interfering spatial channels to every user). If enough data rate is available for every user (note, the terms "user" and "client" are used herein interchangeably), however, it may be desirable to exploit channel spatial diversity to create non-interfering channels to multiple users (rather than single user), according to multiuser MIMO (MU-MIMO) techniques. *See, e.g.*, the following references:

[0008] G. Caire and S. Shamai, "On the achievable throughput of a multiantenna Gaussian broadcast channel," IEEE Trans. Info.Th., vol. 49, pp. 1691–1706, July 2003.

[0009] P. Viswanath and D. Tse, "Sum capacity of the vector Gaussian broadcast channel and uplink-downlink duality," IEEE Trans. Info. Th., vol. 49, pp. 1912–1921, Aug. 2003.

[0010] S. Vishwanath, N. Jindal, and A. Goldsmith, "Duality, achievable rates, and sum-rate capacity of Gaussian MIMO broadcast channels," IEEE Trans. Info. Th., vol. 49, pp. 2658–2668, Oct. 2003.

[0011] W. Yu and J. Cioffi, "Sum capacity of Gaussian vector broadcast channels," IEEE Trans. Info. Th., vol. 50, pp. 1875–1892, Sep. 2004.

[0012] M. Costa, "Writing on dirty paper," IEEE Transactions on Information Theory, vol. 29, pp. 439–441, May 1983.

[0013] M. Bengtsson, "A pragmatic approach to multi-user spatial multiplexing," Proc. of Sensor Array and Multichannel Sign.Proc. Workshop, pp. 130–134, Aug. 2002.

[0014] K.-K. Wong, R. D. Murch, and K. B. Letaief, "Performance enhancement of multiuser MIMO wireless communication systems," IEEE Trans. Comm., vol. 50, pp. 1960–1970, Dec. 2002.

[0015] M. Sharif and B. Hassibi, "On the capacity of MIMO broadcast channel with partial side information," IEEE Trans. Info.Th., vol. 51, pp. 506–522, Feb. 2005.

[0016] For example, in MIMO 4x4 systems (i.e., four transmit and four receive antennas), 10MHz bandwidth, 16-QAM modulation and forward error correction (FEC) coding with rate 3/4 (yielding spectral efficiency of 3bps/Hz), the ideal peak data rate achievable at the physical layer for every user is 4x30Mbps=120Mbps, which is much higher than required to deliver high definition video content (which may only require ~10Mbps). In MU-MIMO systems with four transmit antennas, four users and single antenna per user, in ideal scenarios (i.e., independent identically distributed, i.i.d., channels) downlink data rate may be shared across the four users and channel spatial diversity may be exploited to create four parallel 30Mbps data links to the users.

Different MU-MIMO schemes have been proposed as part of the LTE standard as described, for example, in 3GPP, "Multiple Input Multiple Output in UTRA", 3GPP TR 25.876 V7.0.0, Mar. 2007; 3GPP, "Base Physical channels and modulation", TS 36.211, V8.7.0, May 2009; and 3GPP, "Multiplexing and channel coding", TS 36.212, V8.7.0, May 2009. However, these schemes can provide only up to 2X improvement in DL data rate with four transmit antennas. Practical implementations of MU-MIMO techniques in standard and proprietary cellular systems by companies like ArrayComm (*see, e.g.*, ArrayComm, "Field-proven results", http://www.arraycomm.com/serve.php?page=proof) have yielded up to a ~3X increase (with four transmit antennas) in DL data rate via space division multiple access (SDMA). A key limitation of MU-MIMO schemes in cellular networks is lack of spatial diversity at the transmit side. Spatial diversity is a function of antenna spacing and multipath angular spread in the wireless links. In cellular systems employing MU-MIMO techniques, transmit antennas at a base station are typically clustered together and placed only one or two wavelengths apart due to limited real estate on antenna support structures (referred to herein as "towers," whether physically tall or not) and due to limitations on where towers may be located. Moreover, multipath angular spread is low since cell towers are typically placed high up (10 meters or more) above obstacles to yield wider coverage.

[0017] Other practical issues with cellular system deployment include excessive cost and limited availability of locations for cellular antenna locations (e.g. due to municipal restrictions on antenna placement, cost of real-estate, physical obstructions, etc.) and the cost and/or availability of network connectivity to the transmitters (referred to herein as "backhaul").

Further, cellular systems often have difficulty reaching clients located deeply in buildings due to losses from walls, ceilings, floors, furniture and other impediments.

[0018] Indeed, the entire concept of a cellular structure for wide-area network wireless presupposes a rather rigid placement of cellular towers, an alternation of frequencies between adjacent cells, and frequently sectorization, so as to avoid interference among transmitters (either base stations or users) that are using the same frequency. As a result, a given sector of a given cell ends up being a shared block of DL and UL spectrum among all of the users in the cell sector, which is then shared among these users primarily in only the time domain. For example, cellular systems based on Time Division Multiple Access (TDMA) and Code Division Multiple Access (CDMA) both share spectrum among users in the time domain. By overlaying such cellular systems with sectorization, perhaps a 2-3X spatial domain benefit can be achieved. And, then by overlaying such cellular systems with a MU-MIMO system, such as those described previously, perhaps another 2-3X space-time domain benefit can be achieved. But, given that the cells and sectors of the cellular system are typically in fixed locations, often dictated by where towers can be placed, even such limited benefits are difficult to exploit if user density (or data rate demands) at a given time does not match up well with tower/sector placement. A cellular smart phone user often experiences the consequence of this today where the user may be talking on the phone or downloading a web page without any trouble at all, and then after driving (or even walking) to a new location will suddenly see the voice quality drop or the web page slow to a crawl, or even lose the connection entirely. But, on a different day, the user may have the exact opposite occur in each location. What the user is probably experiencing, assuming the environmental conditions are the same, is the fact that user density (or data rate demands) is highly variable, but the available total spectrum (and thereby total data rate, using prior art techniques) to be shared among users at a given location is largely fixed.

[0019] Further, prior art cellular systems rely upon using different frequencies in different adjacent cells, typically 3 different frequencies. For a given amount of spectrum, this reduces the available data rate by 3X.

[0020] So, in summary, prior art cellular systems may lose perhaps 3X in spectrum utilization due to cellularization, and may improve spectrum utilization by perhaps 3X through sectorization and perhaps 3X more through MU-MIMO techniques, resulting in a net 3*3/3 = 3X potential spectrum utilization. Then, that bandwidth is typically divided up among users in the time domain, based upon what sector of what cell the users fall into at a given time. There are even further inefficiencies that result due to the fact that a given user's data rate demands are typically independent of the user's location, but the available data rate varies depending on the link quality between the user and the base station. For example, a user further from a cellular

base station will typically have less available data rate than a user closer to a base station. Since the data rate is typically shared among all of the users in a given cellular sector, the result of this is that all users are impacted by high data rate demands from distant users with poor link quality (e.g. on the edge of a cell) since such users will still demand the same amount of data rate, yet they will be consuming more of the shared spectrum to get it.

[0021] Other proposed spectrum sharing systems, such as that used by WiFi (e.g., 802.11b, g, and n) and those proposed by the White Spaces Coalition, share spectrum very inefficiently since simultaneous transmissions by base stations within range of a user result in interference, and as such, the systems utilize collision avoidance and sharing protocols. These spectrum sharing protocols are within the time domain, and so, when there are a large number of interfering base stations and users, no matter how efficient each base station itself is in spectrum utilization, collectively the base stations are limited to time domain sharing of the spectrum among each other. Other prior art spectrum sharing systems similarly rely upon similar methods to mitigate interference among base stations (be they cellular base stations with antennas on towers or small scale base stations, such as WiFi Access Points (APs)). These methods include limiting transmission power from the base station so as to limit the range of interference, beamforming (via synthetic or physical means) to narrow the area of interference, time-domain multiplexing of spectrum and/or MU-MIMO techniques with multiple clustered antennas on the user device, the base station or both. And, in the case of advanced cellular networks in place or planned today, frequently many of these techniques are used at once.

[0022] But, what is apparent by the fact that even advanced cellular systems can achieve only about a 3X increase in spectrum utilization compared to a single user utilizing the spectrum is that all of these techniques have done little to increase the aggregate data rate among shared users for a given area of coverage. In particular, as a given coverage area scales in terms of users, it becomes increasingly difficult to scale the available data rate within a given amount of spectrum to keep pace with the growth of users. For example, with cellular systems, to increase the aggregate data rate within a given area, typically the cells are subdivided into smaller cells (often called nano-cells or femto-cells). Such small cells can become extremely expensive given the limitations on where towers can be placed, and the requirement that towers must be placed in a fairly structured pattern so as to provide coverage with a minimum of "dead zones", yet avoid interference between nearby cells using the same frequencies. Essentially, the coverage area must be mapped out, the available locations for placing towers or base stations must be identified, and then given these constraints, the designers of the cellular system must make do with the best they can. And, of course, if user data rate demands grow over time, then the designers of the cellular system must yet again remap the coverage area, try to find locations for

towers or base stations, and once again work within the constraints of the circumstances. And, very often, there simply is no good solution, resulting in dead zones or inadequate aggregate data rate capacity in a coverage area. In other words, the rigid physical placement requirements of a cellular system to avoid interference among towers or base stations utilizing the same frequency results in significant difficulties and constraints in cellular system design, and often is unable to meet user data rate and coverage requirements.

[0023] So-called prior art "cooperative" and "cognitive" radio systems seek to increase the spectral utilization in a given area by using intelligent algorithms within radios such that they can minimize interference among each other and/or such that they can potentially "listen" for other spectrum use so as to wait until the channel is clear. Such systems are proposed for use particularly in unlicensed spectrum in an effort to increase the spectrum utilization of such spectrum.

[0024] A mobile ad hoc network (MANET) (see http://en.wikipedia.org/wiki/Mobile_ad_hoc_network) is an example of a cooperative self-configuring network intended to provide peer-to-peer communications, and could be used to establish communication among radios without cellular infrastructure, and with sufficiently low-power communications, can potentially mitigate interference among simultaneous transmissions that are out of range of each other. A vast number of routing protocols have been proposed and implemented for MANET systems (see http://en.wikipedia.org/wiki/List_of_ad-hoc_routing_protocols for a list of dozens of routing protocols in a wide range of classes), but a common theme among them is they are all techniques for routing (e.g. repeating) transmissions in such a way to minimize transmitter interference within the available spectrum, towards the goal of particular efficiency or reliability paradigms.

[0025] All of the prior art multi-user wireless systems seek to improve spectrum utilization within a given coverage area by utilizing techniques to allow for simultaneous spectrum utilization among base stations and multiple users. Notably, in all of these cases, the techniques utilized for simultaneous spectrum utilization among base stations and multiple users achieve the simultaneous spectrum use by multiple users by mitigating interference among the waveforms to the multiple users. For example, in the case of 3 base stations each using a different frequency to transmit to one of 3 users, there interference is mitigated because the 3 transmissions are at 3 different frequencies. In the case of sectorization from a base station to 3 different users, each 180 degrees apart relative to the base station, interference is mitigated because the beamforming prevents the 3 transmissions from overlapping at any user.

[0026] When such techniques are augmented with MU-MIMO, and, for example, each base station has 4 antennas, then this has the potential to increase downlink throughput by a factor of

4, by creating four non-interfering spatial channels to the users in given coverage area. But it is still the case that some technique must be utilized to mitigate the interference among multiple simultaneous transmissions to multiple users in different coverage areas.

[0027] And, as previously discussed, such prior art techniques (e.g. cellularization, sectorization) not only typically suffer from increasing the cost of the multi-user wireless system and/or the flexibility of deployment, but they typically run into physical or practical limitations of aggregate throughput in a given coverage area. For example, in a cellular system, there may not be enough available locations to install more base stations to create smaller cells. And, in an MU-MIMO system, given the clustered antenna spacing at each base station location, the limited spatial diversity results in asymptotically diminishing returns in throughput as more antennas are added to the base station.

[0028] And further, in the case of multi-user wireless systems where the user location and density is unpredictable, it results in unpredictable (with frequently abrupt changes) in throughput, which is inconvenient to the user and renders some applications (e.g. the delivery of services requiring predictable throughput) impractical or of low quality. Thus, prior art multi-user wireless systems still leave much to be desired in terms of their ability to provide predictable and/or high-quality services to users.

[0029] Despite the extraordinary sophistication and complexity that has been developed for prior art multi-user wireless systems over time, there exist common themes: transmissions are distributed among different base stations (or ad hoc transceivers) and are structured and/or controlled so as to avoid the RF waveform transmissions from the different base stations and/or different ad hoc transceivers from interfering with each other at the receiver of a given user.

[0030] Or, to put it another way, it is taken as a given that if a user happens to receive transmissions from more than one base station or ad hoc transceiver at the same time, the interference from the multiple simultaneous transmissions will result in a reduction of the SNR and/or bandwidth of the signal to the user which, if severe enough, will result in loss of all or some of the potential data (or analog information) that would otherwise have been received by the user.

[0031] Thus, in a multiuser wireless system, it is necessary to utilize one or more spectrum sharing approaches or another to avoid or mitigate such interference to users from multiple base stations or ad hoc transceivers transmitting at the same frequency at the same time. There are a vast number of prior art approaches to avoiding such interference, including controlling base stations' physical locations (e.g. cellularization), limiting power output of base stations and/or ad hoc transceivers (e.g. limiting transmit range), beamforming/sectorization, and time domain multiplexing. In short, all of these spectrum sharing systems seek to address the limitation of

multiuser wireless systems that when multiple base stations and/or ad hoc transceivers transmitting simultaneously at the same frequency are received by the same user, the resulting interference reduces or destroys the data throughput to the affected user. If a large percentage, or all, of the users in the multi-user wireless system are subject to interference from multiple base stations and/or ad hoc transceivers (e.g. in the event of the malfunction of a component of a multi-user wireless system), then it can result in a situation where the aggregate throughput of the multi-user wireless system is dramatically reduced, or even rendered non-functional..

[0032] Prior art multi-user wireless systems add complexity and introduce limitations to wireless networks and frequently result in a situation where a given user's experience (e.g. available bandwidth, latency, predictability, reliability) is impacted by the utilization of the spectrum by other users in the area. Given the increasing demands for aggregate bandwidth within wireless spectrum shared by multiple users, and the increasing growth of applications that can rely upon multi-user wireless network reliability, predictability and low latency for a given user, it is apparent that prior art multi-user wireless technology suffers from many limitations. Indeed, with the limited availability of spectrum suitable for particular types of wireless communications (e.g. at wavelengths that are efficient in penetrating building walls), it may be the case that prior art wireless techniques will be insufficient to meet the increasing demands for bandwidth that is reliable, predictable and low-latency.

[0033] Prior art related to the current invention describes beamforming systems and methods for null-steering in multiuser scenarios. Beamforming was originally conceived to maximize received signal-to-noise ratio (SNR) by dynamically adjusting phase and/or amplitude of the signals (i.e., beamforming weights) fed to the antennas of the array, thereby focusing energy toward the user's direction. In multiuser scanarios, beamforming can be used to suppress interfering sources and maximize signal-to-interference-plus-noise ratio (SINR). For example, when beamforming is used at the receiver of a wireless link, the weights are computed to create nulls in the direction of the interfering sources. When beamforming is used at the transmitter in multiuser downlink scenarios, the weights are calculated to pre-cancel inter-user interfence and maximize the SINR to every user. Alternative techniques for multiuser systems, such as BD precoding, compute the precoding weights to maximize throughput in the downlink broadcast channel. The co-pending applications, which are incorporated herein by reference, describe the foregoing techniques (see co-pending applications for specific citations).

BRIEF DESCRIPTION OF THE DRAWINGS

[0034] A better understanding of the present invention can be obtained from the following detailed description in conjunction with the drawings, in which:

[0035] **FIG. 1** illustrates a main DIDO cluster surrounded by neighboring DIDO clusters in one embodiment of the invention.

[0036] **FIG. 2** illustrates frequency division multiple access (FDMA) techniques employed in one embodiment of the invention.

[0037] **FIG. 3** illustrates time division multiple access (TDMA) techniques employed in one embodiment of the invention.

[0038] **FIG. 4** illustrates different types of interfering zones addressed in one embodiment of the invention.

[0039] **FIG. 5** illustrates a framework employed in one embodiment of the invention.

[0040] **FIG. 6** illustrates a graph showing SER as a function of the SNR, assuming SIR=10dB for the target client in the interfering zone.

[0041] **FIG. 7** illustrates a graph showing SER derived from two IDCI-precoding techniques.

[0042] **FIG. 8** illustrates an exemplary scenario in which a target client moves from a main DIDO cluster to an interfering cluster.

[0043] **FIG. 9** illustrates the signal-to-interference-plus-noise ratio (SINR) as a function of distance (D).

[0044] **FIG. 10** illustrates the symbol error rate (SER) performance of the three scenarios for 4-QAM modulation in flat-fading narrowband channels.

[0045] **FIG. 11** illustrates a method for IDCI precoding according to one embodiment of the invention.

[0046] **FIG. 12** illustrates the SINR variation in one embodiment as a function of the client's distance from the center of main DIDO clusters.

[0047] **FIG. 13** illustrates one embodiment in which the SER is derived for 4-QAM modulation.

[0048] **FIG. 14** illustrates one embodiment of the invention in which a finite state machine implements a handoff algorithm.

[0049] **FIG. 15** illustrates depicts one embodiment of a handoff strategy in the presence of shadowing.

[0050] **FIG. 16** illustrates a hysteresis loop mechanism when switching between any two states in Fig. 93.

[0051] **FIG. 17** illustrates one embodiment of a DIDO system with power control.

[0052] **FIG. 18** illustrates the SER versus SNR assuming four DIDO transmit antennas and four clients in different scenarios.

[0053] **FIG. 19** illustrates MPE power density as a function of distance from the source of RF radiation for different values of transmit power according to one embodiment of the invention.

[0054] **FIGS. 20a-b** illustrate different distributions of low-power and high-power DIDO distributed antennas.

[0055] **FIGS. 21a-b** illustrate two power distributions corresponding to the configurations in Figs. 20a and 20b, respectively.

[0056] **FIG. 22a-b** illustrate the rate distribution for the two scenarios shown in Figs. 99a and 99b, respectively.

[0057] **FIG. 23** illustrates one embodiment of a DIDO system with power control.

[0058] **FIG. 24** illustrates one embodiment of a method which iterates across all antenna groups according to Round-Robin scheduling policy for transmitting data.

[0059] **FIG. 25** illustrates a comparison of the uncoded SER performance of power control with antenna grouping against conventional eigenmode selection in U.S. Patent No. 7,636,381.

[0060] **FIGS. 26a-c** illustrate three scenarios in which BD precoding dynamically adjusts the precoding weights to account for different power levels over the wireless links between DIDO antennas and clients.

[0061] **FIG. 27** illustrates the amplitude of low frequency selective channels (assuming $\beta = 1$) over delay domain or instantaneous PDP (upper plot) and frequency domain (lower plot) for DIDO 2x2 systems

[0062] **FIG. 28** illustrates one embodiment of a channel matrix frequency response for DIDO 2x2, with a single antenna per client.

[0063] **FIG. 29** illustrates one embodiment of a channel matrix frequency response for DIDO 2x2, with a single antenna per client for channels characterized by high frequency selectivity (e.g., with $\beta = 0.1$).

[0064] **FIG. 30** illustrates exemplary SER for different QAM schemes (i.e., 4-QAM, 16-QAM, 64-QAM).

[0065] **FIG. 31** illustrates one embodiment of a method for implementing link adaptation (LA) techniques.

[0066] **FIG. 32** illustrates SER performance of one embodiment of the link adaptation (LA) techniques.

[0067] **FIG. 33** illustrates the entries of the matrix in equation (28) as a function of the OFDM tone index for DIDO 2x2 systems with $N_{FFT} = 64$ and $L_0 = 8$.

[0068] **FIG. 34** illustrates the SER versus SNR for $L_0 = 8$, M=N_t=2 transmit antennas and a variable number of P.

[0069] **FIG. 35** illustrates the SER performance of one embodiment of an interpolation method for different DIDO orders and $L_0 = 16$.

[0070] **FIG. 36** illustrates one embodiment of a system which employs super-clusters, DIDO-clusters and user-clusters.

[0071] **FIG. 37** illustrates a system with user clusters according to one embodiment of the invention.

[0072] **FIGS. 38a-b** illustrate link quality metric thresholds employed in one embodiment of the invention.

[0073] **FIGS. 39-41** illustrate examples of link-quality matrices for establishing user clusters.

[0074] **FIG. 42** illustrates an embodiment in which a client moves across different different DIDO clusters.

[0075] **FIGS. 43-46** illustrate relationships between the resolution of spherical arrays and their area A in one embodiment of the invention.

[0076] **FIG. 47** illustrates the degrees of freedom of MIMO systems in practical indoor and outdoor propagation scenarios.

[0077] **FIG. 48** illustrates the degrees of freedom in DIDO systems as a function of the array diameter.

[0078] **FIG. 49** illustrates one embodiment which includes multiple centralized processors (CP) and distributed nodes (DN) that communicate via wireline or wireless connections.

[0079] **FIG. 50** illustrates one embodiment in which CPs exchange control information with the unlicensed DNs and reconfigure them to shut down the frequency bands for licensed use.

[0080] **FIG. 51** illustrates one embodiment in which an entire spectrum is allocated to the new service and control information is used by the CPs to shut down all unlicensed DNs to avoid interference with the licensed DNs.

[0081] **FIG. 52** illustrates one embodiment of a cloud wireless system including multiple CPs, distributed nodes and a network interconnecting the CPs to the DNs.

[0082] **FIGS. 53-59** illustrate embodiments of a multiuser (MU) multiple antenna system (MAS) that adaptively reconfigures parameters to compensate for Doppler effects due to user mobility or changes in the propagation environment.

[0083] **FIG 60** illustrates a plurality of BTSs, some of which have good SNR and some of which have low Doppler with respect to a UE.

[0084] **FIG. 61** illustrates one embodiment of a matrix containing values of SNR and Doppler recorded by a CP for a plurality of BTS-UE links.

[0085] **FIG. 62** illustrates the channel gain (or CSI) at different times in accordance with one embodiment of the invention.

DETAILED DESCRIPTION

[0086] One solution to overcome many of the above prior art limitations is an embodiment of Distributed-Input Distributed-Output (DIDO) technology. DIDO technology is described in the following patents and patent applications, all of which are assigned the assignee of the present patent and are incorporated by reference. The present application is a continuation in part (CIP) to these patent applications. These patents and applications are sometimes referred to collectively herein as the "related patents and applications":

[0087] U.S. Application Serial No. 13/232,996, filed September 14, 2011, entitled "Systems And Methods To Exploit Areas of Coherence in Wirless Systems"

[0088] U.S. Application Serial No. 13/233,006, filed filed September 14, 2011, entitled "Systems and Methods for Planned Evoluation and Obsolescence of Multiuser Spectrum."

[0089] U.S. Application Serial No. 12/917,257, filed November 1, 2010, entitled "Systems And Methods To Coordinate Transmissions In Distributed Wireless Systems Via User Clustering"

[0090] U.S. Application Serial No. 12/802,988, filed June 16, 2010, entitled "Interference Management, Handoff, Power Control And Link Adaptation In Distributed-Input Distributed-Output (DIDO) Communication Systems"

[0091] U.S. Application Serial No. 12/802,976, filed June 16, 2010, entitled "System And Method For Adjusting DIDO Interference Cancellation Based On Signal Strength Measurements"

[0092] U.S. Application Serial No. 12/802,974, filed June 16, 2010, entitled "System And Method For Managing Inter-Cluster Handoff Of Clients Which Traverse Multiple DIDO Clusters"

[0093] U.S. Application Serial No. 12/802,989, filed June 16, 2010, entitled "System And Method For Managing Handoff Of A Client Between Different Distributed-Input-Distributed-Output (DIDO) Networks Based On Detected Velocity Of The Client"

[0094] U.S. Application Serial No. 12/802,958, filed June 16, 2010, entitled "System And Method For Power Control And Antenna Grouping In A Distributed-Input-Distributed-Output (DIDO) Network"

[0095] U.S. Application Serial No. 12/802,975, filed June 16, 2010, entitled "System And Method For Link adaptation In DIDO Multicarrier Systems"

[0096] U.S. Application Serial No. 12/802,938, filed June 16, 2010, entitled "System And Method For DIDO Precoding Interpolation In Multicarrier Systems"

[0097] U.S. Application Serial No. 12/630,627, filed December 2, 2009, entitled "System and Method For Distributed Antenna Wireless Communications"

[0098] U.S. Patent No. 7,599,420, filed August 20, 2007, issued Oct. 6, 2009, entitled "System and Method for Distributed Input Distributed Output Wireless Communication";

[0099] U.S. Patent No. 7,633,994, filed August 20, 2007, issued Dec. 15, 2009, entitled "System and Method for Distributed Input Distributed Output Wireless Communication";

[00100] U.S. Patent No. 7,636,381, filed August 20, 2007, issued Dec. 22, 2009, entitled "System and Method for Distributed Input Distributed Output Wireless Communication";

[00101] U.S. Application Serial No. 12/143,503, filed June 20, 2008 entitled, "System and Method For Distributed Input-Distributed Output Wireless Communications";

[00102] U.S. Application Serial No. 11/256,478, filed October 21, 2005 entitled "System and Method For Spatial-Multiplexed Tropospheric Scatter Communications";

[00103] U.S. Patent No. 7,418,053, filed July 30, 2004, issued August 26, 2008, entitled "System and Method for Distributed Input Distributed Output Wireless Communication";

[00104] U.S. Application Serial No. 10/817,731, filed April 2, 2004 entitled "System and Method For Enhancing Near Vertical Incidence Skywave ("NVIS") Communication Using Space-Time Coding.

[00105] To reduce the size and complexity of the present patent application, the disclosure of some of the related patents and applications is not explicitly set forth below. Please see the related patents and applications for a full detailed description of the disclosure.

[00106] Note that section I below (Disclosure From Related Application Serial No. 12/802,988) utilizes its own set of endnotes which refer to prior art references and prior applications assigned to the assignee of the present application. The endnote citations are listed at the end of section I (just prior to the heading for Section II). Citations in Section II uses may have numerical designations for its citations which overlap with those used in Section I even through these numerical designations identify different references (listed at the end of Section II). Thus, references identified by a particular numerical designation may be identified within the section in which the numerical designation is used.

I. Disclosure From Related Application Serial No. 12/802,988

1. Methods to Remove Inter-cluster Interference

[00121] Described below are wireless radio frequency (RF) communication systems and methods employing a plurality of distributed transmitting antennas to create locations in space with zero RF energy. When M transmit antennas are employed, it is possible to create up to (M-1) points of zero RF energy in predefined locations. In one embodiment of the invention, the points of zero RF energy are wireless devices and the transmit antennas are aware of the channel

state information (CSI) between the transmitters and the receivers. In one embodiment, the CSI is computed at the receivers and fed back to the transmitters. In another embodiment, the CSI is computed at the transmitter via training from the receivers, assuming channel reciprocity is exploited. The transmitters may utilize the CSI to determine the interfering signals to be simultaneously transmitted. In one embodiment, block diagonalization (BD) precoding is employed at the transmit antennas to generate points of zero RF energy.

[00122] The system and methods described herein differ from the conventional receive/transmit beamforming techniques described above. In fact, receive beamforming computes the weights to suppress interference at the receive side (via null-steering), whereas some embodiments of the invention described herein apply weights at the transmit side to create interference patters that result in one or multiple locations in space with "zero RF energy." Unlike conventional transmit beamforming or BD precoding designed to maximize signal quality (or SINR) to every user or downlink throughput, respectively, the systems and methods described herein minimize signal quality under certain conditions and/or from certain transmitters, thereby creating points of zero RF energy at the client devices (sometimes referred to herein as "users"). Moreover, in the context of distributed-input distributed-output (DIDO) systems (described in our related patents and applications), transmit antennas distributed in space provide higher degrees of freedom (i.e., higher channel spatial diversity) that can be exploited to create multiple points of zero RF energy and/or maximum SINR to different users. For example, with M transmit antennas it is possible to create up to (M-1) points of RF energy. By contrast, practical beamforming or BD multiuser systems are typically designed with closely spaced antennas at the transmit side that limit the number of simultaneous users that can be serviced over the wireless link, for any number of transmit antennas M.

[00123] Consider a system with M transmit antennas and K users, with K<M. We assume the transmitter is aware of the CSI ($\mathbf{H} \in \mathbb{C}^{K\text{x}M}$) between the M transmit antennas and K users. For simplicity, every user is assumed to be equipped with single antenna, but the same method can be extended to multiple receive antennas per user. The precoding weights ($\mathbf{w} \in \mathbb{C}^{M\text{x}1}$) that create zero RF energy at the K users' locations are computed to satisfy the following condition

$$\mathbf{H}\mathbf{w} = \mathbf{0}^{K\text{x}1}$$

where $\mathbf{0}^{K\text{x}1}$ is the vector with all zero entries and $\mathbf{H}$ is the channel matrix obtained by combining the channel vectors ($\mathbf{h}_k \in \mathbb{C}^{1\text{x}M}$) from the M transmit antennas to the K users as

$$\mathbf{H} = \begin{bmatrix} \mathbf{h}_1 \\ \vdots \\ \mathbf{h}_k \\ \vdots \\ \mathbf{h}_K \end{bmatrix}.$$

In one embodiment, singular value decomposition (SVD) of the channel matrix **H** is computed and the precoding weight **w** is defined as the right singular vector corresponding to the null subspace (identified by zero singular value) of **H**.

The transmit antennas employ the weight vector defined above to transmit RF energy, while creating K points of zero RF energy at the locations of the K users such that the signal received at the k^{th} user is given by

$$r_k = \mathbf{h}_k \mathbf{w} s_k + n_k = 0 + n_k$$

where $n_k \in C^{1x1}$ is the additive white Gaussian noise (AWGN) at the k^{th} user.

In one embodiment, singular value decomposition (SVD) of the channel matrix **H** is computed and the precoding weight **w** is defined as the right singular vector corresponding to the null subspace (identified by zero singular value) of **H**.

[00124] In another embodiment, the wireless system is a DIDO system and points of zero RF energy are created to pre-cancel interference to the clients between different DIDO coverage areas. In U.S. Application Serial No. 12/630,627, a DIDO system is described which includes:

- DIDO clients
- DIDO distributed antennas
- DIDO base transceiver stations (BTS)
- DIDO base station network (BSN)

Every BTS is connected via the BSN to multiple distributed antennas that provide service to given coverage area called *DIDO cluster*. In the present patent application we describe a system and method for removing interference between adjacent DIDO clusters. As illustrated in **Figure 1**, we assume the *main* DIDO cluster hosts the client (i.e. a user device served by the multi-user DIDO system) affected by interference (or *target client*) from the *neighbor* clusters.

[00125] In one embodiment, neighboring clusters operate at different frequencies according to frequency division multiple access (FDMA) techniques similar to conventional cellular systems. For example, with frequency reuse factor of 3, the same carrier frequency is reused every third DIDO cluster as illustrated in **Figure 2**. In **Figure 2**, the different carrier frequencies are identified as F_1, F_2 and F_3. While this embodiment may be used in some implementations, this solution yields loss in spectral efficiency since the available spectrum is divided in multiple subbands and only a subset of DIDO clusters operate in the same subband. Moreover, it requires complex cell planning to associate different DIDO clusters to different frequencies, thereby preventing interference. Like prior art cellular systems, such cellular planning requires specific placement of antennas and limiting of transmit power to as to avoid interference between clusters using the same frequency.

[00126] In another embodiment, neighbor clusters operate in the same frequency band, but at different time slots according to time division multiple access (TDMA) technique. For example, as illustrated in **Figure 3** DIDO transmission is allowed only in time slots T_1, T_2, and T_3 for certain clusters, as illustrated. Time slots can be assigned equally to different clusters, such that different clusters are scheduled according to a Round-Robin policy. If different clusters are characterized by different data rate requirements (i.e., clusters in crowded urban environments as opposed to clusters in rural areas with fewer number of clients per area of coverage), different priorities are assigned to different clusters such that more time slots are assigned to the clusters with larger data rate requirements. While TDMA as described above may be employed in one embodiment of the invention, a TDMA approach may require time synchronization across different clusters and may result in lower spectral efficiency since interfering clusters cannot use the same frequency at the same time.

[00127] In one embodiment, all neighboring clusters transmit at the same time in the same frequency band and use spatial processing across clusters to avoid interference. In this embodiment, the multi-cluster DIDO system: (i) uses conventional DIDO precoding within the main cluster to transmit simultaneous non-interfering data streams within the same frequency band to multiple clients (such as described in the related patents and applications, including 7,599,420; 7,633,994; 7,636,381; and Application Serial No. 12/143,503); (ii) uses DIDO precoding with interference cancellation in the neighbor clusters to avoid interference to the clients lying in the *interfering zones* 8010 in **Figure 4**, by creating points of zero radio frequency (RF) energy at the locations of the target clients. If a target client is in an interfering zone 410, it will receive the sum of the RF containing the data stream from the main cluster 411 and the zero RF energy from the interfering cluster 412-413, which will simply be the RF containing the data stream from the main cluster. Thus, adjacent clusters can utilize the same frequency simultaneously without target clients in the interfering zone suffering from interference.

[00128] In practical systems, the performance of DIDO precoding may be affected by different factors such as: channel estimation error or Doppler effects (yielding obsolete channel state information at the DIDO distributed antennas); intermodulation distortion (IMD) in multicarrier DIDO systems; time or frequency offsets. As a result of these effects, it may be impractical to achieve points of zero RF energy. However, as long as the RF energy at the target client from the interfering clusters is negligible compared to the RF energy from the main cluster, the link performance at the target client is unaffected by the interference. For example, let us assume the client requires 20dB signal-to-noise ratio (SNR) to demodulate 4-QAM constellations using forward error correction (FEC) coding to achieve target bit error rate (BER) of 10^{-6}. If the RF energy at the target client received from the interfering cluster is 20dB below

the RF energy received from the main cluster, the interference is negligible and the client can demodulate data successfully within the predefined BER target. Thus, the term "zero RF energy" as used herein does not necessarily mean that the RF energy from interfering RF signals is zero. Rather, it means that the RF energy is sufficiently low relative to the RF energy of the desired RF signal such that the desired RF signal may be received at the receiver. Moreover, while certain desirable thresholds for interfering RF energy relative to desired RF energy are described, the underlying principles of the invention are not limited to any particular threshold values.

[00129] There are different types of interfering zones 8010 as shown in **Figure 4**. For example, "type A" zones (as indicated by the letter "A" in Figure 80) are affected by interference from only one neighbor cluster, whereas "type B" zones (as indicated by the letter "B") account for interference from two or multiple neighbor clusters.

[00130] **Figure 5** depicts a framework employed in one embodiment of the invention. The dots denote DIDO distributed antennas, the crosses refer to the DIDO clients and the arrows indicate the directions of propagation of RF energy. The DIDO antennas in the main cluster transmit precoded data signals to the clients MC 501 in that cluster. Likewise, the DIDO antennas in the interfering cluster serve the clients IC 502 within that cluster via conventional DIDO precoding. The green cross 503 denotes the target client TC 503 in the interfering zone. The DIDO antennas in the main cluster 511 transmit precoded data signals to the target client (black arrows) via conventional DIDO precoding. The DIDO antennas in the interfering cluster 512 use precoding to create zero RF energy towards the directions of the target client 503 (green arrows).

[00131] The received signal at target client k in any interfering zone 410A, B in **Figure 4** is given by

$$\mathbf{r}_k = \mathbf{H}_k \mathbf{W}_k \mathbf{s}_k + \mathbf{H}_k \sum_{\substack{u=1 \\ u \neq k}}^{U} \mathbf{W}_u \mathbf{s}_u + \sum_{c=1}^{C} \mathbf{H}_{c,k} \sum_{i=1}^{I_c} \mathbf{W}_{c,i} \mathbf{s}_{c,i} + \mathbf{n}_k \qquad (1)$$

where k=1,…,K, with K being the number of clients in the interfering zone 8010A, B, U is the number of clients in the main DIDO cluster, C is the number of interfering DIDO clusters 412-413 and I_c is the number of clients in the interfering cluster c. Moreover, $\mathbf{r}_k \in \mathbb{C}^{N \times M}$ is the vector containing the receive data streams at client k, assuming M transmit DIDO antennas and N receive antennas at the client devices; $\mathbf{s}_k \in \mathbb{C}^{N \times 1}$ is the vector of transmit data streams to client k in the main DIDO cluster; $\mathbf{s}_u \in \mathbb{C}^{N \times 1}$ is the vector of transmit data streams to client u in the main DIDO cluster; $\mathbf{s}_{c,i} \in \mathbb{C}^{N \times 1}$ is the vector of transmit data streams to client i in the c^{th} interfering DIDO cluster; $\mathbf{n}_k \in \mathbb{C}^{N \times 1}$ is the vector of additive white Gaussian noise (AWGN) at the N receive antennas of client k; $\mathbf{H}_k \in \mathbb{C}^{N \times M}$ is the DIDO channel matrix from the M transmit DIDO antennas to the N receive antennas at client k in the main DIDO cluster; $\mathbf{H}_{c,k} \in \mathbb{C}^{N \times M}$ is the

DIDO channel matrix from the M transmit DIDO antennas to the N receive antennas t client k in the c^{th} interfering DIDO cluster; $\mathbf{W}_k \in \mathbb{C}^{M\text{x}N}$ is the matrix of DIDO precoding weights to client k in the main DIDO cluster; $\mathbf{W}_k \in \mathbb{C}^{M\text{x}N}$ is the matrix of DIDO precoding weights to client u in the main DIDO cluster; $\mathbf{W}_{c,i} \in \mathbb{C}^{M\text{x}N}$ is the matrix of DIDO precoding weights to client i in the c^{th} interfering DIDO cluster.

[00132] To simplify the notation and without loss of generality, we assume all clients are equipped with N receive antennas and there are M DIDO distributed antennas in every DIDO cluster, with $M \geq (N \cdot U)$ and $M \geq (N \cdot I_c), \forall c = 1, \ldots, C$. If M is larger than the total number of receive antennas in the cluster, the extra transmit antennas are used to pre-cancel interference to the target clients in the interfering zone or to improve link robustness to the clients within the same cluster via diversity schemes described in the related patents and applications, including 7,599,420; 7,633,994; 7,636,381; and Application Serial No. 12/143,503.

[00133] The DIDO precoding weights are computed to pre-cancel inter-client interference within the same DIDO cluster. For example, block diagonalization (BD) precoding described in the related patents and applications, including 7,599,420; 7,633,994; 7,636,381; and Application Serial No. 12/143,503 and [7] can be used to remove inter-client interference, such that the following condition is satisfied in the main cluster

$$\mathbf{H}_k \mathbf{W}_u = \mathbf{0}^{N\text{x}N}; \quad \forall\, u = 1, \ldots, U; \text{ with } u \neq k. \tag{2}$$

The precoding weight matrices in the neighbor DIDO clusters are designedsuch that the following condition is satisfied

$$\mathbf{H}_{c,k} \mathbf{W}_{c,i} = \mathbf{0}^{N\text{x}N}; \quad \forall\, c = 1, \ldots, C \text{ and } \forall\, i = 1, \ldots, I_c. \tag{3}$$

To compute the precoding matrices $\mathbf{W}_{c,i}$, the downlink channel from the M transmit antennas to the I_c clients in the interfering cluster as well as to client k in the interfering zone is estimated and the precoding matrix is computed by the DIDO BTS in the interfering cluster. If BD method is used to compute the precoding matrices in the interfering clusters, the following effective channel matrix is built to compute the weights to the i^{th} client in the neighbor clusters

$$\bar{\mathbf{H}}_{c,i} = \begin{bmatrix} \mathbf{H}_{c,k} \\ \widetilde{\mathbf{H}}_{c,i} \end{bmatrix} \tag{4}$$

where $\widetilde{\mathbf{H}}_{c,i}$ is the matrix obtained from the channel matrix $\mathbf{H}_c \in \mathbb{C}^{(N \cdot I_c)\text{x}M}$ for the interfering cluster c, where the rows corresponding to the i^{th} client are removed.

Substituting conditions (2) and (3) into (1), we obtain the received data streams for target client k, where intra-cluster and inter-cluster interference is removed

$$\mathbf{r}_k = \mathbf{H}_k \mathbf{W}_k \mathbf{s}_k + \mathbf{n}_k. \tag{5}$$

The precoding weights $\mathbf{W}_{c,i}$ in (1) computed in the neighbor clusters are designed to transmit precoded data streams to all clients in those clusters, while pre-cancelling interference to the

target client in the interfering zone. The target client receives precoded data only from its main cluster. In a different embodiment, the same data stream is sent to the target client from both main and neighbor clusters to obtain diversity gain. In this case, the signal model in (5) is expressed as

$$\mathbf{r}_k = \left(\mathbf{H}_k \mathbf{W}_k + \sum_{c=1}^{C} \mathbf{H}_{c,k}\, \mathbf{W}_{c,k}\right)\mathbf{s}_k + \mathbf{n}_k \quad (6)$$

where $\mathbf{W}_{c,\mathrm{k}}$ is the DIDO precoding matrix from the DIDO transmitters in the c^{th} cluster to the target client k in the interfering zone. Note that the method in (6) requires time synchronization across neighboring clusters, which may be complex to achieve in large systems, but nonetheless, is quite feasible if the diversity gain benefit justifies the cost of implementation.

[00134] We begin by evaluating the performance of the proposed method in terms of symbol error rate (SER) as a function of the signal-to-noise ratio (SNR). Without loss of generality, we define the following signal model assuming single antenna per client and reformulate (1) as

$$r_k = \sqrt{\mathrm{SNR}}\, \mathbf{h}_k \mathbf{w}_k s_k + \sqrt{\mathrm{INR}}\, \mathbf{h}_{c,k} \sum_{i=1}^{I} \mathbf{w}_{c,i}\, s_{c,i} + n_k \quad (7)$$

where INR is the interference-to-noise ratio defined as INR=SNR/SIR and SIR is the signal-to-interference ratio.

[00135] **Figure 6** shows the SER as a function of the SNR, assuming SIR=10dB for the target client in the interfering zone. Without loss of generality, we measured the SER for 4-QAM and 16-QAM without forwards error correction (FEC) coding. We fix the target SER to 1% for uncoded systems. This target corresponds to different values of SNR depending on the modulation order (i.e., SNR=20dB for 4-QAM and SNR=28dB for 16-QAM). Lower SER targets can be satisfied for the same values of SNR when using FEC coding due to coding gain. We consider the scenario of two clusters (one main cluster and one interfering cluster) with two DIDO antennas and two clients (equipped with single antenna each) per cluster. One of the clients in the main cluster lies in the interfering zone. We assume flat-fading narrowband channels, but the following results can be extended to frequency selective multicarrier (OFDM) systems, where each subcarrier undergoes flat-fading. We consider two scenarios: (i) one with *inter-DIDO-cluster interference* (IDCI) where the precoding weights $\mathbf{w}_{c,\mathrm{i}}$ are computed without accounting for the target client in the interfering zone; and (ii) the other where the IDCI is removed by computing the weights $\mathbf{w}_{c,\mathrm{i}}$ to cancel IDCI to the target client. We observe that in presence of IDCI the SER is high and above the predefined target. With IDCI-precoding at the neighbor cluster the interference to the target client is removed and the SER targets are reached for SNR>20dB.

[00136] The results in **Figure 6** assumes IDCI-precoding as in (5). If IDCI-precoding at the neighbor clusters is also used to precode data streams to the target client in the interfering zone as in (6), additional diversity gain is obtained. **Figure 7** compares the SER derived from two

techniques: (i) "Method 1" using the IDCI-precoding in (5); (ii) "Method 2" employing IDCI-precoding in (6) where the neighbor clusters also transmit precoded data stream to the target client. Method 2 yields ~3dB gain compared to conventional IDCI-precoding due to additional array gain provided by the DIDO antennas in the neighbor cluster used to transmit precoded data stream to the target client. More generally, the array gain of Method 2 over Method 1 is proportional to 10*log10(C+1), where C is the number of neighbor clusters and the factor "1" refers to the main cluster.

[00137] Next, we evaluate the performance of the above method as a function of the target client's location with respect to the interfering zone. We consider one simple scenario where a target client 8401 moves from the main DIDO cluster 802 to the interfering cluster 803, as depicted in **Figure 8**. We assume all DIDO antennas 812 within the main cluster 802 employ BD precoding to cancel intra-cluster interference to satisfy condition (2). We assume single interfering DIDO cluster, single receiver antenna at the client device 801 and equal pathloss from all DIDO antennas in the main or interfering cluster to the client (i.e., DIDO antennas placed in circle around the client). We use one simplified pathloss model with pathloss exponent 4 (as in typical urban environments) [11].

The analysis hereafter is based on the following simplified signal model that extends (7) to account for pathloss

$$r_k = \sqrt{\frac{\mathrm{SNR}\cdot \mathrm{D_o^4}}{\mathrm{D^4}}}\mathbf{h}_k\mathbf{w}_k s_k + \sqrt{\frac{\mathrm{SNR}\cdot \mathrm{D_o^4}}{(1-\mathrm{D})^4}}\mathbf{h}_{c,k}\sum_{i=1}^{I}\mathbf{w}_{c,i}\, s_{c,i} + n_k \qquad (8)$$

where the signal-to-interference (SIR) is derived as SIR=((1-D)/D)^4. In modeling the IDCI, we consider three scenarios: i) ideal case with no IDCI; ii) IDCI pre-cancelled via BD precoding in the interfering cluster to satisfy condition (3); iii) with IDCI, not pre-cancelled by the neighbor cluster.

[00138] **Figure 9** shows the signal-to-interference-plus-noise ratio (SINR) as a function of D (i.e., as the target client moves from the main cluster 802 towards the DIDO antennas 813 in the interfering cluster 8403). The SINR is derived as the ratio of signal power and interference plus noise power using the signal model in (8). We assume that D_o=0.1 and SNR=50dB for D=D_o. In absence of IDCI the wireless link performance is only affected by noise and the SINR decreases due to pathloss. In presence of IDCI (i.e., without IDCI-precoding) the interference from the DIDO antennas in the neighbor cluster contributes to reduce the SINR.

[00139] **Figure 10** shows the symbol error rate (SER) performance of the three scenarios above for 4-QAM modulation in flat-fading narrowband channels. These SER results correspond to the SINR in **Figure 9**. We assume SER threshold of 1% for uncoded systems (i.e., without FEC) corresponding to SINR threshold $\mathrm{SINR_T}$=20dB in **Figure 9**. The SINR threshold depends

on the modulation order used for data transmission. Higher modulation orders are typically characterized by higher $SINR_T$ to achieve the same target error rate. With FEC, lower target SER can be achieved for the same SINR value due to coding gain. In case of IDCI without precoding, the target SER is achieved only within the range $D<0.25$. With IDCI-precoding at the neighbor cluster the range that satisfies the target SER is extended up to $D<0.6$. Beyond that range, the SINR increases due to pathloss and the SER target is not satisfied.

[00140] One embodiment of a method for IDCI precoding is shown in **Figure 11** and consists of the following steps:

- **SIR estimate 1101**: Clients estimate the signal power from the main DIDO cluster (i.e., based on received precoded data) and the interference-plus-noise signal power from the neighbor DIDO clusters. In single-carrier DIDO systems, the frame structure can be designed with short periods of silence. For example, periods of silence can be defined between training for channel estimation and precoded data transmissions during channel state information (CSI) feedback. In one embodiment, the interference-plus-noise signal power from neighbor clusters is measured during the periods of silence from the DIDO antennas in the main cluster. In practical DIDO multicarrier (OFDM) systems, null tones are typically used to prevent direct current (DC) offset and attenuation at the edge of the band due to filtering at transmit and receive sides. In another embodiment employing multicarrier systems, the interference-plus-noise signal power is estimated from the null tones. Correction factors can be used to compensate for transmit/receive filter attenuation at the edge of the band. Once the signal-plus-interference-and-noise power (P_S) from the main cluster and the interference-plus-noise power from neighbor clusters (P_{IN}) are estimated, the client computes the SINR as

$$\mathrm{SINR} = \frac{P_S - P_{IN}}{P_{IN}}. \quad (9)$$

Alternatively, the SINR estimate is derived from the received signal strength indication (RSSI) used in typical wireless communication systems to measure the radio signal power.

We observe the metric in (9) cannot discriminate between noise and interference power level. For example, clients affected by shadowing (i.e., behind obstacles that attenuate the signal power from all DIDO distributed antennas in the main cluster) in interference-free environments may estimate low SINR even though they are not affected by inter-cluster interference.

A more reliable metric for the proposed method is the SIR computed as

$$\mathrm{SIR} = \frac{P_S - P_{IN}}{P_{IN} - P_N} \quad (10)$$

where P_N is the noise power. In practical multicarrier OFDM systems, the noise power P_N in (10) is estimated from the null tones, assuming all DIDO antennas from main and neighbor clusters use the same set of null tones. The interference-plus-noise power (P_{IN}), is estimated from the period of silence as mentioned above. Finally, the signal-plus-interference-and-noise power (P_S) is derived from the data tones. From these estimates, the client computes the SIR in (10).

- **Channel estimation at neighbor clusters 1102-1103**: If the estimated SIR in (10) is below predefined threshold (SIR_T), determined at 8702 in **Figure 11**, the client starts listening to training signals from neighbor clusters. Note that SIR_T depends on the modulation and FEC coding scheme (MCS) used for data transmission. Different SIR targets are defined depending on the client's MCS. When DIDO distributed antennas from different clusters are time-synchronized (i.e., locked to the same pulse-per-second, PPS, time reference), the client exploits the training sequence to deliver its channel estimates to the DIDO antennas in the neighbor clusters at 8703. The training sequence for channel estimation in the neighbor clusters are designed to be orthogonal to the training from the main cluster. Alternatively, when DIDO antennas in different clusters are not time-synchronized, orthogonal sequences (with good cross-correlation properties) are used for time synchronization in different DIDO clusters. Once the client locks to the time/frequency reference of the neighbor clusters, channel estimation is carried out at 1103.
- **IDCI Precoding 1104**: Once the channel estimates are available at the DIDO BTS in the neighbor clusters, IDCI-precoding is computed to satisfy the condition in (3). The DIDO antennas in the neighbor clusters transmit precoded data streams only to the clients in their cluster, while pre-cancelling interference to the clients in the interfering zone 410 in **Figure 4**. We observe that if the client lies in the type B interfering zone 410 in **Figure 4**, interference to the client is generated by multiple clusters and IDCI-precoding is carried out by all neighbor clusters at the same time.

Methods for Handoff

[00141] Hereafter, we describe different handoff methods for clients that move across DIDO clusters populated by distributed antennas that are located in separate areas or that provide different kinds of services (i.e., low- or high-mobility services).

a. Handoff Between Adjacent DIDO Clusters

[00142] In one embodiment, the IDCI-precoder to remove inter-cluster interference described above is used as a baseline for handoff methods in DIDO systems. Conventional handoff in cellular systems is conceived for clients to switch seamlessly across cells served by different base stations. In DIDO systems, handoff allows clients to move from one cluster to another without loss of connection.

[00143] To illustrate one embodiment of a handoff strategy for DIDO systems, we consider again the example in **Figure 8** with only two clusters 802 and 803. As the client 801 moves from the main cluster (C1) 802 to the neighbor cluster (C2) 803, one embodiment of a handoff method dynamically calculates the signal quality in different clusters and selects the cluster that yields the lowest error rate performance to the client.

[00144] **Figure 12** shows the SINR variation as a function of the client's distance from the center of clusters C1. For 4-QAM modulation without FEC coding, we consider target SINR=20dB. The line identified by circles represents the SINR for the target client being served by the DIDO antennas in C1, when both C1 and C2 use DIDO precoding without interference cancellation. The SINR decreases as a function of D due to pathloss and interference from the neighboring cluster. When IDCI-precoding is implemented at the neighboring cluster, the SINR loss is only due to pathloss (as shown by the line with triangles), since interference is completely removed. Symmetric behavior is experienced when the client is served from the neighboring cluster. One embodiment of the handoff strategy is defined such that, as the client moves from C1 to C2, the algorithm switches between different DIDO schemes to maintain the SINR above predefined target.

[00145] From the plots in **Figure 12**, we derive the SER for 4-QAM modulation in **Figure 13**. We observe that, by switching between different precoding strategies, the SER is maintained within predefined target.

[00146] One embodiment of the handoff strategy is as follows.

- **C1-DIDO and C2-DIDO precoding**: When the client lies within C1, away from the interfering zone, both clusters C1 and C2 operate with conventional DIDO precoding independently.
- **C1-DIDO and C2-IDCI precoding**: As the client moves towards the interfering zone, its SIR or SINR degrades. When the target $SINR_{T1}$ is reached, the target client starts estimating the channel from all DIDO antennas in C2 and provides the CSI to the BTS of C2. The BTS in C2 computes IDCI-precoding and transmits to all clients in C2 while preventing interference to the target client. For as long as the target client is within the interfering zone, it will continue to provide its CSI to both C1 and C2.

- **C1-IDCI and C2-DIDO precoding**: As the client moves towards C2, its SIR or SINR keeps decreasing until it again reaches a target. At this point the client decides to switch to the neighbor cluster. In this case, C1 starts using the CSI from the target client to create zero interference towards its direction with IDCI-precoding, whereas the neighbor cluster uses the CSI for conventional DIDO-precoding. In one embodiment, as the SIR estimate approaches the target, the clusters C1 and C2 try both DIDO- and IDCI-precoding schemes alternatively, to allow the client to estimate the SIR in both cases. Then the client selects the best scheme, to maximize certain error rate performance metric. When this method is applied, the cross-over point for the handoff strategy occurs at the intersection of the curves with triangles and rhombus in **Figure 12**. One embodiment uses the modified IDCI-precoding method described in (6) where the neighbor cluster also transmits precoded data stream to the target client to provide array gain. With this approach the handoff strategy is simplified, since the client does not need to estimate the SINR for both strategies at the cross-over point.
- **C1-DIDO and C2-DIDO precoding**: As the client moves out of the interference zone towards C2, the main cluster C1 stops pre-cancelling interference towards that target client via IDCI-precoding and switches back to conventional DIDO-precoding to all clients remaining in C1. This final cross-over point in our handoff strategy is useful to avoid unnecessary CSI feedback from the target client to C1, thereby reducing the overhead over the feedback channel. In one embodiment a second target $SINR_{T2}$ is defined. When the SINR (or SIR) increases above this target, the strategy is switched to C1-DIDO and C2-DIDO. In one embodiment, the cluster C1 keeps alternating between DIDO- and IDCI-precoding to allow the client to estimate the SINR. Then the client selects the method for C1 that more closely approaches the target $SINR_{T1}$ from above.

[00147] The method described above computes the SINR or SIR estimates for different schemes in real time and uses them to select the optimal scheme. In one embodiment, the handoff algorithm is designed based on the finite-state machine illustrated in **Figure 14**. The client keeps track of its current state and switches to the next state when the SINR or SIR drops below or above the predefined thresholds illustrated in **Figure 12**. As discussed above, in state 1201, both clusters C1 and C2 operate with conventional DIDO precoding independently and the client is served by cluster C1; in state 1202, the client is served by cluster C1, the BTS in C2 computes IDCI-precoding and cluster C1 operates using conventional DIDO precoding; in state 1203, the client is served by cluster C2, the BTS in C1 computes IDCI-precoding and cluster C2

operates using conventional DIDO precoding; and in state 1204, the client is served by cluster C2, and both clusters C1 and C2 operate with conventional DIDO precoding independently.

[00148] In presence of shadowing effects, the signal quality or SIR may fluctuate around the thresholds as shown in **Figure 15**, causing repetitive switching between consecutive states in **Figure 14**. Changing states repetitively is an undesired effect, since it results in significant overhead on the control channels between clients and BTSs to enable switching between transmission schemes. **Figure 15** depicts one example of a handoff strategy in the presence of shadowing. In one embodiment, the shadowing coefficient is simulated according to log-normal distribution with variance 3 [3]. Hereafter, we define some methods to prevent repetitive switching effect during DIDO handoff.

[00149] One embodiment of the invention employs a *hysteresis loop* to cope with state switching effects. For example, when switching between "C1-DIDO,C2-IDCI" 9302 and "C1-IDCI,C2-DIDO" 9303 states in **Figure 14** (or vice versa) the threshold $SINR_{T1}$ can be adjusted within the range A_1. This method avoids repetitive switches between states as the signal quality oscillates around $SINR_{T1}$. For example, **Figure 16** shows the hysteresis loop mechanism when switching between any two states in **Figure 14**. To switch from state B to A the SIR must be larger than $(SIR_{T1}+A_1/2)$, but to switch back from A to B the SIR must drop below $(SIR_{T1}-A_1/2)$.

[00150] In a different embodiment, the threshold $SINR_{T2}$ is adjusted to avoid repetitive switching between the first and second (or third and fourth) states of the finite-state machine in **Figure 14**. For example, a range of values A_2 may be defined such that the threshold $SINR_{T2}$ is chosen within that range depending on channel condition and shadowing effects.

[00151] In one embodiment, depending on the variance of shadowing expected over the wireless link, the SINR threshold is dynamically adjusted within the range $[SINR_{T2}, SINR_{T2}+A_2]$. The variance of the log-normal distribution can be estimated from the variance of the received signal strength (or RSSI) as the client moves from its current cluster to the neighbor cluster.

[00152] The methods above assume the client triggers the handoff strategy. In one embodiment, the handoff decision is deferred to the DIDO BTSs, assuming communication across multiple BTSs is enabled.

[00153] For simplicity, the methods above are derived assuming no FEC coding and 4-QAM. More generally, the SINR or SIR thresholds are derived for different modulation coding schemes (MCSs) and the handoff strategy is designed in combination with link adaptation (*see, e.g.*, U.S. Patent No. 7,636,381) to optimize downlink data rate to each client in the interfering zone.

b. Handoff Between Low- and High-Doppler DIDO Networks

[00154] DIDO systems employ closed-loop transmission schemes to precode data streams over the downlink channel. Closed-loop schemes are inherently constrained by latency over the feedback channel. In practical DIDO systems, computational time can be reduced by transceivers with high processing power and it is expected that most of the latency is introduced by the DIDO BSN, when delivering CSI and baseband precoded data from the BTS to the distributed antennas. The BSN can be comprised of various network technologies including, but not limited to, digital subscriber lines (DSL), cable modems, fiber rings, T1 lines, hybrid fiber coaxial (HFC) networks, and/or fixed wireless (e.g., WiFi). Dedicated fiber typically has very large bandwidth and low latency, potentially less than a millisecond in local region, but it is less widely deployed than DSL and cable modems. Today, DSL and cable modem connections typically have between 10-25ms in last-mile latency in the United States, but they are very widely deployed.

[00155] The maximum latency over the BSN determines the maximum Doppler frequency that can be tolerated over the DIDO wireless link without performance degradation of DIDO precoding. For example, in [1] we showed that at the carrier frequency of 400MHz, networks with latency of about 10msec (i.e., DSL) can tolerate clients' velocity up to 8mph (running speed), whereas networks with 1msec latency (i.e., fiber ring) can support speed up to 70mph (i.e., freeway traffic).

[00156] We define two or multiple DIDO sub-networks depending on the maximum Doppler frequency that can be tolerated over the BSN. For example, a BSN with high-latency DSL connections between the DIDO BTS and distributed antennas can only deliver low mobility or fixed-wireless services (i.e., *low-Doppler network*), whereas a low-latency BSN over a low-latency fiber ring can tolerate high mobility (i.e., *high-Doppler network*). We observe that the majority of broadband users are not moving when they use broadband, and further, most are unlikely to be located near areas with many high speed objects moving by (e.g., next to a highway) since such locations are typically less desirable places to live or operate an office. However, there are broadband users who will be using broadband at high speeds (e.g., while in a car driving on the highway) or will be near high speed objects (e.g., in a store located near a highway). To address these two differing user Doppler scenarios, in one embodiment, a low-Doppler DIDO network consists of a typically larger number of DIDO antennas with relatively low power (i.e., 1W to 100W, for indoor or rooftop installation) spread across a wide area, whereas a high-Doppler network consists of a typically lower number of DIDO antennas with high power transmission (i.e., 100W for rooftop or tower installation). The low-Doppler DIDO network serves the typically larger number of low-Doppler users and can do so at typically lower

connectivity cost using inexpensive high-latency broadband connections, such as DSL and cable modems. The high-Doppler DIDO network serves the typically fewer number of high-Doppler users and can do so at typically higher connectivity cost using more expensive low-latency broadband connections, such as fiber.

[00157] To avoid interference across different types of DIDO networks (e.g. low-Doppler and high-Doppler), different multiple access techniques can be employed such as: time division multiple access (TDMA), frequency division multiple access (FDMA), or code division multiple access (CDMA).

[00158] Hereafter, we propose methods to assign clients to different types of DIDO networks and enable handoff between them. The network selection is based on the type of mobility of each client. The client's velocity (v) is proportional to the maximum Doppler shift according to the following equation [6]

$$f_d = \frac{v}{\lambda}\sin\theta \tag{11}$$

where f_d is the maximum Doppler shift, λ is the wavelength corresponding to the carrier frequency and θ is the angle between the vector indicating the direction transmitter-client and the velocity vector.

[00159] In one embodiment, the Doppler shift of every client is calculated via blind estimation techniques. For example, the Doppler shift can be estimated by sending RF energy to the client and analyzing the reflected signal, similar to Doppler radar systems.

[00160] In another embodiment, one or multiple DIDO antennas send training signals to the client. Based on those training signals, the client estimates the Doppler shift using techniques such as counting the zero-crossing rate of the channel gain, or performing spectrum analysis. We observe that for fixed velocity v and client's trajectory, the angular velocity $v\sin\theta$ in (11) may depend on the relative distance of the client from every DIDO antenna. For example, DIDO antennas in the proximity of a moving client yield larger angular velocity and Doppler shift than faraway antennas. In one embodiment, the Doppler velocity is estimated from multiple DIDO antennas at different distances from the client and the average, weighted average or standard deviation is used as an indicator for the client's mobility. Based on the estimated Doppler indicator, the DIDO BTS decides whether to assign the client to low- or high-Doppler networks.

[00161] The Doppler indicator is periodically monitored for all clients and sent back to the BTS. When one or multiple clients change their Doppler velocity (i.e., client riding in the bus versus client walking or sitting), those clients are dynamically re-assigned to different DIDO network that can tolerate their level of mobility.

[00162] Although the Doppler of low-velocity clients can be affected by being in the vicinity of high-velocity objects (e.g. near a highway), the Doppler is typically far less than the Doppler of clients that are in motion themselves. As such, in one embodiment, the velocity of the client is estimated (e.g. by using a means such as monitoring the clients position using GPS), and if the velocity is low, the client is assigned to a low-Doppler network, and if the velocity if high, the client is assigned to a high-Doppler network.

Methods for Power Control and Antenna Grouping

[00163] The block diagram of DIDO systems with power control is depicted in **Figure 17**. One or multiple data streams (s_k) for every client (1,…,U) are first multiplied by the weights generated by the DIDO precoding unit. Precoded data streams are multiplied by power scaling factor computed by the power control unit, based on the input channel quality information (CQI). The CQI is either fed back from the clients to DIDO BTS or derived from the uplink channel assuming uplink-downlink channel reciprocity. The U precoded streams for different clients are then combined and multiplexed into M data streams (t_m), one for each of the M transmit antennas. Finally, the streams t_m are sent to the digital-to-analog converter (DAC) unit, the radio frequency (RF) unit, power amplifier (PA) unit and finally to the antennas.

[00164] The power control unit measures the CQI for all clients. In one embodiment, the CQI is the average SNR or RSSI. The CQI varies for different clients depending on pathloss or shadowing. Our power control method adjusts the transmit power scaling factors P_k for different clients and multiplies them by the precoded data streams generated for different clients. Note that one or multiple data streams may be generated for every client, depending on the number of clients' receive antennas.

[00165] To evaluate the performance of the proposed method, we defined the following signal model based on (5), including pathloss and power control parameters

$$\mathbf{r}_k = \sqrt{\mathrm{SNR}\,\mathrm{P_k}\,\alpha_\mathrm{k}}\,\mathbf{H}_k\mathbf{W}_k\mathbf{s}_k + \mathbf{n}_k \qquad (12)$$

where k=1,…,U, U is the number of clients, SNR=P_o/N_o, with P_o being the average transmit power, N_o the noise power and α_k the pathloss/shadowing coefficient. To model pathloss/shadowing, we use the following simplified model

$$\alpha_\mathrm{k} = \mathrm{e}^{-a\frac{k-1}{U}} \qquad (13)$$

where a=4 is the pathloss exponent and we assume the pathloss increases with the clients' index (i.e., clients are located at increasing distance from the DIDO antennas).

[00166] **Figure 18** shows the SER versus SNR assuming four DIDO transmit antennas and four clients in different scenarios. The ideal case assumes all clients have the same pathloss (i.e., a=0), yielding P_k=1 for all clients. The plot with squares refers to the case where clients have different pathloss coefficients and no power control. The curve with dots is derived from the

same scenario (with pathloss) where the power control coefficients are chosen such that $P_k = 1/\alpha_k$. With the power control method, more power is assigned to the data streams intended to the clients that undergo higher pathloss/shadowing, resulting in 9dB SNR gain (for this particular scenario) compared to the case with no power control.

[00167] The Federal Communications Commission (FCC) (and other international regulatory agencies) defines constraints on the maximum power that can be transmitted from wireless devices to limit the exposure of human body to electromagnetic (EM) radiation. There are two types of limits [2]: i) "occupational/controlled" limit, where people are made fully aware of the radio frequency (RF) source via fences, warnings or labels; ii) "general population/uncontrolled" limit where there is no control over the exposure.

[00168] Different emission levels are defined for different types of wireless devices. In general, DIDO distributed antennas used for indoor/outdoor applications qualify for the FCC category of "mobile" devices, defined as [2]:

"transmitting devices designed to be used in other than fixed locations that would normally be used with radiating structures maintained 20 cm or more from the body of the user or nearby persons."

[00169] The EM emission of "mobile" devices is measured in terms of maximum permissible exposure (MPE), expressed in mW/cm^2. **Figure 19** shows the MPE power density as a function of distance from the source of RF radiation for different values of transmit power at 700MHz carrier frequency. The maximum allowed transmit power to meet the FCC "uncontrolled" limit for devices that typically operate beyond 20cm from the human body is 1W.

[00170] Less restrictive power emission constraints are defined for transmitters installed on rooftops or buildings, away from the "general population". For these "rooftop transmitters" the FCC defines a looser emission limit of 1000W, measured in terms of effective radiated power (ERP).

[00171] Based on the above FCC constraints, in one embodiment we define two types of DIDO distributed antennas for practical systems:

- **Low-power (LP)** transmitters: located anywhere (i.e., indoor or outdoor) at any height, with maximum transmit power of **1W** and 5Mbps consumer-grade broadband (e.g. DSL, cable modem, Fibe To The Home (FTTH)) backhaul connectivity.
- **High-power (HP)** transmitters: rooftop or building mounted antennas at height of approximately 10 meters, with transmit power of **100W** and a commercial-grade broadband (e.g. optical fiber ring) backhaul (with effectively "unlimited" data rate compared to the throughput available over the DIDO wireless links).

[00172] Note that LP transmitters with DSL or cable modem connectivity are good candidates for low-Doppler DIDO networks (as described in the previous section), since their clients are mostly fixed or have low mobility. HP transmitters with commercial fiber connectivity can tolerate higher client's mobility and can be used in high-Doppler DIDO networks.

[00173] To gain practical intuition on the performance of DIDO systems with different types of LP/HP transmitters, we consider the practical case of DIDO antenna installation in downtown Palo Alto, CA. **Figure 20a** shows a random distribution of N_{LP}=100 low-power DIDO distributed antennas in Palo Alto. In **Figure 20b**, 50 LP antennas are substituted with N_{HP}=50 high-power transmitters.

[00174] Based on the DIDO antenna distributions in **Figures 20a-b**, we derive the coverage maps in Palo Alto for systems using DIDO technology. **Figures 21a** and **21b** show two power distributions corresponding to the configurations in **Figure 20a** and **Figure 20b**, respectively. The received power distribution (expressed in dBm) is derived assuming the pathloss/shadowing model for urban environments defined by the 3GPP standard [3] at the carrier frequency of 700MHz. We observe that using 50% of HP transmitters yields better coverage over the selected area.

[00175] **Figures 22a-b** depict the rate distribution for the two scenarios above. The throughput (expressed in Mbps) is derived based on power thresholds for different modulation coding schemes defined in the 3GPP long-term evolution (LTE) standard in [4,5]. The total available bandwidth is fixed to 10MHz at 700MHz carrier frequency. Two different frequency allocation plans are considered: i) 5MHz spectrum allocated only to the LP stations; ii) 9MHz to HP transmitters and 1MHz to LP transmitters. Note that lower bandwidth is typically allocated to LP stations due to their DSL backhaul connectivity with limited throughput. **Figures 22a-b** shows that when using 50% of HP transmitters it is possible to increase significantly the rate distribution, raising the average per-client data rate from 2.4Mbps in **Figure 22a** to 38Mbps in **Figure 22b**.

[00176] Next, we defined algorithms to control power transmission of LP stations such that higher power is allowed at any given time, thereby increasing the throughput over the downlink channel of DIDO systems in **Figure 22b**. We observe that the FCC limits on the power density is defined based on average over time as [2]

$$S = \frac{\sum_{n=1}^{N} s_n t_n}{T_{MPE}} \tag{14}$$

where $T_{MPE} = \sum_{n=1}^{N} t_n$ is the MPE averaging time, t_n is the period of time of exposure to radiation with power density S_n. For "controlled" exposure the average time is 6 minutes, whereas for "uncontrolled" exposure it is increased up to 30 minutes. Then, any power source is allowed to transmit at larger power levels than the MPE limits, as long as the average power density in (14) satisfies the FCC limit over 30 minute average for "uncontrolled" exposure.

[00177] Based on this analysis, we define adaptive power control methods to increase instantaneous per-antenna transmit power, while maintaining average power per DIDO antenna below MPE limits. We consider DIDO systems with more transmit antennas than active clients. This is a reasonable assumption given that DIDO antennas can be conceived as inexpensive wireless devices (similar to WiFi access points) and can be placed anywhere there is DSL, cable modem, optical fiber, or other Internet connectivity.

[00178] The framework of DIDO systems with adaptive per-antenna power control is depicted in **Figure 23**. The amplitude of the digital signal coming out of the multiplexer 234 is dynamically adjusted with power scaling factors $S_1,\ldots,S_M$, before being sent to the DAC units 235. The power scaling factors are computed by the power control unit 232 based on the CQI 233.

[00179] In one embodiment, N_g DIDO antenna groups are defined. Every group contains at least as many DIDO antennas as the number of active clients (K). At any given time, only one group has $N_a > K$ active DIDO antennas transmitting to the clients at larger power level (S_o) than MPE limit ($\overline{MPE}$). One method iterates across all antenna groups according to Round-Robin scheduling policy depicted in **Figure 24**. In another embodiment, different scheduling techniques (i.e., proportional-fair scheduling [8]) are employed for cluster selection to optimize error rate or throughput performance.

[00180] Assuming Round-Robin power allocation, from (14) we derive the average transmit power for every DIDO antenna as

$$S = S_o \frac{t_o}{T_{MPE}} \leq \overline{MPE} \tag{15}$$

where t_o is the period of time over which the antenna group is active and T_{MPE}=30min is the average time defined by the FCC guidelines [2]. The ratio in (15) is the *duty factor* (DF) of the groups, defined such that the average transmit power from every DIDO antenna satisfies the MPE limit ($\overline{MPE}$). The duty factor depends on the number of active clients, the number of groups and active antennas per-group, according to the following definition

$$DF \triangleq \frac{K}{N_g N_a} = \frac{t_o}{T_{MPE}}. \tag{16}$$

The SNR gain (in dB) obtained in DIDO systems with power control and antenna grouping is expressed as a function of the duty factor as

$$G_{dB} = 10\log_{10}\left(\frac{1}{DF}\right). \quad (17)$$

We observe the gain in (17) is achieved at the expense of G_{dB} additional transmit power across all DIDO antennas.

In general, the total transmit power from all N_a of all N_g groups is defined as

$$\bar{P} = \sum_{j=1}^{N_g}\sum_{i=1}^{N_a} P_{ij} \quad (18)$$

where the P_{ij} is the average per-antenna transmit power given by

$$P_{ij} = \frac{1}{T_{MPE}}\int_0^{T_{MPE}} S_{ij}(t)\,dt \leq \overline{MPE} \quad (19)$$

and $S_{ij}(t)$ is the power spectral density for the i^{th} transmit antenna within the j^{th} group. In one embodiment, the power spectral density in (19) is designed for every antenna to optimize error rate or throughput performance.

[00181] To gain some intuition on the performance of the proposed method, consider 400 DIDO distributed antennas in a given coverage area and 400 clients subscribing to a wireless Internet service offered over DIDO systems. It is unlikely that every Internet connection will be fully utilized all the time. Let us assume that 10% of the clients will be actively using the wireless Internet connection at any given time. Then, 400 DIDO antennas can be divided in N_g=10 groups of N_a=40 antennas each, every group serving K=40 active clients at any given time with duty factor DF=0.1. The SNR gain resulting from this transmission scheme is $G_{dB}=10\log_{10}(1/DF)$=10dB, provided by 10dB additional transmit power from all DIDO antennas. We observe, however, that the average per-antenna transmit power is constant and is within the MPE limit.

[00182] **Figure 25** compares the (uncoded) SER performance of the above power control with antenna grouping against conventional eigenmode selection in U.S. Patent No. 7,636,381. All schemes use BD precoding with four clients, each client equipped with single antenna. The SNR refers to the ratio of per-transmit-antenna power over noise power (i.e., per-antenna transmit SNR). The curve denoted with DIDO 4x4 assumes four transmit antenna and BD precoding. The curve with squares denotes the SER performance with two extra transmit antennas and BD with eigenmode selection, yielding 10dB SNR gain (at 1% SER target) over conventional BD precoding. Power control with antenna grouping and DF=1/10 yields 10dB gain at the same SER target as well. We observe that eigenmode selection changes the slope of the SER curve due to diversity gain, whereas our power control method shifts the SER curve to the left (maintaining the same slope) due to increased average transmit power. For comparison, the SER with larger duty factor DF=1/50 is shown to provide additional 7dB gain compared to DF=1/10.

[00183] Note that our power control may have lower complexity than conventional eigenmode selection methods. In fact, the antenna ID of every group can be pre-computed and shared among DIDO antennas and clients via lookup tables, such that only K channel estimates are required at any given time. For eigenmode selection, $(K+2)$ channel estimates are computed and additional computational processing is required to select the eigenmode that minimizes the SER at any given time for all clients.

[00184] Next, we describe another method involving DIDO antenna grouping to reduce CSI feedback overhead in some special scenarios. **Figure 26a** shows one scenario where clients (dots) are spread randomly in one area covered by multiple DIDO distributed antennas (crosses). The average power over every transmit-receive wireless link can be computed as

$$\mathbf{A} = \{|\mathbf{H}|^2\}. \quad (20)$$

where **H** is the channel estimation matrix available at the DIDO BTS.

[00185] The matrices **A** in **Figures 26a-c** are obtained numerically by averaging the channel matrices over 1000 instances. Two alternative scenarios are depicted in **Figure 26b** and **Figure 26c**, respectively, where clients are grouped together around a subset of DIDO antennas and receive negligible power from DIDO antennas located far away. For example, **Figure 26b** shows two groups of antennas yielding block diagonal matrix **A**. One extreme scenario is when every client is very close to only one transmitter and the transmitters are far away from one another, such that the power from all other DIDO antennas is negligible. In this case, the DIDO link degenerates in multiple SISO links and **A** is a diagonal matrix as in **Figure 26c**.

[00186] In all three scenarios above, the BD precoding dynamically adjusts the precoding weights to account for different power levels over the wireless links between DIDO antennas and clients. It is convenient, however, to identify multiple *groups* within the DIDO cluster and operate DIDO precoding only within each group. Our proposed grouping method yields the following advantages:

- **Computational gain**: DIDO precoding is computed only within every group in the cluster. For example, if BD precoding is used, singular value decomposition (SVD) has complexity $O(n^3)$, where n is the minimum dimension of the channel matrix **H**. If **H** can be reduced to a block diagonal matrix, the SVD is computed for every block with reduced complexity. In fact, if the channel matrix is divided into two block matrices with dimensions n_1 and n_2 such that $n=n_1+n_2$, the complexity of the SVD is only $O(n_1^3)+O(n_2^3)<O(n^3)$. In the extreme case, if **H** is diagonal matrix, the DIDO link reduce to multiple SISO links and no SVD calculation is required.
- **Reduced CSI feedback overhead**: When DIDO antennas and clients are divided into groups, in one embodiment, the CSI is computed from the clients to the antennas only

within the same group. In TDD systems, assuming channel reciprocity, antenna grouping reduces the number of channel estimates to compute the channel matrix **H**. In FDD systems where the CSI is fed back over the wireless link, antenna grouping further yields reduction of CSI feedback overhead over the wireless links between DIDO antennas and clients.

Multiple Access Techniques for the DIDO Uplink Channel

[00187] In one embodiment of the invention, different multiple access techniques are defined for the DIDO uplink channel. These techniques can be used to feedback the CSI or transmit data streams from the clients to the DIDO antennas over the uplink. Hereafter, we refer to feedback CSI and data streams as *uplink streams*.

- **Multiple-input multiple-output (MIMO)**: the uplink streams are transmitted from the client to the DIDO antennas via open-loop MIMO multiplexing schemes. This method assumes all clients are time/frequency synchronized. In one embodiment, synchronization among clients is achieved via training from the downlink and all DIDO antennas are assumed to be locked to the same time/frequency reference clock. Note that variations in delay spread at different clients may generate jitter between the clocks of different clients that may affect the performance of MIMO uplink scheme. After the clients send uplink streams via MIMO multiplexing schemes, the receive DIDO antennas may use non-linear (i.e., maximum likelihood, ML) or linear (i.e., zeros-forcing, minimum mean squared error) receivers to cancel co-channel interference and demodulate the uplink streams individually.
- **Time division multiple access (TDMA)**: Different clients are assigned to different time slots. Every client sends its uplink stream when its time slot is available.
- **Frequency division multiple access (FDMA)**: Different clients are assigned to different carrier frequencies. In multicarrier (OFDM) systems, subsets of tones are assigned to different clients that transmit the uplink streams simultaneously, thereby reducing latency.
- **Code division multiple access (CDMA)**: Every client is assigned to a different pseudo-random sequence and orthogonality across clients is achieved in the code domain.

[00188] In one embodiment of the invention, the clients are wireless devices that transmit at much lower power than the DIDO antennas. In this case, the DIDO BTS defines client sub-groups based on the uplink SNR information, such that interference across sub-groups is minimized. Within every sub-group, the above multiple access techniques are employed to create

orthogonal channels in time, frequency, space or code domains thereby avoiding uplink interference across different clients.

[00189] In another embodiment, the uplink multiple access techniques described above are used in combination with antenna grouping methods presented in the previous section to define different client groups within the DIDO cluster.

System and Method for Link Adaptation in DIDO Multicarrier Systems

[00190] Link adaptation methods for DIDO systems exploiting time, frequency and space selectivity of wireless channels were defined in U.S. Patent No. 7,636,381. Described below are embodiments of the invention for link adaptation in multicarrier (OFDM) DIDO systems that exploit time/frequency selectivity of wireless channels.

[00191] We simulate Rayleigh fading channels according to the exponentially decaying power delay profile (PDP) or Saleh-Valenzuela model in [9]. For simplicity, we assume single-cluster channel with multipath PDP defined as

$$P_n = e^{-\beta n} \tag{21}$$

where n=0,…,L-1, is the index of the channel tap, L is the number of channel taps and $\beta = 1/\sigma_{DS}$ is the PDP exponent that is an indicator of the channel coherence bandwidth, inverse proportional to the channel delay spread (σ_{DS}). Low values of β yield frequency-flat channels, whereas high values of β produce frequency selective channels. The PDP in (21) is normalized such that the total average power for all L channel taps is unitary

$$\overline{P_n} = \frac{P_n}{\sum_{i=0}^{L-1} P_i} . \tag{22}$$

Figure 27 depicts the amplitude of low frequency selective channels (assuming $\beta = 1$) over delay domain or instantaneous PDP (upper plot) and frequency domain (lower plot) for DIDO 2x2 systems. The first subscript indicates the client, the second subscript the transmit antenna. High frequency selective channels (with $\beta = 0.1$) are shown in **Figure 28**.

[00192] Next, we study the performance of DIDO precoding in frequency selective channels. We compute the DIDO precoding weights via BD, assuming the signal model in (1) that satisfies the condition in (2). We reformulate the DIDO receive signal model in (5), with the condition in (2), as

$$\mathbf{r}_k = \mathbf{H}_{ek}\mathbf{s}_k + \mathbf{n}_k. \tag{23}$$

[00193] where $\mathbf{H}_{ek} = \mathbf{H}_k\mathbf{W}_k$ is the *effective channel matrix* for user k. For DIDO 2x2, with a single antenna per client, the effective channel matrix reduces to one value with a frequency response shown in **Figure 29** and for channels characterized by high frequency selectivity (e.g., with $\beta = 0.1$) in **Figure 28**. The continuous line in **Figure 29** refers to client 1, whereas the line

with dots refers to client 2. Based on the channel quality metric in **Figure 29** we define time/frequency domain link adaptation (LA) methods that dynamically adjust MCSs, depending on the changing channel conditions.

[00194] We begin by evaluating the performance of different MCSs in AWGN and Rayleigh fading SISO channels. For simplicity, we assume no FEC coding, but the following LA methods can be extended to systems that include FEC.

[00195] **Figure 30** shows the SER for different QAM schemes (i.e., 4-QAM, 16-QAM, 64-QAM). Without loss of generality, we assume target SER of 1% for uncoded systems. The SNR thresholds to meet that target SER in AWGN channels are 8dB, 15.5dB and 22dB for the three modulation schemes, respectively. In Rayleigh fading channels, it is well known the SER performance of the above modulation schemes is worse than AWGN [13] and the SNR thresholds are: 18.6dB, 27.3dB and 34.1dB, respectively. We observe that DIDO precoding transforms the multi-user downlink channel into a set of parallel SISO links. Hence, the same SNR thresholds as in **Figure 30** for SISO systems hold for DIDO systems on a client-by-client basis. Moreover, if instantaneous LA is carried out, the thresholds in AWGN channels are used.

[00196] The key idea of the proposed LA method for DIDO systems is to use low MCS orders when the channel undergoes deep fades in the time domain or frequency domain (depicted in **Figure 28**) to provide link-robustness. Contrarily, when the channel is characterized by large gain, the LA method switches to higher MCS orders to increase spectral efficiency. One contribution of the present application compared to U.S. Patent No. 7,636,381 is to use the effective channel matrix in (23) and in **Figure 29** as a metric to enable adaptation.

[00197] The general framework of the LA methods is depicted in **Figure 31** and defined as follows:

- **CSI estimation**: At 3171 the DIDO BTS computes the CSI from all users. Users may be equipped with single or multiple receive antennas.
- **DIDO precoding**: At 3172, the BTS computes the DIDO precoding weights for all users. In one embodiment, BD is used to compute these weights. The precoding weights are calculated on a tone-by-tone basis.
- **Link-quality metric calculation**: At 3173 the BTS computes the frequency-domain link quality metrics. In OFDM systems, the metrics are calculated from the CSI and DIDO precoding weights for every tone. In one embodiment of the invention, the link-quality metric is the average SNR over all OFDM tones. We define this method as **LA1** (based on average SNR performance). In another embodiment, the link quality metric is the frequency response of the effective channel in (23). We define this method as **LA2** (based on tone-by-tone performance to exploit frequency diversity). If every client has

single antenna, the frequency-domain effective channel is depicted in **Figure 29**. If the clients have multiple receive antennas, the link-quality metric is defined as the Frobenius norm of the effective channel matrix for every tone. Alternatively, multiple link-quality metrics are defined for every client as the singular values of the effective channel matrix in (23).

- **Bit-loading algorithm**: At 3174, based on the link-quality metrics, the BTS determines the MCSs for different clients and different OFDM tones. For LA1 method, the same MCS is used for all clients and all OFDM tones based on the SNR thresholds for Rayleigh fading channels in **Figure 30**. For LA2, different MCSs are assigned to different OFDM tones to exploit channel frequency diversity.
- **Precoded data transmission**: At 3175, the BTS transmits precoded data streams from the DIDO distributed antennas to the clients using the MCSs derived from the bit-loading algorithm. One header is attached to the precoded data to communicate the MCSs for different tones to the clients. For example, if eight MCSs are available and the OFDM symbols are defined with N=64 tone, $\log_2(8)*N=192$ bits are required to communicate the current MCS to every client. Assuming 4-QAM (2 bits/symbol spectral efficiency) is used to map those bits into symbols, only 192/2/N=1.5 OFDM symbols are required to map the MCS information. In another embodiment, multiple subcarriers (or OFDM tones) are grouped into subbands and the same MCS is assigned to all tones in the same subband to reduce the overhead due to control information. Moreover, the MCS are adjusted based on temporal variations of the channel gain (proportional to the coherence time). In fixed-wireless channel (characterized by low Doppler effect) the MCS are recalculated every fraction of the channel coherence time, thereby reducing the overhead required for control information.

[00198] **Figure 32** shows the SER performance of the LA methods described above. For comparison, the SER performance in Rayleigh fading channels is plotted for each of the three QAM schemes used. The LA2 method adapts the MCSs to the fluctuation of the effective channel in the frequency domain, thereby providing 1.8bps/Hz gain in spectral efficiency for low SNR (i.e., SNR=20dB) and 15dB gain in SNR (for SNR>35dB) compared to LA1.

System and Method for DIDO Precoding Interpolation in Multicarrier Systems

[00199] The computational complexity of DIDO systems is mostly localized at the centralized processor or BTS. The most computationally expensive operation is the calculation of the precoding weights for all clients from their CSI. When BD precoding is employed, the BTS has to carry out as many singular value decomposition (SVD) operations as the number of

clients in the system. One way to reduce complexity is through parallelized processing, where the SVD is computed on a separate processor for every client.

[00200] In multicarrier DIDO systems, each subcarrier undergoes flat-fading channel and the SVD is carried out for every client over every subcarrier. Clearly the complexity of the system increases linearly with the number of subcarriers. For example, in OFDM systems with 1MHz signal bandwidth, the cyclic prefix (L_0) must have at least eight channel taps (i.e., duration of 8 microseconds) to avoid intersymbol interference in outdoor urban macrocell environments with large delay spread [3]. The size (N_{FFT}) of the fast Fourier transform (FFT) used to generate the OFDM symbols is typically set to multiple of L_0 to reduce loss of data rate. If N_{FFT}=64, the effective spectral efficiency of the system is limited by a factor $N_{FFT}/(N_{FFT}+L_0)$=89%. Larger values of N_{FFT} yield higher spectral efficiency at the expense of higher computational complexity at the DIDO precoder.

[00201] One way to reduce computational complexity at the DIDO precoder is to carry out the SVD operation over a subset of tones (that we call *pilot tones*) and derive the precoding weights for the remaining tones via interpolation. Weight interpolation is one source of error that results in inter-client interference. In one embodiment, optimal weight interpolation techniques are employed to reduce inter-client interference, yielding improved error rate performance and lower computational complexity in multicarrier systems. In DIDO systems with M transmit antennas, U clients and N receive antennas per clients, the condition for the precoding weights of the k^{th} client ($\mathbf{W}_k$) that guarantees zero interference to the other clients u is derived from (2) as

$$\mathbf{H}_u\mathbf{W}_k = \mathbf{0}^{N\text{x}N}; \quad \forall\, u = 1, \ldots, U; \text{ with } u \neq k \tag{24}$$

where $\mathbf{H}_u$ are the channel matrices corresponding to the other DIDO clients in the system.

[00202] In one embodiment of the invention, the objective function of the weight interpolation method is defined as

$$\mathrm{f}(\boldsymbol{\theta}_k) = \sum_{\substack{u=1 \\ u\neq k}}^{U} \left\| \mathbf{H}_u \widehat{\mathbf{W}}_k(\boldsymbol{\theta}_k) \right\|_F \tag{25}$$

where $\boldsymbol{\theta}_k$ is the set of parameters to be optimized for user k, $\widehat{\mathbf{W}}_k(\boldsymbol{\theta}_k)$ is the *weight interpolation matrix* and $\|\cdot\|_F$ denotes the Frobenius norm of a matrix. The optimization problem is formulated as

$$\boldsymbol{\theta}_{k,\text{opt}} = \arg\min_{\boldsymbol{\theta}_k \square \Theta_k} \mathrm{f}(\boldsymbol{\theta}_k) \tag{26}$$

where Θ_k is the feasible set of the optimization problem and $\boldsymbol{\theta}_{k,\text{opt}}$ is the optimal solution.

[00203] The objective function in (25) is defined for one OFDM tone. In another embodiment of the invention, the objective function is defined as linear combination of the

Frobenius norm in (25) of the matrices for all the OFDM tones to be interpolated. In another embodiment, the OFDM spectrum is divided into subsets of tones and the optimal solution is given by

$$\boldsymbol{\theta}_{k,\mathrm{opt}} = \arg\min_{\boldsymbol{\theta}_k \in \Theta_k} \max_{n \in A} \mathrm{f}(\mathrm{n}, \boldsymbol{\theta}_k) \tag{27}$$

where n is the OFDM tone index and A is the subset of tones.

[00204] The weight interpolation matrix $\mathbf{W}_k(\boldsymbol{\theta}_k)$ in (25) is expressed as a function of a set of parameters $\boldsymbol{\theta}_k$. Once the optimal set is determined according to (26) or (27), the optimal weight matrix is computed. In one embodiment of the invention, the weight interpolation matrix of given OFDM tone n is defined as linear combination of the weight matrices of the pilot tones. One example of weight interpolation function for beamforming systems with single client was defined in [11]. In DIDO multi-client systems we write the weight interpolation matrix as

$$\widehat{\mathbf{W}}_k(lN_0 + n, \theta_k) = (1 - c_n) \cdot \mathbf{W}(l) + c_n \mathrm{e}^{j\theta_k} \cdot \mathbf{W}(l+1) \tag{28}$$

where $0 \leq l \leq (L_0\text{-}1)$, L_0 is the number of pilot tones and $c_n = (n-1)/N_0$, with $N_0 = N_{FFT}/L_0$. The weight matrix in (28) is then normalized such that $\|\widehat{\mathbf{W}}_k\|_{\mathrm{F}} = \sqrt{NM}$ to guarantee unitary power transmission from every antenna. If N=1 (single receive antenna per client), the matrix in (28) becomes a vector that is normalized with respect to its norm. In one embodiment of the invention, the pilot tones are chosen uniformly within the range of the OFDM tones. In another embodiment, the pilot tones are adaptively chosen based on the CSI to minimize the interpolation error.

[00205] We observe that one key difference of the system and method in [11] against the one proposed in this patent application is the objective function. In particular, the systems in [11] assumes multiple transmit antennas and single client, so the related method is designed to maximize the product of the precoding weight by the channel to maximize the receive SNR for the client. This method, however, does not work in multi-client scenarios, since it yields inter-client interference due to interpolation error. By contrast, our method is designed to minimize inter-client interference thereby improving error rate performance to all clients.

[00206] **Figure 33** shows the entries of the matrix in (28) as a function of the OFDM tone index for DIDO 2x2 systems with $N_{FFT} = 64$ and $L_0 = 8$. The channel PDP is generated according to the model in (21) with $\beta = 1$ and the channel consists of only eight channel taps. We observe that L_0 must be chosen to be larger than the number of channel taps. The solid lines in **Figure 33** represent the ideal functions, whereas the dotted lines are the interpolated ones. The interpolated weights match the ideal ones for the pilot tones, according to the definition in (28). The weights computed over the remaining tones only approximate the ideal case due to estimation error.

[00207] One way to implement the weight interpolation method is via exhaustive search over the feasible set Θ_k in (26). To reduce the complexity of the search, we quantize the feasible set into P values uniformly in the range $[0,2\pi]$. **Figure 34** shows the SER versus SNR for $L_0 = 8$, $M=N_t=2$ transmit antennas and variable number of P. As the number of quantization levels increases, the SER performance improves. We observe the case P=10 approaches the performance of P=100 for much lower computational complexity, due to reduced number of searches.

[00208] **Figure 35** shows the SER performance of the interpolation method for different DIDO orders and $L_0 = 16$. We assume the number of clients is the same as the number of transmit antennas and every client is equipped with single antenna. As the number of clients increases the SER performance degrades due to increase inter-client interference produced by weight interpolation errors.

[00209] In another embodiment of the invention, weight interpolation functions other than those in (28) are used. For example, linear prediction autoregressive models [12] can be used to interpolate the weights across different OFDM tones, based on estimates of the channel frequency correlation.

References

[00210] [1] A. Forenza and S. G. Perlman, "System and method for distributed antenna wireless communications", U.S. Application Serial No. 12/630,627, filed December 2, 2009, entitled "System and Method For Distributed Antenna Wireless Communications"

[00211] [2] FCC, "Evaluating compliance with FCC guidelines for human exposure to radiofrequency electromagnetic fields," OET Bulletin 65, Ed. 97-01, Aug. 1997

[00212] [3] 3GPP, "Spatial Channel Model AHG (Combined ad-hoc from 3GPP & 3GPP2)", SCM Text V6.0, April 22, 2003

[00213] [4] 3GPP TR 25.912, "Feasibility Study for Evolved UTRA and UTRAN", V9.0.0 (2009-10)

[00214] [5] 3GPP TR 25.913, "Requirements for Evolved UTRA (E-UTRA) and Evolved UTRAN (E-UTRAN)", V8.0.0 (2009-01)

[00215] [6] W. C. Jakes, *Microwave Mobile Communications*, IEEE Press, 1974

[00216] [7] K. K. Wong, et al., "A joint channel diagonalization for multiuser MIMO antenna systems," IEEE Trans. Wireless Comm., vol. 2, pp. 773-786, July 2003;

[00217] [8] P. Viswanath, et al., "Opportunistic beamforming using dump antennas," IEEE Trans. On Inform. Theory, vol. 48, pp. 1277–1294, June 2002.

[00218] [9] A. A. M. Saleh, et al., "A statistical model for indoor multipath propagation," IEEE Jour. Select. Areas in Comm., vol. 195 SAC-5, no. 2, pp. 128–137, Feb. 1987.

[00219] [10] A. Paulraj, et al., *Introduction to Space-Time Wireless Communications*, Cambridge University Press, 40 West 20th Street, New York, NY, USA, 2003.

[00220] [11] J. Choi, et al., ``Interpolation Based Transmit Beamforming for MIMO-OFDM with Limited Feedback," *IEEE Trans. on Signal Processing*, vol. 53, no. 11, pp. 4125-4135, Nov. 2005.

[00221] [12] I. Wong, et al., ``Long Range Channel Prediction for Adaptive OFDM Systems," *Proc. of the IEEE Asilomar Conf. on Signals, Systems, and Computers*, vol. 1,pp. 723-736, Pacific Grove, CA, USA, Nov. 7-10, 2004.

[00222] [13] J. G. Proakis, *Communication System Engineering*, Prentice Hall, 1994

[00223] [14] B.D.Van Veen, et al., ``Beamforming: a versatile approach to spatial filtering," *IEEE ASSP Magazine*, Apr. 1988.

[00224] [15] R.G. Vaughan, "On optimum combining at the mobile," *IEEE Trans. On Vehic. Tech.*, vol37, n.4, pp.181-188, Nov. 1988

[00225] [16] F.Qian, "Partially adaptive beamforming for correlated interference rejection," *IEEE Trans. On Sign. Proc.*, vol.43, n.2, pp.506-515, Feb.1995

[00226] [17] H.Krim, et. al., "Two decades of array signal processing research," *IEEE Signal Proc. Magazine*, pp.67-94, July 1996

[00227] [19] W.R. Remley, "Digital *beamforming* system", US Patent N. 4,003,016, Jan. 1977

[00228] [18] R.J. Masak, "*Beamforming/null-steering adaptive array*", US Patent N. 4,771,289, Sep.1988

[00229] [20] K.-B.Yu, et. al., "Adaptive digital *beamforming* architecture and algorithm for nulling mainlobe and multiple sidelobe radar jammers while preserving monopulse ratio angle estimation accuracy", US Patent 5,600,326, Feb.1997

[00230] [21] H.Boche, et al., "Analysis of different precoding/decoding strategies for multiuser beamforming", IEEE Vehic. Tech. Conf., vol.1, Apr. 2003

[00231] [22] M.Schubert, et al., "Joint 'dirty paper' pre-coding and downlink beamforming," vol.2, pp.536-540, Dec. 2002

[00232] [23] H.Boche, et al." A general duality theory for uplink and downlink beamformingc", vol.1, pp.87-91, Dec. 2002

[00233] [24] K. K. Wong, R. D. Murch, and K. B. Letaief, "A joint channel diagonalization for multiuser MIMO antenna systems," IEEE Trans. Wireless Comm., vol. 2, pp. 773–786, Jul 2003;

[00234] [25] Q. H. Spencer, A. L. Swindlehurst, and M. Haardt, "Zero forcing methods for downlink spatial multiplexing in multiuser MIMO channels," IEEE Trans. Sig. Proc., vol. 52, pp. 461–471, Feb. 2004.

II. DISCLOSURE FROM RELATED APPLICATION SERIAL NO. 12/917,257

[00235] Described below are wireless radio frequency (RF) communication systems and methods employing a plurality of distributed transmitting antennas operating cooperatively to create wireless links to given users, while suppressing interference to other users. Coordination across different transmitting antennas is enabled via *user-clustering*. The user cluster is a subset of transmitting antennas whose signal can be reliably detected by given user (i.e., received signal strength above noise or interference level). Every user in the system defines its own user-cluter. The waveforms sent by the transmitting antennas within the same user-cluster coherently combine to create RF energy at the target user's location and points of zero RF interference at the location of any other user reachable by those antennas.

[00236] Consider a system with M transmit antennas within one user-cluster and K users reachable by those M antennas, with $K \leq M$. We assume the transmitters are aware of the CSI ($\mathbf{H} \in \mathbb{C}^{K \times M}$) between the M transmit antennas and K users. For simplicity, every user is assumed to be equipped with a single antenna, but the same method can be extended to multiple receive antennas per user. Consider the channel matrix $\mathbf{H}$ obtained by combining the channel vectors ($\mathbf{h}_k \in \mathbb{C}^{1 \times M}$) from the M transmit antennas to the K users as

$$\mathbf{H} = \begin{bmatrix} \mathbf{h}_1 \\ \vdots \\ \mathbf{h}_k \\ \vdots \\ \mathbf{h}_K \end{bmatrix}.$$

The precoding weights ($\mathbf{w}_k \in \mathbb{C}^{M \times 1}$) that create RF energy to user k and zero RF energy to all other K-1 users are computed to satisfy the following condition

$$\tilde{\mathbf{H}}_k \mathbf{w}_k = \mathbf{0}^{K \times 1}$$

where $\tilde{\mathbf{H}}_k$ is the effective channel matrix of user k obtained by removing the k-th row of matrix $\mathbf{H}$ and $0^{K \times 1}$ is the vector with all zero entries

[00237] In one embodiment, the wireless system is a DIDO system and user clustering is employed to create a wireless communication link to the target user, while pre-cancelling interference to any other user reachable by the antennas lying within the user-cluster. In U.S. Application Serial No. 12/630,627, a DIDO system is described which includes:

- **DIDO clients**: user terminals equipped with one or multiple antennas;

- **DIDO distributed antennas**: transceiver stations operating cooperatively to transmit precoded data streams to multiple users, thereby suppressing inter-user interference;
- **DIDO base transceiver stations (BTS)**: centralized processor generating precoded waveforms to the DIDO distributed antennas;
- **DIDO base station network (BSN)**: wired backhaul connecting the BTS to the DIDO distributed antennas or to other BTSs.

The DIDO distributed antennas are grouped into different subsets depending on their spatial distribution relative to the location of the BTSs or DIDO clients. We define three types of clusters, as depicted in **Figure 36**:

- **Super-cluster 3640**: is the set of DIDO distributed antennas connected to one or multiple BTSs such that the round-trip latency between all BTSs and the respective users is within the constraint of the DIDO precoding loop;
- **DIDO-cluster 3641**: is the set of DIDO distributed antennas connected to the same BTS. When the super-cluster contains only one BTS, its definition coincides with the DIDO-cluster;
- **User-cluster 3642**: is the set of DIDO distributed antennas that cooperatively transmit precoded data to given user.

[00238] For example, the BTSs are local hubs connected to other BTSs and to the DIDO distributed antennas via the BSN. The BSN can be comprised of various network technologies including, but not limited to, digital subscriber lines (DSL), ADSL, VDSL [6], cable modems, fiber rings, T1 lines, hybrid fiber coaxial (HFC) networks, and/or fixed wireless (e.g., WiFi). All BTSs within the same super-cluster share information about DIDO precoding via the BSN such that the round-trip latency is within the DIDO precoding loop.

[00239] In **Figure 37**, the dots denote DIDO distributed antennas, the crosses are the users and the dashed lines indicate the user-clusters for users U1 and U8, respectively. The method described hereafter is designed to create a communication link to the target user U1 while creating points of zero RF energy to any other user (U2-U8) inside or outside the user-cluster.

[00240] We proposed similar method in [5], where points of zero RF energy were created to remove interference in the overlapping regions between DIDO clusters. Extra antennas were required to transmit signal to the clients within the DIDO cluster while suppressing inter-cluster interference. One embodiment of a method proposed in the present application does not attempt to remove inter-DIDO-cluster interference; rather it assumes the cluster is bound to the client (i.e., user-cluster) and guarantees that no interference (or negligible interference) is generated to any other client in that neighborhood.

[00241] One idea associated with the proposed method is that users far enough from the user-cluster are not affected by radiation from the transmit antennas, due to large pathloss. Users close or within the user-cluster receive interference-free signal due to precoding. Moreover, additional transmit antennas can be added to the user-cluster (as shown in **Figure 37**) such that the condition $K \leq M$ is satisfied.

[00242] One embodiment of a method employing user clustering consists of the following steps:

a. **Link-quality measurements**: the link quality between every DIDO distributed antenna and every user is reported to the BTS. The link-quality metric consists of signal-to-noise ratio (SNR) or signal-to-interference-plus-noise ratio (SINR).

In one embodiment, the DIDO distributed antennas transmit training signals and the users estimate the received signal quality based on that training. The training signals are designed to be orthogonal in time, frequency or code domains such that the users can distinguish across different transmitters. Alternatively, the DIDO antennas transmit narrowband signals (i.e., single tone) at one particular frequency (i.e., a beacon channel) and the users estimate the link-quality based on that beacon signal. One threshold is defined as the minimum signal amplitude (or power) above the noise level to demodulate data successfully as shown in **Figure 38a**. Any link-quality metric value below this threshold is assumed to be zero. The link-quality metric is quantized over a finite number of bits and fed back to the transmitter.

In a different embodiment, the training signals or beacons are sent from the users and the link quality is estimated at the DIDO transmit antennas (as in **Figure 38b**), assuming reciprocity between uplink (UL) and downlink (DL) pathloss. Note that pathloss reciprocity is a realistic assumption in time division duplexing (TDD) systems (with UL and DL channels at the same frequency) and frequency division duplexing (FDD) systems when the UL and DL frequency bands are reatively close.

Information about the link-quality metrics is shared across different BTSs through the BSN as depicted in **Figure 37** such that all BTSs are aware of the link-quality between every antenna/user couple across different DIDO clusters.

b. **Definition of user-clusters**: the link-quality metrics of all wireless links in the DIDO clusters are the entries to the *link-quality matrix* shared across all BTSs via the BSN. One example of link-quality matrix for the scenario in **Figure 37** is depicted in **Figure 39**.

The link-quality matrix is used to define the user clusters. For example, **Figure 39** shows the selection of the user cluster for user U8. The subset of transmitters with non-zero link-quality metrics (i.e., *active transmitters*) to user U8 is first identified. These transmitters populate the *user-cluster* for the user U8. Then the sub-matrix containing non-zero entries from the

transmitters within the user-cluster to the other users is selected. Note that since the link-quality metrics are only used to select the user cluster, they can be quantized with only two bits (i.e., to identify the state above or below the thresholds in **Figure 38**) thereby reducing feedback overhead.

[00243] Another example is depicted in **Figure 40** for user U1. In this case the number of active transmitters is lower than the number of users in the sub-matrix, thereby violating the condition $K \leq \mathrm{M}$. Therefore, one or more columns are added to the sub-matrix to satisfy that condition. If the number of transmitters exceeds the number of users, the extra antennas can be used for diversity schemes (i.e., antenna or eigenmode selection).

[00244] Yet another example is shown in **Figure 41** for user U4. We observe that the sub-matrix can be obtained as combination of two sub-matrices.

c. **CSI report to the BTSs**: Once the user clusters are selected, the CSI from all transmitters within the user-cluster to every user reached by those transmitters is made available to all BTSs. The CSI information is shared across all BTSs via the BSN. In TDD systems, UL/DL channel reciprocity can be exploited to derive the CSI from training over the UL channel. In FDD systems, feedback channels from all users to the BTSs are required. To reduce the amount of feedback, only the CSI corresponding to the non-zero entries of the link-quality matrix are fed back.

d. **DIDO precoding**: Finally, DIDO precoding is applied to every CSI sub-matrix corresponding to different user clusters (as described, for example, in the related U.S. Patent Applications).

In one embodiment, singular value decomposition (SVD) of the effective channel matrix $\widetilde{\mathbf{H}}_{\mathbf{k}}$ is computed and the precoding weight $\mathbf{w}_k$ for user k is defined as the right sigular vector corresponding to the null subspace of $\widetilde{\mathbf{H}}_k$. Alternatively, if $M>K$ and the SVD decomposes the effective channel matrix as $\widetilde{\mathbf{H}}_k = \mathbf{V}_k \mathbf{\Sigma}_k {\mathbf{U}_k}^H$, the DIDO precoding weight for user k is given by

$$\mathbf{w}_k = \mathbf{U}_{\mathrm{o}} \left({\mathbf{U}_{\mathrm{o}}}^H \cdot {\mathbf{h}_k}^T\right)$$

where $\mathbf{U}_{\mathrm{o}}$ is the matrix with columns being the singular vectors of the null subspace of $\widetilde{\mathbf{H}}_k$.

From basic linear algebra considerations, we observe that the right singular vector in the null subspace of the matrix $\widetilde{\mathbf{H}}$ is equal to the eigenvetor of C corresponding to the zero eigenvalue

$$\mathbf{C} = \widetilde{\mathbf{H}}^H \widetilde{\mathbf{H}} = (\mathbf{V\Sigma U}^H)^H (\mathbf{V\Sigma U}^H) = \mathbf{U}\,\mathbf{\Sigma}^2\,\mathbf{U}^H$$

where the effective channel matrix is decomposed as $\widetilde{\mathbf{H}} = \mathbf{V\Sigma U}^H$, according to the SVD. Then, one alternative to computing the SVD of $\widetilde{\mathbf{H}}_{\mathbf{k}}$ is to calculate the eigenvalue decomposition of $\mathbf{C}$. There are several methods to compute eigenvalue decomposition such as the power method.

Since we are only interested to the eigenvector corresponding to the null subspace of **C**, we use the inverse power method described by the iteration

$$\mathbf{u}_{i+1} = \frac{(\mathbf{C} - \lambda\mathbf{I})^{-1}\,\mathbf{u}_i}{\|(\mathbf{C} - \lambda\mathbf{I})^{-1}\,\mathbf{u}_i\|}$$

where the vector $(\mathbf{u}_i)$ at the first iteration is a random vector.

Given that the eigenvalue (λ) of the null subspace is known (i.e., zero) the inverse power method requires only one iteration to converge, thereby reducing computational complexity. Then, we write the precoding weight vector as

$$\mathbf{w} = \mathbf{C}^{-1}\,\mathbf{u}_1$$

where $\mathbf{u}_1$ is the vector with real entries equal to 1 (i.e., the precoding weight vector is the sum of the columns of $\mathbf{C}^{-1}$).

The DIDO precoding calculation requires one matrix inversion. There are several numerical solutions to reduce the complexity of matrix inversions such as the Strassen's algorithm [1] or the Coppersmith-Winograd's algorithm [2,3]. Since **C** is Hermitian matrix by definition, an alternative solution is to decompose **C** in its real and imaginary components and compute matrix inversion of a real matrix, according to the method in [4, Section 11.4].

[00245] Another feature of the proposed method and system is its reconfigurability. As the client moves across different DIDO clusters as in **Figure 42**, the user-cluster follows its moves. In other words, the subset of transmit antennas is constantly updated as the client changes its position and the effective channel matrix (and corresponding precoding weights) are recomputed.

[00246] The method proposed herein works within the super-cluster in **Figure 36**, since the links between the BTSs via the BSN must be low-latency. To suppress interference in the overlapping regions of different super-clusters, it is possible to use our method in [5] that uses extra antennas to create points of zero RF energy in the interfering regions between DIDO clusters.

[00247] It should be noted that the terms "user" and "client" are used interchangeably herein.

References

[00248] [1] S. Robinson, "Toward an Optimal Algorithm for Matrix Multiplication", SIAM News, Volume 38, Number 9, November 2005.

[00249] [2] D. Coppersmith and S. Winograd, "Matrix Multiplication via Arithmetic Progression", J. Symb. Comp. vol.9, p.251-280, 1990.

[00250] [3] H. Cohn, R. Kleinberg, B. Szegedy, C. Umans, "Group-theoretic Algorithms for Matrix Multiplication", p. 379-388, Nov. 2005.

[00251] [4] W.H. Press, S.A. Teukolsky, W. T. Vetterling, B.P. Flannery "NUMERICAL RECIPES IN C: THE ART OF SCIENTIFIC COMPUTING", Cambridge University Press, 1992.

[00252] [5] A. Forenza and S.G.Perlman, "INTERFERENCE MANAGEMENT, HANDOFF, POWER CONTROL AND LINK ADAPTATION IN DISTRIBUTED-INPUT DISTRIBUTED-OUTPUT (DIDO) COMMUNICATION SYSTEMS", Patent Application Serial No. 12/802,988, filed June 16, 2010.

[00253] [6] Per-Erik Eriksson and Björn Odenhammar, "VDSL2: Next important broadband technology", Ericsson Review No. 1, 2006.

III. SYSTEMS AND METHODS TO EXPLOIT AREAS OF COHERENCE IN WIRELESS SYSTEMS

[00254] The capacity of multiple antenna systems (MAS) in practical propagation environments is a function of the spatial diversity available over the wireless link. Spatial diversity is determined by the distribution of scattering objects in the wireless channel as well as the geometry of transmit and receive antenna arrays.

[00255] One popular model for MAS channels is the so called clustered channel model, that defines groups of scatterers as clusters located around the transmitters and receivers. In general, the more clusters and the larger their angular spread, the higher spatial diversity and capacity achievable over wireless links. Clustered channel models have been validated through practical measurements [1-2] and variations of those models have been adopted by different indoor (i.e., IEEE 802.11n Technical Group [3] for WLAN) and outdoor (3GPP Technical Specification Group for 3G cellular systems [4]) wireless standards.

[00256] Other factors that determine the spatial diversity in wireless channels are the characteristics of the antenna arrays, including: antenna element spacing [5-7], number of antennas [8-9], array aperture [10-11], array geometry [5,12,13], polarization and antenna pattern [14-28].

[00257] A unified model describing the effects of antenna array design as well as the characteristics of the propagation channel on the spatial diversity (or degrees of freedom) of wireless links was presented in [29]. The received signal model in [29] is given by

$$\mathbf{y}(\mathbf{q}) = \int \mathbf{C}(\mathbf{q},\mathbf{p})\mathbf{x}(\mathbf{p})d\mathbf{p} + \mathbf{z}(\mathbf{q})$$

where $\mathbf{x}(\mathbf{p}) \in C^3$ is the polarized vector describing the transmit signal, $\mathbf{p},\mathbf{q} \in R^3$ are the polarized vector positions describing the transmit and receive arrays, respectively, and $\mathbf{C}(\cdot,\cdot) \in C^{3x3}$ is the matrix describing the system response between transmit and receive vector positions given by

$$\mathbf{C}(\mathbf{q},\mathbf{p}) = \iint \mathbf{A_r}(\mathbf{q},\hat{\mathbf{m}})\mathbf{H}(\hat{\mathbf{m}},\hat{\mathbf{n}})\mathbf{A_t}(\hat{\mathbf{n}},\mathbf{p})d\hat{\mathbf{n}}d\hat{\mathbf{m}}$$

where $\mathbf{A_t}(\cdot,\cdot), \mathbf{A_r}(\cdot,\cdot) \in C^{3x3}$ are the transmit and receive array responses respectively and $\mathbf{H}(\hat{\mathbf{m}},\hat{\mathbf{n}}) \in C^{3x3}$ is the channel response matrix with entries being the complex gains between transmit direction $\hat{\mathbf{n}}$ and receive direction $\hat{\mathbf{m}}$. In DIDO systems, user devices may have single or multiple antennas. For the sake of simplicity, we assume single antenna receivers with ideal isotropic patterns and rewrite the system response matrix as

$$\mathbf{C}(\mathbf{q},\mathbf{p}) = \int \mathbf{H}(\mathbf{q},\hat{\mathbf{n}})\mathbf{A}(\hat{\mathbf{n}},\mathbf{p})d\hat{\mathbf{n}}$$

where only the transmit antenna pattern $\mathbf{A}(\hat{\mathbf{n}},\mathbf{p})$ is considered.

[00258] From the Maxwell equations and the far-field term of the Green function, the array response can be approximated as [29]

$$\mathbf{A}(\hat{\mathbf{n}},\mathbf{p}) = \frac{j\eta e^{j2\pi d_o}}{2\lambda^2 d_o}(\mathbf{I} - \hat{\mathbf{n}}\hat{\mathbf{n}}^H)\, a(\hat{\mathbf{n}},\mathbf{p})$$

with $\mathbf{p}$□P, P is the space that defines the antenna array and where

$$a(\hat{\mathbf{n}},\mathbf{p}) = \exp(-j2\pi\, \hat{\mathbf{n}}^H\mathbf{p})$$

with $(\hat{\mathbf{n}},\mathbf{p})$□ $\Omega \times$ P. For unpolarized antennas, studying the array response is equivalent to study the integral kernel above. Hereafter, we show closed for expressions of the integral kernels for different types of arrays.

Unpolarized Linear Arrays

[00259] For unpolarized linear arrays of length L (normalized by the wavelength) and antenna elements oriented along the z-axis and centered at the origin, the integral kernel is given by [29]

$$a(\cos\theta, p_z) = \exp(-j2\pi\, p_z \cos\theta)\,.$$

[00260] Expanding the above equation into a series of shifted dyads, we obtain that the sinc function have resolution of 1/L and the dimension of the array-limited and approximately wavevector-limited subspace (i.e., degrees of freedom) is

$$D_F = L\,|\Omega_\theta|$$

where $\Omega_\theta = \{\cos\theta : \theta\epsilon\Theta\}$. We observe that for broadside arrays $|\Omega_\theta| = |\Theta|$ whereas for endfire $|\Omega_\theta| \approx |\Theta|^2/2$.

Unpolarized Spherical Arrays

[00261] The integral kernel for a spherical array of radius R (normalized by the wavelength) is given by [29]

$$a(\hat{\mathbf{n}},\mathbf{p}) = \exp\{-j2\pi R\,[\sin\theta\ \sin\theta'\cos(\phi-\phi') + \cos\theta\cos\theta']\}.$$

[00262] Decomposing the above function with sum of spherical Bessel functions of the first kind we obtain the resolution of spherical arrays is $1/(\pi R^2)$ and the degrees of freedom are given by

$$D_F = A|\Omega| = \pi R^2|\Omega|$$

[00263] where A is the area of the spherical array and $|\Omega| \subset [0,\pi) \times [0,2\pi)$.

Areas of Coherence in Wireless Channels

[00264] The relation between the resolution of spherical arrays and their area A is depicted in **Figure 43**. The sphere in the middle is the spherical array of area A. The projection of the channel clusters on the unit sphere defines different scattering regions of size proportional to the angular spread of the clusters. The area of size $1/A$ within each cluster, which we call "area of coherence", denotes the projection of the basis functions of the radiated field of the array and defines the resolution of the array in the wavevector domain.

[00265] Comparing **Figure 43** with **Figure 44**, we observe that the size of the area of coherence decreases as the inverse of the size of the array. In fact, larger arrays can focus energy into smaller areas, yielding larger number of degrees of freedom D_F. Note that to total number of degrees of freedom depends also on the angular spread of the cluster, as shown in the definition above.

[00266] **Figure 45** depicts another example where the array size covers even larger area than **Figure 44**, yielding additional degrees of freedom. In DIDO systems, the array aperture can be approximated by the total area covered by all DIDO transmitters (assuming antennas are spaced fractions of wavelength apart). Then **Figure 45** shows that DIDO systems can achieve increasing numbers of degrees of freedom by distributing antennas in space, thereby reducing the size of the areas of coherence. Note that these figures are generated assuming ideal spherical arrays. In practical scenarios, DIDO antennas spread random across wide areas and the resulting shape of the areas of coherence may not be as regular as in the figures.

[00267] **Figure 46** shows that, as the array size increases, more clusters are included within the wireless channel as radio waves are scatterered by increasing number of objects between DIDO transmitters. Hence, it is possible to excite an increasing number of basis functions (that span the radiated field) , yielding additional degrees of freedom, in agreement with the definition above.

[00268] The multi-user (MU) multiple antenna systems (MAS) described in this patent application exploit the area of coherence of wireless channels to create multiple simultaneous independent non-interfering data streams to different users. For given channel conditions and user distribution, the basis functions of the radiated field are selected to create independent and

simultaneous wireless links to different users in such a way that every user experiences interference-free links. As the MU-MAS is aware of the channel between every transmitter and every user, the precoding transmission is adjusted based on that information to create separate areas of coherence to different users.

[00269] In one embodiment of the invention, the MU-MAS employs non-linear precoding, such as dirty-paper coding (DPC) [30-31] or Tomlinson-Harashima (TH) [32-33] precoding. In another embodiment of the invention, the MU-MAS employs non-linear precoding, such as block diagonalization (BD) as in our previous patent applications [0003-0009] or zero-forcing beamforming (ZF-BF) [34].

[00270] To enable precoding, the MU-MAS requires knowledge of the channel state information (CSI). The CSI is made available to the MU-MAS via a feedback channel or estimated over the uplink channel, assuming uplink/downlink channel reciprocity is possible in time division duplex (TDD) systems. One way to reduce the amount of feedback required for CSI, is to use limited feedback techniques [35-37]. In one embodiment, the MU-MAS uses limited feedback techniques to reduce the CSI overhead of the control channel. Codebook design is critical in limited feedback techniques. One embodiment defines the codebook from the basis functions that span the radiated field of the transmit array.

[00271] As the users move in space or the propagation environment changes over time due to mobile objects (such as people or cars), the areas of coherence change their locations and shape. This is due to well know Doppler effect in wireless communications. The MU-MAS described in this patent application adjusts the precoding to adapt the areas of coherence constantly for every user as the environment changes due to Doppler effects. This adaptation of the areas of coherence is such to create simultaneous non-interfering channels to different users.

[00272] Another embodiment of the invention adaptively selects a subset of antennas of the MU-MAS system to create areas of coherence of different sizes. For example, if the users are sparsely distributed in space (i.e., rural area or times of the day with low usage of wireless resources), only a small subset of antennas is selected and the size of the area of coherence are large relative to the array size as in **Figure 43**. Alternatively, in densely populated areas (i.e., urban areas or time of the day with peak usage of wireless services) more antennas are selected to create small areas of coherence for users in direct vicinity of each other.

[00273] In one embodiment of the invention, the MU-MAS is a DIDO system as described in previous patent applications [0003-0009]. The DIDO system uses linear or non-linear precoding and/or limited feedback techniques to create area of coherence to different users.

Numerical Results

[00274] We begin by computing the number of degrees of freedom in conventional multiple-input multiple-output (MIMO) systems as a function of the array size. We consider unpolarized linear arrays and two types of channel models: indoor as in the IEEE 802.11n standard for WiFi systems and outdoor as in the 3GPP-LTE standard for cellular systems. The indoor channel mode in [3] defines the number of clusters in the range [2, 6] and angular spread in the range [15^o, 40^o]. The outdoor channel model for urban micro defines about 6 clusters and the angular spread at the base station of about 20^o.

[00275] **Figure 47** shows the degrees of freedom of MIMO systems in practical indoor and outdoor propagation scenarios. For example, considering linear arrays with ten antennas spaced one wavelength apart, the maximum degrees of freedom (or number of spatial channels) available over the wireless link is limited to about 3 for outdoor scenarios and 7 for indoor. Of course, indoor channels provide more degrees of freedom due to the larger angular spread.

[00276] Next we compute the degrees of freedom in DIDO systems. We consider the case where the antennas distributed over 3D space, such as downtown urban scenarios where DIDO access points may be distributed on different floors of adjacent building. As such, we model the DIDO transmit antennas (all connected to each other via fiber or DSL backbone) as a spherical array. Also, we assume the clusters are uniformly distributed across the solid angle.

[00277] **Figure 48** shows the degrees of freedom in DIDO systems as a function of the array diameter. We observe that for a diameter equal to ten wavelengths, about 1000 degrees of freedom are available in the DIDO system. In theory, it is possible to create up to 1000 non-interfering channels to the users. The increased spatial diversity due to distributed antennas in space is the key to the multiplexing gain provided by DIDO over conventional MIMO systems.

[00278] As a comparison, we show the degrees of freedom achievable in suburban environments with DIDO systems. We assume the clusters are distributed within the elevation angles $[\alpha, \pi - \alpha]$, and define the solid angle for the clusters as $|\Omega| = 4\pi \cos\alpha$. For example, in suburban scenarios with two-story buildings, the elevation angle of the scatterers can be $\alpha = 60^o$. In that case, the number of degrees of freedom as a function of the wavelength is shown in **Figure 48**.

References

[00279] [1] A. A. M. Saleh and R. A. Valenzuela, "A statistical model for indoor multipath propagation," IEEE Jour. Select. Areas in Comm., vol.195 SAC-5, no. 2, pp. 128–137, Feb. 1987.

[00280] [2] J. W. Wallace and M. A. Jensen, "Statistical characteristics of measured MIMO wireless channel data and comparison to conventional models," Proc. IEEE Veh. Technol. Conf., vol. 2, no. 7-11, pp. 1078–1082, Oct. 2001.

[00281] [3] V. Erceg et al., "TGn channel models," IEEE 802.11-03/940r4, May 2004.

[00282] [4] 3GPP Technical Specification Group, "Spatial channel model, SCM-134 text V6.0," Spatial Channel Model AHG (Combined ad-hoc from 3GPP and 3GPP2), Apr. 2003.

[00283] [5] D.-S. Shiu, G. J. Foschini, M. J. Gans, and J. M. Kahn, "Fading correlation and its effect on the capacity of multielement antenna systems," IEEE Trans. Comm., vol. 48, no. 3, pp. 502–513, Mar. 2000.

[00284] [6] V. Pohl, V. Jungnickel, T. Haustein, and C. von Helmolt, "Antenna spacing in MIMO indoor channels," Proc. IEEE Veh. Technol. Conf., vol. 2, pp. 749–753, May 2002.

[00285] [7] M. Stoytchev, H. Safar, A. L. Moustakas, and S. Simon, "Compact antenna arrays for MIMO applications," Proc. IEEE Antennas and Prop. Symp., vol. 3, pp. 708–711, July 2001.

[00286] [8] K. Sulonen, P. Suvikunnas, L. Vuokko, J. Kivinen, and P. Vainikainen, "Comparison of MIMO antenna configurations in picocell and microcell environments," IEEE Jour. Select. Areas in Comm., vol. 21, pp. 703–712, June 2003.

[00287] [9] Shuangqing Wei, D. L. Goeckel, and R. Janaswamy, "On the asymptoticcapacity of MIMO systems with fixed length linear antenna arrays," Proc. IEEE Int. Conf. on Comm., vol. 4, pp. 2633–2637, 2003.

[00288] [10] T. S. Pollock, T. D. Abhayapala, and R. A. Kennedy, "Antenna saturation effects on MIMO capacity," Proc. IEEE Int. Conf. on Comm., 192 vol. 4, pp. 2301–2305, May 2003.

[00289] [11] M. L. Morris and M. A. Jensen, "The impact of array configuration on MIMO wireless channel capacity," Proc. IEEE Antennas and Prop. Symp., vol. 3, pp. 214–217, June 2002.

[00290] [12] Liang Xiao, Lin Dal, Hairuo Zhuang, Shidong Zhou, and Yan Yao, "A comparative study of MIMO capacity with different antenna topologies," IEEE ICCS'02, vol. 1, pp. 431–435, Nov. 2002.

[00291] [13] A. Forenza and R. W. Heath Jr., "Impact of antenna geometry on MIMO communication in indoor clustered channels," Proc. IEEE Antennas and Prop. Symp., vol. 2, pp. 1700–1703, June 2004.

[00292] [14] M. R. Andrews, P. P. Mitra, and R. deCarvalho, "Tripling the capacity of wireless communications using electromagnetic polarization," Nature, vol. 409, pp. 316–318, Jan. 2001.

[00293] [15] D.D. Stancil, A. Berson, J.P. Van't Hof, R. Negi, S. Sheth, and P. Patel, "Doubling wireless channel capacity using co-polarised, co-located electric and magnetic dipoles," Electronics Letters, vol. 38, pp. 746–747, July 2002.

[00294] [16] T. Svantesson, "On capacity and correlation of multi-antenna systems employing multiple polarizations," Proc. IEEE Antennas and Prop. Symp., vol. 3, pp. 202–205, June 2002.

[00295] [17] C. Degen and W. Keusgen, "Performance evaluation of MIMO systems using dual-polarized antennas," Proc. IEEE Int. Conf. on Telecommun., vol. 2, pp. 1520–1525, Feb. 2003.

[00296] [18] R. Vaughan, "Switched parasitic elements for antenna diversity," IEEE Trans. Antennas Propagat., vol. 47, pp. 399–405, Feb. 1999.

[00297] [19] P. Mattheijssen, M. H. A. J. Herben, G. Dolmans, and L. Leyten, "Antenna-pattern diversity versus space diversity for use at handhelds," IEEE Trans. on Veh. Technol., vol. 53, pp. 1035–1042, July 2004.

[00298] [20] L. Dong, H. Ling, and R. W. Heath Jr., "Multiple-input multiple-output wireless communication systems using antenna pattern diversity," Proc. IEEE Glob. Telecom. Conf., vol. 1, pp. 997–1001, Nov. 2002.

[00299] [21] J. B. Andersen and B. N. Getu, "The MIMO cube-a compact MIMO antenna," IEEE Proc. of Wireless Personal Multimedia Communications Int. Symp., vol. 1, pp. 112–114, Oct. 2002.

[00300] [22] C. Waldschmidt, C. Kuhnert, S. Schulteis, and W. Wiesbeck, "Compact MIMO-arrays based on polarisation-diversity," Proc. IEEE Antennas and Prop. Symp., vol. 2, pp. 499–502, June 2003.

[00301] [23] C. B. Dietrich Jr, K. Dietze, J. R. Nealy, and W. L. Stutzman, "Spatial, polarization, and pattern diversity for wireless handheld terminals," Proc. IEEE Antennas and Prop. Symp., vol. 49, pp. 1271–1281, Sep. 2001.

[00302] [24] S. Visuri and D. T. Slock, "Colocated antenna arrays: design desiderata for wireless communications," Proc. of Sensor Array and Multichannel Sign. Proc. Workshop, pp. 580–584, Aug. 2002.

[00303] [25] A. Forenza and R. W. Heath Jr., "Benefit of pattern diversity via 2-element array of circular patch antennas in indoor clustered MIMO channels," IEEE Trans. on Communications, vol. 54, no. 5, pp. 943-954, May 2006.

[00304] [26] A. Forenza and R. W. Heath, Jr., ``Optimization Methodology for Designing 2-CPAs Exploiting Pattern Diversity in Clustered MIMO Channels", IEEE Trans. on Communications, Vol. 56, no. 10, pp. 1748 -1759, Oct. 2008.

[00305] [27] D. Piazza, N. J. Kirsch, A. Forenza, R. W. Heath, Jr., and K. R. Dandekar, ``Design and Evaluation of a Reconfigurable Antenna Array for MIMO Systems," IEEE Transactions on Antennas and Propagation, vol. 56, no. 3, pp. 869-881, March 2008.

[00306] [28] R. Bhagavatula, R. W. Heath, Jr., A. Forenza, and S. Vishwanath, ``Sizing up MIMO Arrays," IEEE Vehicular Technology Magazine, vol. 3, no. 4, pp. 31-38, Dec. 2008.

[00307] [29] Ada Poon, R. Brodersen and D. Tse, "Degrees of Freedom in Multiple Antenna Channels: A Signal Space Approach" , IEEE Transactions on Information Theory, vol. 51(2), Feb. 2005, pp. 523-536.

[00308] [30] M. Costa, "Writing on dirty paper," *IEEE Transactions on Information Theory*, Vol. 29, No. 3, Page(s): 439 - 441, May 1983.

[00309] [31] U. Erez, S. Shamai (Shitz), and R. Zamir, "Capacity and lattice-strategies for cancelling known interference," *Proceedings of International Symposium on Information Theory*, Honolulu, Hawaii, Nov. 2000.

[00310] [32] M. Tomlinson, "New automatic equalizer employing modulo arithmetic," *Electronics Letters*, Page(s): 138 - 139, March 1971.

[00311] [33] H. Miyakawa and H. Harashima, "A method of code conversion for digital communication channels with intersymbol interference," *Transactions of the Institute of Electronic*

[00312] [34] R. A. Monziano and T. W. Miller, *Introduction to Adaptive Arrays*, New York: Wiley, 1980.

[00313] [35] T. Yoo, N. Jindal, and A. Goldsmith, "Multi-antenna broadcast channels with limited feedback and user selection," IEEE Journal on Sel. Areas in Communications, vol. 25, pp. 1478-91, July 2007.

[00314] [36] P. Ding, D. J. Love, and M. D. Zoltowski, "On the sum rate of channel subspace feedback for multi-antenna broadcast channels," in Proc., IEEE Globecom, vol. 5, pp. 2699-2703, November 2005.

[00315] [37] N. Jindal, "MIMO broadcast channels with finite-rate feedback," IEEE Trans. on Info. Theory, vol. 52, pp. 5045-60, November 2006.

IV. SYSTEM AND METHODS FOR PLANNED EVOLUTION AND OBSOLESCENCE OF MULTIUSER SPECTRUM

[00316] The growing demand for high-speed wireless services and the increasing number of cellular telephone subscribers has produced a radical technology revolution in the wireless industry over the past three decades from initial analog voice services (AMPS [1-2]) to standards that support digital voice (GSM [3-4], IS-95 CDMA [5]), data traffic (EDGE [6], EV-DO [7]) and Internet browsing (WiFi [8-9], WiMAX [10-11], 3G [12-13], 4G [14-15]). This wireless technology growth throughout the years has been enabled by two major efforts:

i) The federal communications commission (FCC) [16] has been allocating new spectrum to support new emerging standards. For example, in the first generation AMPS systems the number of channels allocated by the FCC grew from the initial 333 in 1983 to 416 in the late 1980s to support the increasing number of cellular clients. More recently, the commercialization of technologies like Wi-Fi, Bluetooth and ZigBee has been possible with the use of the unlicensed ISM band allocated by the FCC back in 1985 [17].

ii) The wireless industry has been producing new technologies that utilize the limited available spectrum more efficiently to support higher data rate links and increased numbers of subscribers. One big revolution in the wireless world was the migration from the analog AMPS systems to digital D-AMPS and GSM in the 1990s, that enabled much higher call volume for a given frequency band due to improved spectral efficiency. Another radical shift was produced in the early 2000s by spatial processing techniques such as multiple-input multiple-output (MIMO), yielding 4x improvement in data rate over previous wireless networks and adopted by different standards (i.e., IEEE 802.11n for Wi-Fi, IEEE 802.16 for WiMAX, 3GPP for 4G-LTE).

[00317] Despite efforts to provide solutions for high-speed wireless connectivity, the wireless industry is facing new challenges: to offer high-definition (HD) video streaming to satisfy the growing demand for services like gaming and to provide wireless coverage everywhere (including rural areas, where building the wireline backbone is costly and impractical). Currently, the most advanced wireless standard systems (i.e., 4G-LTE) cannot provide data rate requirements and latency constraints to support HD streaming services, particularly when the network is overloaded with a high volume of concurrent links. Once again, the main drawbacks have been the limited spectrum availability and lack of spectrally efficient technologies that can truly enhance data rate and provide complete coverage.

[00318] A new technology has emerged in recent years called distributed-input distributed-output (DIDO) [18-21] and described in our previous patent applications [0002-0009]. DIDO technology promises orders of magnitude increase in spectral efficiency, making HD wireless streaming services possible in overloaded networks.

[00319] At the same time, the US government has been addressing the issue of spectrum scarcity by launching a plan that will free 500MHz of spectrum over the next 10 years. This plan was released on June 28th, 2010 with the goal of allowing new emerging wireless technologies to operate in the new frequency bands and providing high-speed wireless coverage in urban and rural areas [22]. As part of this plan, on September 23rd, 2010 the FCC opened up about 200MHz of the VHF and UHF spectrum for unlicensed use called “white spaces” [23]. One restriction to operate in those frequency bands is that harmful interference must not be created with existing

wireless microphone devices operating in the same band. As such, on July 22nd, 2011 the IEEE 802.22 working group finalized the standard for a new wireless system employing cognitive radio technology (or spectrum sensing) with the key feature of dynamically monitoring the spectrum and operating in the available bands, thereby avoiding harmful interference with coexisting wireless devices [24]. Only recently has there been debates to allocate part of the white spaces to licensed use and open it up to spectrum auction [25].

[00320] The coexistence of unlicensed devices within the same frequency bands and spectrum contention for unlicensed versus licensed use have been two major issues for FCC spectrum allocation plans throughout the years. For example, in white spaces, coexistence between wireless microphones and wireless communications devices has been enabled via cognitive radio technology. Cognitive radio, however, can provide only a fraction of the spectral efficiency of other technologies using spatial processing like DIDO. Similarly, the performance of Wi-Fi systems have been degrading significantly over the past decade due to increasing number of access points and the use of Bluetooth/ZigBee devices that operate in the same unlicensed ISM band and generate uncontrolled interference. One shortcoming of the unlicensed spectrum is unregulated use of RF devices that will continue to pollute the spectrum for years to come. RF pollution also prevents the unlicensed spectrum from being used for future licensed operations, thereby limiting important market opportunities for wireless broadband commercial services and spectrum auctions.

[00321] We propose a new system and methods that allow dynamic allocation of the wireless spectrum to enable coexistence and evolution of different services and standards. One embodiment of our method dynamically assigns entitlements to RF transceivers to operate in certain parts of the spectrum and enables obsolescence of the same RF devices to provide:

i) Spectrum reconfigurability to enable new types of wireless operations (i.e., licensed vs. unlicensed) and/or meet new RF power emission limits. This feature allows spectrum auctions whenever is necessary, without need to plan in advance for use of licensed versus unlicensed spectrum. It also allows transmit power levels to be adjusted to meet new power emission levels enforced by the FCC.

ii) Coexistence of different technologies operating in the same band (i.e., white spaces and wireless microphones, WiFi and Bluetooth/ZigBee) such that the band can be dynamically reallocated as new technologies are created, while avoiding interference with existing technologies.

iii) Seamless evolution of wireless infrastructure as systems migrate to more advanced technologies that can offer higher spectral efficiency, better coverage and improved

performance to support new types of services demanding higher QoS (i.e., HD video streaming).

[00322] Hereafter, we describe a system and method for planned evolution and obsolescence of a multiuser spectrum. One embodiment of the system consists of one or multiple centralized processors (CP) 4901-4904 and one or multiple distributed nodes (DN) 4911-4913 that communicate via wireline or wireless connections as depicted in **Figure 49**. For example, in the context of 4G-LTE networks [26], the centralized processor is the access core gateway (ACGW) connected to several Node B transceivers. In the context of Wi-Fi, the centralized processor is the internet service provider (ISP) and the distributed nodes are Wi-Fi access points connected to the ISP via modems or direct connection to cable or DSL. In another embodiment of the invention, the system is a distributed-input distributed-output (DIDO) system [0002-0009] with one centralized processor (or BTS) and distributed nodes being the DIDO access points (or DIDO distributed antennas connected to the BTS via the BSN).

[00323] The DNs 4911-4913 communicate with the CPs 4901-4904. The information exchanged from the DNs to the CP is used to dynamically adjust the configuration of the nodes to the evolving design of the network architecture. In one embodiment, the DNs 4911-4913 share their identification number with the CP. The CP store the identification numbers of all DNs connected through the network into lookup tables or shared database. Those lookup tables or database can be shared with other CPs and that information is synchronized such that all CPs have always access to the most up to date information about all DNs on the network.

[00324] For example, the FCC may decide to allocate a certain portion of the spectrum to unlicensed use and the proposed system may be designed to operate within that spectrum. Due to scarcity of spectrum, the FCC may subsequently need to allocate part of that spectrum to licensed use for commercial carriers (i.e., AT&T, Verizon, or Sprint), defense, or public safety. In conventional wireless systems, this coexistence would not be possible, since existing wireless devices operating in the unlicensed band would create harmful interference to the licensed RF transceivers. In our proposed system, the distributed nodes exchange control information with the CPs 4901-4903 to adapt their RF transmission to the evolving band plan. In one embodiment, the DNs 4911-4913 were originally designed to operate over different frequency bands within the available spectrum. As the FCC allocates one or multiple portions of that spectrum to licensed operation, the CPs exchange control information with the unlicensed DNs and reconfigure them to shut down the frequency bands for licensed use, such that the unlicensed DNs do not interfere with the licensed DNs. This scenario is depicted in **Figure 50** where the unlicensed nodes (e.g., 5002) are indicated with solid circles and the licensed nodes with empty circles (e.g., 5001). In another embodiment, the whole spectrum can be allocated to the new

licensed service and the control information is used by the CPs to shut down all unlicensed DNs to avoid interference with the licensed DNs. This scenario is shown in **Figure 51** where the obsolete unlicensed nodes are covered with a cross.

[00325] By way of another example, it may be necessary to restrict power emissions for certain devices operating at given frequency band to meet the FCC exposure limits [27]. For instance, the wireless system may originally be designed for fixed wireless links with the DNs 4911-4913 connected to outdoor rooftop transceiver antennas. Subsequently, the same system may be updated to support DNs with indoor portable antennas to offer better indoor coverage. The FCC exposure limits of portable devices are more restrictive than rooftop transmitters, due to possibly closer proximity to the human body. In this case, the old DNs designed for outdoor applications can be re-used for indoor applications as long as the transmit power setting is adjusted. In one embodiment of the invention the DNs are designed with predefined sets of transmit power levels and the CPs 4901-4903 send control information to the DNs 4911-4913 to select new power levels as the system is upgraded, thereby meeting the FCC exposure limits. In another embodiment, the DNs are manufactured with only one power emission setting and those DNs exceeding the new power emission levels are shut down remotely by the CP.

[00326] In one embodiment, the CPs 4901-4903 monitor periodically all DNs 4911-4913 in the network to define their entitlement to operate as RF transceivers according to a certain standard. Those DNs that are not up to date can be marked as obsolete and removed from the network. For example, the DNs that operate within the current power limit and frequency band are kept active in the network, and all the others are shut down. Note that the DN parameters controlled by the CP are not limited to power emission and frequency band; it can be any parameter that defines the wireless link between the DN and the client devices.

[00327] In another embodiment of the invention, the DNs 4911-4913 can be reconfigured to enable the coexistence of different standard systems within the same spectrum. For example, the power emission, frequency band or other configuration parameters of certain DNs operating in the context of WLAN can be adjusted to accommodate the adoption of new DNs designed for WPAN applications, while avoiding harmful interference.

[00328] As new wireless standards are developed to enhance data rate and coverage in the wireless network, the DNs 4911-4913 can be updated to support those standards. In one embodiment, the DNs are software defined radios (SDR) equipped with programmable computational capability such as FPGA, DSP, CPU, GPU and/or GPGPU that run algorithms for baseband signal processing. If the standard is upgraded, new baseband algorithms can be remotely uploaded from the CP to the DNs to reflect the new standard. For example, in one embodiment the first standard is CDMA-based and subsequently it is replaced by OFDM

technology to support different types of systems. Similarly, the sample rate, power and other parameters can be updated remotely to the DNs. This SDR feature of the DNs allows for continuous upgrades of the network as new technologies are developed to improve overall system performance.

[00329] In another embodiment, the system described herein is a cloud wireless system consisting of multiple CPs, distributed nodes and a network interconnecting the CPs to the DNs. **Figure 52** shows one example of cloud wireless system where the nodes identified with solid circles (e.g., 5203) communicate to CP 5206, the nodes identified with empty circles communicate to CP 5205 and the CPs 5205-5206 communicate between each other all through the network 5201. In one embodiment of the invention, the cloud wireless system is a DIDO system and the DNs are connected to the CP and exchange information to reconfigure periodically or instantly system parameters, and dynamically adjust to the changing conditions of the wireless architecture. In the DIDO system, the CP is the DIDO BTS, the distributed nodes are the DIDO distributed antennas, the network is the BSN and multiple BTSs are interconnected with each other via the DIDO centralized processor as described in our previous patent applications [0002-0009].

[00330]

All DNs 5202-5203 within the cloud wireless system can be grouped in different sets. These sets of DNs can simultaneously create non-interfering wireless links to the multitude of client devices, while each set supporting a different multiple access techniques (e.g., TDMA, FDMA, CDMA, OFDMA and/or SDMA), different modulations (e.g., QAM, OFDM) and/or coding schemes (e.g., convolutional coding, LDPC, turbo codes). Similarly, every client may be served with different multiple access techniques and/or different modulation/coding schemes. Based on the active clients in the system and the standard they adopt for their wireless links, the CPs 5205-5206 dynamically select the subset of DNs that can support those standards and that are within range of the client devices.

Reference

[00331] [1] Wikipedia, "Advanced Mobile Phone System"
http://en.wikipedia.org/wiki/Advanced_Mobile_Phone_System

[00332] [2] AT&T, "1946: First Mobile Telephone Call"
http://www.corp.att.com/attlabs/reputation/timeline/46mobile.html

[00333] [3] GSMA, "GSM technology"
http://www.gsmworld.com/technology/index.htm

[00334] [4] ETSI, "Mobile technologies GSM"
http://www.etsi.org/WebSite/Technologies/gsm.aspx

[00335] [5] Wikipedia, "IS-95"
http://en.wikipedia.org/wiki/IS-95

[00336] [6] Ericsson, "The evolution of EDGE"
http://www.ericsson.com/res/docs/whitepapers/evolution_to_edge.pdf

[00337] [7] Q. Bi (2004-03). "A Forward Link Performance Study of the 1xEV-DO Rel. 0 System Using Field Measurements and Simulations" (PDF). Lucent Technologies.
http://www.cdg.org/resources/white_papers/files/Lucent%201xEV-DO%20Rev%20O%20Mar%2004.pdf

[00338] [8] Wi-Fi alliance, http://www.wi-fi.org/

[00339] [9] Wi-Fi alliance, "Wi-Fi certified makes it Wi-Fi"
http://www.wi-fi.org/files/WFA_Certification_Overview_WP_en.pdf

[00340] [10] WiMAX forum, http://www.wimaxforum.org/

[00341] [11] C. Eklund, R. B. Marks, K. L. Stanwood and S. Wang, "IEEE Standard 802.16: A Technical Overview of the WirelessMAN™Air Interface for Broadband Wireless Access"
http://ieee802.org/16/docs/02/C80216-02_05.pdf

[00342] [12] 3GPP, "UMTS", http://www.3gpp.org/article/umts

[00343] [13] H. Ekström, A. Furuskär, J. Karlsson, M. Meyer, S. Parkvall, J. Torsner, and M. Wahlqvist "Technical Solutions for the 3G Long-Term Evolution", IEEE Communications Magazine, pp.38-45, Mar. 2006

[00344] [14] 3GPP, "LTE", http://www.3gpp.org/LTE

[00345] [15] Motorola, "Long Term Evolution (LTE): A Technical Overview", http://business.motorola.com/experiencelte/pdf/LTETechnicalOverview.pdf

[00346] [16] Federal Communications Commission, "Authorization of Spread Spectrum Systems Under Parts 15 and 90 of the FCC Rules and Regulations", June 1985.

[00347] [17] ITU, "ISM band" http://www.itu.int/ITU-R/terrestrial/faq/index.html#g013

[00348] [18] S. Perlman and A. Forenza "Distributed-input distributed-output (DIDO) wireless technology: a new approach to multiuser wireless", Aug. 2011
http://www.rearden.com/DIDO/DIDO_White_Paper_110727.pdf

[00349] [19] Bloomberg Businessweek, "Steve Perlman's Wireless Fix", July 27, 2011
http://www.businessweek.com/magazine/the-edison-of-silicon-valley-07272011.html

[00350] [20] Wired, "Has OnLive's Steve Perlman Discovered Holy Grail of Wireless?", June 30, 2011
http://www.wired.com/epicenter/2011/06/perlman-holy-grail-wireless/

[00351] [21] The Wall Street Journal "Silicon Valley Inventor's Radical Rewrite of Wireless", July 28, 2011
http://blogs.wsj.com/digits/2011/07/28/silicon-valley-inventors-radical-rewrite-of-wireless/

[00352] [22] The White House, "Presidential Memorandum: Unleashing the Wireless Broadband Revolution", June 28, 2010
http://www.whitehouse.gov/the-press-office/presidential-memorandum-unleashing-wireless-broadband-revolution

[00353] [23] FCC, "Open commission meeting", Sept. 23rd, 2010
http://reboot.fcc.gov/open-meetings/2010/september

[00354] [24] IEEE 802.22, "IEEE 802.22 Working Group on Wireless Regional Area Networks", http://www.ieee802.org/22/

[00355] [25] "A bill",112th congress, 1st session, July 12, 2011
http://republicans.energycommerce.house.gov/Media/file/Hearings/Telecom/071511/Discussion Draft.pdf

[00356] [26] H. Ekström, A. Furuskär, J. Karlsson, M. Meyer, S. Parkvall, J. Torsner, and M. Wahlqvist "Technical Solutions for the 3G Long-Term Evolution", IEEE Communications Magazine, pp.38-45, Mar. 2006

[00357] [27] FCC, "Evaluating compliance with FCC guidelines for human exposure to radiofrequency electromagnetic fields," OET Bulletin 65, Edition 97-01, Aug. 1997

V. SYSTEM AND METHOD TO COMPENSATE FOR DOPPLER EFFECTS IN DISTRIBUTED-INPUT DISTRIBUTED-OUTPUT WIRELESS SYSTEMS

[00358] In this portion of the detailed description we describe a multiuser (MU) multiple antenna system (MAS) for multiuser wireless transmissions that adaptively reconfigures its parameters to compensate for Doppler effects due to user mobility or changes in the propagation environment. In one embodiment, the MAS is a distributed-input distributed-output (DIDO) system as described the co-pending patent applications [0002-0016] and depicted in **Figure 53**. The DIDO system of one embodiment includes the following components:

- **User Equipment (UE)**: The UE 5301 of one embodiment includes an RF transceiver for fixed or mobile clients receiving data streams over the downlink (DL) channel from the DIDO backhaul and transmitting data to the DIDO backhaul via the uplink (UL) channel
- **Base Transceiver Station (BTS)**: The BTSs 5310-5314 of one embodiment interface the DIDO backhaul with the wireless channel. BTSs 5310-5314 are access points consisting of DAC/ADC and radio frequency (RF) chain to convert the baseband signal to RF. In some cases, the BTS is a simple RF transceiver equipped with power amplifier/antenna

and the RF signal is carried to the BTS via RF-over-fiber technology as described in our patent application [0010].

- **Controller (CTR)**: The CTR 5320 in one embodiment is one particular type of BTS designed for certain specialized features such as transmitting training signals for time/frequency synchronization of the BTSs and/or the UEs, receiving/transmitting control information from/to the UEs, receiving the channel state information (CSI) or channel quality information from the UEs.
- **Centralized Processor (CP)**: The CP 5340 of one embodiment is a DIDO server interfacing the Internet or other types of external networks 5350 with the DIDO backhaul. The CP computes the DIDO baseband processing and sends the waveforms to the distributed BTSs for DL transmission
- **Base Station Network (BSN)**: The BSN 5330 of one embodiment is the network connecting the CP to the distributed BTSs carrying information for either the DL or the UL channel. The BSN is a wireline or a wireless network or a combination of the two. For example, the BSN is a DSL, cable, optical fiber network, or line-of-sight or non-line-of-sight wireless link. Furthermore, the BSN is a proprietary network, or a local area network, or the Internet.

[00359] As described in the co-pending applications, the DIDO system creates independent channels to multiple users, such that each user receives interference-free channels. In DIDO systems, this is achieved by employing distributed antennas or BTSs to exploit spatial diversity. In one embodiment, the DIDO system exploits spatial, polarization and/or pattern diversity to increase the degrees of freedom within each channel. The increased degrees of freedom of the wireless link are used to transmit independent data streams to an increased number of UEs (i.e., multiplexing gain) and/or improve coverage (i.e., diversity gain).

[00360] The BTSs 5310-5314 are placed anywhere that is convenient where there is access to the Internet or BSN. In one embodiment of the invention, the UEs 5301-5305 are placed randomly between, around and/or surrounded by the BTSs or distributed antennas as depicted in **Figure 54**.

[00361] In one embodiment, the BTSs 5310-5314 send a training signal and/or independent data streams to the UEs 5301 over the DL channel as depicted in **Figure 55**. The training signal is used by the UEs for different purposes, such as time/frequency synchronization, channel estimation and/or estimation of the channel state information (CSI). In one embodiment of the invention, the MU-MAS DL employs non-linear precoding, such as dirty-paper coding (DPC) [1-2] or Tomlinson-Harashima (TH) [3-4] precoding. In another embodiment of the invention, the MU-MAS DL employs non-linear precoding, such as block diagonalization (BD) as

described in the co-pending patent applications [0003-0009] or zero-forcing beamforming (ZF-BF) [5]. If the number of BTSs is larger than the UEs, the extra BTSs are used to increase link quality to every UE via diversity schemes such as antenna selection or eigenmode selection described in [0002-0016]. If the number of BTSs is smaller than the UEs, the extra UEs share the wireless links with the other UEs via conventional multiplexing techniques (e.g., TDMA, FDMA, CDMA, OFDMA).

[00362] The UL channel is used to transmit data from the UEs 5301 to the CP 5340 and/or the CSI (or channel quality information) employed by the DIDO precoder. In one embodiment, the UL channels from the UEs are multiplexed via conventional multiplexing techniques (e.g., TDMA, FDMA, CDMA, OFDMA) to the CTR as depicted in **Figure 56** or to the closest BTS. In another embodiment of the invention, spatial processing techniques are used to separate the UL channels from the UEs 5301 to the distributed BTSs 5310-5314 as depicted in **Figure 57**. For example, UL streams are transmitted from the client to the DIDO antennas via multiple-input multiple-output (MIMO) multiplexing schemes. The MIMO multiplexing schemes include transmitting independent data streams from the clients and using linear or non-linear receivers at the DIDO antennas to remove co-channel interference. In another embodiment, the downlink weights are used over the uplink to demodulate the uplink streams, assuming UL/DL channel reciprocity holds and the channel does not vary significantly between DL and UL transmission due to Doppler effects. In another embodiment, a maximum ratio combining (MRC) receiver is used over the UL channel to increase signal quality at the DIDO antennas from every client.

[00363] The data, control information and CSI sent over the DL/UL channels is shared between the CP 5340 and the BTSs 5310-5314 via the BSN 5330. The known training signals for the DL channel can be stored in memory at the BTSs 5310-5314 to reduce overhead over the BSN 5330. Depending on the type of network (i.e., wireless versus wireline, DSL versus cable or fiber optic), there may not be a sufficient data rate available over the BSN 5330 to exchange information between the CP 5340 and the BTSs 5310-5314, especially when the baseband signal is delivered to the BTSs. For example, let us assume the BTSs transmit 10Mbps independent data streams to every UE over 5MHz bandwidth (depending on the digital modulation and FEC coding scheme used over the wireless link). If 16 bits of quantization are used for the real and 16 for the imaginary components, the baseband signal requires 160Mbps of data throughput from the CP to the BTSs over the BSN. In one embodiment, the CP and the BTSs are equipped with encoders and decoders to compress and decompress information sent over the BSN. In the forward link, the precoded baseband data sent from the CP to the BTSs is compressed to reduce the amount of bits and overhead sent over the BSN. Similarly, in the reverse link, the CSI as well as data (sent over the uplink channel from the UEs to the BTSs) are compressed before being

transmitted over the BSN from the BTSs to the CP. Different compression algorithms are employed to reduce the amount of bits and overhead sent over the BSN, including but not limited to lossless and/or lossy techniques [6].

[00364] One feature of DIDO systems employed in one embodiment is making the CP 5340 aware of the CSI or channel quality information between all BTSs 53105314 and UEs 5301 to enable precoding. As explained in [0006], the performance of DIDO depends on the rate at which the CSI is delivered to the CP relative to the rate of change of the wireless links. It is well known that variations of the channel complex gain are due to UE mobility and/or changes in the propagation environment that cause Doppler effects. The rate of change of the channel is measured in terms of channel coherence time (T_c) that is inversely proportional to the maximum Doppler shift. For DIDO transmissions to perform reliably, the latency due to CSI feedback must be a fraction (e.g., 1/10 or less) of the channel coherence time. In one embodiment, the latency over the CSI feedback loop is measured as the time between the time at which the CSI training is sent and the time the precoded data is demodulated at the UE side, as depicted in **Figure 58**.

[00365] In frequency division duplex (FDD) DIDO systems the BTSs 5310-5314 send CSI training to the UEs 5301, that estimate the CSI and feedback to the BTSs. Then the BTSs send the CSI via the BSN to the CP 5340, that computes the DIDO precoded data streams and sends those back to the BTSs via the BSN 5330. Finally the BTSs send precoded streams to the UEs that demodulate the data. Referring to **Figure 58**, the overall latency for the DIDO feedback loop is given by

$$2*T_{DL} + T_{UL} + T_{BSN} + T_{CP}$$

where T_{DL} and T_{UL} include the times to build, send and process the downlink and uplink frames, respectively, T_{BSN} is the round-trip delay over the BSN and T_{CP} is the time taken by the CP to process the CSI, generate the precoded data streams for the UEs and schedule different UEs for the current transmission. In this case, T_{DL} is multiplied by 2 to account for the training signal time (from the BTS to the UE) and the feedback signal time (from the UE to the BTS). In time division duplex (TDD), if channel reciprocity can be exploited, the first step is skipped (i.e., transitting a CSI training signal from the BTS to the UE) as the UEs send CSI training to the BTSs that compute the CSI and send it to the CP. Hence, in this embodiment, the overall latency for the DIDO feedback loop is

$$T_{DL} + T_{UL} + T_{BSN} + T_{CP}$$

[00366] The latency T_{BSN} depends on the type of BSN whether dedicated cable, DSL, fiber optic connection or general Internet. Typical values may vary between fractions of 1msec to 50msec. The computational time at the CP can be reduced if the DIDO processing is implemented at the CP on dedicated processors such as ASIC, FPGA, DSP, CPU, GPU and/or

GPGPU. Moreover, if the number of BTSs 5310-5314 exceeds the number of UEs 5301, all the UEs can be served at the same time, thereby removing latency due to multiuser scheduling. Hence, the latency T_{CP} is negligible compared to T_{BSN}. Finally, transmit and receive processing for the DL and UL is typically implemented on ASIC, FPGA or DSP with negligible computational time and if the signal bandwidth is relatively large (e.g. more than 1MHz) the frame duration can be made very small (i.e., less than 1msec). Therefore, also T_{DL} and T_{UL} are negligible compared to T_{BSN}.

[00367] In one embodiment of the invention, the CP 5340 tracks the Doppler velocity of all UEs 5301 and dynamically assigns the BTSs 5310-5314 with the lowest T_{BSN} to the UEs with higher Doppler. This adaptation is based on different criteria:

- Type of BSN: For example, dedicated fiber optic links typically experience lower latency than cable modems or DSL. Then the lower latency BSNs are used for high-mobility UEs (e.g., cars on freeways, trains), whereas the higher-latency BSNs are used for the fixed-wireless or low-mobility UEs (e.g., home equipment, pedestrians, cars in residential areas)
- Type of QoS: For example, the BSN can support different types of DIDO or non-DIDO traffic. It is possible to define quality of service (QoS) with different priorities for different types of traffic. For example, the BSN assigns high priority to DIDO traffic and low priority to non-DIDO traffic. Alternatively, high priority QoS is assigned to traffic for high-mobility UEs and low priority QoS to UEs with low-mobility.
- Long-term statistics: For example, the traffic over the BSN may vary significantly depending on the time of the day (e.g., night use for homes and day use for offices). Higher traffic load may result in higher latency. Then, in different times of the day, the BSNs with higher traffic, if it results in higher latency, are used for low-mobility UEs, whereas the BSNs with lower traffic, if it results in lower latency, are used for the high-mobility UEs
- Short-term statistics: For example, any BSN can be affected by temporary network congestion that can result in higher latency. Then the CP can adaptively select the BTSs from congested BSNs, if the congestion cause higher latency, for the low-mobility UEs and the remaining BSNs, if they are lower latency, for the high-mobility UEs.

[00368] In another embodiment of the invention, the BTSs 5310-5314 are selected based on the Doppler experienced on each individual BTS-UE link. For example, in the line-of-sight (LOS) link B in **Figure 59**, the maximum Doppler shift is a function of the angle (ϕ) between the BTS-UE link and the vehicular velocity (v), according to the well known equation

$$f_d = \frac{v}{\lambda} \cdot \cos\phi$$

where λ is the wavelength corresponding to the carrier frequency. Hence, in LOS channels the Doppler shift is maximum for link A and nearly zero for link C in **Figure 59**. In non-LOS (NLOS) the maximum Doppler shift depends on the direction of the multipaths around the UEs, but in general because of the distributed nature of the BTSs in DIDO systems, some BTSs will experience higher Doppler for a given UE (e.g., BTS 5312) whereas other BTSs will experience lower Doppler for that given UE (e.g., BTS 5314).

[00369] In one embodiment, the CP tracks the Doppler velocity over every BTS-UE link and selects only the links with the lowest Doppler effect for every UE. Similarly to the techniques described in [0002], the CP 5340 defines the "user cluster" for every UE 5301. The user cluster is the set of BTSs with good link quality (defined based on certain signal-to-noise ratio, SNR, threshold) to the UE and low Doppler (defined, for example, based on a predefined Doppler threshold) as depicted in **Figure 60**. In **Figure 60**, BTSs 5 through 10 all have good SNR to the UE1, but only BTSs 6 through 9 experience low Doppler effect (e.g., below the specified threshold).

[00370] The CP of this embodiement records all of the values of SNR and Doppler for every BTS-UE link into a matrix and for each UE it selects the submatrix that satisfies the SNR and Doppler thresholds. In the example depicted in **Figure 61**, the submatrix is identified by the green dotted line surrounding $C_{2,6}$, $C_{2,7}$, $C_{3,9}$, $C_{4,7}$, $C_{4,8}$, $C_{4,9}$, and $C_{5,6}$. DIDO precoding weights are computed for that UE based on that submatrix. Note that BTSs 5 and 10 are reachable by UEs 2,3,4,5 and 7 as shown in the table in **Figure 61**. Then, to avoid interference to UE1 when transmitting to those other UEs, the BTSs 5 and 10 either must switched off or assigned to different orthogonal channels based on conventional multiplexing techniques such as TDMA, FDMA, CDMA or OFDMA.

[00371] In another embodiment, the adverse effect of Doppler on the performance of DIDO precoding systems is reduced via linear prediction, which is one technique to estimate the complex channel coefficients in the future based on past channel estimates. By way of example and not limitation, different prediction algorithms for single-input single-output (SISO) and OFDM wireless systems were proposed in [7-11]. Knowing the future channel complex coefficients it is possible to reduce the error due to outdated CSI. For example, **Figure 62** shows the channel gain (or CSI) at different times: i) t_{CTR} is the time at which the CTR in **Figure 58** receives the CSI from the UEs in FDD systems (or equivalently the BTSs estimate the CSI from the UL channel exploiting DL/UL reciprocity in TDD systems); ii) t_{CP} is the time at which the CSI is delivered to the CP via the BSN; iii) t_{BTS} is the time at which the CSI is used for

precoding over the wireless link. In **Figure 62** we observe that due to the delay T_{BSN} (also depicted in **Figure 58**), the CSI estimated at time t_{CTR} will be outdated (i.e., complex channel gain has changed) by the time is used for wireless transmission over the DL channel at time t_{BTS}. One way to avoid this effect due to Doppler is to run the prediction method at the CP. The CSI estimates available at the CP at time t_{CTR} is delayed of $T_{BSN}/2$ due to CTR-to-CP latency and corresponds to the channel gain at time t_0 in **Figure 62**. Then, the CP uses all or part of the CSI estimated before time t_0 and stored in memory to predict the future channel coefficient at time $t_0+T_{BSN} = t_{CP}$. If the prediction algorithm has minimal error propagation, the predicted CSI at time t_{CP} reproduces reliably the channel gain in the future. The time difference between the predicted CSI and the current CSI is called prediction horizon and in SISO systems typically scales with the channel coherence time.

[00372] In DIDO systems the prediction algorithm is more complex since it estimates the future channel coefficients both in time and space domains. Linear prediction algorithms exploiting spatio-temporal characteristics of MIMO wireless channels were described in [12-13]. In [13] it was shown that the performance of the prediction algorithms in MIMO systems (measured in terms of mean squared error, or MSE) improves for higher channel coherence time (i.e., reduce Doppler effect) and lower channel coherence distance (due to lower spatial correlation). Hence the prediction horizon (expressed in seconds) of spatial-temporal methods is directly proportional to the channel coherence time and inversely proportional to the channel coherence distance. In DIDO systems the coherence distance is low due to high spatial selectivity produce by the distributed antennas.

[00373] Described herein is are prediction techniques that exploit temporal and spatial diversity of DIDO systems to predict the vector channel (i.e., CSI from the BTSs to the UEs) in the future. These embodiments exploit spatial diversity available in wireless channels to obtain negligible CSI prediction error and an extended prediction horizon over any existing SISO and MIMO prediction algorithms. One important feature of these techniques is to exploit distributed antennas given that they receive uncorrelated complex channel coefficients from the distributed UEs.

[00374] In one embodiment of the invention, the spatial and temporal predictor is combined with estimator in the frequency domain to allow CSI prediction over all the available subcarriers in the system, such as in OFDM systems. In another embodiment of the invention, the DIDO precoding weights are predicted (rather than the CSI) based on previous estimates of the DIDO weights.

References

[00375] [1] M. Costa, "Writing on dirty paper," *IEEE Transactions on Information Theory*, Vol. 29, No. 3, Page(s): 439 - 441, May 1983.

[00376] [2] U. Erez, S. Shamai (Shitz), and R. Zamir, "Capacity and lattice-strategies for cancelling known interference," *Proceedings of International Symposium on Information Theory*, Honolulu, Hawaii, Nov. 2000.

[00377] [3] M. Tomlinson, "New automatic equalizer employing modulo arithmetic," *Electronics Letters*, Page(s): 138 - 139, March 1971.

[00378] [4] H. Miyakawa and H. Harashima, "A method of code conversion for digital communication channels with intersymbol interference," *Transactions of the Institute of Electronic*

[00379] [5] R. A. Monziano and T. W. Miller, *Introduction to Adaptive Arrays*, New York: Wiley, 1980.

[00380] [6] Guy E. Blelloch, "Introduction to Data Compression", Carnegie Mellon University Tech. Report Sept. 2010

[00381] [7] A. Duel-Hallen, S. Hu, and H. Hallen, "Long-Range Prediction of Fading Signals," *IEEE Signal Processing Mag.*, vol. 17, no. 3, pp. 62–75, May 2000.

[00382] [8] A. Forenza and R. W. Heath, Jr., "Link Adaptation and Channel Prediction in Wireless OFDM Systems," in *Proc. IEEE Midwest Symp. on Circuits and Sys.*, Aug 2002, pp. 211–214.

[00383] [9] M. Sternad and D. Aronsson, "Channel estimation and prediction for adaptive OFDM downlinks [vehicular applications]," in *Proc. IEEE Vehicular Technology Conference*, vol. 2, Oct 2003, pp. 1283–1287.

[00384] [10] D. Schafhuber and G. Matz, "MMSE and Adaptive Prediction of Time-Varying Channels for OFDM Systems," *IEEE Trans. Wireless Commun.*, vol. 4, no. 2, pp. 593–602, Mar 2005.

[00385] [11] I. C. Wong and B. L. Evans, "Joint Channel Estimation and Prediction for OFDM Systems," in *Proc. IEEE Global Telecommunications Conference*, St. Louis, MO, Dec 2005.

[00386] [12] M. Guillaud and D. Slock, "A specular approach to MIMO frequencyselective channel tracking and prediction," in *Proc. IEEE Signal Processing Advances in Wireless Communications*, July 2004, pp. 59–63.

[00387] [13] Wong, I.C. Evans, B.L., "Exploiting Spatio-Temporal Correlations in MIMO Wireless Channel Prediction", IEEE Globecom Conf., pp.1-5, Dec. 2006

[00388] Embodiments of the invention may include various steps as set forth above. The steps may be embodied in machine-executable instructions which cause a general-purpose or

special-purpose processor to perform certain steps. For example, the various components within the Base Stations/APs and Client Devices described above may be implemented as software executed on a general purpose or special purpose processor. To avoid obscuring the pertinent aspects of the invention, various well known personal computer components such as computer memory, hard drive, input devices, etc., have been left out of the figures.

[00389] Alternatively, in one embodiment, the various functional modules illustrated herein and the associated steps may be performed by specific hardware components that contain hardwired logic for performing the steps, such as an application-specific integrated circuit ("ASIC") or by any combination of programmed computer components and custom hardware components.

[00390] In one embodiment, certain modules such as the Coding, Modulation and Signal Processing Logic 903 described above may be implemented on a programmable digital signal processor ("DSP") (or group of DSPs) such as a DSP using a Texas Instruments' TMS320x architecture (e.g., a TMS320C6000, TMS320C5000, . . . etc). The DSP in this embodiment may be embedded within an add-on card to a personal computer such as, for example, a PCI card. Of course, a variety of different DSP architectures may be used while still complying with the underlying principles of the invention.

[00391] Elements of the present invention may also be provided as a machine-readable medium for storing the machine-executable instructions. The machine-readable medium may include, but is not limited to, flash memory, optical disks, CD-ROMs, DVD ROMs, RAMs, EPROMs, EEPROMs, magnetic or optical cards, propagation media or other type of machine-readable media suitable for storing electronic instructions. For example, the present invention may be downloaded as a computer program which may be transferred from a remote computer (e.g., a server) to a requesting computer (e.g., a client) by way of data signals embodied in a carrier wave or other propagation medium via a communication link (e.g., a modem or network connection).

[00392] Throughout the foregoing description, for the purposes of explanation, numerous specific details were set forth in order to provide a thorough understanding of the present system and method. It will be apparent, however, to one skilled in the art that the system and method may be practiced without some of these specific details. Accordingly, the scope and spirit of the present invention should be judged in terms of the claims which follow.

[00393] Moreover, throughout the foregoing description, numerous publications were cited to provide a more thorough understanding of the present invention. All of these cited references are incorporated into the present application by reference.

APPENDIX

U.S. Application No. 11/256,487 filed on 21 October 2005
U.S. Issued Patent 7711030 issued on 04 May 2010
"System and Method for Spatial-Multiplexed Tropospheric Scatter Communications"
Attorney Docket No. 6181P514X (corrected from 6181P014X)

U.S. Application No. 12/630,627 filed on 03 December 2009
"System and Method for Distributing Antenna Wireless Communications"
Attorney Docket No. 6181P515X

06181.P014X *Patent*

UNITED STATES PATENT APPLICATION

for

SYSTEM AND METHOD FOR SPATIAL-MULTIPLEXED TROPOSPHERIC SCATTER COMMUNICATIONS

INVENTOR:

Steve Perlman

Prepared by:

BLAKELY, SOKOLOFF, TAYLOR & ZAFMAN, LLP
12400 WILSHIRE BOULEVARD
SEVENTH FLOOR
LOS ANGELES, CALIFORNIA 90025
(408) 720-8598

Attorney's Docket No. 06181.P014X

SYSTEM AND METHOD FOR SPATIAL-MULTIPLEXED TROPOSPHERIC SCATTER COMMUNICATIONS

BACKGROUND OF THE INVENTION

Field of the Invention

[0001] This application is a continuation-in-part of co-pending U.S. Patent Application No. 10/902,978, entitled, "System And Method For Distributed Input-Distributed Output Wireless Communications" filed on July 30, 2004.

[0002] This invention relates generally to the field of communication systems. More particularly, the invention relates to a system and method for distributed input-distributed output wireless communications using space-time coding techniques.

Description of the Related Art

Space-Time Coding of Communication Signals

[0003] A relatively new development in wireless technology is known as spatial multiplexing and space-time coding. One particular type of space-time coding is called MIMO for "Multiple Input Multiple Output" because several antennas are used on each end. By using multiple antennas to send and receive, multiple independent radio waves may be transmitted at the same time within the same frequency range. The following articles provide an overview of MIMO:

IEEE JOURNAL ON SELECTED AREAS IN COMMUNICATIONS, VOL. 21, NO. 3, APRIL 2003 : "From Theory to Practice: An Overview of MIMO Space–Time Coded Wireless Systems", by David Gesbert, Member, IEEE,

Mansoor Shafi, Fellow, IEEE, Da-shan Shiu, Member, IEEE, Peter J. Smith, Member, IEEE, and Ayman Naguib, Senior Member, IEEE.

IEEE TRANSACTIONS ON COMMUNICATIONS, VOL. 50, NO. 12, DECEMBER 2002: "Outdoor MIMO Wireless Channels: Models and Performance Prediction", David Gesbert, Member, IEEE, Helmut Bölcskei, Member, IEEE, Dhananjay A. Gore, and Arogyaswami J. Paulraj, Fellow, IEEE.

[0004] Fundamentally, MIMO technology is based on the use of spatially distributed antennas for creating parallel spatial data streams within a common frequency band. The radio waves are transmitted in such a way that the individual signals can be separated at the receiver and demodulated, even though they are transmitted within the same frequency band, which can result in multiple statistically independent (i.e. effectively separate) communications channels. Thus, in contrast to standard wireless communication systems which attempt to inhibit multi-path signals (i.e., multiple signals at the same frequency delayed in time, and modified in amplitude and phase), MIMO can rely on uncorrelated or weakly-correlated multi-path signals to achieve a higher throughput and improved signal-to-noise ratio within a given frequency band. By way of example, using MIMO technology within an 802.11g system, Airgo Networks was recently able to achieve 108 Mbps in the same spectrum where a conventional 802.11g system can achieve only 54 Mbps (this is described on Airgo's website, currently at http://www.airgonetworks.com).

[0005] MIMO systems typically face a practical limitation of fewer than 10 antennas per device (and therefore less than 10X throughput improvement in the network) for several reasons:

1. Physical limitations: MIMO antennas on a given device must have sufficient separation between them so that each receives a statistically independent signal. Although MIMO bandwidth improvements can be seen with antenna spacing of even one-sixth wavelength (λ/6), the efficiency rapidly deteriorates as the antennas get closer, resulting in lower MIMO bandwidth multipliers. Also, as the antennas are crowded together, the antennas typically must be made smaller, which can impact bandwidth efficiency as well. Finally, with lower frequencies and longer wavelengths, the physical size of a single MIMO device can become unmanageable. An extreme example is in the HF band, where MIMO device antennas may have to be separated from each other by 10 meters or more.

2. Noise limitations. Each MIMO receiver/transmitter subsystem produces a certain level of noise. As more and more of these subsystems are placed in close proximity to each other, the noise floor increases. Meanwhile, as increasingly more distinct signals need to be distinguished from each other in a many-antenna MIMO system, an increasingly lower noise floor is required.

3. Cost and power limitations. Although there are MIMO applications where cost and power consumption are not at issue, in a typical wireless product, both cost and power consumption are critical constraints in developing a

successful product. A separate RF subsystem is required for each MIMO antenna, including separate Analog-to-Digital (A/D) and Digital-to-Analog (D/A) converters. Unlike many aspects of digital systems which scale with Moore's Law, such analog-intensive subsystems typically have certain physical structural size and power requirements, and scale in cost and power linearly. So, a many-antenna MIMO device would become prohibitively expensive and power consumptive compared to a single-antenna device.

[0006] As a result of the above, most MIMO systems contemplated today are on the order of 2-to-4 antennas, resulting in a 2-to-4X increase in bandwidth, and some increase in SNR due to the diversity benefits of a multi-antenna system. Up to 10 antenna MIMO systems have been contemplated (particularly at higher microwave frequencies due to shorter wavelengths and closer antenna spacing), but much beyond that is impractical except for very specialized and cost-insensitive applications.

Virtual Antenna Arrays

[0007] One particular application of MIMO-type technology is a virtual antenna array. Such a system is proposed in a research paper presented at European Cooperation in the field of Scientific and Technical Research, EURO-COST, Barcelona, Spain, Jan 15-17, 2003: Center for Telecommunications Research, King's College London, UK: "A step towards MIMO: Virtual Antenna Arrays", Mischa Dohler & Hamid Aghvami.

[0008] Virtual antenna arrays, as presented in this paper, are systems of cooperative wireless devices (such as cell phones), which communicate amongst each other (if and when they are near enough to each other) on a separate communications channel than their primary communications channel to the their base station so as to operate cooperatively (e.g. if they are GSM cellular phones in the UHF band, this might be a 5 GHz Industrial Scientific and Medical (ISM) wireless band). This allows single antenna devices, for example, to potentially achieve MIMO-like increases in bandwidth by relaying information among several devices in range of each other (in addition to being in range of the base station) to operate as if they are physically one device with multiple antennas.

[0009] In practice, however, such a system is extremely difficult to implement and of limited utility. For one thing, there are now a minimum of two distinct communications paths per device that must be maintained to achieve improved throughput, with the second relaying link often of uncertain availability. Also, the devices are more expensive, physically larger, and consume more power since they have at a minimum a second communications subsystem and greater computational needs. In addition, the system is reliant on very sophisticated real-time of coordination of all devices, potentially through a variety of communications links. Finally, as the simultaneous channel utilization (e.g. the simultaneous phone call transmissions utilizing MIMO techniques) grows, the computational burden for each device grows (potentially exponentially as channel utilization increases linearly), which may very well be impractical for portable devices with tight power and size constraints.

SUMMARY OF THE INVENTION

[0010] A method is described comprising: transmitting a training signal from each antenna of a base station to each of a plurality of client devices utilizing tropospheric scatter, each of the client devices analyzing each training signal to generate channel characterization data, and transmitting the channel characterization data back to the base station utilizing tropospheric scatter; storing the channel characterization data for each of the plurality of client devices; receiving data to be transmitted to each of the client devices; and precoding the data using the channel characterization data associated with each respective client device to generate precoded data signals for each antenna of the base station; and transmitting the precoded data signals through each antenna of the base station to each respective client device.

BRIEF DESCRIPTION OF THE DRAWINGS

[0011] A better understanding of the present invention can be obtained from the following detailed description in conjunction with the drawings, in which:

[0012] FIG. 1 illustrates a prior art MIMO system.

[0013] FIG. 2 illustrates an N-antenna Base Station communicating with a plurality of Single-antenna Client Devices.

[0014] FIG. 3 illustrates a three Antenna Base Station communicating with three Single-Antenna Client Devices

[0015] FIG. 4 illustrates training signal techniques employed in one embodiment of the invention.

[0016] FIG. 5 illustrates channel characterization data transmitted from a client device to a base station according to one embodiment of the invention.

[0017] FIG. 6 illustrates a Multiple-Input Distributed-Output ("MIDO") downstream transmission according to one embodiment of the invention.

[0018] FIG. 7 illustrates a Multiple-Input Multiple Output ("MIMO") upstream transmission according to one embodiment of the invention.

[0019] FIG. 8 illustrates a base station cycling through different client groups to allocate bandwidth according to one embodiment of the invention.

[0020] FIG. 9 illustrates a grouping of clients based on proximity according to one embodiment of the invention.

[0021] FIG. 10 illustrates an embodiment of the invention employed within an NVIS system.

[0022] FIG. 11 illustrates an embodiment of the invention employing the use of tropospheric scatter.

[0023] FIG. 12 illustrates a prior art tropospheric scatter transmission system.

[0024] FIG. 13 illustrates an embodiment of the invention employing the use of a tropospheric scatter transmission system over a coverage area.

[0025] FIG. 14 illustrates a Direct Broadcast Satellite dish and RF signal paths in an embodiment of the invention.

[0026] FIG. 15 illustrates an embodiment of the invention employing the use of conventional MIMO with tropospheric scatter.

[0027] Figure 16 illustrates an overhead view of a coverage area surrounded by 12 clusters of 3 antennas.

[0028] Figures 17a-c illustrates 3 client antennas in a coverage area from different elevation views.

DETAILED DESCRIPTION OF PREFERRED EMBODIMENTS

[0029] In the following description, for the purposes of explanation, numerous specific details are set forth in order to provide a thorough understanding of the present invention. It will be apparent, however, to one skilled in the art that the present invention may be practiced without some of these specific details. In other instances, well-known structures and devices are shown in block diagram form to avoid obscuring the underlying principles of the invention.

[0030] **Figure 1** shows a prior art MIMO system with transmit antennas 104 and receive antennas 105. Such a system can achieve up to 3X the throughput that would normally be achievable in the available channel. There are a number of different approaches in which to implement the details of such a MIMO system which are described in published literature on the subject, and the following explanation describes one such approach.

[0031] Before data is transmitted in the MIMO system of **Figure 1**, the channel is "characterized." This is accomplished by initially transmitting a "training signal" from each of the transmit antennas 104 to each of the receivers 105. The training signal is generated by the coding and modulation subsystem 102, converted to analog by a D/A converter (not shown), and then converted from baseband to RF by each transmitter 103, in succession. Each receive antenna 105 coupled to its RF Receiver 106 receives each training signal and converts it to baseband. The baseband signal is converted to digital by a D/A converter (not shown), and the signal processing subsystem 107 characterizes the training

signal. Each signal's characterization may include many factors including, for example, phase and amplitude relative to a reference internal to the receiver, an absolute reference, a relative reference, characteristic noise, or other factors. Each signal's characterization is typically defined as a vector that characterizes phase and amplitude changes of several aspects of the signal when it is transmitted across the channel. For example, in a quadrature amplitude modulation ("QAM")-modulated signal the characterization might be a vector of the phase and amplitude offsets of several multipath images of the signal. As another example, in an orthogonal frequency division multiplexing ("OFDM")-modulated signal, it might be a vector of the phase and amplitude offsets of several or all of the individual sub-signals in the OFDM spectrum.

[0032] The signal processing subsystem 107 stores the channel characterization received by each receiving antenna 105 and corresponding receiver 106. After all three transmit antennas 104 have completed their training signal transmissions, then the signal processing subsystem 107 will have stored three channel characterizations for each of three receiving antennas 105, resulting in a 3x3 matrix 108, designated as the channel characterization matrix, "H." Each individual matrix element $H_{i,j}$ is the channel characterization (which is typically a vector, as described above) of the training signal transmission of transmit antenna 104 i as received by the receive antenna 105 j.

[0033] At this point, the signal processing subsystem 107 inverts the matrix H 108, to produce H^{-1}, and awaits transmission of actual data from transmit

antennas 104. Note that various prior art MIMO techniques described in available literature, can be utilized to ensure that the H matrix 108 can be inverted.

[0034] In operation, a payload of data to be transmitted is presented to the data Input subsystem 100. It is then divided up into three parts by splitter 101 prior to being presented to coding and modulation subsystem 102. For example, if the payload is the ASCII bits for "abcdef," it might be divided up into three sub-payloads of ASCII bits for "ad," "be," and "cf" by Splitter 101. Then, each of these sub-payloads is presented individually to the coding and modulation subsystem 102.

[0035] Each of the sub-payloads is individually coded by using a coding system suitable for both statistical independence of each signal and error correction capability. These include, but are not limited to Reed-Solomon coding, Viterbi coding, and Turbo Codes. Finally, each of the three coded sub-payloads is modulated using an appropriate modulation scheme for the channel. Example modulation schemes are differential phase shift key ("DPSK") modulation, 64-QAM modulation and OFDM. It should be noted here that the diversity gains provided by MIMO allow for higher-order modulation constellations that would otherwise be feasible in a SISO (Single Input-Single Output) system utilizing the same channel. Each coded and modulated signal is then transmitted through its own antenna 104 following D/A conversion by a D/A conversion unit (not shown) and RF generation by each transmitter 103.

[0036] Assuming that adequate spatial diversity exists amongst the transmit and receive antennas, each of the receiving antennas 105 will receive a different combination of the three transmitted signals from antennas 104. Each signal is received and converted down to baseband by each RF receiver 106, and digitized by an A/D converter (not shown). If y_n is the signal received by the nth receive antenna 105, and x_n is the signal transmitted by nth transmit antenna 104, and N is noise, this can be described by the following three equations.

$$y_1 = x_1 H_{11} + x_2 H_{21} + x_3 H_{31} + N$$

$$y_2 = x_1 H_{12} + x_2 H_{22} + x_3 H_{32} + N$$

$$y_3 = x_1 H_{13} + x_2 H_{23} + x_3 H_{33} + N$$

[0037] Given that this is a system of three equations with three unknowns, it is a matter of linear algebra for the signal processing subsystem 107 to derive x_1, x_2, and x_3 (assuming that N is at a low enough level to permit decoding of the signals):

$$x_1 = y_1 H^{-1}{}_{11} + y_2 H^{-1}{}_{12} + y_3 H^{-1}{}_{13}$$

$$x_2 = y_1 H^{-1}{}_{21} + y_2 H^{-1}{}_{22} + y_3 H^{-1}{}_{23}$$

$$x_3 = y_1 H^{-1}{}_{31} + y_2 H^{-1}{}_{32} + y_3 H^{-1}{}_{33}$$

[0038] Once the three transmitted signals x_n are thus derived, they are then demodulated, decoded, and error-corrected by signal processing subsystem 107 to recover the three bit streams that were originally separated out by splitter 101. These bit streams are combined in combiner unit 108, and output as a single

data stream from the data output 109. Assuming the robustness of the system is able to overcome the noise impairments, the data output 109 will produce the same bit stream that was introduced to the data Input 100.

[0039] Although the prior art system just described is generally practical up to four antennas, and perhaps up to as many as 10, for the reasons described in the Background section of this disclosure, it becomes impractical with large numbers of antennas (e.g. 25, 100, or 1000).

[0040] Typically, such a prior art system is two-way, and the return path is implemented exactly the same way, but in reverse, with each side of the communications channels having both transmit and receive subsystems.

[0041] **Figure 2** illustrates one embodiment of the invention in which a Base Station 200 is configured with a Wide Area Network interface (e.g. to the Internet through a T1 or other high speed connection) 201 and is provisioned with a number (n) of antennas 202. There are a number of Client Devices 203-207, each with a single antenna, which are served wirelessly from the Base Station 200. Although for the purposes of this example it is easiest to think about such a Base Station as being located in an office environment where it is serving Client Devices 203-207 that are wireless-network equipped personal computers, this architecture will apply to a large number of applications, both indoor and outdoor, where a Base Station is serving wireless clients. For example, the Base Station could be based at a cellular phone tower, or on a television broadcast tower. In one embodiment, the Base Station 200 is positioned on the ground and is

configured to transmit upward at HF frequencies (e.g., frequencies up to 24MHz) to bounce signals off the ionosphere as described in co-pending application entitled SYSTEM AND METHOD FOR ENHANCING NEAR VERTICAL INCIDENCE SKYWAVE ("NVIS") COMMUNICATION USING SPACE-TIME CODING, Serial No. 10/817,731, Filed April 2, 2004 which is assigned to the assignee of the present application and which is incorporated herein by reference. In another embodiment, the Base Station 200 is positioned on the ground and is configured to transmit at angle into the troposphere using tropospheric scatter ("troposcatter") techniques.

[0042] Certain details associated with the Base Station 200 and Client Devices 203-207 set forth above are for the purpose of illustration only and are not required for complying with the underlying principles of the invention. For example, the Base Station may be connected to a variety of different types of wide area networks via WAN interface 201 including application-specific wide area networks such as those used for digital video distribution. Similarly, the Client Devices may be any variety of wireless data processing and/or communication devices including, but not limited to cellular phones, personal digital assistants ("PDAs"), receivers, and wireless cameras.

[0043] In one embodiment, the Base Station's n Antennas 202 are separated spatially such that each is transmitting and receiving signals which are not spatially correlated, just as if the Base Station was a prior art MIMO transceiver. As described in the Background, experiments have been done where antennas

placed within λ/6 (i.e. 1/6 wavelength) apart successfully achieve an increase in bandwidth from MIMO, but generally speaking, the further apart these Base Station antennas are placed, the better the system performance, and λ/2 is a desirable minimum. Of course, the underlying principles of the invention are not limited to any particular separation between antennas.

[0044] Note that a single Base Station 200 may very well have its antennas located very far apart. For example, in the HF spectrum, the antennas may be 10 meters apart or more (e.g., in an NVIS implementation mentioned above). If 100 such antennas are used, the Base Station's antenna array could well occupy several square kilometers.

[0045] In addition to spatial diversity techniques, one embodiment of the invention polarizes the signal in order to increase the effective bandwidth of the system. Increasing channel bandwidth through polarization is a well known technique which has been employed by satellite television providers for years. Using polarization, it is possible to have multiple (e.g., three) Base Station antennas very close to each other, and still be not spatially correlated. Although conventional RF systems usually will only benefit from the diversity of two dimensions (e.g. x and y) of polarization, the architecture descried herein may further benefit from the diversity of three dimensions of polarization (x, y and z).

[0046] **Figure 3** provides additional detail of one embodiment of the Base Station 200 and Client Devices 203-207 shown in **Figure 2**. For the purposes of simplicity, the Base Station 300 is shown with only three antennas 305 and only

three Client Devices 306-308. It will be noted, however, that the embodiments of the invention described herein may be implemented with a virtually unlimited number of antennas 305 (i.e., limited only by available space and noise) and Client Devices 306-308.

[0047] **Figure 3** is similar to the prior art MIMO architecture shown in **Figure 1** in that both have three antennas on each sides of a communication channel. A notable difference is that in the prior art MIMO system the three antennas 105 on the right side of **Figure 1** are all a fixed distance from one another (e.g., integrated on a single device), and the received signals from each of the antennas 105 are processed together in the Signal Processing subsystem 107. By contrast, in **Figure 3**, the three antennas 309 on the right side of the diagram are each coupled to a different Client Device 306-308, each of which may be distributed anywhere within range of the Base Station 305. As such, the signal that each Client Device receives is processed independently from the other two received signals in its Coding, Modulation, Signal Processing subsystem 311. Thus, in contrast to a Multiple-Input (i.e. antennas 105) Multiple-Output (i.e. antennas 104) "MIMO" system, **Figure 3** illustrates a Multiple Input (i.e. antennas 309) Distributed Output (i.e. antennas 305) system, referred to hereinafter as a "MIDO" system.

[0048] The MIDO architecture shown in **Figure 3** achieves a similar bandwidth increase as MIMO over a SISO system for a given number of transmitting antennas. However, one difference between MIMO and the particular MIDO

embodiment illustrated in **Figure 3** is that, to achieve the bandwidth increase provided by multiple base station antennas, each MIDO Client Device 306-308 requires only a *single* receiving antenna, whereas with MIMO, each Client Device requires *as least as many* receiving antennas as the bandwidth multiple that is hoped to be achieved. Given that there is usually a practical limit to how many antennas can be placed on a Client Device (as explained in the Background), this typically limits MIMO systems to between four to ten antennas (and 4X to 10X bandwidth multiple). Since the Base Station 300 is typically serving many Client Devices from a fixed and powered location, is it practical to expand it to far more antennas than ten, and to separate the antennas by a suitable distance to achieve spatial diversity. As illustrated, each antenna is equipped with a transceiver 304 and a portion of the processing power of a Coding, Modulation, and Signal Processing section 303. Significantly, in this embodiment, no matter how much Base Station 300 is expanded, each Client Device 306-308 only will require one antenna 309, so the cost for an individual user Client Device 306-308 will be low, and the cost of Base Station 300 can be shared among a large base of users.

[0049] An example of how a MIDO transmission from the Base Station 300 to the Client Devices 306-308 can be accomplished is illustrated in **Figures 4** through **6**.

[0050] In one embodiment of the invention, before a MIDO transmission begins, the channel is characterized. As with a MIMO system, a training signal is

transmitted (in the embodiment herein described), one-by-one, by each of the antennas 405. **Figure 4** illustrates only the first training signal transmission, but with three antennas 405 there are three separate transmissions in total. Each training signal is generated by the Coding, Modulation, and Signal Processing subsystem 403, converted to analog through a D/A converter, and transmitted as RF through each RF Transceiver 404. Various different coding, modulation and signal processing techniques may be employed including, but not limited to, those described above (e.g., Reed Solomon, Viterbi coding; QAM, DPSK, QPSK modulation, . . . etc).

[0051] Each Client Device 406-408 receives a training signal through its antenna 409 and converts the training signal to baseband by Transceiver 410. An A/D converter (not shown) converts the signal to digital where is it processed by each Coding, Modulation, and Signal Processing subsystem 411. Signal characterization logic 320 then characterizes the resulting signal (e.g., identifying phase and amplitude distortions as described above) and stores the characterization in memory. This characterization process is similar to that of prior art MIMO systems, with a notable difference being that the each client device only computes the characterization vector for its one antenna, rather than for n antennas. For example, the Coding Modulation and Signal Processing subsystem 420 of client device 406 is initialized with a known pattern of the training signal (either at the time of manufacturing, by receiving it in a transmitted message, or through another initialization process). When antenna 405 transmits the training signal with this known pattern, Coding Modulation and Signal

Processing subsystem 420 uses correlation methods to find the strongest received pattern of the training signal, it stores the phase and amplitude offset, then it subtracts this pattern from the received signal. Next, it finds then second strongest received pattern that correlates to the training signal, it stores the phase and amplitude offset, then it subtracts this second strongest pattern from the received signal. This process continues until either some fixed number of phase and amplitude offsets are stored (e.g. eight), or a detectable training signal pattern drops below a given noise floor. This vector of phase/amplitude offsets becomes element H_{11} of the vector 413. Simultaneously, Coding Modulation and Signal Processing subsystems for Client Devices 407 and 408 implement the same processing to produce their vector elements H_{21} and H_{31}.

[0052] The memory in which the characterization is stored may be a non-volatile memory such as a Flash memory or a hard drive and/or a volatile memory such as a random access memory (e.g., SDRAM, RDAM). Moreover, different Client Devices may concurrently employ different types of memories to store the characterization information (e.g., PDA's may use Flash memory whereas notebook computers may use a hard drive). The underlying principles of the invention are not limited to any particular type of storage mechanism on the various Client Devices or the Base Station.

[0053] As mentioned above, depending on the scheme employed, since each Client Device 406-408 has only one antenna, each only stores a 1x3 column 413-415 of the H matrix. **Figure 4** illustrates the stage after the first training

signal transmission where the first row of 1x3 columns 413-415 has been stored with channel characterization information for the first of the three Base Station antennas 405. The remaining two columns are stored following the channel characterization of the next two training signal transmissions from the remaining two base station antennas. Note that for the sake of illustration the three training signals are transmitted at separate times. If the three training signal patterns are chosen such as not to be correlated to one another, they may be transmitted simultaneously, thereby reducing training time.

[0054] As indicated in **Figure 5**, after all three pilot transmissions are complete, each Client Device 506-508 transmits back to the Base Station 500 the 1x3 column 513-515 of matrix H that it has stored. To the sake of simplicity, only one Client Device 506 is illustrated transmitting its characterization information in **Figure 5**. An appropriate modulation scheme (e.g. DPSK, 64QAM, OFDM) for the channel combined with adequate error correction coding (e.g. Reed Solomon, Viterbi, and/or Turbo codes) may be employed to make sure that the Base Station 500 receives the data in the columns 513-515 accurately.

[0055] Although all three antennas 505 are shown receiving the signal in **Figure 5**, it is sufficient for a single antenna and transceiver of the Base Station 500 to receive each 1x3 column 513-515 transmission. However, utilizing many or all of antennas 505 and Transceivers 504 to receive each transmission (i.e., utilizing prior art Single-Input Multiple-Output ("SIMO") processing techniques in the Coding, Modulation and Signal Processing subsystem 503) may yield a better

signal-to-noise ratio ("SNR") than utilizing a single antenna 505 and Transceiver 504 under certain conditions.

[0056] As the Coding, Modulation and Signal Processing subsystem 503 of Base Station 500 receives the 1x3 column 513-515, from each Client Device 507-508, it stores it in a 3x3 H matrix 516. As with the Client Devices, the Base Station may employ various different storage technologies including, but not limited to non-volatile mass storage memories (e.g., hard drives) and/or volatile memories (e.g., SDRAM) to store the matrix 516. **Figure 5** illustrates a stage at which the Base Station 500 has received and stored the 1x3 column 513 from Client Device 509. The 1x3 columns 514 and 515 may be transmitted and stored in H matrix 516 as they are received from the remaining Client Devices, until the entire H matrix 516 is stored.

[0057] One embodiment of a MIDO transmission from a Base Station 600 to Client Devices 606-608 will now be described with reference to **Figure 6**. Because each Client Device 606-608 is an independent device, typically each device is receiving a different data transmission. As such, one embodiment of a Base Station 600 includes a Router 602 communicatively positioned between the WAN Interface 601 and the Coding, Modulation and Signal Processing subsystem 603 that sources multiple data streams (formatted into bit streams) from the WAN interface 601 and routes them as separate bit streams u_1- u_3 intended for each Client Device 606-608, respectively. Various well known routing techniques may be employed by the router 602 for this purpose.

[0058] The three bit streams, u_1- u_3, shown in **Figure 6** are then routed into the Coding, Modulation and Signal Processing subsystem 603 and coded into statistically distinct, error correcting streams (e.g. using Reed Solomon, Viterbi, or Turbo Codes) and modulated using an appropriate modulation scheme for the channel (such as DPSK, 64QAM or OFDM). In addition, the embodiment illustrated in **Figure 6** includes signal precoding logic 630 for uniquely coding the signals transmitted from each of the antennas 605 based on the signal characterization matrix 616. More specifically, rather than routing each of the three coded and modulated bit streams to a separate antenna (as is done in **Figure 1**), in one embodiment, the precoding logic 630 multiplies the three bit streams u_1- u_3 in **Figure 6** by the inverse of the H matrix 616, producing three new bit streams, u'_1- u'_3. The three precoded bit streams are then converted to analog by D/A converters (not shown) and transmitted as RF by Transceivers 604 and antennas 605.

[0059] Before explaining how the bit streams are received by the Client Devices 606-608, the operations performed by the precoding module 630 will be described. Similar to the MIMO example from **Figure 1** above, the coded and modulated signal for each of the three source bit streams will be designated with u_n. In the embodiment illustrated in **Figure 6**, each u_i contains the data from one of the three bit streams routed by the Router 602, and each such bit stream is intended for one of the three Client Devices 606-608.

[0060] However, unlike the MIMO example of **Figure 1**, where each x_i is *transmitted* by each antenna 104, in the embodiment of the invention illustrated in **Figure 6**, each u_i is *received* at each Client Device antenna 609 (plus whatever noise N there is in the channel). To achieve this result, the output of each of the three antennas 605 (each of which we will designate as v_i) is a function of u_i and the H matrix that characterizes the channel for each Client Device. In one embodiment, each v_i is calculated by the precoding logic 630 within the Coding, Modulation and Signal Processing subsystem 603 by implementing the following formulas:

$$v_1 = u_1H^{-1}{}_{11} + u_2H^{-1}{}_{12} + u_3H^{-1}{}_{13} v_2 = u_1H^{-1}{}_{21} + u_2H^{-1}{}_{22} + u_3H^{-1}{}_{23}$$

$$v_3 = u_1H^{-1}{}_{31} + u_2H^{-1}{}_{32} + u_3H^{-1}{}_{33}$$

[0061] Thus, unlike MIMO, where each x_i is calculated at the receiver after the signals have been transformed by the channel, the embodiments of the invention described herein solve for each v_i at the transmitter *before* the signals have been transformed by the channel. Each antenna 609 receives u_i *already separated* from the other u_{n-1} bit streams intended for the other antennas 609. Each Transceiver 610 converts each received signal to baseband, where it is digitized by an A/D converter (now shown), and each Coding, Modulation and Signal Processing subsystem 611, demodulates and decodes the x_i bit stream intended for it, and sends its bit stream to a Data Interface 612 to be used by the Client Device (e.g., by an application on the client device).

[0062] The embodiments of the invention described herein may be implemented using a variety of different coding and modulation schemes. For example, in an OFDM implementation, where the frequency spectrum is separated into a plurality of sub-bands, the techniques described herein may be employed to characterize each individual sub-band. As mentioned above, however, the underlying principles of the invention are not limited to any particular modulation scheme.

[0063] If the Client Devices 606-608 are portable data processing devices such as PDAs, notebook computers, and/or wireless telephones the channel characterization may change frequently as the Client Devices may move from one location to another. As such, in one embodiment of the invention, the channel characterization matrix 616 at the Base Station is continually updated. In one embodiment, the Base Station 600 periodically (e.g., every 250 milliseconds) sends out a new training signal to each Client Device, and each Client Device continually transmits its channel characterization vector back to the Base Station 600 to ensure that the channel characterization remains accurate (e.g. if the environment changes so as to affect the channel or if a Client Device moves). In one embodiment, the training signal is interleaved within the actual data signal sent to each client device. Typically, the training signals are much lower bandwidth than the data signals, so this would have little impact on the overall throughput of the system. Accordingly, in this embodiment, the channel characterization matrix 616 may be updated continuously as the Base Station actively communicates with each Client Device, thereby maintaining an accurate

channel characterization as the Client Devices move from one location to the next or if the environment changes so as to affect the channel.

[0064] One embodiment of the invention illustrated in **Figure 7** employs MIMO techniques to improve the upstream communication channel (i.e., the channel from the Client Devices 706-708 to the Base Station 700). In this embodiment, the channel from each of the Client Devices is continually analyzed and characterized by upstream channel characterization logic 741 within the Base Station. More specifically, each of the Client Devices 706-708 transmits a training signal to the Base Station 700 which the channel characterization logic 741 analyzes (e.g., as in a typical MIMO system) to generate an *N* x *M* channel characterization matrix 741, where *N* is the number of Client Devices and *M* is the number of antennas employed by the Base Station. The embodiment illustrated in **Figure 7** employs three antennas 705 at the Base Station and three Client Devices 706-608, resulting in a 3x3 channel characterization matrix 741 stored at the Base Station 700. The MIMO upstream transmission illustrated in **Figure 7** may be used by the Client Devices both for transmitting data back to the Base Station 700, and for transmitting channel characterization vectors back to the Base Station 700 as illustrated in **Figure 5**. But unlike the embodiment illustrated in **Figure 5** in which each Client Device's channel characterization vector is transmitted at a separate time, the method shown in **Figure 7** allows for the simultaneous transmission of channel characterization vectors from multiple Client Devices back to the Base Station 700, thereby dramatically reducing the channel characterization vectors' impact on return channel throughput.

[0065] As mentioned above, each signal's characterization may include many factors including, for example, phase and amplitude relative to a reference internal to the receiver, an absolute reference, a relative reference, characteristic noise, or other factors. For example, in a quadrature amplitude modulation ("QAM")-modulated signal the characterization might be a vector of the phase and amplitude offsets of several multipath images of the signal. As another example, in an orthogonal frequency division multiplexing ("OFDM")-modulated signal, it might be a vector of the phase and amplitude offsets of several or all of the individual sub-signals in the OFDM spectrum. The training signal may be generated by each Client Device's coding and modulation subsystem 711, converted to analog by a D/A converter (not shown), and then converted from baseband to RF by each Client Device's transmitter 709. In one embodiment, in order to ensure that the training signals are synchronized, Client Devices only transmit training signals when requested by the Base Station (e.g., in a round robin manner). In addition, training signals may be interleaved within or transmitted concurrently with the actual data signal sent from each client device. Thus, even if the Client Devices 706-708 are mobile, the training signals may be continuously transmitted and analyzed by the upstream channel characterization logic 741, thereby ensuring that the channel characterization matrix 741 remains up-to-date.

[0066] The total channel bandwidth supported by the foregoing embodiments of the invention may be defined as *min (N, M)* where *N* is the number of Client Devices and *M* is the number of Base Station antennas. That is, the capacity is

limited by the number of antennas on either the Base Station side or the Client side. As such, one embodiment of the invention employs synchronization techniques to ensure that no more than *min (N, M)* antennas are transmitting/ receiving at a given time.

[0067] In a typical scenario, the number of antennas 705 on the Base Station 700 will be less than the number of Client Devices 706-708. An exemplary scenario is illustrated in **Figure 8** which shows five Client Devices 804-808 communicating with a base station having three antennas 802. In this embodiment, after determining the total number of Client Devices 804-808, and collecting the necessary channel characterization information (e.g., as described above), the Base Station 800 chooses a first group of three clients 810 with which to communicate (three clients in the example because *min (N, M)* = 3). After communicating with the first group of clients 810 for a designated period of time, the Base Station then selects another group of three clients 811 with which to communicate. To distribute the communication channel evenly, the Base Station 800 selects the two Client Devices 807, 808 which were not included in the first group. In addition, because an extra antenna is available, the Base Station 800 selects an additional client device 806 included in the first group. In one embodiment, the Base Station 800 cycles between groups of clients in this manner such that each client is effectively allocated the same amount of bandwidth over time. For example, to allocate bandwidth evenly, the Base Station may subsequently select any combination of three Client Devices which

excludes Client Device 806 (i.e., because Client Device 806 was engaged in communication with the Base Station for the first two cycles).

[0068] In one embodiment, in addition to standard data communications, the Base Station may employ the foregoing techniques to transmit training signals to each of the Client Devices and receive training signals and signal characterization data from each of the Client Devices.

[0069] In one embodiment, certain Client Devices or groups of client devices may be allocated different levels of bandwidth. For example, Client Devices may be prioritized such that relatively higher priority Client Devices may be guaranteed more communication cycles (i.e., more bandwidth) than relatively lower priority client devices. The "priority" of a Client Device may be selected based on a number of variables including, for example, the designated level of a user's subscription to the wireless service (e.g., user's may be willing to pay more for additional bandwidth) and/or the type of data being communicated to/from the Client Device (e.g., real-time communication such as telephony audio and video may take priority over non-real time communication such as email).

[0070] In one embodiment of the Base Station dynamically allocates bandwidth based on the Current Load required by each Client Device. For example, if Client Device 804 is streaming live video and the other devices 805-808 are performing non-real time functions such as email, then the Base Station 800 may allocate relatively more bandwidth to this client 804. It should be noted, however,

that the underlying principles of the invention are not limited to any particular bandwidth allocation technique.

[0071] As illustrated in **Figure 9**, two Client Devices 907, 908 may be so close in proximity, that the channel characterization for the clients is effectively the same. As a result, the Base Station will receive and store effectively equivalent channel characterization vectors for the two Client Devices 907, 908 and therefore will not be able to create unique, spatially distributed signals for each Client Device. Accordingly, in one embodiment, the Base Station will ensure that any two or more Client Devices which are in close proximity to one another are allocated to different groups. In **Figure 9**, for example, the Base Station 900 first communicates with a first group 910 of Client Devices 904, 905 and 908; and then with a second group 911 of Client Devices 905, 906, 907, ensuring that Client Devices 907 and 908 are in different groups.

[0072] Alternatively, in one embodiment, the Base Station 900 communicates with both Client Devices 907 and 908 concurrently, but multiplexes the communication channel using known channel multiplexing techniques. For example, the Base Station may employ time division multiplexing ("TDM"), frequency division multiplexing ("FDM") or code division multiple access ("CDMA") techniques to divide the single, spatially-correlated signal between Client Devices 907 and 908.

[0073] Although each Client Device described above is equipped with a single antenna, the underlying principles of the invention may be employed using Client

Devices with multiple antennas to increase throughput. For example, when used on the wireless systems described above, a client with 2 antennas will realize a 2x increase in throughput, a client with 3 antennas will realize a 3x increase in throughput, and so on (i.e., assuming that the spatial and angular separation between the antennas is sufficient). The Base Station may apply the same general rules when cycling through Client Devices with multiple antennas. For example, it may treat each antenna as a separate client and allocate bandwidth to that "client" as it would any other client (e.g., ensuring that each client is provided with an adequate or equivalent period of communication).

[0074] As mentioned above, one embodiment of the invention employs the MIDO and/or MIMO signal transmission techniques described above to increase the signal-to-noise ratio and transmission bandwidth within a Near Vertical Incidence Skywave ("NVIS") system. Referring to **Figure 10**, in one embodiment of the invention, a first NVIS station 1001 equipped with a matrix of *N* antennas 1002 is configured to communicate with *M* client devices 1004. The NVIS antennas 1002 and antennas of the various client devices 1004 transmit signals upward to within about 15 degrees of vertical in order to achieve the desired NVIS and minimize ground wave interference effects. In one embodiment, the antennas 1002 and client devices 1004, support multiple independent data streams 1006 using the various MIDO and MIMO techniques described above at a designated frequency within the NVIS spectrum (e.g., at a carrier frequency at or below 23 MHz, but typically below 10 MHz), thereby significantly increasing

the bandwidth at the designated frequency (i.e., by a factor proportional to the number of statistically independent data streams).

[0075] The NVIS antennas serving a given station may be physically very far apart from each other. Given the long wavelengths below 10 MHz and the long distance traveled for the signals (as much as 300 miles round trip), physical separation of the antennas by 100s of yards, and even miles, can provide advantages in diversity. In such situations, the individual antenna signals may be brought back to a centralized location to be processed using conventional wired or wireless communications systems. Alternatively, each antenna can have a local facility to process its signals, then use conventional wired or wireless communications systems to communicate the data back to a centralized location. In one embodiment of the invention, NVIS Station 1001 has a broadband link 1015 to the Internet 1010 (or other wide area network), thereby providing the client devices 1003 with remote, high speed, wireless network access.

[0076] As mentioned above, one embodiment of the invention employs the MIDO and/or MIMO signal transmission techniques described above (collective referred to heretofore as "DIDO") to increase the signal-to-noise ratio and transmission bandwidth within a tropospheric scatter ("troposcatter") system. Referring to **Figure 11**, in one embodiment of the invention, a first troposcatter station 1101 equipped with a matrix of *N* antennas 1102 is configured to communicate with *M* client devices 1104. (The upward angle of transmission is exaggerated for illustration purposes in **Figure 11**. A more typical low angle for

troposcatter transmission is shown in prior art **Figure 12**.) The antennas of the various client devices 1104 transmit signals back through tropospheric scatter, and they are received by base station antennas 1102.

[0077] The troposcatter base station antennas 1102 are aimed at an upward angle so that part of the transmission scatters and reflects off the troposphere so as to hit the target area where the *M* client devices 1104 are located. Calculating specific antenna elevation angles and optimizing antennas for troposcatter is well understood to those skilled in the art, and several online calculators exist for making such calculations. As an example, one such calculator can be downloaded at http://home.planet.nl/~alphe078/propagat1.htm. This particular troposcatter calculator's input parameters include distance between the transmit and receive antennas, transmission frequency, antenna heights, output power, station noise characteristics, obstacle distance/heights, antenna gain, and bandwidth.

[0078] An exemplary prior art troposcatter radio terminal (i.e. transceiver and antenna) that is currently in use by the US Military is the AN/TRC-170V3 Tropospheric Microwave Radio Terminal. The system has a nominal transmission range of 100 miles. Such a system typically transmits less than 1 Mbps. Newer troposcatter modems such as the General Dynamics and Radyne Corporation TM-20 modem can achieve up to 20 Mbps. But, both systems only can achieve such data rates with a single data stream in a given channel,

[0079] In one embodiment, the antennas 1102 and client devices 1104, support multiple independent data streams 1106 using the various DIDO techniques described herein at a designated frequency within the troposcatter spectrum (e.g., at a carrier frequency from below 50 MHz to above 10 GHz). These DIDO techniques include, but are not limited to, the transmission of training signals, the characterization of the channel vectors, and the transmission back to the troposcatter base station 1101 of the channel vectors so as to form a channel matrix.

[0080] The troposcatter antennas served by a given troposcatter base station 1101 may be close (e.g. as close as $\lambda/6$) or physically very far apart (10s or 100s of miles) from each other and/or they may be clustered in groups. So, the term "troposcatter base station 1101" as used herein refers to a common channel matrix computation system, similar to **Figure 2**'s Base Station 200, but one in which the transmitting antennas 1102 may in fact be distributed very far from a given site. The specific configuration will depend on the desired coverage area, the need to avoid obstacles in the terrain, and if necessary, the need to achieve more diversity and/or a wider angle between transmit antennas. As previously described, a DIDO base station, by utilizing channel state information feedback from the client devices after sending training signals, will produce a combination of transmitted signals from its antennas 1102, such that the client devices will receive independent signals. And, when the client devices 1104 transmit back to the base stations antennas 1102, the base station will use the channel state information determined from client device training signals.

[0081] Because troposcatter largely preserves polarization, 2D and 3D polarization can be used with antennas 1102 and 1104 to achieve further diversity.

[0082] In one embodiment of the invention, troposcatter Station 1101 has a broadband link 1115 to the Internet 1110 (or other wide area network), thereby providing the client devices 1103 with remote, high speed, wireless network access.

[0083] The troposcatter base station antennas 1102 and the client device antennas 1104 will work best if they each have a line-of-sight (LOS) view of the troposphere to the common volume 1121. The common volume 1121 is an area of the troposphere where tropospheric scattering will cause some of the transmitted signal to reflect back to the ground. Typically, most of the transmitted signal will pass through the troposphere as indicated by 1120. Perfect LOS transmissions over long distances with very narrow angles between antennas may result in poor diversity. This can be mitigated by separating the base station antennas 1102 by large distances, but the scattering effect of the troposphere itself may also create diversity.

[0084] While a LOS path to the common volume 1121 can be planned for when the base station antennas 1102 are installed, it is more difficult to guarantee that a client device antenna 1104 has a LOS view of the common volume 1121. In particular, the common volume 1121 is often going to be at a low angle in the sky. If, for example, a consumer wishes to place a client device antenna 1104 in

a window of her house, or on the roof of her house, even though the antenna may have a view of some of the sky, it may be obstructed from having a view of the particular patch of the sky which contains the common volume 1121.

[0085] This issue can be mitigated by having multiple troposcatter base station antennas 1102 transmitting from various directions over a coverage area. One such configuration is illustrated in **Figure 13** from an overhead ("plan") view. Troposcatter base station 1301 serves the same function as troposcatter base station 1101, but its antennas are deliberately distributed far apart in antenna clusters 1341-1344. The antenna clusters 1341-1344 are aimed such that their transmissions reflect from the troposphere to a common ground coverage area 1360. This coverage area may be a town, a city, a rural area, or an uninhabited area under exploration. It may also be an area on a body of water. Antenna cluster 1341 transmits RF transmission 1330, which scatters in common volume 1321 and then reflects back to earth as RF reflection 1331 into coverage area 1360 where it then is received in coverage area 1360 by one or more client antennas 1361-1363. Simultaneously, antenna clusters 1342-1344 transmit RF that scatters in common volumes 1322-1324, respectively, and then the RF reflects back to earth in to coverage area 1360 where it is then received by one or more client antennas 1361-1363. And, one or more client antennas 1361-1363 transmit back through common volumes 1321-1324 to antenna clusters 1341-1344 as a return path.

[0086] Some or all client antennas 1361-1363 may not have a LOS view the sky to see all common volumes 1321-1324. But so long as each client antenna 1361-1363 can see at least one common volume 1321-1324, then it will be able to have communications with the troposcatter base station 1301. Clearly, the more antenna clusters 1341-1344 that are established around the coverage area 1360, the less chance that a client antenna 1361 will be unable to see at least one common volume 1321-1324.

[0087] The troposcatter base station 1101 communicates to the antenna clusters 1341-1344 through communication links 1351-1354. These communications links 1351-1354 may be physically implemented via various means, including optical fiber, leased communications lines, such as DS3 lines, or they may be implemented through wireless communications. In fact, communication links 1351-1354 may be implemented utilizing troposcatter communications.

[0088] Because of the long distances required for the communications links 1351-1354, in the presently preferred embodiment, each of the antenna clusters 1341-1344 will have its own local RF transceivers which are directed by the troposcatter base 1301 as to precisely what RF signals are to be generated in synchrony so that all antenna clusters 1341-1344 work in a coordinated fashion as a single DIDO system.

[0089] In an alternative embodiment, each antenna cluster 1341-1344 will have its own base station 1301 and will operate independently from the other antenna clusters 1341-1344. In this situation each antenna cluster may transmit at a

different frequency so as to avoid interfering with the others, or directional antennas maybe used for client antennas 1361-1363 may so as to reject transmission from all but a signal antenna cluster 1341-1344.

[0090] An alternative embodiment of the system illustrated in **Figure 13** is illustrated in **Figures 16** and **Figures 17a-c**. The communications links, then base station and the common volumes from **Figure 13** are not shown in **Figures 16** and **Figures 17a-c** for the sake of clarity, but such components still exist, and are implemented as previously described.

[0091] **Figure 16** shows an overhead (plan) view of a coverage area 1360 surrounded by 12 clusters 1611-1643 of 3 antennas 1651-1653 each, for a total of 36 antennas. All of these antennas are aimed such that when they scatter off of their respective common volumes, the reflected RF reaches the coverage area 1360. Coverage area 1360 has many client antennas, of which 3, 1361-1363 are illustrated. **Figure 16** also indicates the north/south/east/west orientation of the illustration.

[0092] **Figures 17a-c** shows the 3 client antennas 1361-1363 in the coverage area 1360 schematically as antennas 1701. **Figure 17a** shows the antennas 1701 in an elevation view from the south; **Figure 17b** shows the antennas 1701 in an elevation view from the west; and **Figure 17c** shows the antennas 1701 in an overhead (plan) view from above. Note the schematic illustration of the antennas 1701 shows them as triangles in the elevation views and as squares in the overhead view, but they are the same antennas. The antennas could be any

of many prior art antenna shapes. And, rather than being in a row, the 3 antennas may be located in many different positions relative to each other, including being miles apart. And finally, in one embodiment, far more than 3 antennas are deployed in a given coverage area.

[0093] **Figure 17a-c** shows how the RF beams from the various antennas in **Figure 16** arrive at a large variety of angles to antennas 1701. For example, antenna cluster 1613's transmission arrives at angle 1713, 1612's transmission arrives at angle 1712, and 1611's transmission arrives at angle 1711. This is due to the fact that the antenna clusters 1613-1615 are positioned successively further from coverage area 1360, but are all aimed to reflect down to coverage area 1360, resulting in varied angles of arrival. Likewise, antenna clusters' 1631-1633's transmission arrive at angles 1731-1733, respectively; clusters 1621-1623 arrive at angles 1721-1723, respectively; and clusters 1641-1643 arrive at angles 1741-1743, respectively.

[0094] Additionally, it can be seen in **Figure 17c** that transmission from each group of antenna clusters in the north, south, east and west of **Figure 16** arrive from their respective directions, and further the 3 antennas 1651-1653 of antenna cluster 1611 arrive at angles 1751-1753, respectively. And the rest of the individual antennas (not numbered) all arrive at different angles.

[0095] All of the varied arrival angles illustrated in **Figure 17a-c** result in significant angular diversity. Such diversity can be exploited using either prior art MIMO techniques or the DIDO techniques described herein, or other spatial

multiplexing techniques to achieve significant improvements in overall channel bandwidth and SNR. Also, if some of the arrival angles are obstructed from reaching some antennas 1701, then with so many arrival angles, there is a high probability that at least some of the RF arrival angles will reach each antenna.

[0096] This same diversity can be exploited in the return path when antennas 1701 transmit back to the various antenna clusters 1611-1643. In one embodiment, some or all of antennas 1701 may be directional and only utilize certain transmission and reception angles. This may be used to either increase the gain off the signal (e.g. using a dish antenna), or can be used to limit the return path transmissions to certain angles to avoid interfering with other receivers using a similar frequency.

[0097] One desirable frequency range to use for tropospheric communications is above 12 GHz. Some of the 12 GHz band is currently used in the US for Direct Broadcast Satellite (DBS) communications. Typically, DBS radio signals are transmitted from geostationary satellites, and a consumer has a dish installed on the roof of his home (or someplace where the dish as a view of the southern sky in the direction of the desired satellite). The satellite signal is received at angle 1410 of **Figure 14**, and then is collected by dish 1401 and reflected to antenna and low-noise block (LNB) 1402. Some satellite dishes 1401 are constructed to receive satellite signals from 2 or 3 angles, and reflect them to multiple LNBs 1402. The 12 GHz band is largely unutilized in the US except for this purpose. Because of the high frequency 12 GHz is easily absorbed by various terrestrial

objects (e.g. tree leaves) and as a result is difficult to use for other than LOS applications.

[0098] In one embodiment of this invention the DIDO troposcatter system described above, and illustrated in **Figures 11** and **13** is used at the same frequency as DBS satellite transmission 1410, but the base station antennas (either 1102 or 1341-1344) are positioned and angled such that the angle(s) of RF reflection from the common volume(s) 1121 or 1321-1324 are such that they will not be reflected by the satellite dishes 1401 into their LNBs 1402. This can be accomplished by placing the base station antennas 1102 or 1341-1344 at angles so that they never transmit in the same direction as the satellite signal 1410 (e.g. always transmit from the north, since all geosynchronous satellites transmit from the south), or choose an elevation angle for the transmission such that the RF reflection 1420 back to the ground bounces away from the LNBs 1402.

[0099] Care must also be used on the return path transmission from the client antennas 1104 or 1361-1363 to the base station so that they do not interfere with LNB 1402. This can be accomplished by using a directional return path antenna, similar to the dish antenna 1401 used to receive the satellite signal.

[00100] In an alternative embodiment the 12 GHz troposcatter approach just described not only applies to DIDO systems, but can be also used for 1-way conventional broadcast without return path or spatial multiplexing. In this case, each client receiver would receive the same signal.

[0100] In an alternative embodiment, conventional 2-way MIMO techniques are used with troposcatter communications, as shown in **Figure 15.** In this embodiment, both the base station 1101 and the client station 1102 have multiple antennas, and each receiver creates a full H matrix after training, and then inverts that matrix and multiplies it by the received data from the multiple antennas. The configuration of a conventional MIMO system is show in **Figure 1**,

[0101] Embodiments of the invention may include various steps as set forth above. The steps may be embodied in machine-executable instructions which cause a general-purpose or special-purpose processor to perform certain steps. For example, the various components within the Base Stations and Client Devices described above may be implemented as software executed on a general purpose or special purpose processor. To avoid obscuring the pertinent aspects of the invention, various well known personal computer components such as computer memory, hard drive, input devices, . . . etc, have been left out of the figures.

[0102] Alternatively, in one embodiment, the various functional modules illustrated herein and the associated steps may be performed by specific hardware components that contain hardwired logic for performing the steps, such as an application-specific integrated circuit ("ASIC") or by any combination of programmed computer components and custom hardware components.

[0103] In one embodiment, certain modules such as the Coding, Modulation and Signal Processing Logic 603 described above may be implemented on a

programmable digital signal processor ("DSP") (or group of DSPs) such as a DSP using a Texas Instruments' TMS320x architecture (e.g., a TMS320C6000, TMS320C5000, . . . etc). The DSP in this embodiment may be embedded within an add-on card to a personal computer such as, for example, a PCI card. Of course, a variety of different DSP architectures may be used while still complying with the underlying principles of the invention.

[0104] Elements of the present invention may also be provided as a machine-readable medium for storing the machine-executable instructions. The machine-readable medium may include, but is not limited to, flash memory, optical disks, CD-ROMs, DVD ROMs, RAMs, EPROMs, EEPROMs, magnetic or optical cards, propagation media or other type of machine-readable media suitable for storing electronic instructions. For example, the present invention may be downloaded as a computer program which may be transferred from a remote computer (e.g., a server) to a requesting computer (e.g., a client) by way of data signals embodied in a carrier wave or other propagation medium via a communication link (e.g., a modem or network connection).

[0105] Throughout the foregoing description, for the purposes of explanation, numerous specific details were set forth in order to provide a thorough understanding of the present system and method. It will be apparent, however, to one skilled in the art that the system and method may be practiced without some of these specific details. Accordingly, the scope and spirit of the present invention should be judged in terms of the claims which follow.

CLAIMS

What is claimed is:

1. A method comprising:

using tropospheric scatter to transmit a training signal from each antenna of a base station to each of a plurality of client devices, each of the client devices analyzing each training signal to generate channel characterization data, and transmitting the channel characterization data back to the base station;

storing the channel characterization data for each of the plurality of client devices;

receiving data to be transmitted to each of the client devices; and

precoding the data using the channel characterization data associated with each respective client device to generate precoded data signals for each antenna of the base station; and

using tropospheric scatter to transmit the precoded data signals through each antenna of the base station to each respective client device.

ABSTRACT

A method is described comprising: transmitting a training signal from each antenna of a base station to each of a plurality of client devices utilizing tropospheric scatter, each of the client devices analyzing each training signal to generate channel characterization data, and transmitting the channel characterization data back to the base station utilizing tropospheric scatter; storing the channel characterization data for each of the plurality of client devices; receiving data to be transmitted to each of the client devices; and precoding the data using the channel characterization data associated with each respective client device to generate precoded data signals for each antenna of the base station; and transmitting the precoded data signals through each antenna of the base station to each respective client device.

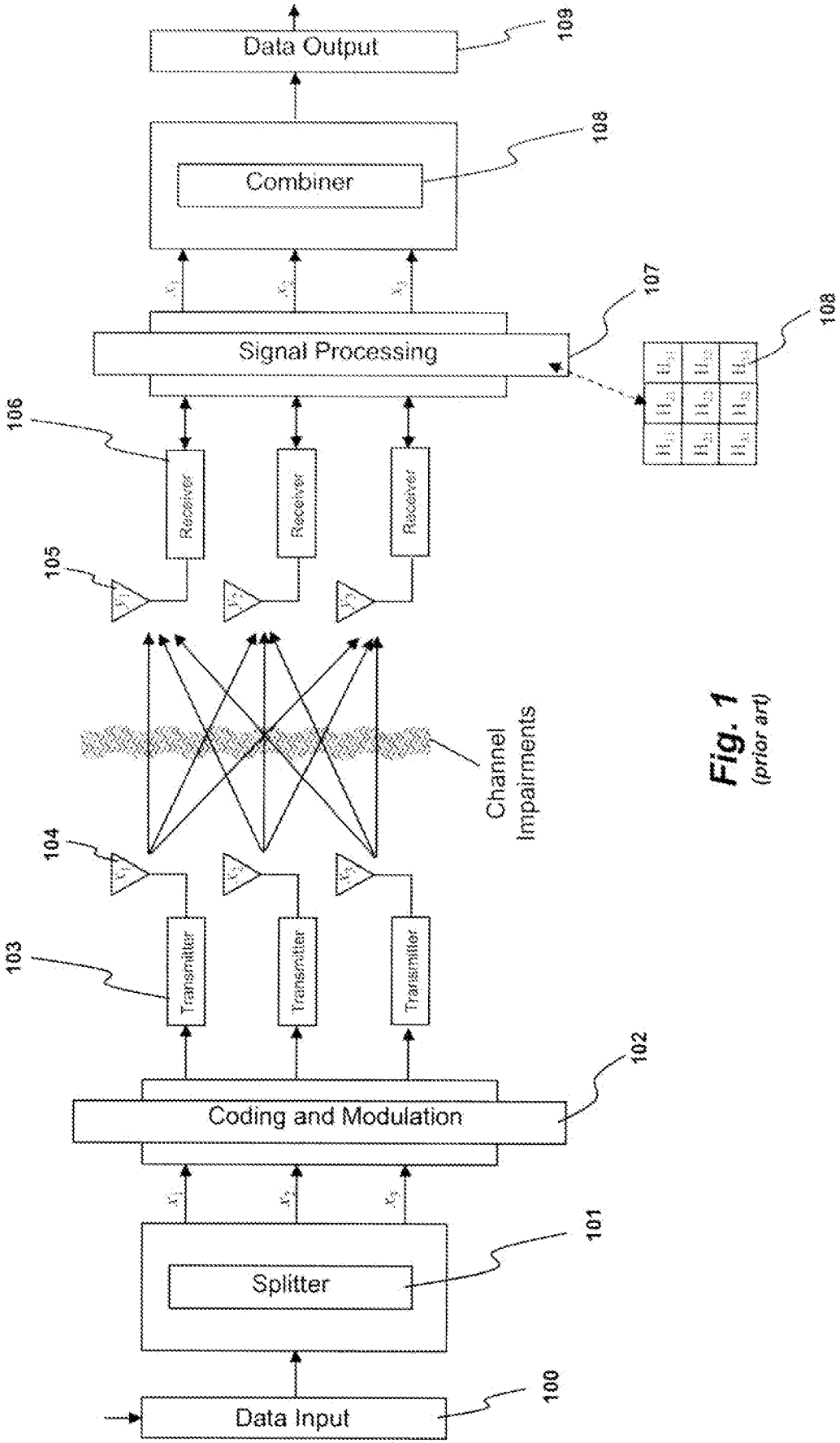

Fig. 1
(prior art)

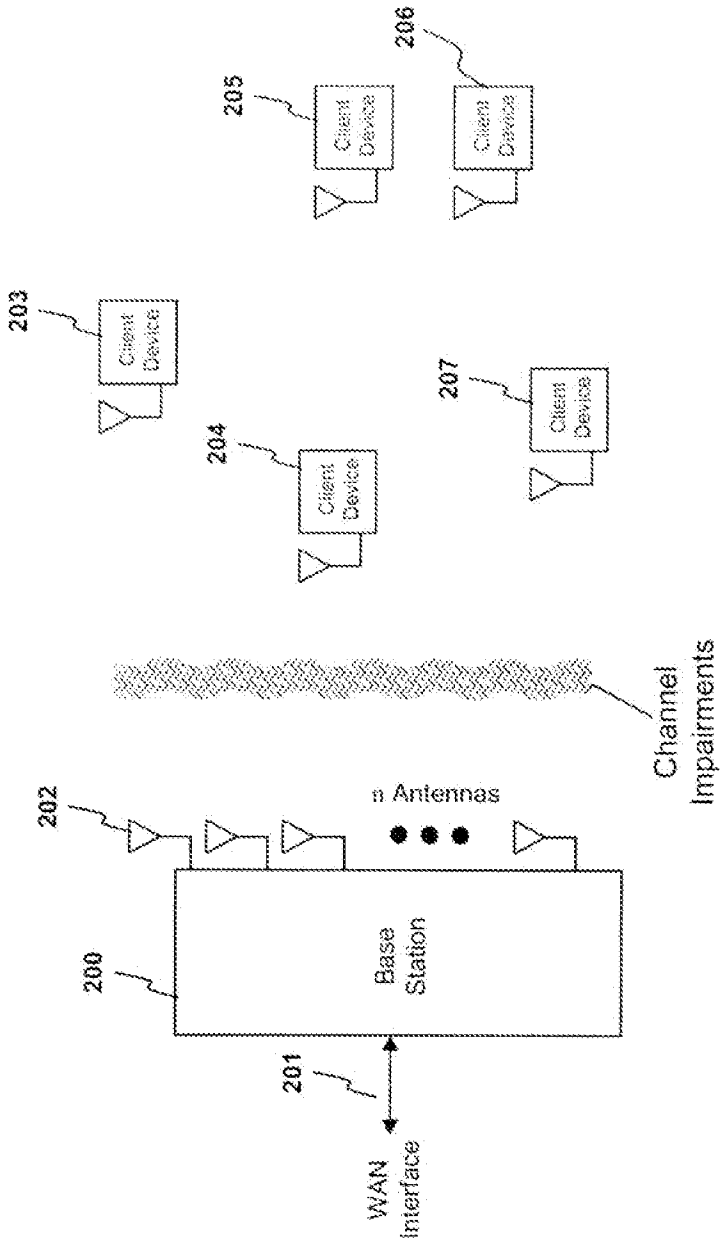

n-antenna Base Station with Single-antenna Client Devices

Fig. 2

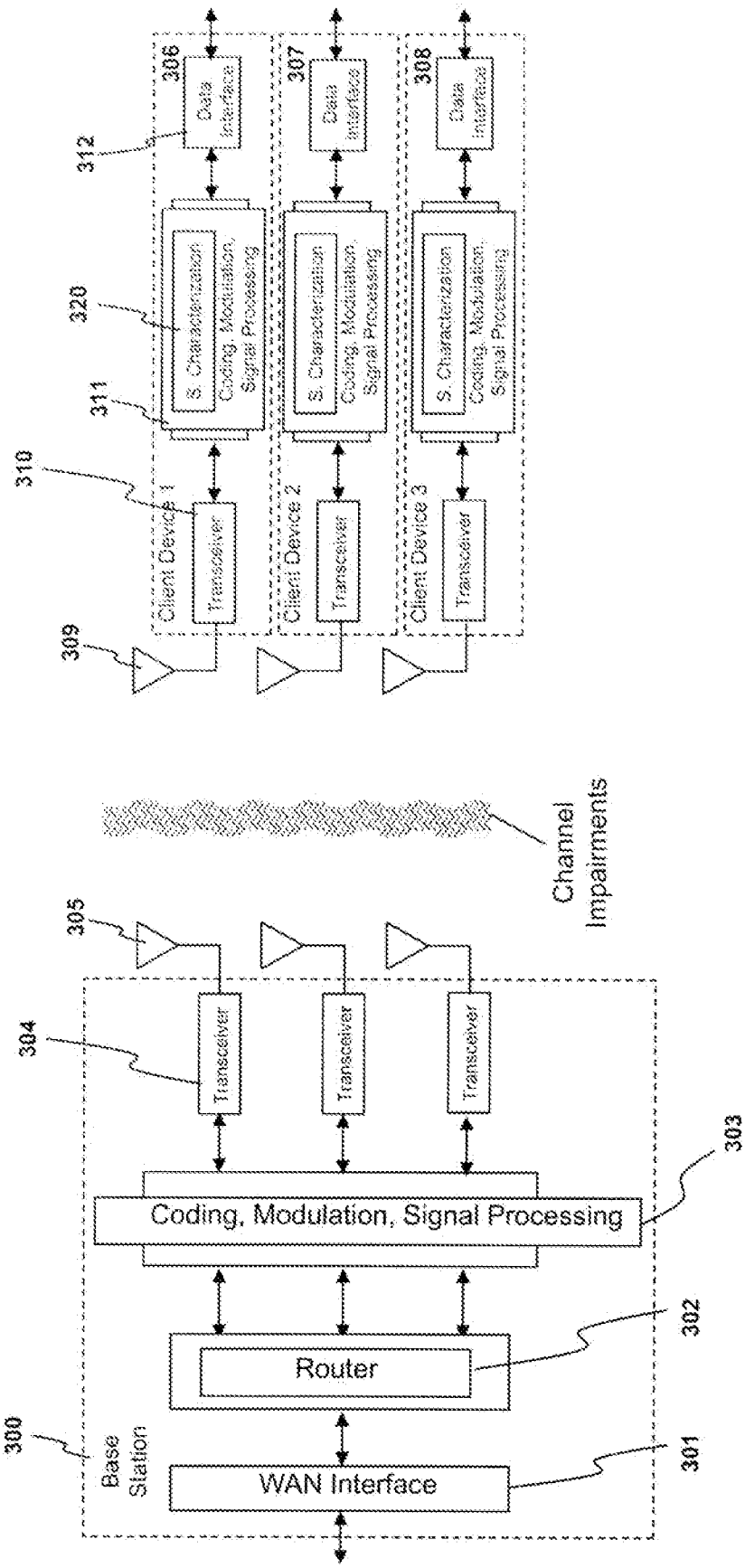

3-Antenna Base Station with 3 Single-Antenna Client Devices

Fig. 3

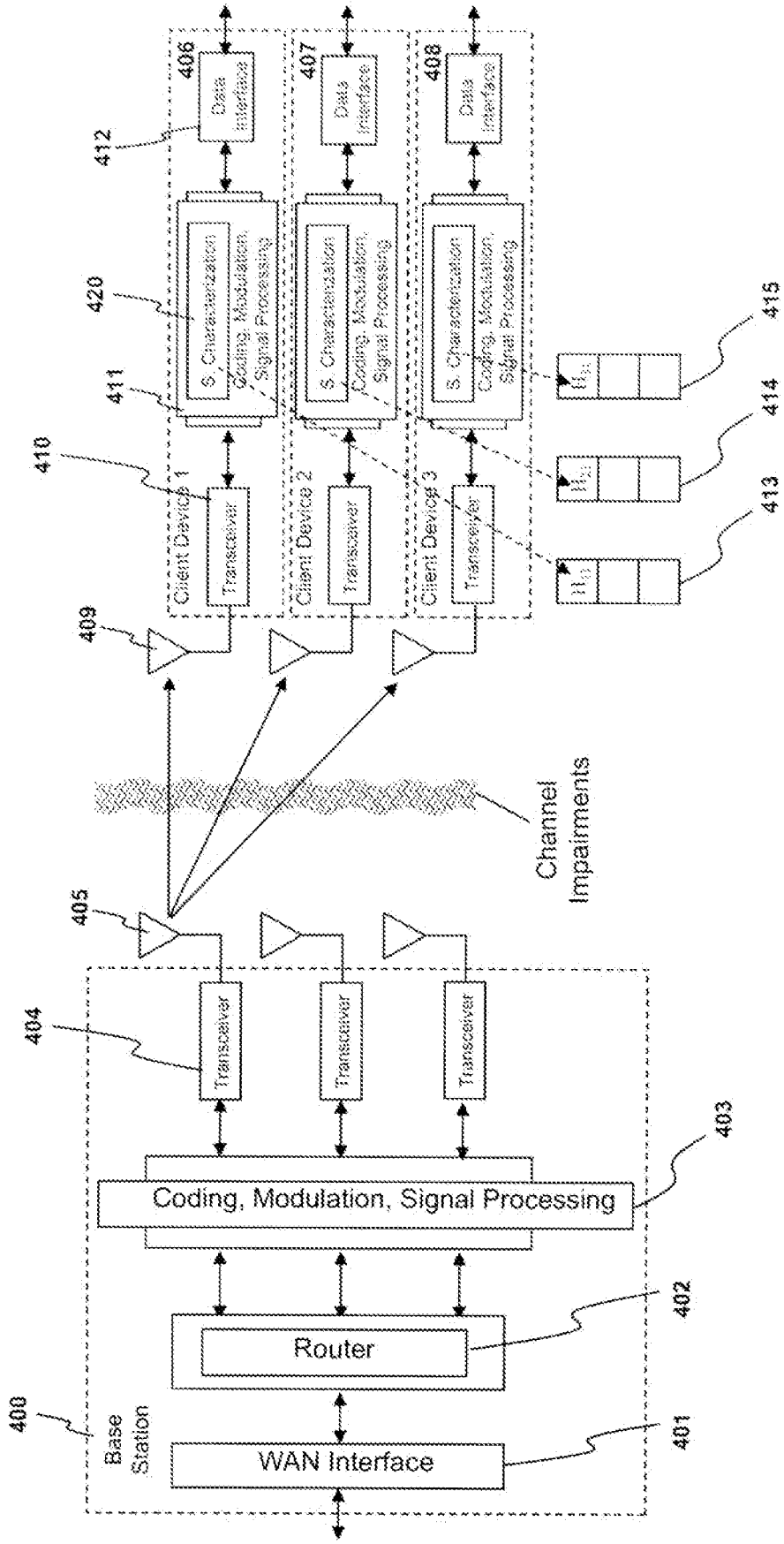
Base Station
400
WAN Interface
401
Router
402
Coding, Modulation, Signal Processing
403
Transceiver
404
405
Channel Impairments
Transceiver
Client Device 1
Client Device 2
Client Device 3
406
407
408
409
410
411
412
413
414
415
420
Data Interface
S. Characterization
Coding, Modulation, Signal Processing
Antenna 1 Pilot Signal Transmission

Fig. 4

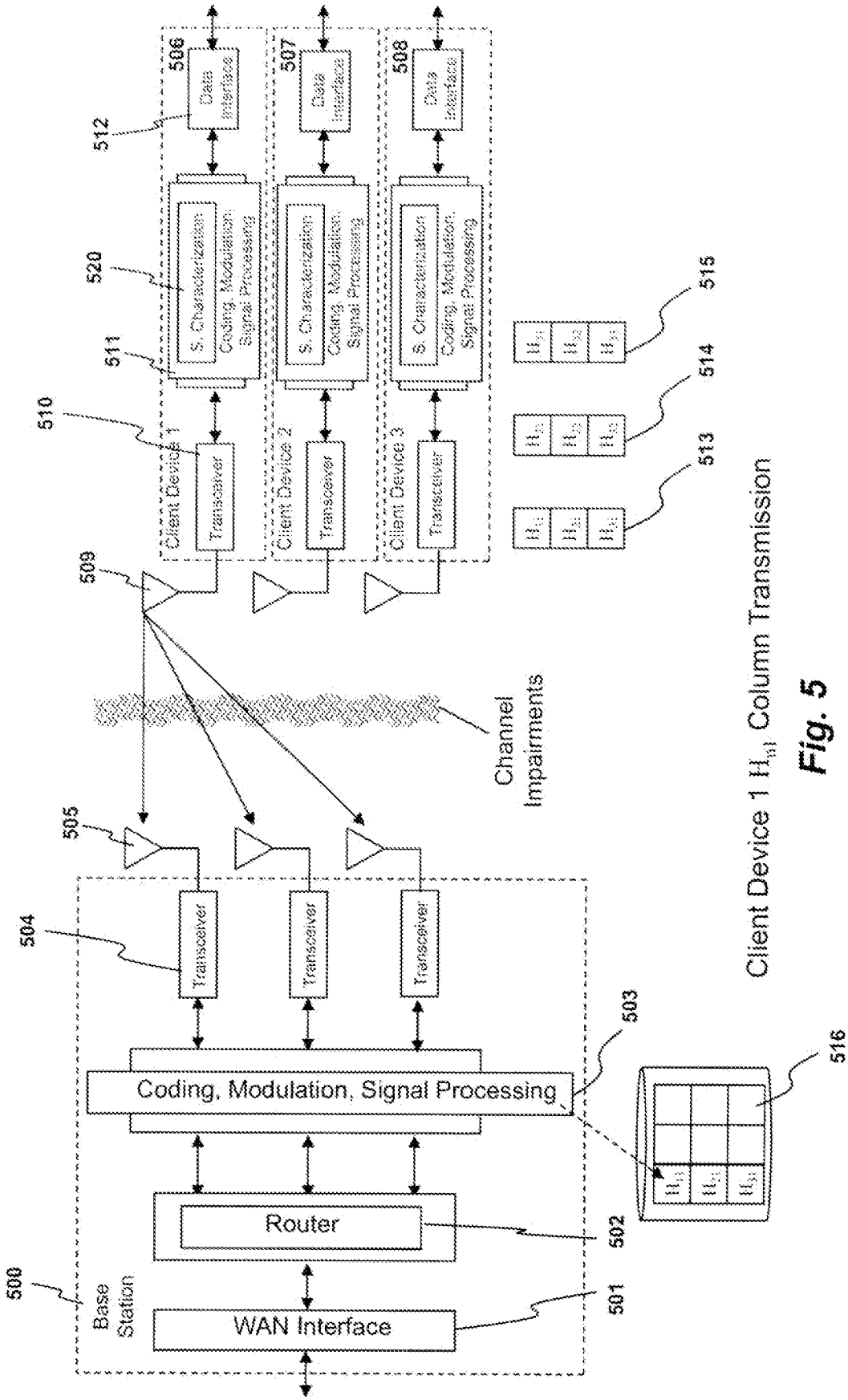
Client Device 1 H_{n1} Column Transmission
Base Station
WAN Interface
Router
Coding, Modulation, Signal Processing
Transceiver
Channel Impairments
Client Device 1
Client Device 2
Client Device 3
S. Characterization
Coding, Modulation, Signal Processing
Data Interface
500
501
502
503
504
505
506
507
508
509
510
511
512
513
514
515
516
520

Fig. 5

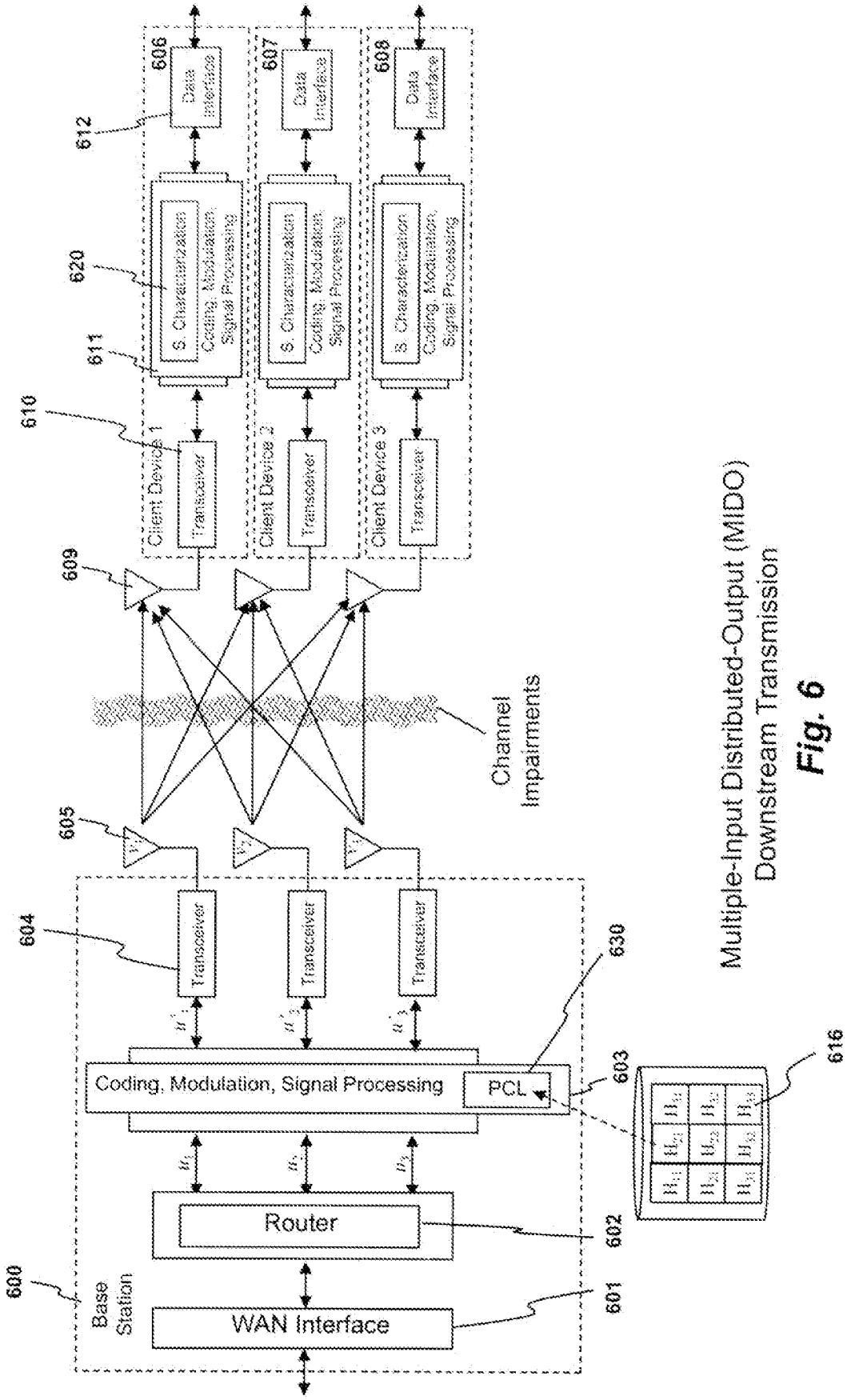
Multiple-Input Distributed-Output (MIDO)
Downstream Transmission
Channel Impairments
Base Station
WAN Interface
Router
Coding, Modulation, Signal Processing
PCL
Transceiver
Client Device 1
Client Device 2
Client Device 3
Data Interface
S. Characterization
Coding, Modulation, Signal Processing
600
601
602
603
604
605
606
607
608
609
610
611
612
616
620
630

Fig. 6

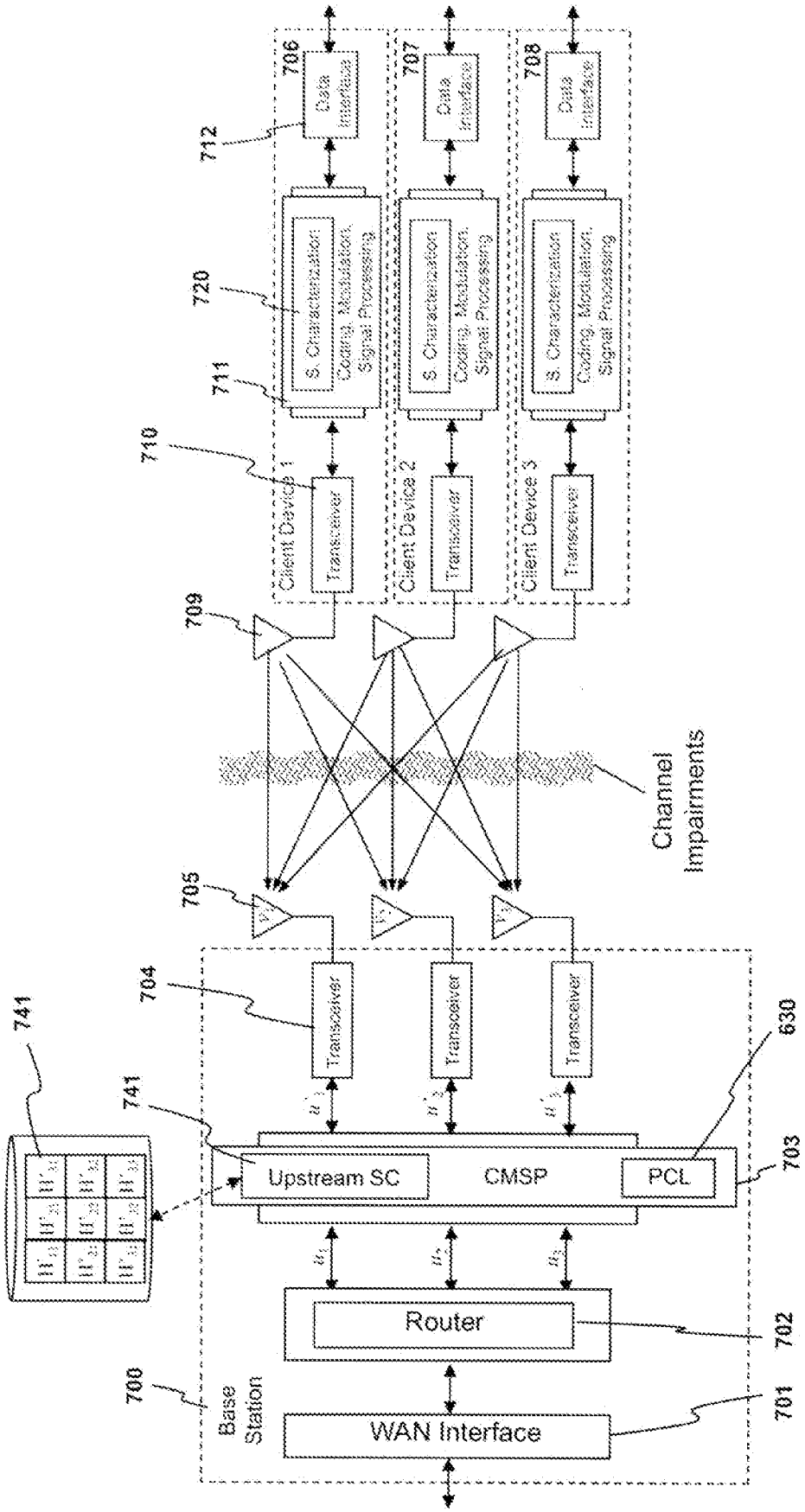
MIMO Upstream Transmission
Channel Impairments
Client Device 1
Client Device 2
Client Device 3
Transceiver
Data Interface
S. Characterization Coding, Modulation, Signal Processing
Upstream SC
CMSP
PCL
Router
WAN Interface
Base Station
700
701
702
703
704
705
706
707
708
709
710
711
712
720
630
741

Fig. 7

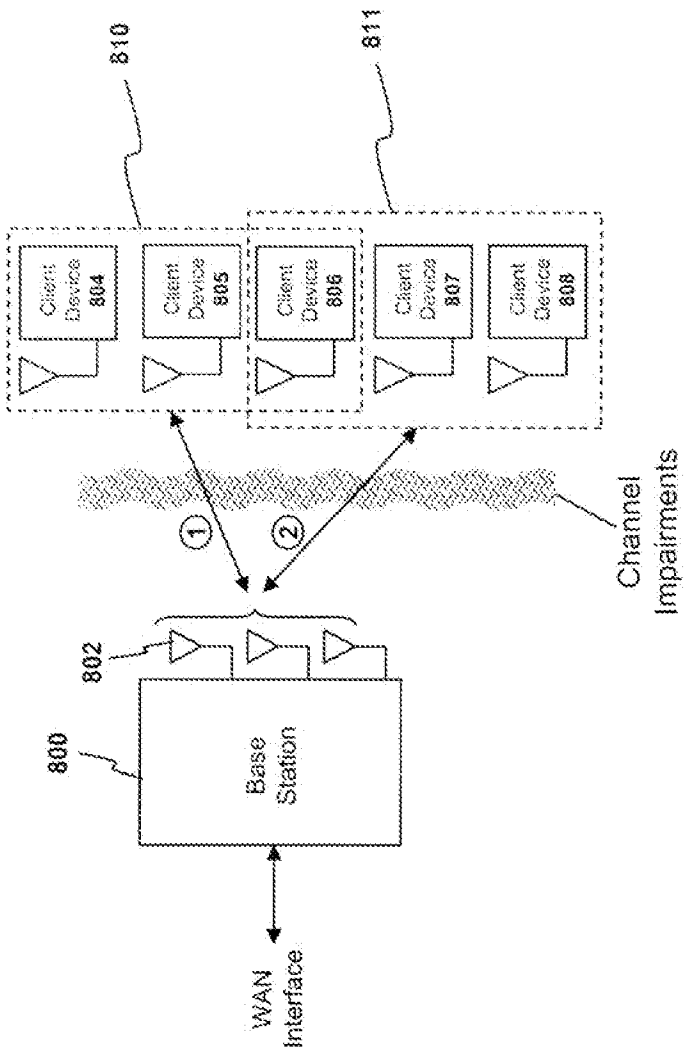

Cycling With Different Client Groups

Fig. 8

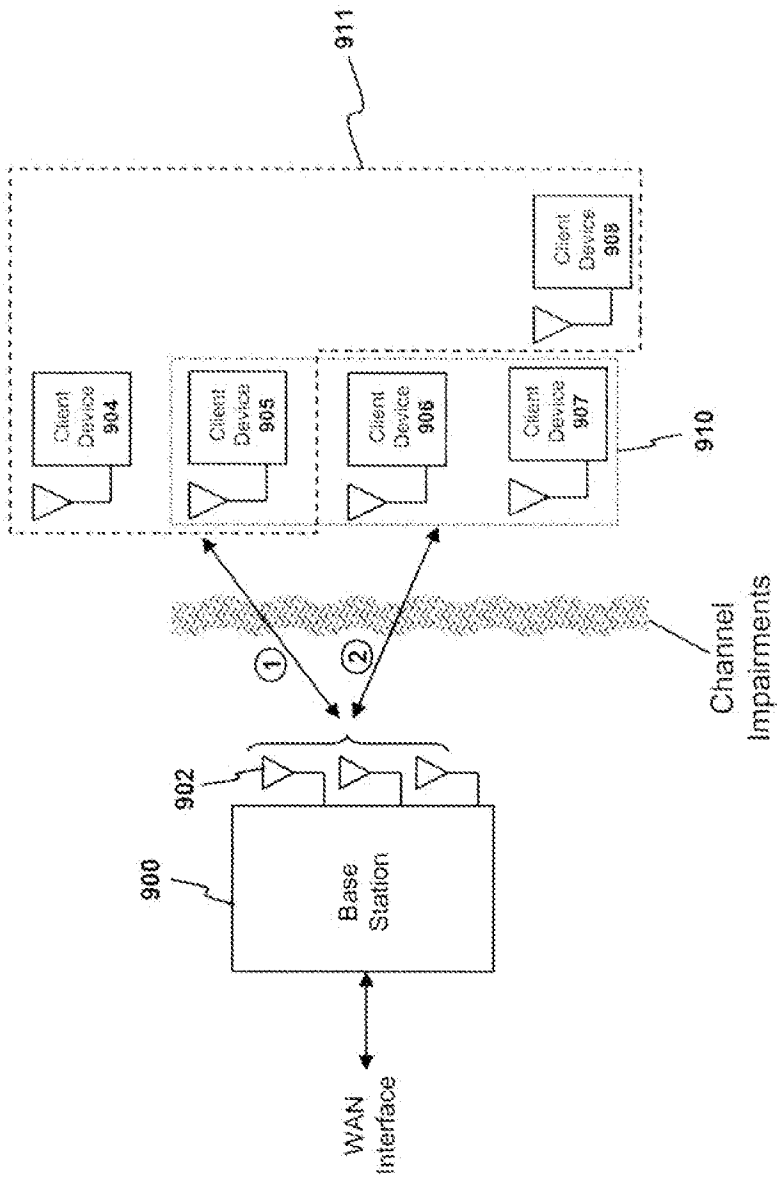

Grouping Clients Based on Proximity

Fig. 9

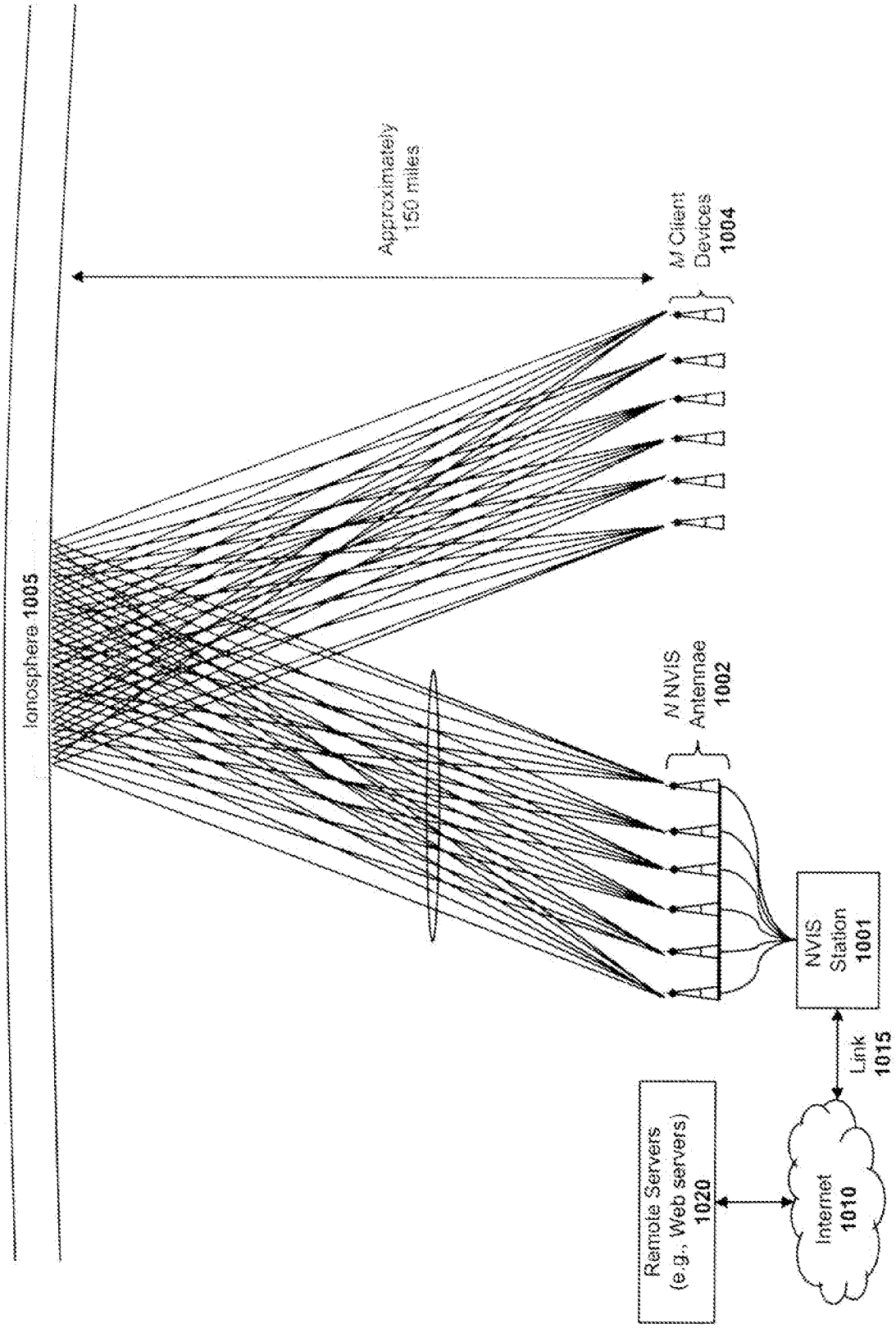
Ionosphere 1005
Approximately 150 miles
M Client Devices 1004
N NVIS Antennae 1002
NVIS Station 1001
Link 1015
Internet 1010
Remote Servers (e.g., Web servers) 1020

Fig. 10

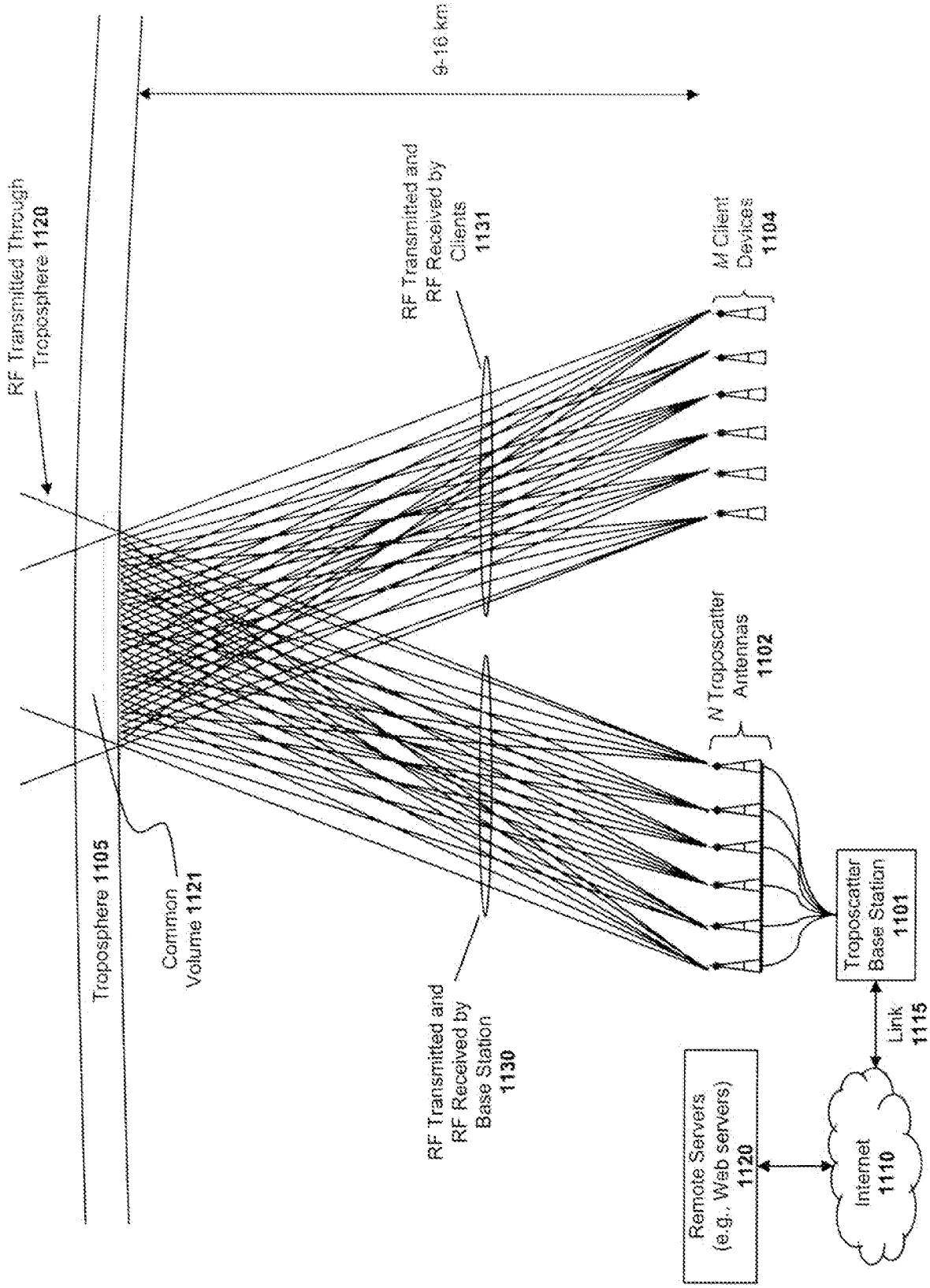
RF Transmitted Through Troposphere 1120
9-16 km
RF Transmitted and RF Received by Clients 1131
M Client Devices 1104
N Troposcatter Antennas 1102
Troposphere 1105
Common Volume 1121
RF Transmitted and RF Received by Base Station 1130
Troposcatter Base Station 1101
Link 1115
Internet 1110
Remote Servers (e.g. Web servers) 1120

Fig. 11

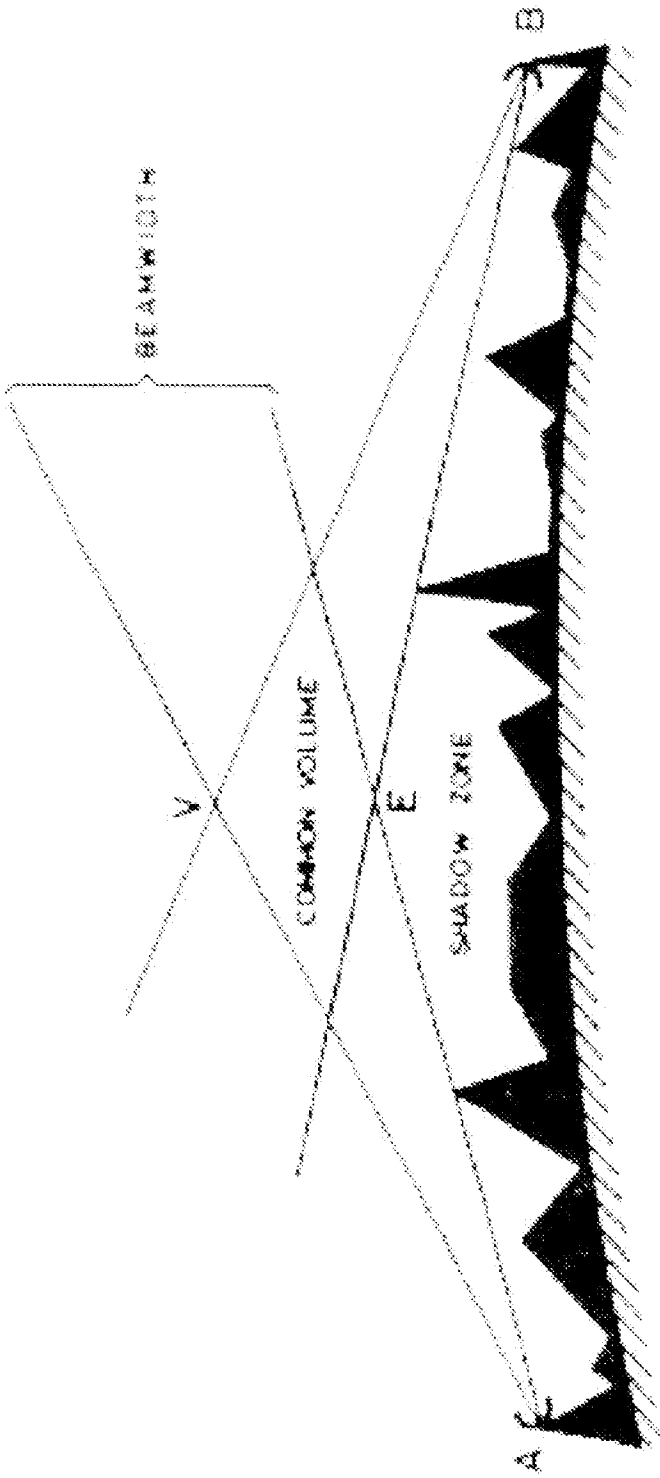

Fig. 4.4 Profile of a typical troposcatter path

Roda, Troposcatter Links

Fig. 12
(prior art)

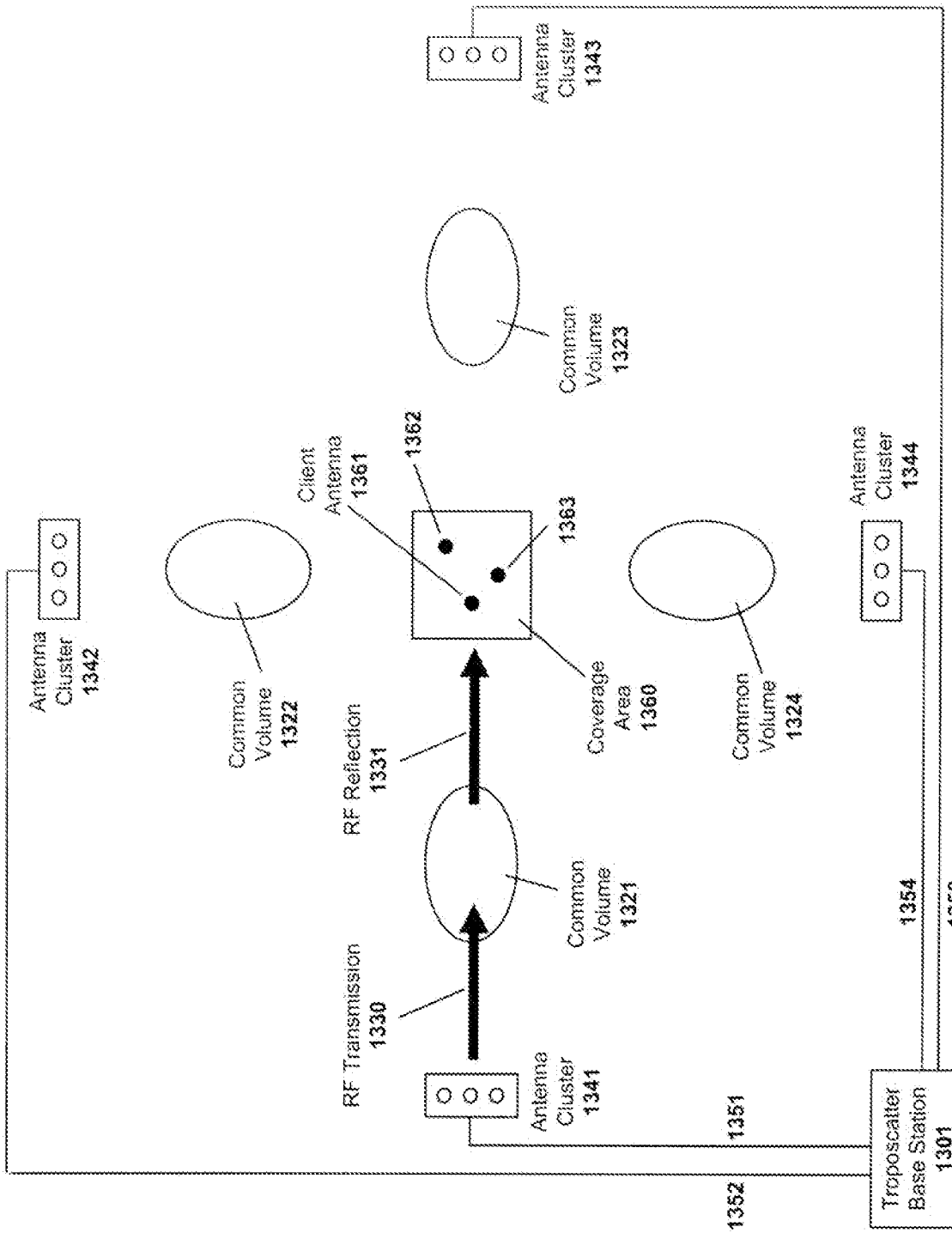
Antenna Cluster 1343
Common Volume 1323
Client Antenna 1361
1362
1363
Antenna Cluster 1344
Antenna Cluster 1342
Common Volume 1322
RF Reflection 1331
Coverage Area 1360
Common Volume 1324
Common Volume 1321
RF Transmission 1330
1354
1353
Antenna Cluster 1341
1351
1352
Troposcatter Base Station 1301

Fig. 13

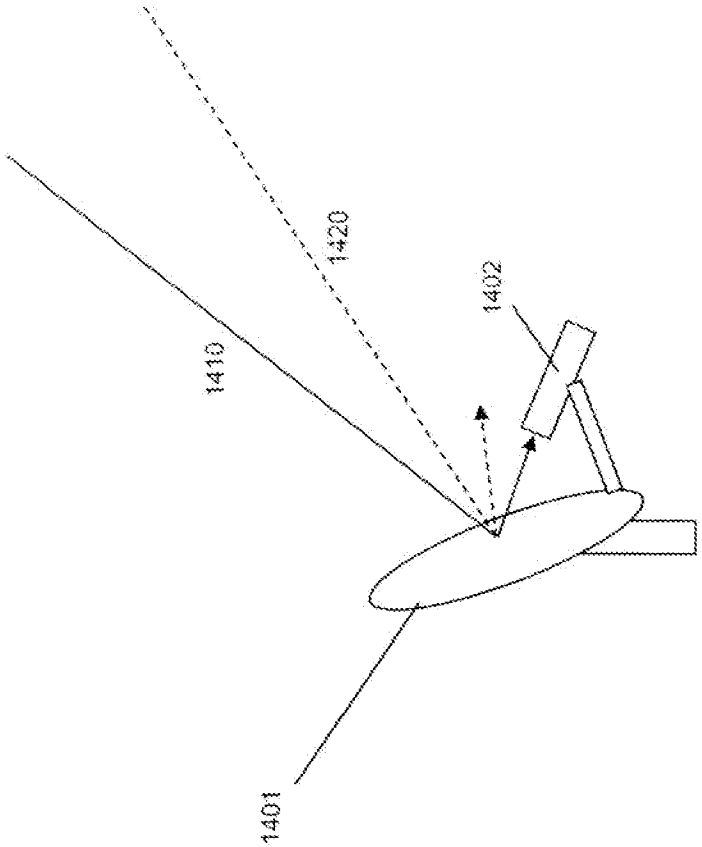

Fig. 14

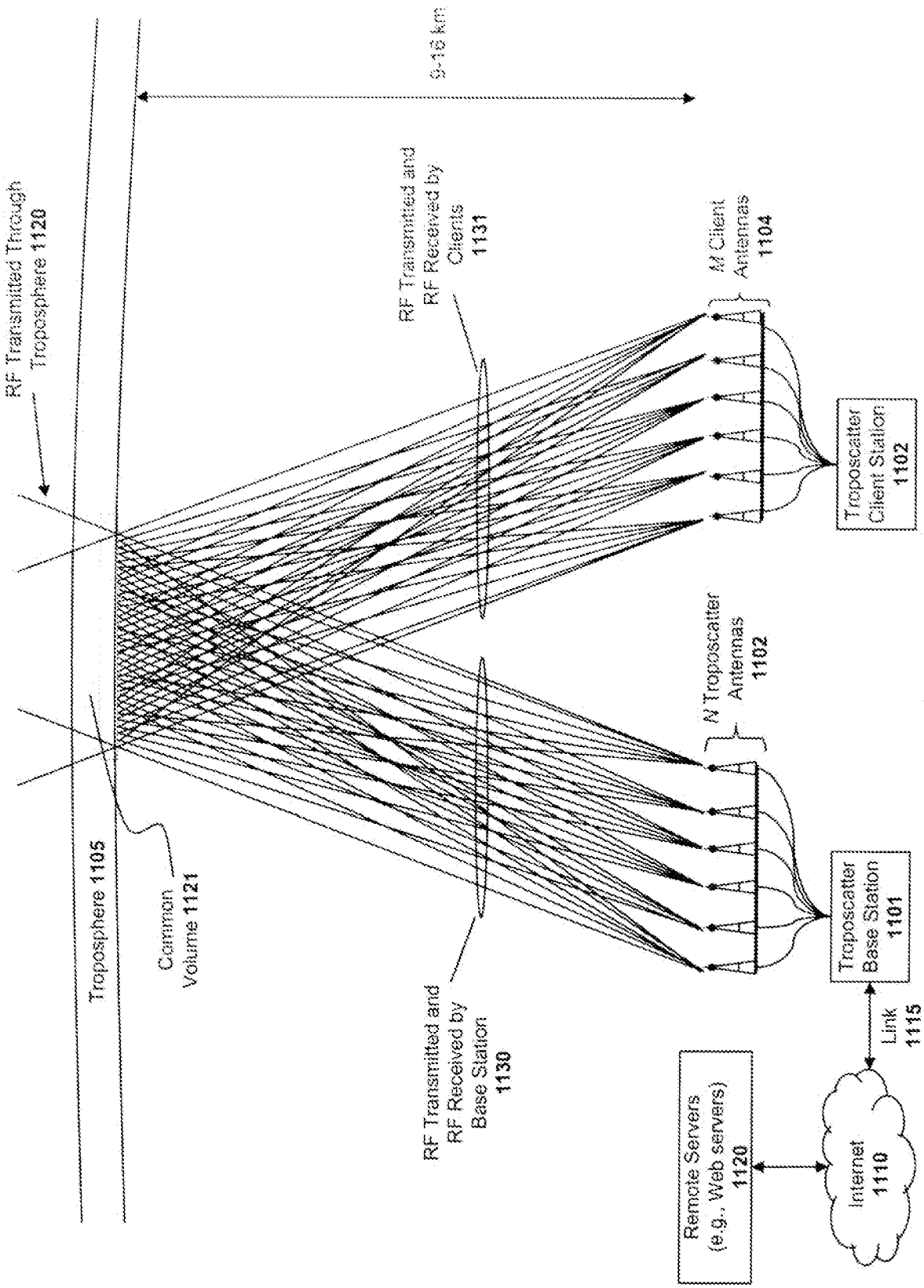
RF Transmitted Through Troposphere 1120
9-18 km
RF Transmitted and RF Received by Clients 1131
M Client Antennas 1104
Troposcatter Client Station 1102
N Troposcatter Antennas 1102
Troposphere 1105
Common Volume 1121
RF Transmitted and RF Received by Base Station 1130
Troposcatter Base Station 1101
Link 1115
Remote Servers (e.g., Web servers) 1120
Internet 1110

Fig. 15

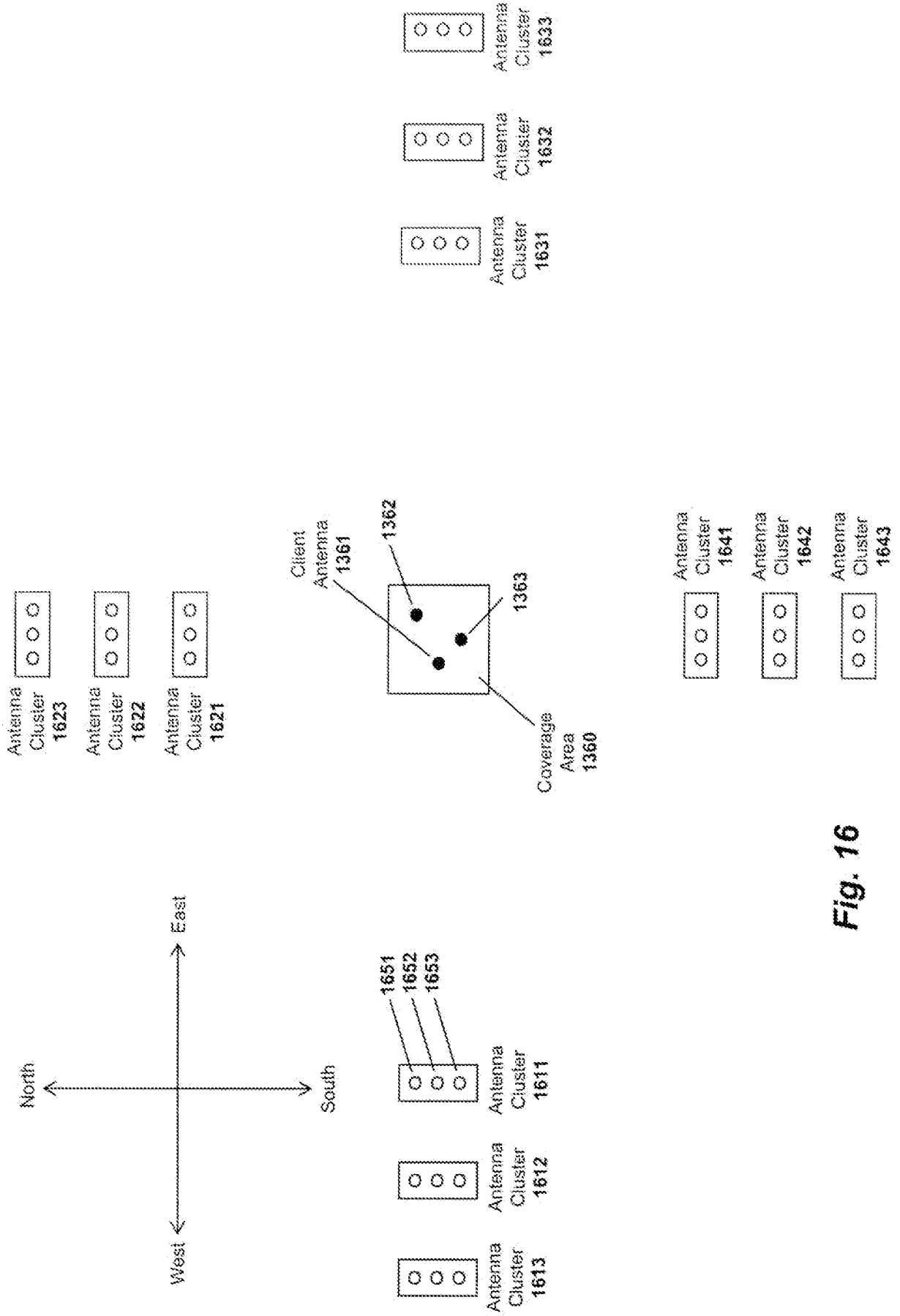
Antenna Cluster 1623
Antenna Cluster 1622
Antenna Cluster 1621
Client Antenna 1361
1362
1363
Coverage Area 1360
Antenna Cluster 1641
Antenna Cluster 1642
Antenna Cluster 1643
Antenna Cluster 1631
Antenna Cluster 1632
Antenna Cluster 1633
North
East
South
West
1651
1652
1653
Antenna Cluster 1611
Antenna Cluster 1612
Antenna Cluster 1613

Fig. 16

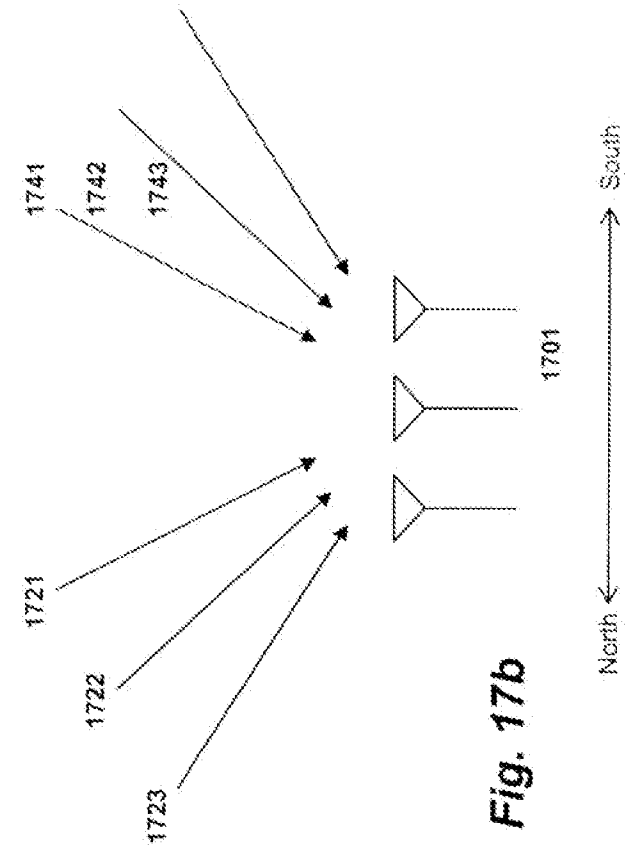

Fig. 17b

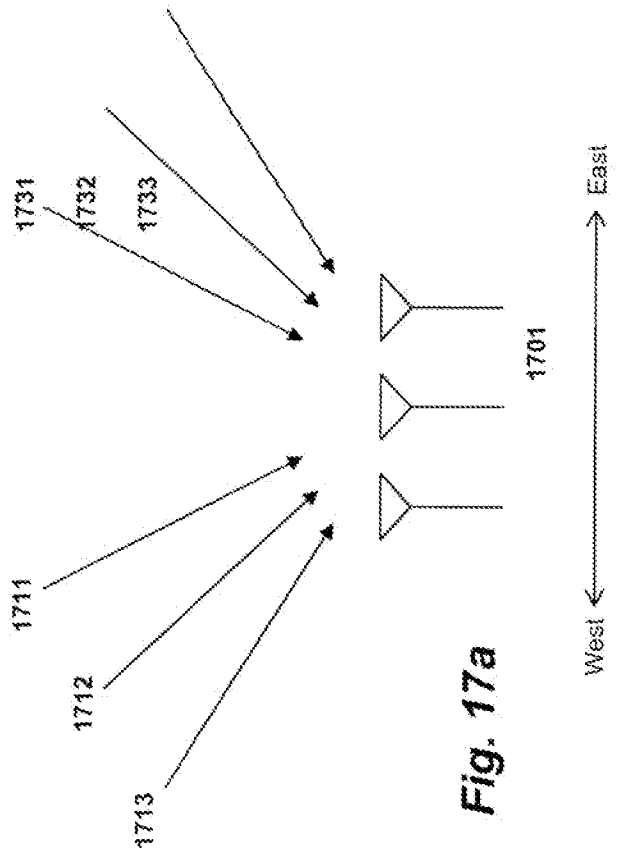

Fig. 17a

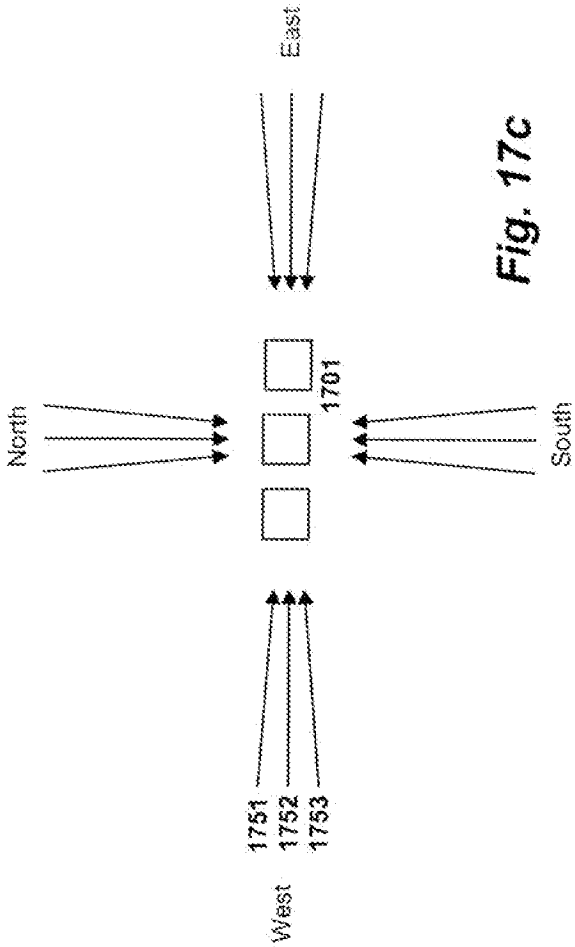

Fig. 17c

Atty. Docket No. 6181P515X *Patent*

UNITED STATES PATENT APPLICATION

for

SYSTEM AND METHOD FOR DISTRIBUTED ANTENNA WIRELESS COMMUNICATIONS

Inventors:

Antonio Forenza
Stephen G. Perlman

Prepared by:

BLAKELY, SOKOLOFF, TAYLOR & ZAFMAN, LLP
1279 OAKMEAD PARKWAY
SUNNYVALE, CALIFORNIA 94085
(408) 720-8300

Attorney's Docket No. 6181P515X

SYSTEM AND METHOD FOR DISTRIBUTED ANTENNA WIRELESS COMMUNICATIONS

RELATED APPLICATIONS

[0001] This application is a continuation-in-part of the following co-pending U.S. Patent Applications:

[0002] U.S. Application Serial No. 12/143,503, filed June 20, 2008 entitled, "System and Method For Distributed Input-Distributed Output Wireless Communications";

[0003] U.S. Application Serial No. 11/894,394, filed August 20, 2007 entitled, "System and Method for Distributed Input Distributed Output Wireless Communications";

[0004] U.S. Application Serial No. 11/894,362, filed August 20, 2007 entitled, "System and method for Distributed Input-Distributed Wireless Communications";

[0005] U.S. Application Serial No. 11/894,540, filed August 20, 2007 entitled "System and Method For Distributed Input-Distributed Output Wireless Communications"

[0006] U.S. Application Serial No. 11/256,478, filed October 21, 2005 entitled "System and Method For Spatial-Multiplexed Tropospheric Scatter Communications";

[0007] U.S. Application Serial No. 10/817,731, filed April 2, 2004 entitled "System and Method For Enhancing Near Vertical Incidence Skywave ("NVIS") Communication Using Space-Time Coding.

BACKGROUND

[0008] Prior art multi-user wireless systems may include only a single base station or several base stations.

[0009] A single WiFi base station (e.g., utilizing 2.4 GHz 802.11b, g or n protocols) attached to a broadband wired Internet connection in an area where there are no other WiFi access points (e.g. a WiFi access point attached to DSL within a rural home) is an example of a relatively simple multi-user wireless system that is a single base station that is shared by one or more users that are within its transmission range. If a user is in the same room as the wireless access point, the user will typically experience a high-speed link with few transmission disruptions (e.g. there may be packet loss from 2.4GHz interferers, like microwave ovens, but not from spectrum sharing with other WiFi devices), If a user is a medium distance away or with a few obstructions in the path between the user and WiFi access point, the user will likely experience a medium-speed link. If a user is approaching the edge of the range of the WiFi access point, the user will likely experience a low-speed link, and may be subject to periodic drop-outs if changes to the channel result in the signal SNR dropping below usable levels. And, finally, if the user is beyond the range of the WiFi base station, the user will have no link at all.

[0010] When multiple users access the WiFi base station simultaneously, then the available data throughput is shared among them. Different users will typically

place different throughput demands on a WiFi base station at a given time, but at times when the aggregate throughput demands exceed the available throughput from the WiFi base station to the users, then some or all users will receive less data throughput than they are seeking. In an extreme situation where a WiFi access point is shared among a very large number of users, throughput to each user can slow down to a crawl, and worse, data throughput to each user may arrive in short bursts separated by long periods of no data throughput at all, during which time other users are served. This “choppy” data delivery may impair certain applications, like media streaming.

[0011] Adding additional WiFi base stations in situations with a large number of users will only help up to a point. Within the 2.4GHz ISM band in the U.S., there are 3 non-interfering channels that can be used for WiFi, and if 3 WiFi base stations in the same coverage area are configured to each use a different non-interfering channel, then the aggregate throughput of the coverage area among multiple users will be increased up to a factor of 3. But, beyond that, adding more WiFi base stations in the same coverage area will not increase aggregate throughput, since they will start sharing the same available spectrum among them, effectually utilizing time-division multiplexed access (TDMA) by “taking turns” using the spectrum. This situation is often seen in coverage areas with high population density, such as within multi-dwelling units. For example, a user in a large apartment building with a WiFi adapter may well experience very poor throughput due to dozens of other interfering WiFi networks (e.g. in other

apartments) serving other users that are in the same coverage area, even if the user's access point is in the same room as the client device accessing the base station. Although the link quality is likely good in that situation, the user would be receiving interference from neighbor WiFi adapters operating in the same frequency band, reducing the effective throughput to the user.

[0012] Current multiuser wireless systems, including both unlicensed spectrum, such as WiFi, and licensed spectrum, suffer from several limitations. These include coverage area, downlink (DL) data rate and uplink (UL) data rate. Key goals of next generation wireless systems, such as WiMAX and LTE, are to improve coverage area and DL and UL data rate via multiple-input multiple-output (MIMO) technology. MIMO employs multiple antennas at transmit and receive sides of wireless links to improve link quality (resulting in wider coverage) or data rate (by creating multiple non-interfering spatial channels to every user). If enough data rate is available for every user (note, the terms "user" and "client" are used herein interchangeably), however, it may be desirable to exploit channel spatial diversity to create non-interfering channels to multiple users (rather than single user), according to multiuser MIMO (MU-MIMO) techniques [20-27]. . For example, in MIMO 4x4 systems (i.e., four transmit and four receive antennas), 10MHz bandwidth, 16-QAM modulation and forward error correction (FEC) coding with rate 3/4 (yielding spectral efficiency of 3bps/Hz), the ideal peak data rate achievable at the physical layer for every user is 4x30Mbps=120Mbps, which is much higher than required to deliver high definition video content (which may

only require ~10Mbps). In MU-MIMO systems with four transmit antennas, four users and single antenna per user, in ideal scenarios (i.e., independent identically distributed, i.i.d., channels) downlink data rate may be shared across the four users and channel spatial diversity may be exploited to create four parallel 30Mbps data links to the users.

[0013] Different MU-MIMO schemes have been proposed as part of the LTE standard [1-3], but they can provide only up to 2X improvement in DL data rate with four transmit antennas. Practical implementations of MU-MIMO techniques in standard and proprietary cellular systems by companies like ArrayComm [4] have yielded up to a ~3X increase (with four transmit antennas) in DL data rate via space division multiple access (SDMA). A key limitation of MU-MIMO schemes in cellular networks is lack of spatial diversity at the transmit side. Spatial diversity is a function of antenna spacing and multipath angular spread in the wireless links. In cellular systems employing MU-MIMO techniques, transmit antennas at a base station are typically clustered together and placed only one or two wavelengths apart due to limited real estate on antenna support structures (referred to herein as “towers,” whether physically tall or not) and due to limitations on where towers may be located. Moreover, multipath angular spread is low since cell towers are typically placed high up (10 meters or more) above obstacles to yield wider coverage.

[0014] Other practical issues with cellular system deployment include excessive cost and limited availability of locations for cellular antenna locations (e.g. due to municipal restrictions on antenna placement, cost of real-estate, physical obstructions, etc.) and the cost and/or availability of network connectivity to the transmitters (referred to herein as "backhaul"). Further, cellular systems often have difficulty reaching clients located deeply in buildings due to losses from walls, ceilings, floors, furniture and other impediments.

[0015] Indeed, the entire concept of a cellular structure for wide-area network wireless presupposes a rather rigid placement of cellular towers, an alternation of frequencies between adjacent cells, and frequently sectorization, so as to avoid interference among transmitters (either base stations or users) that are using the same frequency. As a result, a given sector of a given cell ends up being a shared block of DL and UL spectrum among all of the users in the cell sector, which is then shared among these users primarily in only the time domain. For example, cellular systems based on Time Division Multiple Access (TDMA) and Code Division Multiple Access (CDMA) both share spectrum among users in the time domain. By overlaying such cellular systems with sectorization, perhaps a 2-3X spatial domain benefit can be achieved. And, then by overlaying such cellular systems with a MU-MIMO system, such as those described previously, perhaps another 2-3X space-time domain benefit can be achieved. But, given that the cells and sectors of the cellular system are typically in fixed locations, often dictated by where towers can be placed, even such limited benefits are difficult to

exploit if user density (or data rate demands) at a given time does not match up well with tower/sector placement. A cellular smart phone user often experiences the consequence of this today where the user may be talking on the phone or downloading a web page without any trouble at all, and then after driving (or even walking) to a new location will suddenly see the voice quality drop or the web page slow to a crawl, or even lose the connection entirely. But, on a different day, the user may have the exact opposite occur in each location. What the user is probably experiencing, assuming the environmental conditions are the same, is the fact that user density (or data rate demands) is highly variable, but the available total spectrum (and thereby total data rate, using prior art techniques) to be shared among users at a given location is largely fixed.

[0016] Further, prior art cellular systems rely upon using different frequencies in different adjacent cells, typically 3 different frequencies. For a given amount of spectrum, this reduces the available data rate by 3X.

[0017] So, in summary, prior art cellular systems may lose perhaps 3X in spectrum utilization due to cellularization, and may improve spectrum utilization by perhaps 3X through sectorization and perhaps 3X more through MU-MIMO techniques, resulting in a net 3*3/3 = 3X potential spectrum utilization. Then, that bandwidth is typically divided up among users in the time domain, based upon what sector of what cell the users fall into at a given time. There are even further inefficiencies that result due to the fact that a given user's data rate demands are

typically independent of the user's location, but the available data rate varies depending on the link quality between the user and the base station. For example, a user further from a cellular base station will typically have less available data rate than a user closer to a base station. Since the data rate is typically shared among all of the users in a given cellular sector, the result of this is that all users are impacted by high data rate demands from distant users with poor link quality (e.g. on the edge of a cell) since such users will still demand the same amount of data rate, yet they will be consuming more of the shared spectrum to get it.

[0018] Other proposed spectrum sharing systems, such as that used by WiFi (e.g., 802.11b, g, and n) and those proposed by the White Spaces Coalition, share spectrum very inefficiently since simultaneous transmissions by base stations within range of a user result in interference, and as such, the systems utilize collision avoidance and sharing protocols. These spectrum sharing protocols are within the time domain, and so, when there are a large number of interfering base stations and users, no matter how efficient each base station itself is in spectrum utilization, collectively the base stations are limited to time domain sharing of the spectrum among each other. Other prior art spectrum sharing systems similarly rely upon similar methods to mitigate interference among base stations (be they cellular base stations with antennas on towers or small scale base stations, such as WiFi Access Points (APs)). These methods include limiting transmission power from the base station so as to limit the range

of interference, beamforming (via synthetic or physical means) to narrow the area of interference, time-domain multiplexing of spectrum and/or MU-MIMO techniques with multiple clustered antennas on the user device, the base station or both. And, in the case of advanced cellular networks in place or planned today, frequently many of these techniques are used at once.

[0019] But, what is apparent by the fact that even advanced cellular systems can achieve only about a 3X increase in spectrum utilization compared to a single user utilizing the spectrum is that all of these techniques have done little to increase the aggregate data rate among shared users for a given area of coverage. In particular, as a given coverage area scales in terms of users, it becomes increasingly difficult to scale the available data rate within a given amount of spectrum to keep pace with the growth of users. For example, with cellular systems, to increase the aggregate data rate within a given area, typically the cells are subdivided into smaller cells (often called nano-cells or femto-cells). Such small cells can become extremely expensive given the limitations on where towers can be placed, and the requirement that towers must be placed in a fairly structured pattern so as to provide coverage with a minimum of “dead zones”, yet avoid interference between nearby cells using the same frequencies. Essentially, the coverage area must be mapped out, the available locations for placing towers or base stations must be identified, and then given these constraints, the designers of the cellular system must make do with the best they can. And, of course, if user data rate demands grow over time, then the designers of the

cellular system must yet again remap the coverage area, try to find locations for towers or base stations, and once again work within the constraints of the circumstances. And, very often, there simply is no good solution, resulting in dead zones or inadequate aggregate data rate capacity in a coverage area. In other words, the rigid physical placement requirements of a cellular system to avoid interference among towers or base stations utilizing the same frequency results in significant difficulties and constraints in cellular system design, and often is unable to meet user data rate and coverage requirements.

[0020] So-called prior art "cooperative" and "cognitive" radio systems seek to increase the spectral utilization in a given area by using intelligent algorithms within radios such that they can minimize interference among each other and/or such that they can potentially "listen" for other spectrum use so as to wait until the channel is clear. Such systems are proposed for use particularly in unlicensed spectrum in an effort to increase the spectrum utilization of such spectrum.

[0021] A mobile ad hoc network (MANET) (see http://en.wikipedia.org/wiki/Mobile_ad_hoc_network) is an example of a cooperative self-configuring network intended to provide peer-to-peer communications, and could be used to establish communication among radios without cellular infrastructure, and with sufficiently low-power communications, can potentially mitigate interference among simultaneous transmissions that are out of range of each other. A vast number of

routing protocols have been proposed and implemented for MANET systems (see http://en.wikipedia.org/wiki/List_of_ad-hoc_routing_protocols for a list of dozens of routing protocols in a wide range of classes), but a common theme among them is they are all techniques for routing (e.g. repeating) transmissions in such a way to minimize transmitter interference within the available spectrum, towards the goal of particular efficiency or reliability paradigms.

[0022] All of the prior art multi-user wireless systems seek to improve spectrum utilization within a given coverage area by utilizing techniques to allow for simultaneous spectrum utilization among base stations and multiple users. Notably, in all of these cases, the techniques utilized for simultaneous spectrum utilization among base stations and multiple users achieve the simultaneous spectrum use by multiple users by mitigating interference among the waveforms to the multiple users. For example, in the case of 3 base stations each using a different frequency to transmit to one of 3 users, there interference is mitigated because the 3 transmissions are at 3 different frequencies. In the case of sectorization from a base station to 3 different users, each 180 degrees apart relative to the base station, interference is mitigated because the beamforming prevents the 3 transmissions from overlapping at any user.

[0023] When such techniques are augmented with MU-MIMO, and, for example, each base station has 4 antennas, then this has the potential to increase downlink throughput by a factor of 4, by creating four non-interfering spatial channels to the users in given coverage area. But it is still the case that some

technique must be utilized to mitigate the interference among multiple simultaneous transmissions to multiple users in different coverage areas.

[0024] And, as previously discussed, such prior art techniques (e.g. cellularization, sectorization) not only typically suffer from increasing the cost of the multi-user wireless system and/or the flexibility of deployment, but they typically run into physical or practical limitations of aggregate throughput in a given coverage area. For example, in a cellular system, there may not be enough available locations to install more base stations to create smaller cells. And, in an MU-MIMO system, given the clustered antenna spacing at each base station location, the limited spatial diversity results in asymptotically diminishing returns in throughput as more antennas are added to the base station.

[0025] And further, in the case of multi-user wireless systems where the user location and density is unpredictable, it results in unpredictable (with frequently abrupt changes) in throughput, which is inconvenient to the user and renders some applications (e.g. the delivery of services requiring predictable throughput) impractical or of low quality. Thus, prior art multi-user wireless systems still leave much to be desired in terms of their ability to provide predictable and/or high-quality services to users.

[0026] Despite the extraordinary sophistication and complexity that has been developed for prior art multi-user wireless systems over time, there exist common themes: transmissions are distributed among different base stations (or ad hoc

transceivers) and are structured and/or controlled so as to avoid the RF waveform transmissions from the different base stations and/or different ad hoc transceivers from interfering with each other at the receiver of a given user.

[0027] Or, to put it another way, it is taken as a given that if a user happens to receive transmissions from more than one base station or ad hoc transceiver at the same time, the interference from the multiple simultaneous transmissions will result in a reduction of the SNR and/or bandwidth of the signal to the user which, if severe enough, will result in loss of all or some of the potential data (or analog information) that would otherwise have been received by the user.

[0028] Thus, in a multiuser wireless system, it is necessary to utilize one or more spectrum sharing approaches or another to avoid or mitigate such interference to users from multiple base stations or ad hoc transceivers transmitting at the same frequency at the same time. There are a vast number of prior art approaches to avoiding such interference, including controlling base stations' physical locations (e.g. cellularization), limiting power output of base stations and/or ad hoc transceivers (e.g. limiting transmit range), beamforming/sectorization, and time domain multiplexing. In short, all of these spectrum sharing systems seek to address the limitation of multiuser wireless systems that when multiple base stations and/or ad hoc transceivers transmitting simultaneously at the same frequency are received by the same user, the resulting interference reduces or destroys the data throughput to the affected user. If a large percentage, or all, of

the users in the multi-user wireless system are subject to interference from multiple base stations and/or ad hoc transceivers (e.g. in the event of the malfunction of a component of a multi-user wireless system), then it can result in a situation where the aggregate throughput of the multi-user wireless system is dramatically reduced, or even rendered non-functional..

[0029] Prior art multi-user wireless systems add complexity and introduce limitations to wireless networks and frequently result in a situation where a given user's experience (e.g. available bandwidth, latency, predictability, reliability) is impacted by the utilization of the spectrum by other users in the area. Given the increasing demands for aggregate bandwidth within wireless spectrum shared by multiple users, and the increasing growth of applications that can rely upon multi-user wireless network reliability, predictability and low latency for a given user, it is apparent that prior art multi-user wireless technology suffers from many limitations. Indeed, with the limited availability of spectrum suitable for particular types of wireless communications (e.g. at wavelengths that are efficient in penetrating building walls), it may be the case that prior art wireless techniques will be insufficient to meet the increasing demands for bandwidth that is reliable, predictable and low-latency.

[0030] What is needed is a multiuser wireless system that does not suffer from the aforementioned limitations:

(a) limitations in aggregate bandwidth in a given amount of spectrum;

(b) lack of reliable, predictable and low-latency communications for a given user;

(c) one user's use of the wireless network negatively impacting another user's use;

(d) lack of flexibility in the placement of transceivers and/or antennas that form the multi-user wireless system;

(e) lack of flexibility allowing transceivers and/or antennas to be installed either by commercial network providers or by individuals; or

(f) impractical or expensive implementations.

BRIEF DESCRIPTION OF THE DRAWINGS

[0001] A better understanding of the present invention can be obtained from the following detailed description in conjunction with the drawings, in which:

[0002] **FIG. 1** illustrates a prior art MIMO system.

[0003] **FIG. 2** illustrates an *N*-antenna Base Station communicating with a plurality of Single-antenna Client Devices.

[0004] **FIG. 3** illustrates a three Antenna Base Station communicating with three Single-Antenna Client Devices

[0005] **FIG. 4** illustrates training signal techniques employed in one embodiment of the invention.

[0006] **FIG. 5** illustrates channel characterization data transmitted from a client device to a base station according to one embodiment of the invention.

[0007] **FIG. 6** illustrates a Multiple-Input Distributed-Output ("MIDO") downstream transmission according to one embodiment of the invention.

[0008] **FIG. 7** illustrates a Multiple-Input Multiple Output ("MIMO") upstream transmission according to one embodiment of the invention.

[0009] **FIG. 8** illustrates a base station cycling through different client groups to allocate throughput according to one embodiment of the invention.

[0010] **FIG. 9** illustrates a grouping of clients based on proximity according to one embodiment of the invention.

[0011] **FIG. 10** illustrates an embodiment of the invention employed within an NVIS system.

[0012] **FIG. 11** illustrates an embodiment of the DIDO transmitter with I/Q compensation functional units.

[0013] **FIG. 12** a DIDO receiver with I/Q compensation functional units.

[0014] **FIG. 13** illustrates one embodiment of DIDO-OFDM systems with I/Q compensation.

[0015] **FIG. 14** illustrates one embodiment of DIDO 2 x 2 performance with and without I/Q compensation.

[0016] **FIG. 15** illustrates one embodiment of DIDO 2 x 2 performance with and without I/Q compensation.

[0017] **FIG. 16** illustrates one embodiment of the SER (Symbol Error Rate) with and without I/Q compensation for different QAM constellations.

[0018] **FIG. 17** illustrates one embodiment of DIDO 2 x 2 performances with and without compensation in different user device locations.

[0019] **FIG. 18** illustrates one embodiment of the SER with and without I/Q compensation in ideal (i.i.d. (independent and identically-distributed)) channels.

[0020] **FIG. 19** illustrates one embodiment of a transmitter framework of adaptive DIDO systems.

[0021] **FIG. 20** illustrates one embodiment of a receiver framework of adaptive DIDO systems.

[0022] **FIG. 21** illustrates one embodiment of a method of adaptive DIDO-OFDM.

[0023] **FIG. 22** illustrates one embodiment of the antenna layout for DIDO measurements.

[0024] **FIG. 23** illustrates embodiments of array configurations for different order DIDO systems.

[0025] **FIG. 24** illustrates the performance of different order DIDO systems.

[0026] **FIG. 25** illustrates one embodiment of the antenna layout for DIDO measurements.

[0027] **FIG. 26** illustrates one embodiment of the DIDO 2 x 2 performance with 4-QAM and FEC rate ½ as function of the user device location.

[0028] **FIG. 27** illustrates one embodiment of the antenna layout for DIDO measurements.

[0029] **FIG. 28** illustrates how, in one embodiment, DIDO 8 x 8 yields larger SE than DIDO 2 x 2 for lower TX power requirement.

[0030] **FIG. 29** illustrates one embodiment of DIDO 2 x 2 performance with antenna selection.

[0031] **FIG. 30** illustrates average bit error rate (BER) performance of different DIDO precoding schemes in i.i.d. channels.

[0032] **FIG. 31** illustrates the signal to noise ratio (SNR) gain of ASel as a function of the number of extra transmit antennas in i.i.d. channels.

[0033] **FIG. 32** illustrates the SNR thresholds as a function of the number of users (*M*) for block diagnalization (BD) and ASel with 1 and 2 extra antennas in i.i.d. channels.

[0034] **FIG. 33** illustrates the BER versus per-user average SNR for two users located at the same angular direction with different values of Angle Spread (AS).

[0035] **FIG. 34** illustrates similar results as FIG. 33, but with higher angular separation between the users.

[0036] **FIG. 35** plots the SNR thresholds as a function of the AS for different values of the mean angles of arrival (AOAs) of the users.

[0037] **FIG. 36** illustrates the SNR threshold for an exemplary case of five users.

[0038] **FIG. 37** provides a comparison of the SNR threshold of BD and ASel, with 1 and 2 extra antennas, for two user case.

[0039] **FIG. 38** illustrates similar results as FIG. 37, but for a five user case.

[0040] **FIG. 39** illustrates the SNR thresholds for a BD scheme with different values of AS.

[0041] **FIG. 40** illustrates the SNR thresholds in spatially correlated channels with AS= 0.1^{o} for BD and ASel with 1 and 2 extra antennas.

[0042] **FIG. 41** illustrates the computation of the SNR thresholds for two more channel scenarios with AS= 5^{o}.

[0043] **FIG. 42** illustrates the computation of the SNR thresholds for two more channel scenarios with AS= 10^{o}.

[0044] **FIGS. 43-44** illustrate the SNR thresholds as a function of the number of users (*M*) and angle spread (AS) for BD and ASel schemes, with 1 and 2 extra antennas, respectively.

[0045] **FIG 45** illustrates a receiver equipped with frequency offset estimator/compensator.

[0046] **FIG. 46** illustrates DIDO 2 × 2 system model according to one embodiment of the invention.

[0047] **FIG. 47** illustrates a method according to one embodiment of the invention.

[0048] **FIG. 48** illustrates SER results of DIDO 2 × 2 systems with and without frequency offset.

[0049] **FIG. 49** compares the performance of different DIDO schemes in terms of SNR thresholds.

[0050] **FIG. 50** compares the amount of overhead required for different embodiments of methods.

[0051] **FIG. 51** illustrates a simulation with a small frequency offset of f_{max} = 2Hz and no integer offset correction.

[0052] **FIG. 52** illustrates results when turning off the integer offset estimator.

[0053] **FIG. 53** illustrates downlink spectral efficiency (SE) in [bps/Hz] as a function of mutual information in [bps/Hz].

[0054] **FIG. 54** illustrates average per-user symbol error rare (SER) performance as a function of the mutual information in [bps/Hz].

[0055] **FIG. 55** illustrates average per-user SER performance as a function of the minimum mutual information in [bps/Hz] and the thresholds used to switch between different DIDO modes.

[0056] **FIG. 56** illustrates average per-user SER vs. SNR for fixed modulation and adaptive DIDO systems.

[0057] **FIG. 57** illustrates downlink SE vs. SNR for fixed modulation and adaptive DIDO systems.

[0058] **FIG. 58** illustrates average per-user SER vs. SNR for adaptive DIDO systems with different thresholds.

[0059] **FIG. 59** illustrates downlink SE vs. SNR for adaptive DIDO systems with different thresholds

[0031] **FIG. 60** illustrates average per-user SER performance as a function of the minimum singular value of the effective channel matrix and the CQI threshold for 4-QAM constellation.

[0032] **FIG. 61** illustrates one embodiment of a circular topology of base transceiver stations (DIDO antennas)

[0033] **FIG. 62** illustrates an one embodiment of an alternate arrangement of DIDO antennas.

[0034] **FIG. 63** illustrates one embodiment in which a base station network (BSN) is used to deliver precoded baseband data from the centralized processors (CPs) to DIDO antennas.

[0035] **FIG. 64** illustrates one embodiment in which the BSN is used to carry modulated signals.

[0036] **FIG. 65** illustrates one embodiment comprised of two DIDO base stations perfectly synchronized and two users with Line Of Sight (LOS) channels

[0037] **FIG. 66** illustrates the path loss of DIDO at 85MHz and 400MHz using the Hata-Okumura model.

[0038] **FIG. 67** illustrates the period maximum delay between channel state information and data transmission as a function of the relative velocity between transmitter and receiver for different frequencies in the UHF band.

[0039] **FIG. 68** illustrates propagation effects in DIDO systems for three different carrier frequencies.

[0040] **FIG. 69** illustrates the areas in the US territory currently covered by transceiver stations operating in the Maritime band. The colors identify the

number of active channels (out of the 146 channels available in the Maritime band) that would cause harmful interference to DIDO-NVIS stations at any location.

[0041] **FIG. 70** illustrates sunspot number from the January 1900 throughout June 2009.

[0042] **FIG. 71** illustrates the path loss of WiMAX, LTE and NVIS systems.

[0043] **FIG. 72** illustrates the locations of DIDO-NVIS transmitter (TX) and receiver (RX) stations

[0044] **FIG. 73** illustrates DIDO-NVIS receive antenna location. “lambda” denotes the wavelength at 3.9MHz (~77meters)

[0045] **FIG. 74** illustrates typical 4-QAM constellations demodulated at three users’ locations over DIDO-NVIS links.

[0046] **FIG. 75** illustrates SER as a function of PU-SNR for DIDO-NVIS 3x3.

[0047] **FIG. 76** illustrates DIDO-NVIS cells across the territory of the 48 contiguous states of the USA.

DETAILED DESCRIPTION

1. DIDO system description

[0048] One solution to overcome many of the above prior art limitations is an embodiment of Distributed-Input Distributed-Output (DIDO) technology. DIDO technology is described in the following patents and patent applications, all of which are assigned the assignee of the present patent and are incorporated by reference:

[0049] U.S. Patent No. 7,599,420, filed August 20, 2007, issued Oct. 6, 2009, entitled “System and Method for Distributed Input Distributed Output Wireless Communication”;

[0050] U.S. Application Serial No. 12/143,503, filed June 20, 2008 entitled, ”System and Method For Distributed Input-Distributed Output Wireless Communications”;

[0051] U.S. Application Serial No. 11/894,394, filed August 20, 2007 entitled, ”System and Method for Distributed Input Distributed Output Wireless Communications”;

[0052] U.S. Application Serial No. 11/894,362, filed August 20, 2007 entitled, “System and method for Distributed Input-Distributed Wireless Communications”:

[0053] U.S. Application Serial No. 11/894,540, filed August 20, 2007 entitled “System and Method For Distributed Input-Distributed Output Wireless Communications”

[0054] U.S. Application Serial No. 11/256,478, filed October 21, 2005 entitled "System and Method For Spatial-Multiplexed Tropospheric Scatter Communications";

[0055] U.S. Patent No. 7,418,053, filed July 30, 2004, issued August 26, 2008, entitled "System and Method for Distributed Input Distributed Output Wireless Communication";

[0056] U.S. Application Serial No. 10/817,731, filed April 2, 2004 entitled "System and Method For Enhancing Near Vertical Incidence Skywave ("NVIS") Communication Using Space-Time Coding.

[0057] The foregoing patent applications are referred to below as the "related applications."

[0058] DIDO systems are described in the related application U.S. Patent 7,418,053, where multiple antennas of the same DIDO base station in **Figure 2** work cooperatively to pre-cancel interference and create parallel non-interfering data streams to multiple users. These antennas, with or without local transmitters and/or receivers may be spread across a wide coverage area and be interconnected to the same DIDO base station via wired or wireless links, including networks such as the Internet. For example, as disclosed in related US Patent 7,418,053 in the paragraph starting at column 6, line 31, a single base station may have its antennas located very far apart, potentially resulting in the base station's antenna array occupying several square kilometers. And, for example as disclosed in related US Patent 7,599,420 in the paragraph starting at column 17 line 4, and in paragraphs [0142] of U.S. Application Serial No.

11/894,362 and U.S. Application Serial No. 11/894,540, the separation of antennas from a single DIDO base station may be physically separated by 100s of yards or even miles, potentially providing diversity advantages, and the signals for each antenna installation may either processed locally at each antenna location or brought back to a centralized location for processing. Further, methods for practical deployment of DIDO systems, including addressing practical issues associated with processing signals with widely distributed DIDO antennas, are described in the related applications U.S. Patent No. 7,599,420, U.S. Application No. 11/894,362 and U.S. Application No. 11/894,540.

[0059] Recent publications [32,33] analyzed theoretically the performance of cooperative base stations in the context of cellular systems. In practice, when those cooperative base stations are connected to one another via wireless, wired, or optical network (i.e., wide area network, WAN backbone, router) to share precoded data, control information and/or time/frequency synchronization information as described in U.S. Patent No. 7,418,053, U.S. Patent No. 7,599,420, U.S. Application Serial No. 11/894,362 and U.S. Application Serial No. 11/894,540 they function as multiple distributed antennas of a single DIDO base station as shown in **Figures 2 and 3**. In the system in [32,33], however, multiple base stations (or distributed antennas of the same DIDO base station) are constrained by their physical placements derived from cell planning, as in conventional cellular systems.

[0060] A significant advantage of DIDO systems over prior art systems is that DIDO systems enable the distribution of multiple cooperative distributed

antennas, all using the same frequency at the same time in the same wide coverage area, without significantly restricting the physical placement of the distributed antennas. In contrast to prior art multi-user systems, which avoid interference from multiple base transmitters at a given user receiver, the simultaneous RF waveform transmissions from multiple DIDO distributed antennas *deliberately* interfere with each other at each user's receiver. The interference is a precisely controlled constructive and destructive interference of RF waveforms incident upon each receiving antenna which, rather than impairing data reception, *enhances* data reception. It also achieves a valuable goal: it results in multiple simultaneous non-interfering channels to the users via space-time precoding techniques, increasing the aggregate throughput in a given coverage area, increasing the throughput to a given user, and significantly increasing the reliability and predictability of throughput to a given user.

[0061] Thus, when using DIDO, multiple distributed antenna RF waveform transmission interference and user channel interference have an *inverse* relationship: multiple distributed antenna RF waveform *interference* results in simultaneous *non-interfering* user channels.

[0062] With prior art multi-user systems, multiple base station (and/or ad hoc transceivers) RF waveform transmission interference and user channel interference have a *direct* relationship: multiple base station (and/or ad hoc transceivers) RF waveform *interference* results in simultaneous *interfering* user channels.

[0063] So, what DIDO utilizes and relies upon to achieve performance far beyond prior art systems is exactly what is avoided by, and results in impairment of, prior art systems.

[0064] And, because the number of non-interfering channels (and aggregate throughput) grows largely proportionately with the number of DIDO distributed antennas (unlike MU-MIMO systems, where the aggregate throughput asymptotically levels off as the number of cluster antennas at a base station is increased), the spectrum utilization of a given coverage area can be scaled as the number of users in an area scales, all without subdividing the coverage area by frequency or sector, and without requiring significant restrictions on the placement of DIDO distributed antennas. This results in enormous efficiencies in spectrum utilization and aggregate user downlink (DL) and uplink (UL) data rates, and enormous placement flexibility for either commercial or consumer base station installation.

[0065] In this way, DIDO opens the door to a very large increase in multi-user wireless spectrum efficiency by specifically doing exactly what prior art systems had been meticulously designed to avoid doing.

[0066] As illustrated in **Figures 61-62**, in one embodiment, DIDO systems consist of:

- **DIDO Clients 6110**: wireless devices that estimate the channel state information (CSI), feedback the CSI to the transmitters and demodulate precoded data. Typically each user would have a DIDO client device.

- **DIDO Distributed Antennas 6113**: wireless devices interconnected via a network that transmit precoded data to all DIDO clients. A wide variety of network types can be used to interconnect the distributed antennas 6113 including, but not limited to, a local area network (LAN), a wire area network (WAN), the Internet, a commercial fiber optic loop, a wireless network, or any combination thereof. In one embodiment, to provide a simultaneous independent channel to each client, the number of DIDO distributed antennas is at least equal to the number of clients that are served via precoding, and thereby avoids sharing channels among clients. More DIDO distributed antennas than clients can be used to improve link reliability via transmit diversity techniques, or can be used in combination with multi-antenna clients to increase data rate and/or improve link reliability. Note that "distributed antenna", as used herein, may not be merely an antenna, but refers to a device capable of transmitting and/or receiving through at least one antenna. For example, the device may incorporate the network interface to the DIDO BTS 6112 (described below) and a transceiver, as well as an antenna attached to the transceiver. The distributed antennas 6113 are the antennas that the DIDO BTS 6112, utilizes to implement the DIDO multi-user system.
- **DIDO Base Transceiver Station ("BTS" or "base station") 6112**: computes the precoding weights based on the CSI obtained from all users in a DIDO system and sends precoded data to the DIDO distributed antennas. The BTS may be connected to the Internet, public switched telephone network (PSTN) or private networks to provide connectivity between users and such

networks . For example, upon clients' requests to access web content, the CP fetches data through the Internet and transmits data to the clients via the DIDO distributed antennas.

- **DIDO Base Station Network (BSN) 6111**: One embodiment of DIDO technology enables precisely controlled cooperation among multiple DIDO distributed antennas spread over wide areas and interconnected by a network. In one embodiment, the network used to interconnect the DIDO distributed antennas is a metro fiber optic ring (preferably, with the DIDO distributed antennas connecting to the metro fiber optic ring at locations where it is convenient), characterized by relatively low latency and reasonably high throughput (e.g. throughput to each DIDO antenna comparable to the wireless throughput achievable from that DIDO antenna). The fiber optic ring is used to share control information and precoded data among different stations. Note that many other communication networks can be used instead of a metro fiber optic ring, including fiber optic networks in different topologies other than a ring, fiber-to-the-home (FFTH), Digital Subscriber Lines (DSL), cable modems, wireless links, data over power line, Ethernet, etc. The communication network interconnecting the DIDO distributed antennas may well be made up of a combination of different network technologies. For example, some DIDO distributed antennas may be connected to DSL, some to fiber, some to cable modems, some on Ethernet, etc. The network may be a private network, the Internet, or a combination. Thus, much like prior art consumer and commercial WiFi base stations are connected via a variety of network technologies, as is

convenient at each location, so may be the DIDO distributed antennas. Whatever form this network takes, be it a uniform technology, or a variety of technologies, it is referred herein as the Base Station Network or "BSN." In one embodiment of the BSN, there is an approximate 10-30msec round trip time (RTT) latency between BTS and the DIDO distributed antennas, due to the packet switched nature of existing fiber or DSL networks. The variance of that latency (i.e., jitter) is of the order of milliseconds. If lower latency (i.e., <1msec) and jitter is required for DIDO systems, the BSN may be designed with dedicated fiber links. Depending on the quality of service offered to different DIDO clients, a combination of low and high latency BSNs can be employed.

[0067] Depending on the layout of the network interconnecting the DIDO distributed antennas 6113, one or multiple DIDO BTSs can be used in a given coverage area. We define a *DIDO cell* as the coverage area served by one DIDO BTS. One embodiment with circular topology is depicted in **Figure 61** (the dots are the DIDO clients 6110, and crosses are the DIDO distributed antennas 6113). In more realistic scenarios the BSN does not have circular shape as in **Figure 61**. In fact, the DIDO distributed antennas may be placed randomly within the DIDO cell, wherever connections to the BSN are available and/or conveniently reached, as depicted in **Figure 62**. If the coverage area is one city, in one embodiment multiple DIDO cells (associated to multiple DIDO BTSs) can be designed to cover the whole city. In that case, cellular planning is required to allocate different frequency channels to adjacent DIDO cells to avoid inter-cell interference. Alternatively, one DIDO cell can be designed to cover the entire

city at the expense of higher computational complexity at the DIDO BTS (e.g., more CSI data from all the users in the same DIDO cell to be processed by the BTS) and larger throughput requirement over the network interconnecting the DIDO distributed antennas.

[0068] In one embodiment of the invention, the BSN 6111 is used to deliver precoded baseband data from the BTS 6112 to the DIDO distributed antennas 6113. As shown in **Figure 63,** the DIDO distributed antenna 6313 includes a radio transceiver 6330 equipped with digital-to-analog converter (DAC), analog-to-digital converter (ADC), mixer and coupled to (or including) a power amplifier 6338. Each DIDO distributed antenna receives the baseband precoded data 6332 over the BSN 6311 (such as fiber optic cable 6331) from the BTS 6312, modulates the signal at the carrier frequency and transmits the modulated signal to the clients over the wireless link via antenna 6339. As illustrated in **Figure 63**, a reference clock signal is provided to the radio transceiver by a reference clock generator 6333.

[0069] In another embodiment of the invention, the BSN is used to carry modulated signals as illustrated in **Figure 64**, which shows the structure of DIDO systems employing RF-over-fiber. For example, if the BSN is a fiber optic channel 6431 with sufficient bandwidth, a radio frequency (RF) modulated signal is sent over the fiber according to a system such as that described in [17,18]. Multiple radios 6440 (up to as many as the number of DIDO distributed antennas) can be employed at the BTS 6412 to modulate the baseband signals carrying precoded data. The RF modulated signal is converted into optical signal

by the radio interface unit (RIU) 6441. One example of an RIU for UHF is the FORAX LOS1 by Syntonics [19]. The optical signal propagates from the BTS to the DIDO distributed antennas 6413 over the BSN 6411. The DIDO distributed antennas are equipped with one amplifier interface unit (AIU) 6445 that converts the optical signal to RF. The RF signal is amplified by amplifier 6448 and sent through the antenna 6449 over the wireless link. An advantage of DIDO with RF-over-fiber solution is significant reduction in complexity and cost of the DIDO distributed antennas. In fact, the DIDO distributed antenna consists only of one AIU 6445, power amplifier 6448 and antenna 6449. Moreover, if the fiber propagation delay is known and fixed, all the radios at the BTS can be locked to the same reference clock 6442 as in **Figure 64**, with an appropriate delay to compensate for the propagation delay, and no time/frequency synchronization is required at the DIDO distributed antenna, thereby simplifying further the complexity of DIDO systems.

[0070] In another embodiment, existing cellular towers with antennas, transceivers, and backhaul connectivity are reconfigured such that the backhauls are connected to a DIDO BTS 6112. The backhaul connectivity becomes functionally equivalent to the BSN 6111. Then, as described previously, the cellular transceivers and antennas become functionally equivalent to the DIDO distributed antennas 6113. Depending on the transceivers and antennas installed in existing cellular phone towers, they may need to be reconfigured or replaced, so as to be able to operate in a DIDO configuration. For example, the transmitters may have been configured to transmit at a low power level so as to

not cause interference with a nearby cell using the same frequency. With DIDO, there is no need to mitigate such waveform interference, and indeed, such waveform interference increases the spectrum utilization of the coverage area beyond that achievable in a prior art cellular configuration.

[0071] In another embodiment, existing cellular towers are partially used for DIDO, as described in the preceding paragraph, and partially used as conventional cellular towers, so as to support compatibility with existing cellular devices. Such a combined system can be implemented in a number of different ways. In one embodiment, TDMA is used to alternate between DIDO use and conventional cellular use. So, at any given time, the cellular towers are used for only DIDO or for conventional cellular communications.

[0072] Some key features and benefits of DIDO systems, compared to typical multi-user wireless systems, including cellular systems employing MU-MIMO techniques, are:

- Large spatial diversity: Because DIDO distributed antennas can be located anywhere within a coverage area, and work cooperatively without channel interference, this results in larger transmit antenna spacing and multipath angular spread. Thus, far more antennas can be used, while still maintaining spatial diversity. Unlike prior art commercial or consumer base stations, DIDO distributed antennas can be placed anywhere there is a reasonably fast Internet (or other network) connection, even if it is only a few feet from the ground, indoor or outdoor. Reduced coverage (e.g., due to lower transmit antenna height or

physical obstacles) can be compensated by larger transmit power (e.g., 100W rather than ~200mW as in typical cellular systems in urban areas or ~250mW in typical WiFi access points) because there is no concern (or far less concern than with prior art cellular systems) about higher-powered transmissions interfering with another cell or WiFi access point using the same frequency. Larger spatial diversity translates into a larger number of non-interfering channels that can be created to multiple users. Theoretically (e.g., due to large antenna spacing and angular spread), the number of spatial channels is equal to the number of transmit DIDO stations. That yields an *n*X improvement in aggregate DL data rate, where *n* is the number of DIDO stations. For example, whereas prior art cellular system might achieve a maximum of net 3X improvement in aggregate spectrum utilization, a DIDO system might achieve a 10X, 100X or even greater improvement in aggregate spectrum utilization.

- Uniform rate distribution: Since the DIDO distributed antennas can be dispersed throughout a wide area, far more users can be characterized by good signal-to-noise ratio (SNR) from one or more DIDO distributed antennas. Then, far more users can experience similar data rates, unlike cellular systems where cell-edge users suffer from poor link-budget and low data rate.
- Cost effective: DIDO distributed antennas can be designed as inexpensive devices with single antenna transceivers (similar to WiFi access points). Moreover, they do not require costly real estate or expensive installation as cell towers because of the ability to flexibly locate them within the coverage area.

2. Methods for Implementation and Deployment of DIDO systems

[0073] The following describes different embodiments of practical deployment of DIDO systems.

a. Downlink channel

[0074] The general algorithm used in one embodiment to enable DIDO communications over wireless links is described as follows.

- CSI Computation: All DIDO clients compute the CSI from all DIDO distributed antenna transmitters based on training sequences received from DIDO distributed antennas as shown in **Figure 4** . The CSI is fed back wirelessly from DIDO clients to DIDO distributed antennas 6113 via TDMA or MIMO techniques as described in the related applications and in **Figure 5**, and then the DIDO distributed antennas 6113 send the CSI via the DIDO BSN 6111 to the DIDO BTS 6112.
- Precoding Computation: the DIDO BTS 6112 computes the precoding weights from the CSI feedback from the entire DIDO cell. Precoded data are sent from the DIDO BTS 6112 to the DIDO distributed antennas in **Figure 6** via the DIDO BSN 6111. One precoded data stream is sent to each of the DIDO distributed antennas.
- Precoded Data Transmission: the DIDO distributed antennas transmit precoded data to all clients over the wireless links.
- Demodulation: the DIDO clients demodulate the precoded data streams.

[0075] In DIDO systems, the *feedback loop* in **Figures 19-20** consists of: transmission of the training sequence for channel estimation from DIDO

distributed antennas to clients; CSI estimation by clients; CSI feedback from clients via the DIDO distributed antennas through the DIDO BSN 6111 to the DIDO BTS 6112; precoded data transmission from DIDO BTS 6112 through the DIDO BSN 6111 to DIDO distributed antennas to clients. To guarantee the CSI is up-to-date for successful DIDO precoding and data demodulation at the client side, the delay over the feedback loop should be lower than the channel coherence time. The feedback loop delay depends on the BTS computational resources relative to the computational complexity of the DIDO precoding as well as latency over the BSN. Processing at each client and DIDO distributed antenna is typically very limited (i.e., on the order of a microsecond or less with a single DSP or CPU), depending on the hardware and processor speed. Most of the feedback loop delay is due the latency for transmission of precoded data from the DIDO BTS 6112 to the DIDO distributed antennas 6113 over the DIDO BSN 6111 (e.g., on the order of milliseconds).

[0076] As discussed above, a low latency or high latency BSN can be used in DIDO systems depending on the available network. In one embodiment, the DIDO BTS 6112 switches among two or more types of BSN network infrastructure based on the each users' channel coherence time. For example, outdoor clients are typically characterized by more severe Doppler effects due to the potential of fast mobility of clients or objects within the channel (i.e., resulting in low channel coherence time). Indoor clients have generally fixed wireless or low mobility links (e.g., high channel coherence time). In one embodiment, DIDO distributed antennas connected to low latency BSN network infrastructure (e.g.,

dedicated fiber rings) are assigned to outdoor clients, whereas DIDO distributed antennas connected to high latency BSN network infrastructure (e.g., consumer Internet connections such as DSL or cable modems) are assigned to serve indoor clients. To avoid interference among transmissions to the different types of clients, indoor and outdoor clients can be multiplexed via TDMA, FDMA or CDMA schemes.

[0077] Moreover, DIDO distributed antennas connected to low latency BSNs can also be used for delay-sensitive algorithms such as those used for client time and frequency synchronization.

[0078] We observe that DIDO provides an inherently secure network when more than one DIDO distributed antenna is used to reach a user. In fact, the precoded streams from the BTS to the DIDO distributed antennas consist of linear combinations of data (for different clients) and DIDO precoding weights. Then, the data stream sent from the BTS to the BSN generally cannot be demodulated at the DIDO distributed antenna, since the DIDO distributed antenna is unaware of the precoding weights used by the BTS. Also, the precoding weights change over time as the complex gain of the wireless channels from DIDO distributed antenna-to-client varies (due to Doppler effects), adding an additional level of security. Moreover, the data stream intended to each client can be demodulated only at the client's location, where the precoded signals from all transmit DIDO distributed antennas recombine to provide user interference-free data. At any other location, demodulation of data intended to one particular user is not possible due to high levels of inter-user interference.

b. Uplink channel

[0079] In the uplink (UL) channel, the clients send data (e.g., to request Web content to the DIDO BTS 6112 from the Internet), CSI and control information (e.g., time/frequency synchronization, channel quality information, modulation scheme, etc.). In one embodiment, there are two alternatives for the UL channel that may be used separately or in combination: i) clients communicate directly to the DIDO BTS 6112 via TDMA, FDMA or CDMA schemes; ii) clients communicate to multiple DIDO distributed antennas by creating spatial channels via MIMO techniques as in **Figure 7** (in the MIMO case, however, transmission time synchronization among clients is required).

c. Time and frequency synchronization

[0080] In one embodiment, the DIDO distributed antennas are synchronized in time and frequency. If RF-over-fiber is employed as in **Figure 64**, all radio transceivers at the BTS are locked to the same reference clock 6442, thereby guaranteeing perfect time and frequency synchronization. Assuming negligible jitter over the DIDO BSN 6111, artificial delays can be added to the transmit RF waveforms at the DIDO BTS 6112 side to compensate for propagation delays over the DIDO BSN 6111 to different DIDO distributed antennas.

[0081] If the DIDO BSN 6111 is used to carry baseband waveforms as in **Figure 63**, time and frequency synchronization is required for the radio transceivers at

different DIDO distributed antennas. There are various methods to achieve this synchronization, and more than one method can be used at once.

i. Time and frequency synchronization via GPSDO

[0082] In one embodiment time/frequency synchronization is achieved by connecting the transmitter in radio transceiver 6330 to a GPS Disciplined Oscillators (GPSDO). A crystal clock with high frequency stability and low jitter (e.g., Oven-Controlled Crystal Oscillator, OCXO) is used in one embodiment.

ii. Time and frequency synchronization via power line reference

[0083] An alternate embodiment utilizes the 60Hz (in the United States, 50Hz in other regions) signal available over power lines as a common clock reference for all transmitters. Based on empirical measurements, the jitter of the 60Hz reference signal (after low pass filtering) can be on the order of 100 nanoseconds. It would be necessary, however, to compensate for deterministic offsets due to variable propagation path length along the power lines at different locations.

iii. Time and frequency synchronization with free-running clocks

[0084] An alternative embodiment is used to compensate the time and frequency offsets across different DIDO distributed antennas whose clocks are not synchronized to an external clock reference, but rather are free-running as described in the related U.S. Patent No. 7,599,420 and in **Figures 45, 46** and **47**.

- Coarse Time Synchronization: In one embodiment, all DIDO distributed antennas have free-running clocks as illustrated in **Figure 46** that can generate a periodic reference signal (one pulse per second (PPS) in one embodiment). The DIDO BTS 6112 sends an initial trigger signal to all DIDO distributed antennas via the DIDO BSN 6111 to trigger their transmission at the next PPS. The roundtrip time (RTT) over the BSN is assumed to be of the order of particular time interval (10msec in one embodiment, or ~5ms in each direction), so all DIDO distributed antennas will start transmitting with a relative time offset of at most 1sec+5msec. Each DIDO distributed antenna sends one training signal (i.e., Zadoff-Chu sequence or methods for GPS systems in [6]) to all users for initial time offset estimation. Alternatively, only a subset of users (those with highest SNR) can be selected to reduce the complexity of the algorithm. Training signals from different DIDO distributed antennas are orthogonal or sent via TDMA/FDMA to avoid interference. The users estimate the relative time of arrival from every transmitter by correlating the receive signal with the known training sequence. The same training sequence can be sent periodically and the correlation can be averaged over a long period of time (e.g., on the order of minutes in one embodiment) to average-out multipath effects, particularly in the case of mobile users. In one embodiment of the invention, time-reversal techniques [31] can be applied to pre-compensate for multipath effects at the transmitter and obtain precise time of arrival estimates. Then, the users compute the delays (i.e., deterministic time offsets) of each transmitter relative to a given

time reference (e.g., one of the DIDO distributed antennas can be chosen as an absolute time reference). The relative time offset is fed back from the clients to the DIDO distributed antennas or directly to the DIDO BTS 6112. Then, each DIDO antenna averages the time offset information obtained from all the users and adjusts its PPS (and clock reference) according to that.

[0085] In one embodiment, the time offset is computed from measurements by many users to average out the difference in propagation delay across users. For example, **Figure 65** shows one case with two DIDO distributed antennas 6551 and 6552 perfectly synchronized (e.g., via GPSDO) and two users 6553 and 6554 with Line Of Sight (LOS) channels. We use TX1 6551 as the absolute time reference. Since we assume the transmitters are perfectly synchronized, the average time offset between users should be zero. However, if we average the offset information only across two users, as in **Figure 65**, the average offset of TX2 6552 relative to TX1 6551 would be (7+(-2))/2 = 2.5usec. By relying on the Monte Carlo method, we can average out this effect as the number of users increases. It is possible to simulate the bias of this algorithm depending on the TX/RX distribution and channel delay spread.

- Fine Time Synchronization: Once the coarse time offset is removed, DIDO distributed antennas can keep running the algorithm periodically to improve the offset estimates. Moreover, the DIDO transmit stations are typically at fixed locations (e.g. transceiver DIDO distributed antennas connected to the DIDO BSN 6111). Hence the algorithm should converge after a period of time. The

same algorithm is rerun every time one DIDO distributed antenna changes its location or a new DIDO distributed antenna is added to the DIDO BSN 6111.

- Frequency Offset Compensation: once the 1 PPS reference signals at all DIDO distributed antennas are synchronized, the DIDO distributed antennas send training to one or multiple users to estimate the relative frequency offset between stations. Then, the frequency offset compensation method described in the related U.S. Patent No. 7,599,420 and **Figure 47** is applied to transmit precoded data to all users while compensating for the offset. Note that for the best performance of this algorithm, two conditions need to be satisfied: i) good SNR between all DIDO transmitters and the user (or users) responsible for frequency offset estimation; ii) good clock stability: if the OCXOs at the DIDO distributed antennas are stable, the frequency offset estimation can be carried out only occasionally, thereby reducing the feedback information.

d. Control channel via the BSN

[0086] In one embodiment, the DIDO BSN 6111 is used for at least the following three purposes:

- CSI Feedback: The DIDO clients feedback the CSI wirelessly to the DIDO distributed antennas. If TDMA, FDMA or CDMA schemes are used for feedback, only one DIDO distributed antenna (the one with best SNR to all users) is selected to receive the CSI. If MIMO techniques are employed, all DIDO distributed antennas are used simultaneously to demodulate the CSI from all clients. Then the CSI is fed back from the DIDO distributed antennas to the DIDO BTS 6112 via the DIDO BSN 6111. Alternatively, the CSI can be fed back

wirelessly directly from the clients (or the DIDO distributed antennas) to a DIDO BTS 6112 equipped with one antenna via TDMA or CDMA schemes. This second solution has the advantage of avoiding latency caused by the DIDO BSN 6111, but may not be achievable if the wireless link between each of the clients (or the DIDO distributed antennas) and the DIDO BTS 6112 is not of high enough SNR and reliability. To reduce the throughput requirement over the UL channel, the CSI may be quantized or any number of limited feedback algorithms known in the art can be applied [28-30].

- Control Information: The DIDO BTS 6112 sends control information to the DIDO distributed antennas via the DIDO BSN 6111. Examples of control information are: transmit power for different DIDO distributed antennas (to enable power control algorithms); active DIDO distributed antenna IDs (to enable antenna selection algorithms); trigger signals for time synchronization and frequency offset values.
- Precoded data: the DIDO BTS 6112 sends precoded data to all DIDO distributed antennas via the DIDO BSN 6111. That precoded data is then sent from the DIDO distributed antennas synchronously to all clients over wireless links.

Case study 1: DIDO in UHF spectrum

a. UHF and microwave spectrum allocation

[0087] Different frequency bands are available in the United States as possible candidates for DIDO system deployment: (i) the unused television frequency

band between 54-698MHz (TV Channels 2-51 with 6MHz channel bandwidth), recommended by the White Spaces Coalition to deliver high speed Internet services; (ii) the 734-746MHz and 746-756MHz planned to be used for future developments of LTE systems by AT&T and Verizon, respectively; (iii) the 2.5GHz band for broadband radio service (BRS), consisting of 67.5MHz of spectrum split in five channels for future deployment of WiMAX systems.

b. Propagation channel in UHF spectrum

[0088] We begin by computing the path loss of DIDO systems in urban environments at different frequencies allocated for White Spaces. We use the Hata-Okumura model described in [7], with transmit and receive antenna heights of 1.5 meter (e.g., indoor installation of the DIDO distributed antennas) and 100W transmit power. To determine the range, we use -90dBm target receive sensitivity of typical wireless devices. **Figure 66** shows the path loss at 85MHz and 400MHz. In one embodiment, the expected range for DIDO systems is between 1Km and 3Km depending on the frequency.

[0089] Some prior art multi-user systems proposed for White Spaces have similar interference avoidance protocols as WiFi, although at UHF frequencies. We compare DIDO UHF results against the path loss for WiFi systems with 250mW transmit power. The range for WiFi extends only between 60 meters (indoor) and 200 meters (outdoor). Wider range achievable by DIDO systems is due to larger transmit power and lower carrier frequency (subject to generally lower attenuation from obstacles at UHF frequencies). But, we observe that WiFi

systems were deliberately limited in power because large transmit power would create harmful interference to other users using WiFi systems (or other users in the 2.4GHz ISM spectrum) because only one interfering access point can be transmitting at once, and by extending the range, increasingly more WiFi access points would interfere with one another. Contrarily, in DIDO systems inter-user interference is suppressed by multiple DIDO distributed antennas transmitting precoded data to the clients.

[0090] Next, we summarize the parameters that characterize time, frequency and space selectivity in UHF channels.

[0091] *Time selectivity* is caused by relative motion of transmitter and receiver that yields shift in the frequency domain of the received waveform, known as the Doppler effect. We model the Doppler spectrum according to the well known Jakes' model for rich scattering environments (e.g., urban areas), and compute the channel coherence time from the maximum Doppler shift according to [14]. As a rule of thumb, the channel complex gain can be considered constant over a period of time corresponding to one tenth of the channel coherence time ($\Delta t = T_C/10$). **Figure 67** shows the period Δt as a function of the relative velocity between transmitter and receiver for different frequencies in the UHF band.

[0092] In DIDO systems, Δt provides the constraint to the maximum delay that can be tolerated between estimation of the channel state information (CSI) and data transmission via DIDO precoding. For example, if the constraint is $\Delta t = 10$msec, the maximum speed that can be tolerated by DIDO systems is 4mph at 700MHz, 7mph at 400MHz, and 57mph at 50MHz. If a low latency network is

used for the BSN and the DIDO BTS 6112 is in the vicinity of the DIDO distributed antennas (so as to minimize network transit delay), far less than 10msec RTT can be achieved Δt. For example, if $\Delta t = 1$msec, at 400MHz, DIDO can tolerate approximately highway speeds of 70Mph.

[0093] *Frequency selectivity* depends on the channel delay spread. Typical values of delay spread for indoor environments are below 300 nsec [8-10]. In urban and suburban areas the delay spread ranges between 1 and 10 usec [11,12]. In rural environments it is typically on the order of 10 to 30 usec [11-13].

[0094] *Space selectivity* depends on the channel angular spread and antenna spacing at transmit/receive side. In urban environments, the channel angular spread is typically large due to rich scattering effects. In rich scattering environments, it was shown that the minimum antenna spacing (either at transmitter or receiver sides) to guarantee good spatial selectivity is about one wavelength [15,16] .

[0095] In **Figure 68** we summarize the main propagation effects in DIDO systems for three different carrier frequencies. We observe that lower frequencies provide better range and robustness to mobile speed at the expense of larger antenna size and distance between transceivers. A good tradeoff is offered by the 400 MHz band. This band can support pedestrian speed at a ~10msec limitation to transmit control information from the centralized processor to the DIDO distributed antennas over the Internet, and it can support highway speeds with a ~1msec limitation.

c. Practical implementation of DIDO systems in UHF spectrum

[0096] Based on the channel parameters and systems constraints described above, we provide one embodiment of DIDO system design in UHF spectrum as follows:

- Bandwidth: 5 to 10MHz, depending on UHF spectrum availability.
- Carrier frequency: 400MHz for best tradeoff between range/Doppler and antenna size/spacing.
- Modulation: orthogonal frequency division multiplexing (OFDM) is used to reduce receiver complexity and exploit channel frequency diversity (via interleaving) as in **Figure 11**. The cyclic prefix is 10usec, based upon the maximum delay spread expected in UHF channels, corresponding to 50 channel taps at 5MHz bandwidth. The OFDM waveform can be designed with 1024 tones, corresponding to ~5% loss in spectral efficiency. The total OFDM symbol length (including cyclic prefix and data) is 215usec.
- Packet Size: is limited by the latency over the DIDO BSN 6111 and Doppler effects. For example, the nominal RTT of one embodiment is 10msec. Then, the time required to send precoded data from the DIDO BST 6112 to the DIDO distributed antennas is ~5msec (half RTT). Assuming maximum users' speed of 7mph at 400MHz as in **Figure 68**, the channel gain can be considered constant for approximately 10msec. Hence, we use the remaining 5msec to send data and define the packet size as (5e-3/215e-6)≈23 OFDM symbols. Note that higher users' speeds yield a larger Doppler effect resulting in a lower number of

OFDM symbols sent per packet, unless the latency over the DIDO BSN 6111 can be reduced.

- CSI Estimation and Precoding: With the system parameters above, training for CSI estimation is sent every 5msec. The users estimate/feedback the CSI and ~5msec later they receive 5msec of precoded data to demodulate.
- DIDO Distributed Antenna Placement Within the Coverage Area: Although DIDO distributed antennas can be placed on existing cell towers, as a practical matter, given limited real estate available at existing cell towers, there may be a limited number of antenna locations available. For example, if a maximum of four antennas were placed on each tower this might yield up to 3x increase in data rate as shown in [4] (due to lack of spatial diversity). In this configuration, latency across DIDO transmitters is negligible, since they are all placed on the same tower, but without additional spatial diversity, the gain in spectral utilization will be limited. In one embodiment, the DIDO distributed antennas are placed in random locations throughout the coverage area all connected to the DIDO BSN 6111. Unlike a the coverage area of given cell in a prior art cellular system, which is based on transmission range from the cell tower, the coverage area of a DIDO cell is based instead on the transmission range of each DIDO distributed antenna, which in accordance with the path loss model in one embodiment is approximately 1Km. Thus, a user within 1Km of at least one DIDO distributed antenna will receive service, and a user within range of several DIDO distributed antennas will get non-interfering service from the DIDO distributed antennas within range.

Case study 2: DIDO in NVIS links

[0097] Another application of DIDO technology is in the HF band. The key advantage of HF systems is extended coverage in the 1-30MHz frequency band due to reflection off of the ionosphere. One example of propagation via the ionosphere is near-vertical incident skywave (NVIS) where signals sent towards the sky with high elevation angles from the horizon bounce off the ionosphere and return back to Earth. NVIS offers unprecedented coverage over conventional terrestrial wireless systems: NVIS links extend between 20 and 300 miles, whereas typical range of terrestrial systems is between 1 and 5 miles.

[0098] Hereafter, we present the characteristics of NVIS links based on results obtained from the literature and our experimental data. Then we present a practical implementation of DIDO systems in NVIS links that were described in the related U.S. Patent No. 7,418,053, U.S. Patent No. 7,599,420, U.S. Application No. 11/894,362, U.S. Application No. 11/894,394 U.S. Application No. 11/143,503 and U.S. Application No. 11/894,540 and in **Figure 10**.

a. HF spectrum allocation

[0099] The HF band is divided into several subbands dedicated to different types of services. For example, the Maritime band is defined between 4MHz and 4.438MHz. According to the Federal Communications Commission (FCC) licensing database (i.e., universal licensing systems, “ULS”), there are 1,070 licenses authorized to operate in this Maritime band. There are 146 channels of 3

KHz bandwidth each, covering 0.438MHz bandwidth. Most of the transceiver stations operating in the Maritime band are located along the coast of the US territory as depicted in **Figure 69**. Hence, DIDO-NVIS distributed antennas operating inland (far away from the coast) would not cause harmful interference to those Maritime stations or vessels at sea. Moreover, along the coast, cognitive radio techniques can be applied to detect channels in use and avoid transmission over DIDO-NVIS links in those channels. For example, if the DIDO-NVIS system is designed to transmit broadband OFDM waveforms (~1MHz bandwidth), the OFDM tones corresponding to active channels in the Maritime band can be suppressed to avoid interference.

[00100] Other portions of the HF spectrum are occupied by the Aeronautical band within [3,3.155] MHz and [3.4,3.5] MHz, and the Amateur radio bands defined in the ranges [1.8,2] MHz, [3.5,4] MHz, [5.3305,5.4035] MHz, [7,7.3] MHz, [10.10,10.15] MHz, [14,14.35] MHz, [18.068,18.168] MHz, [21,21.450] MHz, [24.89,24.99] MHz, [28,29.7] MHz. Our experimental measurements have shown that the Amateur radio band is mostly unutilized, particularly during daytime, allowing DIDO-NVIS links without causing harmful interference. Moreover, similarly to the Maritime band, coexistence of DIDO-NVIS systems with Amateur radio transceivers may be enabled by cognitive radio techniques.

b. NVIS propagation channel

[00101] We provide an overview of radio wave propagation through the ionosphere. Then we describe path loss, noise and time/frequency/space selectivity in typical NVIS channels.

[00102] The ionosphere consists of ionized gas or plasma. The plasma behaves as an electromagnetic shield for radio waves propagating from Earth upwards that are refracted and reflected back to Earth as in **Figure 10**. The stronger the level of ionization, the higher the critical frequency of the plasma and number of reflections in the ionosphere, resulting in improved signal quality over NVIS links. The ionization level depends on the intensity of solar radiations that strike the ionosphere producing plasma. One empirical measure of the solar activity is the *sunspot number* (SSN) that varies on 11-year cycles as shown in **Figure 70**. Hence, the performance of DIDO-NVIS systems is expected to vary throughout every 11-year cycle, yielding highest SNR and largest number of usable HF bands at the peak of the cycle.

[00103] Due to the absence of obstacles in NVIS links, the propagation loss is mostly due to free space *path loss* (i.e., Friis formula), without additional attenuation factors as in standard terrestrial wireless systems. Depending on the time of the day and incident angle to the ionosphere, propagating waveforms may suffer from additional 10-25dB loss due to attenuation from the D layer (i.e., lowest layer of the ionosphere). **Figure 71** compares the path loss in NVIS links against next generation wireless systems such as WiMAX and 3GPP long term evolution (LTE) in macrocells with 43dBm transmit power. For WiMAX and LTE

we used 2.5GHz and 700MHz carrier frequencies, respectively. NVIS links yield better signal quality (i.e., wider coverage) than standard systems for distances greater than ~1 mile.

[00104] Any wireless system is affected by thermal *noise* produced internally to radio receivers. In contrast to standard wireless systems, HF links are severely affected by other external noise sources such as: atmospheric noise, man-made noise and galactic noise. Man-made noise is due to environmental sources such as power lines, machinery, ignition systems, and is the main source of noise in the HF band. Its typical values range between -133 and -110 dBm/Hz depending on the environment (i.e., remote versus industrial).

[00105] From our Doppler measurements, we observed typical channel coherence time in NVIS links is of the order of seconds, That is about 100 times larger than the $\Delta t = 10$msec constraint on the DIDO feedback loop over the DIDO BSN 6111. Hence, in DIDO-NVIS systems a long feedback delay over the DIDO BSN 6111 can be tolerated due to extremely high channel coherence time. Note that our measurements assumed fixed wireless links. In case of mobile stations, the channel coherence time is expected to be of the order of 2sec in a very high speed scenario (i.e., vehicle or airplane moving at 200mph) that is still orders of magnitude higher than the latency over the DIDO BSN 6111.

[00106] Typical values of delay spreads in NVIS channels are around 2ms corresponding, corresponding to the roundtrip propagation delay Earth-ionosphere (about 300Km high). That value may be larger (~5msec) in presence of multilayer refractions in the ionosphere.

[00107] The angular spread in NVIS links is typically very small (less than 1 degree, based on our measurements and simulations). Hence, large antenna spacing is required to obtain spatially selective channels and exploit spatial diversity via DIDO techniques. Strangeways' simulator points to around twenty wavelengths required for a long distance HF skywave link [34,35]. Some experimental results for HF skywave with a spacing of around 0.7 wavelengths indicated high correlation [36,37]. Similar results were obtained from our measurements in NVIS links.

c. DIDO-NVIS experimental results

[00108] We measured the performance of DIDO-NVIS systems with a practical testbed consisting of three DIDO distributed antennas 6113 for transmission and three DIDO clients 6110 for reception . The transmitters are located in the area of Austin, Texas, as depicted in **Figure 72**: TX1 in central Austin, TX2 in Pflugerville, TX3 in Lake Austin. All three receivers are installed with antenna spacing of about 10 wavelengths as in **Figure 73**. All six transmit and receive antennas have the same orientation with respect to the direction of the North, since our goal was to evaluate DIDO-NVIS performance when only space diversity is available, without polarization diversity.

[00109] The three transmitting distributed antennas are locked to the same GPSDO that provide time and frequency reference. The three receiving DIDO clients have free-running clocks and synchronization algorithms are implemented

to compensate for time/frequency offsets. The carrier frequency is 3.9MHz, bandwidth is 3.125KHz and we use OFDM modulation with 4-QAM.

[00110] Typical 4-QAM constellations demodulated at the three DIDO client locations are depicted in **Figure 74**. Our DIDO-NVIS 3x3 testbed creates three simultaneous spatial channels over NVIS links by pre-cancelling inter-user interference at the transmit side and enabling successful demodulation at the users' side.

[00111] We compute the symbol error rate (SER) performance as a function of the per-user SNR (PU-SNR) over about 1000 channel realizations as in **Figure 75**. The dots are individual measurements for all three DIDO clients 6112 and the solid lines are the average per-user SER (PU-SER). The average SER across all three DIDO clients 6112 is denoted as A-SER. About 40dB receive SNR is require to successfully demodulate 4-QAM constellations in DIDO-NIVS 3x3 links with A-SER<1%. In fact, the transmit/receive antenna configuration in our experiments yields very low spatial diversity (due to relatively close proximity of the receive antennas, given the wavelength, and transmitters being all located on one side of the recevers rather than around the users). In more favorable conditions (i.e., transmitters placed around the users in circle and at larger distance as in **Figure 61**) much lower SNR (~20dB) is required to demodulate QAM constellations with DIDO-NVIS, as derived via simulations in realistic NVIS propagation channels.

d. Practical implementation of DIDO systems in NVIS links

[00112] Similarly to the case study 1, we provide one embodiment of DIDO-NVIS system design as follows:

- Bandwidth: 1-3 MHz, depending on HF spectrum availability. Larger bandwidths are less practical, since they require more challenging broadband antenna designs. For example, 3MHz bandwidth at 4MHz carrier frequency corresponds to fractional antenna bandwidth of 75%.
- Carrier Frequency: The HF frequencies corresponding to the plasma critical frequency of the ionosphere are between 1 and 10 MHz. Radio waves at lower frequencies (~1MHz) are typically reflected by the ionosphere at nighttime, whereas higher frequencies (~10MHz) at daytime. The frequency of optimal transmission (FOT) at given time of the day varies with the SSN. In practical DIDO-NVIS systems, the carrier frequency can be adjusted throughout the day depending on the FOT provided by the ionospheric maps.
- Transmit Power: Based on the path loss results in **Figure 71**, the average transmit power requirement for 1MHz bandwidth with receivers in remote areas (i.e., man-made noise level of -133dBm/Hz) is between 10dBm and 30dBm, depending on QAM modulation and forward error correction (FEC) coding schemes. In industrial areas (i.e., man-made noise level of -110dBm/Hz) those levels increase of about 23dB up to 33-53dBm, depending on QAM modulation and FEC coding schemes.
- Modulation: We assume OFDM modulation as in **Figure 11**. The cyclic prefix is 2msec (based upon typical delay spread expected in NVIS links)

corresponding to 2000 channel taps at 1MHz bandwidth. The OFDM waveform can be designed with 2^{14} tones, corresponding to ~10% loss in spectral efficiency due to cyclic prefix. The total OFDM symbol duration (including cyclic prefix and data) at 1MHz bandwidth is 18.4msec.

- Packet Size: is limited by the minimum channel coherence time expected in NVIS links. The minimum coherence time is approximately 1 sec and the channel gain can be considered constant over one tenth of that duration (~100msec) in the worst case scenario. Then, the packet size is about five OFDM symbols. The packet size can be dynamically adjusted as the coherence time varies over time.

- CSI Estimation and Precoding: With the system parameters above, training for CSI estimation is sent every ~100msec (or higher, when the coherence time increases). The users estimate/feedback the CSI and ~5msec later (i.e., latency over the BSN feedback loop) they receive 100msec of precoded data to demodulate.

- DIDO Distributed Antenna Placement Within the Coverage Area: One practical solution to implement DIDO-NVIS systems is to place multiple DIDO distributed antennas along the circumference of a circular region of radius ~100 miles as in **Figure 61**. These stations are connected to each other via a BSN that carries control information. At the speed of light through optical fiber, the propagation latency along the circumference of radius 100 miles is ~3.4 msec. This delay is much smaller than typical channel coherence time in NVIS channels and can be tolerated without any significant performance degradation

for the DIDO precoder. Note that if the optical fiber is shared across different operators, that delay may be larger (i.e., 10-30msec) due to the packet switched nature of the Internet. Multiple DIDO-NVIS cells as in **Figure 76** can be distributed to provide full coverage over the USA. For example, **Figure 76** shows that 109 DIDO cells of radius 125 miles are required to cover the entire territory of the 48 contiguous states in the USA.

References

[00113] The following references are referred to in the above detailed description, as indicated by the numbered brackets:

[1] 3GPP, "Multiple Input Multiple Output in UTRA", 3GPP TR 25.876 V7.0.0, Mar. 2007

[2] 3GPP, "Base Physical channels and modulation", TS 36.211, V8.7.0, May 2009

[3] 3GPP, "Multiplexing and channel coding", TS 36.212, V8.7.0, May 2009

[4] ArrayComm, "Field-proven results", http://www.arraycomm.com/serve.php?page=proof

[6] http://www.jackson-labs.com/docs/HP_GPS_Apps.pdf

[7] Oda, Y.; Tsuchihashi, R.; Tsunekawa, K.; Hata, M., "Measured path loss and multipath propagation characteristics in UHF and microwave frequency bands for urban mobile communications", Vehicular Technology Conference, Vol. 1, pp.337-341, 2001

[8] Devasirvatham, D.M.J.; Krain, M.J.; Rappaport, D.A.; Banerjee, C., "Radio propagation measurements at 850 MHz, 1.7 GHz and 4 GHz inside two dissimilar office buildings", IEEE Electronics Letters, Vol. 26, n 7, pp.445 - 447March 1990

[9] Devasirvatham, D., "Time delay spread and signal level measurements of 850 MHz radio waves in building environments", IEEE Trans. on Ant. and Prop., Vol. 34, n. 11, pp.1300 – 1305, Nov 1986

[10] Devasirvatham, D.M.J.; Murray, R.R.; Banerjee, C., "Time delay spread measurements at 850 MHz and 1.7 GHz inside a metropolitan office building", IEEE Electronics Letters, Vol. 25, n 3, pp.194-196, Feb. 1989

[11] Garcia, C.R.; Lehner, A.; Strang, T.; Frank, K., "Channel Model for Train to Train Communication Using the 400 MHz Band", in Proc. of IEEE Vehicular Technology Conference, pp.3082-3086, May 2008

[12] John Proakis, "Digital Communications", Mc Graw Hill, 4th Edition, 2001.

[13] Zogg, A., "Multipath delay spread in a hilly region at 210 MHz", IEEE Transactions on Vehicular Technology, Vol. 36, n 4, Page(s): 184 – 187, Nov 1987

[14] T.S. Rappaport, *Wireless Communications*, Prentice Hall, 2002

[15] A. Forenza and R. W. Heath, Jr., ``Impact of Antenna Geometry on MIMO Communication in Indoor Clustered Channels, (invited) *Proc. of the IEEE AP-S Intern. Symp.*, vol. 2, pp. 1700-1703, June 20-26, 2004.

[16] M. L. Morris and M. A. Jensen, "Network Model for MIMO Systems With Coupled Antennas and Noisy Amplifiers", IEEE TRANS. ON ANTENNAS AND PROPAGATION, VOL. 53, NO. 1, pp. 545-552, Jan. 2005

[17] B.G. Montgomery, "Analog RF-over-fiber technology", Syntonics LLC, Jan. 2008 http://chesapeakebayaoc.org/documents/Syntonics_AOC_RF_over-Fiber_19_Jan_08.pdf

[18] J. Daniel, "Introduction to public safety: RF signal distribution using fiber optics", 2009, http://www.rfsolutions.com/fiber.pdf

[19] Syntonics, "FORAX RF-over-fiber communications systems", http://www.syntonicscorp.com/products/products-foraxRF.html

[20] G. Caire and S. Shamai, "On the achievable throughput of a multiantenna Gaussian broadcast channel," *IEEE Trans. Info.Th.*, vol. 49, pp. 1691–1706, July 2003.

[21] P. Viswanath and D. Tse, "Sum capacity of the vector Gaussian broadcast channel and uplink-downlink duality," *IEEE Trans. Info. Th.*, vol. 49, pp. 1912–1921, Aug. 2003.

[22] S. Vishwanath, N. Jindal, and A. Goldsmith, "Duality, achievable rates, and sum-rate capacity of Gaussian MIMO broadcast channels," *IEEE Trans. Info. Th.*, vol. 49, pp. 2658–2668, Oct. 2003.

[23] W. Yu and J. Cioffi, "Sum capacity of Gaussian vector broadcast channels," *IEEE Trans. Info. Th.*, vol. 50, pp. 1875–1892, Sep. 2004.

[24] M. Costa, "Writing on dirty paper," *IEEE Transactions on Information Theory*, vol. 29, pp. 439–441, May 1983.[25] M. Bengtsson, "A pragmatic approach to multi-user spatial multiplexing," *Proc. of Sensor Array and Multichannel Sign.Proc. Workshop*, pp. 130–134, Aug. 2002.

[26] K.-K. Wong, R. D. Murch, and K. B. Letaief, "Performance enhancement of multiuser MIMO wireless communication systems," *IEEE Trans. Comm.*, vol. 50, pp. 1960–1970, Dec. 2002.

[27] M. Sharif and B. Hassibi, "On the capacity of MIMO broadcast channel with partial side information," *IEEE Trans. Info.Th.*, vol. 51, pp. 506–522, Feb. 2005.

[28] T. Yoo, N. Jindal, and A. Goldsmith, "Multi-antenna broadcast channels with limited feedback and user selection," *IEEE Journal on Sel. Areas in Communications*, vol. 25, pp. 1478–91, July 2007.

[29] P. Ding, D. J. Love, and M. D. Zoltowski, "On the sum rate of channel subspace feedback for multi-antenna broadcast channels," in *Proc., IEEE Globecom*, vol. 5, pp. 2699–2703, Nov. 2005.

[30] N. Jindal, "MIMO broadcast channels with finite-rate feedback," *IEEE Trans. on Info. Theory*, vol. 52, pp. 5045–60, Nov. 2006.

[31] T. Strohmer, M. Emami, J. Hansen, G. Papanicolaou, A. J. Paulraj, "Application of Time-Reversal with MMSE Equalizer to UWB Communications", Proc. of IEEE Globecom, vol.5, pp.3123-3127, Nov. 2004.

[32] J. Zhang, R. Chen, J. G. Andrews, A. Ghosh, and R. W. Heath, Jr., ``Coordinated Multi-cell MIMO Systems with Cellular Block Diagonalization,"

Proc. of the IEEE Asilomar Conf. on Signals, Systems, and Computers, pp. 1669-1673, Pacific Grove, CA, Nov. 4-7, 2007

[33] J. Zhang, R. Chen, J. G. Andrews, A. Ghosh, and R. W. Heath, Jr., ``Networked MIMO with Clustered Linear Precoding," *IEEE Trans. on Wireless* vol. 8, no. 4, pp. 1910-1921, April 2009.

[34] H. J. Strangeways, "Determination of the correlation distance for spaced antennas on multipath HF links and implications for design of SIMO and MIMO systems,"

www.esaspaceweather.net/spweather/workshops/eswwII/proc/Session3/Strangeways HFMIMOposter.pdf

[35] H. J. Strangeways, "Investigation of signal correlation for spaced and co-located antennas on multipath hf links and implications for the design of SIMO and MIMO systems", IEEE First European Conf. on Antennas and Propagation (EuCAP 2006), Vol. , n. 6-10, pp.1-6, Nov. 2006

[36] N. Abbasi, S.D. Gunashekar, E.M. Warrington, S. Salous, S. Feeney, L. Bertel, D. Lemur and M. Oger, "Capacity estimation of HF-MIMO systems", International Conference on Ionospheric Systems and Techniques, Apr. 2009

[37] S. Gunashekar, E.M. Warrington, S. Salous, S.M. Feeney, N.M. Abbasi, L. Bertel, D. Lemur, M. Oger, "Investigations into the Feasibility of MIMO Techniques within the HF Band: Preliminary Results", Radio Science (Special Issue), 2009, (In Press)

DISCLOSURE FROM RELATED APPLICATIONS

[00114] **Figure 1** shows a prior art MIMO system with transmit antennas 104 and receive antennas 105. Such a system can achieve up to 3X the throughput that would normally be achievable in the available channel. There are a number of different approaches in which to implement the details of such a MIMO system which are described in published literature on the subject, and the following explanation describes one such approach.

[00115] Before data is transmitted in the MIMO system of **Figure 1**, the channel is "characterized." This is accomplished by initially transmitting a "training signal" from each of the transmit antennas 104 to each of the receivers 105. The training signal is generated by the coding and modulation subsystem 102, converted to analog by a D/A converter (not shown), and then converted from baseband to RF by each transmitter 103, in succession. Each receive antenna 105 coupled to its RF Receiver 106 receives each training signal and converts it to baseband. The baseband signal is converted to digital by a D/A converter (not shown), and the signal processing subsystem 107 characterizes the training signal. Each signal's characterization may include many factors including, for example, phase and amplitude relative to a reference internal to the receiver, an absolute reference, a relative reference, characteristic noise, or other factors. Each signal's characterization is typically defined as a vector that characterizes phase and amplitude changes of several aspects of the signal when it is transmitted across the channel. For example, in a quadrature amplitude modulation ("QAM")-modulated signal the characterization might be a

vector of the phase and amplitude offsets of several multipath images of the signal. As another example, in an orthogonal frequency division multiplexing ("OFDM")-modulated signal, it might be a vector of the phase and amplitude offsets of several or all of the individual sub-signals in the OFDM spectrum.

[00116] The signal processing subsystem 107 stores the channel characterization received by each receiving antenna 105 and corresponding receiver 106. After all three transmit antennas 104 have completed their training signal transmissions, then the signal processing subsystem 107 will have stored three channel characterizations for each of three receiving antennas 105, resulting in a 3x3 matrix 108, designated as the channel characterization matrix, "H." Each individual matrix element $H_{i,j}$ is the channel characterization (which is typically a vector, as described above) of the training signal transmission of transmit antenna 104 i as received by the receive antenna 105 j.

[00117] At this point, the signal processing subsystem 107 inverts the matrix H 108, to produce H^{-1}, and awaits transmission of actual data from transmit antennas 104. Note that various prior art MIMO techniques described in available literature, can be utilized to ensure that the H matrix 108 can be inverted.

[00118] In operation, a payload of data to be transmitted is presented to the data Input subsystem 100. It is then divided up into three parts by splitter 101 prior to being presented to coding and modulation subsystem 102. For example, if the payload is the ASCII bits for "abcdef," it might be divided up into

three sub-payloads of ASCII bits for “ad,” “be,” and “cf” by Splitter 101. Then, each of these sub-payloads is presented individually to the coding and modulation subsystem 102.

[00119] Each of the sub-payloads is individually coded by using a coding system suitable for both statistical independence of each signal and error correction capability. These include, but are not limited to Reed-Solomon coding, Viterbi coding, and Turbo Codes. Finally, each of the three coded sub-payloads is modulated using an appropriate modulation scheme for the channel. Examples of modulation schemes are differential phase shift key (“DPSK”) modulation, 64-QAM modulation and OFDM. It should be noted here that the diversity gains provided by MIMO allow for higher-order modulation constellations that would otherwise be feasible in a SISO (Single Input-Single Output) system utilizing the same channel. Each coded and modulated signal is then transmitted through its own antenna 104 following D/A conversion by a D/A conversion unit (not shown) and RF generation by each transmitter 103.

[00120] Assuming that adequate spatial diversity exists amongst the transmit and receive antennas, each of the receiving antennas 105 will receive a different combination of the three transmitted signals from antennas 104. Each signal is received and converted down to baseband by each RF receiver 106, and digitized by an A/D converter (not shown). If y_n is the signal received by the

nth receive antenna 105, and x_n is the signal transmitted by nth transmit antenna 104, and N is noise, this can be described by the following three equations:

$$y_1 = x_1 H_{11} + x_2 H_{12} + x_3 H_{13} + N$$

$$y_2 = x_1 H_{21} + x_2 H_{22} + x_3 H_{23} + N$$

$$y_3 = x_1 H_{31} + x_2 H_{32} + x_3 H_{33} + N$$

[00121] Given that this is a system of three equations with three unknowns, it is a matter of linear algebra for the signal processing subsystem 107 to derive x_1, x_2, and x_3 (assuming that N is at a low enough level to permit decoding of the signals):

$$x_1 = y_1 H^{-1}{}_{11} + y_2 H^{-1}{}_{12} + y_3 H^{-1}{}_{13}$$

$$x_2 = y_1 H^{-1}{}_{21} + y_2 H^{-1}{}_{22} + y_3 H^{-1}{}_{23}$$

$$x_3 = y_1 H^{-1}{}_{31} + y_2 H^{-1}{}_{32} + y_3 H^{-1}{}_{33}$$

[00122] Once the three transmitted signals x_n are thus derived, they are then demodulated, decoded, and error-corrected by signal processing subsystem 107 to recover the three bit streams that were originally separated out by splitter 101. These bit streams are combined in combiner unit 108, and output as a single data stream from the data output 109. Assuming the robustness of the system is able to overcome the noise impairments, the data output 109 will produce the same bit stream that was introduced to the data Input 100.

[00123] Although the prior art system just described is generally practical up to four antennas, and perhaps up to as many as 10, for the reasons described in the Background section of this disclosure, it becomes impractical with large numbers of antennas (e.g. 25, 100, or 1000) .

[00124] Typically, such a prior art system is two-way, and the return path is implemented exactly the same way, but in reverse, with each side of the communications channels having both transmit and receive subsystems.

[00125] **Figure 2** illustrates one embodiment of the invention in which a Base Station (BS) 200 is configured with a Wide Area Network (WAN) interface (e.g. to the Internet through a T1 or other high speed connection) 201 and is provisioned with a number (*N*) of antennas 202. For the time being, we use the term "Base Station" to refer to any wireless station that communicates wirelessly with a set of clients from a fixed location. Examples of Base Stations are access points in wireless local area networks (WLANs) or WAN antenna tower or antenna array. There are a number of Client Devices 203-207, each with a single antenna, which are served wirelessly from the Base Station 200. Although for the purposes of this example it is easiest to think about such a Base Station as being located in an office environment where it is serving Client Devices 203-207 that are wireless-network equipped personal computers, this architecture will apply to a large number of applications, both indoor and outdoor, where a Base Station is serving wireless clients. For example, the Base Station could be based at a cellular phone tower, or on a television broadcast tower. In one embodiment, the Base Station 200 is positioned on the ground and is configured to transmit upward at HF frequencies (e.g., frequencies up to 24MHz) to bounce signals off the ionosphere as described in co-pending application entitled SYSTEM AND METHOD FOR ENHANCING NEAR VERTICAL INCIDENCE SKYWAVE ("NVIS") COMMUNICATION USING SPACE-TIME CODING, Serial

No. 10/817,731, Filed April 2, 2004, which is assigned to the assignee of the present application and which is incorporated herein by reference.

[00126] Certain details associated with the Base Station 200 and Client Devices 203-207 set forth above are for the purpose of illustration only and are not required for complying with the underlying principles of the invention. For example, the Base Station may be connected to a variety of different types of wide area networks via WAN interface 201 including application-specific wide area networks such as those used for digital video distribution. Similarly, the Client Devices may be any variety of wireless data processing and/or communication devices including, but not limited to cellular phones, personal digital assistants ("PDAs"), receivers, and wireless cameras.

[00127] In one embodiment, the Base Station's n Antennas 202 are separated spatially such that each is transmitting and receiving signals which are not spatially correlated, just as if the Base Station was a prior art MIMO transceiver. As described in the Background, experiments have been done where antennas placed within λ/6 (i.e. 1/6 wavelength) apart successfully achieve an increase in throughput from MIMO, but generally speaking, the further apart these Base Station antennas are placed, the better the system performance, and λ/2 is a desirable minimum. Of course, the underlying

principles of the invention are not limited to any particular separation between antennas.

[00128] Note that a single Base Station 200 may very well have its antennas located very far apart. For example, in the HF spectrum, the antennas may be 10 meters apart or more (e.g., in an NVIS implementation mentioned above). If 100 such antennas are used, the Base Station's antenna array could well occupy several square kilometers.

[00129] In addition to spatial diversity techniques, one embodiment of the invention polarizes the signal in order to increase the effective throughput of the system. Increasing channel capacity through polarization is a well known technique which has been employed by satellite television providers for years. Using polarization, it is possible to have multiple (e.g., three) Base Station or users' antennas very close to each other, and still be not spatially correlated. Although conventional RF systems usually will only benefit from the diversity of two dimensions (e.g. *x* and *y*) of polarization, the architecture described herein may further benefit from the diversity of three dimensions of polarization (*x*, *y* and *z*).

[00130] In addition to space and polarization diversity, one embodiment of the invention employs antennas with near-orthogonal radiation patterns to

improve link performance via pattern diversity. Pattern diversity can improve the capacity and error-rate performance of MIMO systems and its benefits over other antenna diversity techniques have been shown in the following papers:

[13] L. Dong, H. Ling, and R. W. Heath Jr., "Multiple-input multiple-output wireless communication systems using antenna pattern diversity," *Proc. IEEE Glob. Telecom. Conf.*, vol. 1, pp. 997 – 1001, Nov. 2002.

[14] R. Vaughan, "Switched parasitic elements for antenna diversity," *IEEE Trans. Antennas Propagat.*, vol. 47, pp. 399 – 405, Feb. 1999.

[15] P. Mattheijssen, M. H. A. J. Herben, G. Dolmans, and L. Leyten, "Antenna-pattern diversity versus space diversity for use at handhelds," *IEEE Trans. on Veh. Technol.*, vol. 53, pp. 1035 – 1042, July 2004.

[16] C. B. Dietrich Jr, K. Dietze, J. R. Nealy, and W. L. Stutzman, "Spatial, polarization, and pattern diversity for wireless handheld terminals," *Proc. IEEE Antennas and Prop. Symp.*, vol. 49, pp. 1271 – 1281, Sep. 2001.

[17] A. Forenza and R. W. Heath, Jr., ``Benefit of Pattern Diversity Via 2-element Array of Circular Patch Antennas in Indoor Clustered MIMO Channels", *IEEE Trans. on Communications*, vol. 54, no. 5, pp. 943-954, May 2006.

[00131] Using pattern diversity, it is possible to have multiple Base Station or users' antennas very close to each other, and still be not spatially correlated.

[00132] **Figure 3** provides additional detail of one embodiment of the Base Station 200 and Client Devices 203-207 shown in **Figure 2**. For the purposes of simplicity, the Base Station 300 is shown with only three antennas 305 and only three Client Devices 306-308. It will be noted, however, that the embodiments of the invention

described herein may be implemented with a virtually unlimited number of antennas 305 (i.e., limited only by available space and noise) and Client Devices 306-308.

[00133] **Figure 3** is similar to the prior art MIMO architecture shown in **Figure 1** in that both have three antennas on each sides of a communication channel. A notable difference is that in the prior art MIMO system the three antennas 105 on the right side of **Figure 1** are all a fixed distance from one another (e.g., integrated on a single device), and the received signals from each of the antennas 105 are processed together in the Signal Processing subsystem 107. By contrast, in **Figure 3**, the three antennas 309 on the right side of the diagram are each coupled to a different Client Device 306-308, each of which may be distributed anywhere within range of the Base Station 305. As such, the signal that each Client Device receives is processed independently from the other two received signals in its Coding, Modulation, Signal Processing subsystem 311. Thus, in contrast to a Multiple-Input (i.e. antennas 105) Multiple-Output (i.e. antennas 104) "MIMO" system, **Figure** 3 illustrates a Multiple Input (i.e. antennas 305) Distributed Output (i.e. antennas 305) system, referred to hereinafter as a "MIDO" system.

[00134] Note that this application uses different terminology than previous applications, so as to better conform with academic and industry practices. In previously cited co-pending application, SYSTEM AND METHOD FOR ENHANCING NEAR VERTICAL INCIDENCE SKYWAVE ("NVIS") COMMUNICATION USING SPACE-TIME CODING, Serial No. 10/817,731, Filed April 2, 2004, and Application No. 10/902,978 filed July 30, 2004 for which this is application is a continuation-in-part, the meaning of "Input" and "Output" (in the

context of SIMO, MISO, DIMO and MIDO) is reversed from how the terms are used in this application. In the prior applications, "Input" referred to the wireless signals as they are input to the receiving antennas (e.g. antennas 309 in Figure 3), and "Output" referred to the wireless signals as they are output by the transmitting antennas (e.g. antennas 305). In academia and the wireless industry, the reverse meaning of "Input" and "Output" is commonly used, in which "Input" refers to the wireless signals as they are input to the channel (i.e. the transmitted wireless signals from antennas 305) and "Output" refers to the wireless signals as they are output from the channel (i.e. wireless signals received by antennas 309). This application adopts this terminology, which is the reverse of the applications cited previously in this paragraph. Thus, the following terminology equivalences shall be drawn between applications:

10/817,731 and 10/902,978		Current Application
SIMO	=	MISO
MISO	=	SIMO
DIMO	=	MIDO
MIDO	=	DIMO

[00135] The MIDO architecture shown in **Figure 3** achieves a similar capacity increase as MIMO over a SISO system for a given number of transmitting antennas. However, one difference between MIMO and the particular MIDO embodiment illustrated in **Figure 3** is that, to achieve the capacity increase provided by multiple base station antennas, each MIDO Client Device 306-308 requires only a *single* receiving antenna, whereas with MIMO, each Client Device requires *as least as many* receiving antennas

as the capacity multiple that is hoped to be achieved. Given that there is usually a practical limit to how many antennas can be placed on a Client Device (as explained in the Background), this typically limits MIMO systems to between four to ten antennas (and 4X to 10X capacity multiple). Since the Base Station 300 is typically serving many Client Devices from a fixed and powered location, is it practical to expand it to far more antennas than ten, and to separate the antennas by a suitable distance to achieve spatial diversity. As illustrated, each antenna is equipped with a transceiver 304 and a portion of the processing power of a Coding, Modulation, and Signal Processing section 303. Significantly, in this embodiment, no matter how much Base Station 300 is expanded, each Client Device 306-308 only will require one antenna 309, so the cost for an individual user Client Device 306-308 will be low, and the cost of Base Station 300 can be shared among a large base of users.

[00136] An example of how a MIDO transmission from the Base Station 300 to the Client Devices 306-308 can be accomplished is illustrated in **Figures 4** through **6**.

[00137] In one embodiment of the invention, before a MIDO transmission begins, the channel is characterized. As with a MIMO system, a training signal is transmitted (in the embodiment herein described), one-by-one, by each of *the an*tennas 405. **Figure 4** illustrates only the first training signal transmission, but with three antennas 405 there are three separate transmissions in total. Each training signal is generated by the Coding, Modulation, and Signal Processing subsystem 403, converted to analog through a D/A converter, and transmitted as RF through each RF Transceiver 404. Various different coding, modulation and signal processing techniques may be employed including, but not limited to, those described above (e.g., Reed Solomon, Viterbi coding; QAM, DPSK, QPSK modulation, . . . etc) .

[00138] Each Client Device 406-408 receives a training signal through its antenna 409 and converts the training signal to baseband by Transceiver 410. An A/D converter (not shown) converts the signal to digital where is it processed by each Coding, Modulation, and Signal Processing subsystem 411. Signal characterization logic 320 then characterizes the resulting signal (e.g., identifying phase and amplitude distortions as described above) and stores the characterization in memory. This characterization process is similar to that of prior art MIMO systems, with a notable difference being that the each client device only computes the characterization vector for its one antenna, rather than for n antennas. For example, the Coding Modulation and Signal Processing subsystem 420 of client device 406 is initialized with a known pattern of the training signal (either at the time of manufacturing, by receiving it in a transmitted message, or through another initialization process). When antenna 405 transmits the training signal with this known pattern, Coding Modulation and Signal Processing subsystem 420 uses correlation methods to find the strongest received pattern of the training signal, it stores the phase and amplitude offset, then it subtracts this pattern from the received signal. Next, it finds then second strongest received pattern that correlates to the training signal, it stores the phase and amplitude offset, then it subtracts this second strongest pattern from the received signal. This process continues until either some fixed number of phase and amplitude offsets are stored (e.g. eight), or a detectable training signal pattern drops below a given noise floor. This vector of phase/amplitude offsets becomes element H_{11} of the vector 413. Simultaneously, Coding Modulation and

Signal Processing subsystems for Client Devices 407 and 408 implement the produce their vector elements H_{21} and H_{31}.

[00139] The memory in which the characterization is stored may be a non-volatile memory such as a Flash memory or a hard drive and/or a volatile memory such as a random access memory (e.g., SDRAM, RDAM). Moreover, different Client Devices may concurrently employ different types of memories to store the characterization information (e.g., PDA's may use Flash memory whereas notebook computers may use a hard drive). The underlying principles of the invention are not limited to any particular type of storage mechanism on the various Client Devices or the Base Station.

[00140] As mentioned above, depending on the scheme employed, since each Client Device 406-408 has only one antenna, each only stores a 1x3 row 413-415 of the H matrix. **Figure** 4 illustrates the stage after the first training signal transmission where the first column of 1x3 rows 413-415 has been stored with channel characterization information for the first of the three Base Station antennas 405. The remaining two columns are stored following the channel characterization of the next two training signal transmissions from the remaining two base station antennas. Note that for the sake of illustration the three training signals are transmitted at separate times. If the three training signal patterns are chosen such as not to be correlated to one another, they may be transmitted simultaneously, thereby reducing training time.

[00141] As indicated in **Figure 5**, after all three pilot transmissions are complete, each Client Device 506-508 transmits back to the Base Station 500 the 1x3 row 513-515 of matrix H that it has stored. To the sake of simplicity, only one Client Device 506 is illustrated transmitting its characterization information in **Figure 5**. An appropriate modulation scheme (e.g. DPSK, 64QAM, OFDM) for the channel combined with adequate error correction coding (e.g. Reed Solomon, Viterbi, and/or Turbo codes) may be employed to make sure that the Base Station 500 receives the data in the rows 513-515 accurately.

[00142] Although all three antennas 505 are shown receiving the signal in **Figure 5**, it is sufficient for a single antenna and transceiver of the Base Station 500 to receive each 1x3 row 513-515 transmission. However, utilizing many or all of antennas 505 and Transceivers 504 to receive each transmission (i.e., utilizing prior art Single-Input Multiple-Output ("SIMO") processing techniques in the Coding, Modulation and Signal Processing subsystem 503) may yield a better signal-to-noise ratio ("SNR") than utilizing a single antenna 505 and Transceiver 504 under certain conditions.

[00143] As the Coding, Modulation and Signal Processing subsystem 503 of Base Station 500 receives the 1x3 row 513-515, from each Client Device 507-508, it stores it in a 3x3 H matrix 516. As with the Client Devices, the Base Station may employ various different storage technologies including, but not limited to non-volatile mass storage memories (e.g., hard drives) and/or volatile memories (e.g., SDRAM) to store the matrix 516. **Figure 5** illustrates a stage at

which the Base Station 500 has received and stored the 1x3 row 513 from Client Device 509. The 1x3 rows 514 and 515 may be transmitted and stored in H matrix 516 as they are received from the remaining Client Devices, until the entire H matrix 516 is stored.

[00144] One embodiment of a MIDO transmission from a Base Station 600 to Client Devices 606-608 will now be described with reference to **Figure 66**. Because each Client Device 606-608 is an independent device, typically each device is receiving a different data transmission. As such, one embodiment of a Base Station 600 includes a Router 602 communicatively positioned between the WAN Interface 601 and the Coding, Modulation and Signal Processing subsystem 603 that sources multiple data streams (formatted into bit streams) from the WAN interface 601 and routes them as separate bit streams u_1- u_3 intended for each Client Device 606-608, respectively. Various well known routing techniques may be employed by the router 602 for this purpose.

[00145] The three bit streams, u_1- u_3, shown in **Figure** 6 are then routed into the Coding, Modulation and Signal Processing subsystem 603 and coded into statistically distinct, error correcting streams (e.g. using Reed Solomon, Viterbi, or Turbo Codes) and modulated using an appropriate modulation scheme for the channel (such as DPSK, 64QAM or OFDM). In addition, the embodiment illustrated in **Figure** 6 includes signal precoding logic 630 for uniquely coding the signals transmitted from each of the antennas 605 based on the signal characterization matrix 616. More specifically, rather than routing each of the

three coded and modulated bit streams to a separate antenna (as is done in **Figure 1**), in one embodiment, the precoding logic 630 multiplies the three bit streams u_1- u_3 in **Figure 6** by the inverse of the H matrix 616, producing three new bit streams, u'_1- u'_3. The three precoded bit streams are then converted to analog by D/A converters (not shown) and transmitted as RF by Transceivers 604 and antennas 605.

[00146] Before explaining how the bit streams are received by the Client Devices 606-608, the operations performed by the precoding module 630 will be described. Similar to the MIMO example from **Figure 1** above, the coded and modulated signal for each of the three source bit streams will be designated with u_n. In the embodiment illustrated in **Figure 6**, each u_i contains the data from one of the three bit streams routed by the Router 602, and each such bit stream is intended for one of the three Client Devices 606-608.

[00147] However, unlike the MIMO example of **Figure 1**, where each x_i is *transmitted* by each antenna 104, in the embodiment of the invention illustrated in **Figure 6**, each u_i is *received* at each Client Device antenna 609 (plus whatever noise N there is in the channel). To achieve this result, the output of each of the three antennas 605 (each of which we will designate as v_i) is a function of u_i and the H matrix that characterizes the channel for each Client Device. In one embodiment, each v_i is calculated by the precoding logic 630 within the Coding, Modulation and Signal Processing subsystem 603 by implementing the following formulas:

$v_1 = u_1H^{-1}{}_{11} + u_2H^{-1}{}_{12} + u_3H^{-1}{}_{13}$

$v_2 = u_1H^{-1}{}_{21} + u_2H^{-1}{}_{22} + u_3H^{-1}{}_{23}$

$v_3 = u_1H^{-1}{}_{31} + u_2H^{-1}{}_{32} + u_3H^{-1}{}_{33}$

[00148] Thus, unlike MIMO, where each x_i is calculated at the receiver after the signals have been transformed by the channel, the embodiments of the invention described herein solve for each v_i at the transmitter *before* the signals have been transformed by the channel. Each antenna 609 receives u_i *already separated* from the other u_{n-1} bit streams intended for the other antennas 609. Each Transceiver 610 converts each received signal to baseband, where it is digitized by an A/D converter (now shown), and each Coding, Modulation and Signal Processing subsystem 611, demodulates and decodes the x_i bit stream intended for it, and sends its bit stream to a Data Interface 612 to be used by the Client Device (e.g., by an application on the client device).

[00149] The embodiments of the invention described herein may be implemented using a variety of different coding and modulation schemes. For example, in an OFDM implementation, where the frequency spectrum is separated into a plurality of sub-bands, the techniques described herein may be employed to characterize each individual sub-band. As mentioned above, however, the underlying principles of the invention are not limited to any particular modulation scheme.

[00150] If the Client Devices 606-608 are portable data processing devices such as PDAs, notebook computers, and/or wireless telephones the channel

characterization may change frequently as the Client Devices may move from one location to another. As such, in one embodiment of the invention, the channel characterization matrix 616 at the Base Station is continually updated. In one embodiment, the Base Station 600 periodically (e.g., every 250 milliseconds) sends out a new training signal to each Client Device, and each Client Device continually transmits its channel characterization vector back to the Base Station 600 to ensure that the channel characterization remains accurate (e.g. if the environment changes so as to affect the channel or if a Client Device moves). In one embodiment, the training signal is interleaved within the actual data signal sent to each client device. Typically, the training signals are much lower throughput than the data signals, so this would have little impact on the overall throughput of the system. Accordingly, in this embodiment, the channel characterization matrix 616 may be updated continuously as the Base Station actively communicates with each Client Device, thereby maintaining an accurate channel characterization as the Client Devices move from one location to the next or if the environment changes so as to affect the channel.

[00151] One embodiment of the invention illustrated in **Figure** 7 employs MIMO techniques to improve the upstream communication channel (i.e., the channel from the Client Devices 706-708 to the Base Station 700). In this embodiment, the channel from each of the Client Devices is continually analyzed and characterized by upstream channel characterization logic 741 within the Base Station. More specifically, each of the Client Devices 706-708 transmits a training signal to the Base Station 700 which the channel characterization logic

741 analyzes (e.g., as in a typical MIMO system) to generate an *N* x *M* channel characterization matrix 741, where *N* is the number of Client Devices and *M* is the number of antennas employed by the Base Station. The embodiment illustrated in **Figure** 7 employs three antennas 705 at the Base Station and three Client Devices 706-608, resulting in a 3x3 channel characterization matrix 741 stored at the Base Station 700. The MIMO upstream transmission illustrated in **Figure** 7 may be used by the Client Devices both for transmitting data back to the Base Station 700, and for transmitting channel characterization vectors back to the Base Station 700 as illustrated in **Figure 5**. But unlike the embodiment illustrated in **Figure 5** in which each Client Device's channel characterization vector is transmitted at a separate time, the method shown in **Figure 7** allows for the simultaneous transmission of channel characterization vectors from multiple Client Devices back to the Base Station 700, thereby dramatically reducing the channel characterization vectors' impact on return channel throughput.

[00152] As mentioned above, each signal's characterization may include many factors including, for example, phase and amplitude relative to a reference internal to the receiver, an absolute reference, a relative reference, characteristic noise, or other factors. For example, in a quadrature amplitude modulation ("QAM")-modulated signal the characterization might be a vector of the phase and amplitude offsets of several multipath images of the signal. As another example, in an orthogonal frequency division multiplexing ("OFDM")-modulated signal, it might be a vector of the phase and amplitude offsets of several or all of the individual sub-signals in the OFDM spectrum. The training signal may be

generated by each Client Device's coding and modulation subsystem 711, converted to analog by a D/A converter (not shown), and then converted from baseband to RF by each Client Device's transmitter 709. In one embodiment, in order to ensure that the training signals are synchronized, Client Devices only transmit training signals when requested by the Base Station (e.g., in a round robin manner). In addition, training signals may be interleaved within or transmitted concurrently with the actual data signal sent from each client device. Thus, even if the Client Devices 706-708 are mobile, the training signals may be continuously transmitted and analyzed by the upstream channel characterization logic 741, thereby ensuring that the channel characterization matrix 741 remains up-to-date.

[00153] The total channel capacity supported by the foregoing embodiments of the invention may be defined as *min (N, M)* where *M* is the number of Client Devices and *N* is the number of Base Station antennas. That is, the capacity is limited by the number of antennas on either the Base Station side or the Client side. As such, one embodiment of the invention employs synchronization techniques to ensure that no more than *min (N, M)* antennas are transmitting/ receiving at a given time.

[00154] In a typical scenario, the number of antennas 705 on the Base Station 700 will be less than the number of Client Devices 706-708. An exemplary scenario is illustrated in **Figure** 8 which shows five Client Devices 804-808 communicating with a base station having three antennas 802. In this

embodiment, after determining the total number of Client Devices 804-808, and collecting the necessary channel characterization information (e.g., as described above), the Base Station 800 chooses a first group of three clients 810 with which to communicate (three clients in the example because *min (N, M)* = 3). After communicating with the first group of clients 810 for a designated period of time, the Base Station then selects another group of three clients 811 with which to communicate. To distribute the communication channel evenly, the Base Station 800 selects the two Client Devices 807, 808 which were not included in the first group. In addition, because an extra antenna is available, the Base Station 800 selects an additional client device 806 included in the first group. In one embodiment, the Base Station 800 cycles between groups of clients in this manner such that each client is effectively allocated the same amount of throughput over time. For example, to allocate throughput evenly, the Base Station may subsequently select any combination of three Client Devices which excludes Client Device 806 (i.e., because Client Device 806 was engaged in communication with the Base Station for the first two cycles).

[00155] In one embodiment, in addition to standard data communications, the Base Station may employ the foregoing techniques to transmit training signals to each of the Client Devices and receive training signals and signal characterization data from each of the Client Devices.

[00156] In one embodiment, certain Client Devices or groups of client devices may be allocated different levels of throughput. For example, Client

Devices may be prioritized such that relatively higher priority Client Devices may be guaranteed more communication cycles (i.e., more throughput) than relatively lower priority client devices. The "priority" of a Client Device may be selected based on a number of variables including, for example, the designated level of a user's subscription to the wireless service (e.g., user's may be willing to pay more for additional throughput) and/or the type of data being communicated to/from the Client Device (e.g., real-time communication such as telephony audio and video may take priority over non-real time communication such as email).

[00157] In one embodiment of the Base Station dynamically allocates throughput based on the Current Load required by each Client Device. For example, if Client Device 804 is streaming live video and the other devices 805-808 are performing non-real time functions such as email, then the Base Station 800 may allocate relatively more throughput to this client 804. It should be noted, however, that the underlying principles of the invention are not limited to any particular throughput allocation technique.

[00158] As illustrated in **Figure 9**, two Client Devices 907, 908 may be so close in proximity, that the channel characterization for the clients is effectively the same. As a result, the Base Station will receive and store effectively equivalent channel characterization vectors for the two Client Devices 907, 908 and therefore will not be able to create unique, spatially distributed signals for each Client Device. Accordingly, in one embodiment, the Base Station will ensure that any two or more Client Devices which are in close proximity to one

another are allocated to different groups. In **Figure 9**, for example, the Base Station 900 first communicates with a first group 910 of Client Devices 904, 905 and 908; and then with a second group 911 of Client Devices 905, 906, 907, ensuring that Client Devices 907 and 908 are in different groups.

[00159] Alternatively, in one embodiment, the Base Station 900 communicates with both Client Devices 907 and 908 concurrently, but multiplexes the communication channel using known channel multiplexing techniques. For example, the Base Station may employ time division multiplexing ("TDM"), frequency division multiplexing ("FDM") or code division multiple access ("CDMA") techniques to divide the single, spatially-correlated signal between Client Devices 907 and 908.

[00160] Although each Client Device described above is equipped with a single antenna, the underlying principles of the invention may be employed using Client Devices with multiple antennas to increase throughput. For example, when used on the wireless systems described above, a client with 2 antennas will realize a 2x increase in throughput, a client with 3 antennas will realize a 3x increase in throughput, and so on (i.e., assuming that the spatial and angular separation between the antennas is sufficient). The Base Station may apply the same general rules when cycling through Client Devices with multiple antennas. For example, it may treat each antenna as a separate client and allocate throughput to that "client" as it would any other client (e.g., ensuring that each client is provided with an adequate or equivalent period of communication).

[00161] As mentioned above, one embodiment of the invention employs the MIDO and/or MIMO signal transmission techniques described above to increase the signal-to-noise ratio and throughput within a Near Vertical Incidence Skywave ("NVIS") system. Referring to **Figure 10**, in one embodiment of the invention, a first NVIS station 1001 equipped with a matrix of *N* antennas 1002 is configured to communicate with *M* client devices 1004. The NVIS antennas 1002 and antennas of the various client devices 1004 transmit signals upward to within about 15 degrees of vertical in order to achieve the desired NVIS and minimize ground wave interference effects. In one embodiment, the antennas 1002 and client devices 1004, support multiple independent data streams 1006 using the various MIDO and MIMO techniques described above at a designated frequency within the NVIS spectrum (e.g., at a carrier frequency at or below 23 MHz, but typically below 10 MHz), thereby significantly increasing the throughput at the designated frequency (i.e., by a factor proportional to the number of statistically independent data streams).

[00162] The NVIS antennas serving a given station may be physically very far apart from each other. Given the long wavelengths below 10 MHz and the long distance traveled for the signals (as much as 300 miles round trip), physical separation of the antennas by 100s of yards, and even miles, can provide advantages in diversity. In such situations, the individual antenna signals may be brought back to a centralized location to be processed using conventional wired or wireless communications systems. Alternatively, each antenna can have a local facility to process its signals, then use conventional wired or wireless

communications systems to communicate the data back to a centralized location. In one embodiment of the invention, NVIS Station 1001 has a broadband link 1015 to the Internet 1010 (or other wide area network), thereby providing the client devices 1003 with remote, high speed, wireless network access.

[00163] In one embodiment, the Base Station and/or users may exploit polarization/pattern diversity techniques described above to reduce the array size and/or users' distance while providing diversity and increased throughput. As an example, in MIDO systems with HF transmissions, the users may be in the same location and yet their signals be uncorrelated because of polarization/pattern diversity. In particular, by using pattern diversity, one user may be communicating to the Base Station via groundwave whereas the other user via NVIS.

ADDITIONAL EMBODIMENTS OF THE INVENTION

DIDO-OFDM Precoding with I/Q Imbalance

[00164] One embodiment of the invention employs a system and method to compensate for in-phase and quadrature (I/Q) imbalance in distributed-input distributed-output (DIDO) systems with orthogonal frequency division multiplexing (OFDM). Briefly, according to this embodiment, user devices estimate the channel and feedback this information to the Base Station; the Base Station computes the precoding matrix to cancel inter-carrier and inter-user interference caused by I/Q imbalance; and parallel data streams are transmitted to multiple user devices via DIDO precoding; the user devices demodulate data

via zero-forcing (ZF), minimum mean-square error (MMSE) or maximum likelihood (ML) receiver to suppress residual interference.

[00165] As described in detail below, some of the significant features of this embodiment of the invention include, but are not limited to:

[00166] Precoding to cancel inter-carrier interference (ICI) from mirror tones (due to I/Q mismatch) in OFDM systems;

[00167] Precoding to cancel inter-user interference and ICI (due to I/Q mismatch) in DIDO-OFDM systems;

[00168] Techniques to cancel ICI (due to I/Q mismatch) via ZF receiver in DIDO-OFDM systems employing block diagonalization (BD) precoder;

[00169] Techniques to cancel inter-user interference and ICI (due to I/Q mismatch) via precoding (at the transmitter) and a ZF or MMSE filter (at the receiver) in DIDO-OFDM systems;

[00170] Techniques to cancel inter-user interference and ICI (due to I/Q mismatch) via pre-coding (at the transmitter) and a nonlinear detector like a maximum likelihood (ML) detector (at the receiver) in DIDO-OFDM systems;

[00171] The use of pre-coding based on channel state information to cancel inter-carrier interference (ICI) from mirror tones (due to I/Q mismatch) in OFDM systems;

[00172] The use of pre-coding based on channel state information to cancel inter-carrier interference (ICI) from mirror tones (due to I/Q mismatch) in DIDO-OFDM systems;

[00173] The use of an I/Q mismatch aware DIDO precoder at the station and an IQ-aware DIDO receiver at the user terminal;

[00174] The use of an I/Q mismatch aware DIDO precoder at the station, an I/Q aware DIDO receiver at the user terminal, and an I/Q aware channel estimator;

[00175] The use of an I/Q mismatch aware DIDO precoder at the station, an I/Q aware DIDO receiver at the user terminal, an I/Q aware channel estimator, and an I/Q aware DIDO feedback generator that sends channel state information from the user terminal to the station;

[00176] The use of an I/Q mismatch-aware DIDO precoder at the station and an I/Q aware DIDO configurator that uses I/Q channel information to perform functions including user selection, adaptive coding and modulation, space-time-frequency mapping, or precoder selection;

[00177] The use of an I/Q aware DIDO receiver that cancels ICI (due to I/Q mismatch) via ZF receiver in DIDO-OFDM systems employing block diagonalization (BD) precoder;

[00178] The use of an I/Q aware DIDO receiver that cancels ICI (due to I/Q mismatch) via pre-coding (at the transmitter) and a nonlinear detector like a maximum likelihood detector (at the receiver) in DIDO-OFDM systems; and

[00179] The use of an I/Q aware DIDO receiver that cancels ICI (due to I/Q mismatch) via ZF or MMSE filter in DIDO-OFDM systems.

a. Background

[00180] The transmit and receive signals of typical wireless communication systems consist of in-phase and quadrature (I/Q) components. In practical systems, the inphase and quadrature components may be distorted due to imperfections in the mixing and baseband operations. These distortions manifest as I/Q phase, gain and delay mismatch. Phase imbalance is caused by the sine and cosine in the modulator/demodulator not being perfectly orthogonal. Gain imbalance is caused by different amplifications between the inphase and quadrature components. There may be an additional distortion, called delay imbalance, due to difference in delays between the I-and Q-rails in the analog circuitry.

[00181] In orthogonal frequency division multiplexing (OFDM) systems, I/Q imbalance causes inter-carrier interference (ICI) from the mirror tones. This effect has been studied in the literature and methods to compensate for I/Q mismatch in single-input single-output SISO-OFDM systems have been proposed in M. D. Benedetto and P. Mandarini, "Analysis of the effect of the I/Q baseband filter mismatch in an OFDM modem," Wireless personal communications, pp. 175–186, 2000; S. Schuchert and R. Hasholzner, "A novel I/Q imbalance compensation scheme for the reception of OFDM signals," IEEE Transaction on Consumer Electronics, Aug. 2001; M. Valkama, M. Renfors, and V. Koivunen, "Advanced methods for I/Q imbalance compensation in communication receivers," IEEE Trans. Sig. Proc., Oct. 2001; R. Rao and B. Daneshrad, "Analysis of I/Q mismatch and a cancellation scheme for OFDM

systems," IST Mobile Communication Summit, June 2004; A. Tarighat, R. Bagheri, and A. H. Sayed, "Compensation schemes and performance analysis of IQ imbalances in OFDM receivers," Signal Processing, IEEE Transactions on [see also Acoustics, Speech, and Signal Processing, IEEE Transactions on], vol. 53, pp. 3257–3268, Aug. 2005.

[00182] An extension of this work to multiple-input multiple-output MIMO-OFDM systems was presented in R. Rao and B. Daneshrad, "I/Q mismatch cancellation for MIMO OFDM systems," in Personal, Indoor and Mobile Radio Communications, 2004; PIMRC 2004. 15th IEEE International Symposium on, vol. 4, 2004, pp. 2710–2714. R. M. Rao, W. Zhu, S. Lang, C. Oberli, D. Browne, J. Bhatia, J. F. Frigon, J. Wang, P; Gupta, H. Lee, D. N. Liu, S. G. Wong, M. Fitz, B. Daneshrad, and O. Takeshita, "Multiantenna testbeds for research and education in wireless communications," IEEE Communications Magazine, vol. 42, no. 12, pp. 72–81, Dec. 2004; S. Lang, M. R. Rao, and B. Daneshrad, "Design and development of a 5.25 GHz software defined wireless OFDM communication platform," IEEE Communications Magazine, vol. 42, no. 6, pp. 6–12, June 2004, for spatial multiplexing (SM) and in A. Tarighat and A. H. Sayed, "MIMO OFDM receivers for systems with IQ imbalances," IEEE Trans. Sig. Proc., vol. 53, pp. 3583–3596, Sep. 2005, for orthogonal space-time block codes (OSTBC).

[00183] Unfortunately, there is currently no literature on how to correct for I/Q gain and phase imbalance errors in a distributed-input distributed-output

(DIDO) communication system. The embodiments of the invention described below provide a solution to these problems.

[00184] DIDO systems consist of one Base Station with distributed antennas that transmits parallel data streams (via pre-coding) to multiple users to enhance downlink throughput, while exploiting the same wireless resources (i.e., same slot duration and frequency band) as conventional SISO systems. A detailed description of DIDO systems was presented in S. G. Perlman and T. Cotter, "System and Method for Distributed Input-Distributed Output Wireless Communications," Serial No. 10/902,978, filed July 30, 2004 ("Prior Application"), which is assigned to the assignee of the present application and which is incorporated herein by reference.

[00185] There are many ways to implement DIDO precoders. One solution is block diagonalization (BD) described in Q. H. Spencer, A. L. Swindlehurst, and M. Haardt, "Zero forcing methods for downlink spatial multiplexing in multiuser MIMO channels," IEEE Trans. Sig. Proc., vol. 52, pp. 461–471, Feb. 2004. K. K. Wong, R. D. Murch, and K. B. Letaief, "A joint channel diagonalization for multiuser MIMO antenna systems," IEEE Trans. Wireless Comm., vol. 2, pp. 773–786, Jul 2003; L. U. Choi and R. D. Murch, "A transmit preprocessing technique for multiuser MIMO systems using a decomposition approach," IEEE Trans. Wireless Comm., vol. 3, pp. 20–24, Jan 2004; Z. Shen, J. G. Andrews, R. W. Heath, and B. L. Evans, "Low complexity user selection algorithms for multiuser MIMO systems with block diagonalization," accepted for publication in IEEE Trans. Sig. Proc., Sep. 2005; Z. Shen, R. Chen, J. G. Andrews, R. W.

Heath, and B. L. Evans, "Sum capacity of multiuser MIMO broadcast channels with block diagonalization," submitted to IEEE Trans. Wireless Comm., Oct. 2005; R. Chen, R. W. Heath, and J. G. Andrews, "Transmit selection diversity for unitary precoded multiuser spatial multiplexing systems with linear receivers," accepted to IEEE Trans. on Signal Processing, 2005. The methods for I/Q compensation presented in this document assume BD precoder, but can be extended to any type of DIDO precoder.

[00186] In DIDO-OFDM systems, I/Q mismatch causes two effects: ICI and inter-user interference. The former is due to interference from the mirror tones as in SISO-OFDM systems. The latter is due to the fact that I/Q mismatch destroys the orthogonality of the DIDO precoder yielding interference across users. Both of these types of interference can be cancelled at the transmitter and receiver through the methods described herein. Three methods for I/Q compensation in DIDO-OFDM systems are described and their performance is compared against systems with and without I/Q mismatch. Results are presented based both on simulations and practical measurements carried out with the DIDO-OFDM prototype.

[00187] The present embodiments are an extension of the Prior Application. In particular, these embodiments relate to the following features of the Prior Application:

[00188] The system as described in the prior application, where the I/Q rails are affected by gain and phase imbalance;

[00189] The training signals employed for channel estimation are used to calculate the DIDO precoder with I/Q compensation at the transmitter; and

[00190] The signal characterization data accounts for distortion due to I/Q imbalance and is used at the transmitter to compute the DIDO precoder according to the method proposed in this document.

b. Embodiments of the Invention

[00191] First, the mathematical model and framework of the invention will be described.

[00192] Before presenting the solution, it is useful to explain the core mathematical concept. We explain it assuming I/Q gain and phase imbalance (phase delay is not included in the description but is dealt with automatically in the DIDO-OFDM version of the algorithm). To explain the basic idea, suppose that we want to multiply two complex numbers $s = s_I + js_Q$ and $h = h_I + jh_Q$ and let $x = h * s$. We use the subscripts to denote inphase and quadrature components. Recall that

$$x_I = s_I h_I - s_Q h_Q$$

and

$$x_Q = s_I h_Q + s_Q h_I .$$

In matrix form this can be rewritten as

$$\begin{bmatrix} x_I \\ x_Q \end{bmatrix} = \begin{bmatrix} h_I & -h_Q \\ h_Q & h_I \end{bmatrix} \begin{bmatrix} s_I \\ s_Q \end{bmatrix}.$$

Note the unitary transformation by the channel matrix (H). Now suppose that s is the transmitted symbol and h is the channel. The presence of I/Q gain

and phase imbalance can be modeled by creating a non-unitary transformation as follows

$$\begin{bmatrix} x_I \\ x_Q \end{bmatrix} = \begin{bmatrix} h_{11} & h_{12} \\ h_{21} & h_{22} \end{bmatrix} \begin{bmatrix} s_I \\ s_Q \end{bmatrix}. \quad \text{(A)}$$

The trick is to recognize that it is possible to write

$$\begin{aligned} \begin{bmatrix} h_{11} & h_{12} \\ h_{21} & h_{22} \end{bmatrix} &= \frac{1}{2}\begin{bmatrix} h_{11}+h_{22} & h_{12}-h_{21} \\ -(h_{12}-h_{21}) & h_{11}+h_{22} \end{bmatrix} + \frac{1}{2}\begin{bmatrix} h_{11}-h_{22} & h_{12}+h_{21} \\ h_{12}+h_{21} & h_{22}-h_{11} \end{bmatrix} \\ &= \frac{1}{2}\begin{bmatrix} h_{11}+h_{22} & h_{12}-h_{21} \\ -(h_{12}-h_{21}) & h_{11}+h_{22} \end{bmatrix} + \frac{1}{2}\begin{bmatrix} h_{11}-h_{22} & -(h_{12}+h_{21}) \\ h_{12}+h_{21} & h_{11}-h_{22} \end{bmatrix} \begin{bmatrix} 1 & 0 \\ 0 & -1 \end{bmatrix}. \end{aligned}$$

Now, rewriting (A)

$$\begin{aligned} \begin{bmatrix} x_I \\ x_Q \end{bmatrix} &= \frac{1}{2}\begin{bmatrix} h_{11}+h_{22} & h_{12}-h_{21} \\ -(h_{12}-h_{21}) & h_{11}+h_{22} \end{bmatrix} \begin{bmatrix} s_I \\ s_Q \end{bmatrix} + \frac{1}{2}\begin{bmatrix} h_{11}-h_{22} & -(h_{12}+h_{21}) \\ h_{12}+h_{21} & h_{11}-h_{22} \end{bmatrix} \begin{bmatrix} 1 & 0 \\ 0 & -1 \end{bmatrix} \begin{bmatrix} s_I \\ s_Q \end{bmatrix} \\ &= \frac{1}{2}\begin{bmatrix} h_{11}+h_{22} & h_{12}-h_{21} \\ -(h_{12}-h_{21}) & h_{11}+h_{22} \end{bmatrix} \begin{bmatrix} s_I \\ s_Q \end{bmatrix} + \frac{1}{2}\begin{bmatrix} h_{11}-h_{22} & -(h_{12}+h_{21}) \\ h_{12}+h_{21} & h_{11}-h_{22} \end{bmatrix} \begin{bmatrix} s_I \\ -s_Q \end{bmatrix} \end{aligned} \quad (5)$$

Let us define

$$\mathcal{H}_e = \frac{1}{2}\begin{bmatrix} h_{11}+h_{22} & h_{12}-h_{21} \\ -(h_{12}-h_{21}) & h_{11}+h_{22} \end{bmatrix}$$

and

$$\mathcal{H}_e = \frac{1}{2}\begin{bmatrix} h_{11}-h_{22} & -(h_{12}+h_{21}) \\ h_{12}+h_{21} & h_{11}-h_{22} \end{bmatrix}.$$

Both of these matrices have a unitary structure thus can be equivalently represented by complex scalars as

$$h_e = h_{11} + h_{22} + j(h_{21} - h_{12})$$

and

$$h_c = h_{11} - h_{22} + j(h_{21} + h_{12}).$$

Using all of these observations, we can put the effective equation back in a scalar form with two channels: the equivalent channel h_e and the conjugate channel h_c. Then the effective transformation in (5) becomes

$$x = h_e s + h_c s^*.$$

We refer to the first channel as the equivalent channel and the second channel as the conjugate channel. The equivalent channel is the one you would observe if there were no I/Q gain and phase imbalance.

Using similar arguments, it can be shown that the input-output relationship of a discrete-time MIMO *NxM* system with I/Q gain and phase imbalance is (using the scalar equivalents to build their matrix counterparts)

$$\mathbf{x}[t] = \sum_{\ell=0}^{L} \mathbf{h}_e[\ell]\mathbf{s}[t-\ell] + \mathbf{h}_c[\ell]\mathbf{s}^*[t-\ell]$$

where t is the discrete time index, $\mathbf{h}_e, \mathbf{h}_c \in C^{MxN}, \mathbf{s} = [s_1, ..., s_N], \mathbf{x} = [x_1, ..., x_M]$ and L is the number of channel taps.

In DIDO-OFDM systems, the received signal in the frequency domain is represented. Recall from signals and systems that if

$FFT_K\{s[t]\} = S[k]$ then $FFT_K\{s^*[t]\} = S^*[(-k)] = S^*[K-k]$ *for* $k = 0,1,...,K-1$.

With OFDM, the equivalent input-output relationship for a MIMO-OFDM system for subcarrier *k* is

$$\bar{\mathbf{x}}[k] = \mathbf{H}_e[k]\bar{\mathbf{s}}[k] + \mathbf{H}_c[k]\bar{\mathbf{s}}^*[K-k] \quad (1)$$

where $k = 0, 1, \ldots, K-1$ is the OFDM subcarrier index, $\mathbf{H}_e$ and $\mathbf{H}_c$ denote the equivalent and conjugate channel matrices, respectively, defined as

$$\mathbf{H}_e[k] = \sum_{\ell=0}^{L} \mathbf{h}_e[\ell] e^{-j\frac{2\Pi k}{K}\ell}$$

and

$$\mathbf{H}_c[k] = \sum_{\ell=0}^{L} \mathbf{h}_c[\ell] e^{-j\frac{2\Pi k}{K}\ell}.$$

The second contribution in (1) is interference from the *mirror tone*. It can be dealt with by constructing the following stacked matrix system (note carefully the conjugates)

$$\begin{bmatrix} \bar{\mathbf{x}}[k] \\ \bar{\mathbf{x}}^*[K-k] \end{bmatrix} = \begin{bmatrix} \mathbf{H}_e[k] & \mathbf{H}_c[k] \\ \mathbf{H}_c^*[K-k] & \mathbf{H}_e^*[K-k] \end{bmatrix} \begin{bmatrix} \bar{\mathbf{s}}[k] \\ \bar{\mathbf{s}}^*[K-k] \end{bmatrix}$$

where $\bar{\mathbf{s}} = [\bar{s}_1, \bar{s}_2]^T$ and $\bar{\mathbf{x}} = [\bar{x}_1, \bar{x}_2]^T$ are the vectors of transmit and receive symbols in the frequency domain, respectively.

Using this approach, an effective matrix is built to use for DIDO operation. For example, with DIDO 2 x 2 the input-output relationship (assuming each user has a single receive antenna) the first user device sees (in the absence of noise)

$$\begin{bmatrix} \bar{x}_1[k] \\ \bar{x}_1^*[K-k] \end{bmatrix} = \begin{bmatrix} \mathbf{H}_e^{(1)}[k] & \mathbf{H}_c^{(1)}[k] \\ \mathbf{H}_c^{(1)*}[K-k] & \mathbf{H}_e^{(1)*}[K-k] \end{bmatrix} \mathbf{W} \begin{bmatrix} \bar{s}_1[k] \\ \bar{s}_1^*[K-k] \\ \bar{s}_2[k] \\ \bar{s}_2^*[K-k] \end{bmatrix} \quad (2)$$

while the second user observes

$$\begin{bmatrix} \bar{x}_2[k] \\ \bar{x}_2^*[K-k] \end{bmatrix} = \begin{bmatrix} \mathbf{H}_e^{(2)}[k] & \mathbf{H}_c^{(2)}[k] \\ \mathbf{H}_c^{(2)*}[K-k] & \mathbf{H}_e^{(2)*}[K-k] \end{bmatrix} \mathbf{W} \begin{bmatrix} \bar{s}_1[k] \\ \bar{s}_1^*[K-k] \\ \bar{s}_2[k] \\ \bar{s}_2^*[K-k] \end{bmatrix} \quad (3)$$

where $\mathbf{H}_e^{(m)}, \mathbf{H}_c^{(m)} \in C^{1x2}$ denote the *m-th* row of the matrices $\mathbf{H}_e$ and $\mathbf{H}_c$, respectively, and $\mathbf{W} \in C^{4x4}$ is the DIDO pre-coding matrix. From (2) and (3) it is observed that the received symbol $\bar{x}_m[k]$ of user *m* is affected by two sources of interference caused by I/Q imbalance: *inter-carrier interference* from the mirror tone (i.e., $\bar{s}_m^*[K-k]$) and *inter-user interference* (i.e., $\bar{s}_p[k]$ and $\bar{s}_p^*[K-k]$ with $p \neq m$). The DIDO precoding matrix **W** in (3) is designed to cancel these two interference terms.

[00193] There are several different embodiments of the DIDO precoder that can be used here depending on joint detection applied at the receiver. In one embodiment, block diagonalization (BD) is employed (see, e.g., Q. H. Spencer, A. L. Swindlehurst, and M. Haardt, "Zeroforcing methods for downlink spatial multiplexing in multiuser MIMO channels," IEEE Trans. Sig. Proc., vol. 52, pp. 461–471, Feb. 2004. K. K. Wong, R. D. Murch, and K. B. Letaief, "A joint - channel diagonalization for multiuser MIMO antenna systems," IEEE Trans. Wireless Comm., vol. 2, pp. 773–786, Jul 2003. L. U. Choi and R. D. Murch, "A transmit preprocessing technique for multiuser MIMO systems using a decomposition approach," IEEE Trans. Wireless Comm., vol. 3, pp. 20–24, Jan 2004. Z. Shen, J. G. Andrews, R. W. Heath, and B. L. Evans, "Low complexity

user selection algorithms for multiuser MIMO systems with block diagonalization," accepted for publication in IEEE Trans. Sig. Proc., Sep. 2005. Z. Shen, R. Chen, J. G. Andrews, R. W. Heath, and B. L. Evans, "Sum capacity of multiuser MIMO broadcast channels with block diagonalization," submitted to IEEE Trans. Wireless Comm., Oct. 2005, computed from the composite channel $\left[\mathbf{H}_e^{(m)}, \mathbf{H}_c^{(m)}\right]$ (rather than $\mathbf{H}_e^{(m)}$). So, the current DIDO system chooses the precoder such that

$$\overset{H}{\boldsymbol{H}}_w \overset{\Delta}{=} \begin{bmatrix} \mathbf{H}_e^{(1)}[k] & \mathbf{H}_c^{(1)}[k] \\ \mathbf{H}_c^{(1)*}[K-k] & \mathbf{H}_e^{(1)*}[K-k] \\ \mathbf{H}_e^{(2)}[k] & \mathbf{H}_c^{(2)}[k] \\ \mathbf{H}_c^{(2)*}[K-k] & \mathbf{H}_e^{(2)*}[K-k] \end{bmatrix} \mathbf{W} = \begin{bmatrix} \alpha_{1,1} & 0 & 0 & 0 \\ 0 & \alpha_{1,2} & 0 & 0 \\ 0 & 0 & \alpha_{2,1} & 0 \\ 0 & 0 & 0 & \alpha_{2,2} \end{bmatrix} \Delta \begin{bmatrix} \overset{H}{\boldsymbol{H}}_w^{(1,1)} & \overset{H}{\boldsymbol{H}}_w^{(1,2)} \\ \overset{H}{\boldsymbol{H}}_w^{(2,1)} & \overset{H}{\boldsymbol{H}}_w^{(2,2)} \end{bmatrix} \quad (4)$$

where $\alpha_{i,j}$ are constants and $\overset{H}{\boldsymbol{H}}_w^{(i,j)} \in C^{2x2}$. This method is beneficial because using this precoder, it is possible to keep other aspects of the DIDO precoder the same as before, since the effects of I/Q gain and phase imbalance are completely cancelled at the transmitter.

[00194] It is also possible to design DIDO precoders that pre-cancel inter-user interference, without pre-cancelling ICI due to IQ imbalance. With this approach, the receiver (instead of the transmitter) compensates for the IQ imbalance by employing one of the receive filters described below. Then, the pre-coding design criterion in (4) can be modified as

$$\overset{H}{\boldsymbol{H}}_{w} \overset{\Delta}{=} \begin{bmatrix} \mathbf{H}_e^{(1)}[k] & \mathbf{H}_c^{(1)}[k] \\ \mathbf{H}_c^{(1)*}[K-k] & \mathbf{H}_e^{(1)*}[K-k] \\ \mathbf{H}_e^{(2)}[k] & \mathbf{H}_c^{(2)}[k] \\ \mathbf{H}_c^{(2)*}[K-k] & \mathbf{H}_e^{(2)*}[K-k] \end{bmatrix} W = \begin{bmatrix} \alpha_{1,1} & \alpha_{1,2} & 0 & 0 \\ \alpha_{2,1} & \alpha_{2,2} & 0 & 0 \\ 0 & 0 & \alpha_{3,3} & \alpha_{3,4} \\ 0 & 0 & \alpha_{4,3} & \alpha_{4,4} \end{bmatrix} \Delta \begin{bmatrix} \overset{H}{\boldsymbol{H}}_{w}^{(1,1)} & \overset{H}{\boldsymbol{H}}_{w}^{(1,2)} \\ \overset{H}{\boldsymbol{H}}_{w}^{(2,1)} & \overset{H}{\boldsymbol{H}}_{w}^{(2,2)} \end{bmatrix} \quad (5)$$

$$\bar{\mathbf{x}}_1[k] = \begin{bmatrix} \overset{H}{\boldsymbol{H}}_{w}^{(1,1)} & \overset{H}{\boldsymbol{H}}_{w}^{(1,2)} \end{bmatrix} \begin{bmatrix} \bar{\mathbf{s}}_1[k] \\ \bar{\mathbf{s}}_2[k] \end{bmatrix} \quad (6)$$

and

$$\bar{\mathbf{x}}_2[k] = \begin{bmatrix} \overset{H}{\boldsymbol{H}}_{w}^{(2,1)} & \overset{H}{\boldsymbol{H}}_{w}^{(2,2)} \end{bmatrix} \begin{bmatrix} \bar{\mathbf{s}}_1[k] \\ \bar{\mathbf{s}}_2[k] \end{bmatrix} \quad (7)$$

where $\bar{\mathbf{s}}_m[k] = [\bar{s}_m[k], \bar{s}_m^*[K-k]]^T$ for the *m*-th transmit symbol and $\bar{\mathbf{x}}_m[k] = [\bar{x}_m[k], \bar{x}_m^*[K-k]]^T$ is the receive symbol vector for user *m*.

At the receive side, to estimate the transmit symbol vector $\bar{s}_m[k]$, user *m* employs ZF filter and the estimated symbol vector is given by

$$\hat{\mathbf{s}}_m^{(ZF)}[k] = [(\overset{H}{\boldsymbol{H}}_{w}^{(m,m)\dagger} \overset{H}{\boldsymbol{H}}_{w}^{(m,m)})^{-1} \overset{H}{\boldsymbol{H}}_{w}^{(m,m)\dagger}] \bar{\mathbf{x}}_m[k] \quad (8)$$

While the ZF filter is the easiest to understand, the receiver may apply any number of other filters known to those skilled in the art. One popular choice is the MMSE filter where

$$\hat{\mathbf{s}}_m^{(MMSE)}[k] = (\overset{H}{\boldsymbol{H}}_{w}^{(m,m)\dagger} + \mathrm{p}^{-1} I)^{-1} \overset{H}{\boldsymbol{H}}_{w}^{(m,m)} \overset{H}{\boldsymbol{H}}_{w}^{(m,m)\dagger} \bar{\mathbf{x}}_m[k] \quad (9)$$

and ρ is the signal-to-noise ratio. Alternatively, the receiver may perform a maximum likelihood symbol detection (or sphere decoder or iterative variation). For example, the first user might use the ML receiver and solve the following optimization

$$\hat{\mathbf{s}}_m^{(ML)}[k] = \arg\min_{\mathbf{s}_1,\mathbf{s}_2 \in S} \left\| \mathbf{y}_1[k] - \begin{bmatrix} \overset{H}{\boldsymbol{H}}_w^{(1,1)} & \overset{H}{\boldsymbol{H}}_w^{(1,2)} \end{bmatrix} \begin{bmatrix} \mathbf{s}_1[k] \\ \mathbf{s}_2[k] \end{bmatrix} \right\| \quad (10)$$

where *S* is the set of all possible vectors s and depends on the constellation size. The ML receiver gives better performance at the expense of requiring more complexity at the receiver. A similar set of equations applies for the second user.

[00195] Note that $\overset{H}{\boldsymbol{H}}_w^{(1,2)}$ and $\overset{H}{\boldsymbol{H}}_w^{(2,1)}$ in (6) and (7) are assumed to have zero entries. This assumption holds only if the transmit precoder is able to cancel completely the inter-user interference as for the criterion in (4). Similarly, $\overset{H}{\boldsymbol{H}}_w^{(1,1)}$ and $\overset{H}{\boldsymbol{H}}_w^{(2,2)}$ are diagonal matrices only if the transmit precoder is able to cancel completely the inter-carrier interference (i.e., from the mirror tones).

[00196] **Figure 13** illustrates one embodiment of a framework for DIDO-OFDM systems with I/Q compensation including IQ-DIDO precoder 1302 within a Base Station (BS), a transmission channel 1304, channel estimation logic 1306 within a user device, and a ZF, MMSE or ML receiver 1308. The channel estimation logic 1306 estimates the channels $\overset{H}{\boldsymbol{H}}_e^{(m)}$ and $\overset{H}{\boldsymbol{H}}_c^{(m)}$ via training symbols and feedbacks these estimates to the precoder 1302 within the AP. The BS computes the DIDO precoder weights (matrix **W**) to pre-cancel the interference due to I/Q gain and phase imbalance as well as inter-user interference and transmits the data to the users through the wireless channel 1304. User device *m* employs the ZF, MMSE or ML receiver 1308, by exploiting the channel estimates provided by the unit 1304, to cancel residual interference and demodulates the data.

[00197] The following three embodiments may be employed to implement this I/Q compensation algorithm:

Method 1 - TX compensation: In this embodiment, the transmitter calculates the pre-coding matrix according to the criterion in (4). At the receiver, the user devices employ a "simplified" ZF receiver, where $\overset{H}{\underset{w}{H}}^{(1,1)}$ and $\overset{H}{\underset{w}{H}}^{(2,2)}$ are assumed to be diagonal matrices. Hence, equation (8) simplifies as

$$\hat{\mathbf{s}}_m[k] = \begin{bmatrix} 1/\alpha_{m,1} & 0 \\ 0 & 1/\alpha_{m,2} \end{bmatrix} \bar{\mathbf{x}}_m[k]. \quad (10)$$

Method 2 - RX compensation: In this embodiment, the transmitter calculates the pre-coding matrix based on the conventional BD method described in R. Chen, R. W. Heath, and J. G. Andrews, "Transmit selection diversity for unitary precoded multiuser spatial multiplexing systems with linear receivers," accepted to IEEE Trans. on Signal Processing, 2005, without canceling inter-carrier and inter-user interference as for the criterion in (4). With this method, the pre-coding matrix in (2) and (3) simplifies as

$$\mathbf{W} = \begin{bmatrix} w_{1,1}[k] & 0 & w_{1,2}[k] & 0 \\ 0 & w_{1,1}^*[K-k] & 0 & w_{1,2}^*[K-k] \\ w_{2,1}[k] & 0 & w_{2,2}[k] & 0 \\ 0 & w_{2,1}^*[K-k] & 0 & w_{2,2}^*[K-k] \end{bmatrix}. \quad (12)$$

At the receiver, the user devices employ a ZF filter as in (8). Note that this method does not pre-cancel the interference at the transmitter as in the method 1 above. Hence, it cancels the inter-carrier interference at the receiver, but it is not able to cancel the inter-user interference. Moreover, in

method 2 the users only need to feedback the vector $\overset{H}{\boldsymbol{H}}_{e}^{(m)}$ for the transmitter to compute the DIDO precoder, as opposed to method 1 that requires feedback of both $\overset{H}{\boldsymbol{H}}_{e}^{(m)}$ and $\overset{H}{\boldsymbol{H}}_{c}^{(m)}$. Therefore, method 2 is particularly suitable for DIDO systems with low rate feedback channels. On the other hand, method 2 requires slightly higher computational complexity at the user device to compute the ZF receiver in (8) rather than (11).

Method 3 - TX-RX compensation: In one embodiment, the two methods described above are combined. The transmitter calculates the pre-coding matrix as in (4) and the receivers estimate the transmit symbols according to (8).

[00198] I/Q imbalance, whether phase imbalance, gain imbalance, or delay imbalance, creates a deleterious degradation in signal quality in wireless communication systems. For this reason, circuit hardware in the past was designed to have very low imbalance. As described above, however, it is possible to correct this problem using digital signal processing in the form of transmit pre-coding and/or a special receiver. One embodiment of the invention comprises a system with several new functional units, each of which is important for the implementation of I/Q correction in an OFDM communication system or a DIDO-OFDM communication system.

[00199] One embodiment of the invention uses pre-coding based on channel state information to cancel inter-carrier interference (ICI) from mirror tones (due to I/Q mismatch) in an OFDM system. As illustrated in **Figure 11**, a DIDO transmitter according to this embodiment includes a user selector unit

1102, a plurality of coding modulation units 1104, a corresponding plurality of mapping units 1106, a DIDO IQ-aware precoding unit 1108, a plurality of RF transmitter units 1114, a user feedback unit 1112 and a DIDO configurator unit 1110.

[00200] The user selector unit 1102 selects data associated with a plurality of users U_1-U_M, based on the feedback information obtained by the feedback unit 1112, and provides this information each of the plurality of coding modulation units 1104. Each coding modulation unit 1104 encodes and modulates the information bits of each user and send them to the mapping unit 1106. The mapping unit 1106 maps the input bits to complex symbols and sends the results to the DIDO IQ-aware precoding unit 1108. The DIDO IQ-aware precoding unit 1108 exploits the channel state information obtained by the feedback unit 1112 from the users to compute the DIDO IQ-aware precoding weights and precoding the input symbols obtained from the mapping units 1106. Each of the precoded data streams is sent by the DIDO IQ-aware precoding unit 1108 to the OFDM unit 1115 that computes the IFFT and adds the cyclic prefix. This information is sent to the D/A unit 1116 that operates the digital to analog conversion and send it to the RF unit 1114. The RF unit 1114 upconverts the baseband signal to intermediate/radio frequency and send it to the transmit antenna.

[00201] The precoder operates on the regular and mirror tones together for the purpose of compensating for I/Q imbalance. Any number of precoder

design criteria may be used including ZF, MMSE, or weighted MMSE design. In a preferred embodiment, the precoder completely removes the ICI due to I/Q mismatch thus resulting in the receiver not having to perform any additional compensation.

[00202] In one embodiment, the precoder uses a block diagonalization criterion to completely cancel inter-user interference while not completely canceling the I/Q effects for each user, requiring additional receiver processing. In another embodiment, the precoder uses a zero-forcing criterion to completely cancel both inter-user interference and ICI due to I/Q imbalance. This embodiment can use a conventional DIDO-OFDM processor at the receiver.

[00203] One embodiment of the invention uses pre-coding based on channel state information to cancel inter-carrier interference (ICI) from mirror tones (due to I/Q mismatch) in a DIDO-OFDM system and each user employs an IQ-aware DIDO receiver. As illustrated in **Figure 12**, in one embodiment of the invention, a system including the receiver 1202 includes a plurality of RF units 1208, a corresponding plurality of A/D units 1210, an IQ-aware channel estimator unit 1204 and a DIDO feedback generator unit 1206.

[00204] The RF units 1208 receive signals transmitted from the DIDO transmitter units 1114, downconverts the signals to baseband and provide the downconverted signals to the A/D units 1210. The A/D units 1210 then convert the signal from analog to digital and send it to the OFDM units 1213. The OFDM units 1213 remove the cyclic prefix and operates the FFT to report the signal to

the frequency domain. During the training period the OFDM units 1213 send the output to the IQ-aware channel estimate unit 1204 that computes the channel estimates in the frequency domain. Alternatively, the channel estimates can be computed in the time domain. During the data period the OFDM units 1213 send the output to the IQ-aware receiver unit 1202. The IQ-aware receiver unit 1202 computes the IQ receiver and demodulates/decodes the signal to obtain the data 1214. The IQ-aware channel estimate unit 1204 sends the channel estimates to the DIDO feedback generator unit 1206 that may quantize the channel estimates and send it back to the transmitter via the feedback control channel 1112.

[00205] The receiver 1202 illustrated in **Figure 12** may operate under any number of criteria known to those skilled in the art including ZF, MMSE, maximum likelihood, or MAP receiver. In one preferred embodiment, the receiver uses an MMSE filter to cancel the ICI caused by IQ imbalance on the mirror tones. In another preferred embodiment, the receiver uses a nonlinear detector like a maximum likelihood search to jointly detect the symbols on the mirror tones. This method has improved performance at the expense of higher complexity.

[00206] In one embodiment, an IQ-aware channel estimator 1204 is used to determine the receiver coefficients to remove ICI. Consequently we claim a DIDO-OFDM system that uses pre-coding based on channel state information to cancel inter-carrier interference (ICI) from mirror tones (due to I/Q mismatch), an IQ-aware DIDO receiver, and an IQ-aware channel estimator. The channel

estimator may use a conventional training signal or may use specially constructed training signals sent on the inphase and quadrature signals. Any number of estimation algorithms may be implemented including least squares, MMSE, or maximum likelihood. The IQ-aware channel estimator provides an input for the IQ-aware receiver.

[00207] Channel state information can be provided to the station through channel reciprocity or through a feedback channel. One embodiment of the invention comprises a DIDO-OFDM system, with I/Q-aware precoder, with an I/Q-aware feedback channel for conveying channel state information from the user terminals to the station. The feedback channel may be a physical or logical control channel. It may be dedicated or shared, as in a random access channel. The feedback information may be generated using a DIDO feedback generator at the user terminal, which we also claim. The DIDO feedback generator takes as an input the output of the I/Q aware channel estimator. It may quantize the channel coefficients or may use any number of limited feedback algorithms known in the art.

[00208] The allocation of users, modulation and coding rate, mapping to space-time-frequency code slots may change depending on the results of the DIDO feedback generator. Thus, one embodiment comprises an IQ-aware DIDO configurator that uses an IQ-aware channel estimate from one or more users to configure the DIDO IQ-aware precoder, choose the modulation rate, coding rate,

subset of users allowed to transmit, and their mappings to space-time-frequency code slots.

[00209] To evaluate the performance of the proposed compensation methods, three DIDO 2 x 2 systems will be compared:

1. With I/Q mismatch: transmit over all the tones (except DC and edge tones), without compensation for I/Q mismatch;
2. With I/Q compensation: transmit over all the tones and compensate for I/Q mismatch by using the "method 1" described above;
3. Ideal: transmit data only over the odd tones to avoid inter-user and inter-carrier (i.e., from the mirror tones) interference caused to I/Q mismatch.

[00210] Hereafter, results obtained from measurements with the DIDO-OFDM prototype in real propagation scenarios are presented. **Figure 14** depicts the 64-QAM constellations obtained from the three systems described above. These constellations are obtained with the same users' locations and fixed average signal-to-noise ratio (~45 dB). The first constellation 1401 is very noisy due to interference from the mirror tones caused by I/Q imbalance. The second constellation 1402 shows some improvements due to I/Q compensations. Note that the second constellation 1402 is not as clean as the ideal case shown as constellation 1403 due to possible phase noise that yields inter-carrier interference (ICI).

[00211] **Figure 15** shows the average SER (Symbol Error Rate) 1501 and per-user goodput 1502 performance of DIDO 2×2 systems with 64-QAM and coding rate 3/4, with and without I/Q mismatch. The OFDM bandwidth is 250 KHz, with 64 tones and cyclic prefix length $L_{cp}=4$. Since in the ideal case we transmit data only over a subset of tones, SER and goodput performance is evaluated as a function of the *average per-tone transmit power* (rather than total transmit power) to guarantee a fair comparison across different cases. Moreover, in the following results, we use normalized values of transmit power (expressed in decibel), since our goal here is to compare the relative (rather than absolute) performance of different schemes. **Figure 15** shows that in presence of I/Q imbalance the SER saturates, without reaching the target SER (~ 10^{-2}), consistently to the results reported in A. Tarighat and A. H. Sayed, "MIMO OFDM receivers for systems with IQ imbalances," IEEE Trans. Sig. Proc., vol. 53, pp. 3583–3596, Sep. 2005. This saturation effect is due to the fact that both signal and interference (from the mirror tones) power increase as the TX power increases. Through the proposed I/Q compensation method, however, it is possible to cancel the interference and obtain better SER performance. Note that the slight increase in SER at high SNR is due to amplitude saturation effects in the DAC, due to the larger transmit power required for 64-QAM modulations.

[00212] Moreover, observe that the SER performance with I/Q compensation is very close to the ideal case. The 2 dB gap in TX power between these two cases is due to possible phase noise that yields additional interference between adjacent OFDM tones. Finally, the goodput curves 1502

show that it is possible to transmit twice as much data when the I/Q method is applied compared to the ideal case, since we use *all the data tones rather than* only the odd tones (as for the ideal case).

[00213] **Figure 16** graphs the SER performance of different QAM constellations with and without I/Q compensation. We observe that, in this embodiment, the proposed method is particularly beneficial for 64-QAM constellations. For 4-QAM and 16-QAM the method for I/Q compensation yields worse performance than the case with I/Q mismatch, possibly because the pro^{po}sed method requires larger power to enable both data transmission and interference cancellation from the mirror tones. Moreover, 4-QAM and 16-QAM are not as affected by I/Q mismatch as 64-QAM due to the larger minimum distance between constellation points. See A. Tarighat, R. Bagheri, and A. H. Sayed, "Compensation schemes and performance analysis of IQ imbalances in OFDM receivers," IEEE Transactions on Signal Processing, vol. 53, pp. 3257–3268, Aug. 2005. This can be also observed in **Figure 16** by comparing the I/Q mismatch against the ideal case for 4-QAM and 16-QAM. Hence, the additional power required by the DIDO precoder with interference cancellation (from the mirror tones) does not justify the small benefit of the I/Q compensation for the cases of 4-QAM and 16-QAM. Note that this issue may be fixed by employing the methods 2 and 3 for I/Q compensation described above.

[00214] Finally, the relative SER performance of the three methods described above is measured in different propagation conditions. For reference,

also described is the SER performance in presence of I/Q mismatch. **Figure 17** depicts the SER measured for a DIDO 2 x 2 system with 64-QAM at carrier frequency of 450.5 MHz and bandwidth of 250 KHz, at two different users' locations. In Location 1 the users are ~6λ from the BS in different rooms and NLOS (Non-Line of Sight)) conditions. In Location 2 the users are ~λ from the BS in LOS (Line of Sight).

[00215] **Figure 17** shows that all three compensation methods always outperform the case of no compensation. Moreover, it should be noted that method 3 outperforms the other two compensation methods in any channel scenario. The relative performance of method 1 and 2 depends on the propagation conditions. It is observed through practical measurement campaigns that method 1 generally outperforms method 2, since it pre-cancels (at the transmitter) the inter-user interference caused by I/Q imbalance. When this inter-user interference is minimal, method 2 may outperform method 1 as illustrated in graph 1702 of **Figure 17**, since it does not suffer from power loss due to the I/Q compensation precoder.

[00216] So far, different methods have been compared by considering only a limited set of propagation scenarios as in Figure 17. Hereafter, the relative performance of these methods in ideal i.i.d.(independent and identically-distributed) channels is measured. DIDO-OFDM systems are simulated with I/Q phase and gain imbalance at the transmit and receive sides. Figure 18 shows the performance of the proposed methods with only gain imbalance at the

transmit side (i.e., with 0.8 gain on the I rail of the first transmit chain and gain 1 on the other rails). It is observed that method 3 outperforms all the other methods. Also, method 1 performs better than method 2 in i.i.d. channels, as opposed to the results obtained in Location 2 in graph 1702 of Figure 17.

[00217] Thus, given the three novel methods to compensate for I/Q imbalance in DIDO-OFDM systems described above, Method 3 outperforms the other proposed compensation methods. In systems with low rate feedback channels, method 2 can be used to reduce the amount of feedback required for the DIDO precoder, at the expense of worse SER performance.

II. Adaptive DIDO Transmission Scheme

[00218] Another embodiment of a system and method to enhance the performance of distributed-input distributed-output (DIDO) systems will now be described. This method dynamically allocates the wireless resources to different user devices, by tracking the changing channel conditions, to increase throughput while satisfying certain target error rate. The user devices estimate the channel quality and feedback it to the Base Station (BS); the Base Station processes the channel quality obtained from the user devices to select the best set of user devices, DIDO scheme, modulation/coding scheme (MCS) and array configuration for the next transmission; the Base Station transmits parallel data to multiple user devices via pre-coding and the signals are demodulated at the receiver.

[00219] A system that efficiently allocates resources for a DIDO wireless link is also described. The system includes a DIDO Base Station with a DIDO configurator, which processes feedback received from the users to select the best set of users, DIDO scheme, modulation/coding scheme (MCS) and array configuration for the next transmission; a receiver in a DIDO system that measures the channel and other relevant parameters to generate a DIDO feedback signal; and a DIDO feedback control channel for conveying feedback information from users to the Base Station.

[00220] As described in detail below, some of the significant features of this embodiment of the invention include, but are not limited to:

[00221] Techniques to adaptively select number of users, DIDO transmission schemes (i.e., antenna selection or multiplexing), modulation/coding scheme (MCS) and array configurations based on the channel quality information, to minimize SER or maximize per-user or downlink spectral efficiency;

[00222] Techniques to define sets of DIDO *transmission modes* as combinations of DIDO schemes and MCSs;

[00223] Techniques to assign different DIDO modes to different time slots, OFDM tones and DIDO substreams, depending on the channel conditions;

[00224] Techniques to dynamically assign different DIDO modes to different users based on their channel quality;

[00225] Criteria to enable adaptive DIDO switching based on link quality metrics computed in the time, frequency and space domains;

[00226] Criteria to enable adaptive DIDO switching based on lookup tables.

[00227] A DIDO system with a DIDO configurator at the Base Station as in **Figure 19** to adaptively select the number of users, DIDO transmission schemes (i.e., antenna selection or multiplexing), modulation/coding scheme (MCS) and array configurations based on the channel quality information, to minimize SER or maximize per user or downlink spectral efficiency;

[00228] A DIDO system with a DIDO configurator at the Base Station and a DIDO feedback generator at each user device as in **Figure 20**, which uses the estimated channel state and/or other parameters like the estimated SNR at the receiver to generate a feedback message to be input into the DIDO configurator.

[00229] A DIDO system with a DIDO configurator at the Base Station, DIDO feedback generator, and a DIDO feedback control channel for conveying DIDO-specific configuration information from the users to the Base Station.

a. Background

[00230] In multiple-input multiple-output (MIMO) systems, diversity schemes such as orthogonal space-time block codes (OSTBC) (See V. Tarokh, H. Jafarkhani, and A. R. Calderbank, "Spacetime block codes from orthogonal designs," IEEE Trans. Info. Th., vol. 45, pp. 1456–467, Jul. 1999) or antenna

selection (See R. W. Heath Jr., S. Sandhu, and A. J. Paulraj, "Antenna selection for spatial multiplexing systems with linear receivers," IEEE Trans. Comm., vol. 5, pp. 142–144, Apr. 2001) are conceived to combat channel fading, providing increased link robustness that translates in better coverage. On the other hand, spatial multiplexing (SM) enables transmission of multiple parallel data streams as a means to enhance systems throughput. See G. J. Foschini, G.D. Golden, R. A. Valenzuela, and P. W. Wolniansky, "Simplified processing for high spectral efficiency wireless communication employing multielement arrays," IEEE Jour. Select. Areas in Comm., vol. 17, no. 11, pp. 1841 – 1852, Nov. 1999. These benefits can be simultaneously achieved in MIMO systems, according to the theoretical diversity/multiplexing tradeoffs derived in L. Zheng and D.N. C. Tse, "Diversity and multiplexing: a fundamental tradeoff in multiple antenna channels," IEEE Trans. Info. Th., vol. 49, no. 5, pp. 1073–1096, May 2003. One practical implementation is to adaptively switch between diversity and multiplexing transmission schemes, by tracking the changing channel conditions.

[00231] A number of adaptive MIMO transmission techniques have been proposed thus far. The diversity/multiplexing switching method in R. W. Heath and A. J. Paulraj, "Switching between diversity and multiplexing in MIMO systems," IEEE Trans. Comm., vol. 53, no. 6, pp. 962 – 968, Jun. 2005, was designed to improve BER (Bit Error Rate) for fixed rate transmission, based on instantaneous channel quality information. Alternatively, statistical channel information can be employed to enable adaptation as in S. Catreux, V. Erceg, D. Gesbert, and R. W. Heath. Jr., "Adaptive modulation and MIMO coding for

broadband wireless data networks," IEEE Comm. Mag., vol. 2, pp. 108–115, June 2002 ("Catreux"), resulting in reduced feedback overhead and number of control messages. The adaptive transmission algorithm in Catreux was designed to enhance spectral efficiency for predefined target error rate in orthogonal frequency division multiplexing (OFDM) systems, based on channel time/frequency selectivity indicators. Similar low feedback adaptive approaches have been proposed for narrowband systems, exploiting the channel spatial selectivity to switch between diversity schemes and spatial multiplexing. See, e.g., A. Forenza, M. R. McKay, A. Pandharipande, R. W. Heath. Jr., and I. B. Collings, "Adaptive MIMO transmission for exploiting the capacity of spatially correlated channels," accepted to the IEEE Trans. on Veh. Tech., Mar. 2007; M. R. McKay, I. B. Collings, A. Forenza, and R. W. Heath. Jr., "Multiplexing/beamforming switching for coded MIMO in spatially correlated Rayleigh channels," accepted to the IEEE Trans. on Veh. Tech., Dec. 2007; A. Forenza, M. R. McKay, R. W. Heath. Jr., and I. B. Collings, "Switching between OSTBC and spatial multiplexing with linear receivers in spatially correlated MIMO channels," Proc. IEEE Veh. Technol. Conf., vol. 3, pp. 1387–1391, May 2006; M. R. McKay, I. B. Collings, A. Forenza, and R. W. Heath Jr., "A throughput-based adaptive MIMO BICM approach for spatially correlated channels," to appear in Proc. IEEE ICC, June 2006

[00232] In this document, we extend the scope of the work presented in various prior publications to DIDO-OFDM systems. See, e.g., R. W. Heath and A. J. Paulraj, "Switching between diversity and multiplexing in MIMO systems,"

IEEE Trans. Comm., vol. 53, no. 6, pp. 962 – 968, Jun. 2005.S. Catreux, V. Erceg, D. Gesbert, and R. W. Heath Jr., "Adaptive modulation and MIMO coding for broadband wireless data networks," IEEE Comm. Mag., vol. 2, pp. 108–115, June 2002; A. Forenza, M. R. McKay, A. Pandharipande, R. W. Heath Jr., and I. B. Collings, "Adaptive MIMO transmission for exploiting the capacity of spatially correlated channels," IEEE Trans. on Veh. Tech., vol.56, n.2, pp.619-630, Mar. 2007. M. R. McKay, I. B. Collings, A. Forenza, and R. W. Heath Jr., "Multiplexing/beamforming switching for coded MIMO in spatially correlated Rayleigh channels," accepted to the IEEE Trans. on Veh. Tech., Dec. 2007; A. Forenza, M. R. McKay, R. W. Heath Jr., and I. B. Collings, "Switching between OSTBC and spatial multiplexing with linear receivers in spatially correlated MIMO channels," Proc. IEEE Veh. Technol. Conf., vol. 3, pp. 1387–1391, May 2006. M. R. McKay, I. B. Collings, A. Forenza, and R. W. Heath Jr., "A throughput-based adaptive MIMO BICM approach for spatially correlated channels," to appear in Proc. IEEE ICC, June 2006.

[00233] A novel adaptive DIDO transmission strategy is described herein that switches between different numbers of users, numbers of transmit antennas and transmission schemes based on channel quality information as a means to improve the system performance. Note that schemes that adaptively select the users in multiuser MIMO systems were already proposed in M. Sharif and B. Hassibi, "On the capacity of MIMO broadcast channel with partial side information," IEEE Trans. Info. Th., vol. 51, p. 506522, Feb. 2005; and W. Choi, A. Forenza, J. G. Andrews, and R. W. Heath Jr., "Opportunistic space division

multiple access with beam selection," to appear in IEEE Trans. on Communications. The opportunistic space division multiple access (OSDMA) schemes in these publications, however, are designed to maximize the sum capacity by exploiting multi-user diversity and they achieve only a fraction of the theoretical capacity of dirty paper codes, since the interference is not completely pre-canceled at the transmitter. In the DIDO transmission algorithm described herein block diagonalization is employed to pre-cancel inter-user interference. The proposed adaptive transmission strategy, however, can be applied to any DIDO system, independently on the type of pre-coding technique.

[00234] The present patent application describes an extension of the embodiments of the invention described above and in the Prior Application, including, but not limited to the following additional features:

1. The training symbols of the Prior Application for channel estimation can be employed by the wireless client devices to evaluate the link-quality metrics in the adaptive DIDO scheme;

2. The base station receives signal characterization data from the client devices as described in the Prior Application. In the current embodiment, the signal characterization data is defined as link-quality metric used to enable adaptation;

3. The Prior Application describes a mechanism to select the number of transmit antennas and users as well as defines throughput allocation. Moreover, different levels of throughput can be dynamically assigned to different

clients as in the Prior Application. The current embodiment of the invention defines novel criteria related to this selection and throughput allocation.

b. Embodiments of the Invention

[00235] The goal of the proposed adaptive DIDO technique is to enhance per-user or downlink spectral efficiency by dynamically allocating the wireless resource in time, frequency and space to different users in the system. The general adaptation criterion is to increase throughput while satisfying the target error rate. Depending on the propagation conditions, this adaptive algorithm can also be used to improve the link quality of the users (or coverage) via diversity schemes. The flowchart illustrated in **Figure 21** describes steps of the adaptive DIDO scheme.

[00236] The Base Station (BS) collects the channel state information (CSI) from all the users in 2102. From the received CSI, the BS computes the link quality metrics in time/frequency/space domains in 2104. These link quality metrics are used to select the users to be served in the next transmission as well as the transmission mode for each of the users in 2106. Note that the transmission modes consist of different combinations of modulation/coding and DIDO schemes. Finally, the BS transmits data to the users via DIDO precoding as in 2108.

[00237] At 2102, the Base Station collects the channel state information (CSI) from all the user devices. The CSI is used by the Base Station to

determine the instantaneous or statistical channel quality for all the user devices at 2104. In DIDO-OFDM systems the channel quality (or link quality metric) can be estimated in the time, frequency and space domains. Then, at 2106, the Base Station uses the link quality metric to determine the best subset of users and *transmission mode* for the current propagation conditions. A set of DIDO transmission modes is defined as combinations of DIDO schemes (i.e., antenna selection or multiplexing), modulation/coding schemes (MCSs) and array configuration. At 2108, data is transmitted to user devices using the selected number of users and transmission modes.

[00238] In one embodiment, the mode selection is enabled by lookup tables (LUTs) pre-computed based on error rate performance of DIDO systems in different propagation environments. These LUTs map channel quality information into error rate performance. To construct the LUTs, the error rate performance of DIDO systems is evaluated in different propagation scenarios as a function of the SNR. From the error rate curves, it is possible to compute the minimum SNR required to achieve certain pre-defined target error rate. We define this SNR requirement as *SNR threshold*. Then, the SNR thresholds are evaluated in different propagation scenarios and for different DIDO transmission modes and stored in the LUTs. For example, the SER results in **Figures 24** and **26** can be used to construct the LUTs. Then, from the LUTs, the Base Station selects the transmission modes for the active users that increase throughput

while satisfying predefined target error rate. Finally, the Base Station transmits data to the selected users via DIDO pre-coding. Note that different DIDO modes can be assigned to different time slots, OFDM tones and DIDO substreams such that the adaptation may occur in time, frequency and space domains.

[00239] One embodiment of a system employing DIDO adaptation is illustrated in **Figures 19-20**. Several new functional units are introduced to enable implementation of the proposed DIDO adaptation algorithms. Specifically, in one embodiment, a DIDO configurator 1910 performs a plurality of functions including selecting the number of users, DIDO transmission schemes (i.e., antenna selection or multiplexing), modulation/coding scheme (MCS), and array configurations based on the channel quality information 1912 provided by user devices.

[00240] The user selector unit 1902 selects data associated with a plurality of users U_1-U_M, based on the feedback information obtained by the DIDO configurator 1910, and provides this information each of the plurality of coding modulation units 1904. Each coding modulation unit 1904 encodes and modulates the information bits of each user and sends them to the mapping unit 1906. The mapping unit 1906 maps the input bits to complex symbols and sends it to the precoding unit 1908. Both the coding modulation units 1904 and the mapping unit 1906 exploit the information obtained from the DIDO configurator unit 1910 to choose the type of modulation/coding scheme to employ for each user. This information is computed by the DIDO configurator unit 1910 by

exploiting the channel quality information of each of the users as provided by the feedback unit 1912. The DIDO precoding unit 1908 exploits the information obtained by the DIDO configurator unit 1910 to compute the DIDO precoding weights and precoding the input symbols obtained from the mapping units 1906. Each of the precoded data streams are sent by the DIDO precoding unit 1908 to the OFDM unit 1915 that computes the IFFT and adds the cyclic prefix. This information is sent to the D/A unit 1916 that operates the digital to analog conversion and sends the resulting analog signal to the RF unit 1914. The RF unit 1914 upconverts the baseband signal to intermediate/radio frequency and send it to the transmit antenna.

[00241] The RF units 2008 of each client device receive signals transmitted from the DIDO transmitter units 1914, downconverts the signals to baseband and provide the downconverted signals to the A/D units 2010. The A/D units 2010 then convert the signal from analog to digital and send it to the OFDM units 2013. The OFDM units 2013 remove the cyclic prefix and carries out the FFT to report the signal to the frequency domain. During the training period the OFDM units 2013 send the output to the channel estimate unit 2004 that computes the channel estimates in the frequency domain. Alternatively, the channel estimates can be computed in the time domain. During the data period the OFDM units 2013 send the output to the receiver unit 2002 which demodulates/decodes the signal to obtain the data 2014. The channel estimate

unit 2004 sends the channel estimates to the DIDO feedback generator unit 2006 that may quantize the channel estimates and send it back to the transmitter via the feedback control channel 1912.

[00242] The DIDO configurator 1910 may use information derived at the Base Station or, in a preferred embodiment, uses additionally the output of a DIDO Feedback Generator 2006 (see **Figure 20**), operating at each user device. The DIDO Feedback Generator 2006 uses the estimated channel state 2004 and/or other parameters like the estimated SNR at the receiver to generate a feedback message to be input into the DIDO Configurator 1910. The DIDO Feedback Generator 2006 may compress information at the receiver, may quantize information, and/or use some limited feedback strategies known in the art.

[00243] The DIDO Configurator 1910 may use information recovered from a DIDO Feedback Control Channel 1912. The DIDO Feedback Control Channel 1912 is a logical or physical control channel that is used to send the output of the DIDO Feedback Generator 2006 from the user to the Base Station. The control channel 1912 may be implemented in any number of ways known in the art and may be a logical or a physical control channel. As a physical channel it may comprise a dedicated time/frequency slot assigned to a user. It may also be a random access channel shared by all users. The control channel may be pre-assigned or it may be created by stealing bits in a predefined way from an existing control channel.

[00244] In the following discussion, results obtained through measurements with the DIDO-OFDM prototype are described in real propagation environments. These results demonstrate the potential gains achievable in adaptive DIDO systems. The performance of different order DIDO systems is presented initially, demonstrating that it is possible to increase the number of antennas/user to achieve larger downlink throughput. The DIDO performance as a function of user device's location is then described, demonstrating the need for tracking the changing channel conditions. Finally, the performance of DIDO systems employing diversity techniques is described.

i. Performance of Different Order DIDO Systems

[00245] The performance of different DIDO systems is evaluated with increasing number of transmit antennas $N = M$, where M is the number of users. The performance of the following systems is compared: SISO, DIDO 2 × 2, DIDO 4 × 4, DIDO 6 × 6 and DIDO 8 × 8. DIDO N x M refers to DIDO with N transmit antennas at the BS and M users.

[00246] **Figure 22** illustrates the transmit/receive antenna layout in a exemplary residential floor plan. The transmit antennas 2201 are placed in squared array configuration and the users are located around the transmit array. In **Figure 22**, T indicates the "transmit" antennas and U refers to the "user devices" 2202.

[00247] Different antenna subsets are active in the 8-element transmit array, depending on the value of *N* chosen for different measurements. For each DIDO order (*N*) the subset of antennas that covers the largest real estate for the fixed size constraint of the 8-element array was chosen. This criterion is expected to enhance the spatial diversity for any given value of *N*.

[00248] **Figure 23** shows the array configurations for different DIDO orders that fit the available real estate (i.e., dashed line and outer walls). The squared dashed box has dimensions of 24"×24", corresponding to ~ λ × λ at the carrier frequency of 450 MHz.

[00249] Based on the comments related to **Figure 23** and with reference to **Figure 22**, the performance of each of the following systems will now be defined and compared:

SISO with T1 and U1 (2301)

DIDO 2 × 2 with T1,2 and U1,2 (2302)

DIDO 4 × 4 with T1,2,3,4 and U1,2,3,4 (2303)

DIDO 6 × 6 with T1,2,3,4,5,6 and U1,2,3,4,,5,6 (2304)

DIDO 8 × 8 with T1,2,3,4,5,6,7,8 and U1,2,3,4,5,6,7,8 (2305)

[00250] **Figure 24** shows the SER, BER, SE (Spectral Efficiency) and goodput performance as a function of the transmit (TX) power for the DIDO systems described above, with 4-QAM and FEC (Forward Error Correction) rate of 1/2. Observe that the SER and BER performance degrades for increasing values of *N*. This effect is due to two phenomena: for fixed TX power, the input

power to the DIDO array is split between increasing number of users (or data streams); the spatial diversity decreases with increasing number of users in realistic (spatially correlated) DIDO channels.

[00251] To compare the relative performance of different order DIDO systems the target BER is fixed to 10^{-4} (this value may vary depending on the system) that corresponds approximately to SER= 10^{-2} as shown in **Figure 24**. We refer to the TX power values corresponding to this target as TX power thresholds (TPT). For any *N*, if the TX power is below the TPT, we assume it is not possible to transmit with DIDO order *N* and we need to switch to lower order DIDO. Also, in **Figure 24**, observe that the SE and goodput performance saturate when the TX power exceeds the TPTs for any value of *N*. From these results, an adaptive transmission strategy may be designed that switches between different order DIDO to enhance SE or goodput for fixed predefined target error rate.

ii. Performance with Variable User Location

[00252] The goal of this experiment is to evaluate the DIDO performance for different users' location, via simulations in spatially correlated channels. DIDO 2 x 2 systems are considered with 4QAM and an FEC rate of 1/2. User 1 is at a broadside direction from the transmit array, whereas user 2 changes locations from broadside to endfire directions as illustrated in **Figure 25**. The transmit antennas are spaced ~λ/2 and separated ~2.5λ from the users.

[00253] **Figure 26** shows the SER and per-user SE results for different locations of user device 2. The user device's angles of arrival (AOAs) range between 0º and 90º, measured from the broadside direction of the transmit array. Observe that, as the user device's angular separation increases, the DIDO performance improves, due to larger diversity available in the DIDO channel. Also, at target SER= 10^{-2} there is a 10dB gap between the cases AOA2= 0º and AOA2= 90º. This result is consistent to the simulation results obtained in Figure 35 for an angle spread of 10º. Also, note that for the case of AOA1=AOA2= 0º there may be coupling effects between the two users (due to the proximity of their antennas) that may vary their performance from the simulated results in **Figure 35**.

iii. Preferred Scenario for DIDO 8 X 8

[00254] **Figure 24** illustrated that DIDO 8 X 8 yields a larger SE than lower order DIDO at the expense of higher TX power requirement. The goal of this analysis is to show there are cases where DIDO 8 x 8 outperforms DIDO 2 x 2, not only in terms of peak spectral efficiency (SE), but also in terms of TX power requirement (or TPT) to achieve that peak SE.

[00255] Note that, in i.i.d. (ideal) channels, there is ~6dB gap in TX power between the SE of DIDO 8 × 8 and DIDO 2 × 2. This gap is due to the fact that DIDO 8 × 8 splits the TX power across eight data streams, whereas DIDO 2 X 2 only between two streams. This result is shown via simulation in **Figure 32**.

[00256] In spatially correlated channels, however, the TPT is a function of the characteristics of the propagation environment (e.g., array orientation, user location, angle spread). For example, Figure 35 shows ~15dB gap for low angle spread between two different user device's locations. Similar results are presented in **Figure 26** of the present application.

[00257] Similarly to MIMO systems, the performance of DIDO systems degrades when the users are located at endfire directions from the TX array (due to lack of diversity). This effect has been observed through measurements with the current DIDO prototype. Hence, one way to show that DIDO 8 × 8 outperforms DIDO 2 × 2 is to place the users at endfire directions with respect to the DIDO 2 × 2 arrays. In this scenario, DIDO 8 × 8 outperforms DIDO 2 × 2 due to the higher diversity provided by the 8-antenna array.

[00258] In this analysis, consider the following systems:

System 1: DIDO 8 × 8 with 4-QAM (transmit 8 parallel data streams every time slot);

System 2: DIDO 2 X 2 with 64-QAM (transmit to users X and Y every 4 time slots). For this system we consider four combinations of TX and RX antenna locations: a) T1,T2 U1,2 (endfire direction); b) T3,T4 U3,4 (endfire direction); c) T5,T6 U5,6 (~30° from the endfire direction); d) T7,T8 U7,8 (NLOS (Non-Line of Sight));

System 3: DIDO 8 × 8 with 64-QAM; and

System 4: MISO 8 × 1 with 64-QAM (transmit to user X every 8 time slots).

For all these cases, an FEC rate of ¾ was used.

The users' locations are depicted in **Figure 27**.

[00259] In **Figure 28** the SER results show a ~15dB gap between Systems 2a and 2c due to different array orientations and user locations (similar to the simulation results in **Figure 35**). The first subplot in the second row shows the values of TX power for which the SE curves saturate (i.e. corresponding to BER 1e-4). We observe that System 1 yields larger per-user SE for lower TX power requirement (~ 5dB less) than System 2. Also, the benefits of DIDO 8 × 8 versus DIDO 2 ×2 are more evident for the DL (downlink) SE and DL goodput due to multiplexing gain of DIDO 8 × 8 over DIDO 2 × 2. System 4 has lower TX power requirement (8dB less) than System 1, due to the array gain of beamforming (i.e., MRC with MISO 8 × 1). But System 4 yields only 1/3 of per-user SE compared to System 1. System 2 performs worse than System 1 (i.e., yields lower SE for larger TX power requirement). Finally, System 3 yields much larger SE (due to larger order modulations) than System 1 for larger TX power requirement (~ 15dB).

[00260] From these results, the following conclusions may be drawn:

One channel scenario was identified for which DIDO 8 × 8 outperforms DIDO 2 × 2 (i.e., yields larger SE for lower TX power requirement);

In this channel scenario, DIDO 8 × 8 yields larger per user SE and DL SE than DIDO 2 × 2 and MISO 8 × 1; and

It is possible to further increase the performance of DIDO 8 × 8 by using higher order modulations (i.e., 64-QAM rather than 4-QAM) at the expense of larger TX power requirements (~15dB more).

iv. DIDO with Antenna Selection

[00261] Hereafter, we evaluate the benefit of the antenna selection algorithm described in R. Chen, R. W. Heath, and J. G. Andrews, "Transmit selection diversity for unitary precoded multiuser spatial multiplexing systems with linear receivers," accepted to IEEE Trans. on Signal Processing, 2005. We present the results for one particular DIDO system with two users, 4-QAM and FEC rate of 1/2. The following systems are compared in **Figure 27**:

DIDO 2 × 2 with T1,2 and U1,2; and

DIDO 3 × 2 using antenna selection with T1,2,3 and U1,2.

[00262] The transmit antenna's and user device locations are the same as in **Figure 27**.

[00263] **Figure 29** shows that DIDO 3 ×2 with antenna selection may provide ~5dB gain compared to DIDO 2 × 2 systems (with no selection). Note that the channel is almost static (i.e., no Doppler), so the selection algorithms adapts to the path-loss and channel spatial correlation rather than the fast-fading.

We should be seeing different gains in scenarios with high Doppler. Also, in this particular experiment it was observed that the antenna selection algorithm selects antennas 2 and 3 for transmission.

iv. SNR thresholds for the LUTs

[00264] In section [0171] we stated that the mode selection is enabled by LUTs. The LUTs can be pre-computed by evaluating the SNR thresholds to achieve certain predefined target error-rate performance for the DIDO transmission modes in different propagation environments. Hereafter, we provide the performance of DIDO systems with and without antenna selection and variable number of users that can be used as guidelines to construct the LUTs. While **Figures 24, 26, 28, 29** were derived from practical measurements with the DIDO prototype, the following Figures are obtained through simulations. The following BER results assume no FEC.

[00265] **Figure 30** shows the average BER performance of different DIDO precoding schemes in i.i.d. channels. The curve labeled as 'no selection' refers to the case when BD is employed. In the same figure the performance of antenna selection (ASel) is shown for different number of extra antennas (with respect to the number of users). It is possible to see that as the number of extra antennas increases, ASel provides better diversity gain (characterized by the slope of the BER curve in high SNR regime), resulting in better coverage. For example, if we fix the target BER to 10^{-2} (practical value for uncoded systems), the SNR gain provided by ASel increases with the number of antennas.

[00266] **Figure 31** shows the SNR gain of ASel as a function of the number of extra transmit antennas in i.i.d. channels, for different targets BER. It is possible to see that, just by adding 1 or 2 antennas, ASel yields significant SNR gains compared to BD. In the following sections, we will evaluate the performance of ASel only for the cases of 1 or 2 extra antennas and by fixing the target BER to 10^{-2} (for uncoded systems).

[00267] **Figure 32** depicts the SNR thresholds as a function of the number of users (M) for BD and ASel with 1 and 2 extra antennas in i.i.d. channels. We observe that the SNR thresholds increase with M due to the larger receive SNR requirement for larger number of users. Note that we assume fixed total transmit power (with variable number of transmit antennas) for any number of users. Moreover, Figure 32 shows that the gain due to antenna selection is constant for any number of users in i.i.d. channels.

[00268] Hereafter, we show the performance of DIDO systems in spatially correlated channels. We simulate each user's channel through the COST-259 spatial channel model described in X. Zhuang, F. W. Vook, K. L. Baum, T. A. Thomas, and M. Cudak, "Channel models for link and system level simulations," IEEE 802.16 Broadband Wireless Access Working Group, Sep. 2004.. We generate single-cluster for each user. As a case study, we assume NLOS channels, uniform linear array (ULA) at the transmitter, with element spacing of 0.5 lambda. For the case of 2-user system, we simulate the clusters with mean angles of arrival AOA1 and AOA2 for the first and second user, respectively. The

AOAs are measured with respect to the broadside direction of the ULA. When more than two users are in the system, we generate the users' clusters with uniformly spaced mean AOAs in the range $[-\phi_m, \phi_m]$, where we define

$$\Phi_M = \frac{\Delta\phi(M-1)}{2} \qquad (13)$$

with K being the number of users and $\Delta\phi$ is the angular separation between the users' mean AOAs. Note that the angular range $[-\phi_m, \phi_m]$ is centered at the 0^o angle, corresponding to the broadside direction of the ULA. Hereafter, we study the BER performance of DIDO systems as a function of the channel angle spread (AS) and angular separation between users, with BD and ASel transmission schemes and different numbers of users.

[00269] **Figure 33** depicts the BER versus per-user average SNR for two users located at the same angular direction (i.e., AOA1 = AOA2 = 0^o, with respect to the broadside direction of the ULA), with different values of AS. It is possible to see that as the AS increases the BER performance improves and approaches the i.i.d. case. In fact, higher AS yields statistically less overlapping between the eigenmodes of the two users and better performance of the BD precoder.

[00270] **Figure 34** shows similar results as **Figure 33**, but with higher angular separation between the users. We consider AOA1 = 0^o and AOA2 = 90^o (i.e., 90^o angular separation). The best performance is now achieved in the low

AS case. In fact, for the case of high angle separation, there is less overlapping between the users' eigenmodes when the angular spread is low. Interestingly, we observe that the BER performance in low AS is better than i.i.d. channels for the same reasons just mentioned.

[00271] Next, we compute the SNR thresholds, for target BER of 10^{-2} in different correlation scenarios. **Figure 35** plots the SNR thresholds as a function of the AS for different values of the mean AOAs of the users. For low users' angular separation reliable transmissions with reasonable SNR requirement (i.e., 18 dB) are possible only for channels characterized by high AS. On the other hand, when the users are spatially separated, less SNR is required to meet the same target BER.

[00272] **Figure 36** shows the SNR threshold for the case of five users. The users' mean AOAs are generated according to the definition in (13), with different values of angular separation $\Delta\phi$. We observe that for $\Delta\phi = 0^o$ and AS< 15°, BD performs poorly due to the small angle separation between users, and the target BER is not satisfied. For increasing AS the SNR requirement to meet the fixed target BER decreases. On the other end, for $\Delta\phi = 30^o$, the smallest SNR requirement is obtained at low AS, consistently to the results in Figure 35. As the AS increases, the SNR thresholds saturate to the one of i.i.d. channels. Note that_$\Delta\phi = 30^o$ with 5 users corresponds to the AOA range of [−60°, 60°], that is typical for base stations in cellular systems with 120° sectorized cells.

[00273] Next, we study the performance of ASel transmission scheme in spatially correlated channels. **Figure 37** compares the SNR threshold of BD and ASel, with 1 and 2 extra antennas, for two user case. We consider two different cases of angular separation between users: {AOA1 = 0^o,AOA2 = 0^o} and {AOA1 = 0^o,AOA2 = 90^o}. The curves for BD scheme (i.e., no antenna selection) are the same as in Figure 35. We observe that ASel yields 8 dB and 10 dB SNR gains with 1 and 2 extra antennas, respectively, for high AS. As the AS decreases, the gain due to ASel over BD becomes smaller due to the reduced number of degrees of freedom in the MIMO broadcast channel. Interestingly, for AS= 0^o (i.e., close to LOS channels) and the case {AOA1 = 0^o,AOA2 = 90^o}, ASel does not provide any gain due to the luck of diversity in the space domain. **Figure 38** shows similar results as Figure 37, but for five user case.

[00274] We compute the SNR thresholds (assuming usual target BER of 10^{-2}) as a function of the number of users in the system (M), for both BD and ASel transmission schemes. The SNR thresholds correspond to the average SNR, such that the total transmit power is constant for any M. We assume maximum separation between the mean AOAs of each user's cluster within the azimuth range $[-\phi_m, \phi_m]$ = [-60^o, 60^o]. Then, the angular separation between users is $\Delta\phi = 120^o/(M-1)$.

[00275] **Figure 39** shows the SNR thresholds for BD scheme with different values of AS. We observe that the lowest SNR requirement is obtained for AS= 0.1^o (i.e., low angle spread) with relatively small number of users (i.e., $K \leq 20$),

due to the large angular separation between users. For $M > 50$, however, the SNR requirement is way above 40 dB, since $\Delta\phi$ is very small, and BD is impractical. Moreover, for AS> 10^{o} the SNR thresholds remain almost constant for any M, and the DIDO system in spatially correlated channels approaches the performance of i.i.d. channels.

[00276] To reduce the values of the SNR thresholds and improve the performance of the DIDO system we apply ASel transmission scheme. **Figure 40** depicts the SNR thresholds in spatially correlated channels with AS= 0.1^{o} for BD and ASel with 1 and 2 extra antennas. For reference we report also the curves for the i.i.d. case shown in Figure 32.. It is possible to see that, for low number of users (i.e., $M \leq 10$), antenna selection does not help reducing the SNR requirement due to the lack of diversity in the DIDO broadcast channel. As the number of users increases, ASel benefits from multiuser diversity yielding SNR gains (i.e., 4 dB for $M = 20$). Moreover, for $M \leq 20$, the performance of ASel with 1 or 2 extra antennas in highly spatially correlated channels is the same.

[00277] We then compute the SNR thresholds for two more channel scenarios: AS= 5^{o} in **Figure 41** and AS= 10^{o} in **Figure 42**. Figure 41 shows that ASel yields SNR gains also for relatively small number of users (i.e., $M \leq 10$) as opposed to Figure 40, due to the larger angle spread. For AS= 10^{o} the SNR thresholds reduce further and the gains due to ASel get higher, as reported in **Figure 42**.

[00278] Finally, we summarize the results presented so far for correlated channels. **Figure 43** and **Figure 44** show the SNR thresholds as a function of the number of users (*M*) and angle spread (AS) for BD and ASel schemes, with 1 and 2 extra antennas, respectively. Note that the case of AS= 30^o corresponds actually to i.i.d. channels, and we used this value of AS in the plot only for graphical representation. We observe that, while BD is affected by the channel spatial correlation, ASel yields almost the same performance for any AS. Moreover, for AS= 0.1^o, ASel performs similarly to BD for low *M*, whereas outperforms BD for large *M* (i.e., $M \geq 20$), due to multiuser diversity.

[00279] **Figure 49** compares the performance of different DIDO schemes in terms of SNR thresholds. The DIDO schemes considered are: BD, ASel, BD with eigenmode selection (BD-ESel) and maximum ratio combining (MRC). Note that MRC, does not pre-cancel interference at the transmitter (unlike the other methods), but does provide larger gain in case the users are spatially separated. In Figure 49 we plot the SNR threshold for target BER= 10−2 for DIDO N × 2 systems when the two users are located at -30 ^{o} and 30 ^{o} from the broadside direction of the transmit array, respectively. We observe that for low AS the MRC scheme provides 3 dB gain compared to the other schemes since the users' spatial channels are well separated and the effect of inter-user interference is low. Note that the gain of MRC over DIDO N × 2 are due to array gain. For AS larger than 20^o the QR-ASel scheme outperforms the other and yields about 10 dB gain compared to BD 2×2 with no selection. QR-ASel and BD-ESel provide about the same performance for any value of AS.

[00280] Described above is a novel adaptive transmission technique for DIDO systems. This method dynamically switches between DIDO transmission modes to different users to enhance throughput for fixed target error rate. The performance of different order DIDO systems was measured in different propagation conditions and it was observed that significant gains in throughput may be achieved by dynamically selecting the DIDO modes and number of users as a function of the propagation conditions.

Pre-compensation of Frequency and Phase Offset

a. Background

[00281] As previously described, wireless communication systems use carrier waves to convey information. These carrier waves are usually sinusoids that are amplitude and/or phase modulated in response to information to be transmitted. The nominal frequency of the sinusoid is known as the carrier frequency. To create this waveform, the transmitter synthesizes one or more sinusoids and uses upconversion to create a modulated signal riding on a sinusoid with the prescribed carrier frequency. This may be done through direct conversion where the signal is directly modulated on the carrier or through multiple upconversion stages. To process this waveform, the receiver must demodulate the received RF signal and effectively remove the modulating carrier. This requires that the receiver synthesize one or more sinusoidal signals to reverse the process of modulation at the transmitter, known as downconversion. Unfortunately, the sinusoidal signals generated at the transmitter and receiver are derived from different reference oscillators. No reference oscillator creates a

perfect frequency reference; in practice there is always some deviation from the true frequency.

[00282] In wireless communication systems, the differences in the outputs of the reference oscillators at the transmitter and receivers create the phenomena known as carrier frequency offset, or simply frequency offset, at the receiver. Essentially there is some residual modulation in the received signal (corresponding to the difference in the transmit and receive carriers), which occurs after downconversion. This creates distortion in the received signal resulting in higher bit error rates and lower throughput.

[00283] There are different techniques for dealing with carrier frequency offset. Most approaches estimate the carrier frequency offset at the receiver and then apply a carrier frequency offset correction algorithm. The carrier frequency offset estimation algorithm may be blind using offset QAM (T. Fusco and M. Tanda, "Blind Frequency-offset Estimation for OFDM/OQAM Systems," IEEE Transactions on Signal Processing, vol. 55, pp. 1828–1838, 2007); periodic properties (E. Serpedin, A. Chevreuil, G. B. Giannakis, and P. Loubaton, "Blind channel and carrier frequency offset estimation using periodic modulation precoders," IEEE Transactions on Signal Processing, vol. 48, no. 8, pp. 2389–2405, Aug. 2000); or the cyclic prefix in orthogonal frequency division multiplexing (OFDM) structure approaches (J. J. van de Beek, M. Sandell, and P. O. Borjesson, "ML estimation of time and frequency offset in OFDM systems," IEEE Transactions on Signal Processing, vol. 45, no. 7, pp. 1800–1805, July 1997; U. Tureli, H. Liu, and M. D. Zoltowski, "OFDM blind carrier offset

estimation: ESPRIT," IEEE Trans. Commun., vol. 48, no. 9, pp. 1459–1461, Sept. 2000; M. Luise, M. Marselli, and R. Reggiannini, "Low-complexity blind carrier frequency recovery for OFDM signals over frequency-selective radio channels," IEEE Trans. Commun., vol. 50, no. 7, pp. 1182–1188, July 2002).

[00284] Alternatively special training signals may be utilized including a repeated data symbol (P. H. Moose, "A technique for orthogonal frequency division multiplexing frequency offset correction," IEEE Trans. Commun., vol. 42, no. 10, pp. 2908–2914, Oct. 1994); two different symbols (T. M. Schmidl and D. C. Cox, "Robust frequency and timing synchronization for OFDM," IEEE Trans. Commun., vol. 45, no. 12, pp. 1613–1621, Dec. 1997); or periodically inserted known symbol sequences (M. Luise and R. Reggiannini, "Carrier frequency acquisition and tracking for OFDM systems," IEEE Trans. Commun., vol. 44, no. 11, pp. 1590–1598, Nov. 1996). The correction may occur in analog or in digital. The receiver can also use carrier frequency offset estimation to precorrect the transmitted signal to eliminate offset. Carrier frequency offset correction has been studied extensively for multicarrier and OFDM systems due to their sensitivity to frequency offset (J. J. van de Beek, M. Sandell, and P. O. Borjesson, "ML estimation of time and frequency offset in OFDM systems," Signal Processing, IEEE Transactions on [see also Acoustics, Speech, and Signal Processing, IEEE Transactions on], vol. 45, no. 7, pp. 1800–1805, July 1997; U. Tureli, H. Liu, and M. D. Zoltowski, "OFDM blind carrier offset estimation: ESPRIT," IEEE Trans. Commun., vol. 48, no. 9, pp. 1459–1461, Sept. 2000; T. M. Schmidl and D. C. Cox, "Robust frequency and timing

synchronization for OFDM," IEEE Trans. Commun., vol. 45, no. 12, pp. 1613–1621, Dec. 1997; M. Luise, M. Marselli, and R. Reggiannini, "Low-complexity blind carrier frequency recovery for OFDM signals over frequency-selective radio channels," IEEE Trans. Commun., vol. 50, no. 7, pp. 1182–1188, July 2002).

[00285] Frequency offset estimation and correction is an important issue for multi-antenna communication systems, or more generally MIMO (multiple input multiple output) systems. In MIMO systems where the transmit antennas are locked to one frequency reference and the receivers are locked to another frequency reference, there is a single offset between the transmitter and receiver. Several algorithms have been proposed to tackle this problem using training signals (K. Lee and J. Chun, "Frequency-offset estimation for MIMO and OFDM systems using orthogonal training sequences," IEEE Trans. Veh. Technol., vol. 56, no. 1, pp. 146–156, Jan. 2007; M. Ghogho and A. Swami, "Training design for multipath channel and frequency offset estimation in MIMO systems," IEEE Transactions on Signal Processing, vol. 54, no. 10, pp. 3957–3965, Oct. 2006, and adaptive tracking C. Oberli and B. Daneshrad, "Maximum likelihood tracking algorithms for MIMOOFDM," in Communications, 2004 IEEE International Conference on, vol. 4, June 20– 24, 2004, pp. 2468–2472). A more severe problem is encountered in MIMO systems where the transmit antennas are not locked to the same frequency reference but the receive antennas are locked together. This happens practically in the uplink of a spatial division multiple access (SDMA) system, which can be viewed as a MIMO system where the different users correspond to different transmit antennas. In this case the

compensation of frequency offset is much more complicated. Specifically, the frequency offset creates interference between the different transmitted MIMO streams. It can be corrected using complex joint estimation and equalization algorithms (A. Kannan, T. P. Krauss, and M. D. Zoltowski, "Separation of cochannel signals under imperfect timing and carrier synchronization," IEEE Trans. Veh. Technol., vol. 50, no. 1, pp. 79–96, Jan. 2001), and equalization followed by frequency offset estimation (T. Tang and R. W. Heath, "Joint frequency offset estimation and interference cancellation for MIMO-OFDM systems [mobile radio]," 2004. VTC2004-Fall. 2004 IEEE 60th Vehicular Technology Conference, vol. 3, pp. 1553–1557, Sept.26–29, 2004; X. Dai, "Carrier frequency offset estimation for OFDM/SDMA systems using consecutive pilots," IEEE Proceedings- Communications, vol. 152, pp. 624–632, Oct.7, 2005). Some work has dealt with the related problem of residual phase off-set and tracking error, where residual phase offsets are estimated and compensated after frequency offset estimation, but this work only consider the uplink of an SDMA OFDMA system (L. Haring, S. Bieder, and A. Czylwik, "Residual carrier and sampling frequency synchronization in multiuser OFDM systems," 2006. VTC 2006-Spring. IEEE 63rd Vehicular Technology Conference, vol. 4, pp. 1937–1941, 2006). The most severe case in MIMO systems occurs when all transmit and receive antennas have different frequency references. The only available work on this topic only deals with asymptotic analysis of estimation error in flat fading channels (O. Besson and P. Stoica, "On parameter estimation of MIMO flat-fading channels with frequency offsets," Signal Processing, IEEE

Transactions on [see also Acoustics, Speech, and Signal Processing, IEEE Transactions on], vol. 51, no. 3, pp. 602–613, Mar. 2003).

[00286] A case that has not been significantly investigated occurs when the different transmit antennas of a MIMO system do not have the same frequency reference and the receive antennas process the signals independently. This happens in what is known as a distributed input distributed-output (DIDO) communication system, also called the MIMO broadcast channel in the literature. DIDO systems consist of one access point with distributed antennas that transmit parallel data streams (via precoding) to multiple users to enhance downlink throughput, while exploiting the same wireless resources (i.e., same slot duration and frequency band) as conventional SISO systems. Detailed description of DIDO systems was presented in, S. G. Perlman and T. Cotter, "System and method for distributed input-distributed output wireless communications," United States Patent Application 20060023803, July 2004. There are many ways to implement DIDO precoders. One solution is block diagonalization (BD) described in, for example, Q. H. Spencer, A. L. Swindlehurst, and M. Haardt, "Zero-forcing methods for downlink spatial multiplexing in multiuser MIMO channels," IEEE Trans. Sig. Proc., vol. 52, pp. 461–471, Feb. 2004; K. K. Wong, R. D. Murch, and K. B. Letaief, "A joint-channel diagonalization for multiuser MIMO antenna systems," IEEE Trans. Wireless Comm., vol. 2, pp. 773–786, Jul 2003; L. U. Choi and R. D. Murch, "A transmit preprocessing technique for multiuser MIMO systems using a decomposition approach," IEEE Trans. Wireless Comm., vol. 3, pp. 20–24, Jan 2004; Z. Shen, J. G. Andrews, R. W. Heath, and B. L. Evans,

"Low complexity user selection algorithms for multiuser MIMO systems with block diagonalization," accepted for publication in IEEE Trans. Sig. Proc., Sep. 2005; Z. Shen, R. Chen, J. G. Andrews, R. W. Heath, and B. L. Evans, "Sum capacity of multiuser MIMO broadcast channels with block diagonalization," submitted to IEEE Trans. Wireless Comm., Oct. 2005; R. Chen, R. W. Heath, and J. G. Andrews, "Transmit selection diversity for unitary precoded multiuser spatial multiplexing systems with linear receivers," accepted to IEEE Trans. on Signal Processing, 2005.

[00287] In DIDO systems, transmit precoding is used to separate data streams intended for different users. Carrier frequency offset causes several problems related to the system implementation when the transmit antenna radio frequency chains do not share the same frequency reference. When this happens, each antenna is effectively transmits at a slightly different carrier frequency. This destroys the integrity of the DIDO precoder resulting in each user experiencing extra interference. Proposed below are several solutions to this problem. In one embodiment of the solution, the DIDO transmit antennas share a frequency reference through a wired, optical, or wireless network. In another embodiment of the solution, one or more users estimate the frequency offset differences (the relative differences in the offsets between pairs of antennas) and send this information back to the transmitter. The transmitter then precorrects for the frequency offset and proceeds with the training and precoder estimation phase for DIDO. There is a problem with this embodiment when there are delays in the feedback channel. The reason is that there may be residual

phase errors created by the correction process that are not accounted for in the subsequent channel estimation. To solve this problem, one additional embodiment uses a novel frequency offset and phase estimator that can correct this problem by estimating the delay. Results are presented based both on simulations and practical measurements carried out with a DIDO-OFDM prototype.

[00288] The frequency and phase offset compensation method proposed in this document may be sensitive to estimation errors due to noise at the receiver. Hence, one additional embodiment proposes methods for time and frequency offset estimation that are robust also under low SNR conditions.

[00289] There are different approaches for performing time and frequency offset estimation. Because of its sensitivity to synchronization errors, many of these approaches were proposed specifically for the OFDM waveform.

[00290] The algorithms typically do not exploit the structure of the OFDM waveform thus they are generic enough for both single carrier and multicarrier waveforms. The algorithm described below is among a class of techniques that employ known reference symbols, e.g. training data, to aid in synchronization. Most of these methods are extensions of Moose's frequency offset estimator (see P. H. Moose, "A technique for orthogonal frequency division multiplexing frequency offset correction," IEEE Trans. Commun., vol. 42, no. 10, pp. 2908–2914, Oct. 1994.). Moose proposed to use two repeated training signals and derived the frequency offset using the phase difference between both received signals. Moose's method can only correct for the fractional frequency offset. An

extension of the Moose method was proposed by Schmidl and Cox (T. M. Schmidl and D. C. Cox, "Robust frequency and timing synchronization for OFDM," IEEE Trans. Commun., vol. 45, no. 12, pp. 1613–1621, Dec. 1997.). Their key innovation was to use one periodic OFDM symbol along with an additional differentially encoded training symbol. The differential encoding in the second symbol enables integer offset correction. Coulson considered a similar setup as described in T. M. Schmidl and D. C. Cox, "Robust frequency and timing synchronization for OFDM," IEEE Trans. Commun., vol. 45, no. 12, pp. 1613–1621, Dec. 1997, and provided a detailed discussion of algorithms and analysis as described in A. J. Coulson, "Maximum likelihood synchronization for OFDM using a pilot symbol: analysis," IEEE J. Select. Areas Commun., vol. 19, no. 12, pp. 2495–2503, Dec. 2001.; A. J. Coulson, "Maximum likelihood synchronization for OFDM using a pilot symbol: algorithms,"IEEE J. Select. Areas Commun., vol. 19, no. 12, pp. 2486–2494, Dec. 2001. One main difference is that Coulson uses repeated maximum length sequences to provide good correlation properties. He also suggests using chirp signals because of their constant envelope properties in the time and frequency domains. Coulson considers several practical details but does not include integer estimation. Multiple repeated training signals were considered by Minn et. al. in H. Minn, V. K. Bhargava, and K. B. Letaief, "A robust timing and frequency synchronization for OFDM systems," IEEE Trans. Wireless Commun., vol. 2, no. 4, pp. 822–839, July 2003, but the structure of the training was not optimized. Shi and Serpedin show that the training structure has some optimality form the perspective of

frame synchronization (K. Shi and E. Serpedin, "Coarse frame and carrier synchronization of OFDM systems: a new metric and comparison," IEEE Trans. Wireless Commun., vol. 3, no. 4, pp. 1271–1284, July 2004). One embodiment of the invention uses the Shi and Serpedin approach to perform frame synchronization and fractional frequency offset estimation.

[00291] Many approaches in the literature focus on frame synchronization and fractional frequency offset correction. Integer offset correction is solved using an additional training symbol as in T. M. Schmidl and D. C. Cox, "Robust frequency and timing synchronization for OFDM," IEEE Trans. Commun., vol. 45, no. 12, pp. 1613–1621, Dec. 1997. For example, Morrelli et. al. derived an improved version of T. M. Schmidl and D. C. Cox, "Robust frequency and timing synchronization for OFDM," IEEE Trans. Commun., vol. 45, no. 12, pp. 1613–1621, Dec. 1997, in M. Morelli, A. N. D'Andrea, and U. Mengali, "Frequency ambiguity resolution in OFDM systems," IEEE Commun. Lett., vol. 4, no. 4, pp. 134–136, Apr. 2000. An alternative approach using a different preamble structure was suggested by Morelli and Mengali (M. Morelli and U. Mengali, "An improved frequency offset estimator for OFDM applications," IEEE Commun. Lett., vol. 3, no. 3, pp. 75–77, Mar. 1999). This approach uses the correlations between M repeated identical training symbols to increase the range of the fractional frequency offset estimator by a factor of M. This is the best linear unbiased estimator and accepts a large offset (with proper design) but does not provide good timing synchronization.

System Description

[00292] One embodiment of the invention uses pre-coding based on channel state information to cancel frequency and phase offsets in DIDO systems. See Figure 11 and the associated description above for a description of this embodiment.

[00293] In one embodiment of the invention, each user employs a receiver equipped with frequency offset estimator/compensator. As illustrated in **Figure 45**, in one embodiment of the invention, a system including the receiver includes a plurality of RF units 4508, a corresponding plurality of A/D units 4510, a receiver equipped with a frequency offset estimator/compensator 4512 and a DIDO feedback generator unit 4506.

[00294] The RF units 4508 receive signals transmitted from the DIDO transmitter units, downconvert the signals to baseband and provide the downconverted signals to the A/D units 4510. The A/D units 4510 then convert the signal from analog to digital and send it to the frequency offset estimator/compensator units 4512. The frequency offset estimator/compensator units 4512 estimate the frequency offset and compensate for it, as described herein, and then send the compensated signal to the OFDM units 4513. The OFDM units 4513 remove the cyclic prefix and operate the Fast Fourier Transform (FFT) to report the signal to the frequency domain. During the training period the OFDM units 4513 send the output to the channel estimate unit 4504 that computes the channel estimates in the frequency domain. Alternatively, the channel estimates can be computed in the time domain. During the data period

the OFDM units 4513 send the output to the DIDO receiver unit 4502 which demodulates/decodes the signal to obtain the data. The channel estimate unit 4504 sends the channel estimates to the DIDO feedback generator unit 4506 that may quantize the channel estimates and send them back to the transmitter via the feedback control channel, as illustrated.

Description of One Embodiment of an Algorithm for a DIDO 2 × 2 Scenario

[00295] Described below are embodiments of an algorithm for frequency/phase offset compensation in DIDO systems. The DIDO system model is initially described with and without frequency/phase offsets. For the sake of the simplicity, the particular implementation of a DIDO 2 × 2 system is provided. However, the underlying principles of the invention may also be implemented on higher order DIDO systems.

DIDO System Model w/o Frequency and Phase Offset

[00296] The received signals of DIDO 2 × 2 can be written for the first user as

$$r_1[t] = h_{11}\left(w_{11}x_1[t] + w_{21}x_2[t]\right) + h_{12}\left(w_{12}x_1[t] + w_{22}x_2[t]\right) \quad (1)$$

and for the second user as

$$r_2[t] = h_{21}\left(w_{11}x_1[t] + w_{21}x_2[t]\right) + h_{22}\left(w_{12}x_1[t] + w_{22}x_2[t]\right) \quad (2)$$

where *t* is the discrete time index, h_{mn} hand w_{mn} are the channel and the DIDO precoding weights between the *m*-th user and *n*-th transmit antenna, respectively, and x_m is the transmit signal to user *m*. Note that h_{mn} and w_{mn} are not a function of *t* since we assume the channel is constant over the period between training and data transmission.

[00297] In the presence of frequency and phase offset, the received signals are expressed as

$$r_1[t] = e^{j(\omega_{U1}-\omega_{T1})T_s(t-t_{11})}h_{11}(w_{11}x_1[t]+w_{21}x_2[t]) + e^{j(\omega_{U1}-\omega_{T2})T_s(t-t_{12})}h_{12}(w_{12}x_1[t]+w_{22}x_2[t]) \quad (3)$$

and

$$r_2[t] = e^{j(\omega_{U2}-\omega_{T1})T_s(t-t_{21})}h_{21}(w_{11}x_1[t]+w_{21}x_2[t]) + e^{j(\omega_{U2}-\omega_{T2})T_s(t-t_{22})}h_{22}(w_{12}x_1[t]+w_{22}x_2[t]) \quad (4)$$

where T_s is the symbol period, $\omega_{Tn} = 2\Pi f_{Tn}$ for the *n*-th transmit antenna, $\omega_{Um} = 2\Pi f_{Um}$ for the *m*-th user, and f_{Tn} and f_{Um} are the actual carrier frequencies (affected by offset) for the *n*-th transmit antenna and *m*-th user, respectively. The values t_{mn} denote random delays that cause phase offset over the channel h_{mn}.

Figure 46 depicts the DIDO 2 × 2 system model.

[00298] For the time being, we use the following definitions:

$$\Delta\omega_{mn} = \omega_{Um} - \omega_{Tn} \quad (5)$$

to denote the frequency offset between the *m*-th user and the *n*-th transmit antenna.

[00299] A method according to one embodiment of the invention is illustrated in **Figure 47**. The method includes the following general steps (which include sub-steps, as illustrated): training period for frequency offset estimation 4701; training period for channel estimation 4702; data transmission via DIDO precoding with compensation 4703. These steps are described in detail below.

(a) Training Period for Frequency Offset Estimation (4701)

During the first training period the base station sends one or more training sequences from each transmit antennas to one of the users (4701a). As described herein "users" are wireless client devices. For the DIDO 2 × 2 case, the signal received by the *m*-th user is given by

$$r_m[t] = e^{j\Delta\omega_{m1}T_s(t-t_{m1})}h_{m1}p_1[t] + e^{j\Delta\omega_{m2}T_s(t-t_{m2})}h_{m2}p_2[t] \quad (6)$$

where p_1 and p_2 are the training sequences transmitted from the first and second antennas, respectively.

The *m*-th user may employ any type of frequency offset estimator (i.e., convolution by the training sequences) and estimates the offsets $\Delta\omega_{m1}$ and $\Delta\omega_{m2}$. Then, from these values the user computes the frequency offset between the two transmit antennas as

$$\Delta\omega_T = \Delta\omega_{m2} - \Delta\omega_{m1} = \omega_{T1} - \omega_{T2} \quad (7)$$

Finally, the value in (7) is fed back to the base station (4701b).

Note that p_1 and p_2 in (6) are designed to be orthogonal, so that the user can estimate $\Delta\omega_{m1}$ and $\Delta\omega_{m2}$. Alternatively, in one embodiment, the same training sequence is used over two consecutive time slots and the user estimates the offset from there. Moreover, to improve the estimate of the offset in (7) the same computations described above can be done for all users of the DIDO systems (not just for the *m*-th user) and the final estimate may be the (weighted) average of the values obtained from all users. This solution, however, requires more computational time and amount of feedback. Finally, updates of the frequency offset estimation are needed only if the frequency offset varies over time. Hence, depending on the stability of the clocks at the transmitter, this step 4701 of the algorithm can be carried out on a long-term basis (i.e., not for every data transmission), resulting in reduction of feedback overhead.

(b) Training Period for Channel Estimation (4702)

(c) During the second training period, the base station first obtains the frequency offset feedback with the value in (7) from the *m*-th user or from the plurality of users. The value in (7) is used to pre-compensate for the frequency offset at the transmit side. Then, the base station sends training data to all the users for channel estimation (4702a).

For DIDO 2 × 2 systems, the signal received at the first user is given by

$$r_1[t] = e^{j\Delta\omega_{11}T_s(t-\tilde{t}_{11})}h_{11}p_1[t] + e^{j\Delta\omega_{12}T_s(t-\tilde{t}_{12})}h_{12}e^{-j\Delta\omega_T T_s t}p_2[t] \qquad (8)$$

and at the second user by

$$r_2[t] = e^{j\Delta\omega_{21}T_s(t-\tilde{t}_{21})}h_{21}p_1[t] + e^{j\Delta\omega_{22}T_s(t-\tilde{t}_{22})}h_{22}e^{-j\Delta\omega_T T_s t}p_2[t] \qquad (9)$$

where $\tilde{t}_{mn} = t_{mn} + \Delta t$ and Δt is random or known delay between the first and second transmissions of the base station. Moreover, p_1 and p_2 are the training sequences transmitted from the first and second antennas, respectively, for frequency offset and channel estimation.

Note that the pre-compensation is applied only to the second antennas in this embodiment.

Expanding (8) we obtain

$$r_1[t] = e^{j\Delta\omega_{11}T_s t} e^{j\theta_{11}} [h_{11} p_1[t] + e^{j(\theta_{12}-\theta_{11})} h_{12} p_2[t]] \quad (10)$$

and similarly for the second user

$$r_2[t] = e^{j\Delta\omega_{21}T_s t} e^{j\theta_{21}} [h_{21} p_1[t] + e^{j(\theta_{22}-\theta_{21})} h_{22} p_2[t]] \quad (11)$$

where $\theta_{mn} = -\Delta\omega_{mn} T_s \tilde{t}_{mn}$.

At the receive side, the users compensate for the residual frequency offset by using the training sequences p_1 and p_2. Then the users estimate via training the vector channels (4702b)

$$h_1 = \begin{bmatrix} h_{11} \\ e^{j(\theta_{12}-\theta_{11})} h_{12} \end{bmatrix} \qquad h_2 = \begin{bmatrix} h_{21} \\ e^{j(\theta_{22}-\theta_{21})} h_{22} \end{bmatrix} \quad (12)$$

These channel in (12) or channel state information (CSI) is fed back to the base station (4702b) that computes the DIDO precoder as described in the following subsection.

(d) DIDO Precoding with Pre-compensation (4703)

The base station receives the channel state information (CSI) in (12) from the users and computes the precoding weights via block diagonalization (BD) (4703a), such that

$$\mathbf{w}_1^T\mathbf{h}_2 = 0, \qquad \mathbf{w}_2^T\mathbf{h}_1 = 0 \tag{13}$$

where the vectors h_1 are defined in (12) and $\mathbf{w}_m = [w_{m1}, w_{m2}]$. Note that the invention presented in this disclosure can be applied to any other DIDO precoding method besides BD. The base station also pre-compensates for the frequency offset by employing the estimate in (7) and phase offset by estimating the delay (Δt_o) between the second training transmission and the current transmission (4703a). Finally, the base station sends data to the users via the DIDO precoder (4703b).

After this transmit processing, the signal received at user 1 is given by

$$\begin{aligned} r_1[t] &= e^{j\Delta\omega_{11}T_s(t-\tilde{t}_{11}-\Delta t_o)}h_{11}[w_{11}x_1[t]+w_{21}x_2[t]] \\ &= e^{j\Delta\omega_{12}T_s(t-\tilde{t}_{12}-\Delta t_o)}h_{12}e^{-j\Delta\omega_T T_S(t-\Delta t_o)}[w_{12}x_1[t]+w_{22}x_2[t]] \\ &= \gamma_1[t]\left|h_{11}(w_{11}x_1[t]+w_{21}x_2[t])+e^{j(\Delta\omega_{11}t_{11}-\Delta\omega_{12}t_{12})T_s}h_{12}(w_{12}x_1[t]+w_{22}x_2[t])\right| \\ &= \gamma_1[t]\left[\left(h_{11}w_{11}+e^{j(\theta_{12}-\theta_{11})}h_{12}w_{12}\right)x_1[t]+\left(h_{11}w_{21}+e^{j(\theta_{12}-\theta_{11})}h_{12}w_{22}\right)x_2[t]\right] \end{aligned} \tag{14}$$

where $\gamma_1[t] = e^{j\Delta\omega_{11}T_s(t-\tilde{t}_{11}-\Delta t_o)}$. Using the property (13) we obtain

$$r_1[t] = \gamma_1[t]\mathbf{w}_1^T\mathbf{h}_1x_1[t]. \tag{15}$$

Similarly, for user 2 we get

$$r_2[t] = e^{j\Delta\omega_{21}T_s(t-\tilde{\tau}_{21}-\Delta t_o)}h_{21}[w_{11}x_1[t] + w_{21}x_2[t]]$$
$$+ e^{j\Delta\omega_{22}T_s(t-\tilde{\tau}_{22}-\Delta t_o)}h_{22}e^{-j\Delta\omega_T T_s(t-\Delta t_o)}[w_{12}x_1[t] + w_{22}x_2[t]] \quad (16)$$

and expanding (16)

$$r_2[t] = \gamma_2[t]\mathbf{w}_2^T\mathbf{h}_2 x_2[t] \quad (17)$$

where $\gamma_2[t] = e^{j\Delta\omega_{21}T_s(t-\tilde{\tau}_{21}-\Delta t_o)}$.

Finally, the users compute the residual frequency offset and the channel estimation to demodulate the data streams $x_1[t]$ and $x_2[t]$ (4703c).

Generalization to DIDO *N* × *M*

[00300] In this section, the previously described techniques are generalized to DIDO systems with *N* transmit antennas and *M* users.

i. Training Period for Frequency Offset Estimation

[00301] During the first training period, the signal received by the *m*-th user as a result of the training sequences sent from the *N* antennas is given by

$$r_m[t] = \sum_{n=1}^{N} e^{j\Delta\omega_{mn}T_s(t-t_{mn})}h_{mn}p_n[t] \quad (18)$$

where p_n is the training sequences transmitted from the *n*-th antenna.

After estimating the offsets $\Delta\omega_{mn}, \forall n = 1,..., N,$ the *m*-th user computes the frequency offset between the first and the *n*-th transmit antenna as

$$\Delta\omega_{T,1n} = \Delta\omega_{mn} - \Delta\omega_{m1} = \omega_{T1} - \omega_{Tn}\,. \qquad (19)$$

Finally, the values in (19) are fed back to the base station.

ii. Training Period for Channel Estimation

[00302] During the second training period, the base station first obtains the frequency offset feedback with the value in (19) from the *m*-th user or from the plurality of users. The value in (19) is used to pre-compensate for the frequency offset at the transmit side. Then, the base station sends training data to all the users for channel estimation.

For DIDO *N* × *M* systems, the signal received at the *m*-th user is given by

$$\begin{aligned} r_m[t] &= e^{j\Delta\omega_{m1}T_S(t-\tilde{t}_{m1})}h_{m1}p_1[t] + \sum_{n=2}^{N} e^{j\Delta\omega_{mn}T_s(t-\tilde{t}_{mn})}h_{mn}e^{-j\Delta\omega_{T,1n}T_s t}p_n[t] \\ &= e^{j\Delta\omega_{m1}T_s(t-\tilde{t}_{m1})}\left[h_{m1}p_1[t] + \sum_{n=2}^{N} e^{j(\theta_{mn}-\theta_{m1})}h_{mn}p_n[t]\right] \\ &= e^{j\Delta\omega_{m1}T_s(t-\tilde{t}_{m1})}\sum_{n=1}^{N} e^{j(\theta_{mn}-\theta_{m1})}h_{mn}p_n[t] \end{aligned} \qquad (20)$$

where $\theta_{mn} = -\Delta\omega_{mn}T_s\tilde{t}_{mn}, \tilde{t}_{mn} = t_{mn} + \Delta t$ and Δt is random or known delay between the first and second transmissions of the base station. Moreover, p_n is the training sequence transmitted from the *n*-th antenna for frequency offset and channel estimation.

At the receive side, the users compensate for the residual frequency offset by using the training sequences p_n. Then, each users *m* estimates via training the vector channel

$$\mathbf{h}_m = \begin{bmatrix} h_{m1} \\ e^{j(\theta_{m2}-\theta_{m1})}h_{m2} \\ \vdots \\ e^{j(\theta_{mN}-\theta_{m1})}h_{mN} \end{bmatrix} \qquad (21)$$

and feeds back to the base station that computes the DIDO precoder as described in the following subsection.

iii. DIDO Precoding with Pre-compensation

[00303] The base station receives the channel state information (CSI) in (12) from the users and computes the precoding weights via block diagonalization (BD), such that

$$\mathbf{w}_m^T \mathbf{h}_l = 0, \qquad \forall m \neq l, \qquad m = 1,...,M \tag{22}$$

where the vectors $\boldsymbol{h}_m$ are defined in (21) and $\mathbf{w}_m = [w_{m1}, w_{m2}, \ldots, w_{mN}]$. The base station also pre-compensates for the frequency offset by employing the estimate in (19) and phase offset by estimating the delay (Δt_o) between the second training transmission and the current transmission. Finally, the base station sends data to the users via the DIDO precoder.

After this transmit processing, the signal received at user *i* is given by

$$
\begin{aligned}
r_i[t] &= e^{j\Delta\omega_{i1}T_s\left(t-\tilde{t}_{i1}-\Delta t_o\right)}h_{i1}\sum_{m=1}^{M}w_{m1}x_m[t]+ \\
&+\sum_{n=2}^{N}e^{j\Delta\omega_{in}T_s\left(t-\tilde{t}_{in}-\Delta t_o\right)}h_{in}e^{-j\Delta\omega_{T,1n}T_s\left(t-\Delta t_o\right)}\sum_{m=1}^{M}w_{mn}x_m[t] \\
&= e^{j\Delta\omega_{i1}T_s\left(t-\Delta t_o\right)}e^{-j\Delta\omega_{i1}T_s\tilde{t}_{i1}}h_{i1}\sum_{m=1}^{M}w_{m1}x_m[t] \\
&+\sum_{n=2}^{N}e^{j\Delta\omega_{i1}T_s\left(t-\Delta t_o\right)}e^{-j\Delta\omega_{in}T_s\tilde{t}_{in}}h_{in}\sum_{m=1}^{M}w_{mn}x_m[t] \\
&= \gamma_i[t]\left[h_{i1}\sum_{m=1}^{M}w_{m1}x_m[t]+\sum_{n=2}^{N}e^{j\left(\theta_{in}-\theta_{i1}\right)}h_{in}\sum_{m=1}^{M}w_{m1}x_m[t]\right] \\
&= \gamma_i[t]\left[\sum_{n=1}^{N}e^{j\left(\theta_{in}-\theta_{i1}\right)}h_{in}\sum_{m=1}^{M}w_{mn}x_m[t]\right] \\
&= \gamma_i[t]\sum_{m=1}^{M}\left[\sum_{n=1}^{N}e^{j\left(\theta_{in}-\theta_{i1}\right)}h_{in}w_{mn}\right]x_m[t] \\
&= \gamma_i[t]\sum_{m=1}^{M}\mathbf{w}_m^T\mathbf{h}_i x_m[t]
\end{aligned}
\tag{23}
$$

Where $\gamma_i[n]=e^{j\Delta\omega_{i1}T_s\left(t-\tilde{t}_{i1}-\Delta t_o\right)}$. Using the property (22) we obtain

$$
r_i[t]=\gamma_i[t]\mathbf{w}_i^T\mathbf{h}_i x_i[t] \tag{24}
$$

Finally, the users compute the residual frequency offset and the channel estimation to demodulate the data streams $x_i[t]$.

Results

[00304] **Figure 48** shows the SER results of DIDO 2 × 2 systems with and without frequency offset. It is possible to see that the proposed method completely cancels the frequency/phase offsets yielding the same SER as systems without offsets.

[00305] Next, we evaluate the sensitivity of the proposed compensation method to frequency offset estimation errors and/or fluctuations of the offset in time. Hence, we re-write (14) as

$$
\begin{aligned}
r_1[t] &= e^{j\Delta\omega_{11}T_s\left(t-\tilde{t}_{11}-\Delta t_o\right)}h_{11}\left[w_{11}x_1[t]+w_{21}x_2[t]\right] \\
&+e^{j\Delta\omega_{12}T_s\left(t-\tilde{t}_{12}-\Delta t_o\right)}h_{12}e^{-j\left(\Delta\omega_T+2\Pi\epsilon\right)T_s\left(t-\Delta t_o\right)}\left[w_{12}x_1[t]+w_{22}x_2[t]\right]
\end{aligned}
\tag{25}
$$

where $\in$ indicates the estimation error and/or variation of the frequency offset between training and data transmission. Note that the effect of $\in$ is to destroy the orthogonality property in (13) such that the interference terms in (14) and (16) are not completely pre-canceled at the transmitter. As a results of that, the SER performance degrades for increasing values of $\in$.

[00306] **Figure 48** shows the SER performance of the frequency offset compensation method for different values of $\in$. These results assume T_s = 0.3 ms (i.e., signal with 3 KHz bandwidth). We observe that for $\in$ = 0.001 Hz (or less) the SER performance is similar to the no offset case.

f. Description of One Embodiment of an Algorithm for Time and Frequency Offset Estimation

[00307] Hereafter, we describe additional embodiments to carry out time and frequency offset estimation (4701b in **Figure 47**). The transmit signal structure under consideration is illustrated in H. Minn, V. K. Bhargava, and K. B. Letaief, "A robust timing and frequency synchronization for OFDM systems," IEEE Trans. Wireless Commun., vol. 2, no. 4, pp. 822–839, July 2003, and studied in more detail in K. Shi and E. Serpedin, "Coarse frame and carrier synchronization of OFDM systems: a new metric and comparison," IEEE Trans. Wireless Commun., vol. 3, no. 4, pp. 1271–1284, July 2004. Generally sequences with good correlation properties are used for training. For example, for our system, Chu sequences are used which are derived as described in D. Chu, "Polyphase codes with good periodic correlation properties (corresp.),"

IEEE Trans. Inform. Theory, vol. 18, no. 4, pp. 531–532, July 1972. These sequences have an interesting property that they have perfect circular correlations. Let L_{cp} denote the length of the cyclic prefix and let N_t denote the length of the component training sequences. Let $N_t = M_t$, where M_t is the length of the training sequence. Under these assumptions the transmitted symbol sequence for the preamble can be written as

$$\begin{array}{rcll} s[n] & = & t[n-N_t] & \text{for } n=-1,\ldots,-L_{cp} \\ s[n] & = & t[n] & \text{for } n=0,\ldots,N_t-1 \\ s[n] & = & t[n-N_t] & \text{for } n=N_t,\ldots,2N_t-1 \\ s[n] & = & -t[n-2N_t] & \text{for } n=2N_t,\ldots,3N_t-1 \\ s[n] & = & t[n-3N_t] & \text{for } n=3N_t,\ldots,4N_t-1. \end{array}$$

Note that the structure of this training signal can be extended to other lengths but repeating the block structure. For example, to use 16 training signals we consider a structure such as:

$$[CP, B, B, -B, B, B, B, -B, B, -B, -B, B, -B, B, B, -B, B,].$$

By using this structure and letting $N_t = 4\ M_t$ all the algorithms to be described can be employed without modification. Effectively we are repeating the training sequence. This is especially useful in cases where a suitable training signal may not be available.

Consider the following received signal, after matched filtering and downsampling to the symbol rate:

$$r[n] = e^{2\pi\epsilon n}\sum_{l=0}^{L} h[l]s[n-l-\Delta] + v[n]$$

where ε is the unknown discrete-time frequency offset, Δ is the unknown frame offset, h[l] are the unknown discrete-time channel coefficients, and v[n] is additive noise. To explain the key ideas in the following sections the presence of additive noise is ignored.

i. Coarse Frame Synchronization

[00308] The purpose of coarse frame synchronization is to solve for the unknown frame offset Δ. Let us make the following definitions

$$\begin{aligned}
\mathbf{r}_1[n] &:= [r[n], r[n+1], \ldots, r[n+N_t-1]]^T, \\
\bar{\mathbf{r}}_1[n] &:= [r[n+L_{cp}], r[n+1], \ldots, r[n+N_t-1]]^T, \\
\mathbf{r}_2[n] &:= [r[n+N_t], r[n+1+N_t], \ldots, r[n+2N_t-1]]^T, \\
\bar{\mathbf{r}}_2[n] &:= [r[n+L_{cp}+N_t], r[n+1+L_{cp}+N_t], \ldots, r[n+L_{cp}+2N_t-1]]^T, \\
\mathbf{r}_3[n] &:= [r[n+2N_t], r[n+1+2N_t], \ldots, r[n+3N_t-1]]^T, \\
\bar{\mathbf{r}}_3[n] &:= [r[n+L_{cp}+2N_t], r[n+L_{cp}+1+2N_t], \ldots, r[n+L_{cp}+3N_t-1]]^T, \\
\mathbf{r}_4[n] &:= [r[n+3N_t], r[n+1+3N_t], \ldots, r[n+4N_t-1]]^T, \\
\bar{\mathbf{r}}_4[n] &:= [r[n+L_{cp}+3N_t], r[n+L_{cp}+1+3N_t], \ldots, r[n+L_{cp}+4N_t-1]]^T.
\end{aligned}$$

The proposed coarse frame synchronization algorithm is inspired from the algorithm in K. Shi and E. Serpedin, "Coarse frame and carrier synchronization of OFDM systems: a new metric and comparison," IEEE Trans. Wireless Commun., vol. 3, no. 4, pp. 1271–1284, July 2004, derived from a maximum likelihood criterion.

Method 1 – **Improved coarse frame synchronization**: *the coarse frame synchronization estimator solves the following optimization*

$$\hat{\Delta} = \arg\max_{k\in\mathbb{Z}} \frac{|P_1(k)| + |P_2(k)| + |P_3(k)|}{\|\mathbf{r}_1\|^2 + \|\mathbf{r}_2\|^2 + \|\mathbf{r}_3\|^2 + \|\mathbf{r}_4\|^2 + \frac{1}{2}\left(\|\bar{\mathbf{r}}_1\|^2 + \|\bar{\mathbf{r}}_2\|^2 + \|\bar{\mathbf{r}}_3\|^2 + \|\bar{\mathbf{r}}_4\|^2\right)}$$

where

$$\begin{aligned} P_1[k] &= \mathbf{r}_1^*[k]\mathbf{r}_2[k] - \mathbf{r}_3^*[k]\mathbf{r}_4[k] - \bar{\mathbf{r}}_2^*[k]\bar{\mathbf{r}}_3[k] \\ P_2[k] &= \mathbf{r}_2^*[k]\mathbf{r}_4[k] - \mathbf{r}_1^*[k]\mathbf{r}_3[k] \\ P_3[k] &= \bar{\mathbf{r}}_1^*[k]\bar{\mathbf{r}}_4[k]. \end{aligned}$$

Let the corrected signal be defined as

$$r_c[n] = r[n - \hat{\Delta} - \lceil L_{cp}/4 \rceil].$$

The additional correction term is used to compensate for small initial taps in the channel and can be adjusted based on the application. This extra delay will be included henceforth in the channel.

ii. Fractional Frequency Offset Correction

[00309] The fractional frequency offset correction follows the coarse frame synchronization block.

Method 2 – Improved fractional frequency offset correction: *the fractional frequency offset is the solution to*

$$\hat{\epsilon}_f = \frac{\text{phase}P_1[\hat{\Delta}]}{2\pi N_t}.$$

This is known as a fractional frequency offset because the algorithm can only correct for offsets

$$|\epsilon_f| < \frac{1}{2N_c}.$$

This problem will be solved in the next section. Let the fine frequency offset corrected signal be defined as

$$r_f[n] = e^{-j2\pi\epsilon_f} r_c[n].$$

Note that the Methods 1 and 2 are an improvement to K. Shi and E. Serpedin, "Coarse frame and carrier synchronization of OFDM systems: a new metric and comparison," IEEE Trans. Wireless Commun., vol. 3, no. 4, pp.1271–1284, July 2004 that works better in frequency-selective channels. One specific innovation here is the use of both r and $\overline{r}$ as described above. The use of $\overline{r}$ improves the prior estimator because it ignores the samples that would be contaminated due to inter-symbol interference.

iii. Integer Frequency Offset Correction

[00310] To correct for the integer frequency offset, it is necessary to write an equivalent system model for the received signal after fine frequency offset correction. Absorbing remaining timing errors into the channel, the received signal in the absence of noise has the following structure:

$$r_f[n] = e^{j2\pi\frac{nk}{N_s}} \sum_{l=0}^{L_g} g[l]s[n-l]$$

for n = 0, 1, . . . , $4N_t - 1$. The integer frequency offset is *k* while the unknown equivalent channel is g[l].

Method 3 - Improved integer frequency offset correction: *the integer frequency offset is the solution to*

$$\hat{k} = \arg \max_{m=0,1,\ldots,N_t-1} \mathbf{r}^* \mathbf{D}[k]\mathbf{S}\left(\mathbf{S}^*\mathbf{S}\right)^{-1}\mathbf{S}^*\mathbf{D}[k]^*\mathbf{r}$$

where

$$\mathbf{r} = \mathbf{D}[k]\mathbf{S}\mathbf{g}$$

$$\mathbf{D}[k] := \operatorname{diag}\left\{1, e^{j2\pi\frac{k}{N_t}}, \ldots, e^{j2\pi\frac{n(4N_t-1)}{N_t}}\right\}$$

$$\mathbf{S} := \begin{bmatrix} s[0] & s[-1] & \cdots & \cdots & s[-L_{cp}] \\ s[1] & s[0] & s[-1] & \cdots & s[-L_{cp}+1] \\ s[4N_t-1] & s[4N_t-2] & s[4N_t-3] & \cdots & s[4N_t-1-L_{cp}] \end{bmatrix}$$

$$\mathbf{g} := \begin{bmatrix} g[0] \\ g[1] \\ \vdots \\ g[L_{cp}] \end{bmatrix}$$

This gives the estimate of the total frequency offset as

$$\hat{\epsilon} = \frac{\hat{k}}{N_t} + \hat{\epsilon}_f.$$

Practically, Method 3 has rather high complexity. To reduce complexity the following observations can be made. First of all, the product S $\mathbf{S}(\mathbf{S}^*\mathbf{S})^{-1}\mathbf{S}^*$ can be precomputed. Unfortunately, this still leaves a rather large matrix multiplication. An alternative is to exploit the observation that with the proposed training sequences, $\mathbf{S}^*\mathbf{S} \approx \mathbf{I}$. This leads to the following reduced complexity method.

Method 4 – Low-complexity improved integer frequency offset correction: *a low complexity integer frequency offset estimator solves*

$$\hat{k} = \arg \max_{m=0,1,\ldots,N_t-1} (\mathbf{S}^*\mathbf{D}[k]^*\mathbf{r})^* (\mathbf{S}^*\mathbf{D}[k]^*\mathbf{r}).$$

iv. Results

[00311] In this section we compare the performance of the different proposed estimators.

[00312] First, in **Figure** 50 we compare the amount of overhead required for each method. Note that both of the new methods reduce the overhead required by 10x to 20x. To compare the performance of the different estimators, Monte Carlo experiments were performed. The setup considered is our usual NVIS transmit waveform constructed from a linear modulation with a symbol rate of 3K

symbols per second, corresponding to a passband bandwidth of 3kHz, and raised cosine pulse shaping. For each Monte Carlo realization, the frequency offset is generated from a uniform distribution on $[-f_{max}, f_{max}]$.

[00313] A simulation with a small frequency offset of f_{max} = 2Hz and no integer offset correction is illustrated in **Figure 51**. It can be seen from this performance comparison that performance with $N_t/ M_t = 1$ is slightly degraded from the original estimator, though still substantially reduces overhead. Performance with $N_t/ M_t = 4$ is much better, almost 10dB. All the curves experience a knee at low SNR points due to errors in the integer offset estimation. A small error in the integer offset can create a large frequency error and thus a large mean squared error. Integer offset correction can be turned off in small offsets to improve performance.

[00314] In the presence of multipath channels, the performance of frequency offset estimators generally degrades. Turning off the integer offset estimator, however, reveals quite good performance in **Figure 52**. Thus, in multipath channels it is even more important to perform a robust coarse correction followed by an improved fine correction algorithm. Notice that the offset performance with $N_t/M_t = 4$ is much better in the multipath case.

Adaptive DIDO Transmission Scheme

[00315] New systems and methods for adaptive DIDO systems are described below. These systems and methods are extensions to the patent applications entitled “System and Method for Distributed Input-Distributed Output

Wireless Communications," Serial Nos. 11/894,394, 11/894,362, and 11/894,540, filed August 20, 2007, of which the present application is a continuation-in-part. The content of these applications has been described above. The adaptive DIDO system and method described in the foregoing applications were designed to exploit instantaneous and/or statistical channel quality information. Described below are additional techniques to enable adaptation between different DIDO modes assuming instantaneous channel knowledge.

[00316] The following prior art references will be discussed below within the context of the embodiments of the invention. Each reference will be identified by its corresponding bracketed number:

[1] K. K. Wong, R. D. Murch, and K. B. Letaief, "A joint-channel diagonalization for multiuser MIMO antenna systems," *IEEE Trans. Commun.*, vol. 2, no. 4, pp. 773-786, July 2003.

[2] R. Chen, R. W. Heath, Jr., and J. G. Andrews, ``Transmit Selection Diversity for Unitary Precoded Multiuser Spatial Multiplexing Systems with Linear Receivers," *IEEE Trans. on Signal Processing*, vol. 55, no. 3, pp. 1159-1171, March 2007.

[3] R. W. Heath, Jr. and A. J. Paulraj, ``Switching Between Diversity and Multiplexing in MIMO Systems," *IEEE Trans. on Communications*, vol. 53, no. 6, pp. 962-968, June 2005.

[00317] A fundamental concept associated with link adaptation (LA) is to adaptively adjust system parameters such as modulation order, FEC coding rate and/or transmission schemes to the changing channel conditions to improve throughput or error rate performance. These system parameters are often combined in sets of "transmission modes," referred to herein as *DIDO modes*. One embodiment of a technique for LA is to measure the channel quality information and predict the best transmission mode based on certain performance criterion. The channel quality consists of statistical channel information, as in *slow LA*, or (instantaneous) CSI, as in *fast LA*. One embodiment of the system and method described herein is employed within the context of fast LA systems and the goal is to increase throughput for fixed predefined target error rate.

[00318] One embodiment of a method for adaptive DIDO transmission is depicted in **Figure 21**. In frequency division duplex (FDD) systems the proposed adaptive algorithm consists of the following steps: i) the users compute the channel quality indicator (CQI) 2102; ii) the users select the best DIDO mode for transmission 2106 based on the CQI in time/frequency/space domains 2104; iii) the base station selects the active users and transmits data with the selected DIDO modes via DIDO precoding. In time division duplex (TDD) systems, where the uplink/downlink channel reciprocity can be exploited, the base station may compute the CQIs and select the best DIDO modes for all the users. Moreover, to compute the DIDO precoding weights, the channel state information (CSI) can be computed at the users side in FDD systems or at the base station in TDD

systems. When the CSI is computed at the users' side and fed back to the base station, the base station can exploit the CSI to compute the CQI for every users to enable the adaptive DIDO algorithm.

[00319] We first define an indicator of channel quality that is used to predict the performance of different DIDO modes and select the optimal one for given transmission. One example of channel quality indicator (CQI) is the mutual information (MI) of DIDO systems defined as [1,2]

$$C = \sum_{k=1}^{K} \log_2 \left| \mathbf{I}_{N_k} + \frac{\gamma_k}{N_k} \widetilde{\mathbf{H}}_k^H \widetilde{\mathbf{H}}_k \right| \qquad (1)$$

where K is the number of users, $\widetilde{\mathbf{H}}_k = \mathbf{H}_k \mathbf{T}_k$ is the equivalent channel transfer matrix, $\mathbf{H}_k$ is the channel matrix for the k-th user, $\mathbf{T}_k$ is the DIDO precoding matrix for the k-th user, γ_k is the per-user SNR and N_k is the number of parallel data streams sent to user k. We observe that the CQI in (1) depends on the SNR and the channel matrix.

[00320] The MI in (1) measures the data rate per unit bandwidth that can be transmitted reliably over the DIDO link (i.e., error-free spectral efficiency). When the spectral efficiency (SE) of given DIDO mode is below the MI in (1) the error rate performance is arbitrarily small, whereas when the SE exceeds (1) the error rate approaches 100%. As an example, we plot the spectral efficiency of three DIDO modes as a function of the MI (1) in **Figure 53**. The DIDO modes consist

of three constellation orders: 4-QAM, 16-QAM and 64-QAM. For simplicity and without loss of generality we assume no FEC coding. The transmitter of the 2x2 DIDO system employs block-diagonalization precoding scheme [1]. The SE is obtained from the symbol error rate as SE=$\log_2$M*(1-SER), where M is the M-QAM constellation size. We simulate the channel according to the block fading i.i.d. channel model. We generate 1000 channel realizations and for each realization we simulate 500 AWGN samples. The SNR values chosen for this simulation are {0, 10, 20, 30} dB.

[00321] In **Figure 53**, each dot corresponds to one combination of mutual information and SE obtained within each AWGN block. Moreover, different colors are associated to different values of SNR. Similar results are expressed in terms of SER as a function of the MI (1) in **Figure 54**. For the case of 4-QAM, we note that when the SE exceeds MI in **Figure 53** the SER is close to 100% in **Figure 54**. Unfortunately, there is a large variance in the SER vs. MI plot that prevent the identification of the thresholds used to define the link-quality regions.

[00322] Next, we define another CQI to reduce this variance. We first expand (1) as

$$C = \sum_{k=1}^{K} \sum_{i=1}^{N_k} \log_2 \left(1 + \frac{\gamma_k}{N_k} \left| \lambda_{k,i} \right|^2 \right)$$

where $\lambda_{k,i}$ is the i-th singular value of the matrix $\widetilde{\mathbf{H}}_k$. We observe that the per-user SER (which is a function of the post-processing SNR) depends on

$\lambda_{\min}^{k} = \min_{i=1,\ldots,N_k}(\lambda_{k,i})$ and the system SER is upper bounded by the user with the smallest singular value $\lambda_{\min} = \min_{k=1,\ldots,K}(\lambda_{\min}^{k})$ among all the users [2]. Then, we define the following CQI

$$C_{\min} = \min_{k=1,\ldots,K}\left\{\min_{i=1,\ldots,N_k}\left[\log_2\left(1+\frac{\gamma_k}{N_k}\left|\lambda_{k,i}\right|^2\right)\right]\right\} \qquad (2)$$

[00323] **Figure 55** shows the SER vs. $C_{\min}$ for different DIDO modes. We observe the reduced variance compared to **Figure 54**. To define the CQI thresholds and link-quality regions, we fix the target SER. For example, if the target SER is 1%, the CQI thresholds are T_1=2.8 bps/Hz, T_2=5 bps/Hz and T_3=7 bps/Hz.

[00324] Finally, we compare the SER and SE performance as a function of SNR for different DIDO modes against the adaptive DIDO algorithm. Results are shown in **Figures 56** and **57**. We observe that the adaptive algorithm maintains the SER below 1% for SNR>20dB while increasing the SE, approaching the ideal sum-rate capacity. **Figures 58** and **59** show the performance of the adaptive DIDO algorithm for different values of the CQI thresholds. We observe that by decreasing the CQI thresholds for fixed SNR the SE increases at the expense of larger SER. In one embodiment, the CQI thresholds are adjusted based on the system performance requirements.

[00325] The proposed method for fast LA in DIDO systems includes different types of adaptation criteria and CQIs. For example, a similar adaptive DIDO algorithm can be designed to minimize error rate performance for fixed rate transmission, similar to the approach described in [3] for MIMO systems. Moreover, different types of CQIs can be employed such as the minimum singular value of the composite channel matrix as

$$\lambda_{\min} = \min_{j=1,\ldots,\bar{N}} \left\{ \lambda_j (\mathbf{H}\mathbf{H}^H) \right\} \qquad (3)$$

where $\bar{N} = \sum_{k=1}^{K} N_k$ is the total number of data streams sent to the users and H is the composite channel matrix obtained by stacking the channel matrices of all the users as

$$\mathbf{H} = \begin{bmatrix} \mathbf{H}_1 \\ \vdots \\ \mathbf{H}_K \end{bmatrix} \qquad (4)$$

[00326] **Figure** 60 shows the SER expressed as a function of the minimum singular value in (3) for 4-QAM constellation, average SNR=15 dB and single-tap channels. The composite channel matrix in (4) is normalized such that $\|\mathbf{H}\|_F^2 = 1$. We observe that, for 4-QAM constellation, the CQI threshold to guarantee SER<1% is -16 dB. Similar results can be obtained for higher order modulations.

[00327] The proposed method can be extended to multicarrier systems, such as orthogonal frequency division multiplexing (OFDM) systems. In multicarrier systems the MI in (1) and (2) is computed for each subcarrier and different MCSs are assigned to different subcarriers, thereby exploiting the frequency selectivity of wireless channels. This method, however, may result in large number of control information to share the CQI or DIDO mode number between transmitters and receivers. An alternative method is to group multiple subcarriers with similar channel quality and compute the average of (1) or (2) over each group of subcarrier. Then, different DIDO modes are assigned to different groups of subcarriers based on the criterion described above.

[00328] Embodiments of the invention may include various steps as set forth above. The steps may be embodied in machine-executable instructions which cause a general-purpose or special-purpose processor *to perf*orm certain steps. For example, *the va*rious components within the Base Stations/APs and Client Devices described above may be implemented as software executed on a general purpose or special purpose processor. To avoid obscuring the pertinent aspects of the invention, various well known personal computer components such as computer memory, hard drive, input devices, etc., have been left out of the figures.

[00329] Alternatively, in one embodiment, the various functional modules illustrated herein and the associated steps may be performed by specific hardware components that contain hardwired logic for performing the steps, such

as an application-specific integrated circuit ("ASIC") or by any combination of programmed computer components and custom hardware components.

[00330] In one embodiment, certain modules such as the Coding, Modulation and Signal Processing Logic 903 described above may be implemented on a programmable digital signal processor ("DSP") (or group of DSPs) such as a DSP using a Texas Instruments' TMS320x architecture (e.g., a TMS320C6000, TMS320C5000, . . . etc). The DSP in this embodiment may be embedded within an add-on card to a personal computer such as, for example, a PCI card. Of course, a variety of different DSP architectures may be used while still complying with the underlying principles of the invention.

[00331] Elements of the present invention may also be provided as a machine-readable medium for storing the machine-executable instructions. The machine-readable medium may include, but is not limited to, flash memory, optical disks, CD-ROMs, DVD ROMs, RAMs, EPROMs, EEPROMs, magnetic or optical cards, propagation media or other type of machine-readable media suitable for storing electronic instructions. For example, the present invention may be downloaded as a computer program which may be transferred from a remote computer (e.g., a server) to a requesting computer (e.g., a client) by way of data signals embodied in a carrier wave or other propagation medium via a communication link (e.g., a modem or network connection).

[00332] Throughout the foregoing description, for the purposes of explanation, numerous specific details were set forth in order to provide a

thorough understanding of the present system and method. It will be apparent, however, to one skilled in the art that the system and method may be practiced without some of these specific details. Accordingly, the scope and spirit of the present invention should be judged in terms of the claims which follow.

[00333] Moreover, throughout the foregoing description, numerous publications were cited to provide a more thorough understanding of the present invention. All of these cited references are incorporated into the present application by reference.

CLAIMS

1. A method implemented within a wireless transmission system comprised of a plurality of wireless client devices, a base station, and a plurality of distributed antennas communicatively coupled to the base station comprising:

simultaneously transmitting radio signals from the plurality of distributed antennas so as to create radio frequency interference resulting in a plurality of non-interfering channels between the plurality of distributed antennas and the plurality of wireless client devices.

ABSTRACT

A system and method are described for distributed antenna wireless communications. For example, a method implemented within a wireless transmission system comprised of a plurality of wireless client devices and a plurality of distributed antennas is described comprising: computing channel state information (CSI) for wireless communication channels between the plurality of base distributed antennas and the wireless client devices; computing precoding weights from the channel state information; precoding data using the precoding weights prior to wireless transmission from the plurality of distributed antennas to the wireless client devices; and wirelessly transmitting the precoded data from the distributed antennas to each of the wireless client devices, wherein the precoding causes radio frequency interference between the plurality of base stations but simultaneously generating a plurality of non-interfering radio frequency user channels between the plurality of distributed antennas and the plurality of wireless client devices.

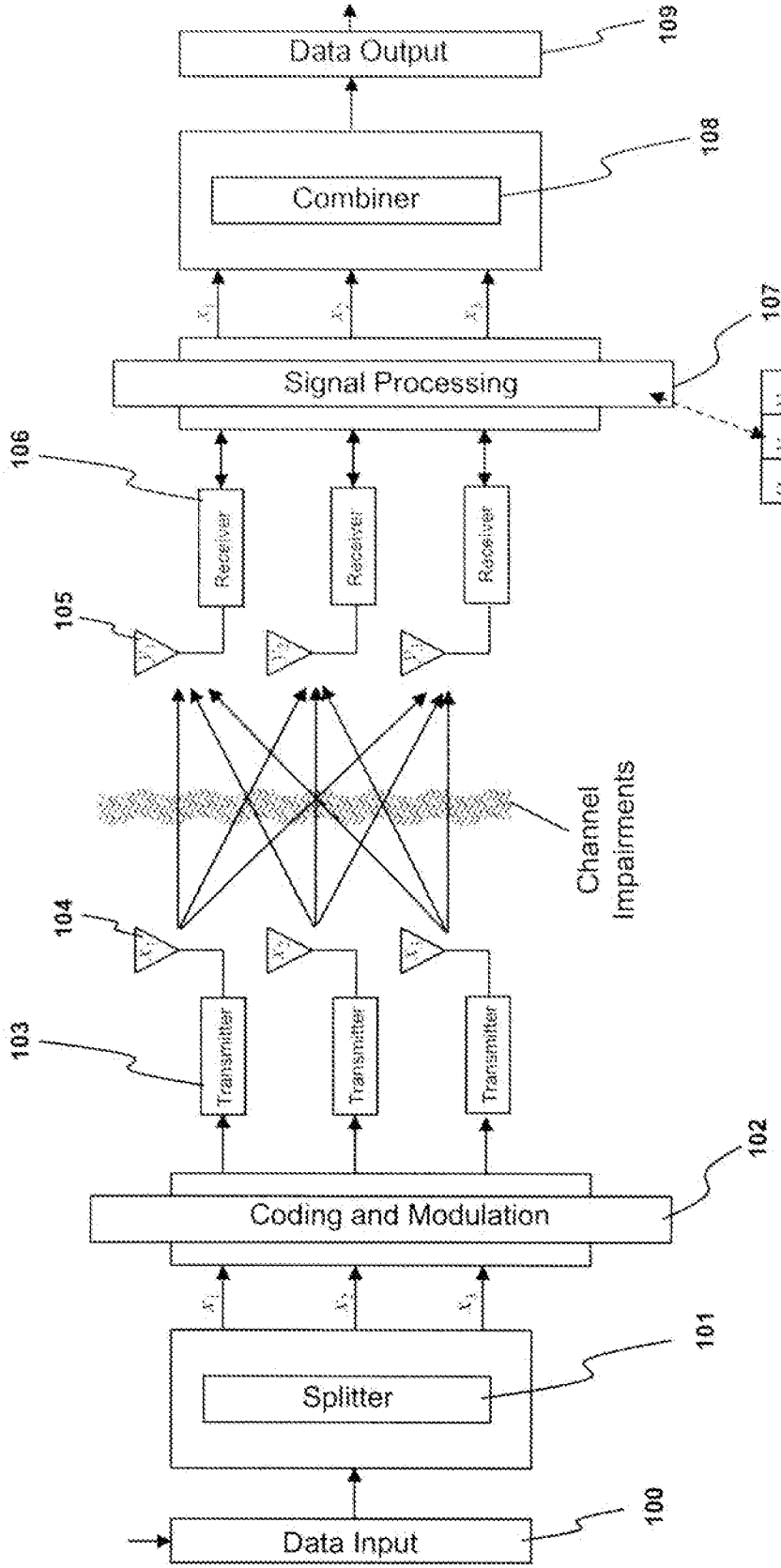

Fig. 1
(prior art)

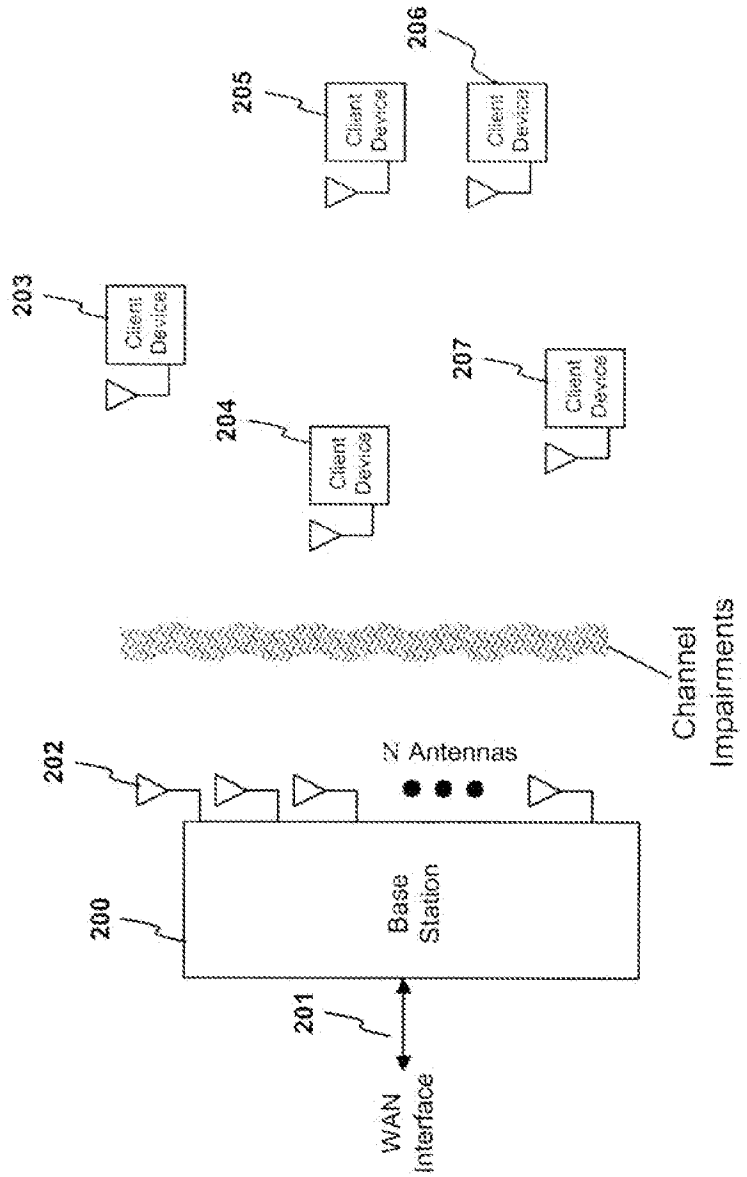

N-antenna Base Station with Single-antenna Client Devices

Fig. 2

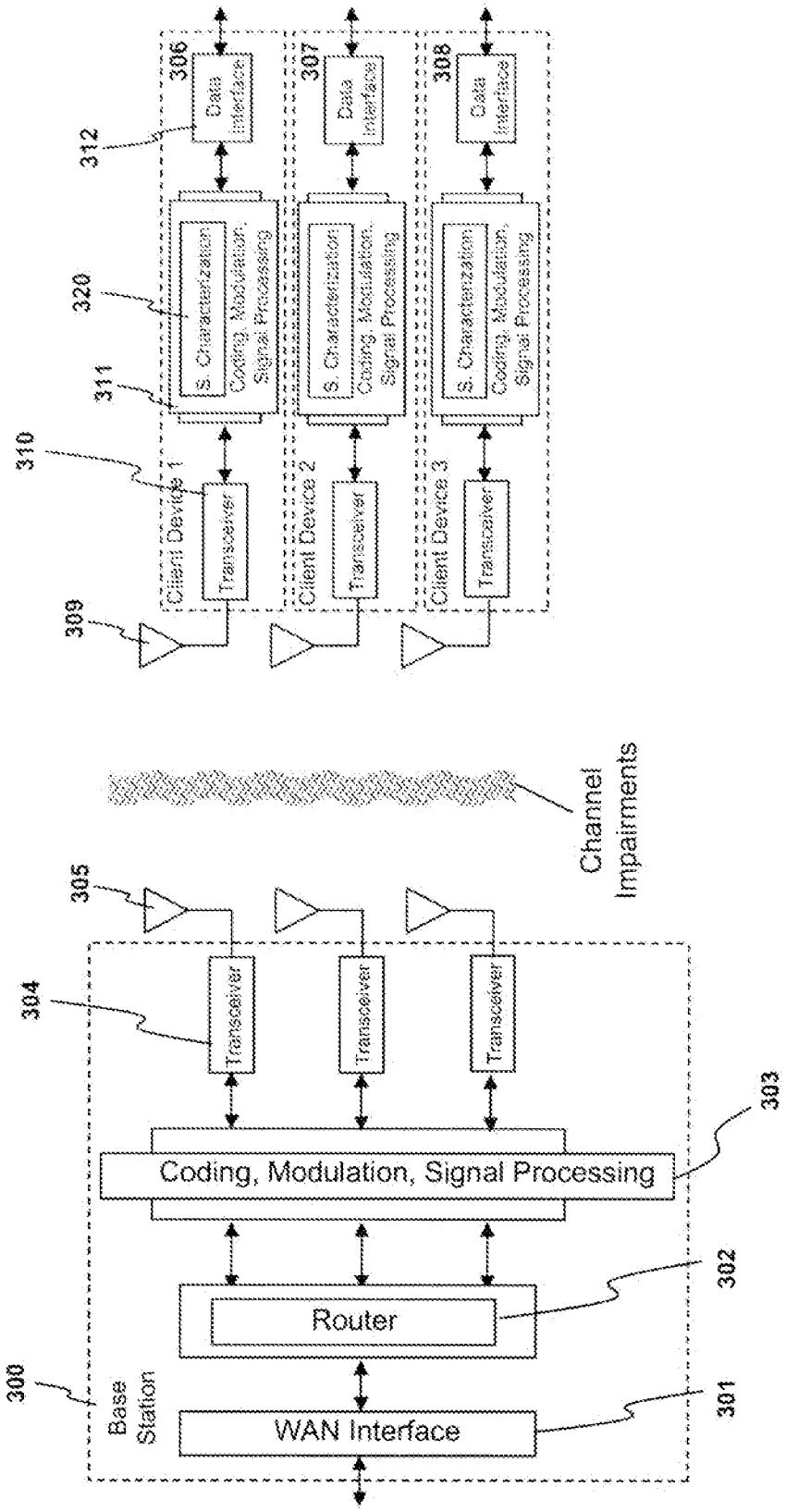

3-Antenna Base Station with 3 Single-Antenna Client Devices

Fig. 3

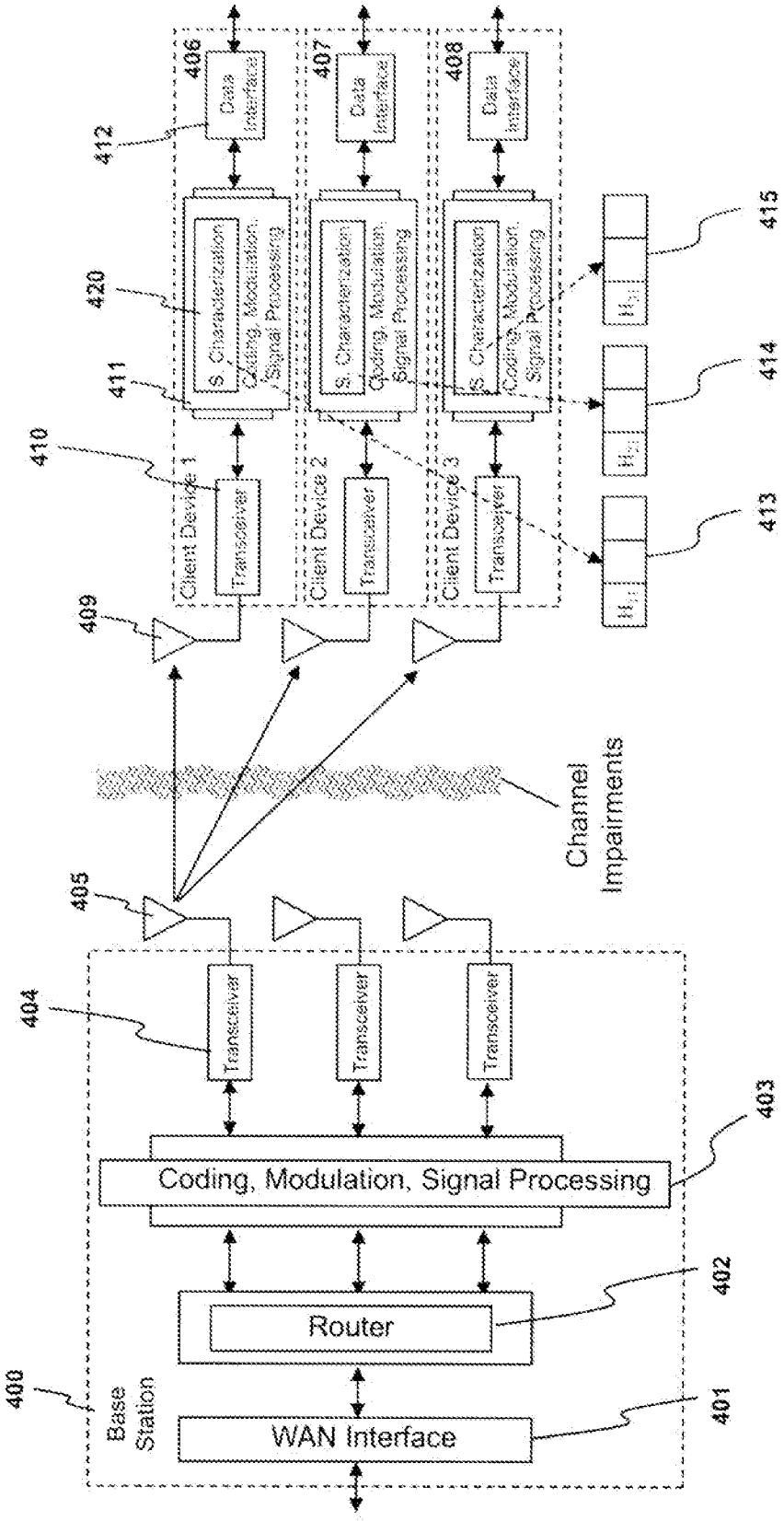
Base Station
400
WAN Interface
401
Router
402
Coding, Modulation, Signal Processing
403
Transceiver
404
405
Channel Impairments
Client Device 1
Client Device 2
Client Device 3
Transceiver
409
410
411
412
Data Interface
406
407
408
S. Characterization
Coding, Modulation, Signal Processing
420
413
414
415
Antenna 1 Pilot Signal Transmission

Fig. 4

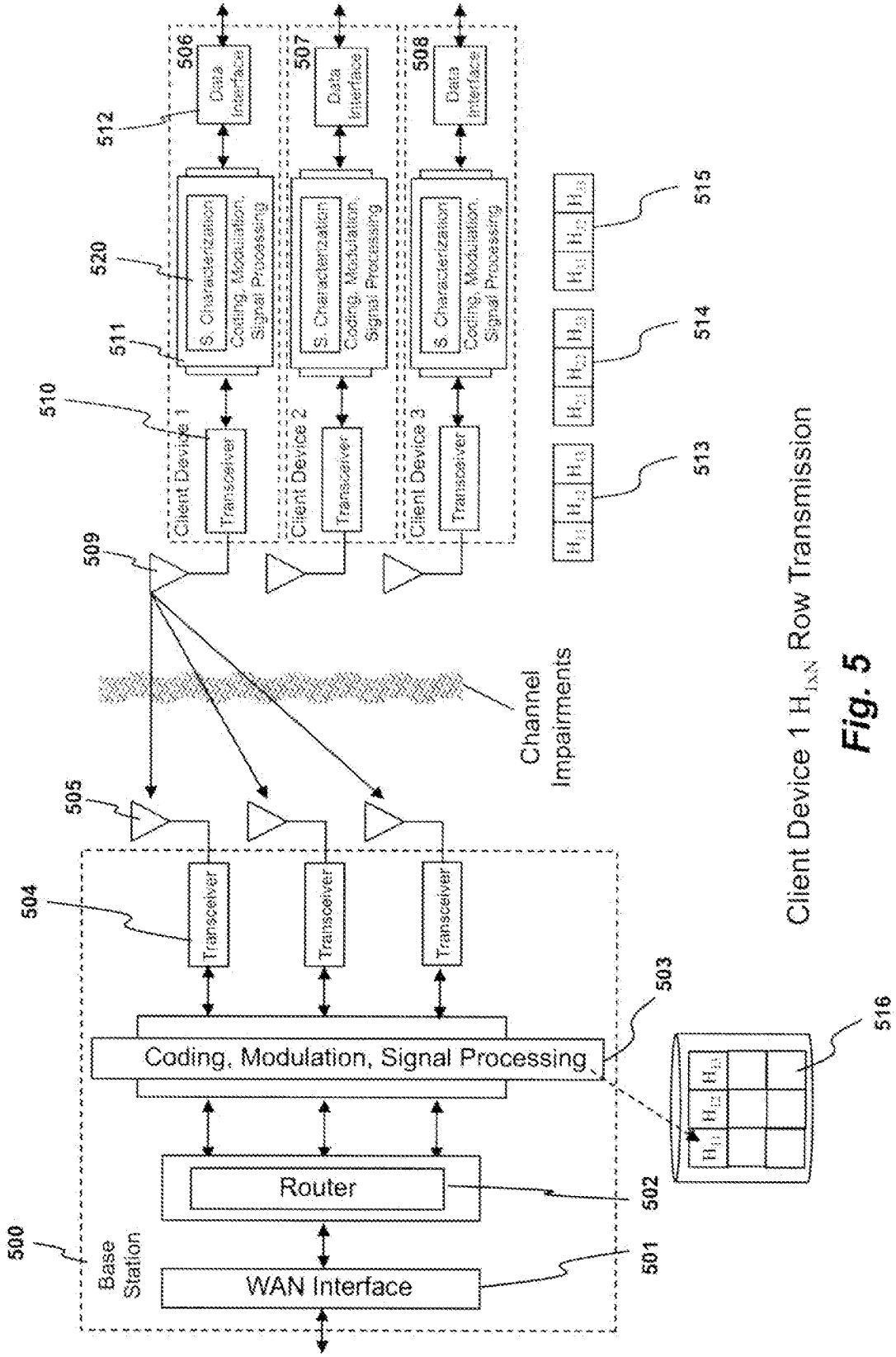
Base Station
WAN Interface
Router
Coding, Modulation, Signal Processing
Transceiver
Transceiver
Transceiver
Channel Impairments
Client Device 1
Client Device 2
Client Device 3
Transceiver
Transceiver
Transceiver
S. Characterization
Coding, Modulation, Signal Processing
S. Characterization
Coding, Modulation, Signal Processing
S. Characterization
Coding, Modulation, Signal Processing
Data Interface
Data Interface
Data Interface
500
501
502
503
504
505
506
507
508
509
510
511
512
513
514
515
516
Client Device 1 $H_{1,N}$ Row Transmission

Fig. 5

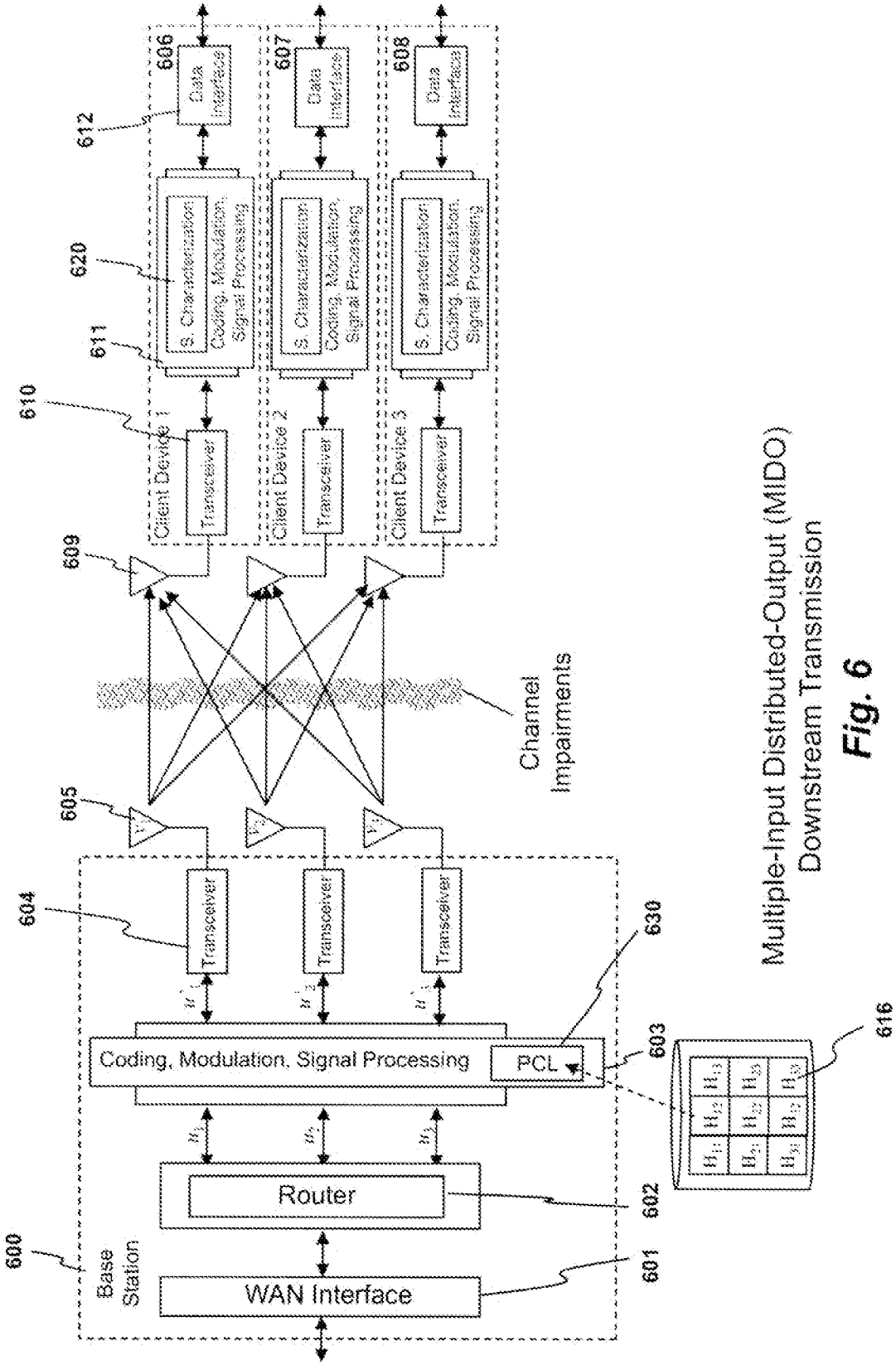
Multiple-Input Distributed-Output (MIDO)
Downstream Transmission
Channel
Impairments
Client Device 1
Client Device 2
Client Device 3
Data Interface
S. Characterization
Coding, Modulation, Signal Processing
Transceiver
Coding, Modulation, Signal Processing
PCL
Router
WAN Interface
Base Station
600
601
602
603
604
605
606
607
608
609
610
611
612
616
620
630

Fig. 6

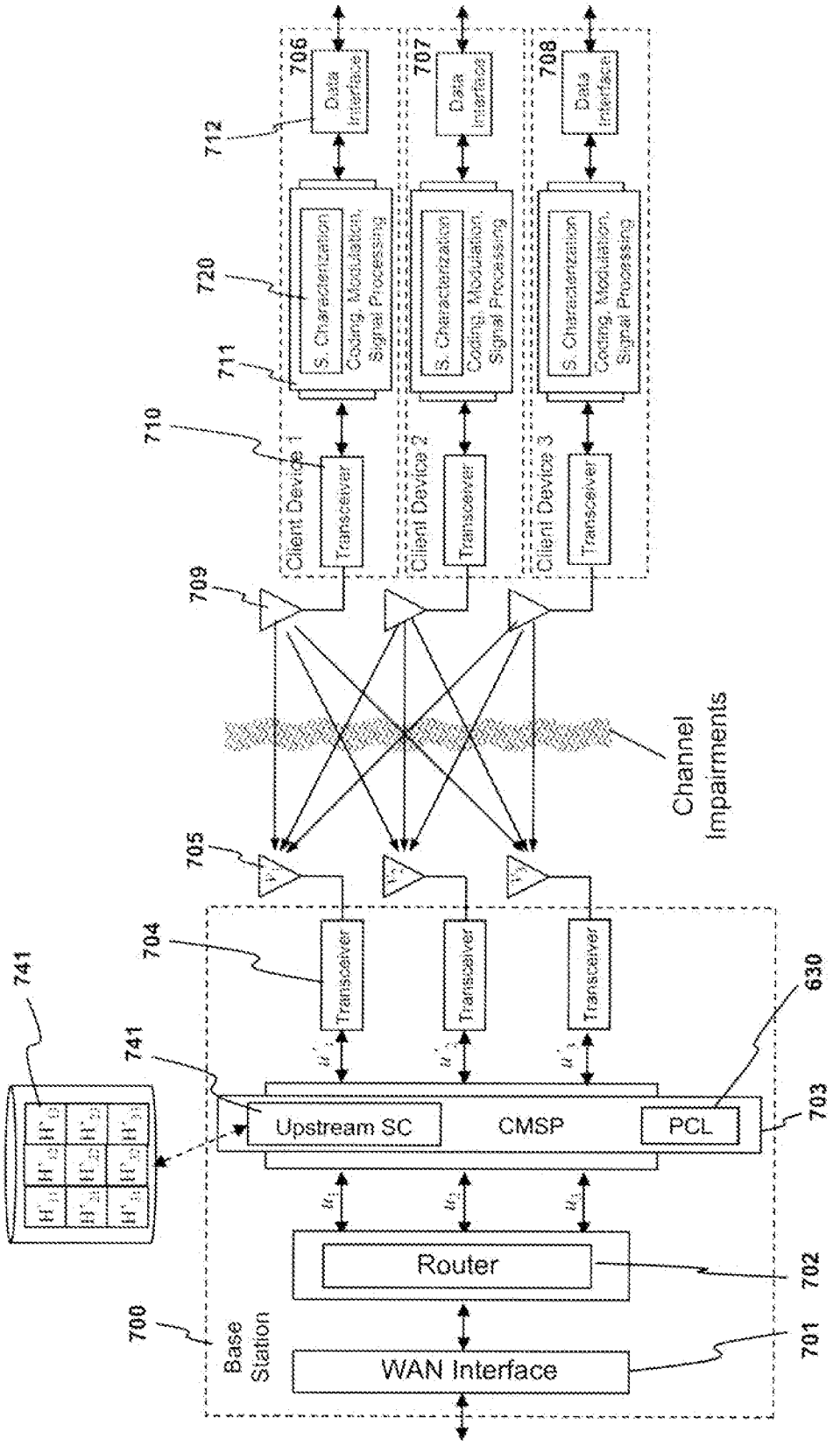
MIMO Upstream Transmission
Channel Impairments
Client Device 1
Client Device 2
Client Device 3
Data Interface
S. Characterization
Coding, Modulation, Signal Processing
Transceiver
Upstream SC
CMSP
PCL
Router
WAN Interface
Base Station
700
701
702
703
704
705
706
707
708
709
710
711
712
720
630
741

Fig. 7

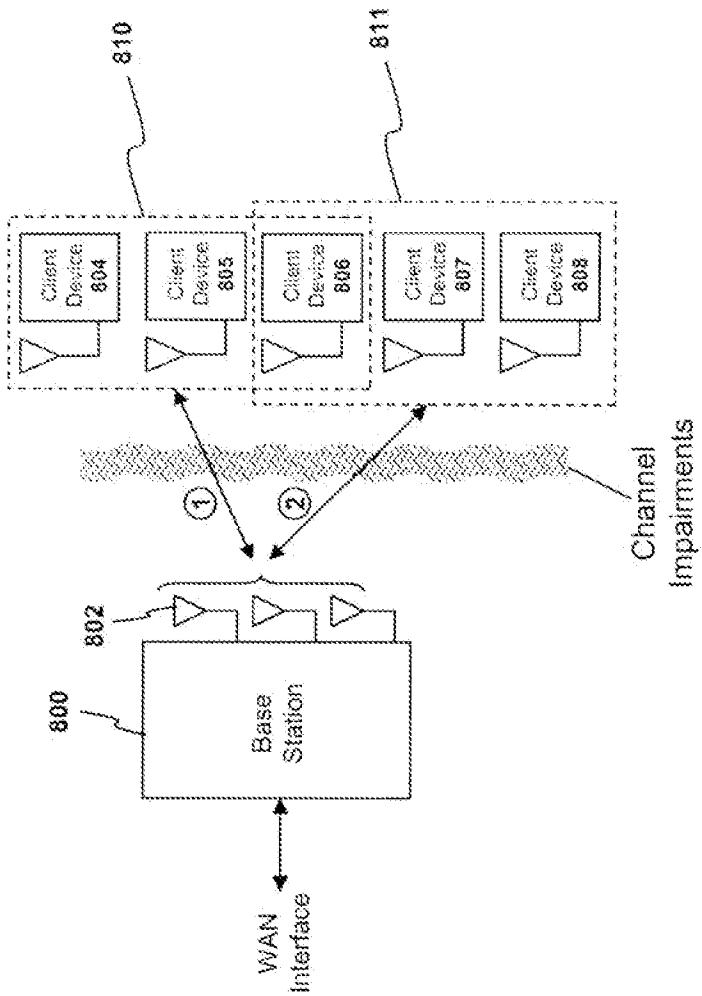

Cycling With Different Client Groups

Fig. 8

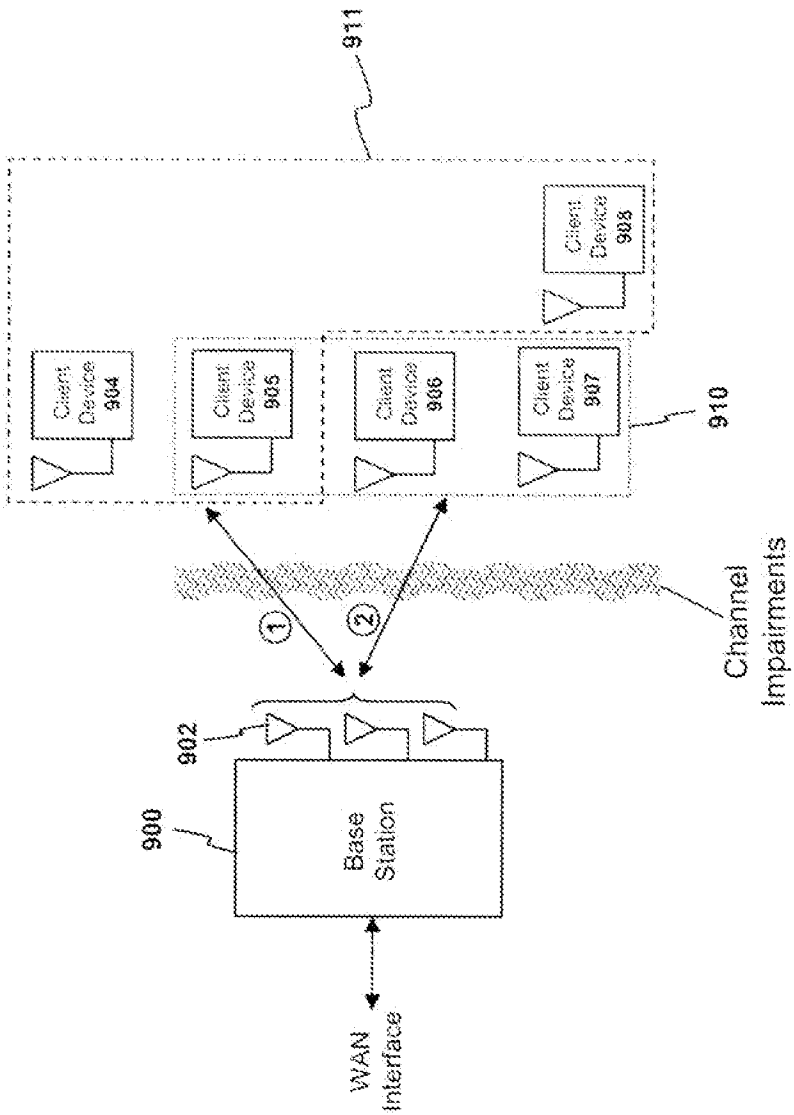

Grouping Clients Based on Proximity

Fig. 9

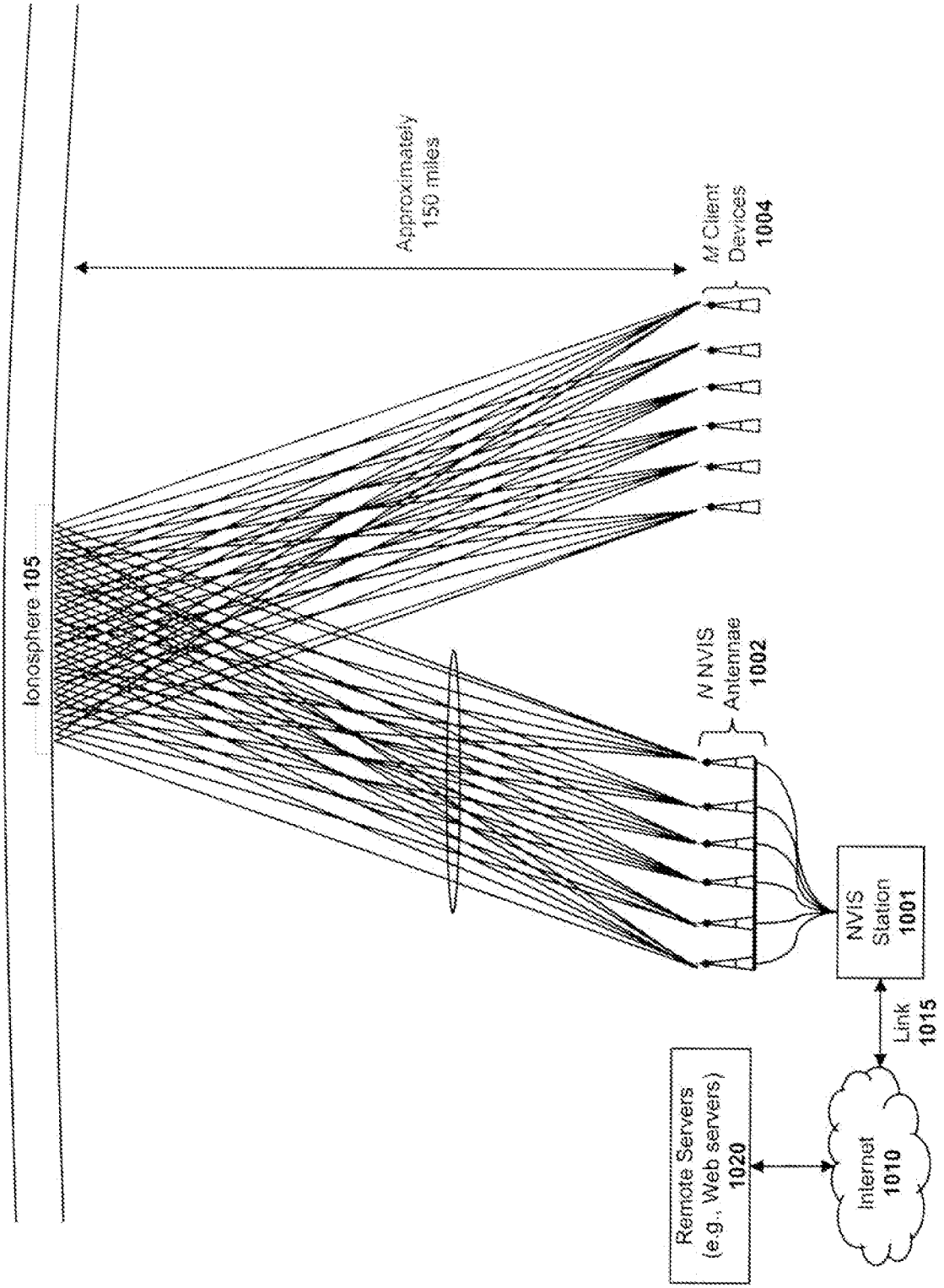
Ionosphere 105
Approximately 150 miles
M Client Devices 1004
N NVIS Antennae 1002
NVIS Station 1001
Link 1015
Internet 1010
Remote Servers (e.g., Web servers) 1020

Fig. 10

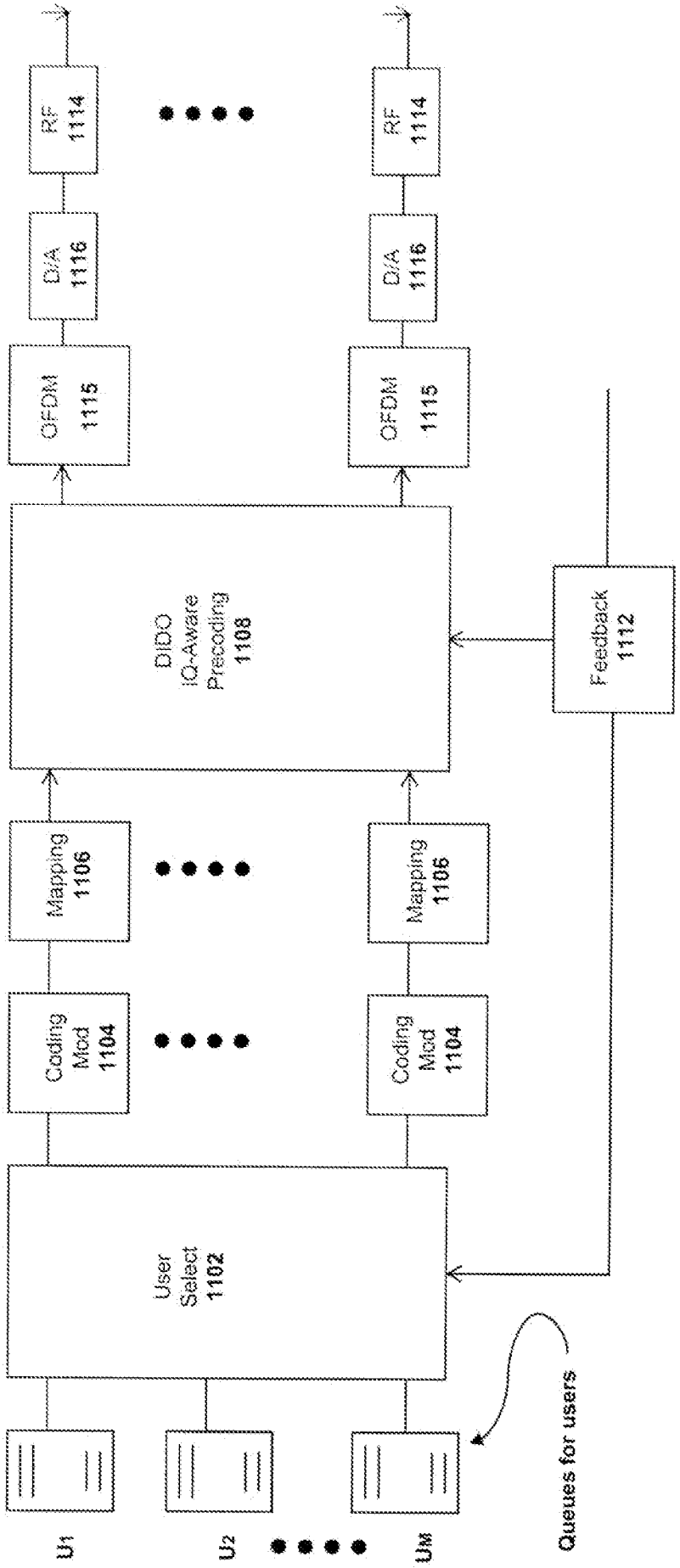
RF 1114
RF 1114
D/A 1116
D/A 1116
OFDM 1115
OFDM 1115
DIDO IQ-Aware Precoding 1108
Feedback 1112
Mapping 1106
Mapping 1106
Coding Mod 1104
Coding Mod 1104
User Select 1102
Queues for users
U1
U2
UM

FIG. 11

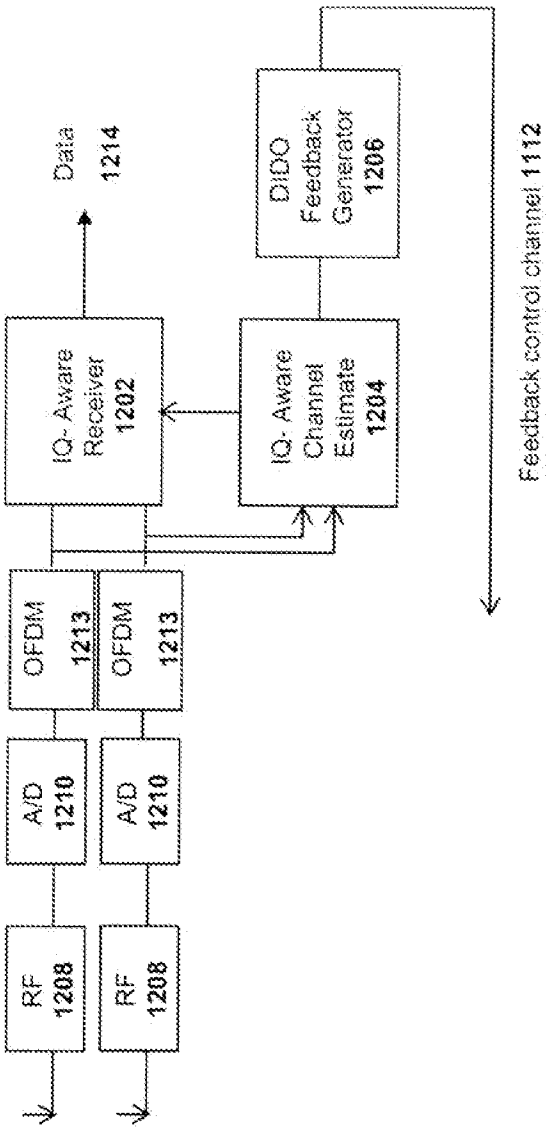
RF 1208
RF 1208
A/D 1210
A/D 1210
OFDM 1213
OFDM 1213
IQ- Aware Receiver 1202
IQ- Aware Channel Estimate 1204
DIDO Feedback Generator 1206
Data 1214
Feedback control channel 1112

FIG. 12

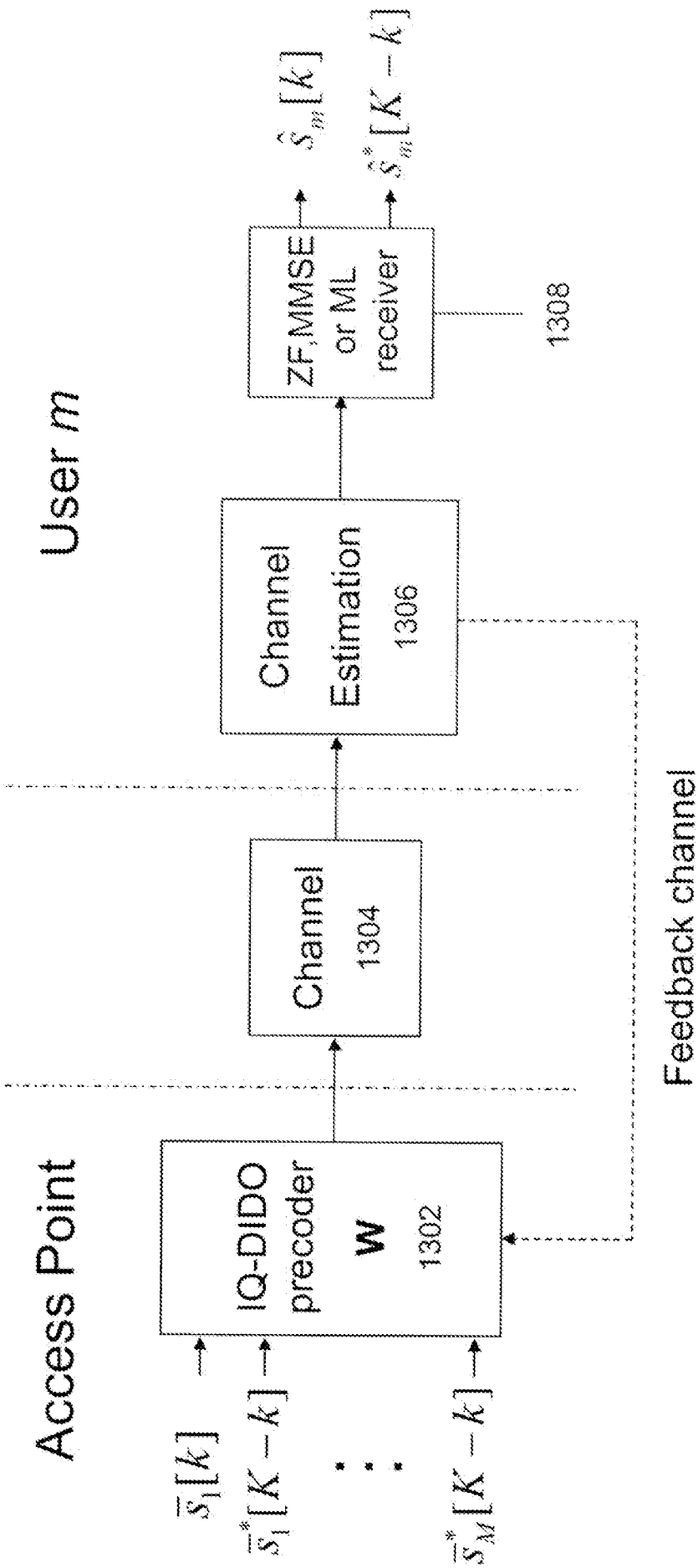
Access Point
IQ-DIDO precoder
W
1302
Channel
1304
Channel Estimation
1306
ZF,MMSE or ML receiver
1308
User m
Feedback channel
$\bar{s}_1[k]$
$\bar{s}_1^*[K-k]$
$\bar{s}_M^*[K-k]$
$\hat{s}_m[k]$
$\hat{s}_m^*[K-k]$

FIG. 13

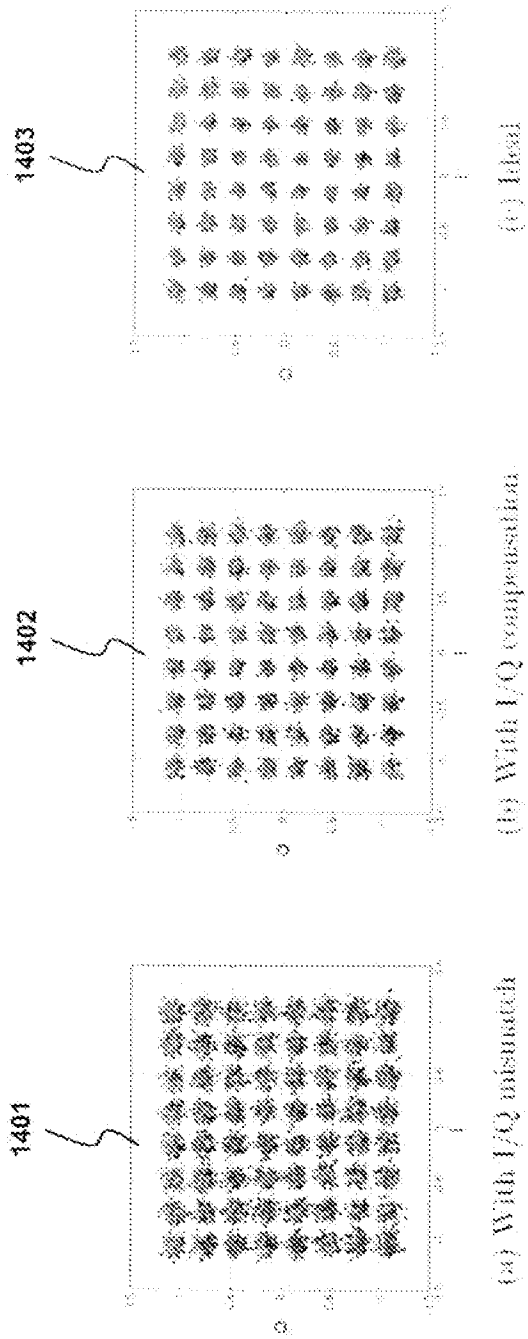
1401
1402
1403
(a) With I/Q mismatch
(b) With I/Q compensation
(c) Ideal

FIG. 14

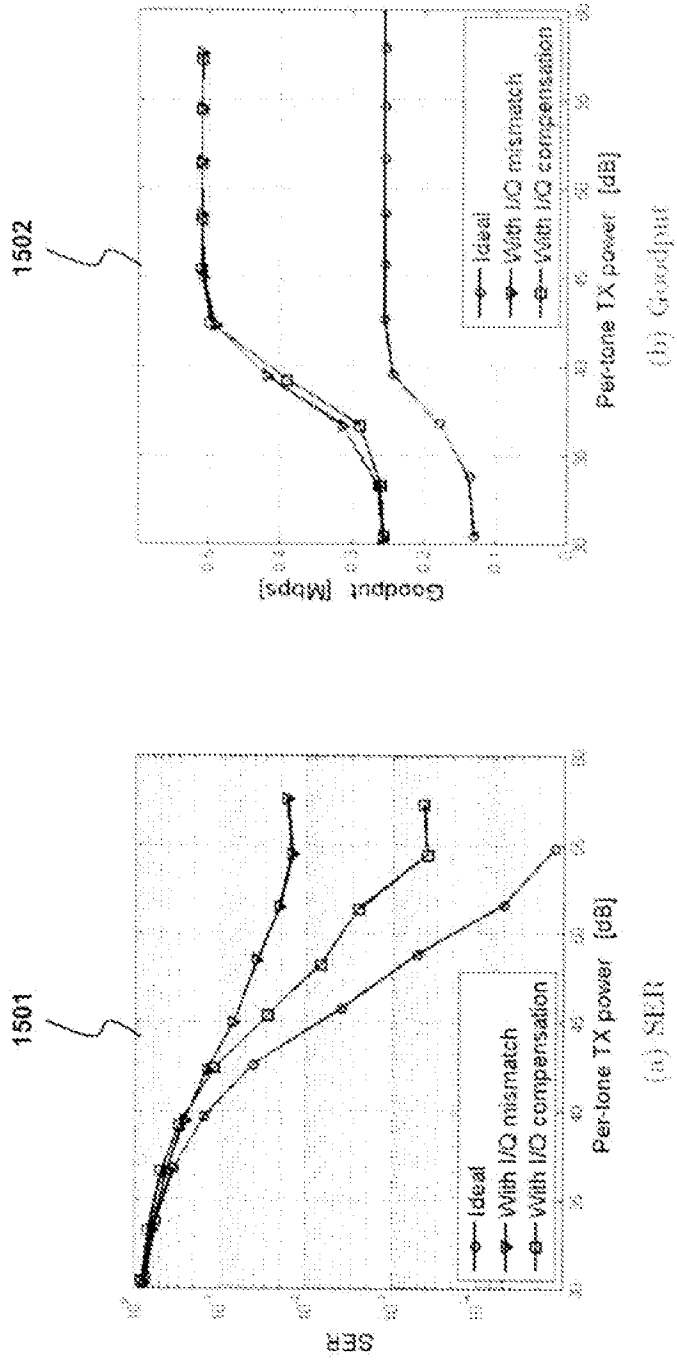
1501
SER
Per-tone TX power [dB]
Ideal
With I/Q mismatch
With I/Q compensation
(a) SER
1502
Goodput [Mbps]
Per-tone TX power [dB]
Ideal
With I/Q mismatch
With I/Q compensation
(b) Goodput

FIG. 15

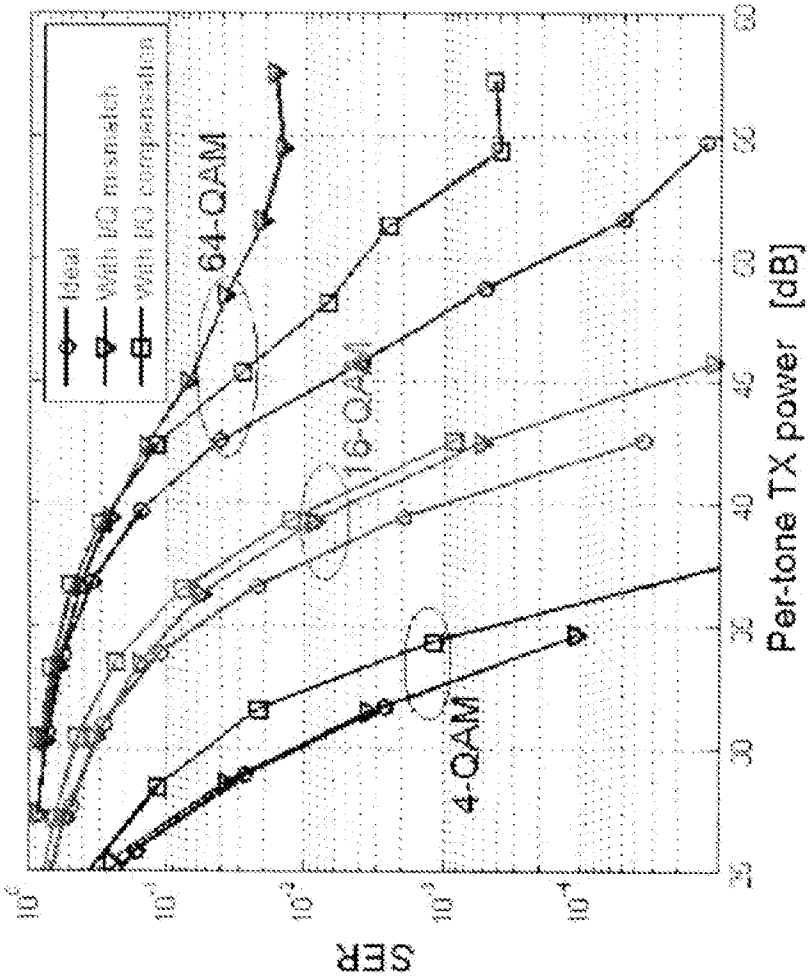
Ideal
With I/Q mismatch
With I/Q compensation
64-QAM
16-QAM
4-QAM
SER
Per-tone TX power [dB]

FIG. 16

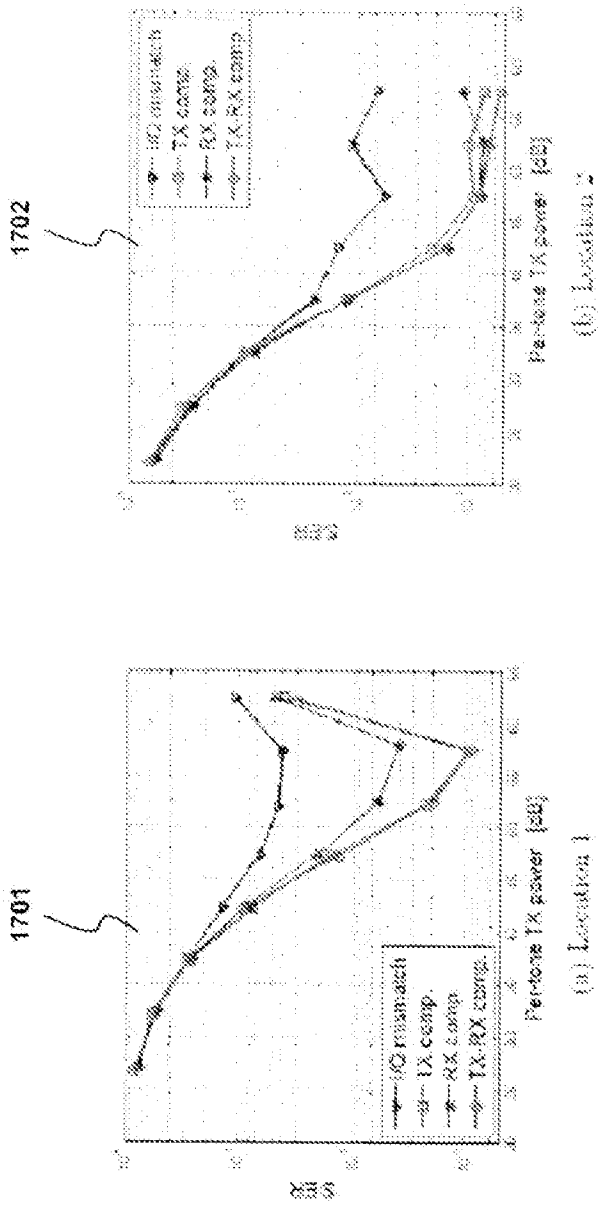
1702
1701
IQ mismatch
TX comp.
RX comp.
TX-RX comp.
Per-tone TX power [dB]
SER
(a) Location 1
(b) Location 2

FIG. 17

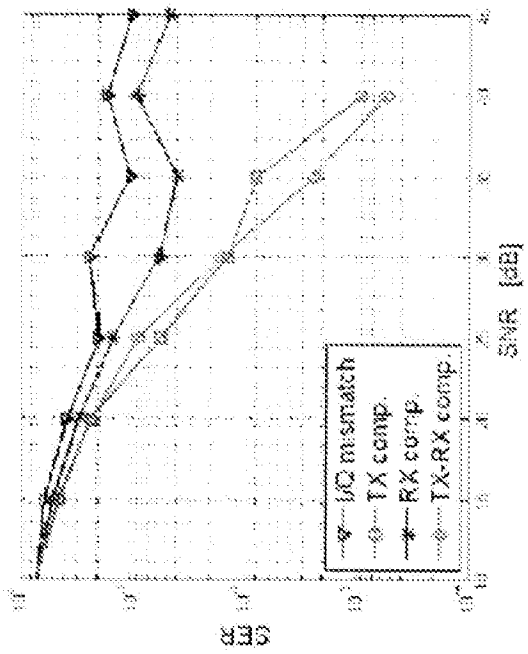

FIG. 18

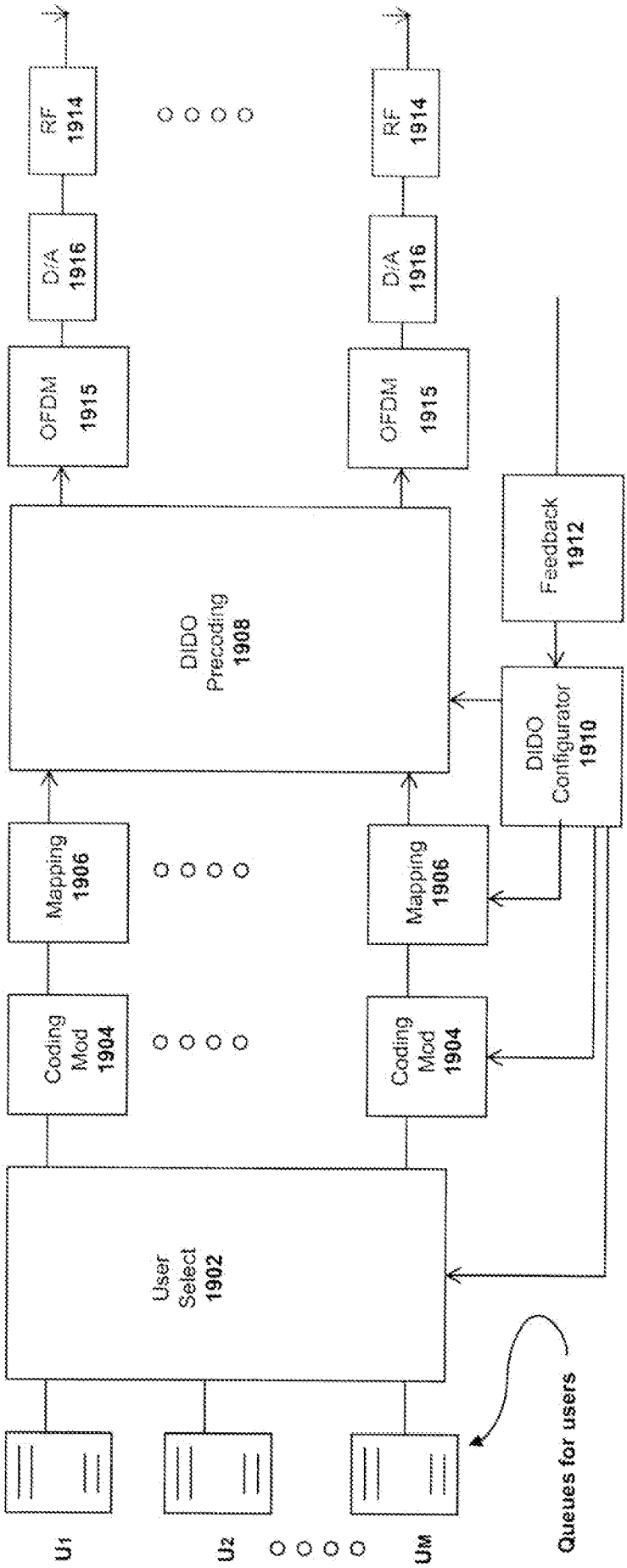
RF 1914
D/A 1916
OFDM 1915
DIDO Precoding 1908
Mapping 1906
Coding Mod 1904
User Select 1902
Feedback 1912
DIDO Configurator 1910
Queues for users
U1
U2
UM

FIG. 19

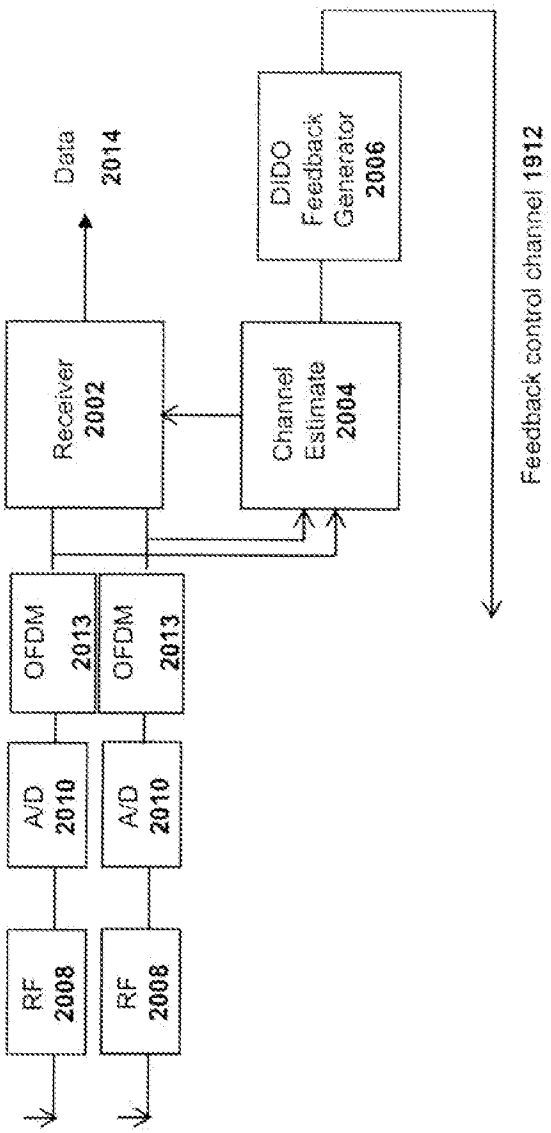
RF 2008
RF 2008
A/D 2010
A/D 2010
OFDM 2013
OFDM 2013
Receiver 2002
Channel Estimate 2004
DiDO Feedback Generator 2006
Data 2014
Feedback control channel 1912

FIG. 20

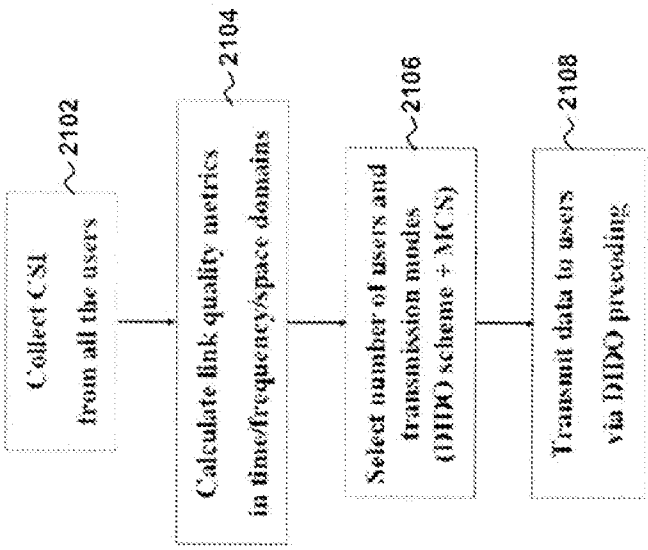
Collect CSI
from all the users
2102
Calculate link quality metrics
in time/frequency/space domains
2104
Select number of users and
transmission modes
(DIDO scheme + MCS)
2106
Transmit data to users
via DIDO precoding
2108

FIG. 21

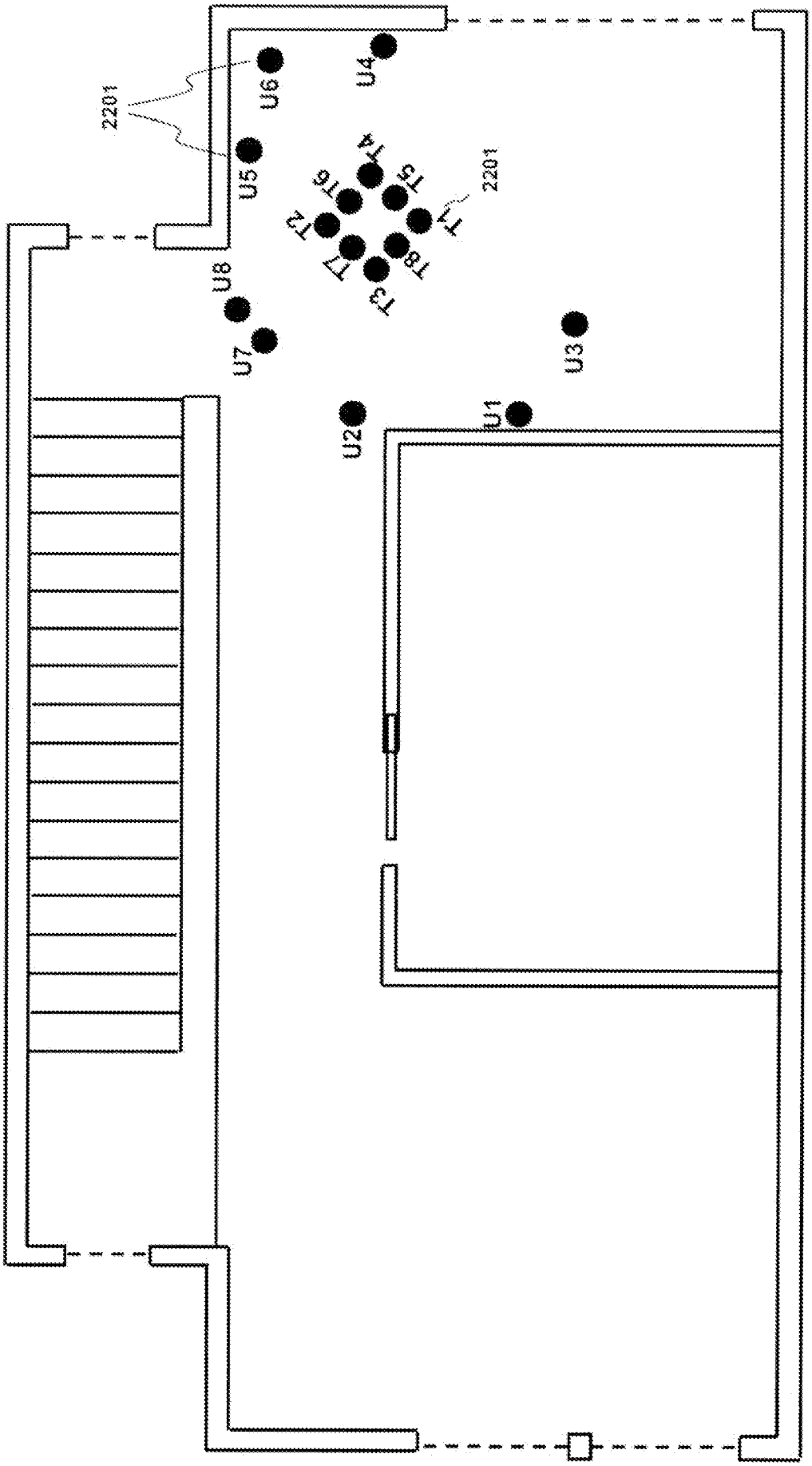

FIG. 22

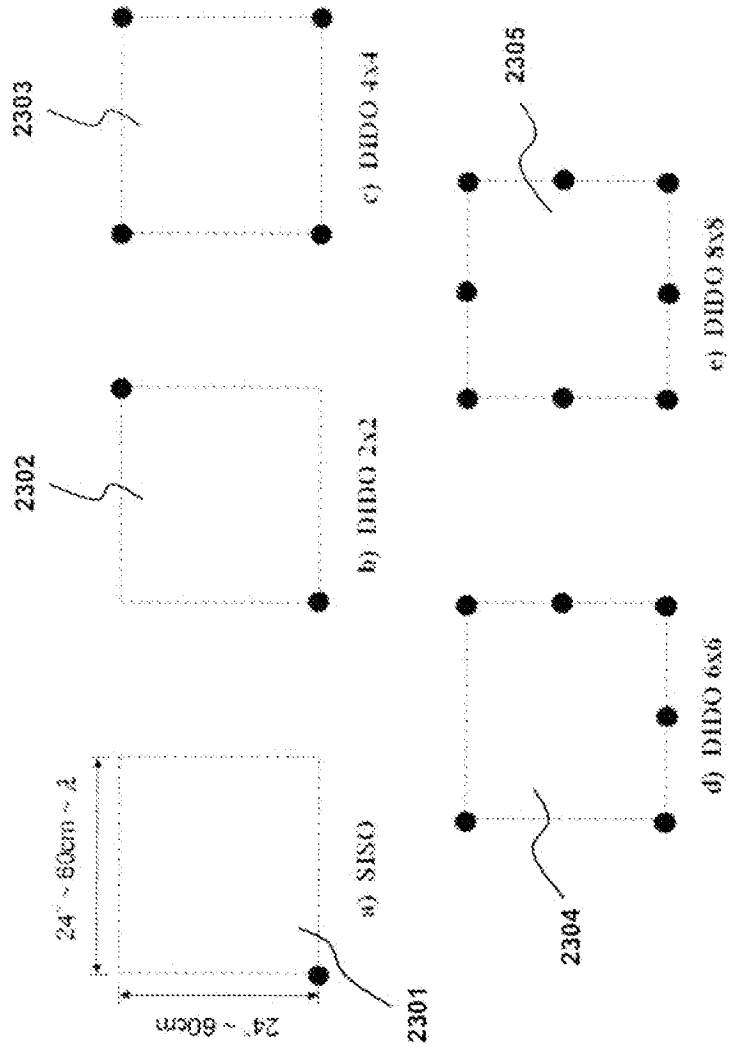
2303
c) DIDO 4x4
2305
e) DIDO 8x8
2302
b) DIDO 2x2
d) DIDO 6x6
2304
24" ~ 60cm ~ λ
24" ~ 60cm
a) SISO
2301

FIG. 23

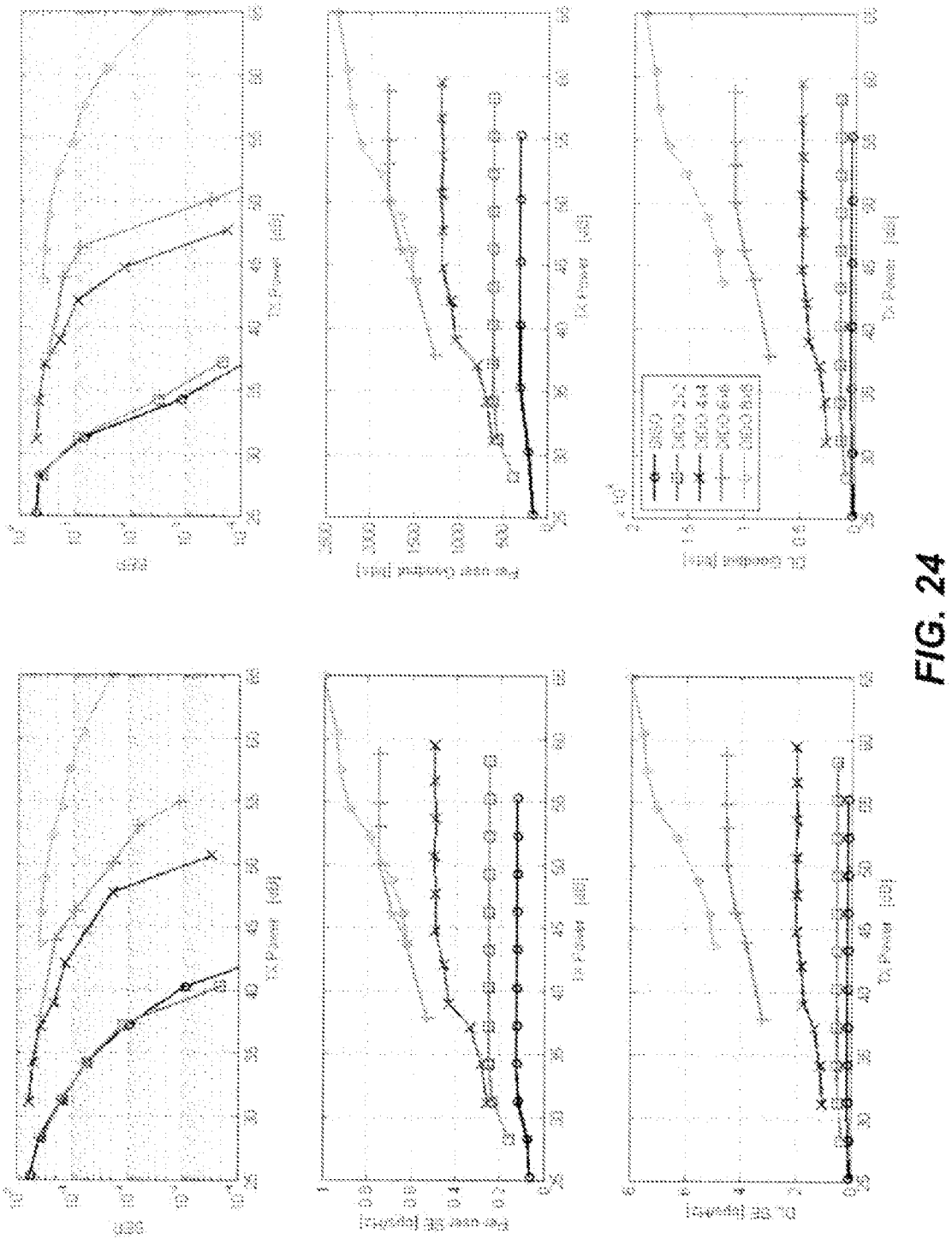

FIG. 24

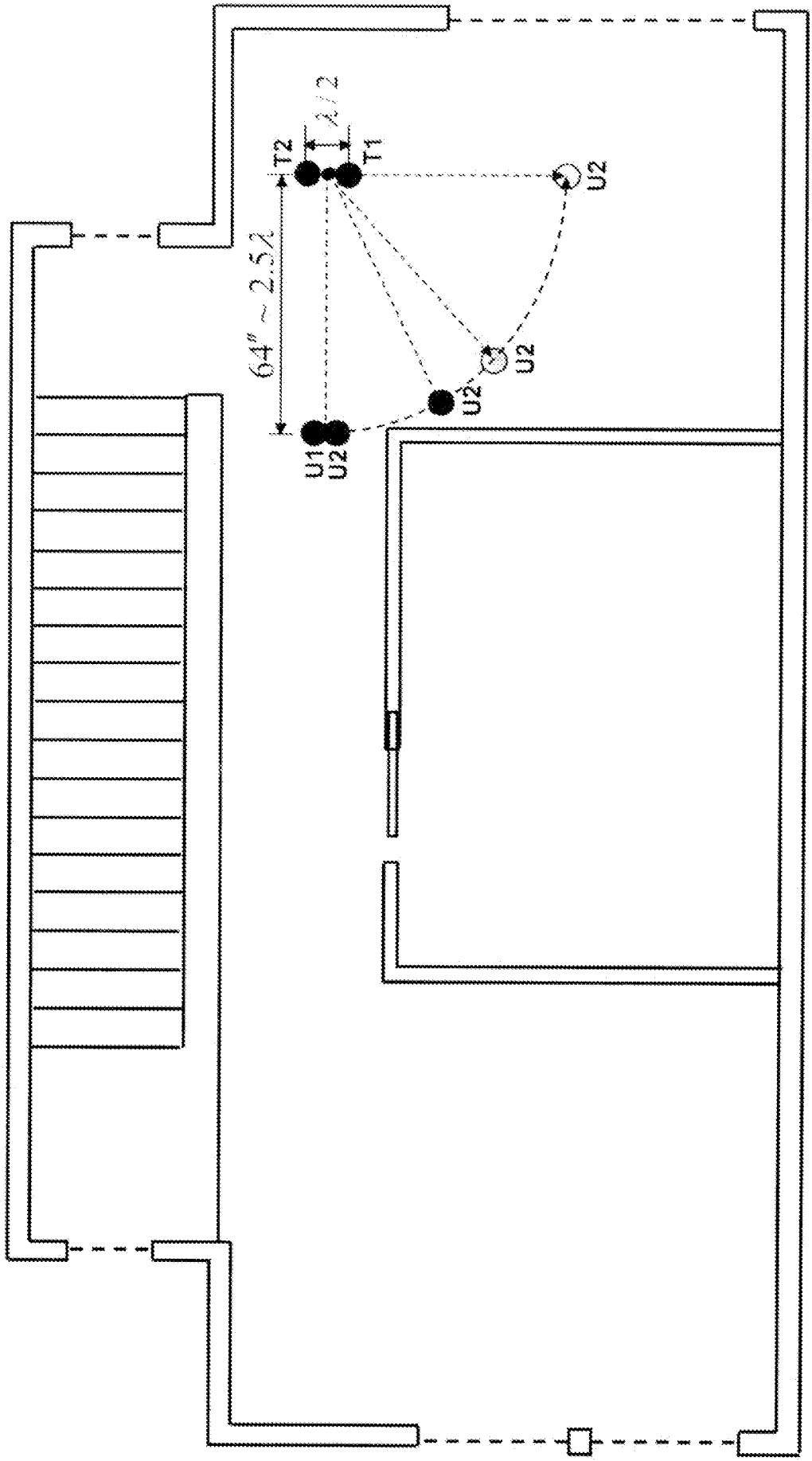

FIG. 25

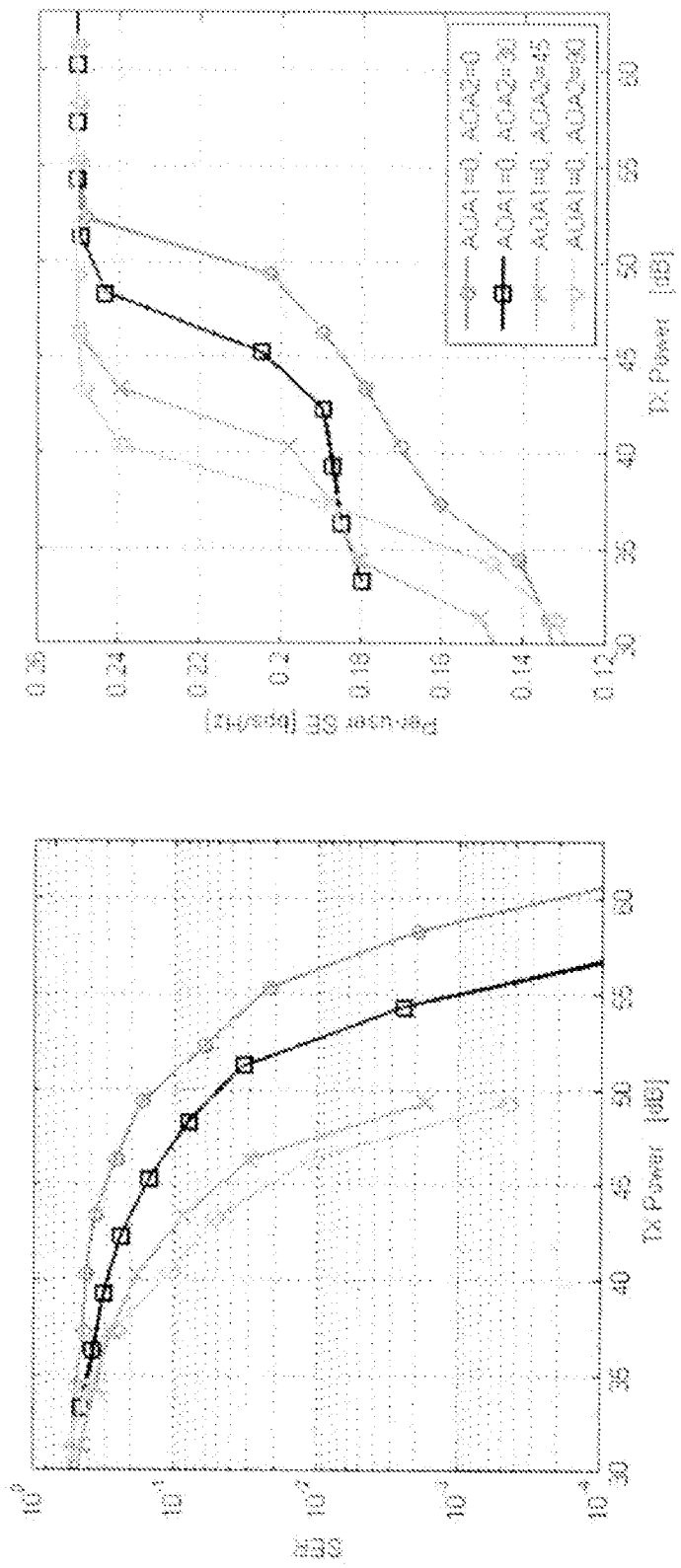
AOA1=0, AOA2=0
AOA1=0, AOA2=30
AOA1=0, AOA2=45
AOA1=0, AOA2=60
Tx Power [dB]
Per-user SE [bps/Hz]
SER

FIG. 26

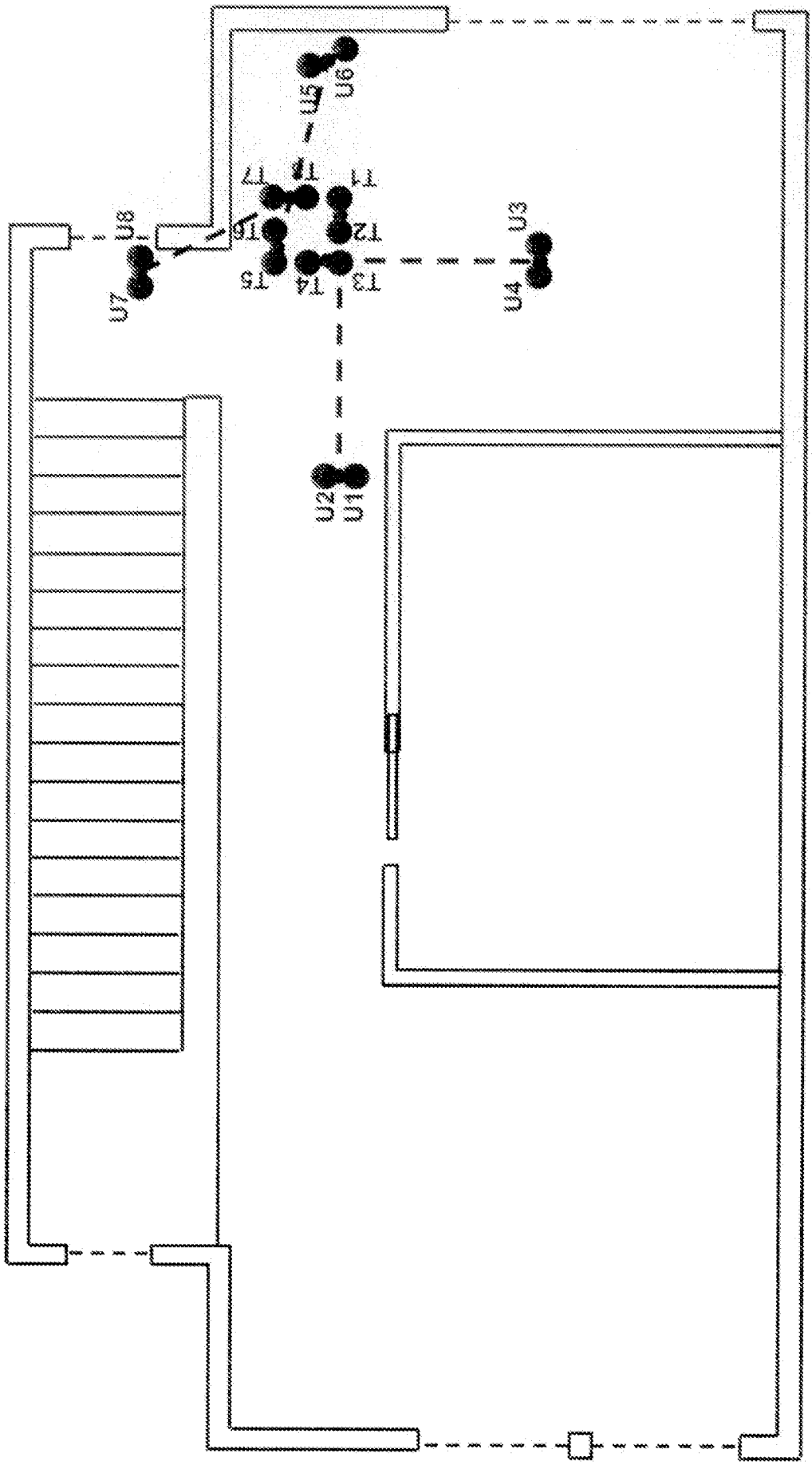

FIG. 27

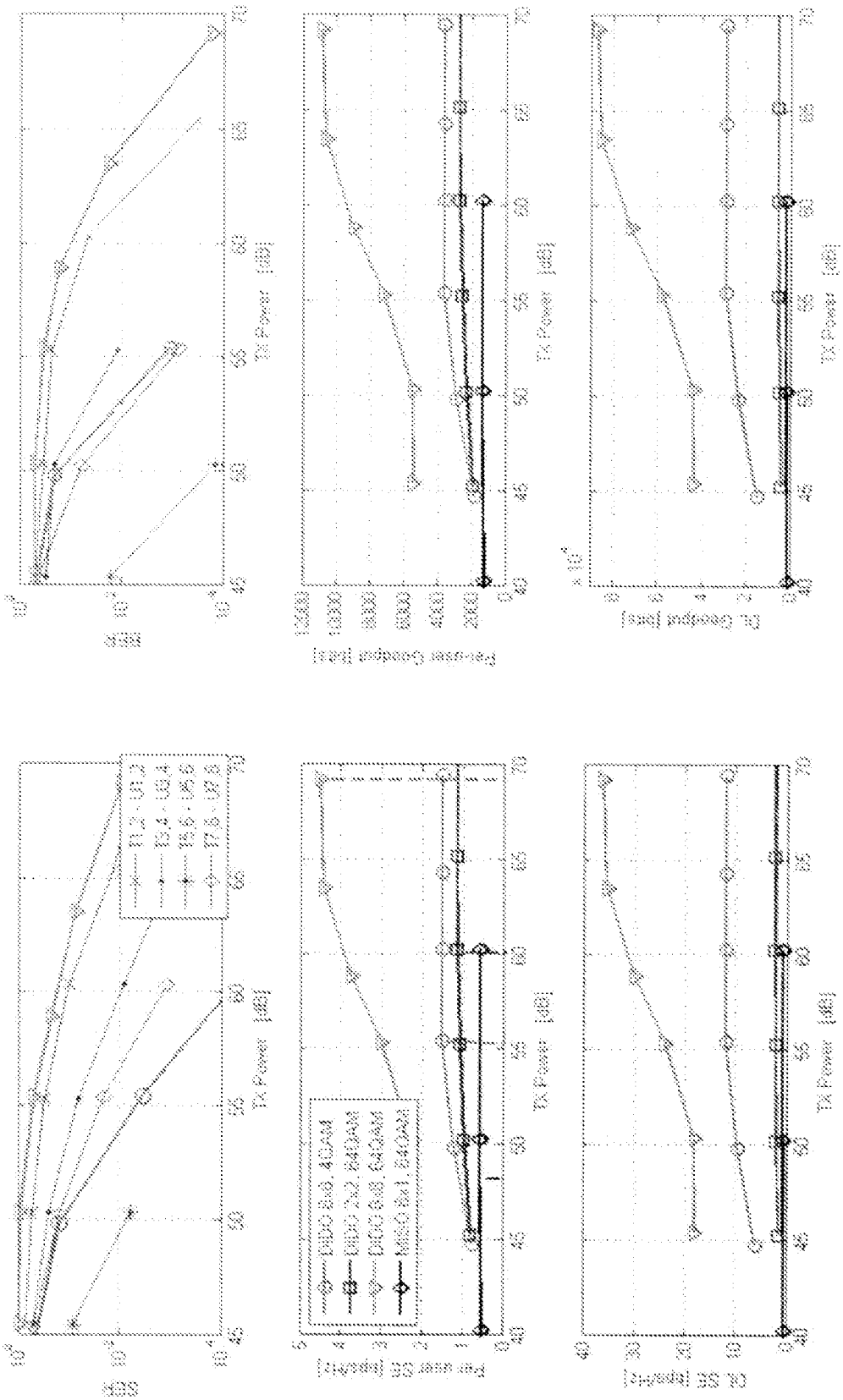
BLER
Tx Power [dB]
Per-user Goodput [bps]
Tx Power [dB]
DL Goodput [bps]
Tx Power [dB]
SCP
Tx Power [dB]
Per-user SE [bps/Hz]
Tx Power [dB]
DL SE [bps/Hz]
Tx Power [dB]
UE1 - UE2
UE4 - UE5
UE6 - UE7
UE8 - UE9
UE10 Bw0, 4QAM
UE3 2x2, 64QAM
UE12 Bw0, QPSK
UE11 Bw1, 64QAM

FIG. 28

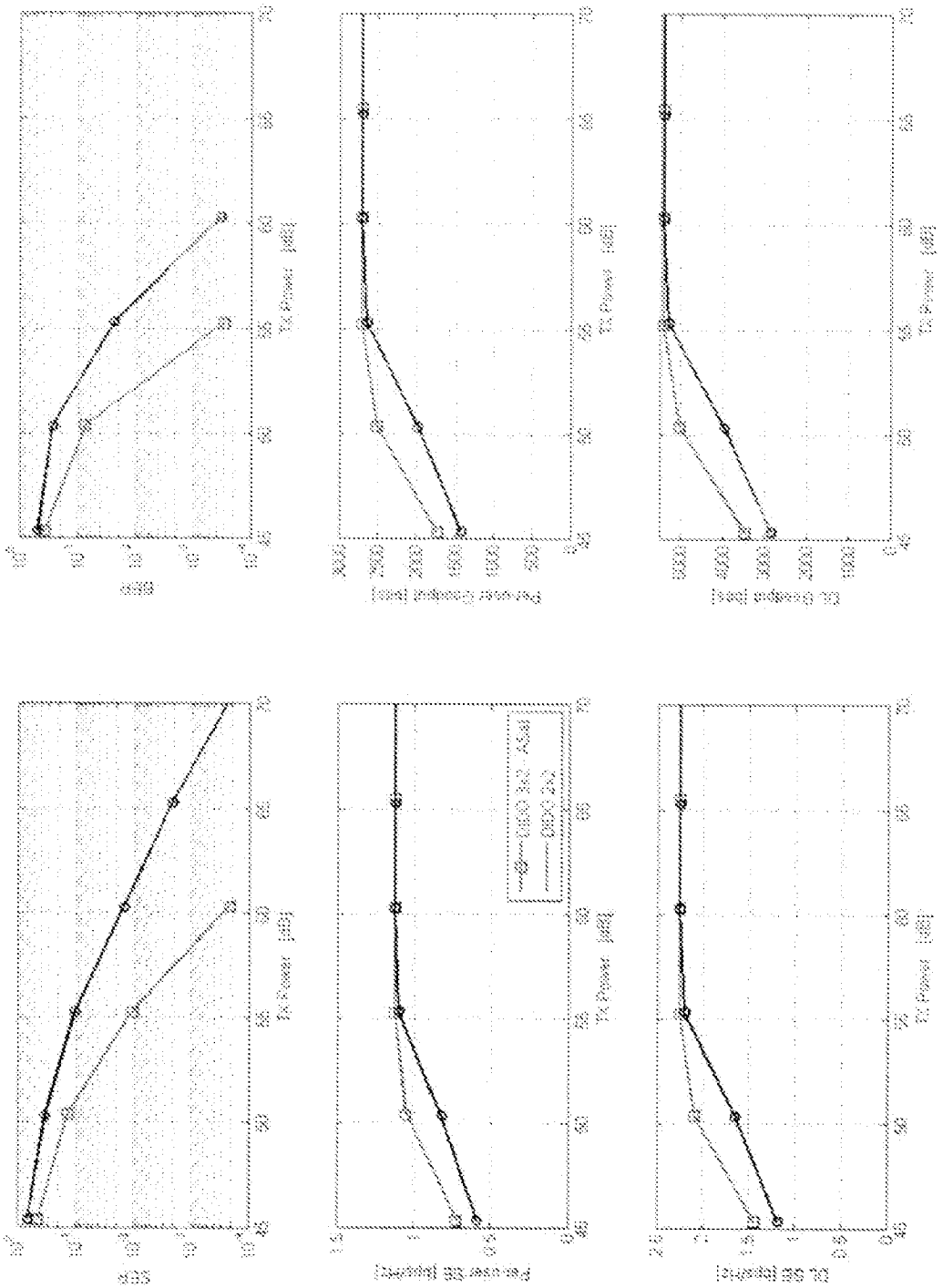

FIG. 29

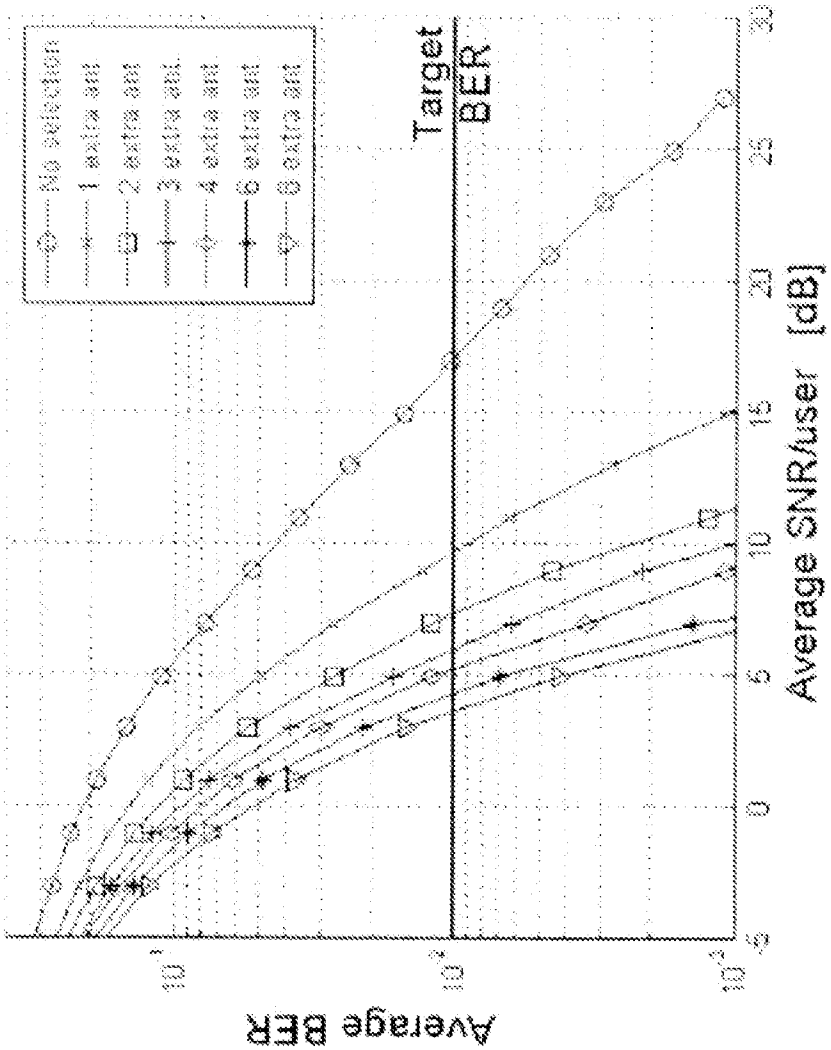
No selection
1 extra ant.
2 extra ant.
3 extra ant.
4 extra ant.
6 extra ant.
8 extra ant.
Target BER
Average BER
Average SNR/user [dB]
10^-1
10^-2
10^-3
0
5
10
15
20
25
30

FIG. 30

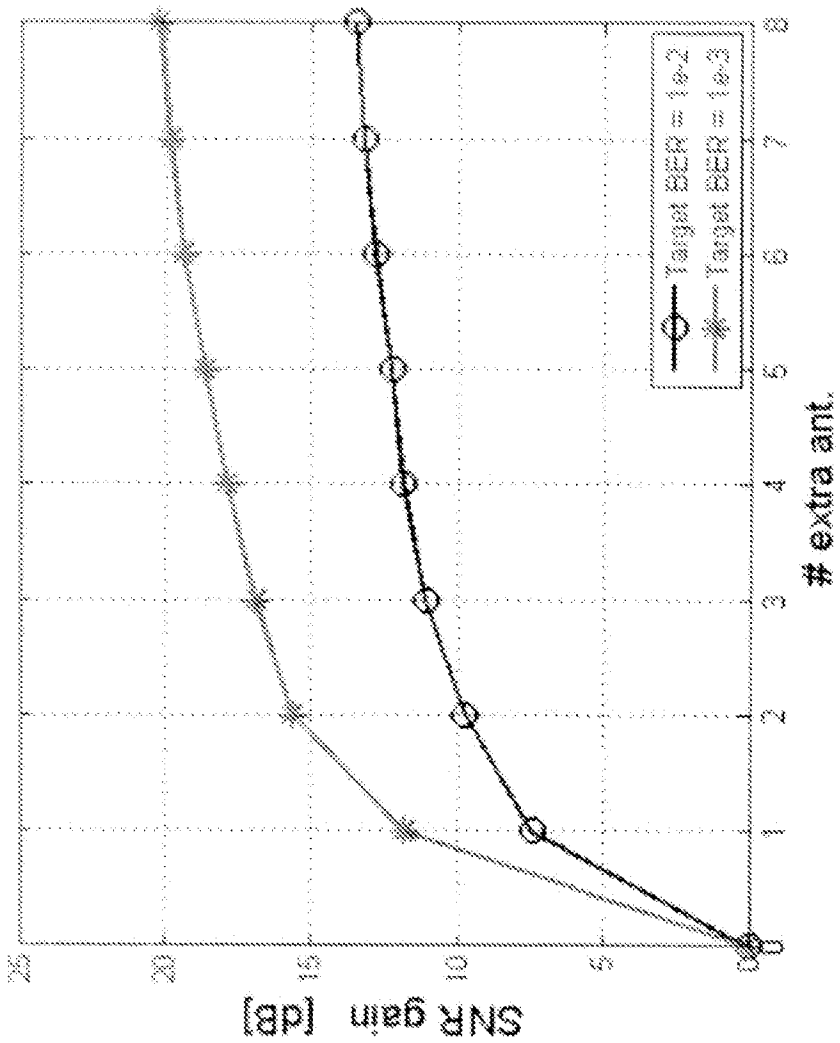
SNR gain [dB]
extra ant.
Target BER = 1e-2
Target BER = 1e-3
0
5
10
15
20
25
1
2
3
4
5
6
7
8

FIG. 31

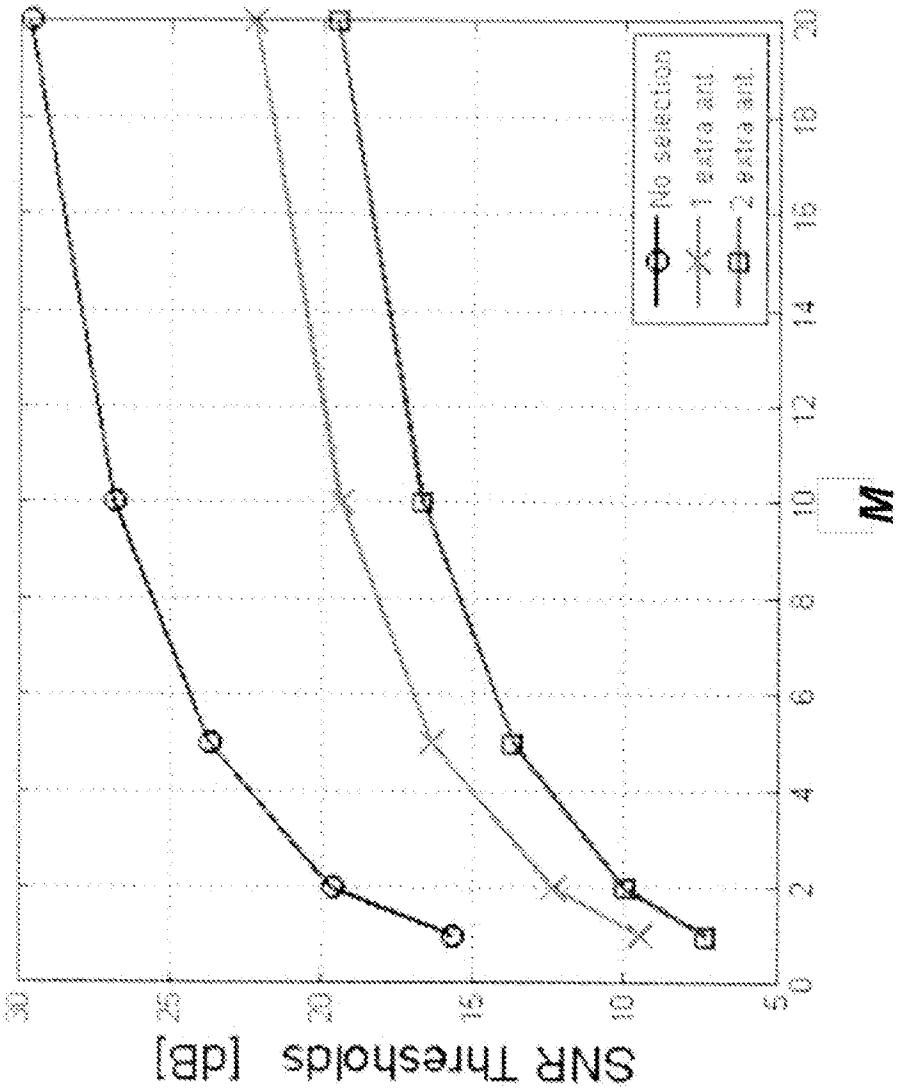

FIG. 32

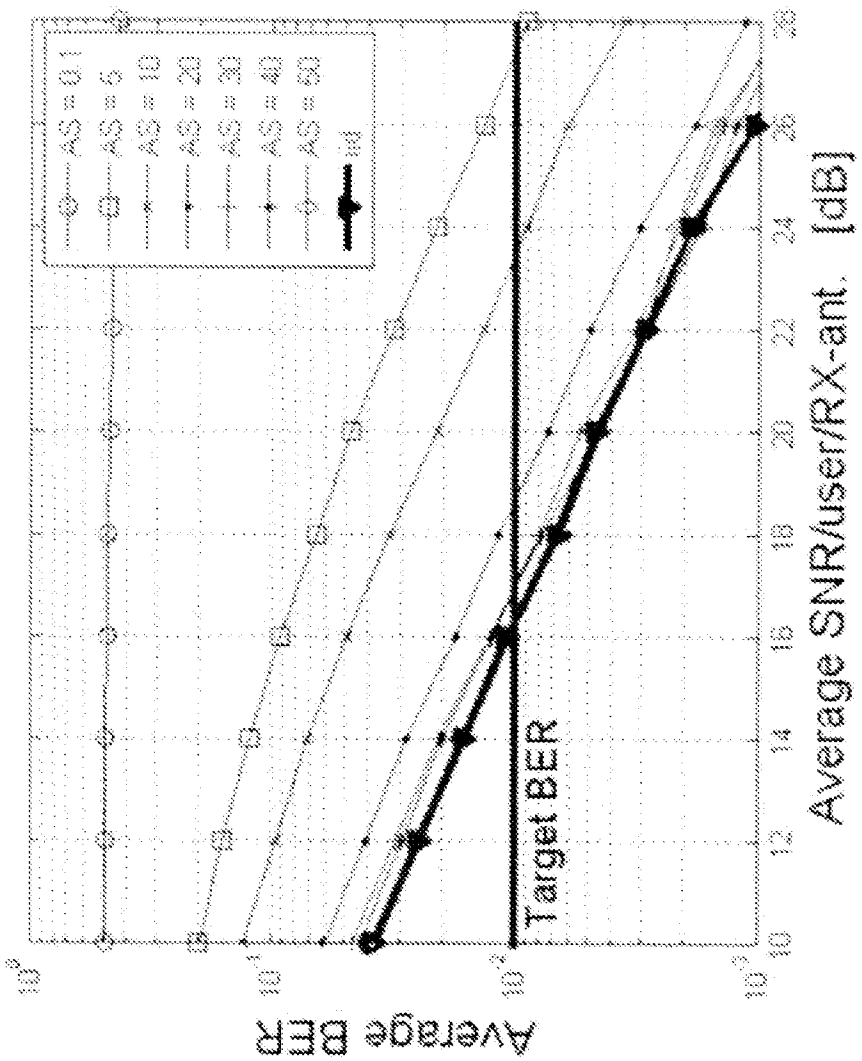
Average BER
Average SNR/user/RX-ant. [dB]
Target BER
ΔS = 0.1
ΔS = 6
ΔS = 10
ΔS = 20
ΔS = 30
ΔS = 40
ΔS = 60
MF

FIG. 33

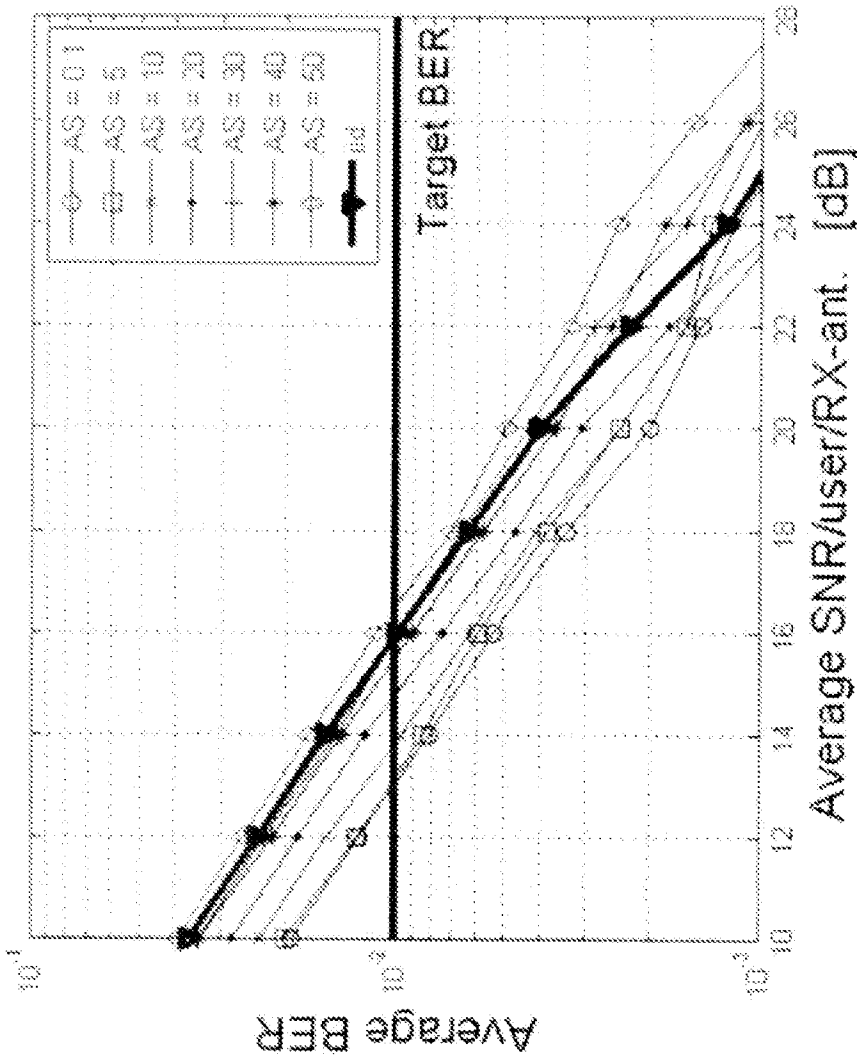
Average BER
Average SNR/user/RX-ant. [dB]
Target BER
AS = 0.1
AS = 6
AS = 10
AS = 20
AS = 30
AS = 40
AS = 60
std

FIG. 34

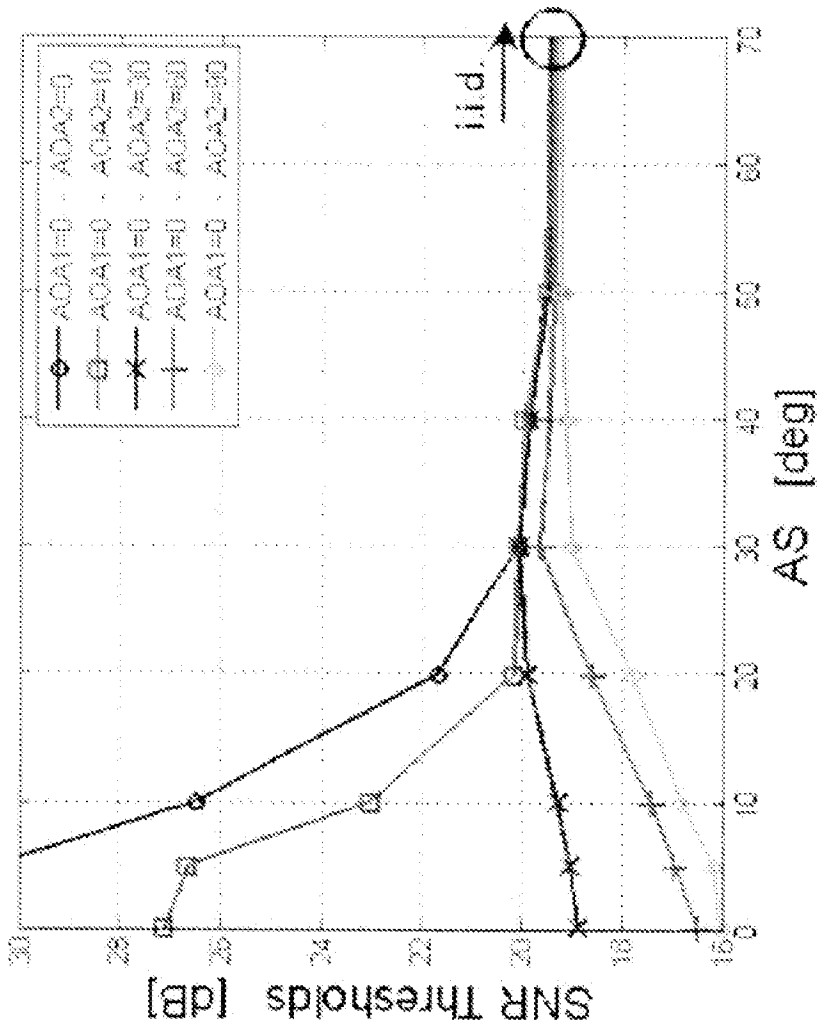
SNR Thresholds [dB]
AS [deg]
i.i.d.
AOA1=0 - AOA2=0
AOA1=0 - AOA2=10
AOA1=0 - AOA2=30
AOA1=0 - AOA2=60
AOA1=0 - AOA2=90

FIG. 35

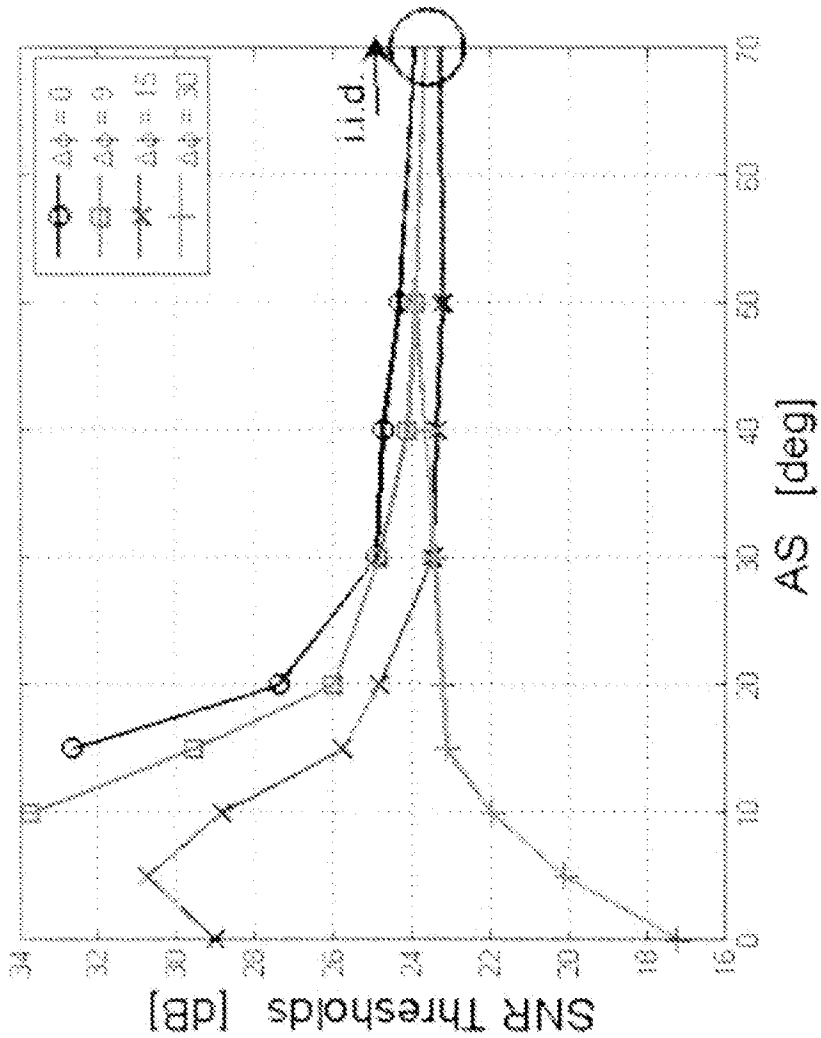

FIG. 36

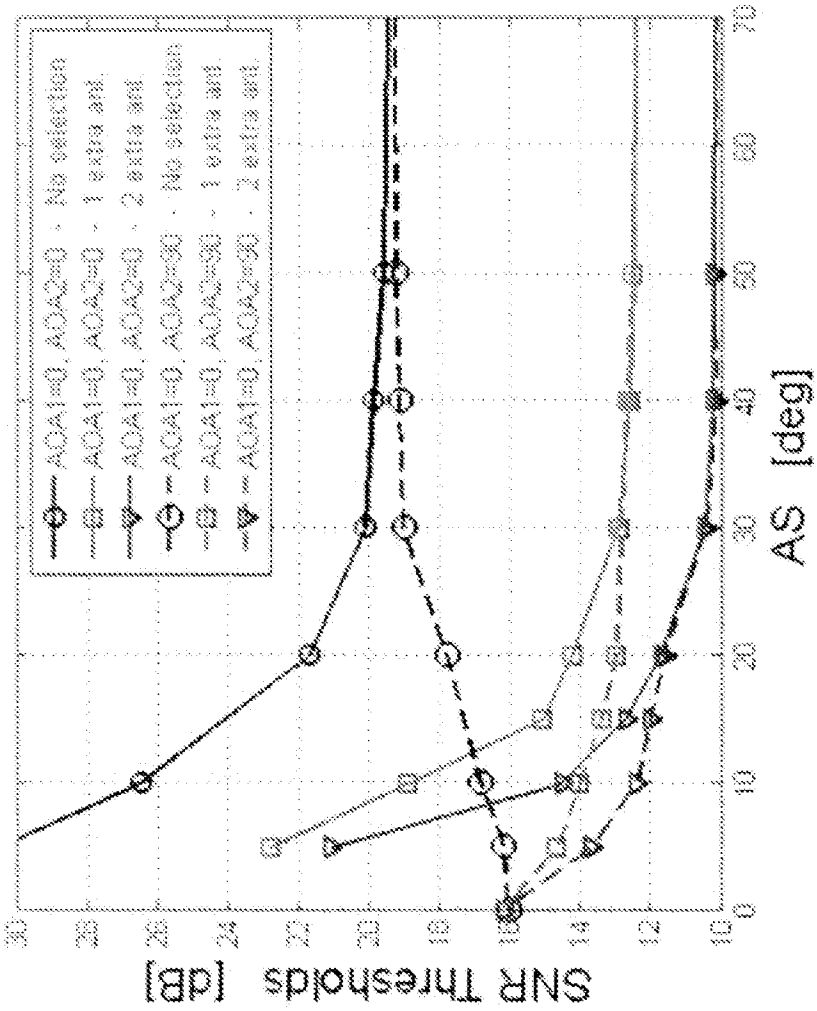
SNR Thresholds [dB]
AS [deg]
AOA1=0, AOA2=0 - No selection
AOA1=0, AOA2=0 - 1 extra ant.
AOA1=0, AOA2=0 - 2 extra ant.
AOA1=0, AOA2=60 - No selection
AOA1=0, AOA2=60 - 1 extra ant.
AOA1=0, AOA2=60 - 2 extra ant.

FIG. 37

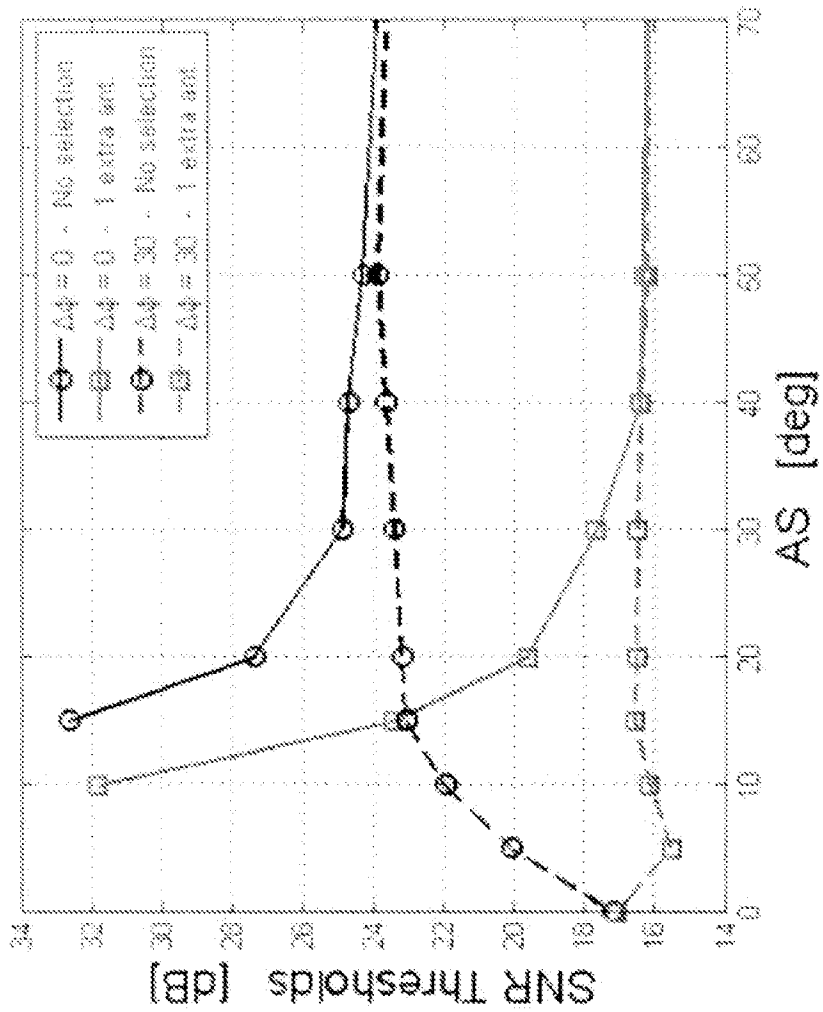
SNR Thresholds [dB]
AS [deg]
Δd = 0 - No selection
Δd = 0 - 1 extra ant.
Δd = 30 - No selection
Δd = 30 - 1 extra ant.

FIG. 38

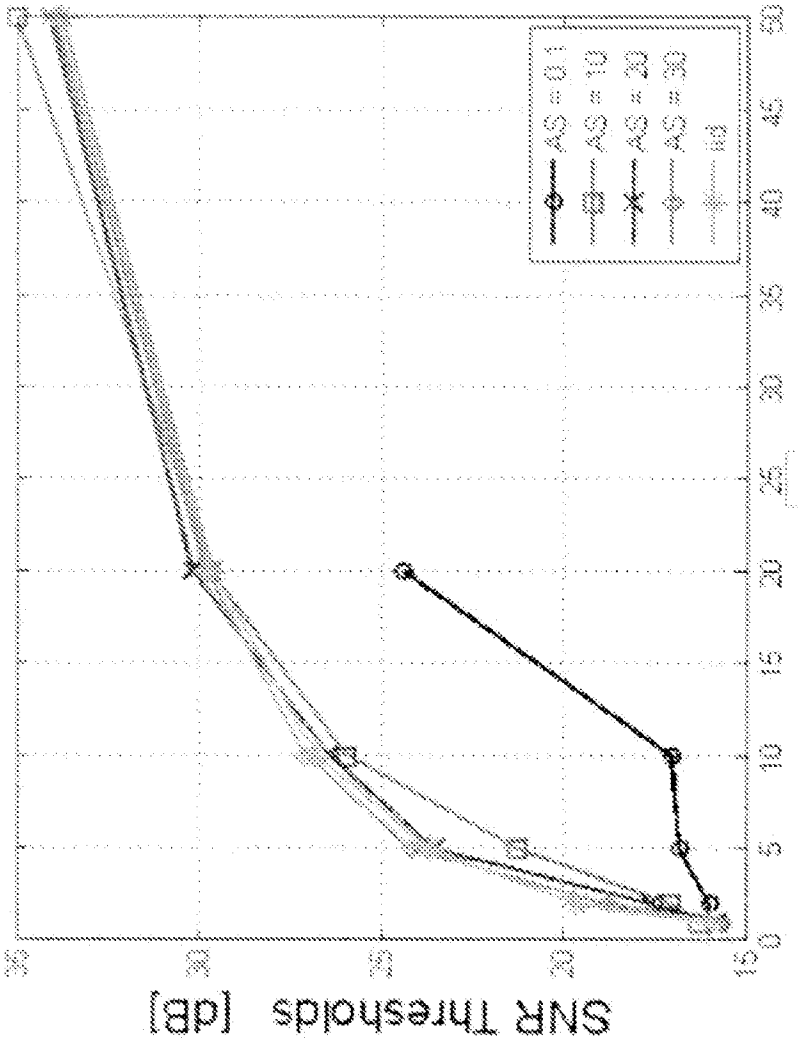

FIG. 39

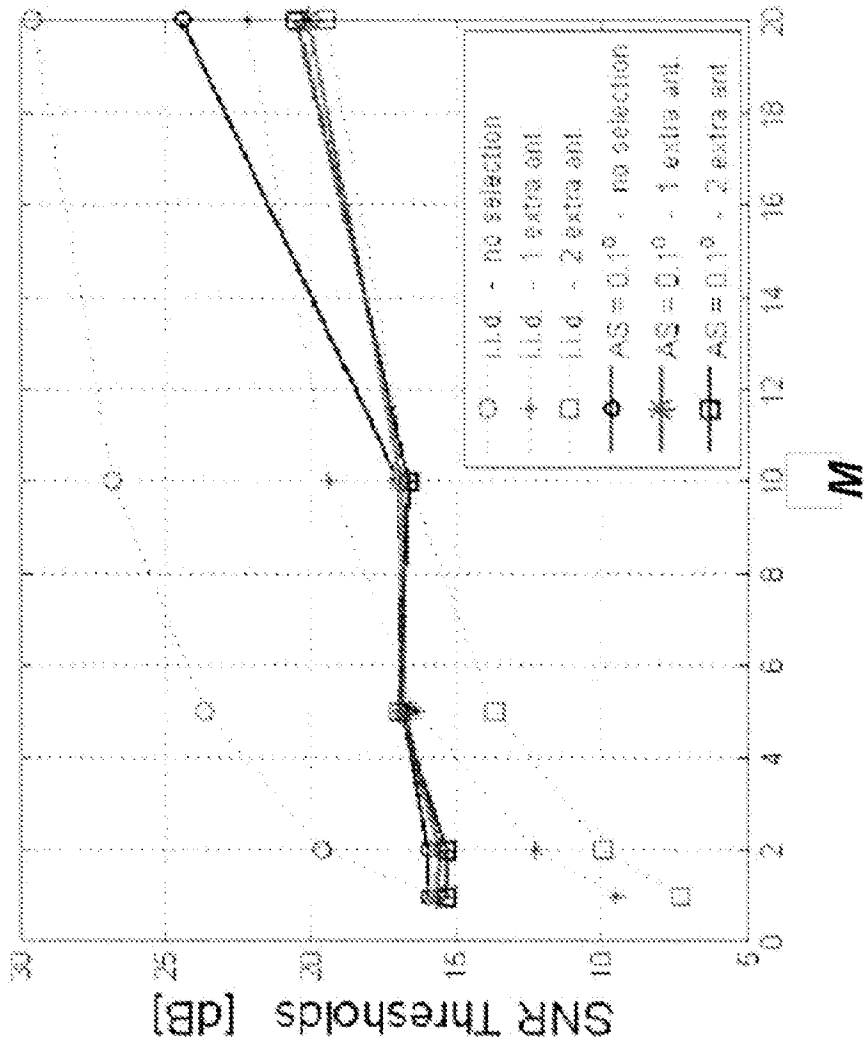
SNR Thresholds [dB]
M
0
2
4
6
8
10
12
14
16
18
20
5
10
15
20
111 - no selection
111 - 1 extra ant.
111 - 2 extra ant.
AS = 0.1° - no selection
AS = 0.1° - 1 extra ant.
AS = 0.1° - 2 extra ant.

FIG. 40

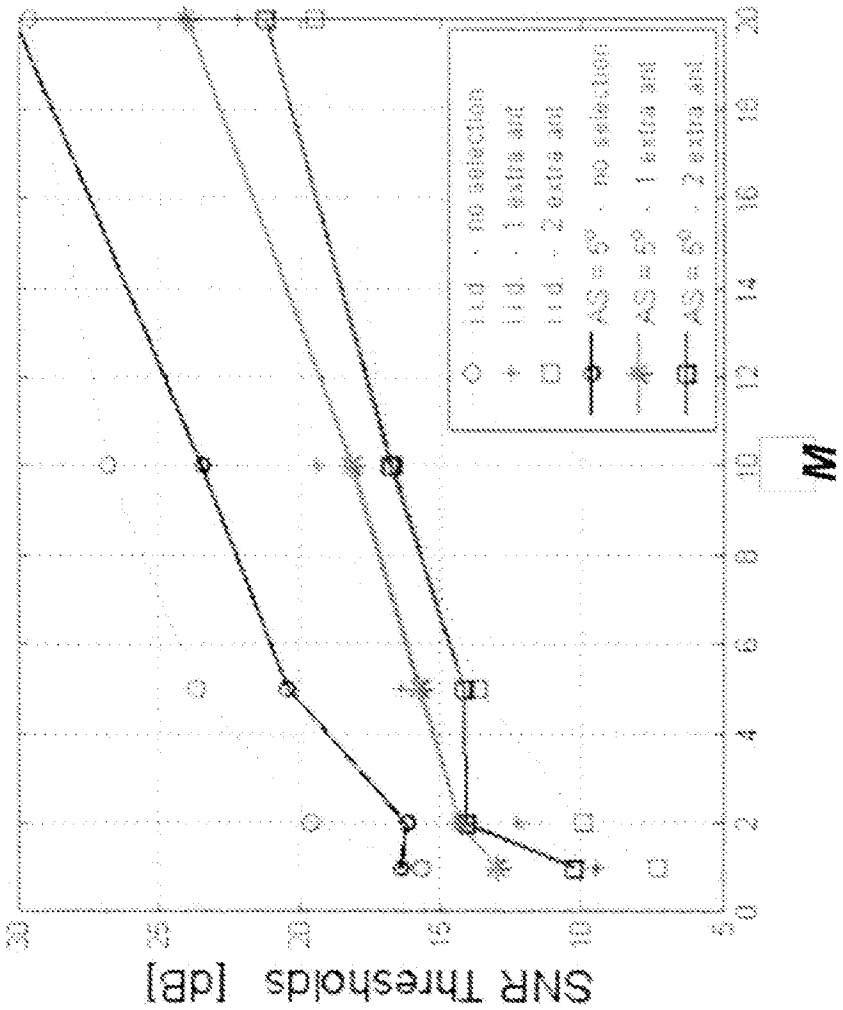
SNR Thresholds [dB]
M
1 rx - no selection
1 rx - 1 extra ant
1 rx - 2 extra ant
2 rx - no selection
2 rx - 1 extra ant
2 rx - 2 extra ant

FIG. 41

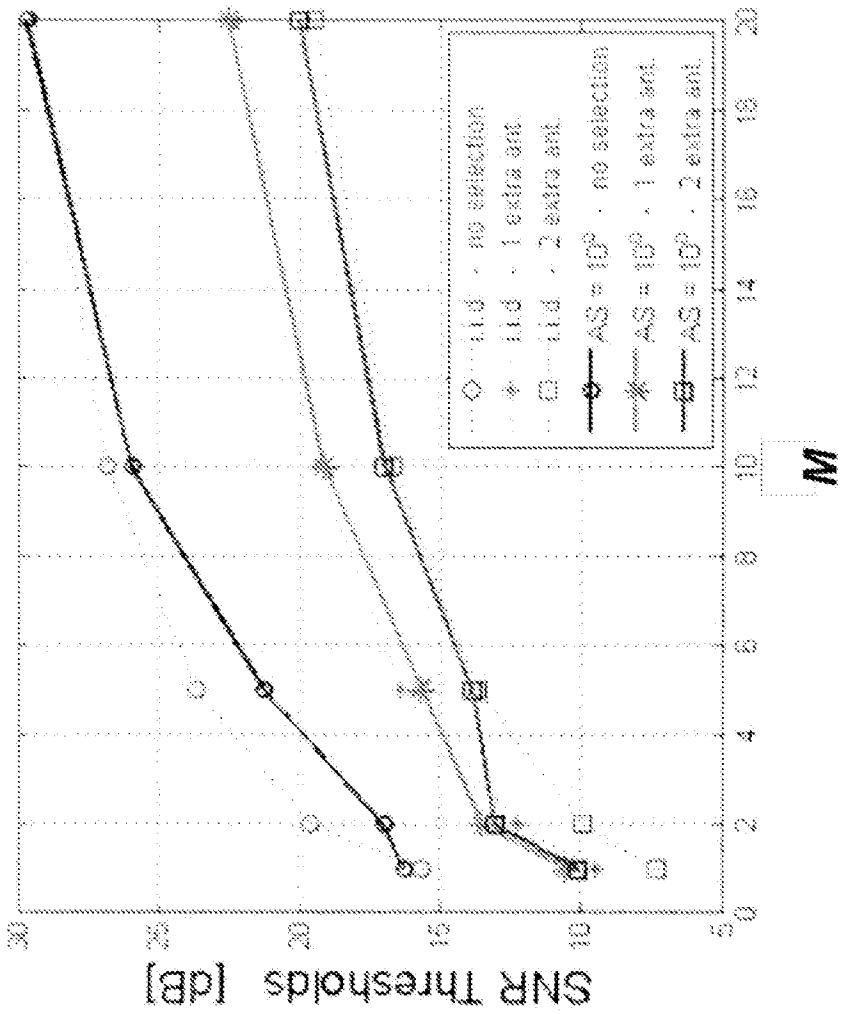
SNR Thresholds [dB]
M
i.i.d. - no selection
i.i.d. - 1 extra ant.
i.i.d. - 2 extra ant.
AS = ID², no selection
AS = ID², 1 extra ant.
AS = ID², 2 extra ant.

FIG. 42

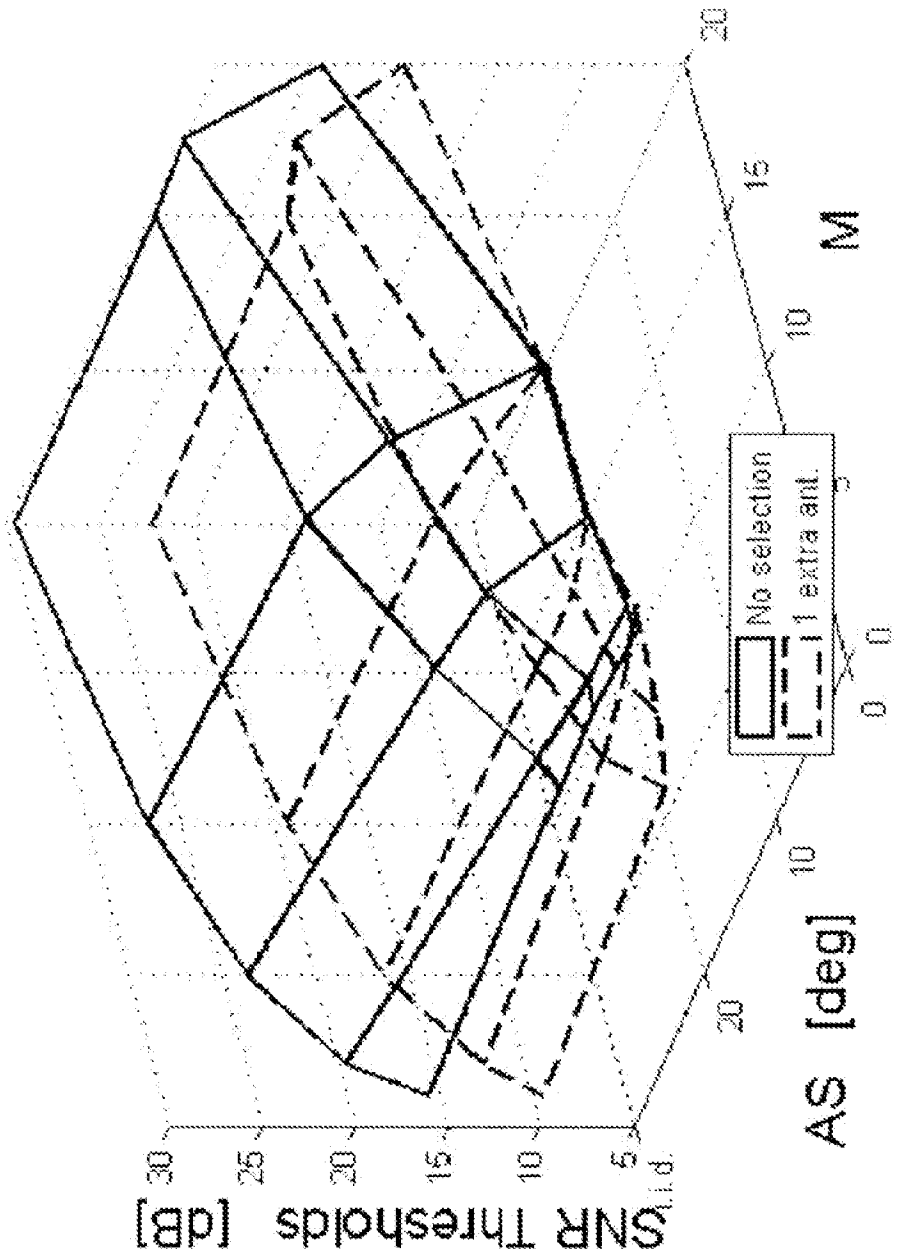
SNR Thresholds [dB]
30
25
20
15
10
5
p.l.d.
AS [deg]
20
10
0
0
5
10
15
20
M
No selection
1 extra ant.

FIG. 43

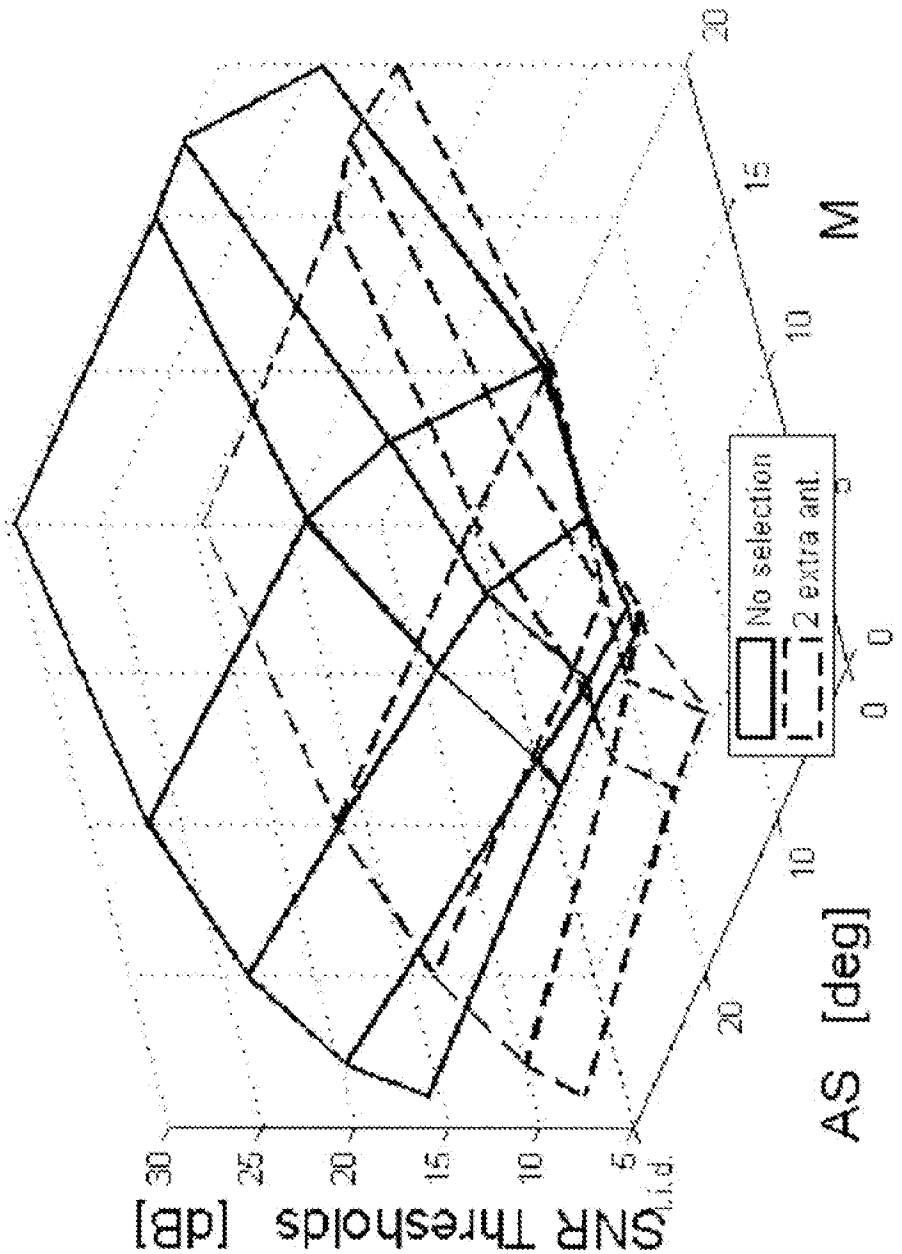
SNR Thresholds [dB]
30
25
20
15
10
5
p.f.d.
AS [deg]
20
10
0
0
5
10
15
20
M
No selection
2 extra ant.

FIG. 44

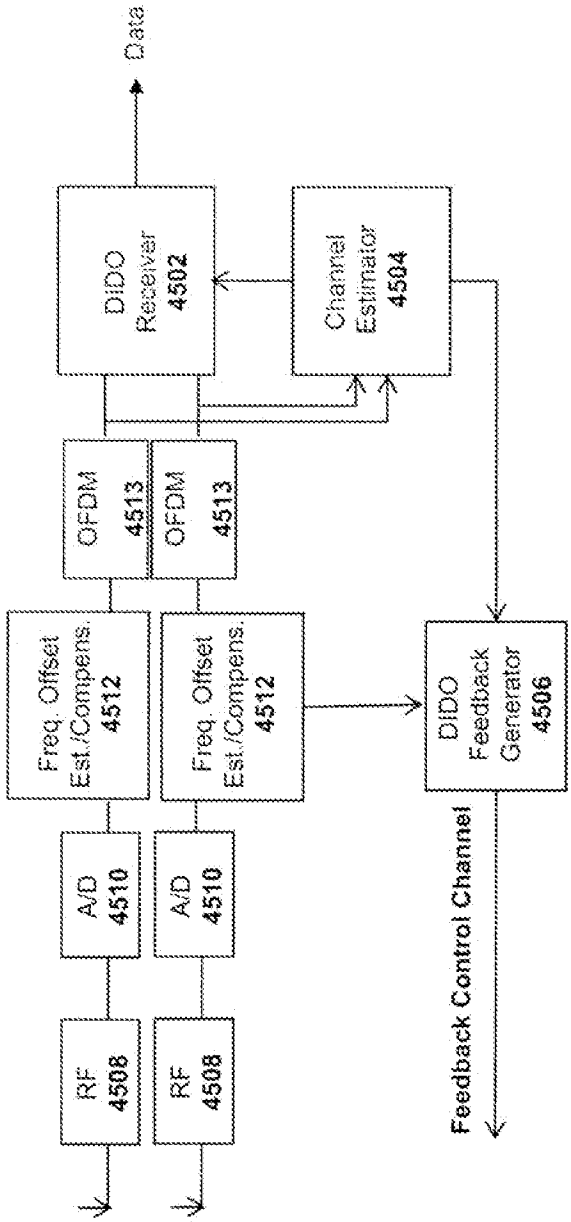
Data
DiDO Receiver 4502
Channel Estimator 4504
OFDM 4513
OFDM 4513
Freq. Offset Est./Compens. 4512
Freq. Offset Est./Compens. 4512
DiDO Feedback Generator 4506
A/D 4510
A/D 4510
RF 4508
RF 4508
Feedback Control Channel

FIG. 45

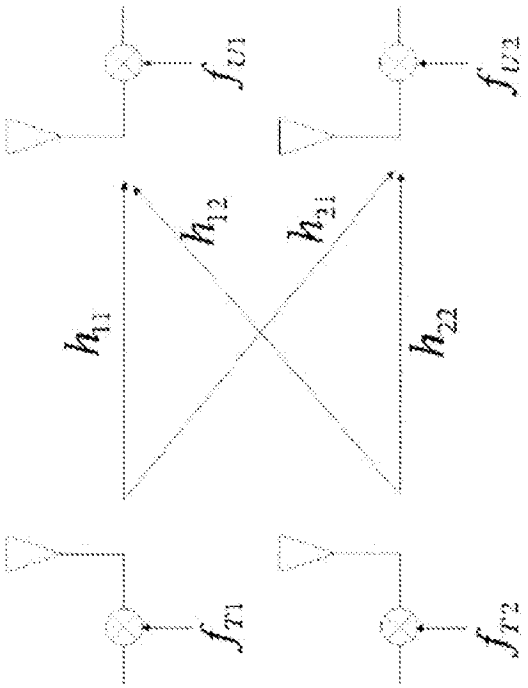

FIG. 46

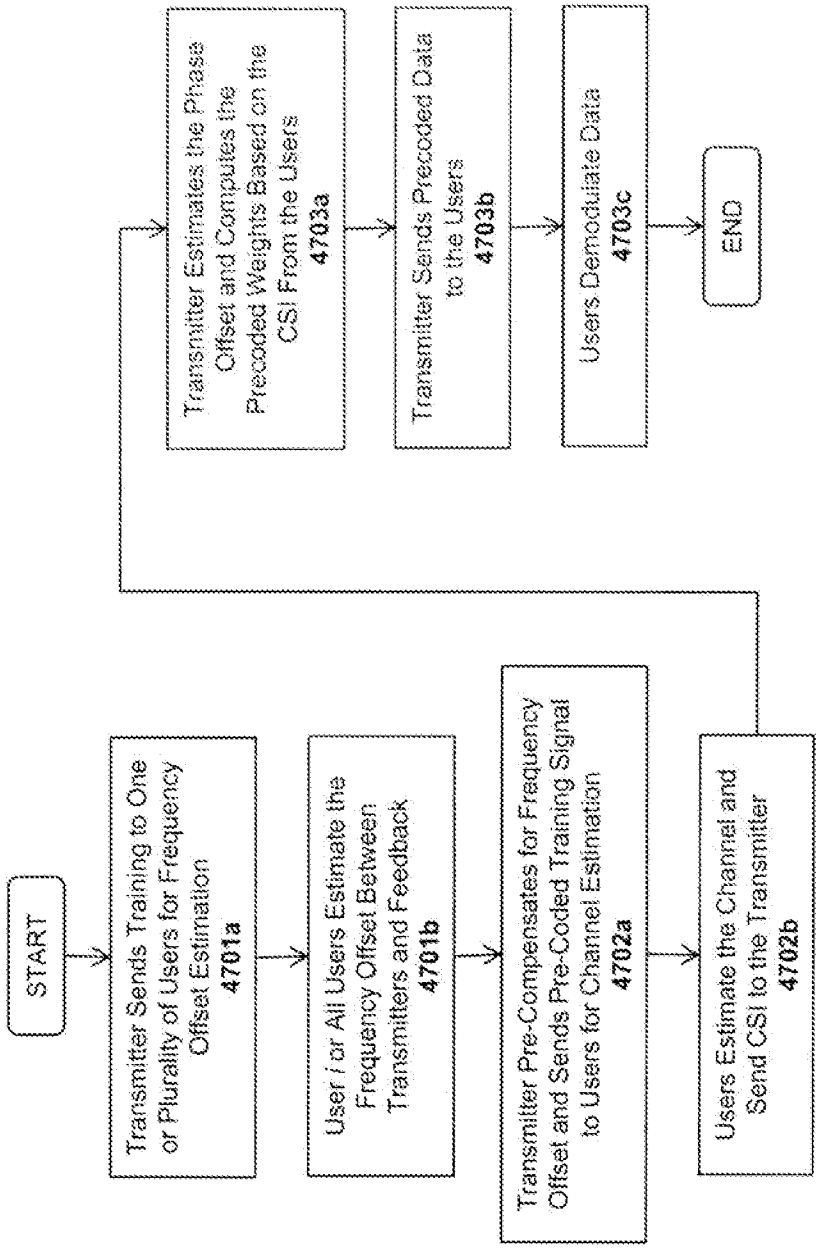
START
Transmitter Sends Training to One or Plurality of Users for Frequency Offset Estimation
4701a
User / or All Users Estimate the Frequency Offset Between Transmitters and Feedback
4701b
Transmitter Pre-Compensates for Frequency Offset and Sends Pre-Coded Training Signal to Users for Channel Estimation
4702a
Users Estimate the Channel and Send CSI to the Transmitter
4702b
Transmitter Estimates the Phase Offset and Computes the Precoded Weights Based on the CSI From the Users
4703a
Transmitter Sends Precoded Data to the Users
4703b
Users Demodulate Data
4703c
END

FIG. 47

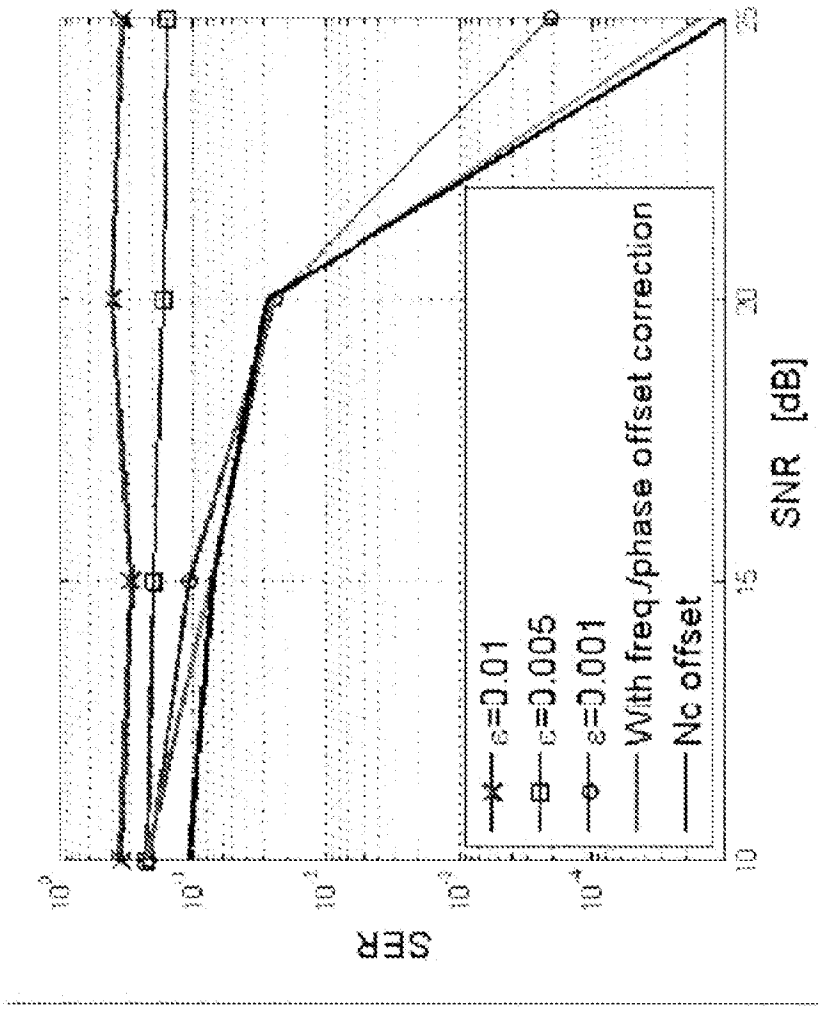
SER
SNR [dB]
10
15
20
10^{-1}
10^{-2}
10^{-3}
10^{-4}
ε=0.01
ε=0.005
ε=0.001
With freq./phase offset correction
Nc offset

FIG. 48

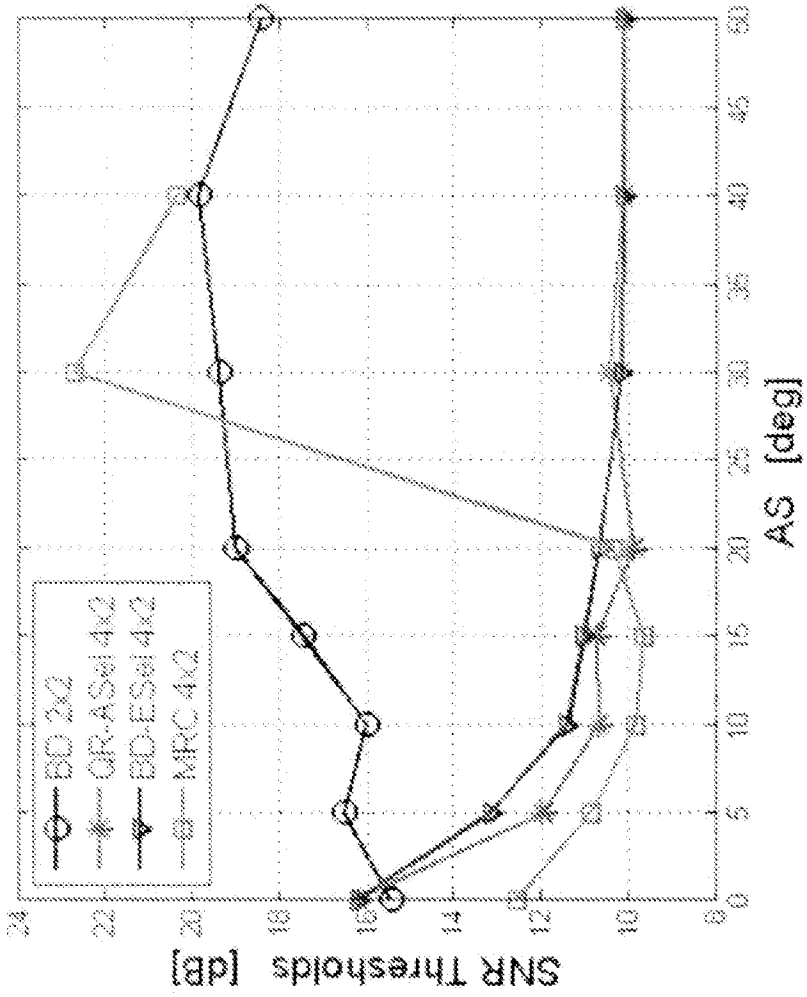

FIG. 49

Method	# of Symbols	Run Time (1,000 iterations)	Max Correct. Offset
Old	14208	600s	?
New ($N_1/M_1 = 1$)	288	60s	150MHz
New ($N_1/M_1 = 4$ length N_1)	1056	600s	150MHz

FIG. 50

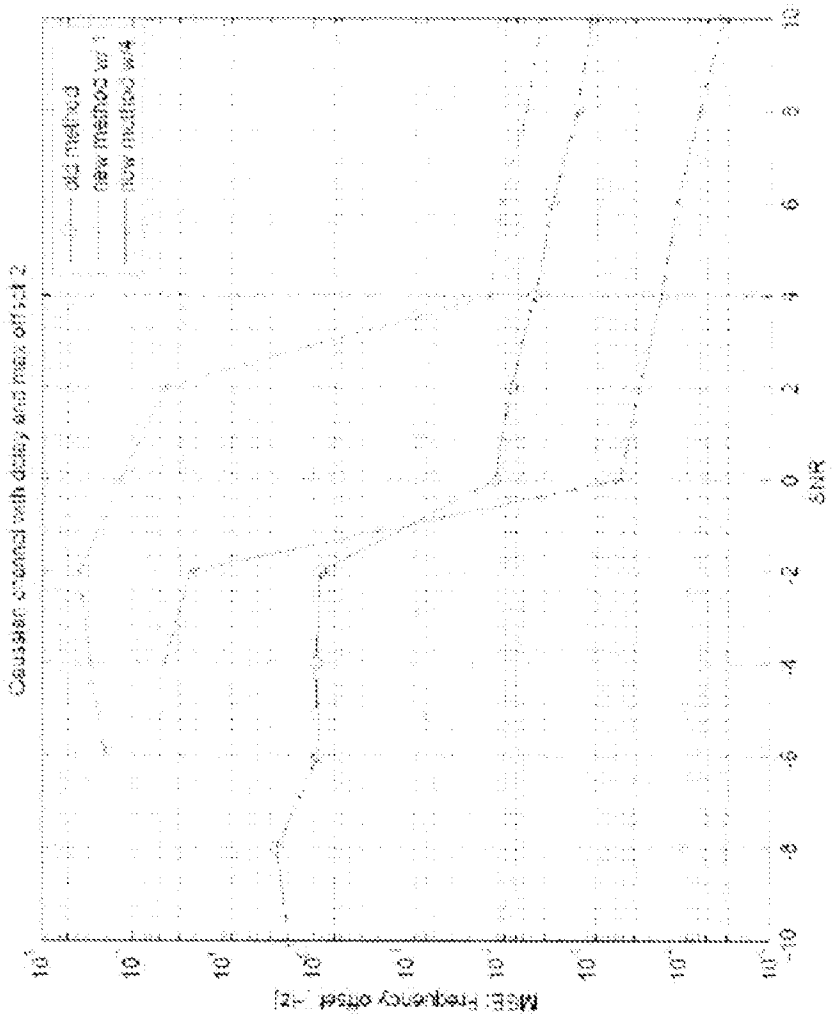
old method
new methods w/ 1
new method w/ 4
SNR
MSE: frequency offset (Hz)

FIG. 51

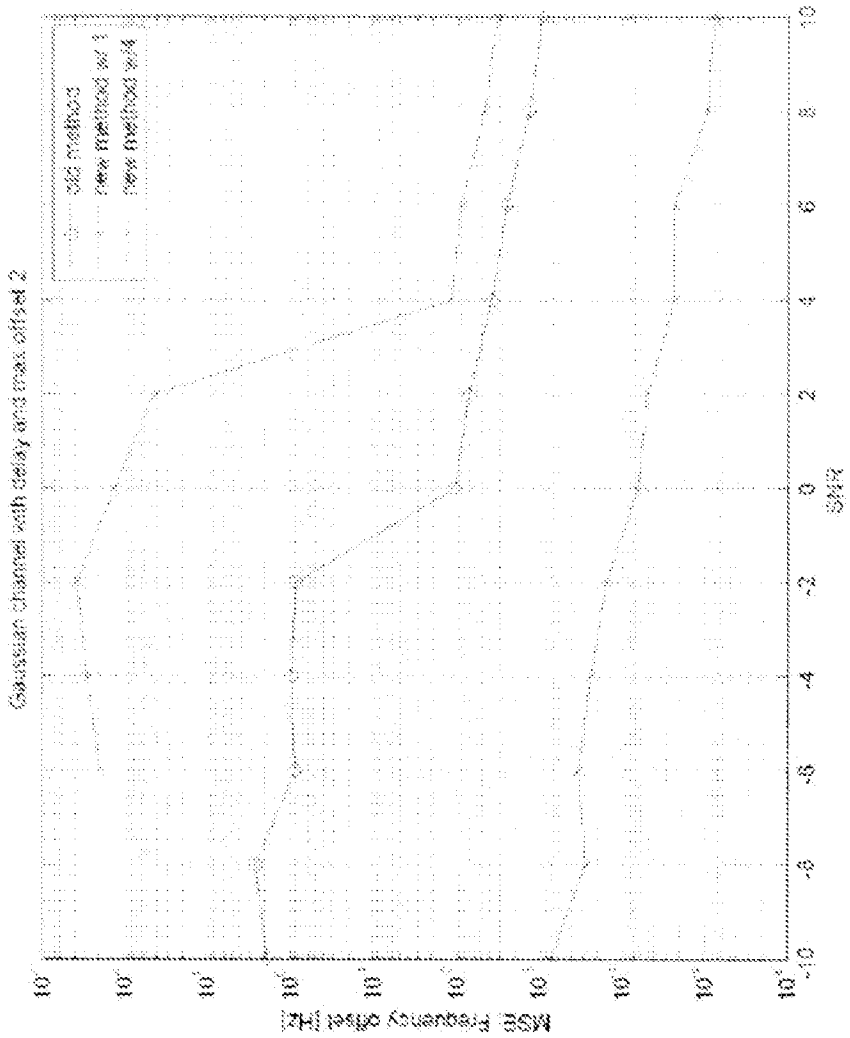
Gaussian channel with delay and max offset 2
MSE Frequency offset [Hz]
SNR
-10
-8
-6
-4
-2
0
2
4
6
8
10

FIG. 52

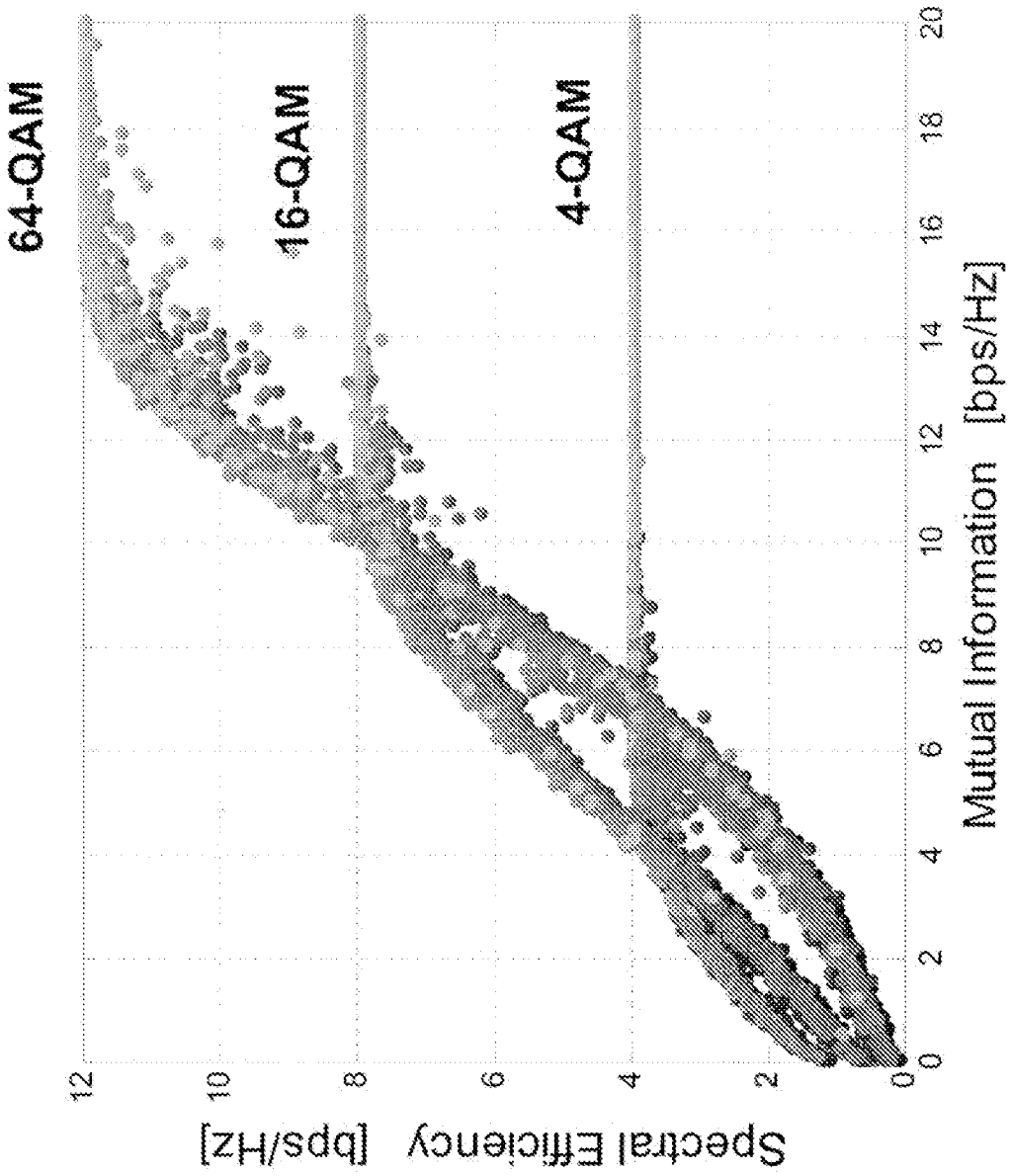
64-QAM
16-QAM
4-QAM
Spectral Efficiency [bps/Hz]
Mutual Information [bps/Hz]
0
2
4
6
8
10
12
14
16
18
20

FIG. 53

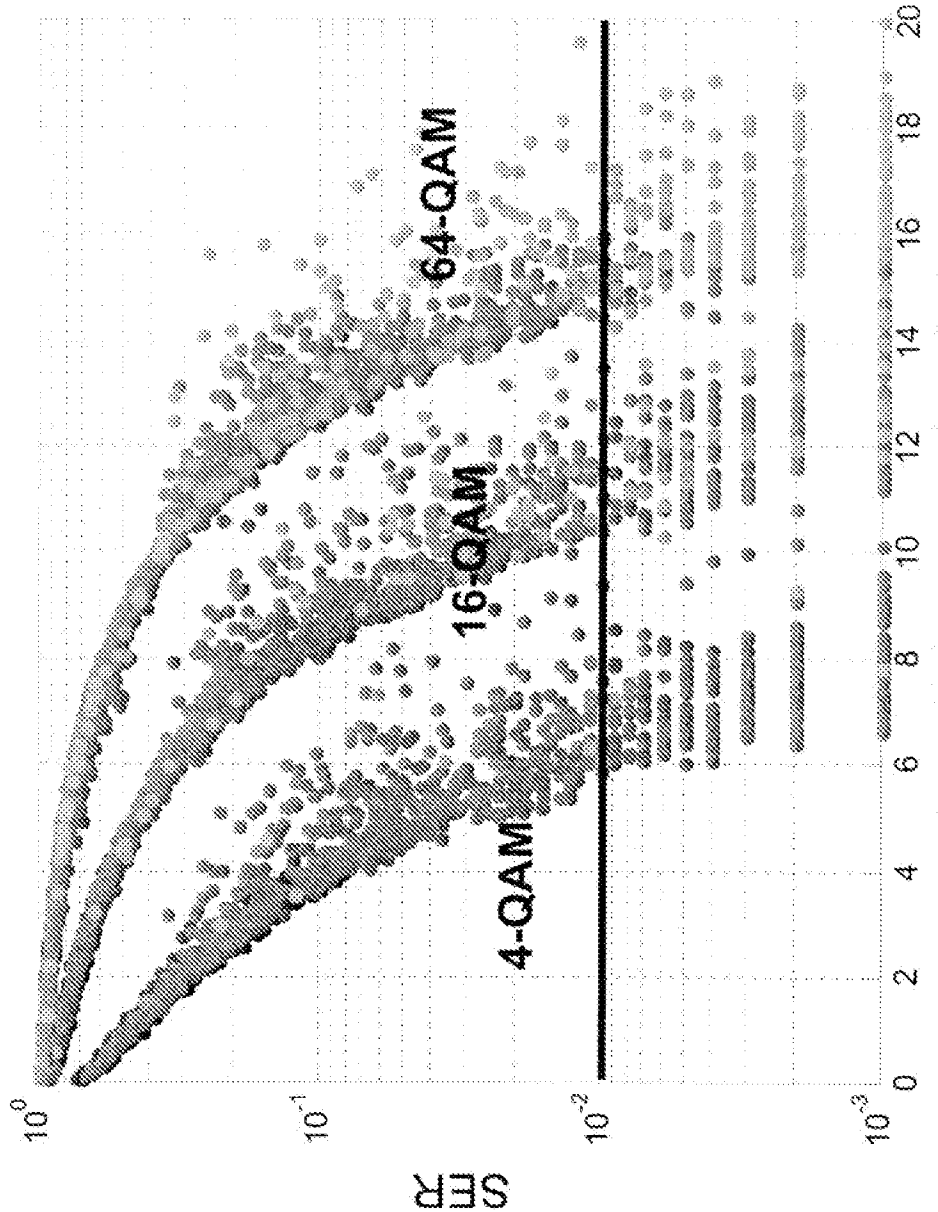
SER
10^{0}
10^{-1}
10^{-2}
10^{-3}
64-QAM
16-QAM
4-QAM
0
2
4
6
8
10
12
14
16
18
20
Mutual Information [bps/Hz]

FIG. 54

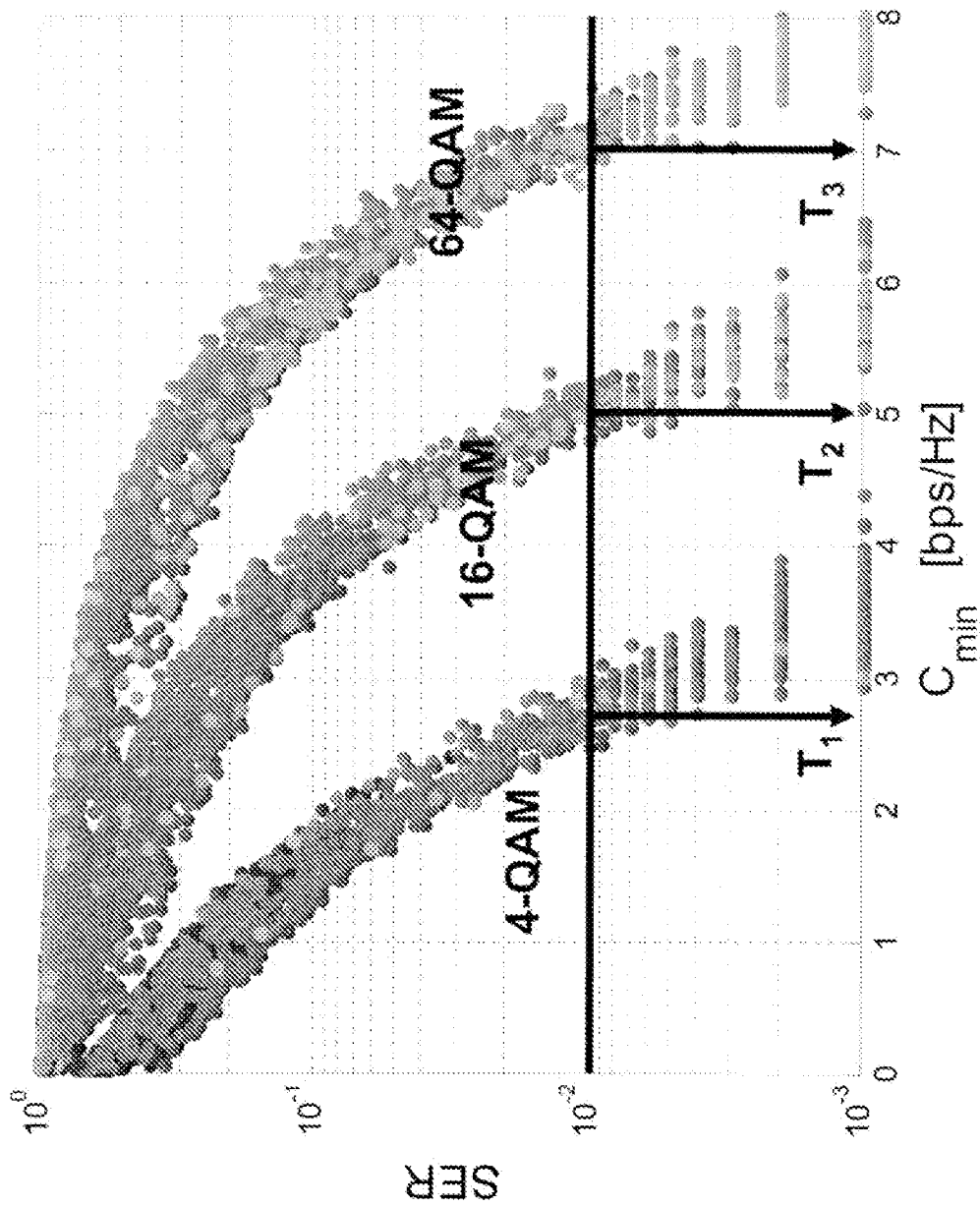
SER
10^{0}
10^{-1}
10^{-2}
10^{-3}
64-QAM
16-QAM
4-QAM
T_1
T_2
T_3
0
1
2
3
4
5
6
7
8
C_{min} [bps/Hz]

FIG. 55

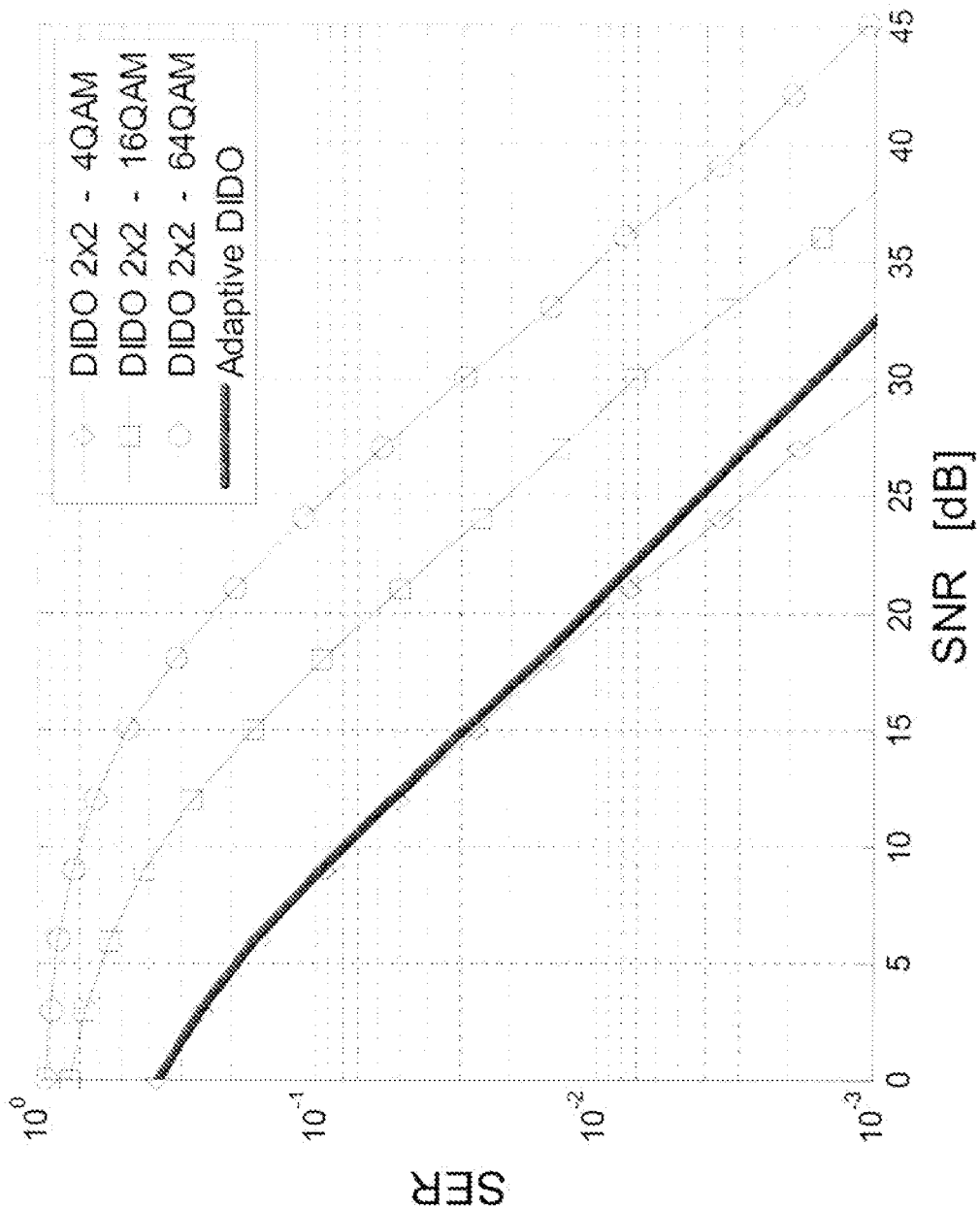
DIDO 2x2 - 4QAM
DIDO 2x2 - 16QAM
DIDO 2x2 - 64QAM
Adaptive DIDO
SER
SNR [dB]
10^0
10^-1
10^-2
10^-3
0
5
10
15
20
25
30
35
40
45

FIG. 56

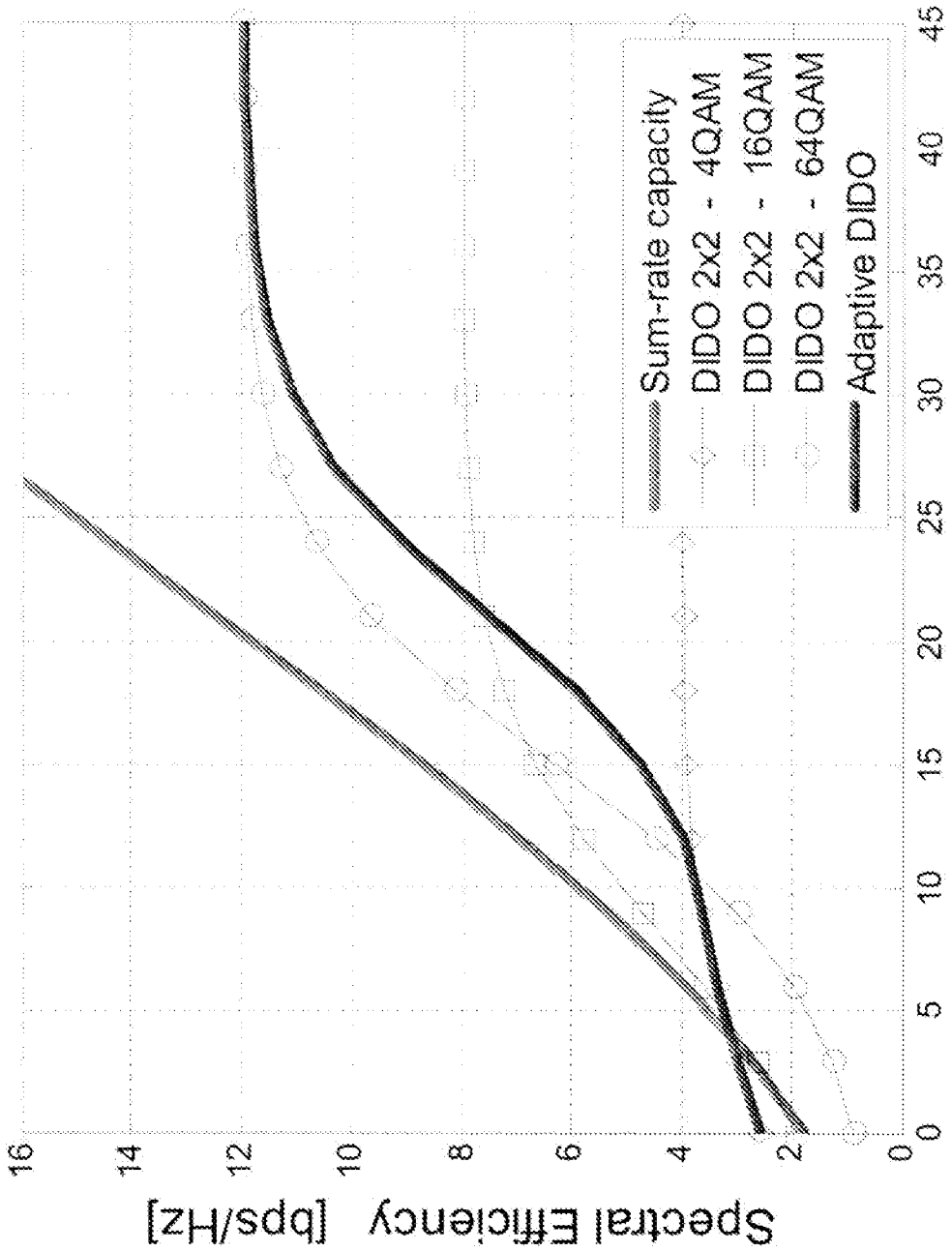
Spectral Efficiency [bps/Hz]
SNR [dB]
Sum-rate capacity
DIDO 2x2 - 4QAM
DIDO 2x2 - 16QAM
DIDO 2x2 - 64QAM
Adaptive DIDO
0
2
4
6
8
10
12
14
16
0
5
10
15
20
25
30
35
40
45

FIG. 57

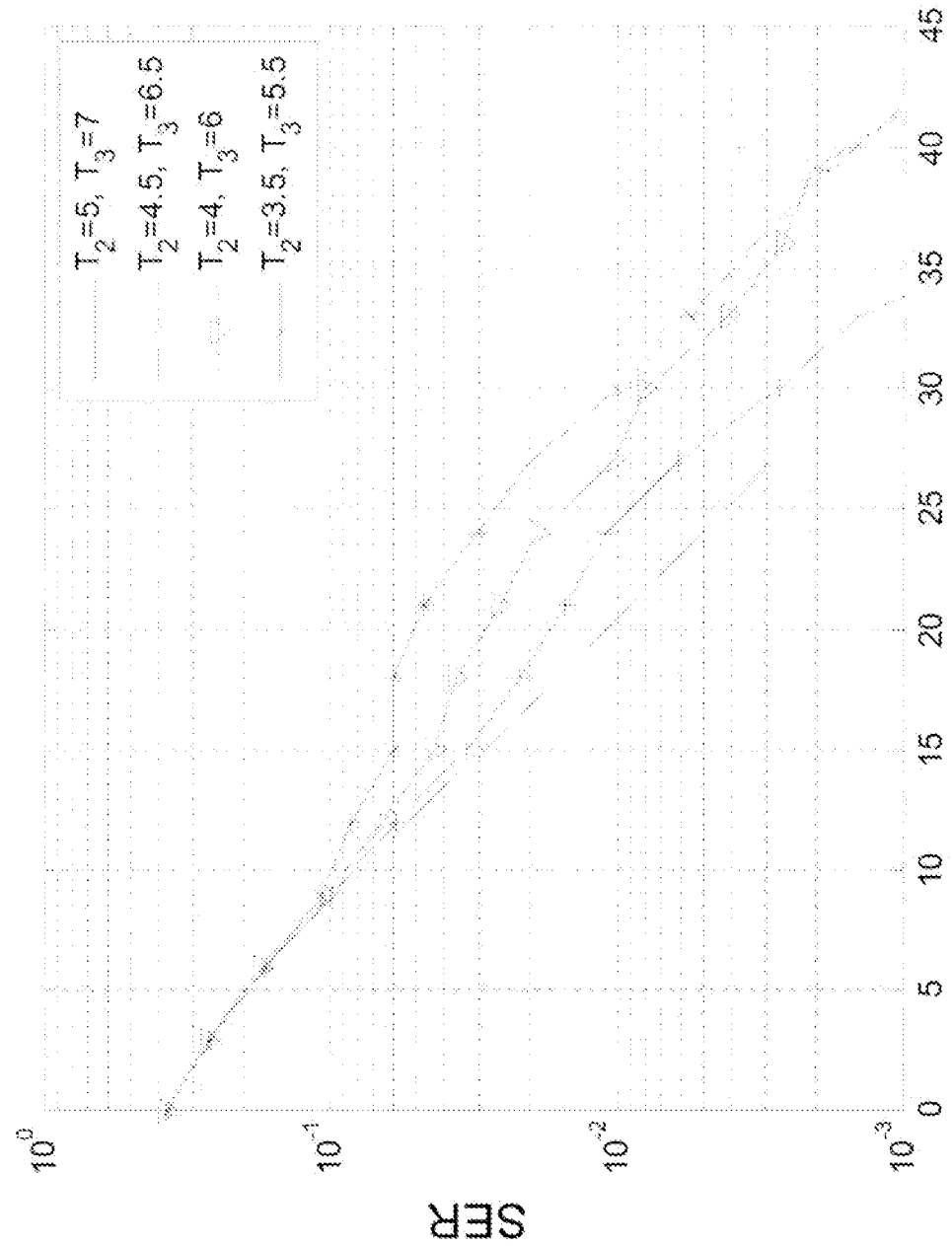
SER
SNR [dB]
10^{0}
10^{-1}
10^{-2}
10^{-3}
0
5
10
15
20
25
30
35
40
45
T_2=5, T_3=7
T_2=4.5, T_3=6.5
T_2=4, T_3=6
T_2=3.5, T_3=5.5

FIG. 58

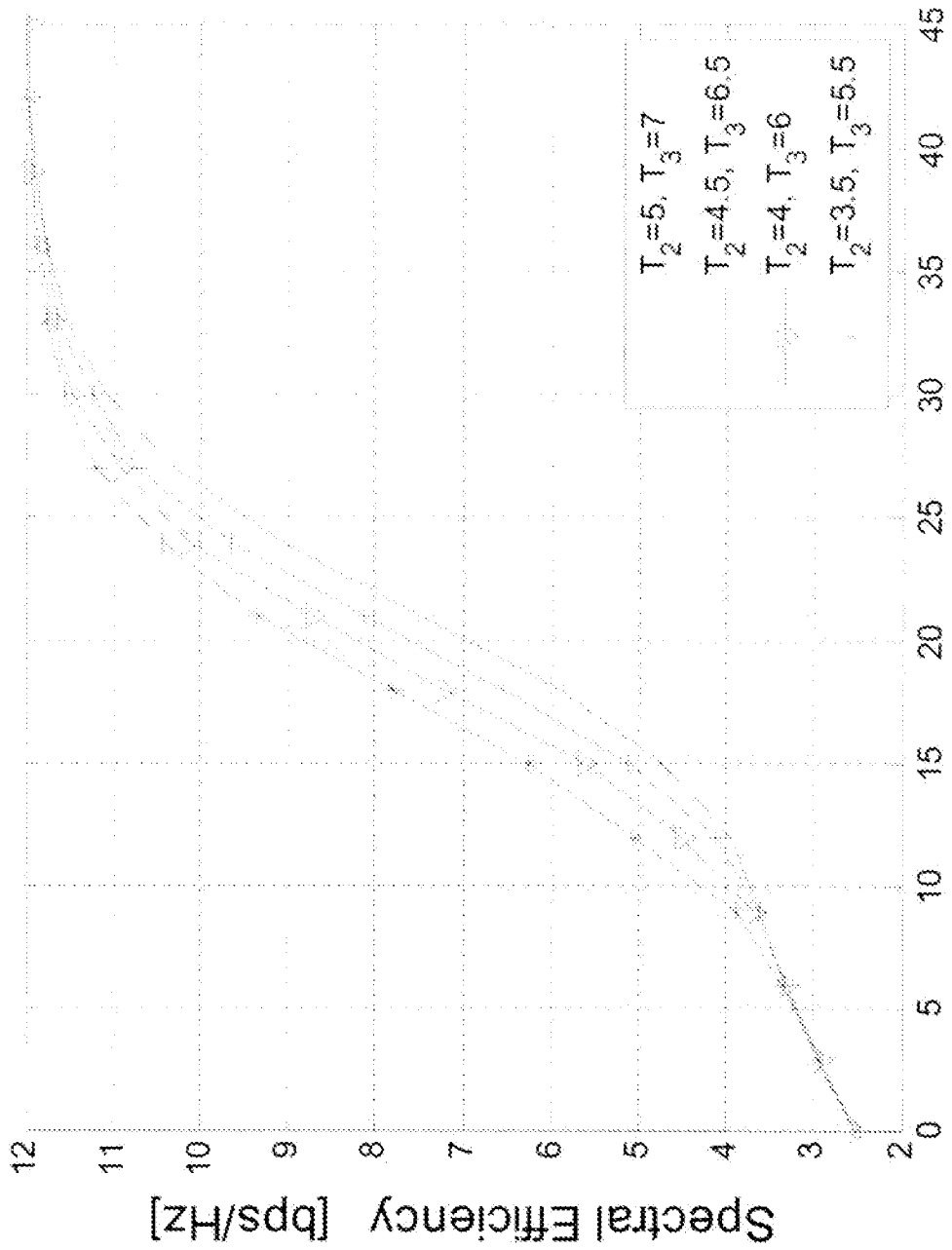
Spectral Efficiency [bps/Hz]
SNR [dB]
T_2=5, T_3=7
T_2=4.5, T_3=6.5
T_2=4, T_3=6
T_2=3.5, T_3=5.5

FIG. 59

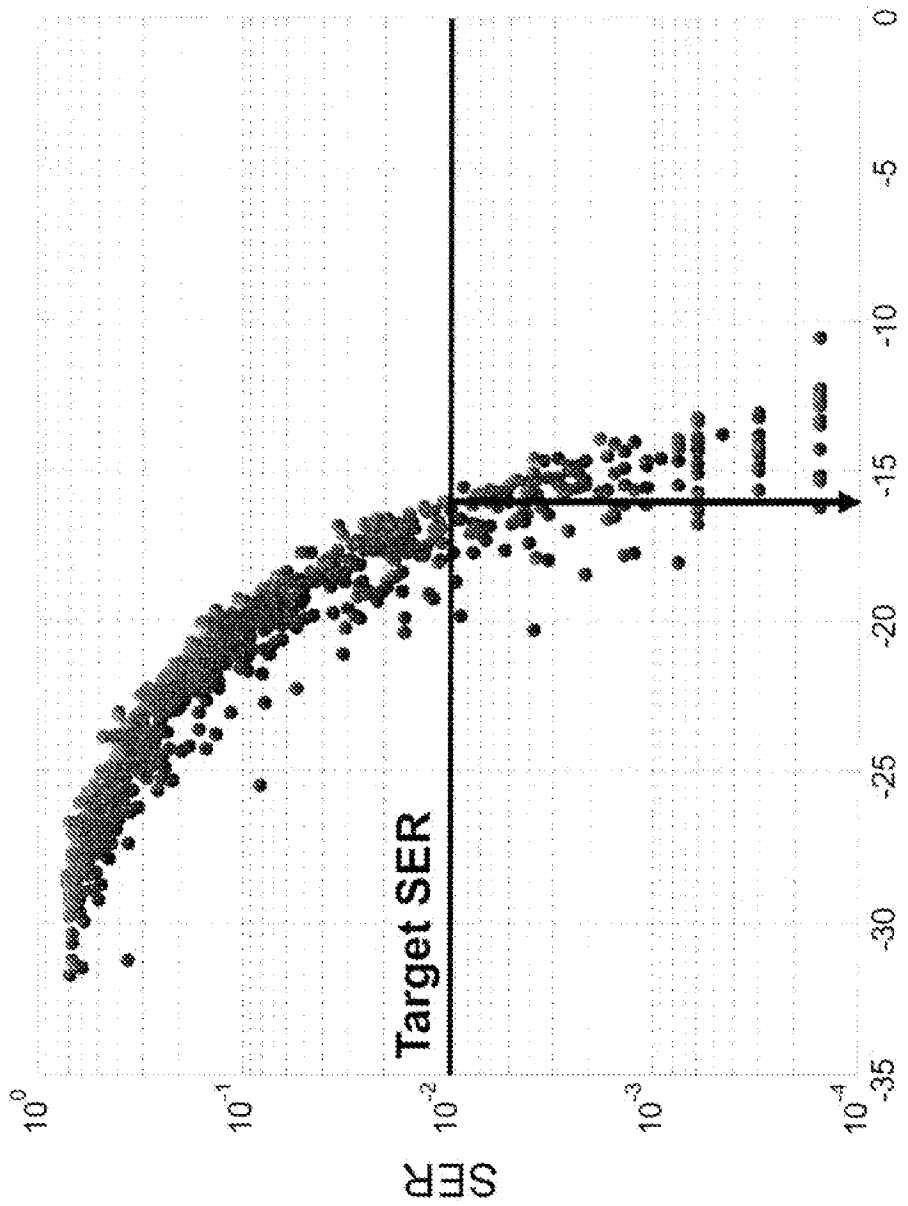
SER
10^{0}
10^{-1}
10^{-2}
10^{-3}
10^{-4}
Target SER
0
-5
-10
-15
-20
-25
-30
-35
λ_{min} [dB]

FIG. 60

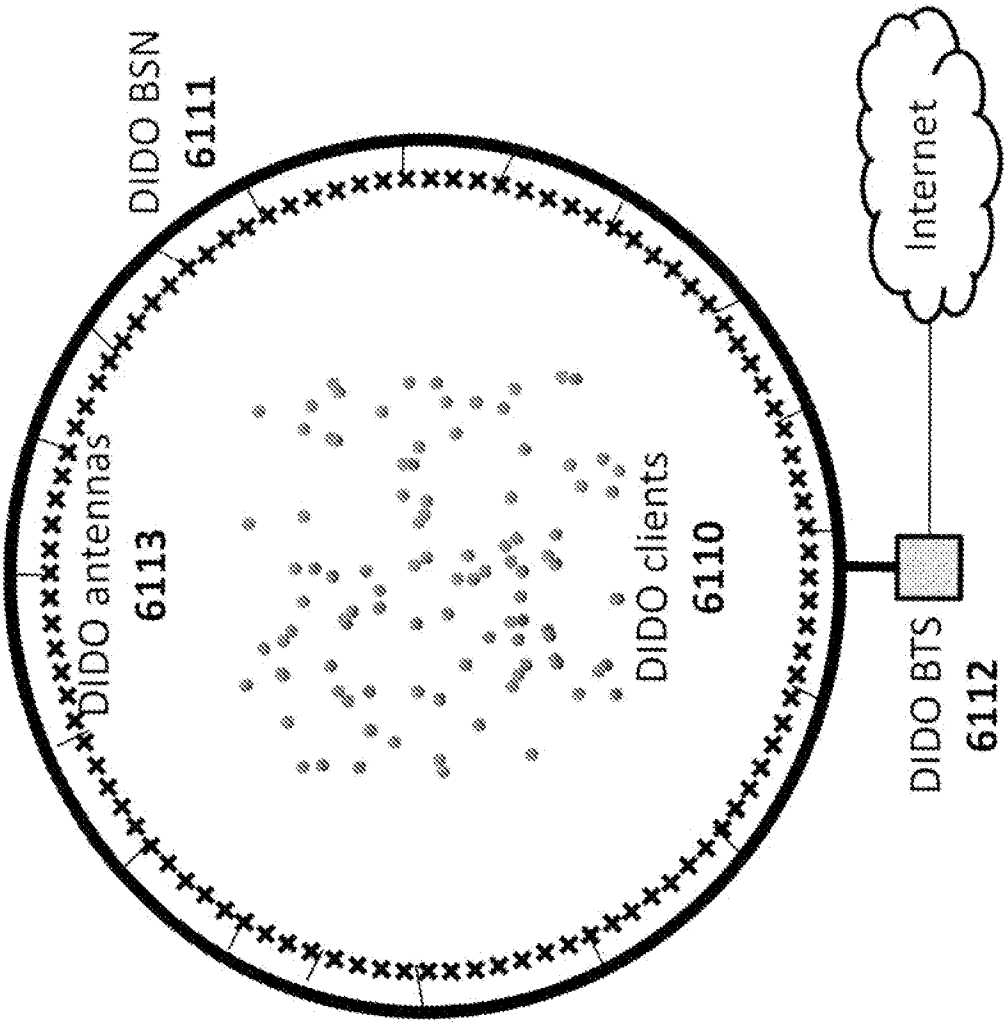
DIDO BSN
6111
DIDO antennas
6113
DIDO clients
6110
DIDO BTS
6112
Internet

Fig. 61

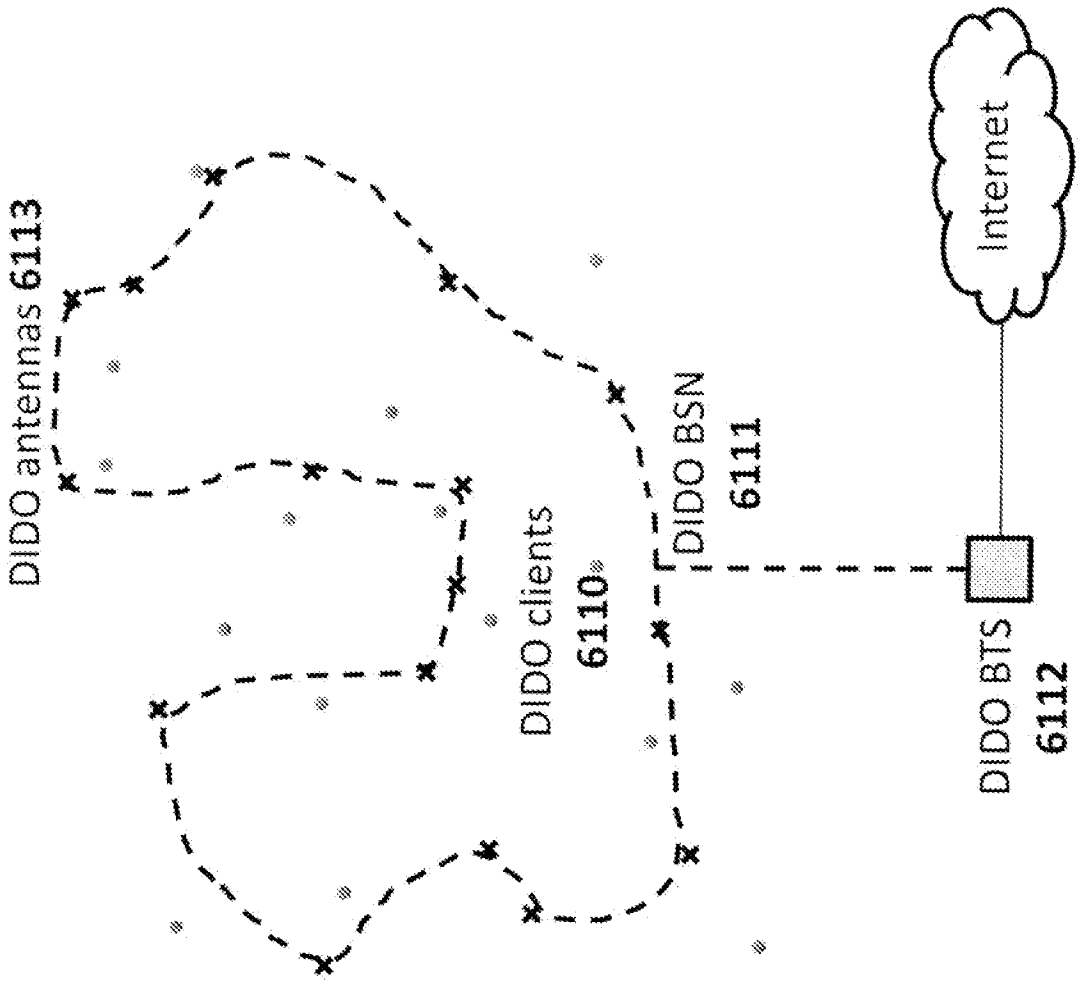
DIDO antennas 6113
DIDO clients 6110
DIDO BSN 6111
DIDO BTS 6112
Internet

Fig. 62

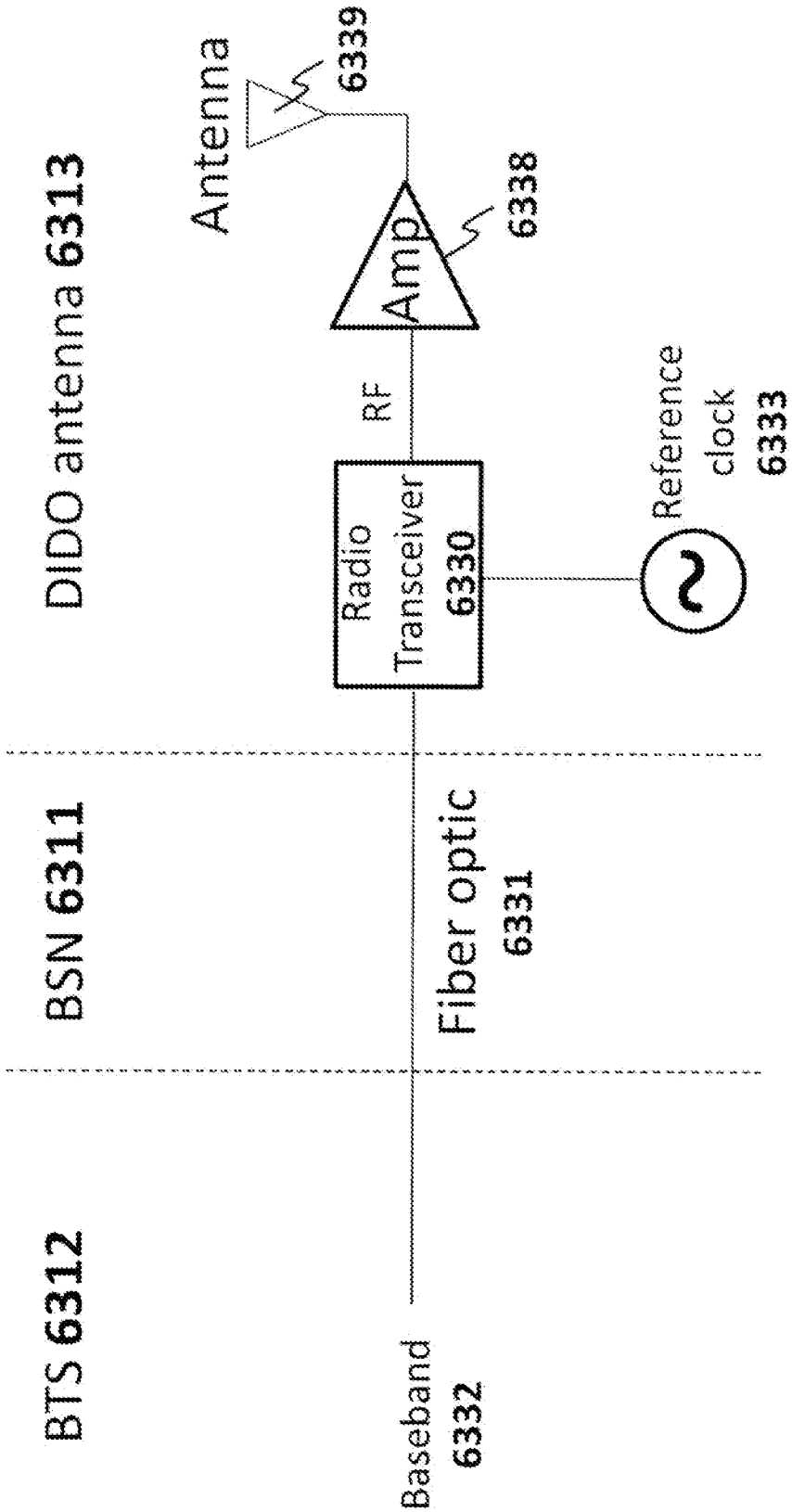
DIDO antenna 6313
Antenna
6339
Amp
6338
RF
Radio Transceiver 6330
Reference clock 6333
BSN 6311
Fiber optic 6331
BTS 6312
Baseband 6332

Fig. 63

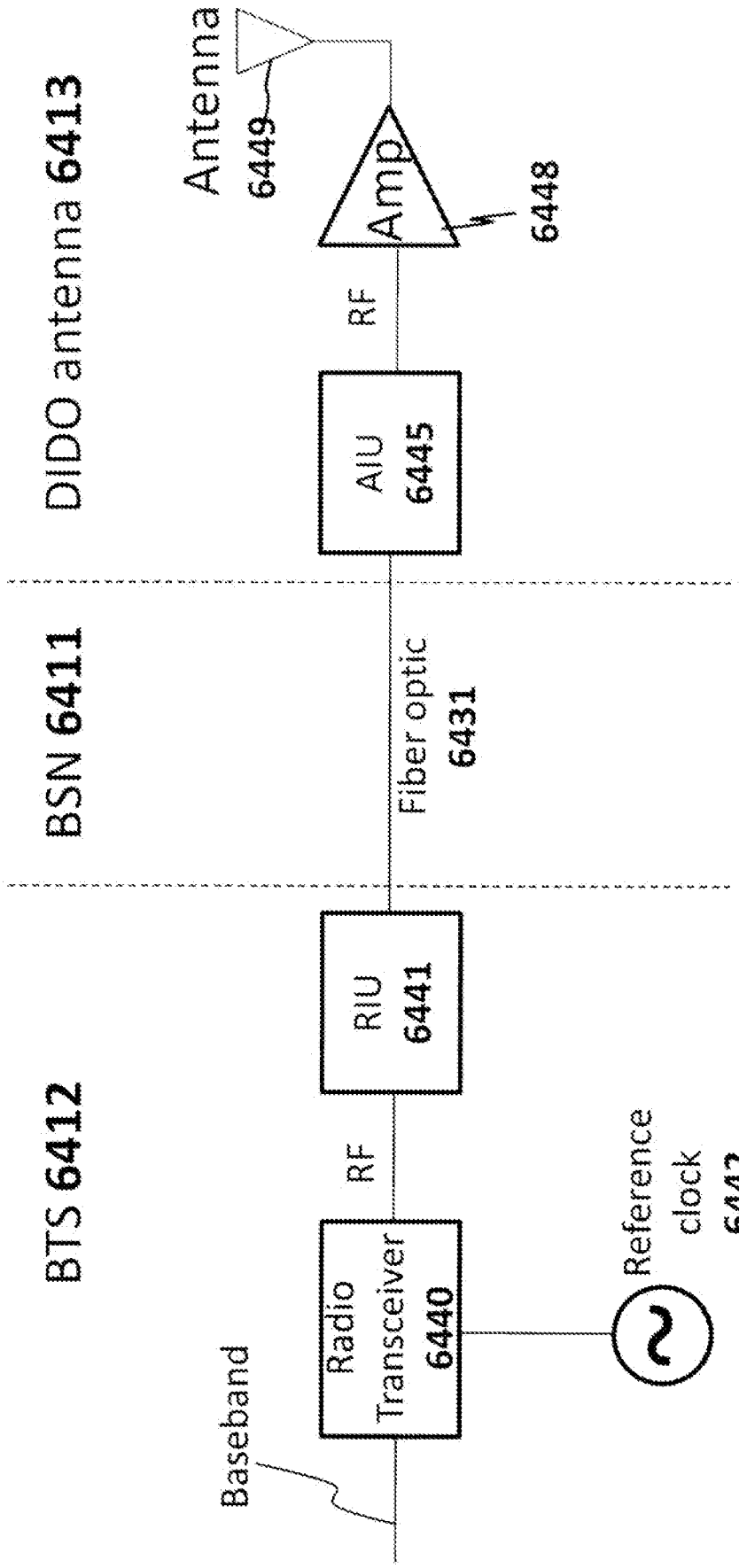
BTS 6412
BSN 6411
DIDO antenna 6413
Baseband
Radio Transceiver 6440
RF
RIU 6441
Fiber optic 6431
AIU 6445
RF
Amp
6448
Antenna 6449
Reference clock 6442

Fig. 64

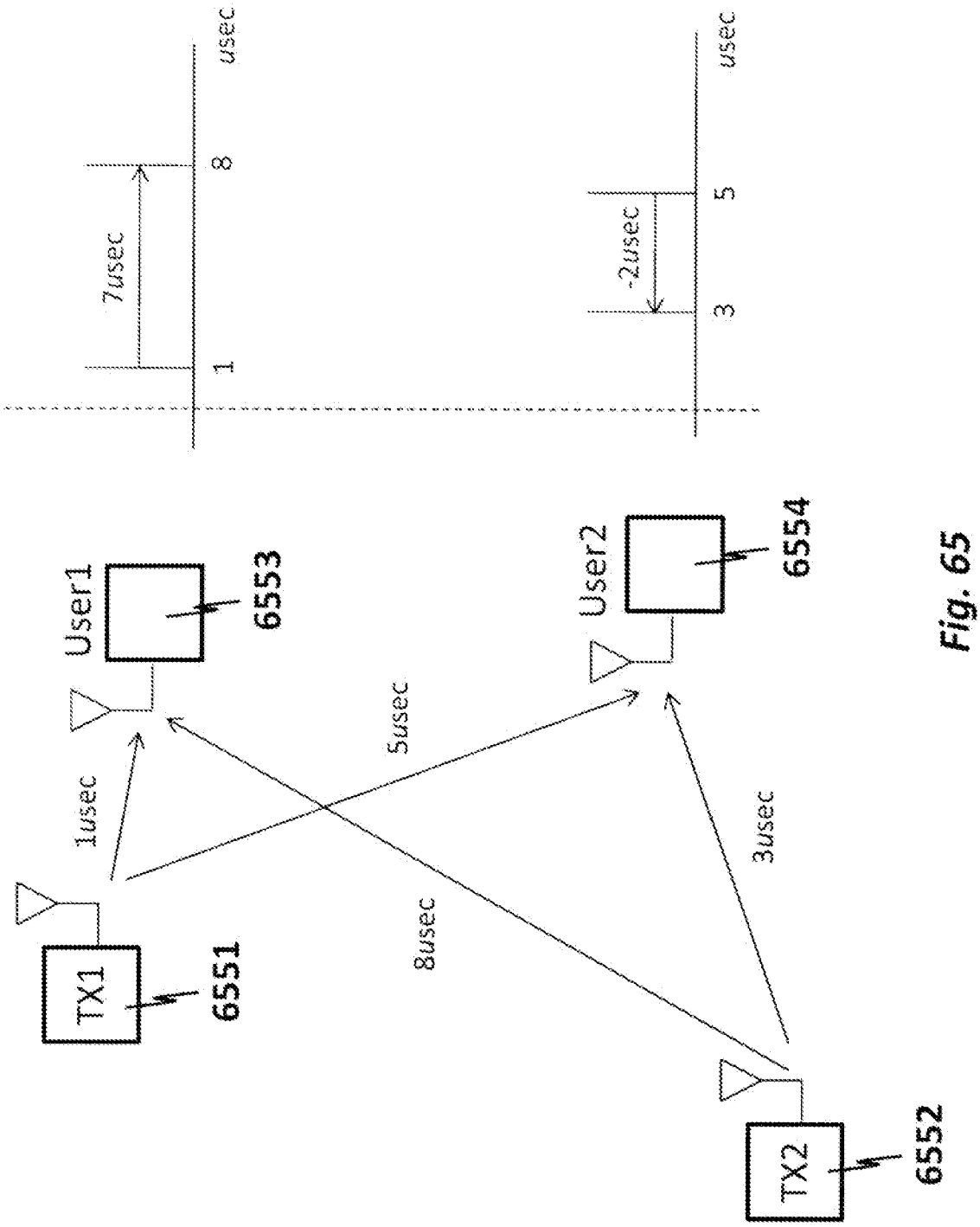
usec
8
1
7usec
usec
5
3
-2usec
User1
6553
User2
6554
5usec
1usec
3usec
8usec
TX1
6551
TX2
6552

Fig. 65

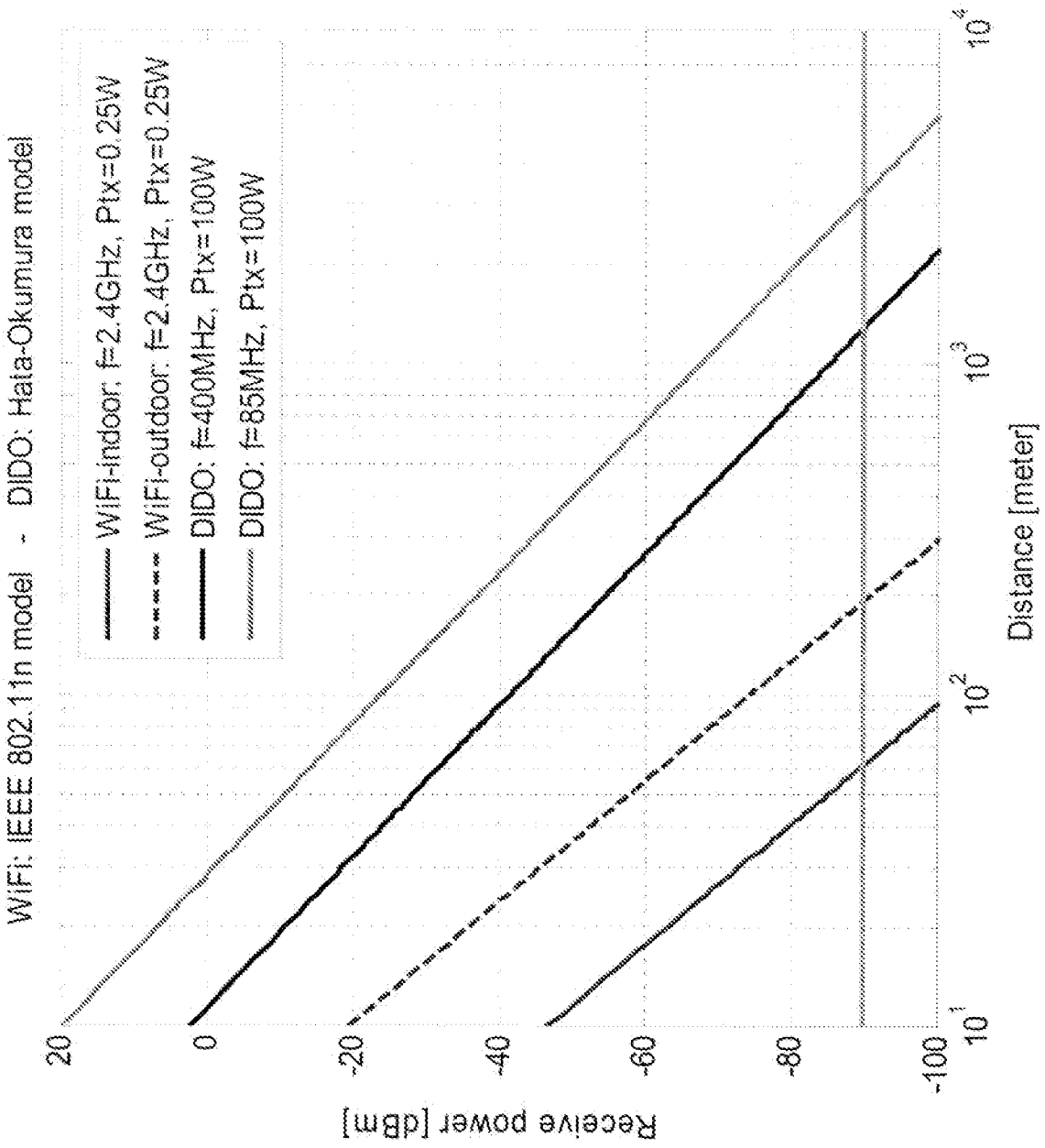
WiFi: IEEE 802.11n model - DIDO: Hata-Okumura model
WiFi-indoor, f=2.4GHz, Ptx=0.25W
WiFi-outdoor, f=2.4GHz, Ptx=0.25W
DIDO: f=400MHz, Ptx=100W
DIDO: f=85MHz, Ptx=100W
Receive power [dBm]
20
0
-20
-40
-60
-80
-100
Distance [meter]
10^1
10^2
10^3
10^4

Fig. 66

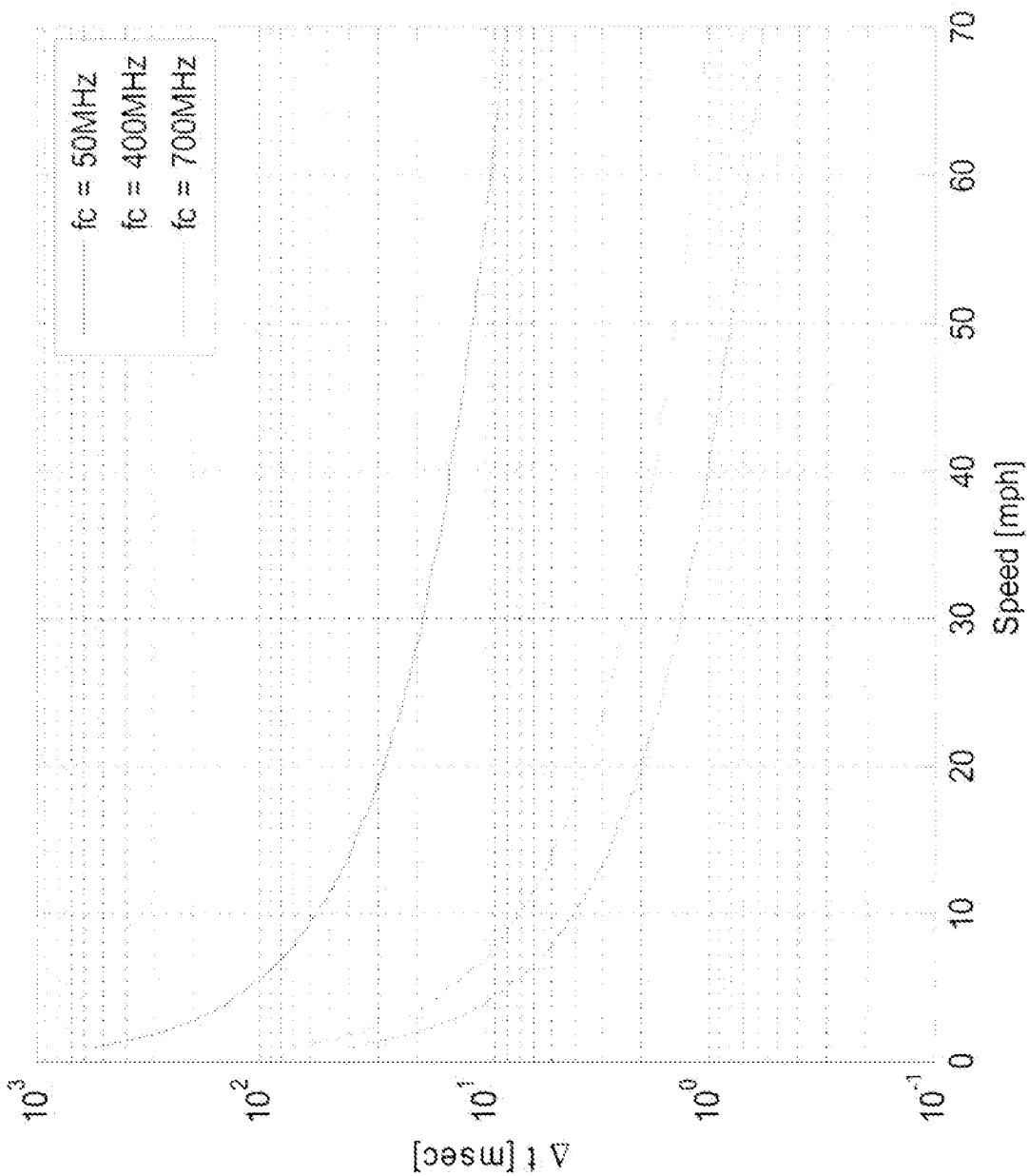
fc = 50MHz
fc = 400MHz
fc = 700MHz
Δ t [msec]
Speed [mph]
10^3
10^2
10^1
10^0
10^-1
0
10
20
30
40
50
60
70

Fig. 67

Carrier frequency	Range (Ptx=100W)	Delay spread (indoor)	Delay spread (outdoor)	Max speed*	Min antenna spacing**	Antenna size***
50 MHz	4 Km	<300 nsec	1-10 usec	57 mph	6 meters	3 meters
400 MHz	1.3 Km	<300 nsec	1-10 usec	7 mph	0.8 meters	0.4 meters
700 MHz	1 Km	<300 nsec	1-10 usec	4 mph	0.4 meters	0.2 meters

* maximum relative TX/RX speed assuming feedback loop delay (RTT base station-to-centralized processor over the Internet) of 10 msec

**minimum TX or RX antenna spacing to gain the benefit of spatial diversity in rich scattering environments (i.e., indoor or urban environments) is one wavelength

***assuming half-wavelength dipole for maximum antenna efficiency

Fig. 68

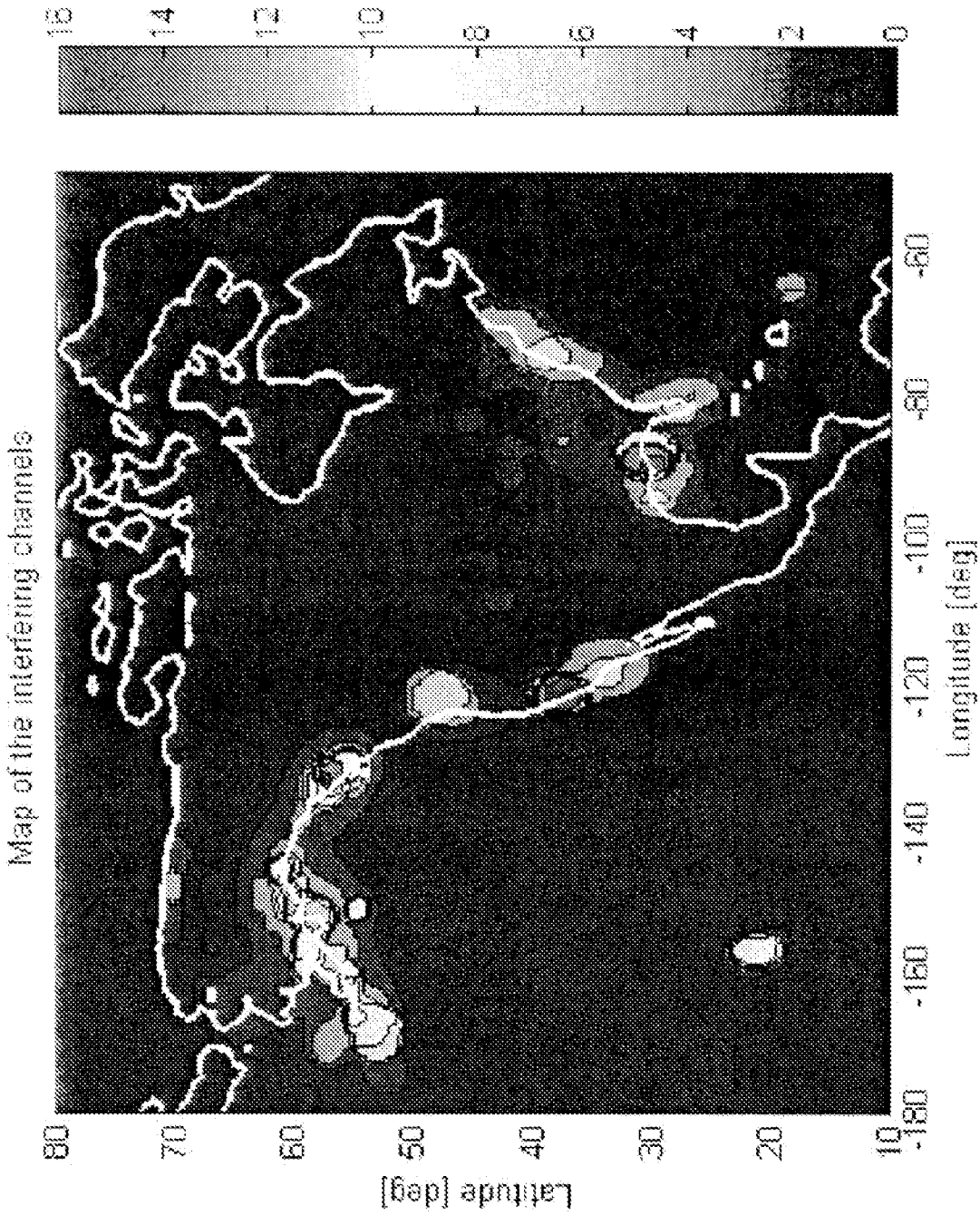
Map of the interfering channels
Latitude [deg]
80
70
60
50
40
30
20
10
-180
-160
-140
-120
-100
-80
-60
Longitude [deg]
16
14
12
10
8
6
4
2
0

Fig. 69

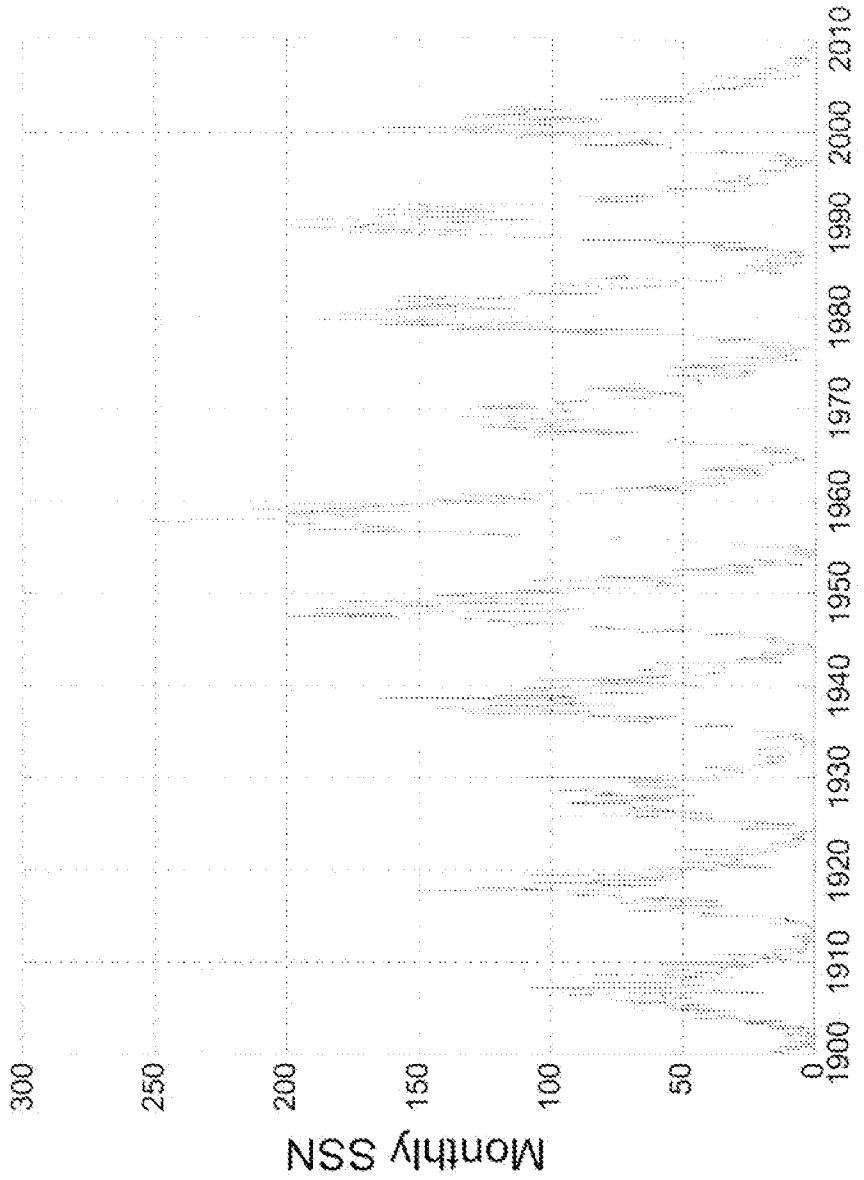
Monthly SSN
300
250
200
150
100
50
0
1900
1910
1920
1930
1940
1950
1960
1970
1980
1990
2000
2010
Year

Fig. 70

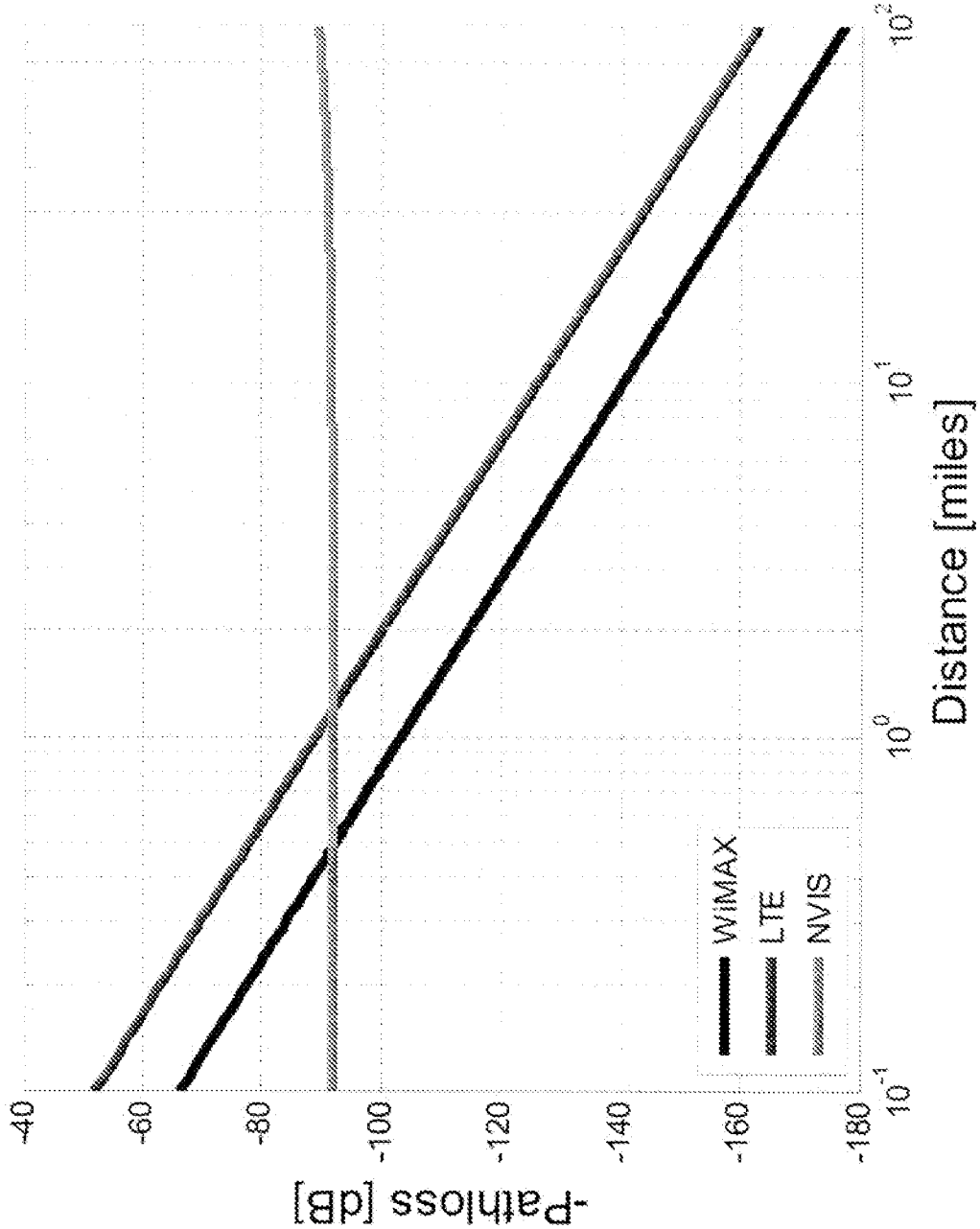
-Pathloss [dB]
-40
-60
-80
-100
-120
-140
-160
-180
Distance [miles]
10^{-1}
10^{0}
10^{1}
10^{2}
WiMAX
LTE
NVIS

Fig. 71

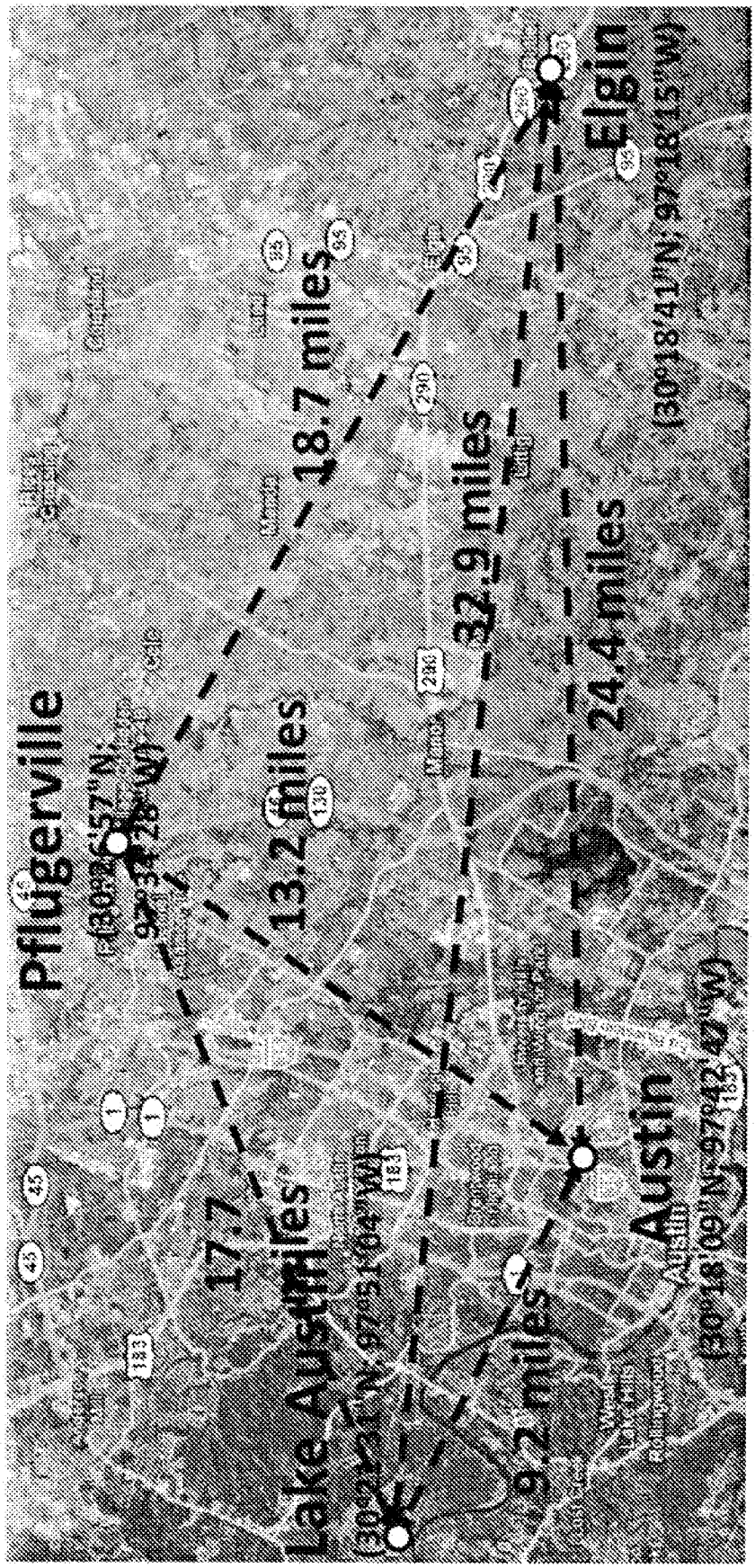
Pflugerville
Lake Austin
Austin
Elgin
17.7 miles
13.2 miles
18.7 miles
32.9 miles
24.4 miles
9.2 miles
(30°18'41"N; 97°18'15"W)

Fig. 72

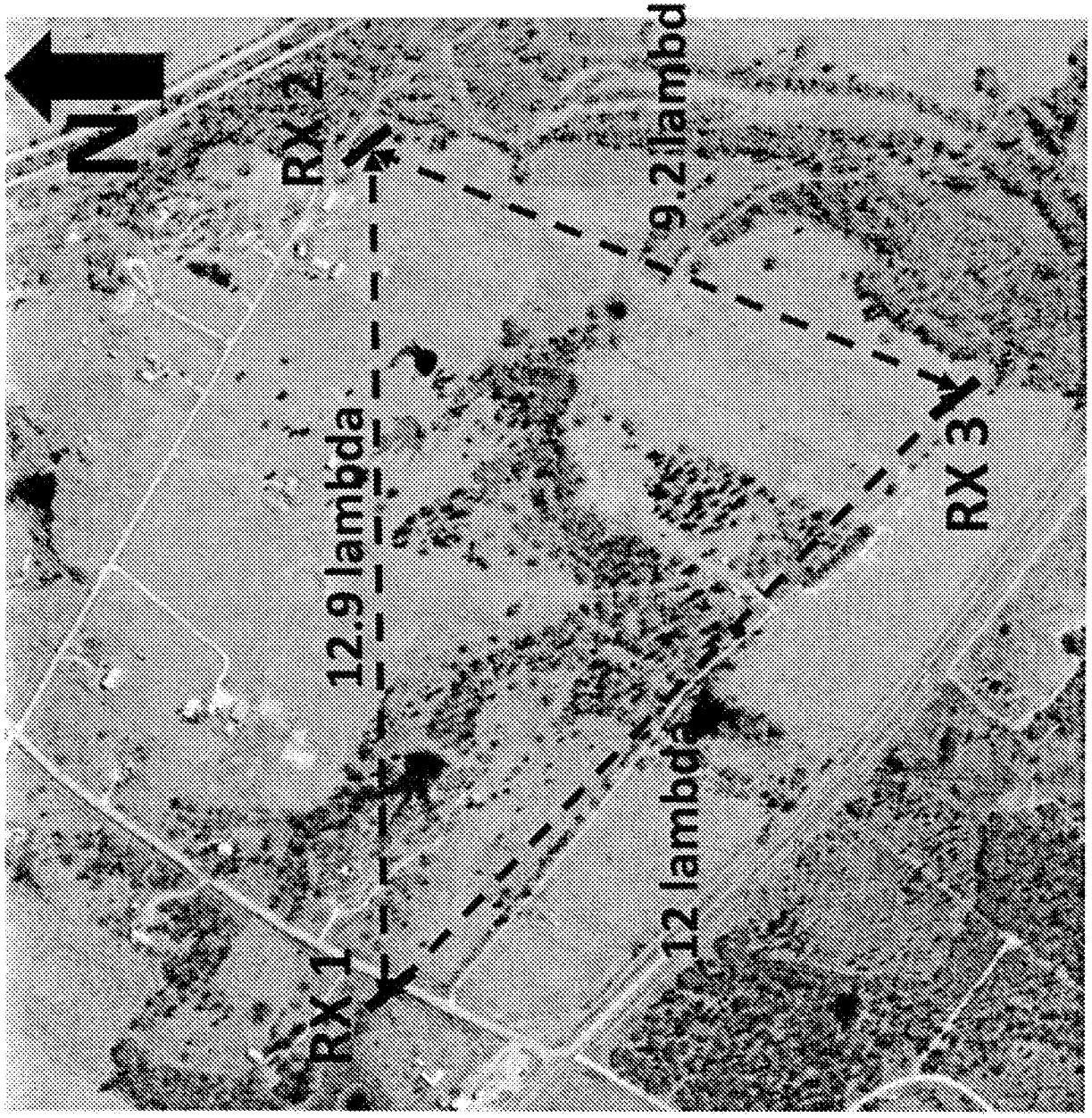

Fig. 73

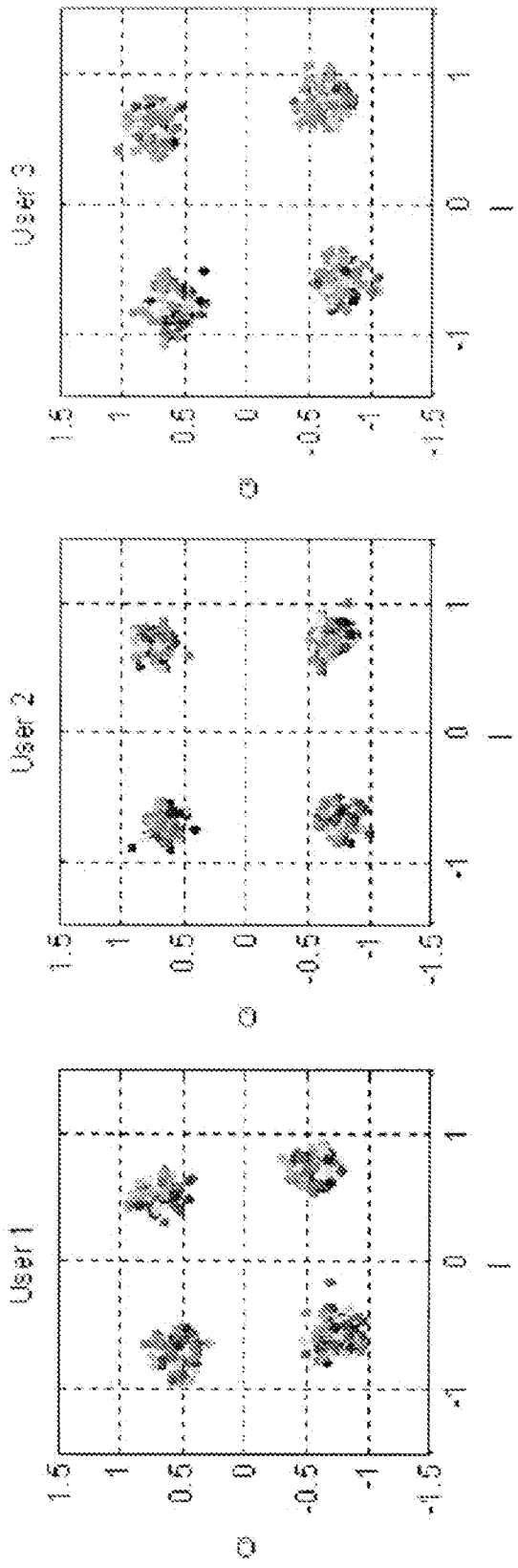

Fig. 74

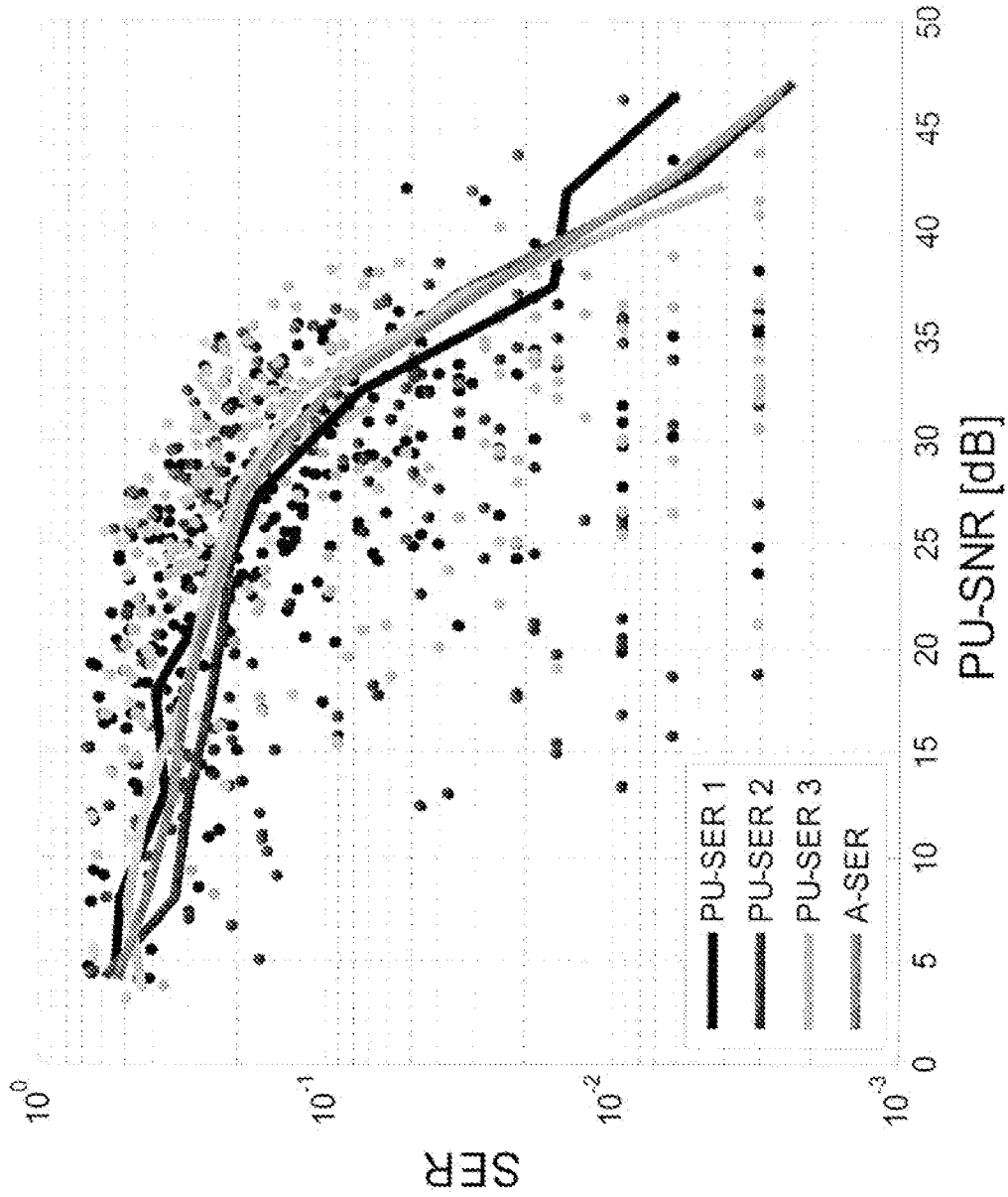
SER
10^{0}
10^{-1}
10^{-2}
10^{-3}
0
5
10
15
20
25
30
35
40
45
50
PU-SNR [dB]
PU-SER 1
PU-SER 2
PU-SER 3
A-SER

Fig. 75

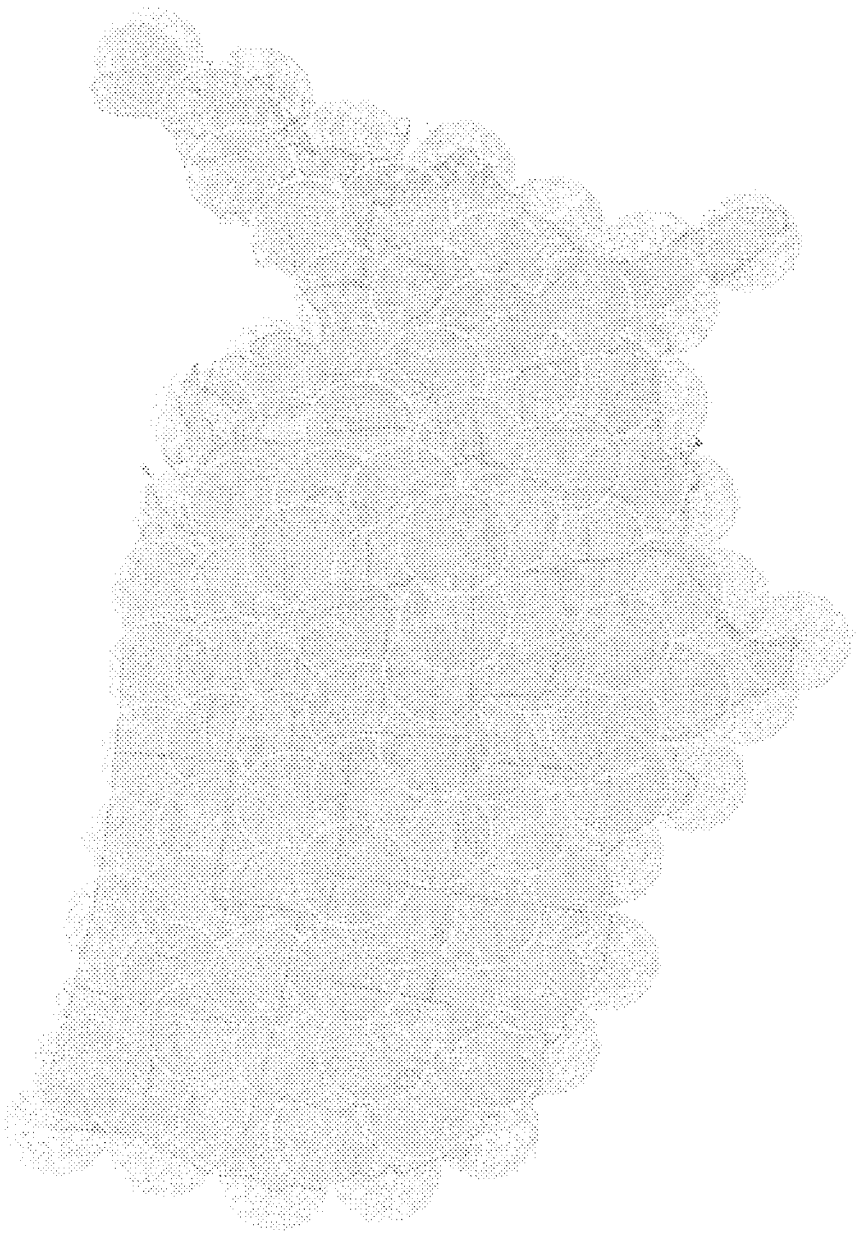

Fig. 76

CLAIMS

1. A multiuser (MU) multiple antenna system (MAS) comprising:
one or more centralized units communicatively coupled to multiple distributed transceiver stations or antennas via a network;
the network consisting of wireline or wireless links or a combination of both, employed as a backhaul communication channel;
the MU-MAS adaptively reconfiguring to compensate for Doppler effects due to user mobility or changes in the propagation environment.

2. The system as in claim 1 wherein the MU-MAS system comprises one or more sets of user equipment (UE), base transceiver stations (BTSs), controllers (CTRs), centralized processors (CPs) and base station networks (BSNs).

3. The system as in claim 1 employing distributed antennas that exploits spatial, polarization and/or pattern diversity to enhance data rate and/or coverage to one or multiple users in wireless systems.

4. The system as in claim 1 wherein the UEs are located around or in between the distributed antennas or surrounded by the distributed antennas.

5. The system as in claim 1 wherein MU-MAS employs complex weights at the receiver of the uplink channel to demodulate independent streams (e.g. data or CSI) from the UEs.

6. The system as in claim 5 wherein the complex weights of the uplink receiver are derived from the downlink precoding weights or computed via maximum ratio combining receiver.

7. The system as in claim 2 wherein the CP and the BTSs are equipped with encoders/decoders to compress/decompress information exchanged among them over the BSN.

8. The system in claim 7 wherein the precoded baseband data streams are compressed, before being transmitted from/to the BTS to/from the MU-MAS distributed antennas, to reduce overhead over the BSN.

9. The system as in claim 2 wherein the CP adaptively selects the BTSs to be used for low- or high-mobility UEs based on latency over the BSN.

10. The system as in claim 9 wherein the adaptation is based on the type of high versus low data rate BSN, or QoS, or average traffic statistics (e.g., daytime or nighttime use of different networks), or instantaneous traffic statistics (e.g., temporary network congestions) over the BSN.

11. The system as in claim 2 wherein the CP adaptively selects the BTSs to be used for low- or high-mobility UEs based on the Doppler velocities of every BTS-UE link.

12. The system as in claim 2 wherein linear prediction is employed to estimate the CSI or MU-MAS precoding weights in the future, thereby eliminating the adverse effect of Doppler on the performance of the MU-MAS.

13. The system as in claim 12 wherein the prediction is employed in the time, frequency and/or space domains.

14. A method implemented within a multiuser (MU) multiple antenna system (MAS) to compensate for Doppler effects comprising:

measuring Doppler velocity of a first mobile user relative to a plurality of base transceiver stations (BTSs); and

dynamically assigning the first mobile user to a first BTS or to a first set of BTSs of the plurality of BTSs based on the measured Doppler velocity for the first BTS relative to other BTSs.

15. The method as in claim 14 wherein if the first mobile user has a measured Doppler velocity which is relatively higher than a second mobile user, then dynamically assigning comprises assigning the first mobile user to a first BTS or to a first set of BTSs and assigning the second mobile user to a second BTS or to a second set of BTSs, the first BTS or the first set of

BTSs having a relatively lower latency associated therewith than the second BTS or second set of BTSs.

16. The method as in claim 14 wherein the latency includes (a) time taken to transmit a first training signal from the first mobile user to a BTS, (b) round-trip delay over a base station network (BSN) connecting the BTSs to a centralized processor (CP), and (c) time taken buy the CP to process channel state information (CSI) for the wireless channel between the BTSs and the first mobile user, generate precoded data streams for the first mobile user based on the CSI, and schedule transmissions to different mobile users including the first user for the current transmission.

17. The method as in claim 16 wherein the latency further includes time taken to transmit a second training signal from the BTS to the first mobile user.

18. The method as in claim 14 wherein dynamically assigning further comprises assigning based on a combination of link quality of a communication channel between each BTS and the first mobile user and the measured Doppler velocity associated with each BTS with respect to the first user.

19. The method as in claim 18 wherein, for a given Doppler velocity, the BTS having the relatively higher link quality is selected.

20. The method as in claim 18 wherein for a given link quality, the BTS having the relatively lower Doppler velocity is selected.

21. The method as in claim 14 further comprising:

estimating future complex channel coefficients based on past complex channel coefficients to compensate for the adverse effect of Doppler on communication between the BTSs and the first mobile user.

22. The method as in claim 21 wherein linear prediction is employed for estimation.

23. The method as in claim 14 wherein the first mobile user is dynamically assigned to the first BTS or a first set of BTSs based on both the Doppler velocity and channel state

information (CSI) defining quality of communication channels between the mobile user and each of the BTSs within the plurality.

24. The method as in claim 23 further comprising:

building a matrix of Doppler velocities and link qualities for each of the BTSs within the plurality with respect to the first mobile user; and

selecting a BTS which has a Doppler velocity below a specified threshold and link quality above a specified threshold.

25. A multiuser (MU) multiple antenna system (MAS) to compensate for Doppler effects comprising:

a plurality of base transceiver stations (BTSs);

a first mobile user establishing a communication link with each of the BTSs;

a centralized processor (CP) measuring Doppler velocity of a first mobile user relative to each of the BTSs and dynamically assigning the first mobile user to a first BTS of the plurality of BTSs based on the measured Doppler velocity for the first BTS relative to other BTSs.

26. The system as in claim 25 wherein if the first mobile user has a measured Doppler velocity which is relatively higher than a second mobile user, then dynamically assigning comprises assigning the first mobile user to a first BTS and assigning the second mobile user to a second BTS, the first BTS having a relatively lower latency associated therewith than the second BTS.

27. The system as in claim 25 wherein the latency includes (a) time taken to transmit a first training signal from the first mobile user to a BTS, (b) round-trip delay over a base station network (BSN) connecting the BTSs to a centralized processor (CP), and (c) time taken buy the CP to process channel state information (CSI) for the wireless channel between the BTSs and the first mobile user, generate precoded data streams for the first mobile user based on the CSI, and schedule transmissions to different mobile users including the first user for the current transmission.

28. The system as in claim 27 wherein the latency further includes time taken to transmit a second training signal from the BTS to the first mobile user.

29. The system as in claim 25 wherein dynamically assigning further comprises assigning based on a combination of link quality of a communication channel between each BTS and the first mobile user and the measured Doppler velocity associated with each BTS with respect to the first user.

30. The system as in claim 29 wherein, for a given Doppler velocity, the BTS having the relatively higher link quality is selected.

31. The system as in claim 29 wherein for a given link quality, the BTS having the relatively lower Doppler velocity is selected.

32. The system as in claim 25 wherein the CP estimates future complex channel coefficients based on past complex channel coefficients to compensate for the adverse effect of Doppler on communication between the BTSs and the first mobile user.

33. The system as in claim 32 wherein linear prediction is employed for estimation.

34. The system as in claim 25 wherein the first mobile user is dynamically assigned to the first BTS based on both the Doppler Velocity and channel state information (CSI) defining quality of communication channels between the mobile user and each of the BTSs within the plurality.

35. The system as in claim 34 wherein the CP performs the additional operations of:

building a matrix of Doppler velocities and link qualities for each of the BTSs within the plurality with respect to the first mobile user; and

selecting a BTS which has a Doppler velocity below a specified threshold and link quality above a specified threshold.

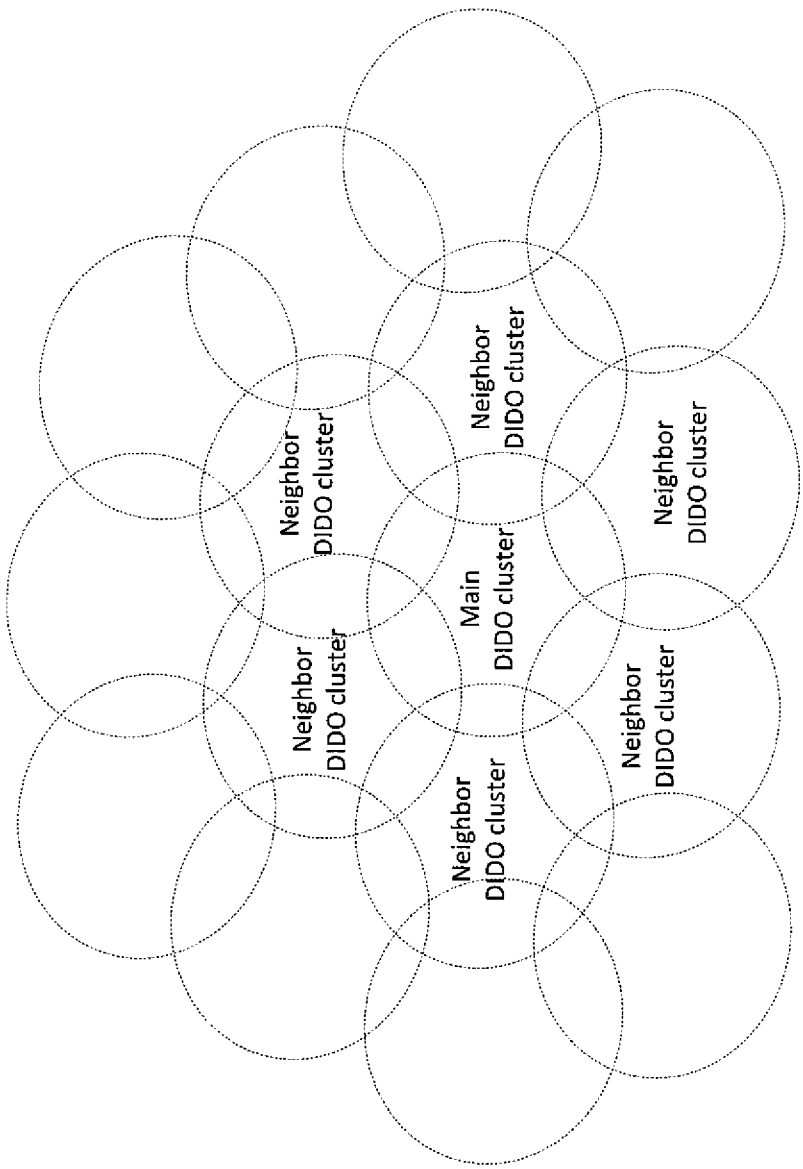
Neighbor DIDO cluster
Neighbor DIDO cluster
Neighbor DIDO cluster
Main DIDO cluster
Neighbor DIDO cluster
Neighbor DIDO cluster
Neighbor DIDO cluster

Fig. 1

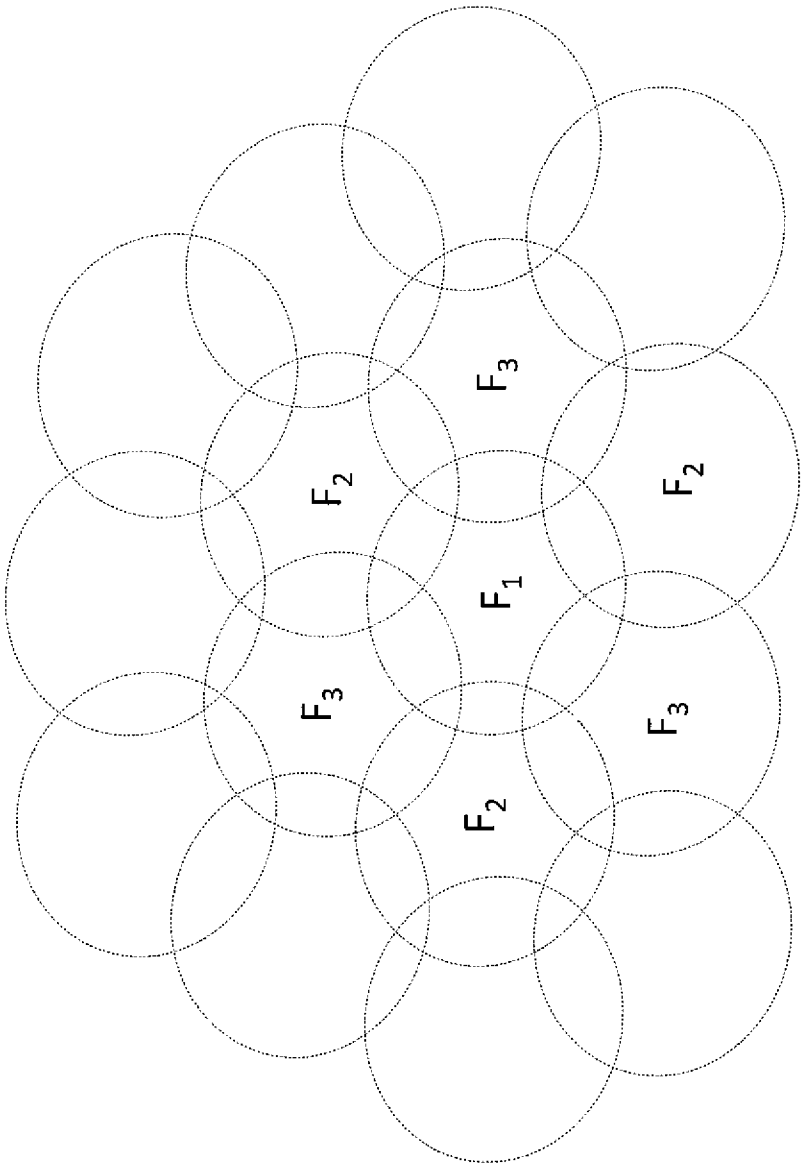

Fig. 2

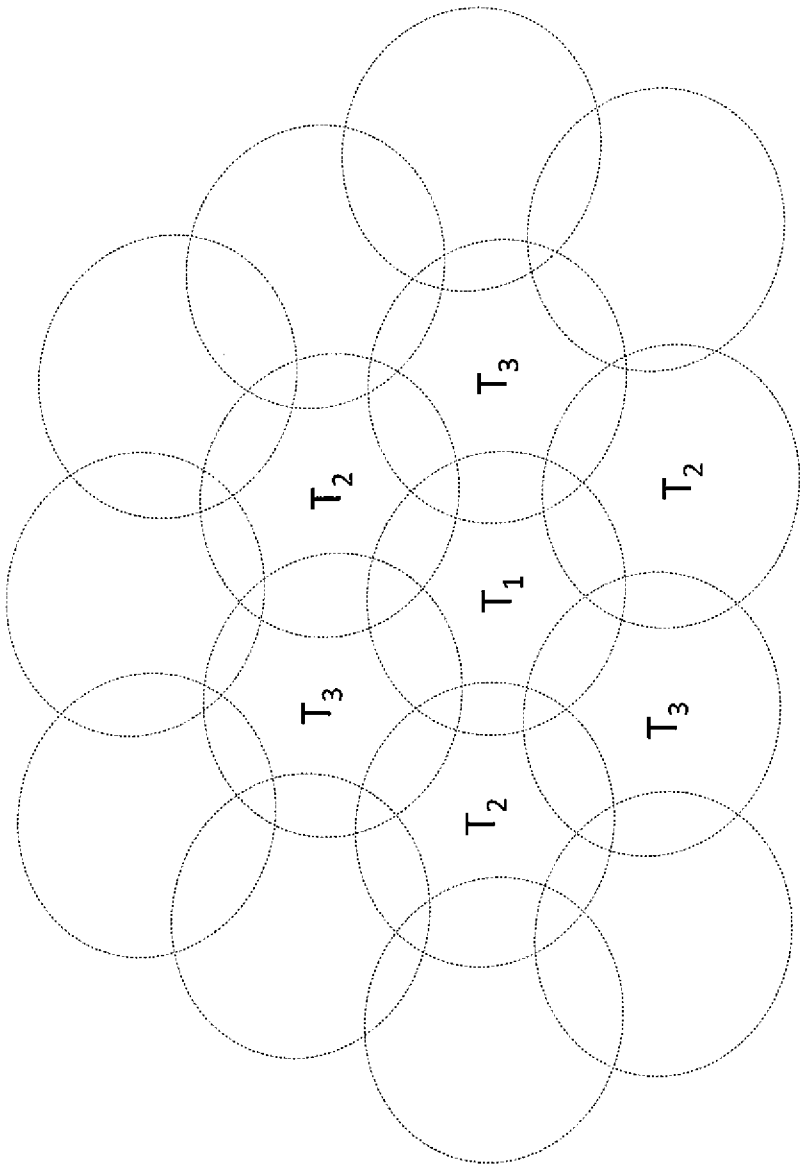

Fig. 3

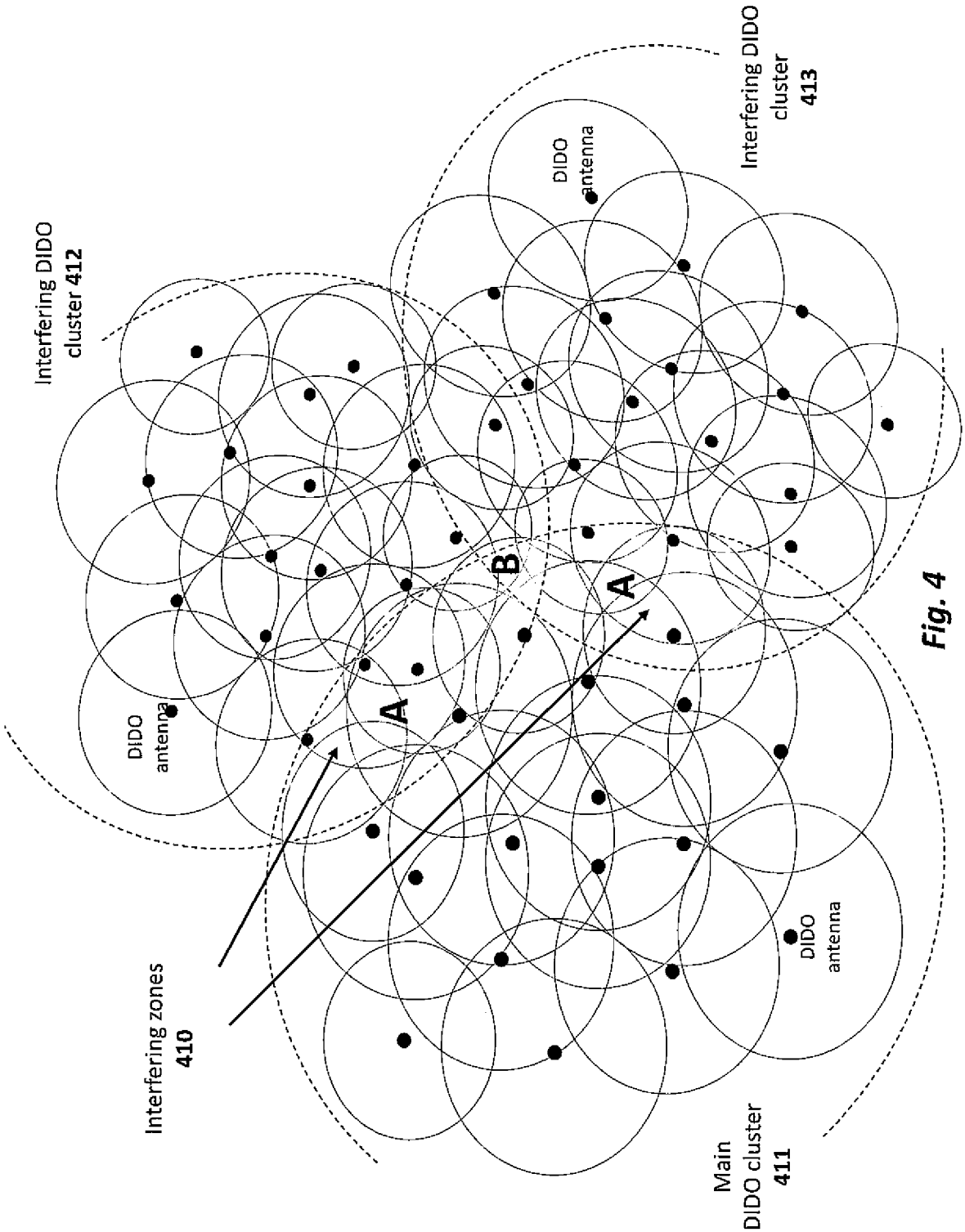
Interfering DIDO cluster 412
Interfering DIDO cluster 413
DIDO antenna
DIDO antenna
DIDO antenna
A
B
A
Interfering zones 410
Main DIDO cluster 411

Fig. 4

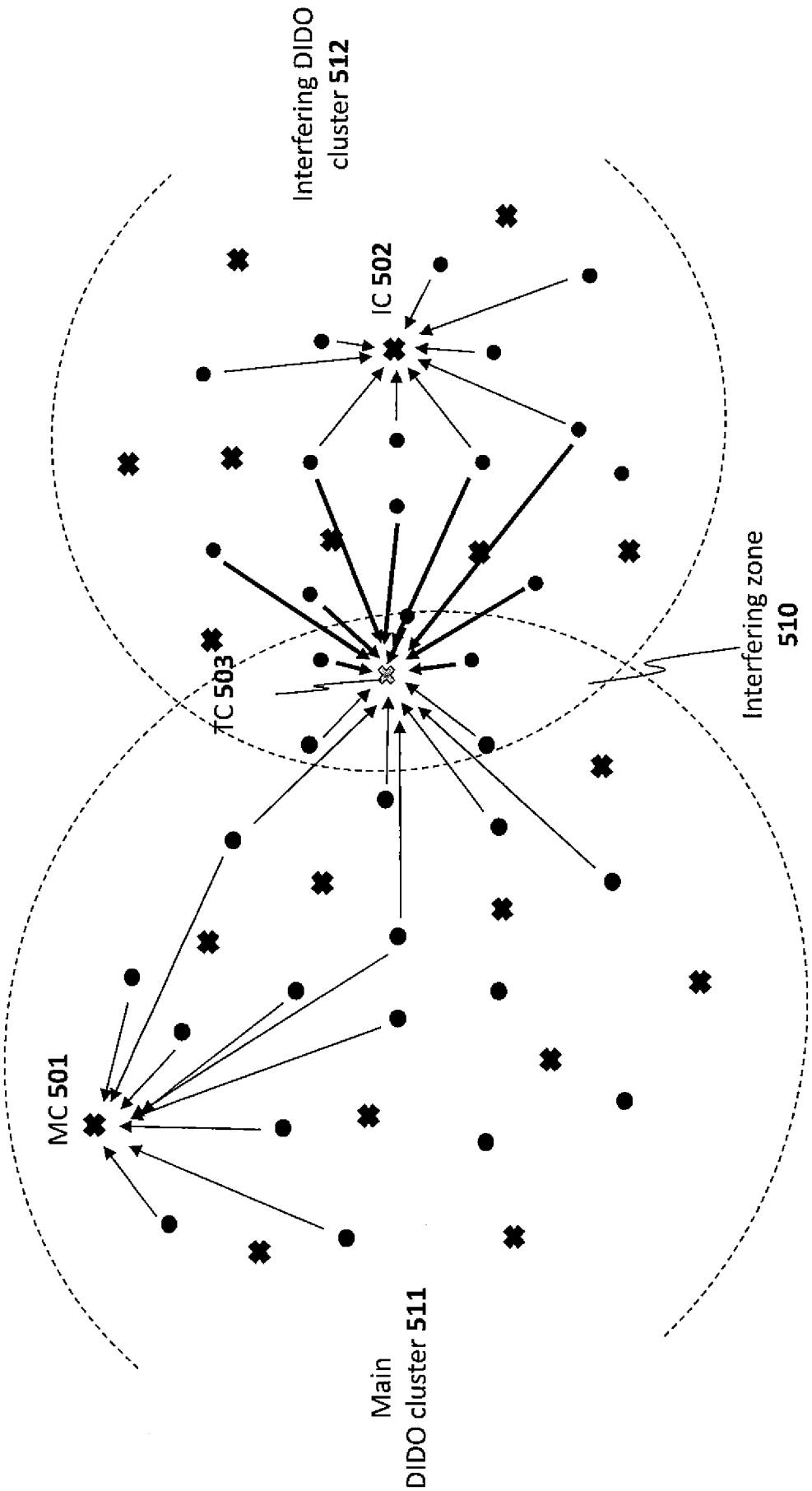
Interfering DIDO cluster 512
IC 502
IC 503
Interfering zone 510
MC 501
Main DIDO cluster 511

Fig. 5

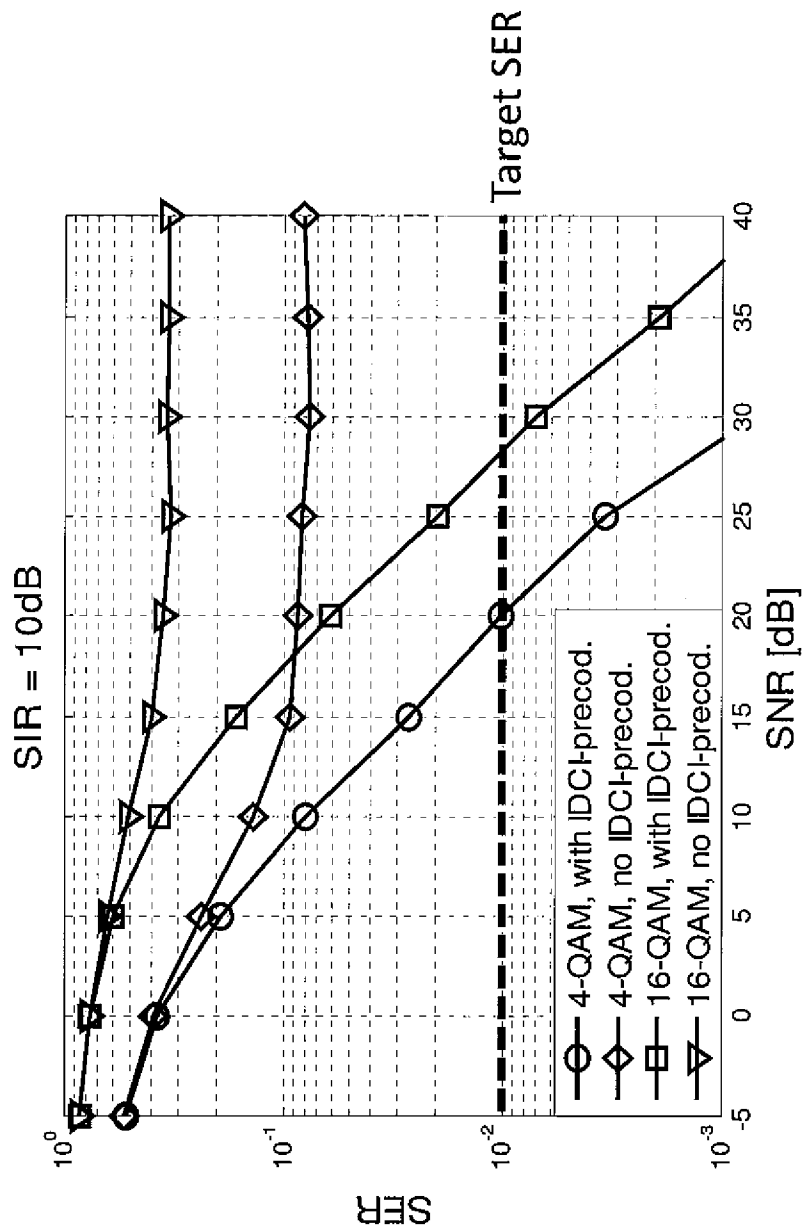
SIR = 10dB
Target SER
SER
SNR [dB]
4-QAM, with IDCI-precod.
4-QAM, no IDCI-precod.
16-QAM, with IDCI-precod.
16-QAM, no IDCI-precod.

Fig. 6

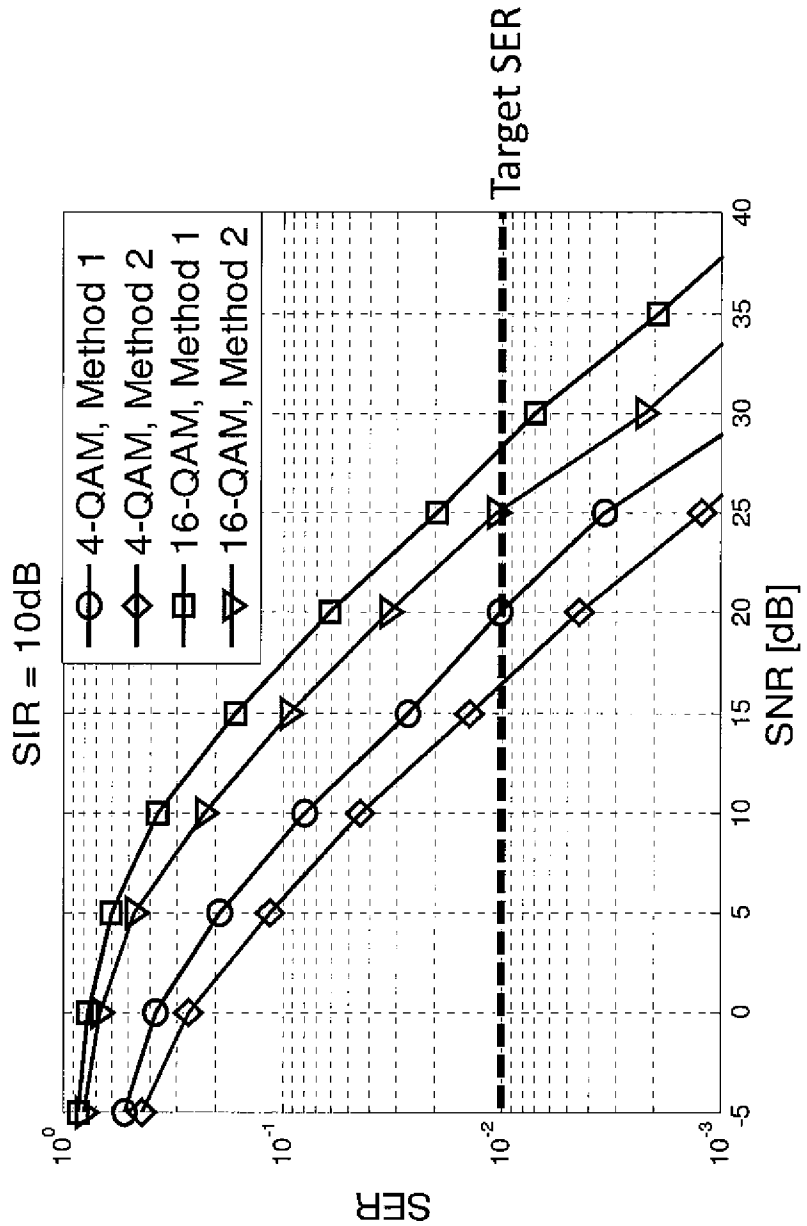
SIR = 10dB
4-QAM, Method 1
4-QAM, Method 2
16-QAM, Method 1
16-QAM, Method 2
Target SER
SER
SNR [dB]
10^0
10^-1
10^-2
10^-3
-5
0
5
10
15
20
25
30
35
40

Fig. 7

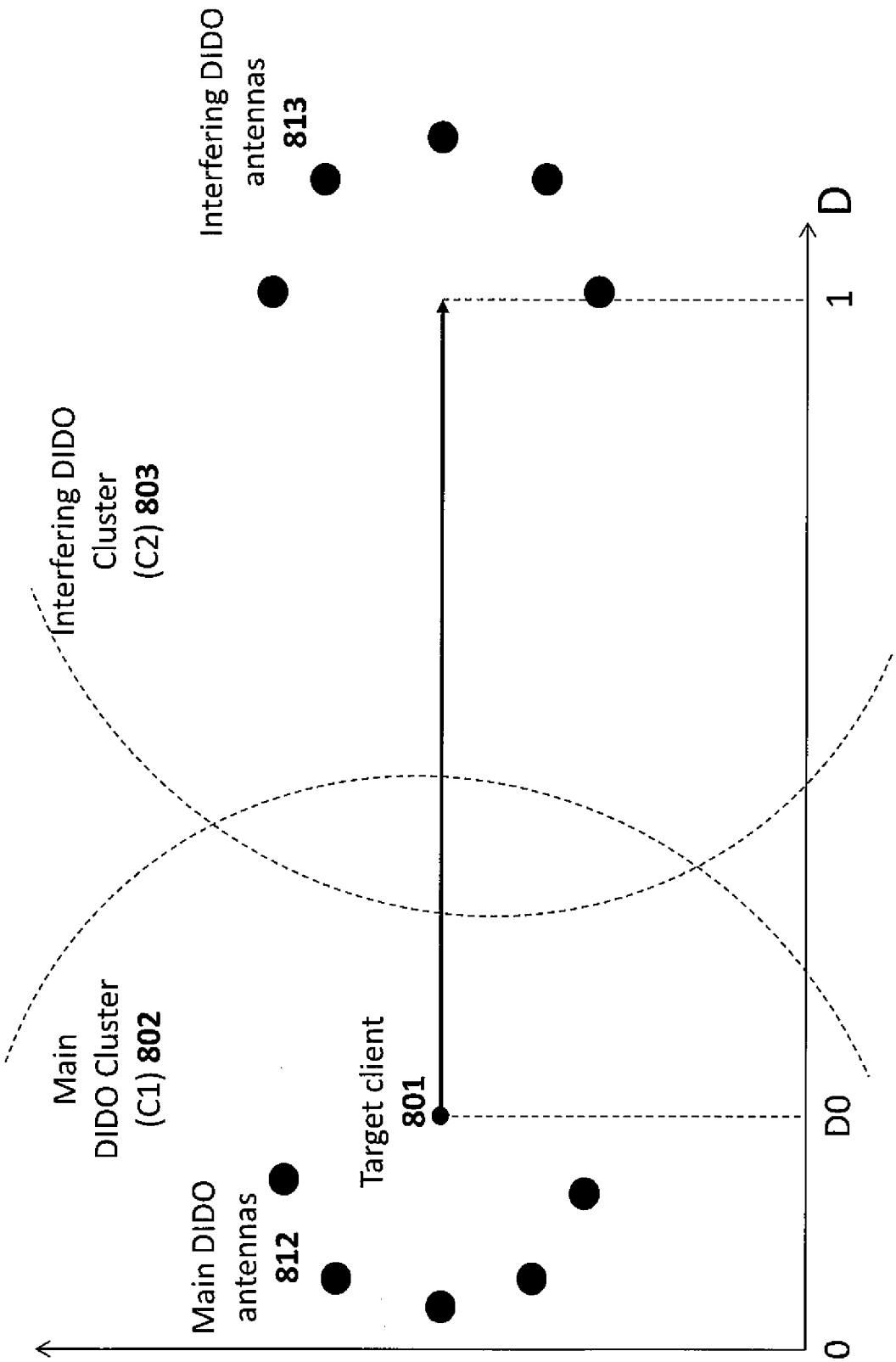
Interfering DIDO antennas 813
Interfering DIDO Cluster (C2) 803
Main DIDO Cluster (C1) 802
Target client 801
Main DIDO antennas 812
D
1
D0
0

Fig. 8

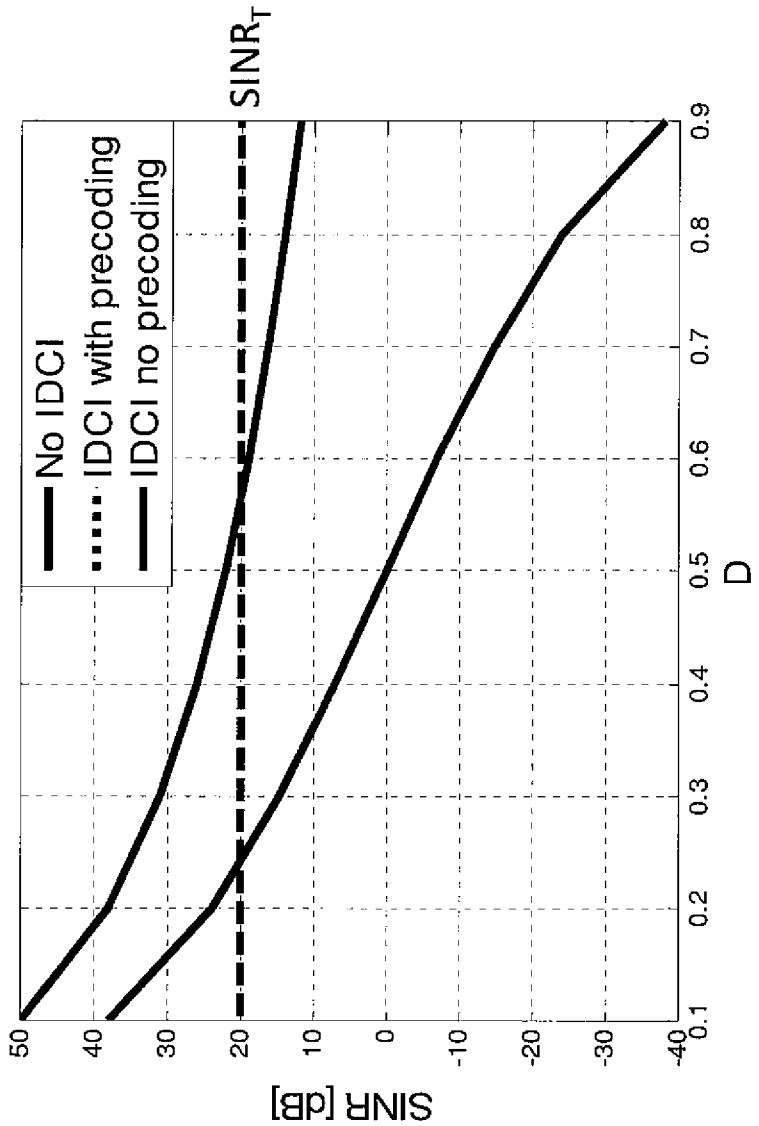
SINR_T
No IDCI
IDCI with precoding
IDCI no precoding
SINR [dB]
D
50
40
30
20
10
0
-10
-20
-30
-40
0.1
0.2
0.3
0.4
0.5
0.6
0.7
0.8
0.9

Fig. 9

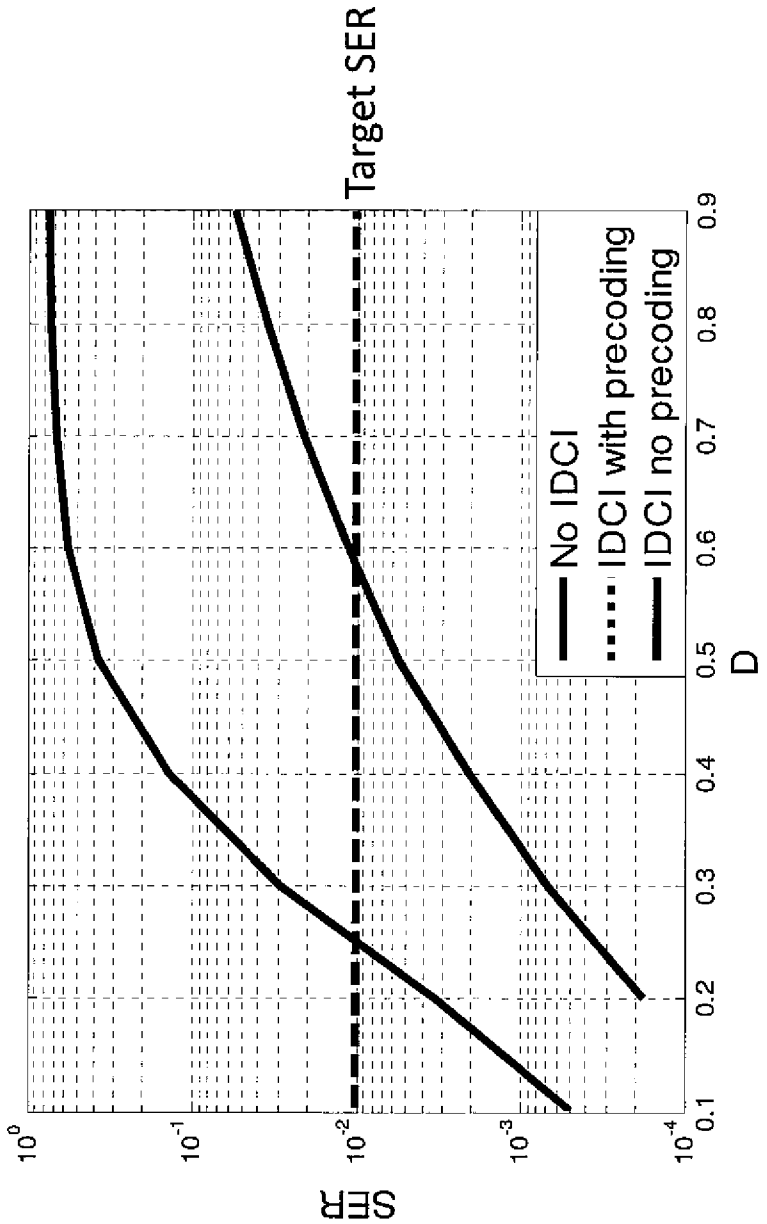
Target SER
No IDCI
IDCI with precoding
IDCI no precoding
SER
D
10^{0}
10^{-1}
10^{-2}
10^{-3}
10^{-4}
0.1
0.2
0.3
0.4
0.5
0.6
0.7
0.8
0.9

Fig. 10

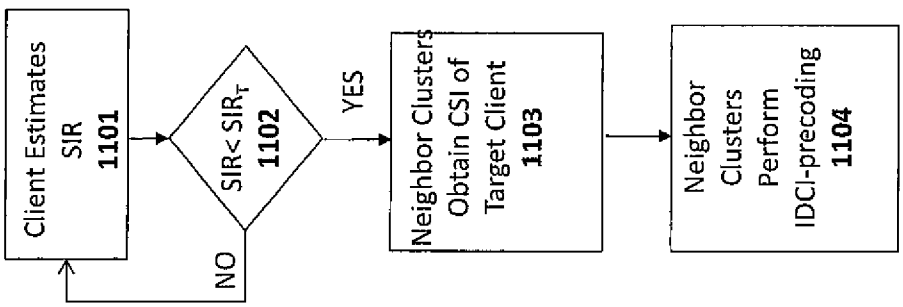
Client Estimates SIR 1101
SIR< SIR$_T$ 1102
YES
NO
Neighbor Clusters Obtain CSI of Target Client 1103
Neighbor Clusters Perform IDCI-precoding 1104

Fig. 11

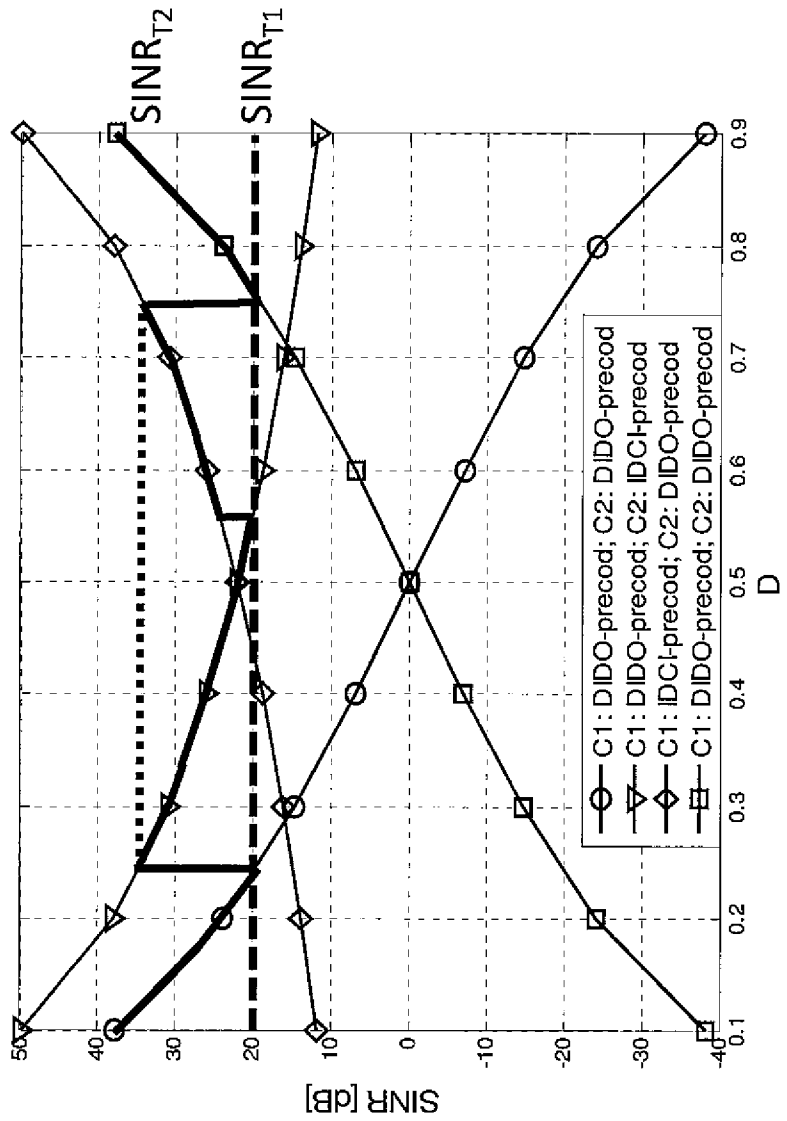
SINR_T2
SINR_T1
SINR [dB]
D
C1: DIDO-precod; C2: DIDO-precod
C1: DIDO-precod; C2: IDCI-precod
C1: IDCI-precod; C2: DIDO-precod
C1: DIDO-precod; C2: DIDO-precod

Fig. 12

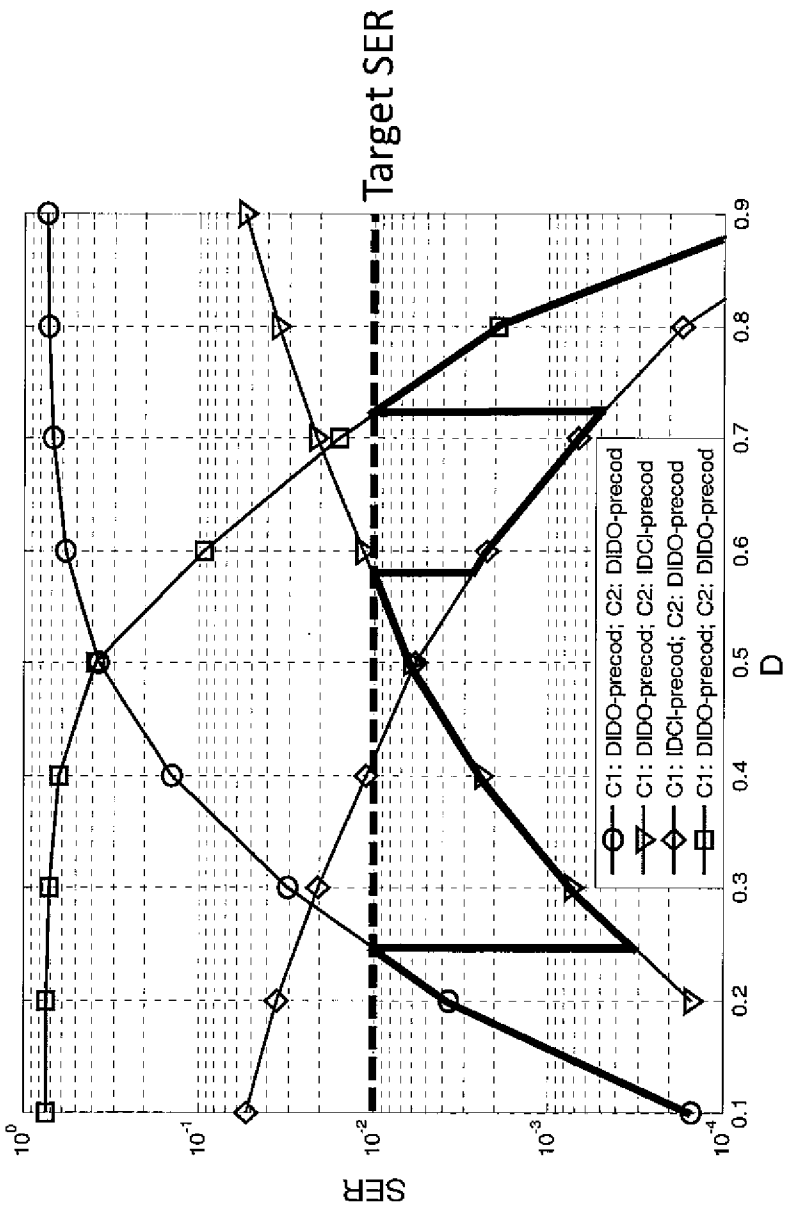
Target SER
SER
D
C1: DIDO-precod; C2: DIDO-precod
C1: DIDO-precod; C2: IDCI-precod
C1: IDCI-precod; C2: DIDO-precod
C1: DIDO-precod; C2: DIDO-precod

Fig. 13

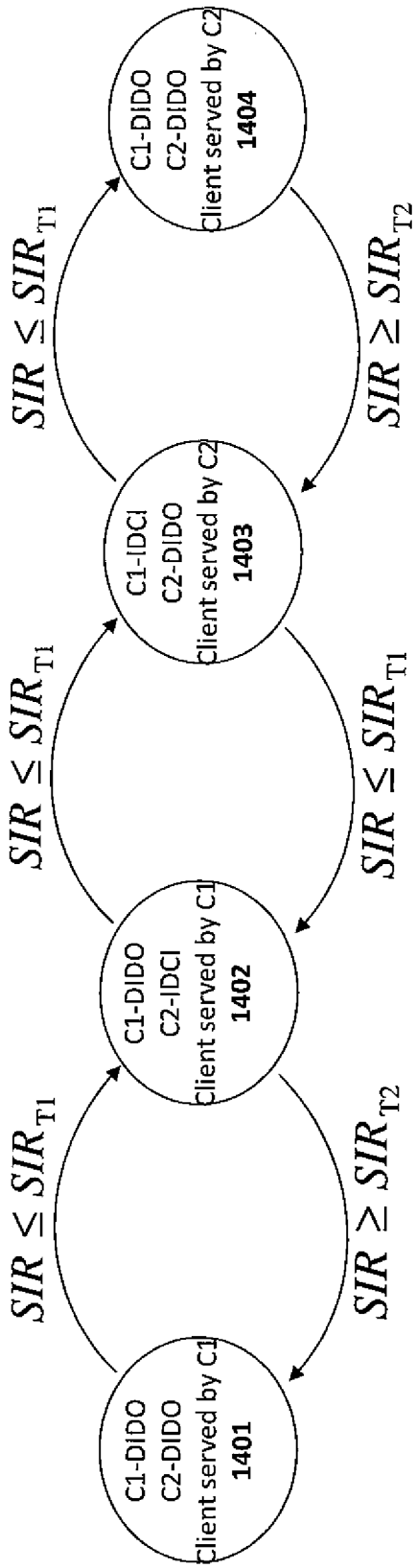
C1-DIDO
C2-DIDO
Client served by C1
1401
C1-DIDO
C2-IDCI
Client served by C1
1402
C1-IDCI
C2-DIDO
Client served by C2
1403
C1-DIDO
C2-DIDO
Client served by C2
1404
$SIR \leq SIR_{T1}$
$SIR \geq SIR_{T2}$
$SIR \leq SIR_{T1}$
$SIR \leq SIR_{T1}$
$SIR \geq SIR_{T2}$

Fig. 14

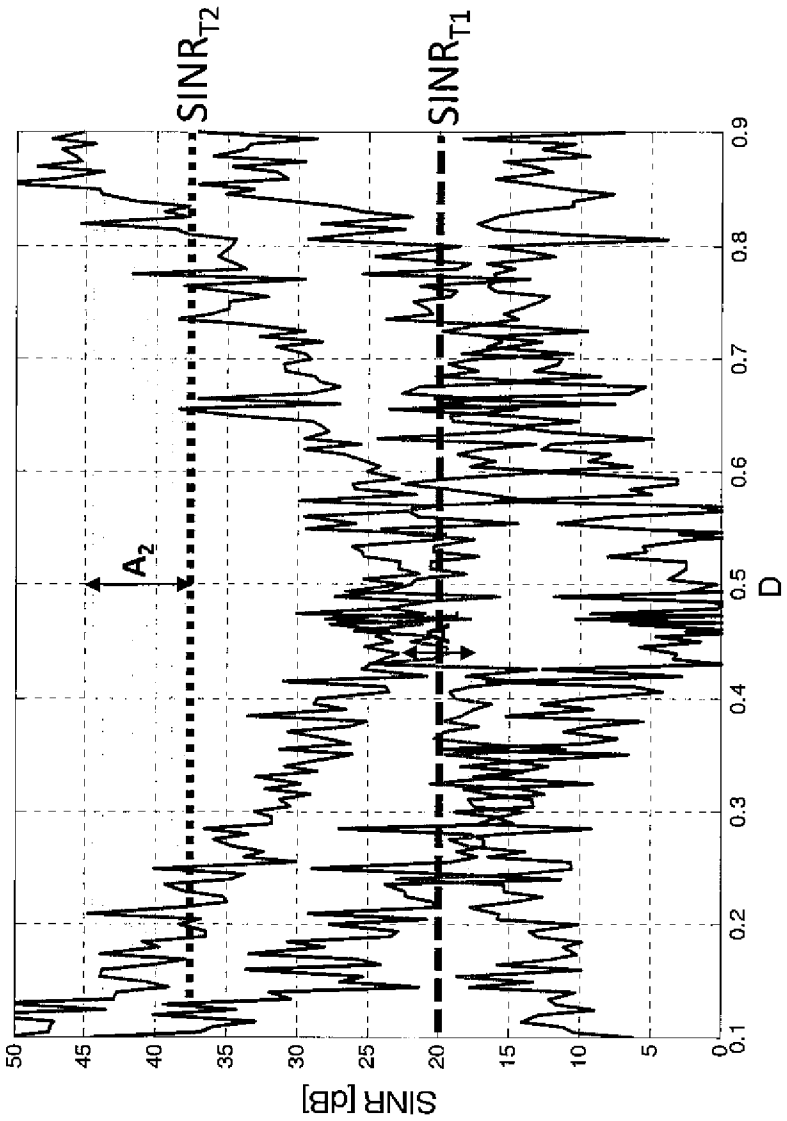
SINR_T2
SINR_T1
A_2
A_1
SINR [dB]
D
50
45
40
35
30
25
20
15
10
5
0
0.1
0.2
0.3
0.4
0.5
0.6
0.7
0.8
0.9

Fig. 15

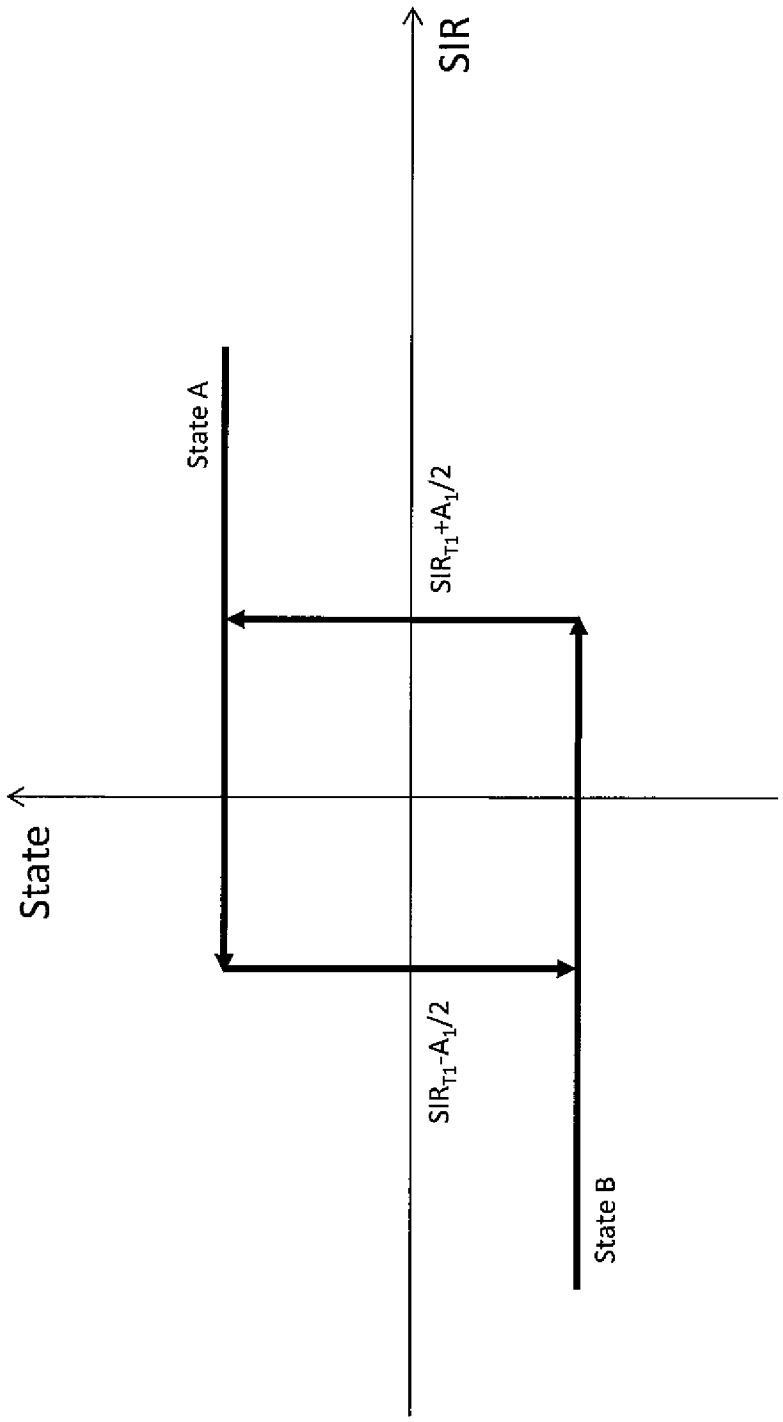

Fig. 16

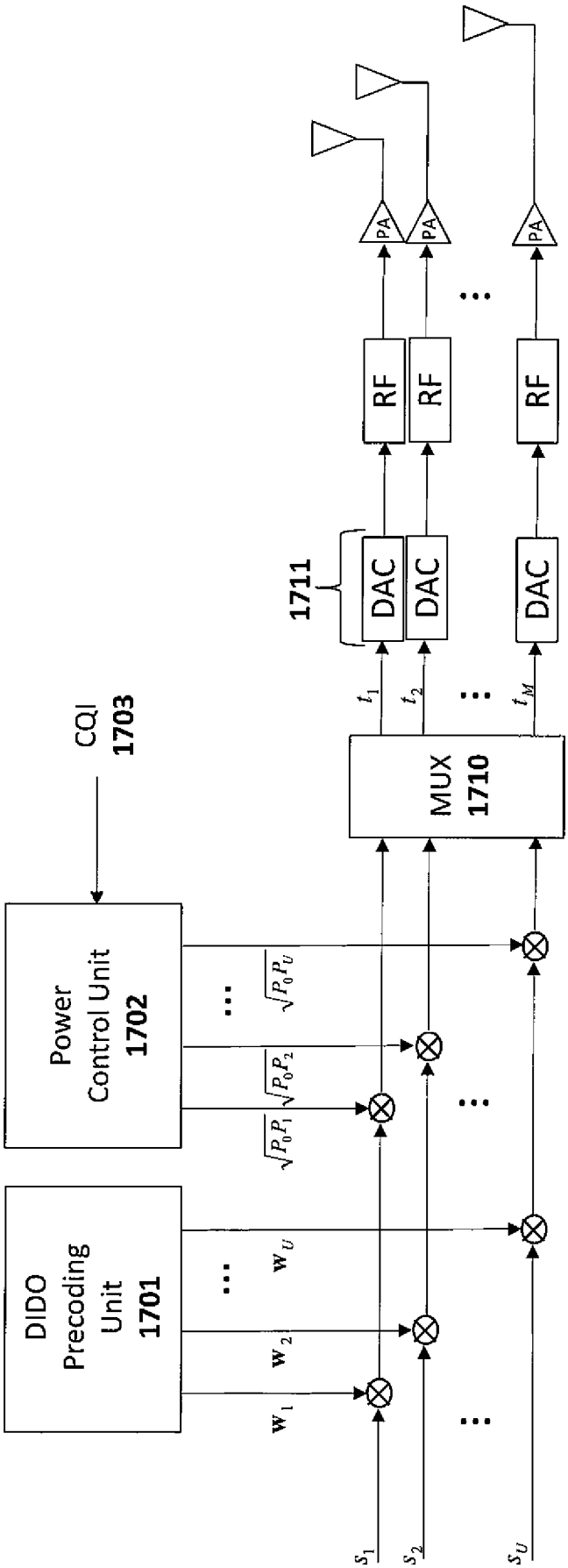
CQI
1703
Power Control Unit
1702
DIDO Precoding Unit
1701
MUX
1710
1711
DAC
RF
PA
$\mathbf{w}_1$
$\mathbf{w}_2$
$\mathbf{w}_U$
$\sqrt{P_0 P_1}$
$\sqrt{P_0 P_2}$
$\sqrt{P_0 P_U}$
t_1
t_2
t_M
s_1
s_2
s_U

Fig. 17

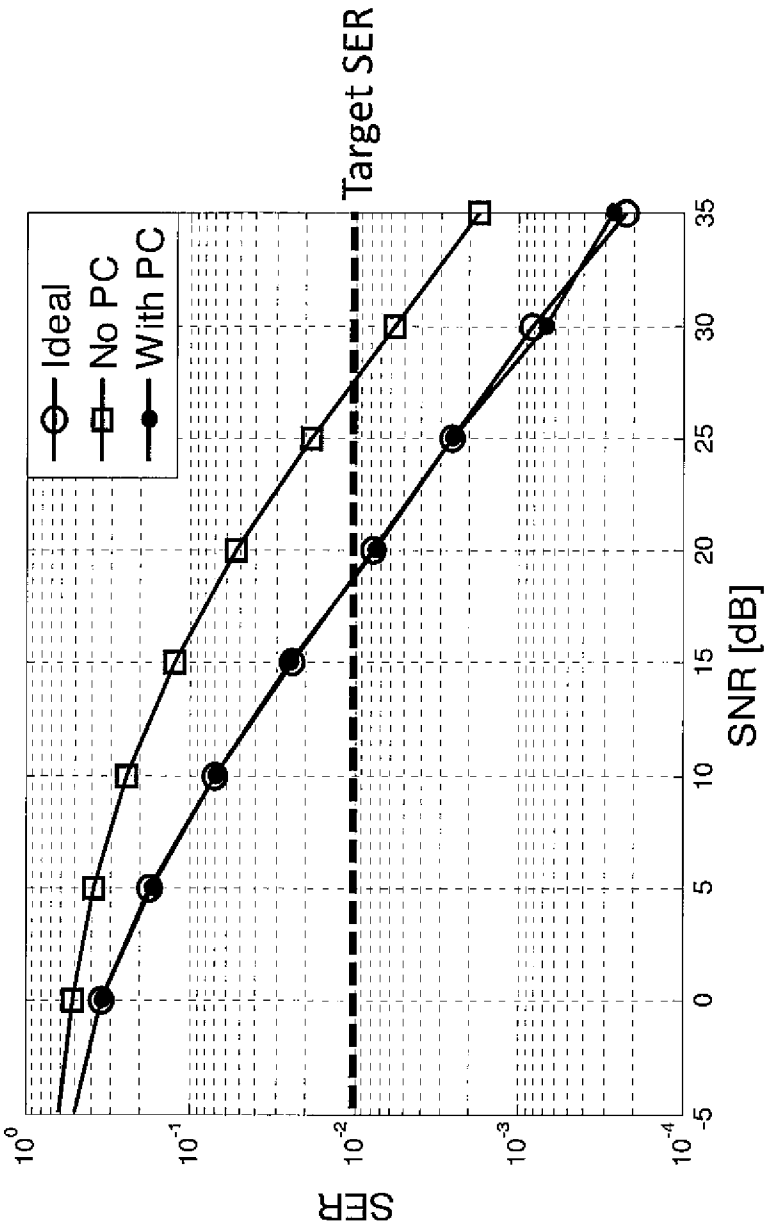
Target SER
Ideal
No PC
With PC
SER
SNR [dB]
10^{0}
10^{-1}
10^{-2}
10^{-3}
10^{-4}
-5
0
5
10
15
20
25
30
35

Fig. 18

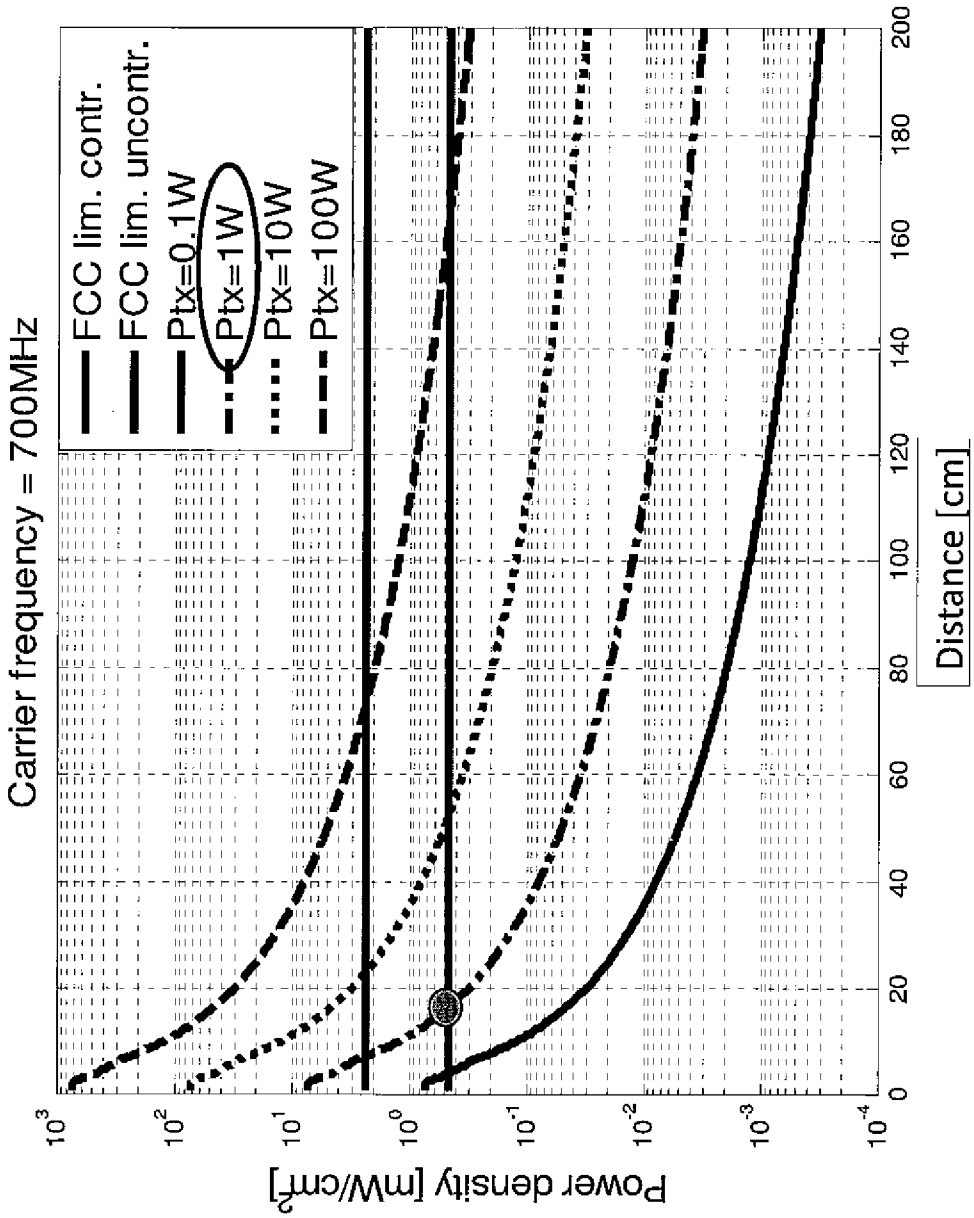
Carrier frequency = 700MHz
FCC lim. contr.
FCC lim. uncontr.
Ptx=0.1W
Ptx=1W
Ptx=10W
Ptx=100W
Power density [mW/cm²]
Distance [cm]
10^3
10^2
10^1
10^0
10^-1
10^-2
10^-3
10^-4
0
20
40
60
80
100
120
140
160
180
200

Fig. 19

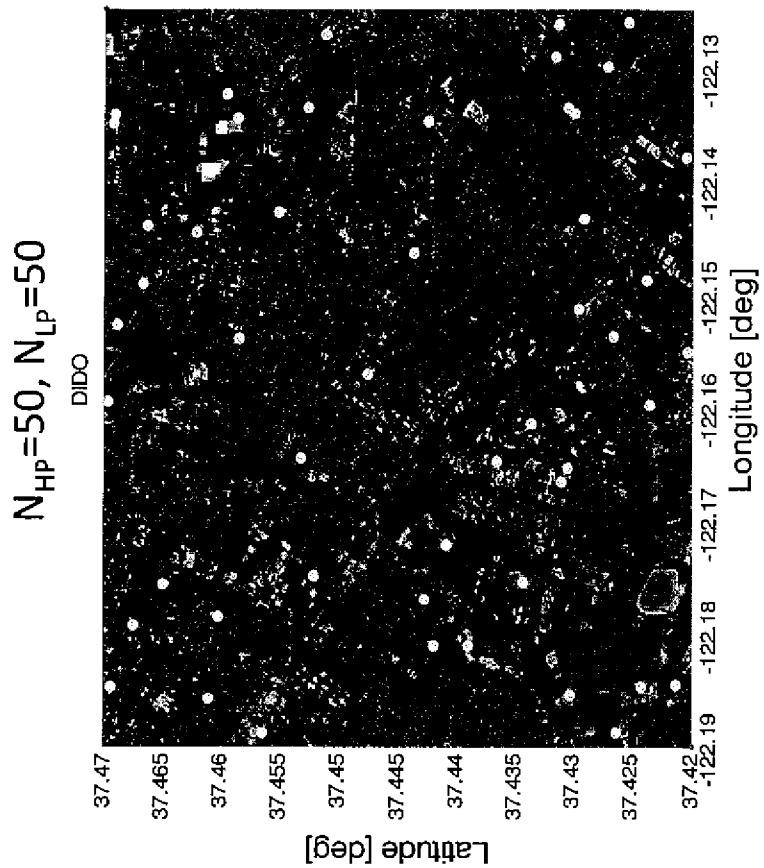

Fig. 20b

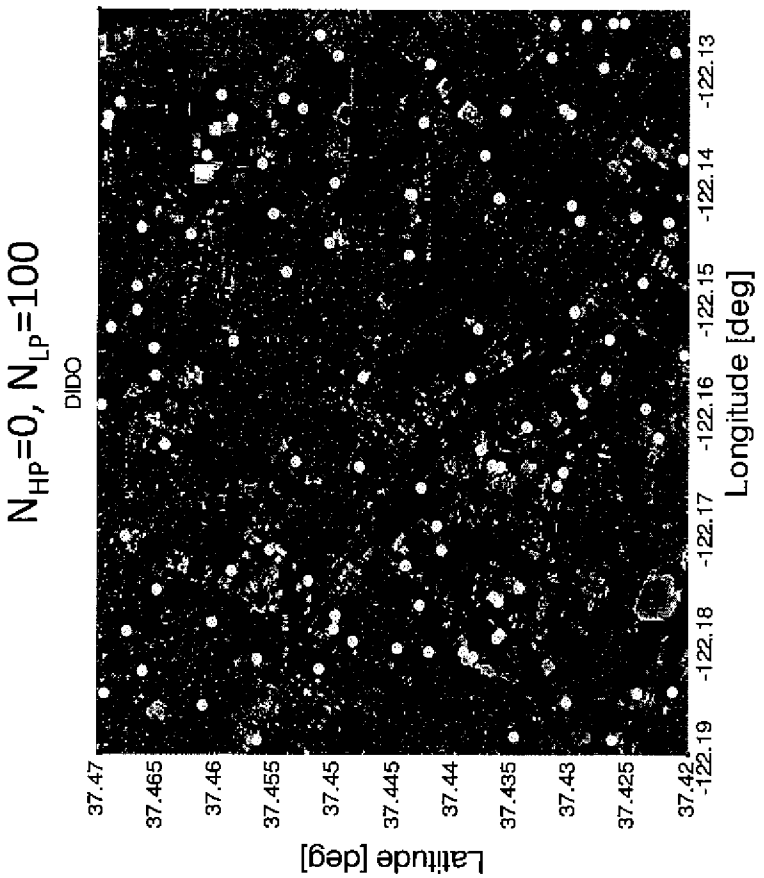

Fig. 20a

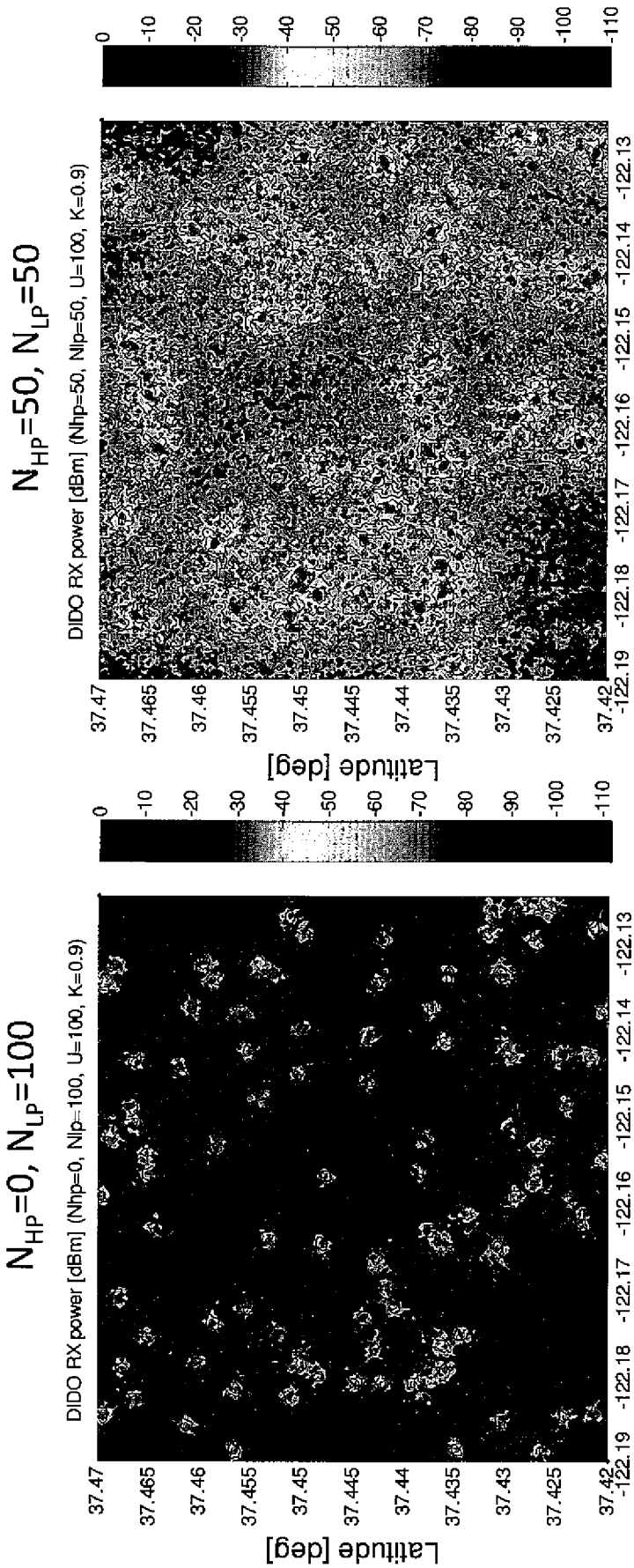

Fig. 21a

Fig. 21b

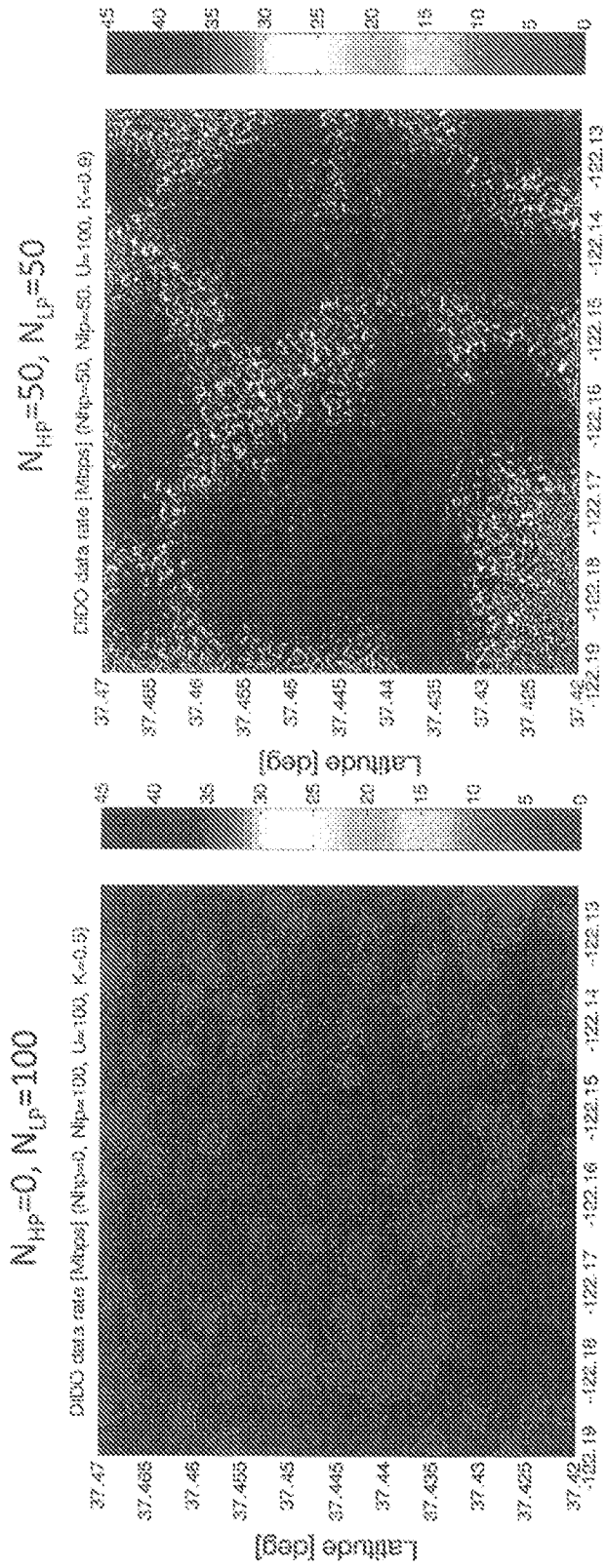

Fig. 22a

Fig. 22b

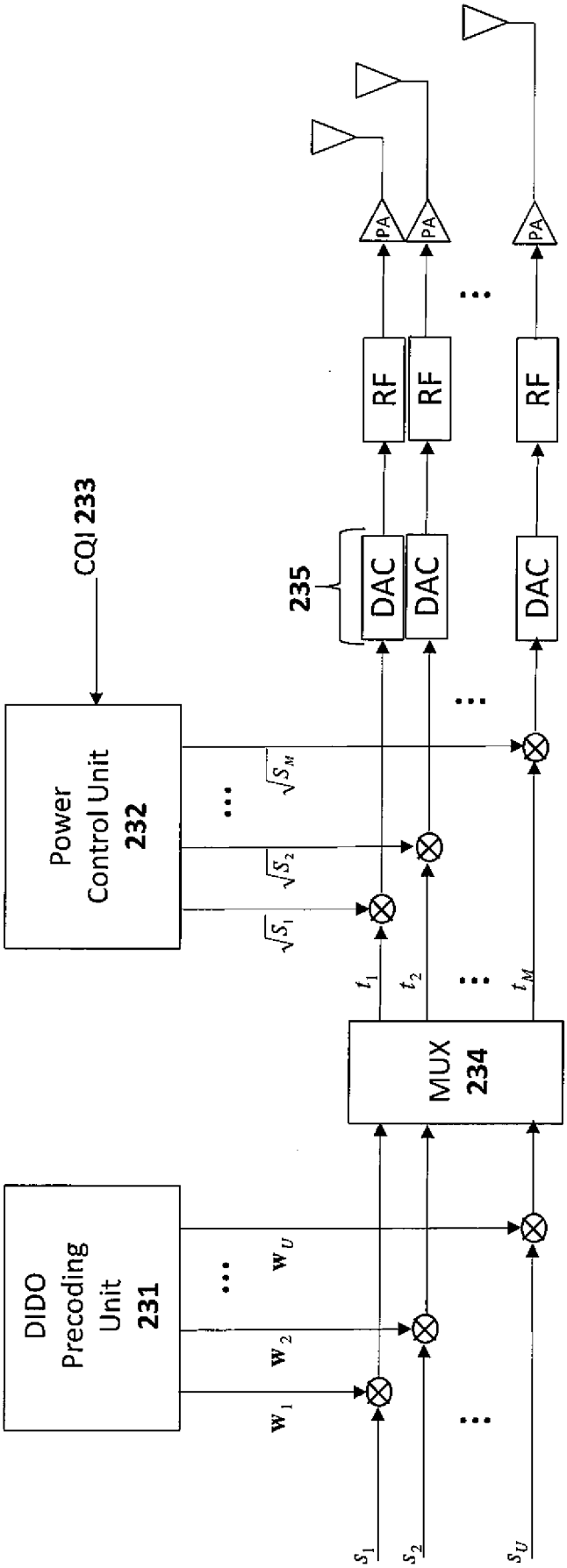
CQI 233
Power Control Unit 232
DIDO Precoding Unit 231
MUX 234
235
DAC
RF
PA
$\sqrt{s_1}$
$\sqrt{s_2}$
$\sqrt{s_M}$
t_1
t_2
t_M
$\mathbf{w}_1$
$\mathbf{w}_2$
$\mathbf{w}_U$
s_1
s_2
s_U

Fig. 23

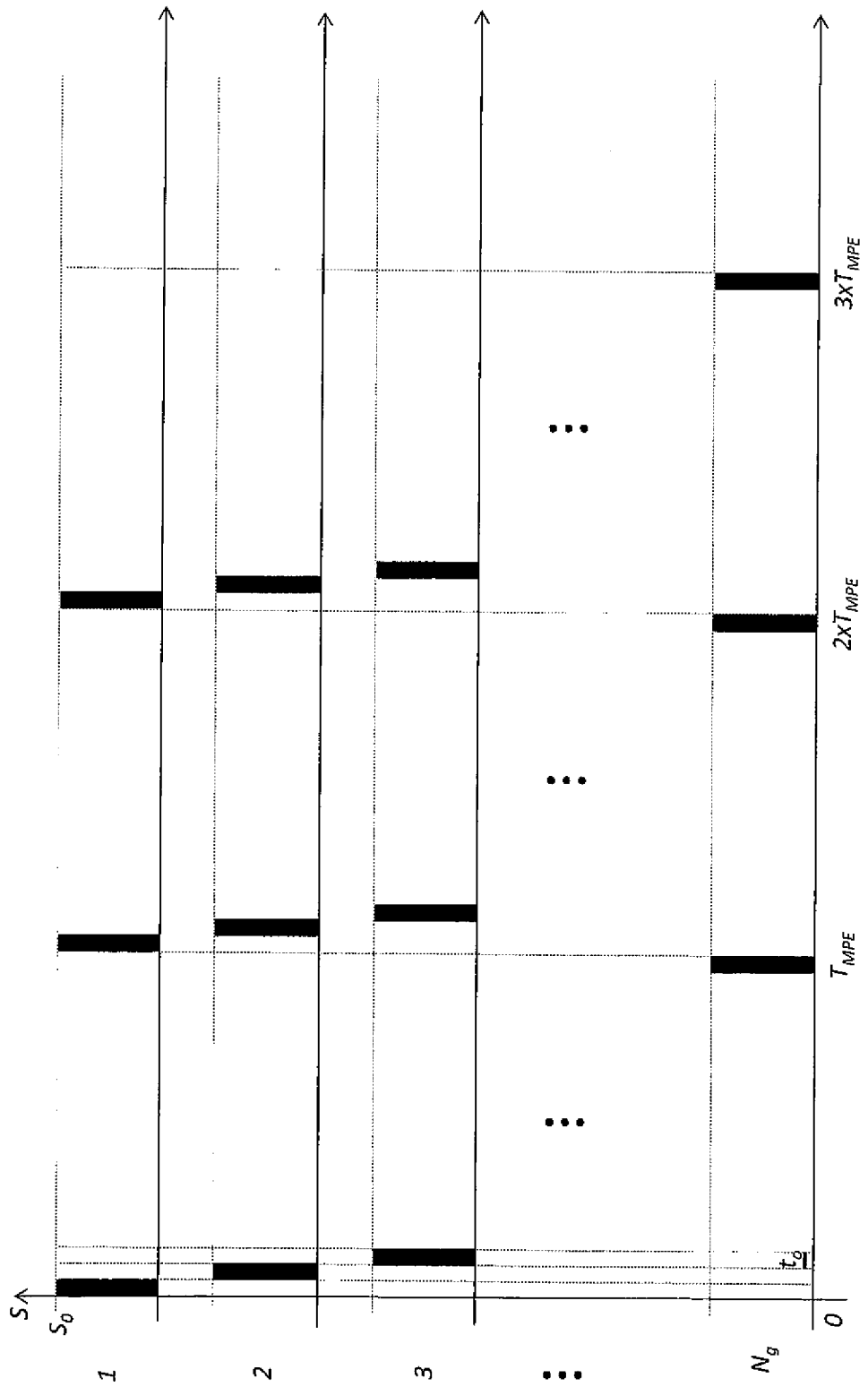

Fig. 24

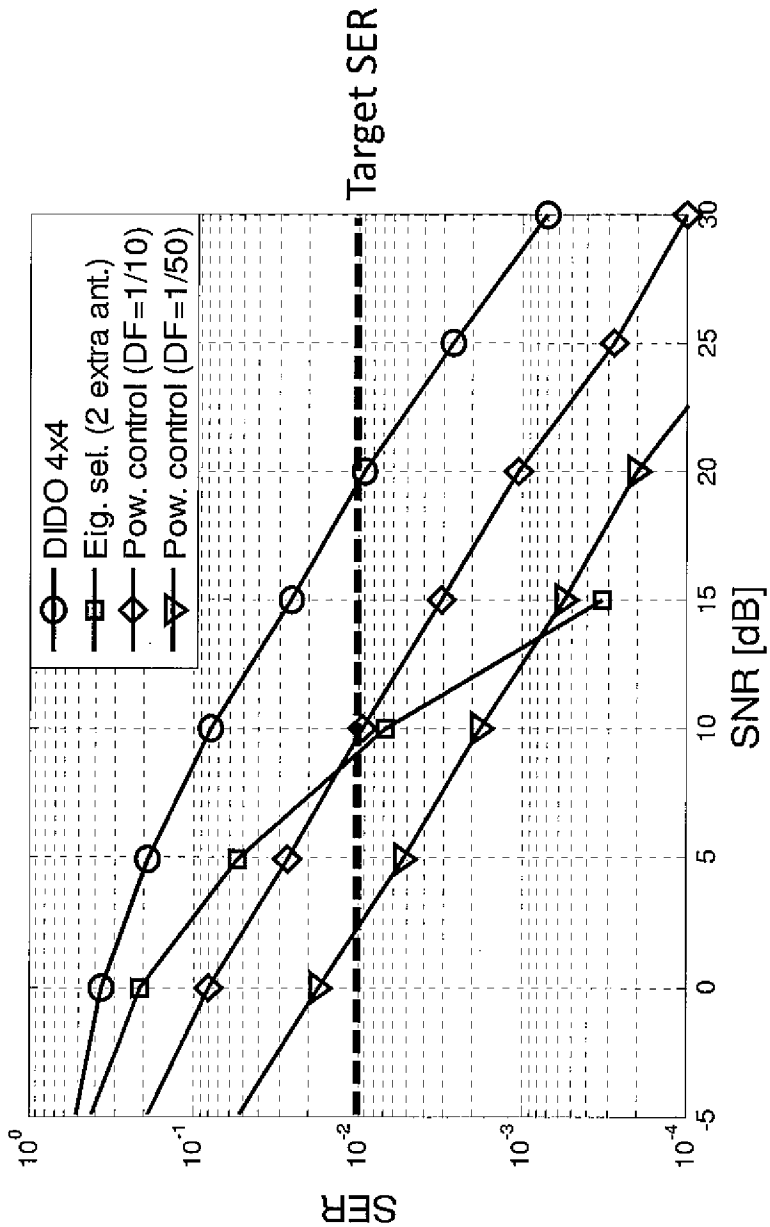
Target SER
DIDO 4x4
Eig. sel. (2 extra ant.)
Pow. control (DF=1/10)
Pow. control (DF=1/50)
SER
SNR [dB]
10^0
10^-1
10^-2
10^-3
10^-4
-5
0
5
10
15
20
25
30

Fig. 25

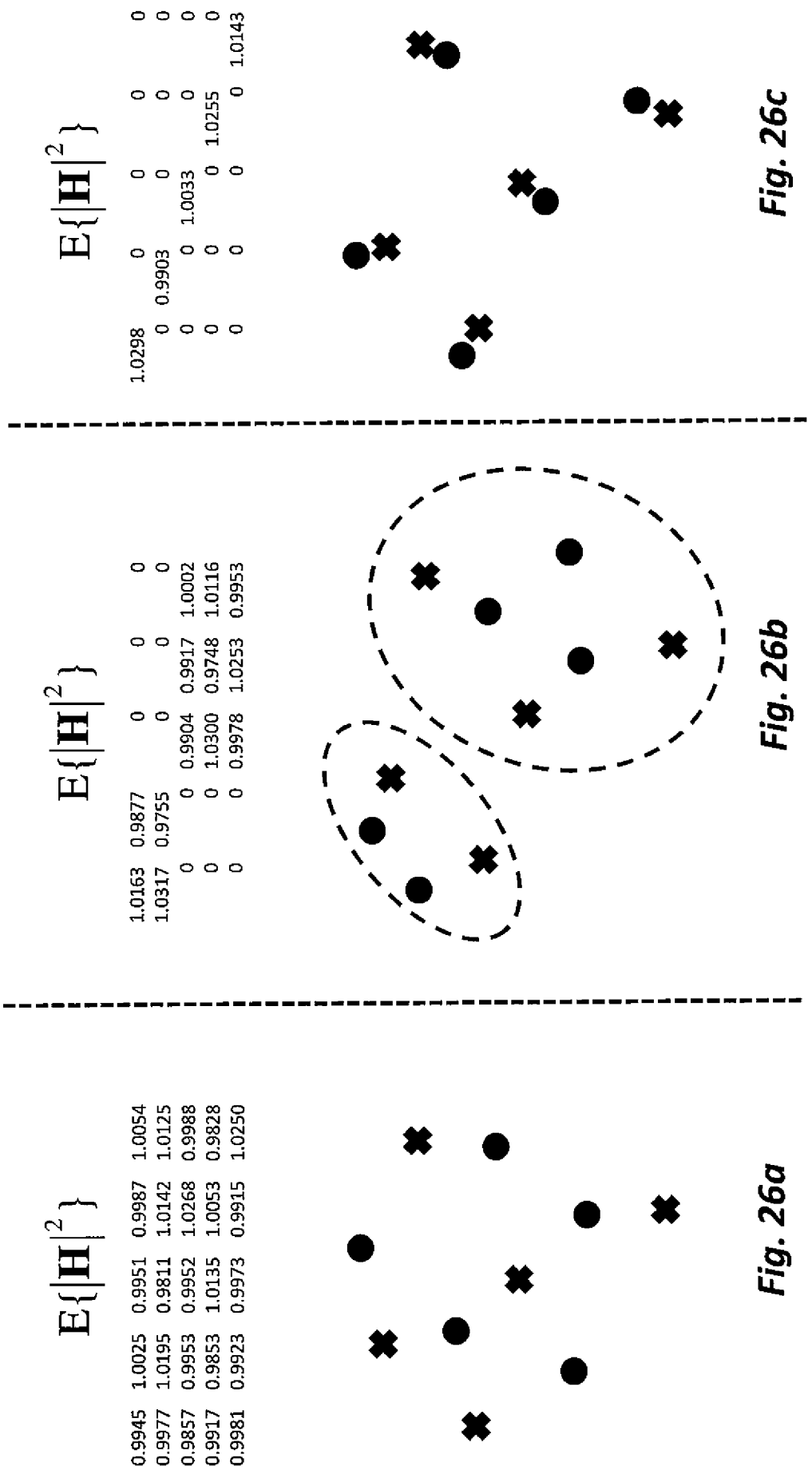

Fig. 26a

Fig. 26b

Fig. 26c

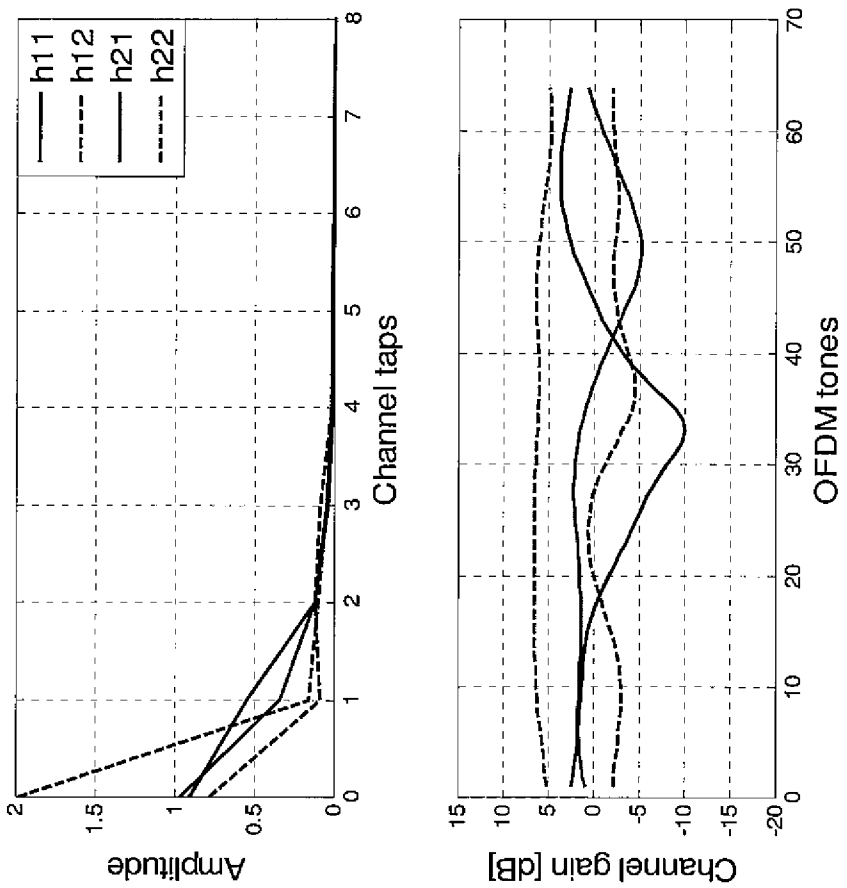
h11
h12
h21
h22
Amplitude
Channel taps
Channel gain [dB]
OFDM tones

Fig. 27

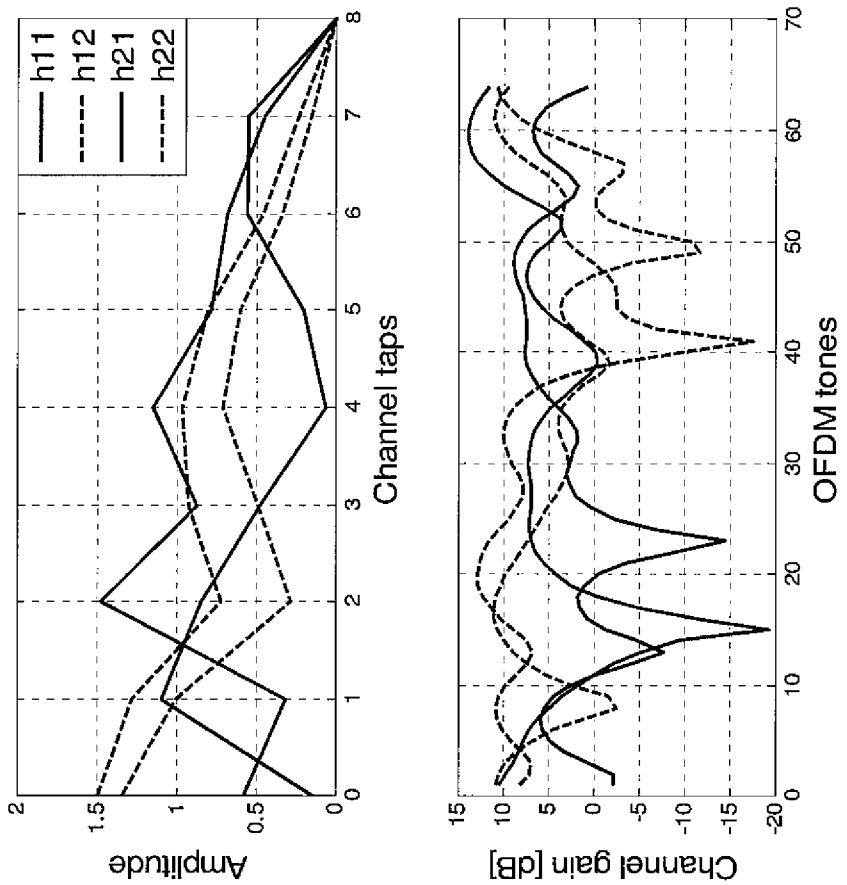
h11
h12
h21
h22
Amplitude
Channel taps
Channel gain [dB]
OFDM tones

Fig. 28

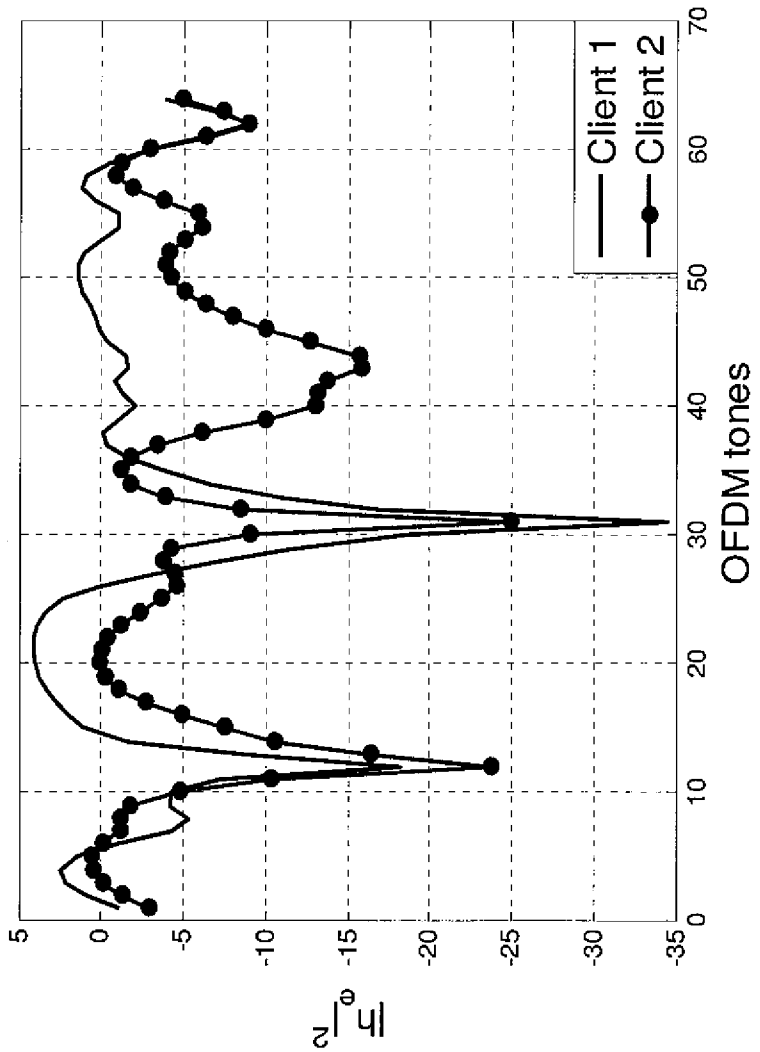
Client 1
Client 2
OFDM tones
$|h_\phi|^2$
5
0
-5
-10
-15
-20
-25
-30
-35
0
10
20
30
40
50
60
70

Fig. 29

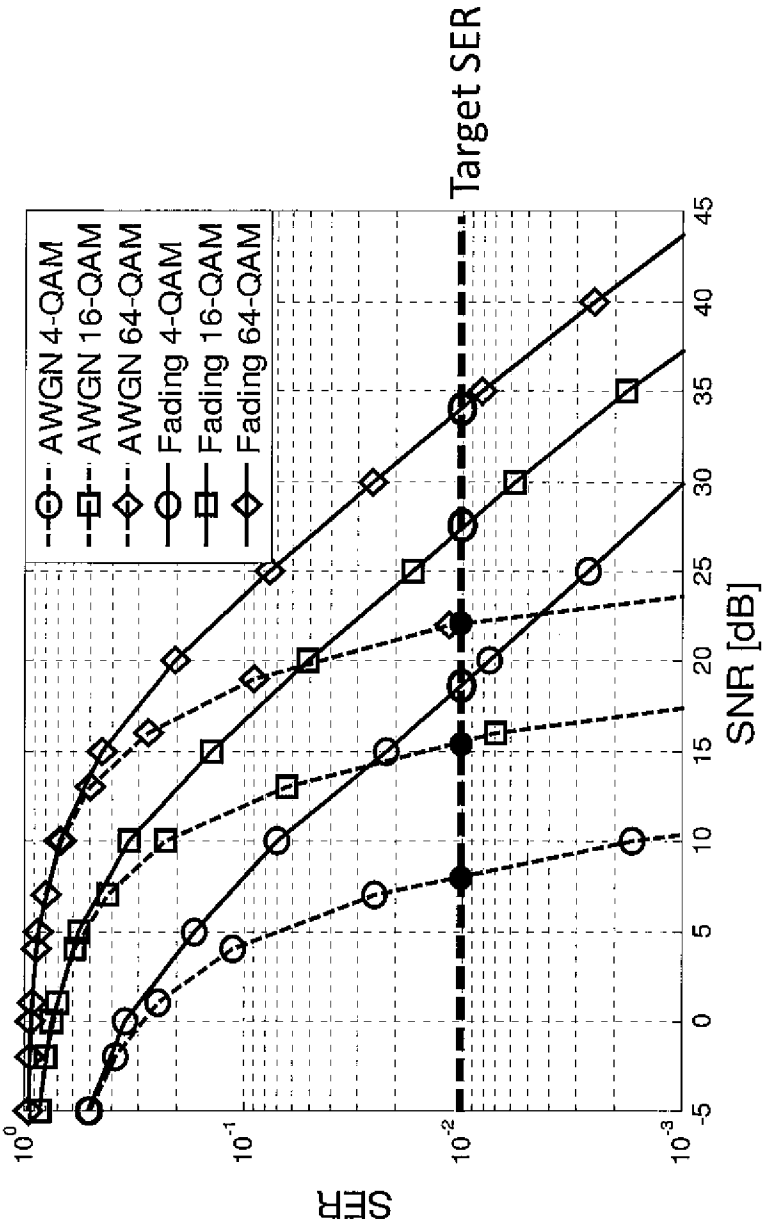
Target SER
AWGN 4-QAM
AWGN 16-QAM
AWGN 64-QAM
Fading 4-QAM
Fading 16-QAM
Fading 64-QAM
SER
SNR [dB]
10^0
10^-1
10^-2
10^-3
-5
0
5
10
15
20
25
30
35
40
45

Fig. 30

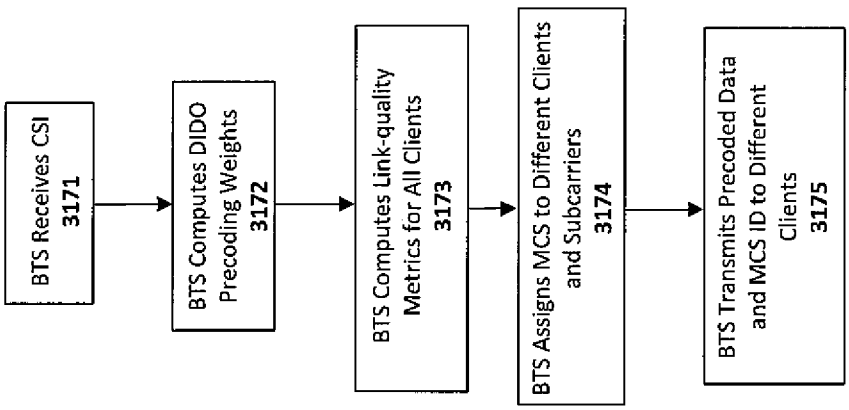
BTS Receives CSI
3171
BTS Computes DIDO Precoding Weights
3172
BTS Computes Link-quality Metrics for All Clients
3173
BTS Assigns MCS to Different Clients and Subcarriers
3174
BTS Transmits Precoded Data and MCS ID to Different Clients
3175

Fig. 31

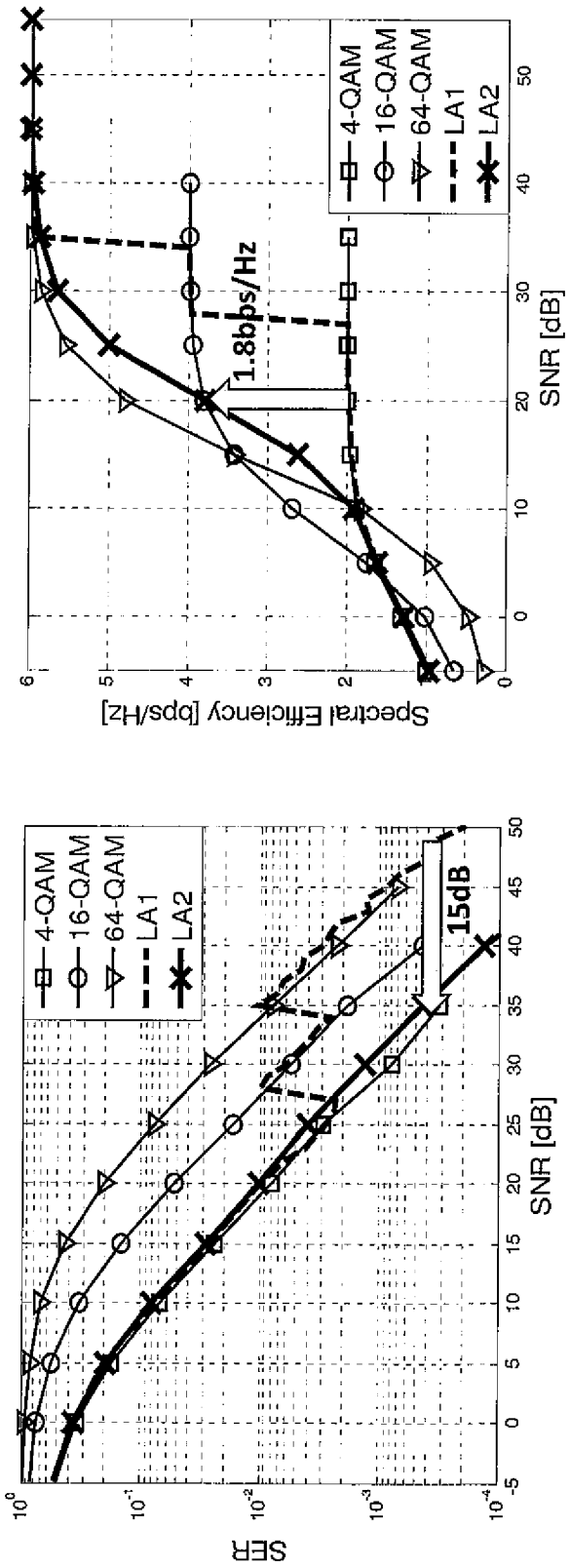
Spectral Efficiency [bps/Hz]
SNR [dB]
4-QAM
16-QAM
64-QAM
LA1
LA2
1.8bps/Hz
SER
SNR [dB]
4-QAM
16-QAM
64-QAM
LA1
LA2
15dB

Fig. 32

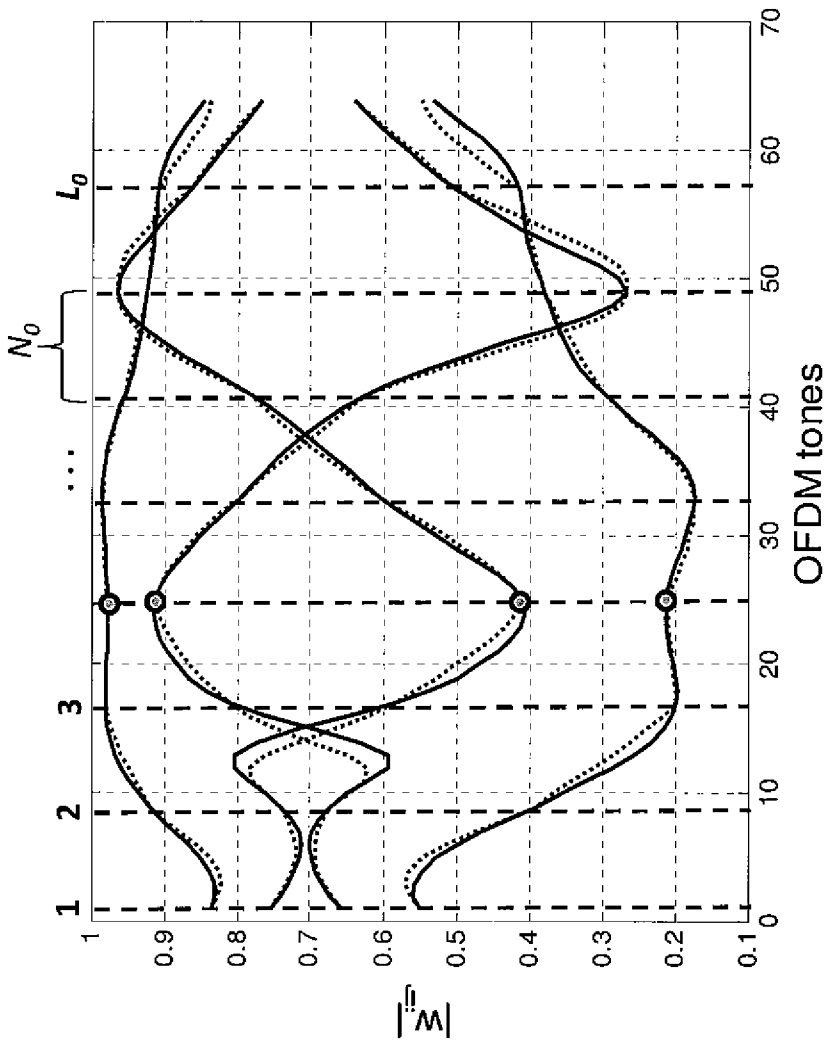
$|W_{ij}|$
1
0.9
0.8
0.7
0.6
0.5
0.4
0.3
0.2
0.1
0
10
20
30
40
50
60
70
OFDM tones
1
2
3
...
N_0
L_0

Fig. 33

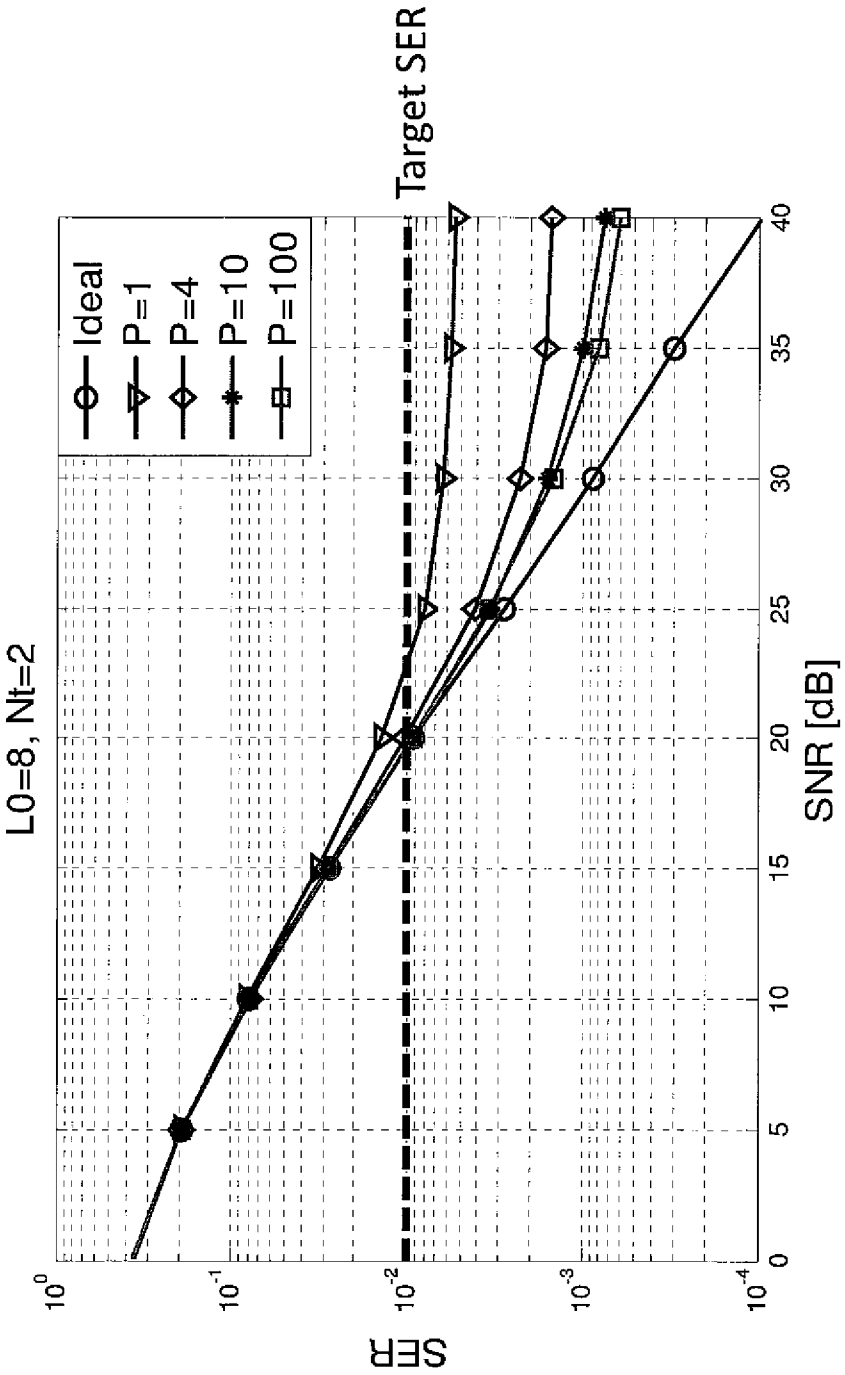
Target SER
Ideal
P=1
P=4
P=10
P=100
L0=8, Nt=2
SER
SNR [dB]
10^{0}
10^{-1}
10^{-2}
10^{-3}
10^{-4}
0
5
10
15
20
25
30
35
40

Fig. 34

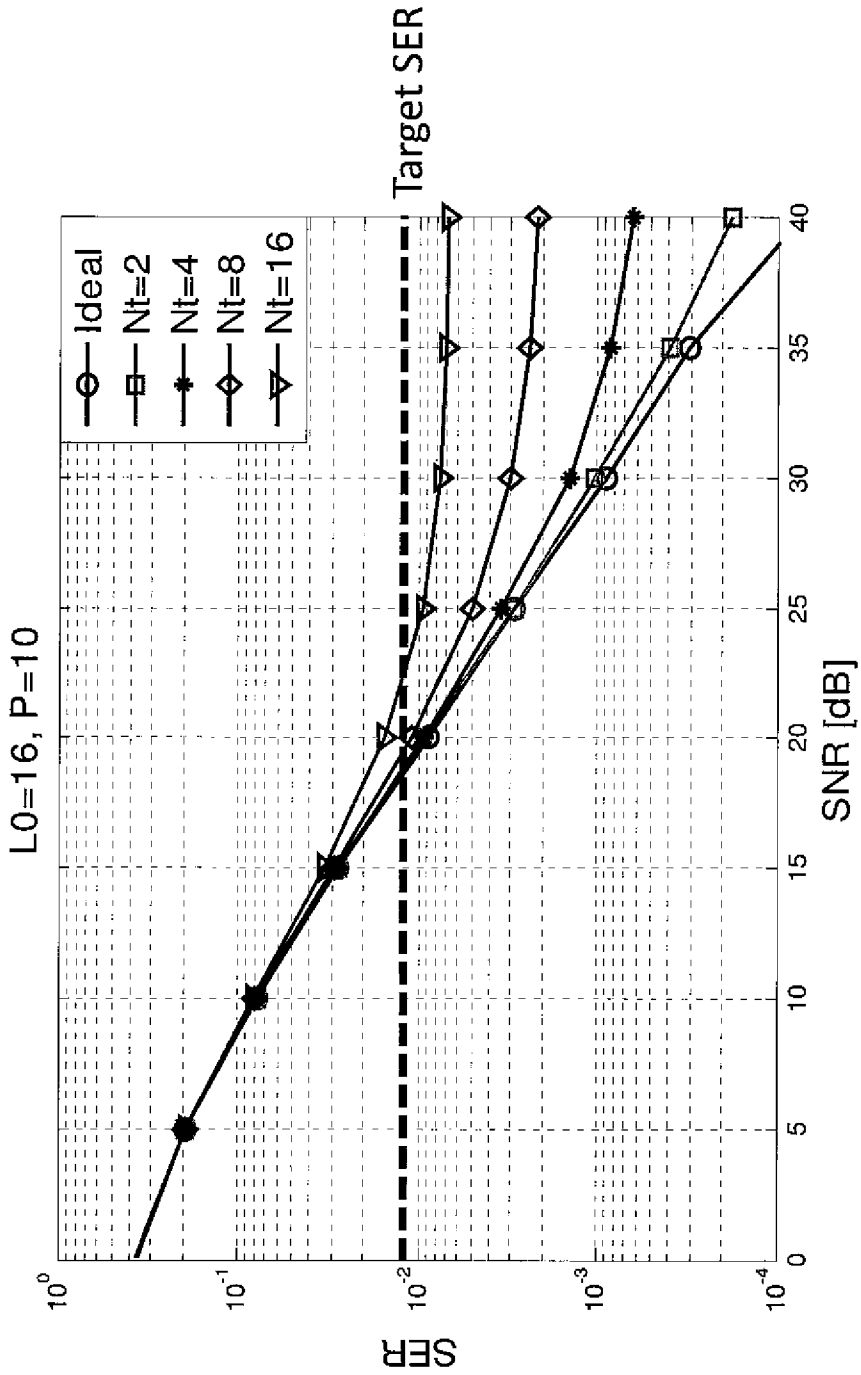
Target SER
Ideal
Nt=2
Nt=4
Nt=8
Nt=16
L0=16, P=10
SER
SNR [dB]
10^0
10^-1
10^-2
10^-3
10^-4
0
5
10
15
20
25
30
35
40

Fig. 35

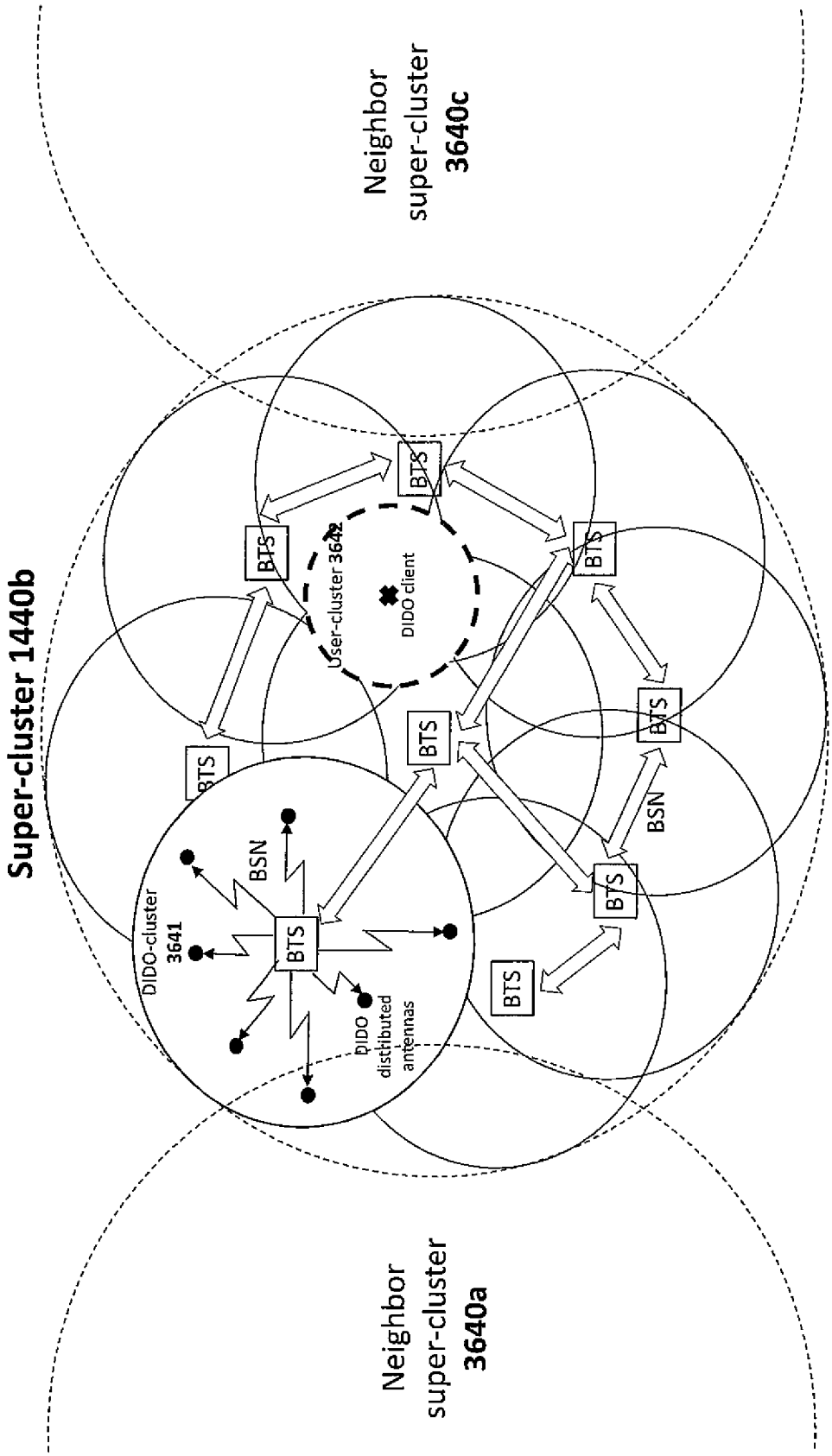
Neighbor super-cluster 3640c
Super-cluster 1440b
User-cluster 3642
DIDO client
BTS
BSN
DIDO-cluster 3641
DIDO distributed antennas
Neighbor super-cluster 3640a

Fig. 36

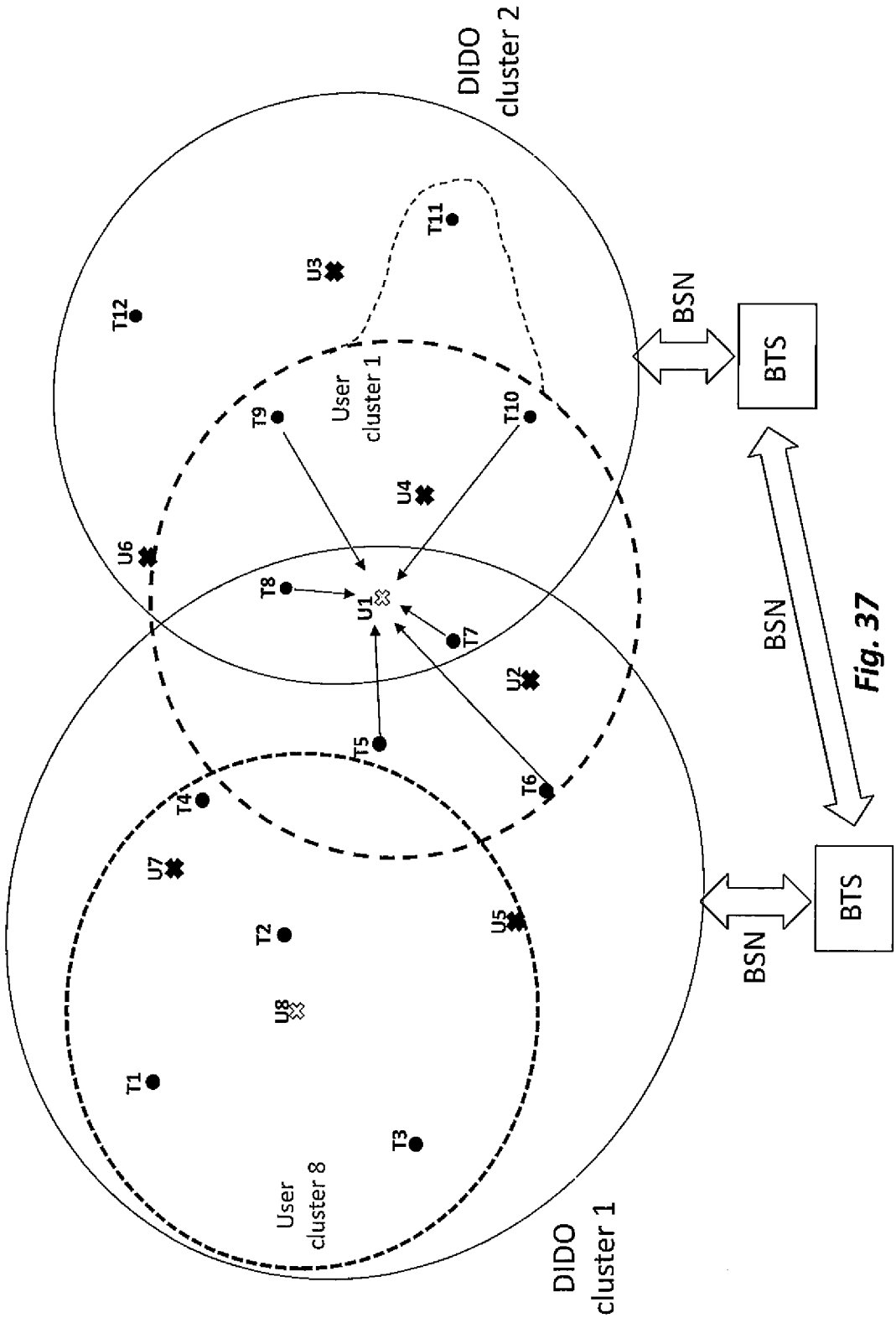
DIDO cluster 2
User cluster 1
User cluster 8
DIDO cluster 1
BSN
BTS
BSN
BTS
BSN
T1
T2
T3
T4
T5
T6
T7
T8
T9
T10
T11
T12
U1
U2
U3
U4
U5
U6
U7
U8

Fig. 37

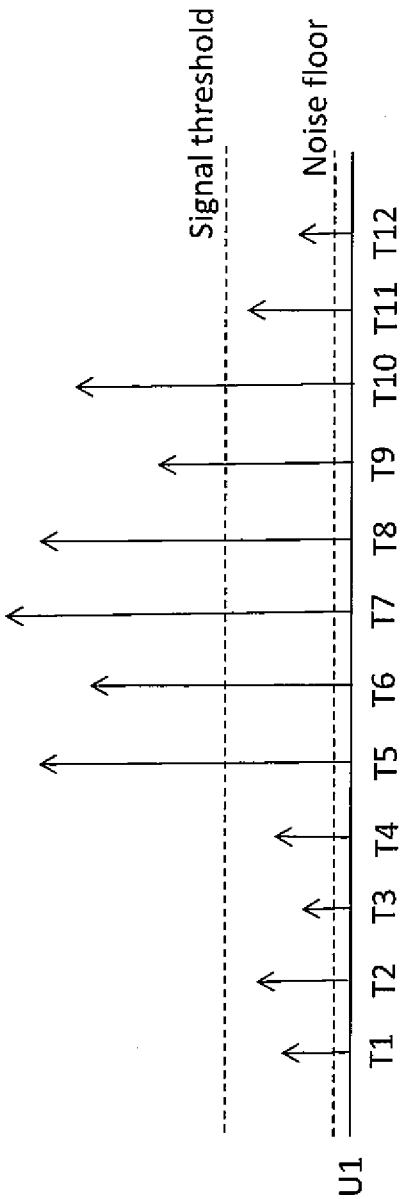

Fig. 38a

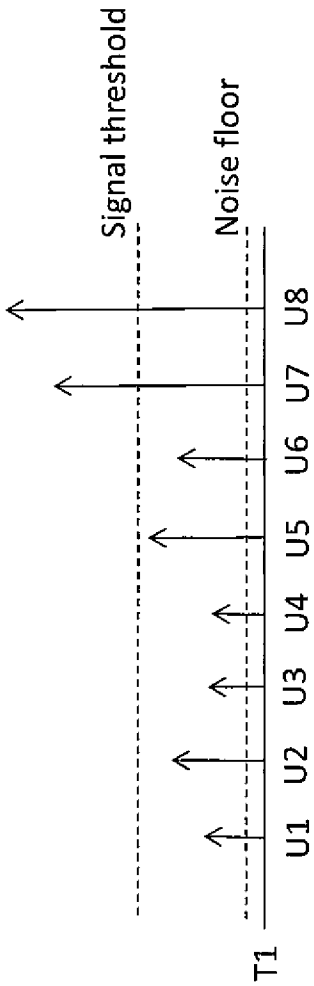

Fig. 38b

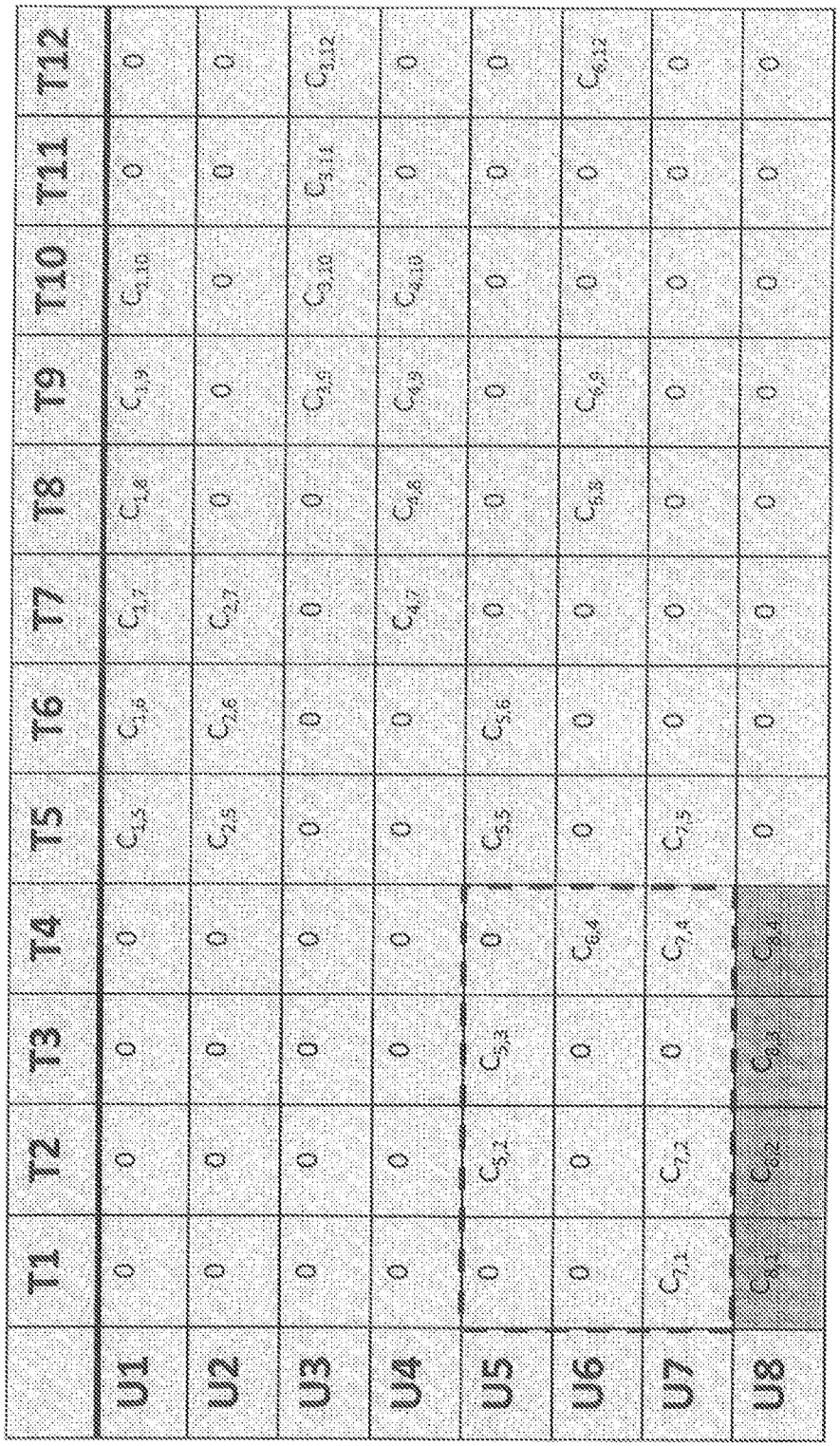

	T1	T2	T3	T4	T5	T6	T7	T8	T9	T10	T11	T12
U1	0	0	0	0	$C_{1,3}$	$C_{1,6}$	$C_{1,7}$	$C_{1,8}$	$C_{1,9}$	$C_{1,10}$	0	0
U2	0	0	0	0	$C_{2,5}$	$C_{2,6}$	$C_{2,7}$	0	0	0	0	0
U3	0	0	0	0	0	0	0	0	$C_{3,9}$	$C_{3,10}$	$C_{3,11}$	$C_{3,12}$
U4	0	0	0	0	0	0	$C_{4,7}$	$C_{4,8}$	$C_{4,9}$	$C_{4,10}$	0	0
U5	0	$C_{5,2}$	$C_{5,3}$	0	$C_{5,5}$	$C_{5,6}$	0	0	0	0	0	0
U6	0	0	0	$C_{6,4}$	0	0	0	$C_{6,8}$	$C_{6,9}$	0	0	$C_{6,12}$
U7	$C_{7,1}$	$C_{7,2}$	0	$C_{7,4}$	$C_{7,5}$	0	0	0	0	0	0	0
U8	$C_{8,1}$	$C_{8,2}$	$C_{8,3}$	$C_{8,4}$	0	0	0	0	0	0	0	0

Fig. 39

	T1	T2	T3	T4	T5	T6	T7	T8	T9	T10	T11	T12
U1	0	0	0	0	$C_{1,5}$	$C_{1,6}$	$C_{1,7}$	$C_{1,8}$	$C_{1,9}$	$C_{1,10}$	0	0
U2	0	0	0	0	$C_{2,5}$	$C_{2,6}$	$C_{2,7}$	0	0	0	0	0
U3	0	0	0	0	0	0	0	0	$C_{3,9}$	$C_{3,10}$	$C_{3,11}$	$C_{3,12}$
U4	0	0	0	0	0	0	$C_{4,7}$	$C_{4,8}$	$C_{4,9}$	$C_{4,10}$	0	0
U5	0	$C_{5,2}$	$C_{5,3}$	0	$C_{5,5}$	$C_{5,6}$	0	0	0	0	0	0
U6	0	0	0	$C_{6,4}$	0	0	0	$C_{6,8}$	$C_{6,9}$	0	0	$C_{6,12}$
U7	$C_{7,1}$	$C_{7,2}$	0	$C_{7,4}$	$C_{7,5}$	0	0	0	0	0	0	0
U8	$C_{8,1}$	$C_{8,2}$	$C_{8,3}$	$C_{8,4}$	0	0	0	0	0	0	0	0

Fig. 40

	T1	T2	T3	T4	T5	T6	T7	T8	T9	T10	T11	T12
U1	0	0	0	0	$C_{3,5}$	$C_{3,6}$	$C_{3,7}$	$C_{1,8}$	$C_{1,9}$	$C_{1,10}$	0	0
U2	0	0	0	0	$C_{2,5}$	$C_{2,6}$	$C_{2,7}$	0	0	0	0	0
U3	0	0	0	0	0	0	0	0	$C_{3,9}$	$C_{3,10}$	$C_{3,11}$	$C_{3,12}$
U4	0	0	0	0	0	0	$C_{4,7}$	$C_{4,8}$	$C_{4,9}$	$C_{4,10}$	0	0
U5	0	$C_{5,2}$	$C_{5,3}$	0	$C_{5,5}$	$C_{5,6}$	0	0	0	0	0	0
U6	0	0	0	$C_{6,4}$	0	0	0	$C_{6,8}$	$C_{6,9}$	0	0	$C_{6,12}$
U7	$C_{7,1}$	$C_{7,2}$	0	$C_{7,4}$	$C_{7,5}$	0	0	0	0	0	0	0
U8	$C_{8,1}$	$C_{8,2}$	$C_{8,3}$	$C_{8,4}$	0	0	0	0	0	0	0	0

Fig. 41

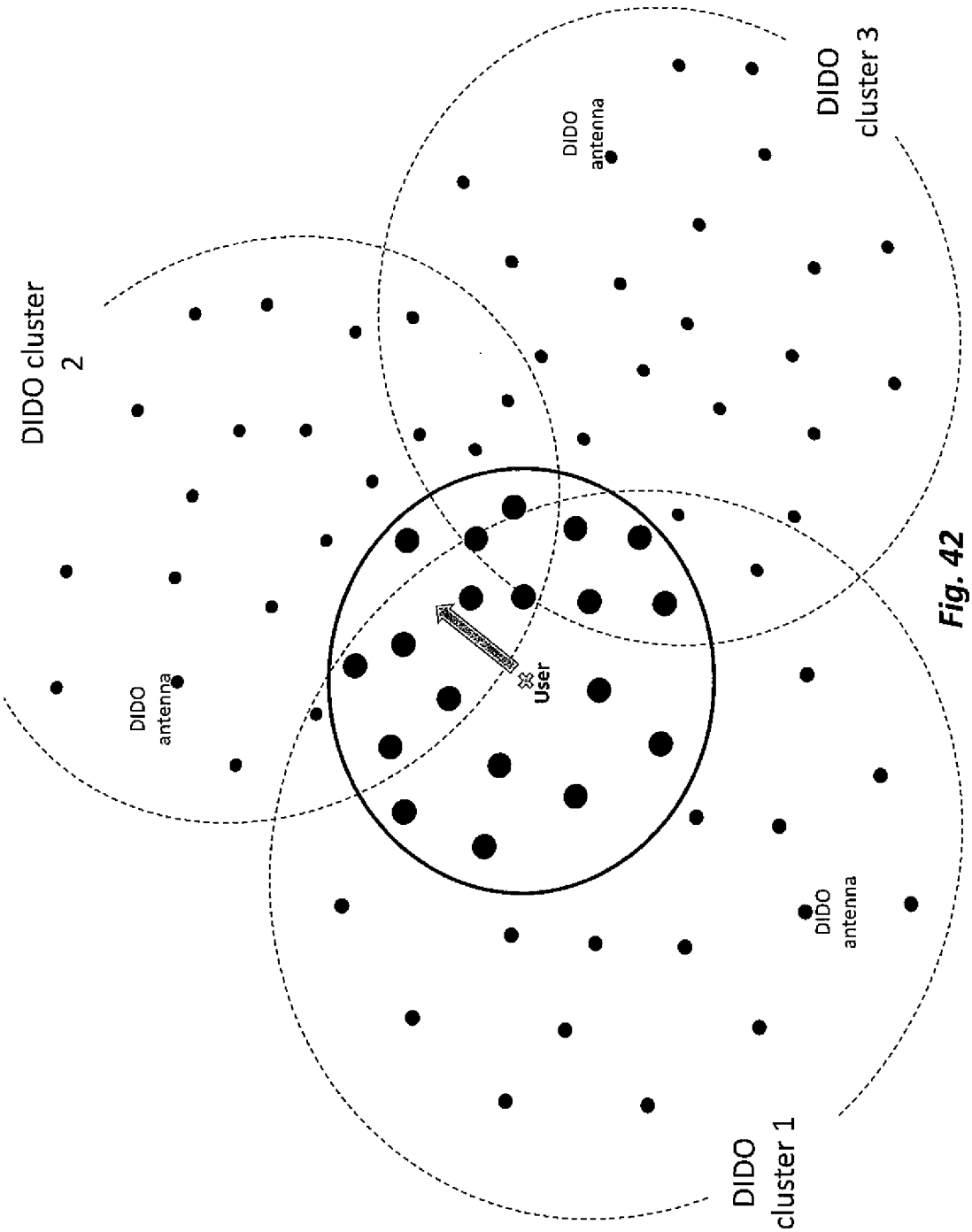
DIDO cluster 2
DIDO cluster 3
DIDO cluster 1
DIDO antenna
DIDO antenna
DIDO antenna
User

Fig. 42

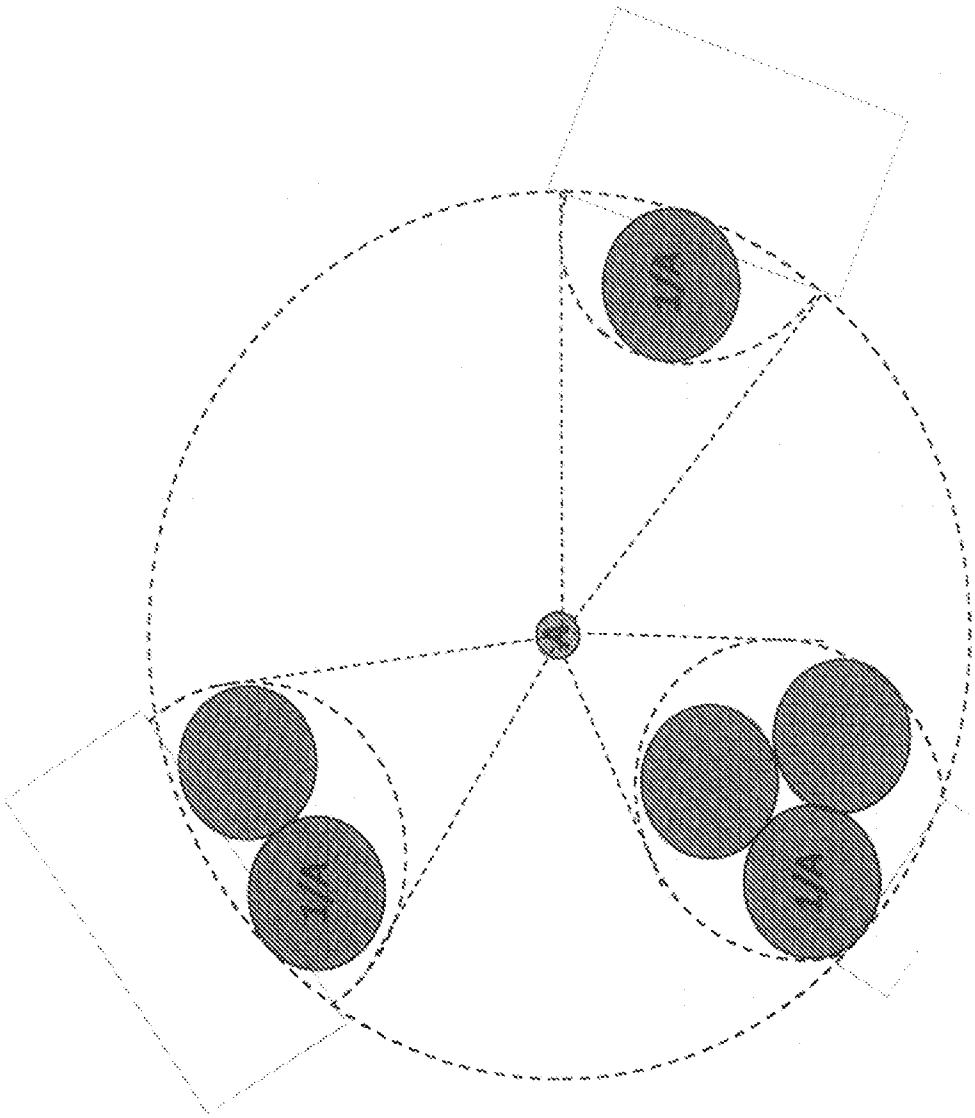

Fig. 43

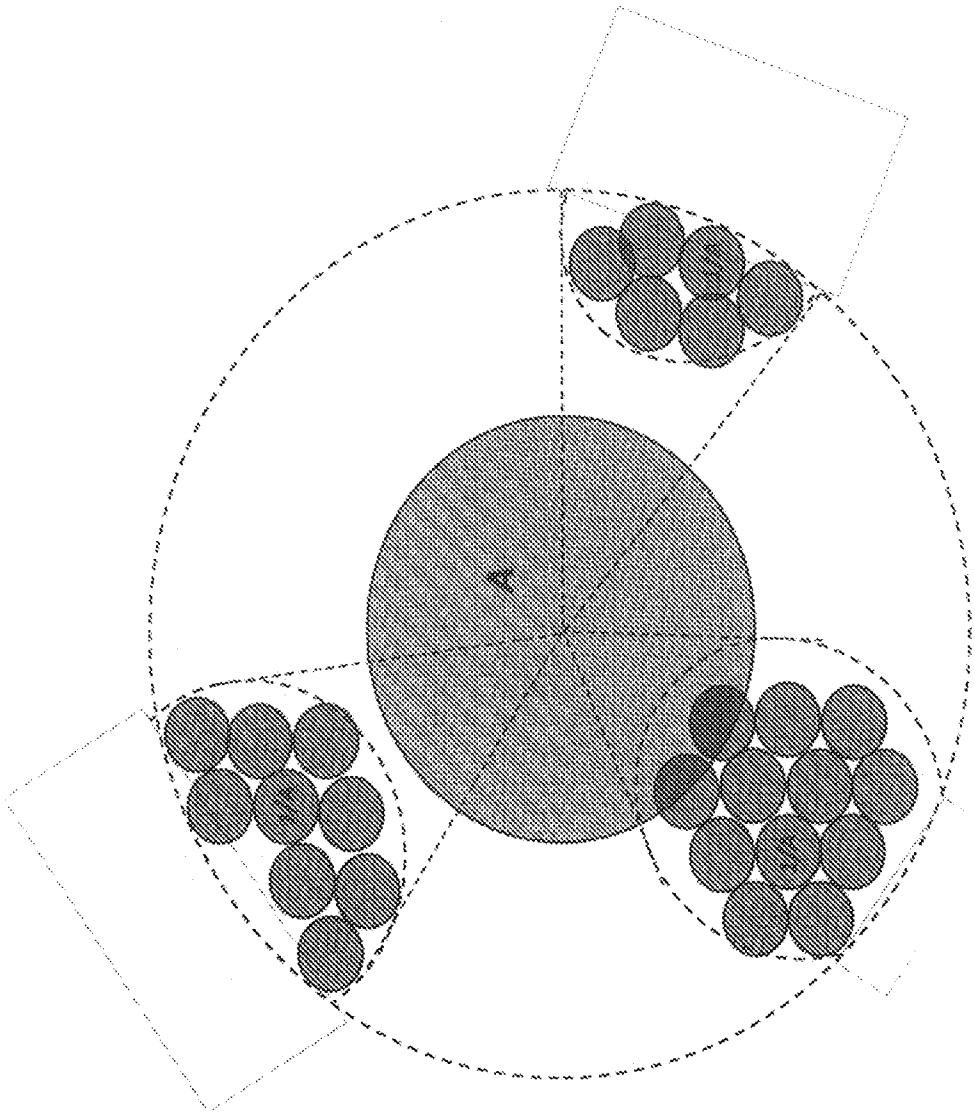

Fig. 44

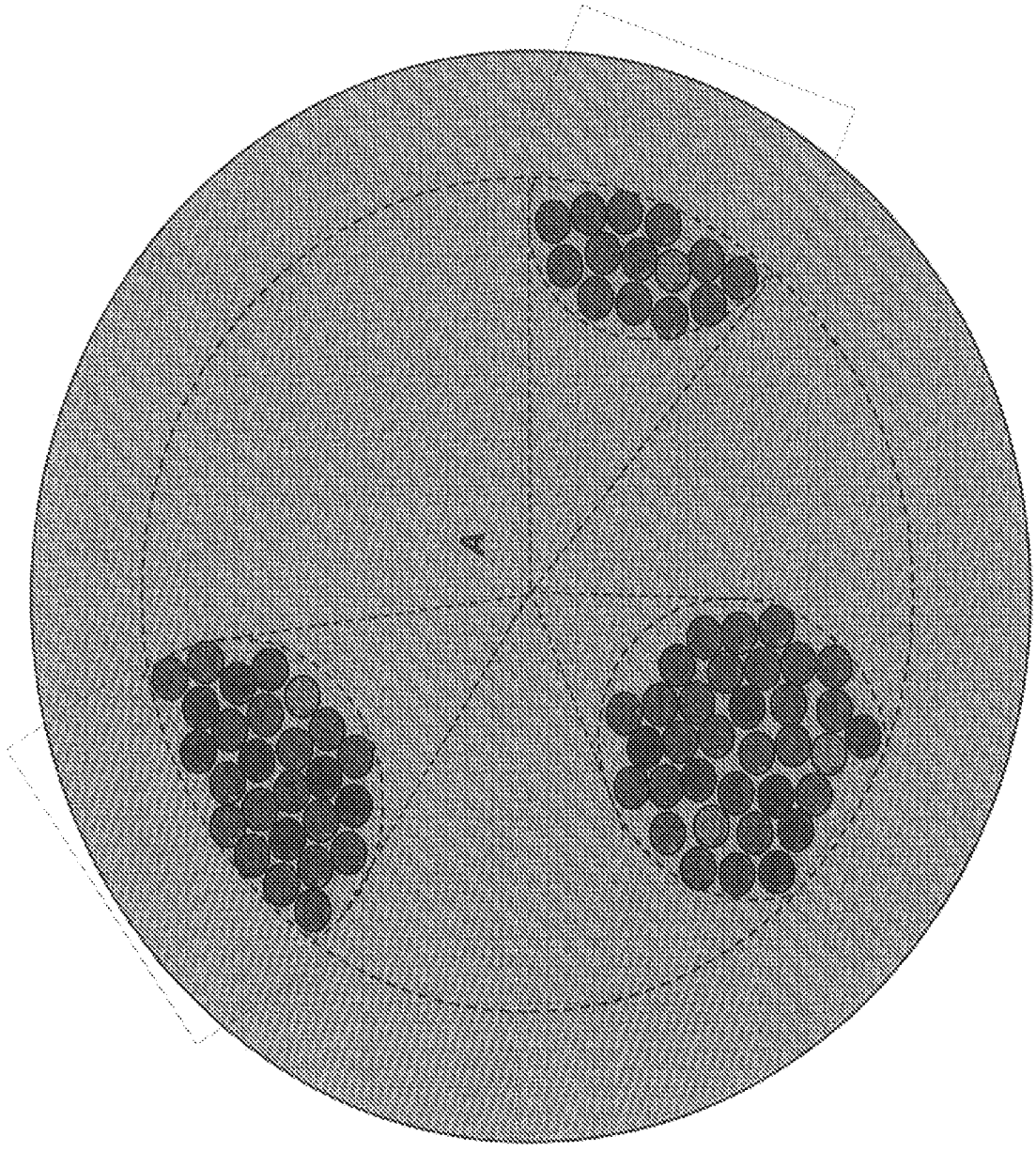

Fig. 45

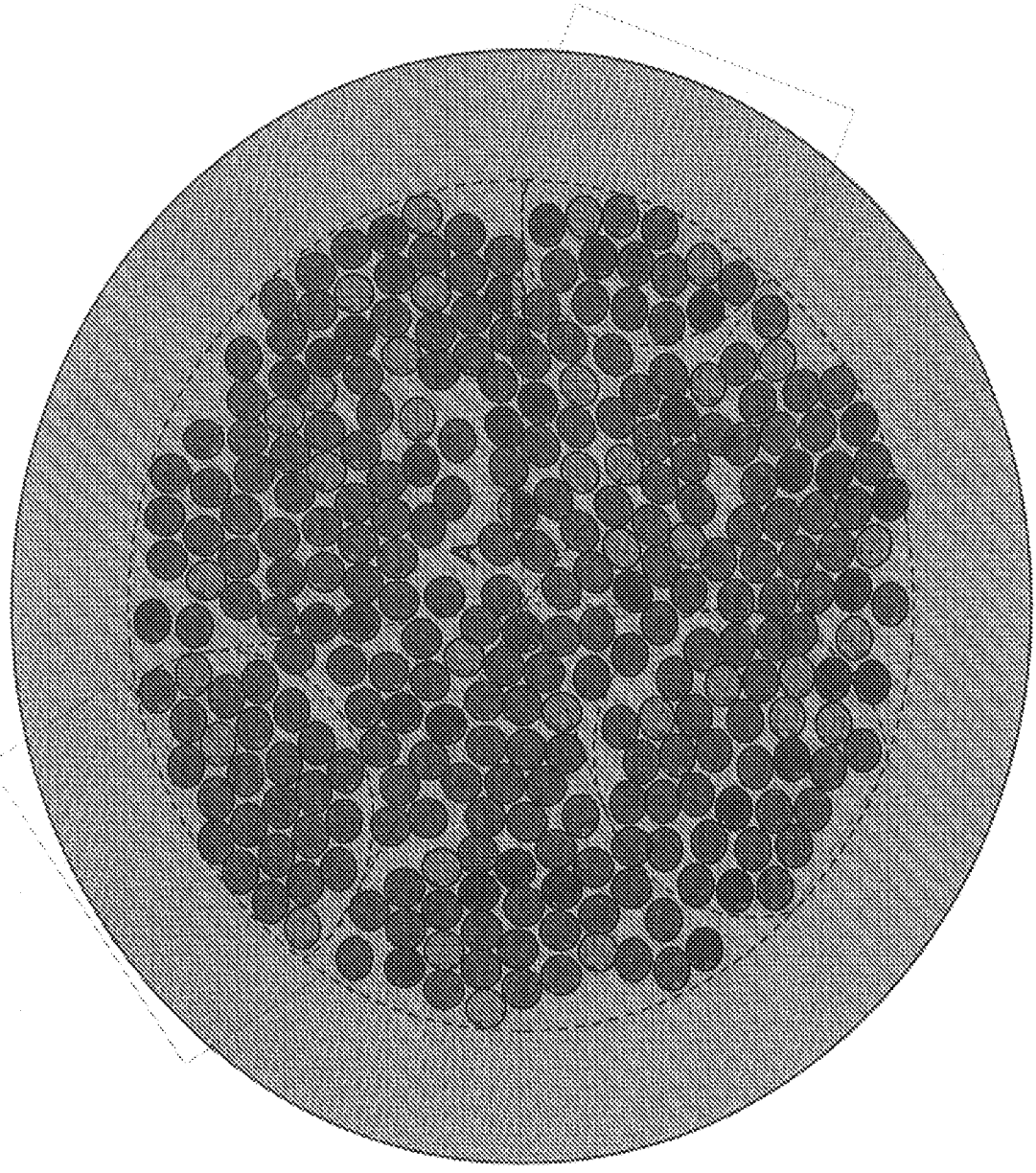

Fig. 46

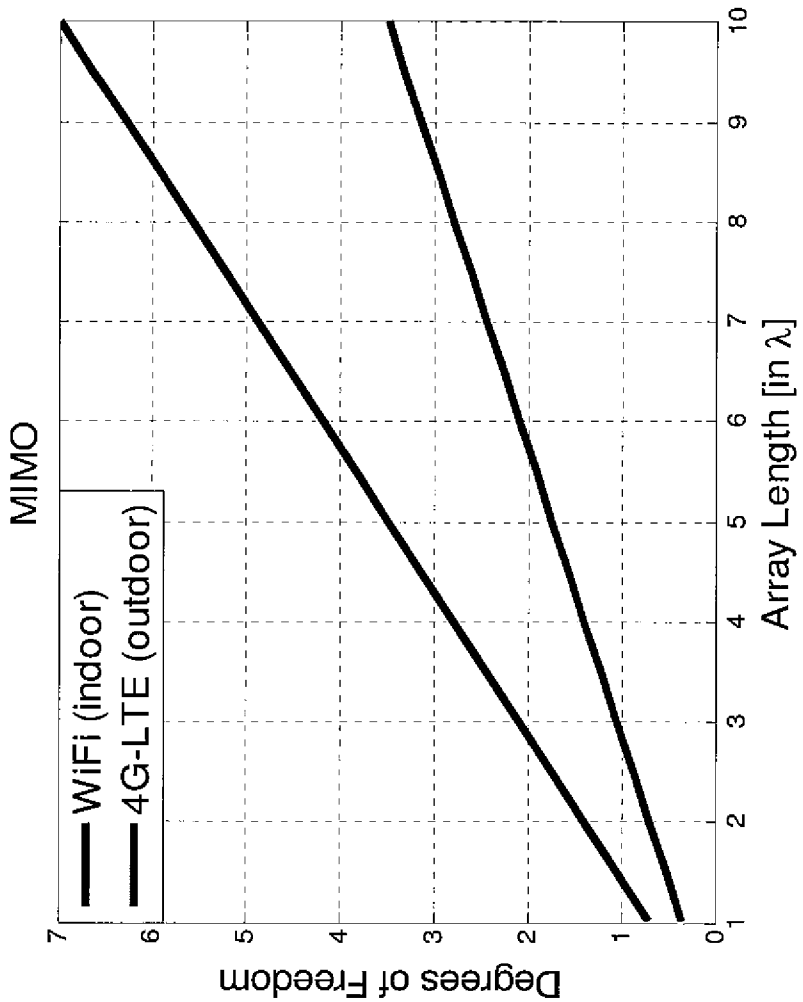
MIMO
WiFi (indoor)
4G-LTE (outdoor)
Degrees of Freedom
Array Length [in λ]
0
1
2
3
4
5
6
7
1
2
3
4
5
6
7
8
9
10

Fig. 47

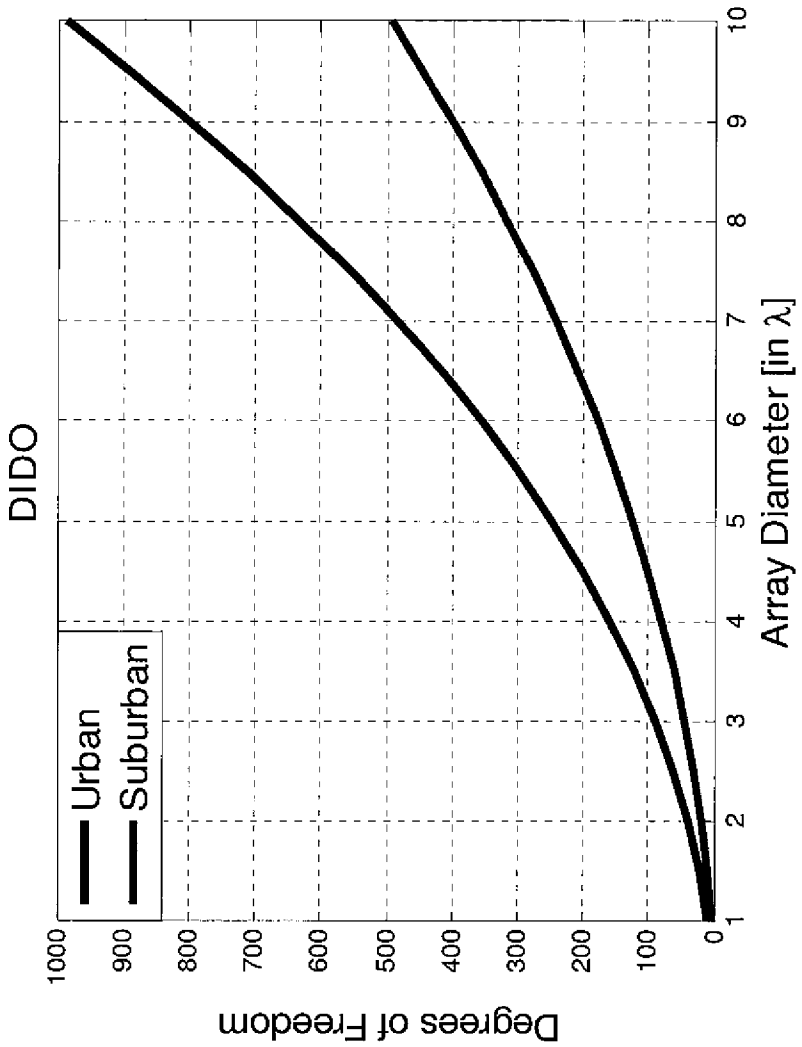
DIDO
Urban
Suburban
Degrees of Freedom
Array Diameter [in λ]
0
100
200
300
400
500
600
700
800
900
1000
1
2
3
4
5
6
7
8
9
10

Fig. 48

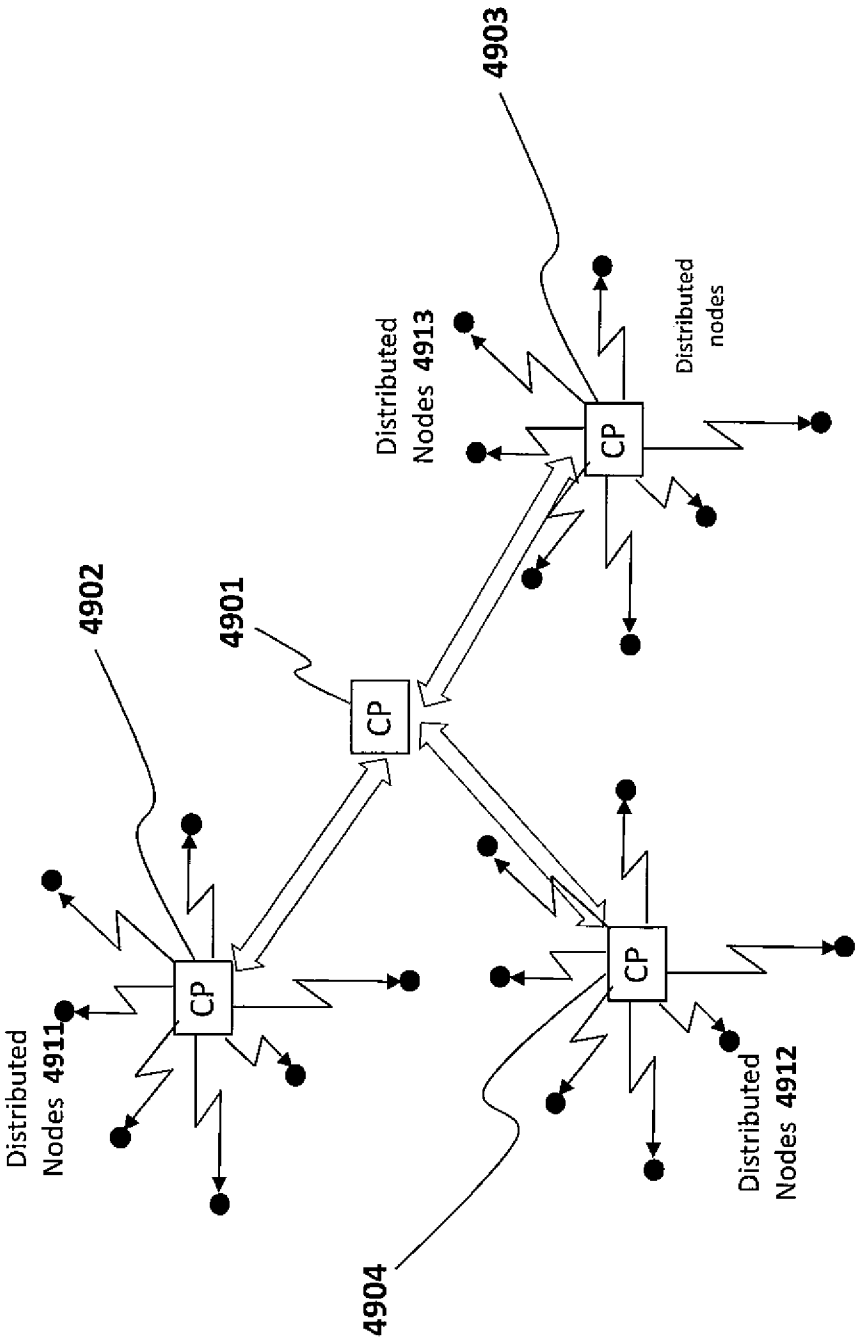
4903
Distributed
Nodes 4913
Distributed
nodes
CP
4902
4901
CP
CP
Distributed
Nodes 4911
Distributed
Nodes 4912
4904

Fig. 49

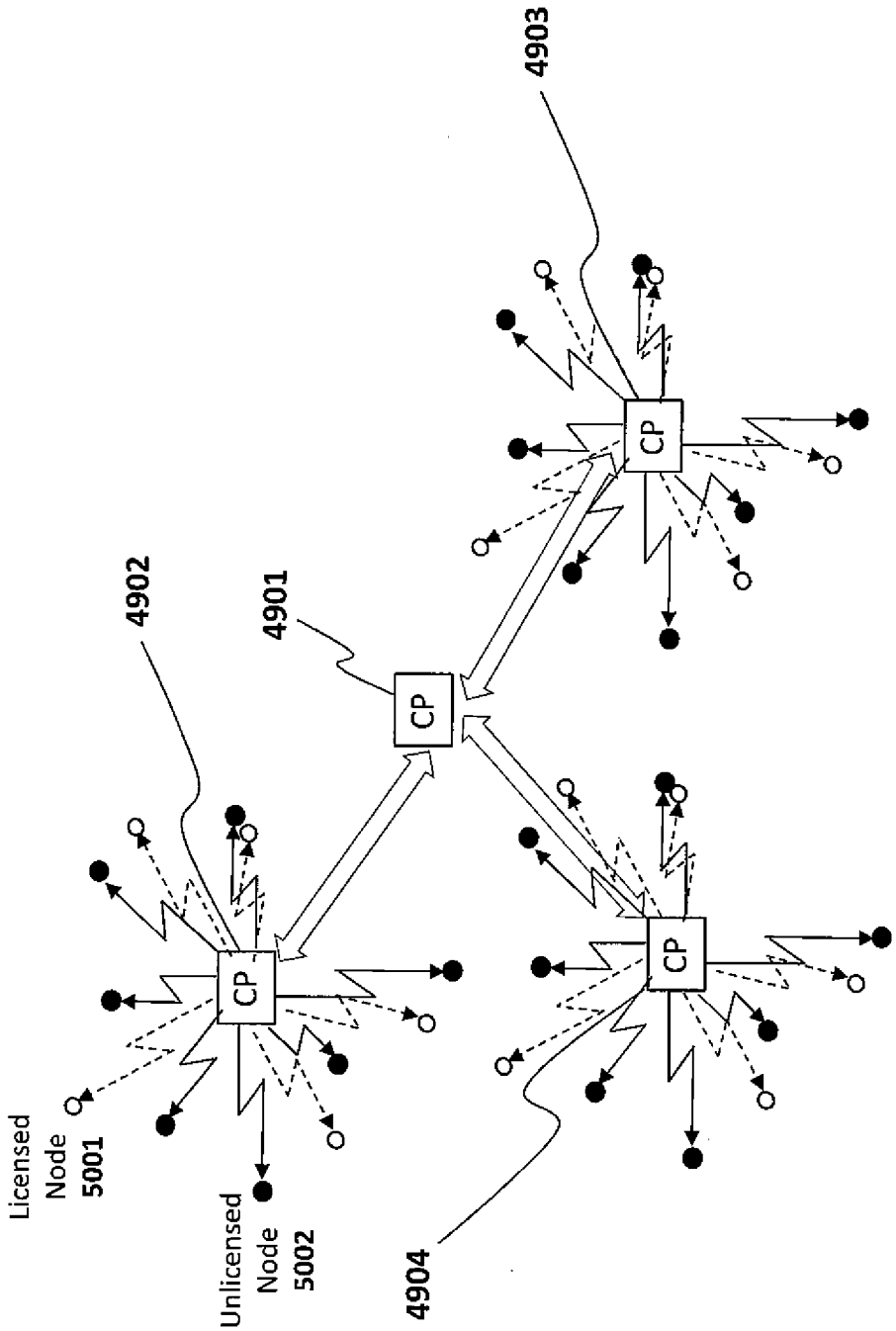
4903
4902
4901
CP
CP
CP
CP
Licensed Node 5001
Unlicensed Node 5002
4904

Fig. 50

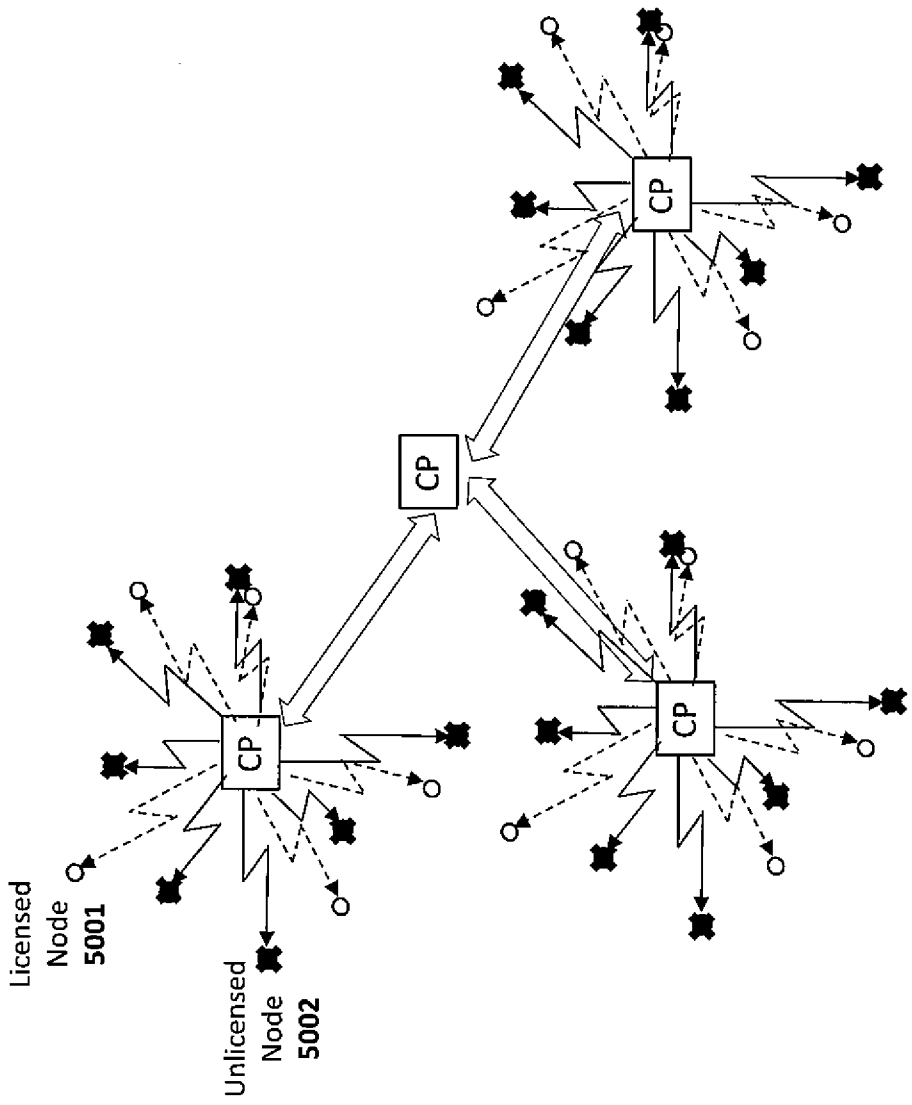

Fig. 51

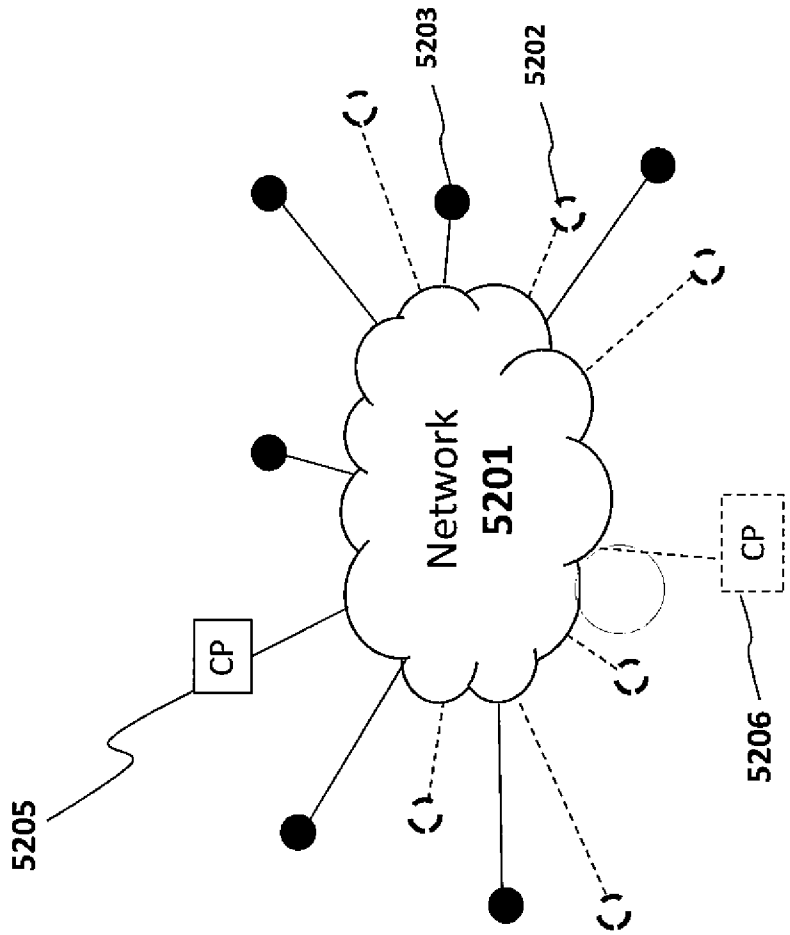

Fig. 52

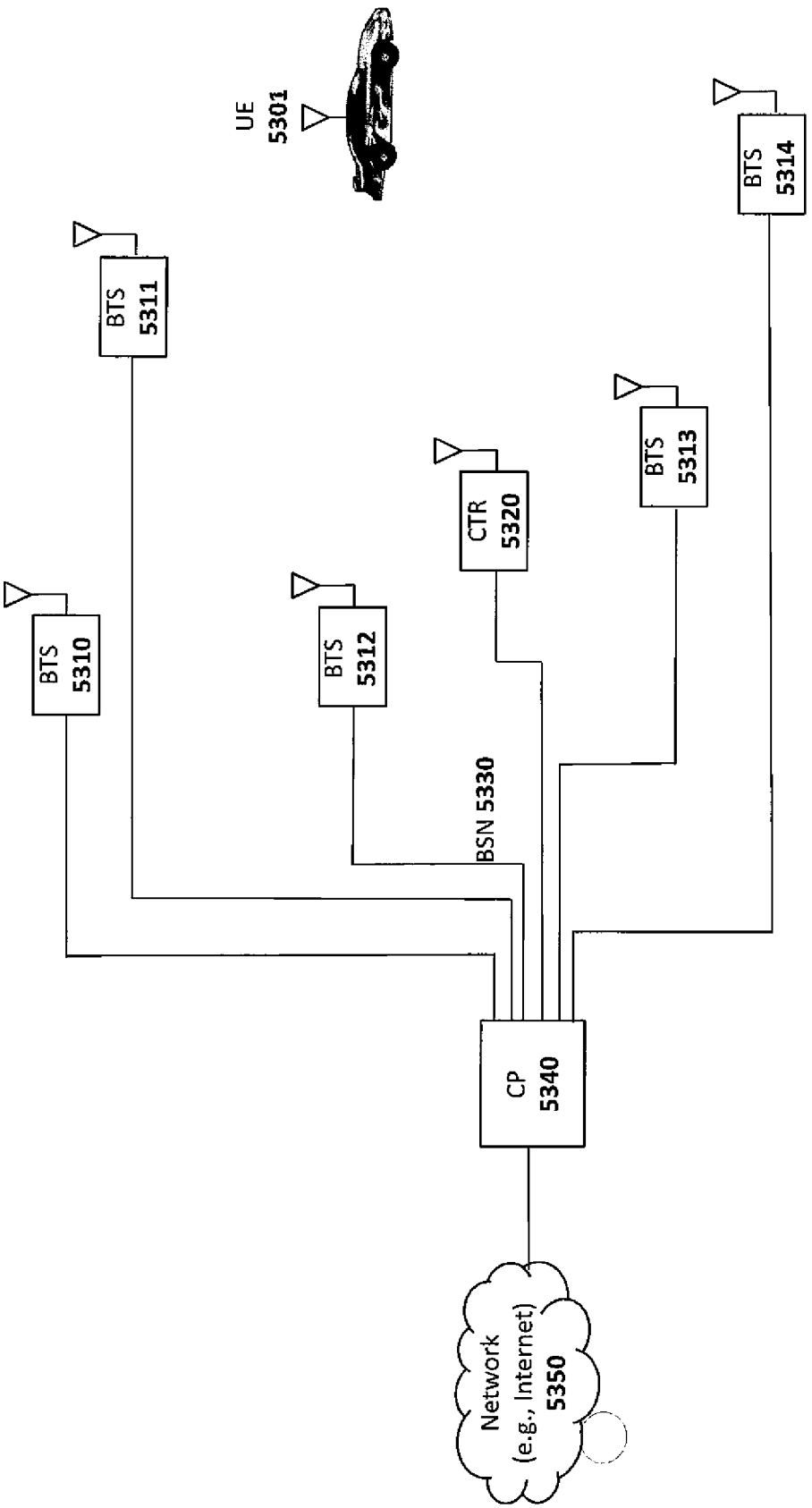
UE
5301
BTS
5311
BTS
5314
BTS
5313
CTR
5320
BTS
5310
BTS
5312
BSN 5330
CP
5340
Network
(e.g., Internet)
5350

Fig. 53

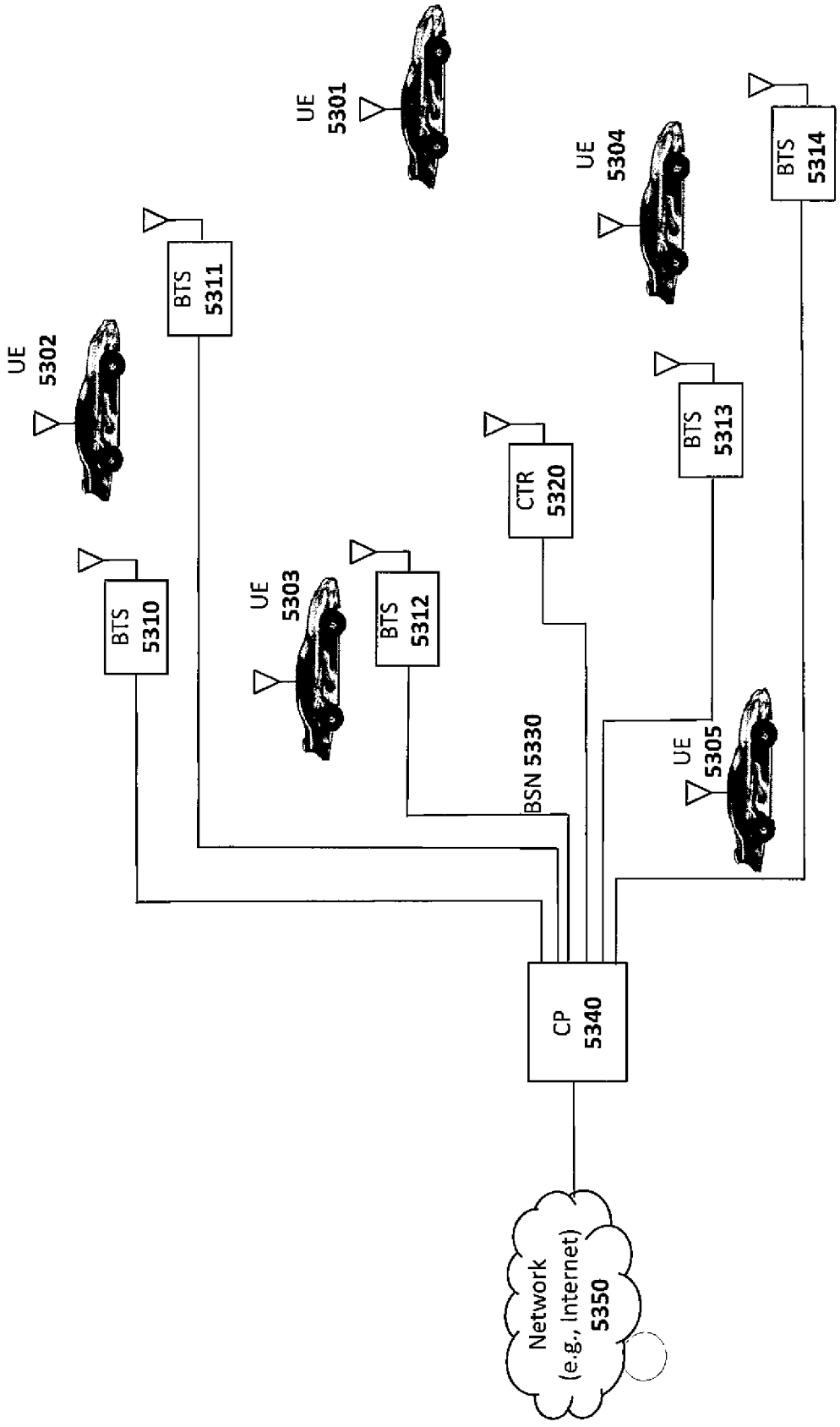
UE 5301
UE 5302
UE 5303
UE 5304
UE 5305
BTS 5310
BTS 5311
BTS 5312
BTS 5313
BTS 5314
CTR 5320
BSN 5330
CP 5340
Network (e.g., Internet) 5350

Fig. 54

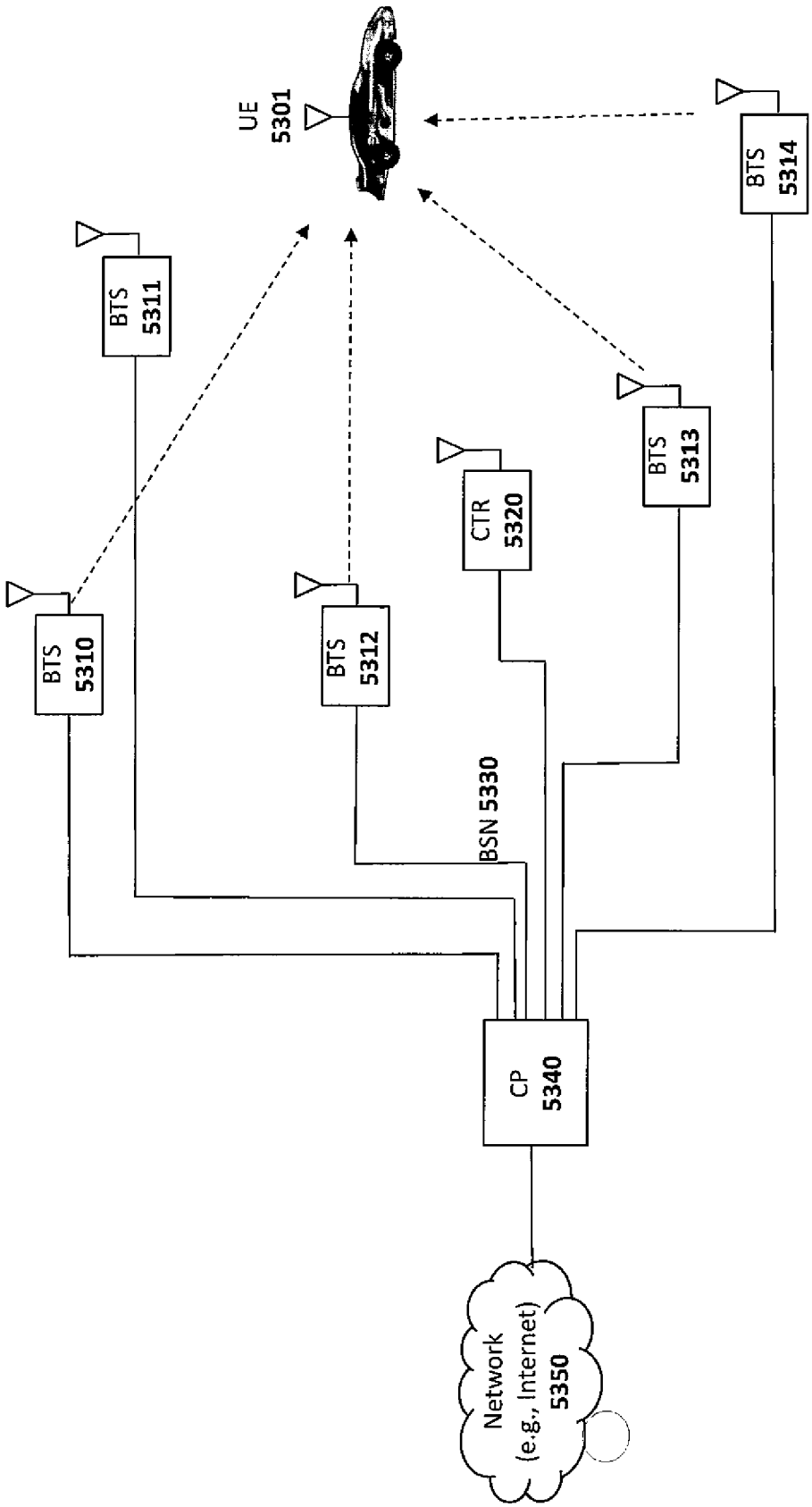
UE
5301
BTS
5310
BTS
5311
BTS
5312
CTR
5320
BTS
5313
BTS
5314
BSN 5330
CP
5340
Network
(e.g., Internet)
5350

Fig. 55

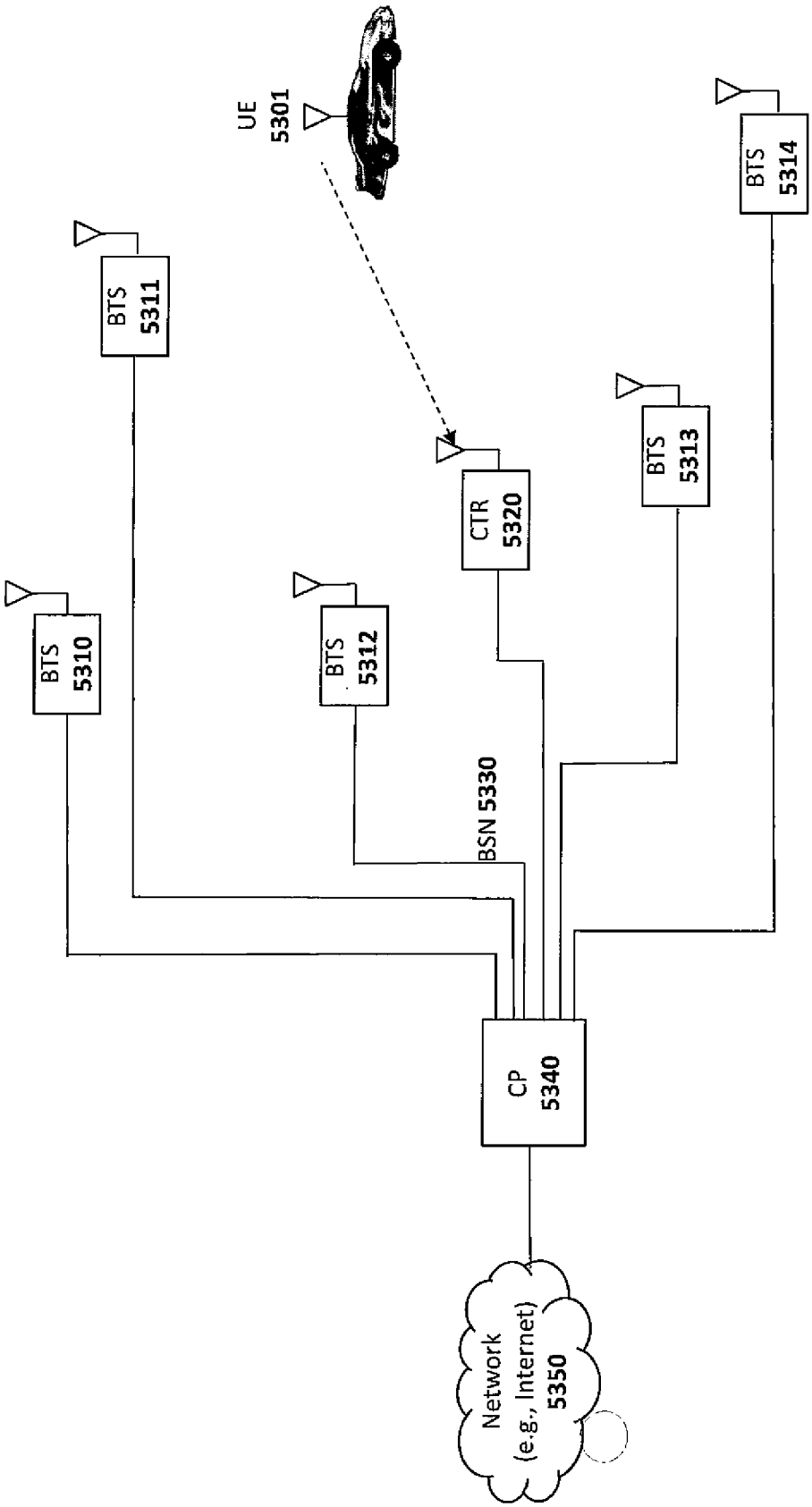
UE
5301
BTS
5311
BTS
5314
CTR
5320
BTS
5313
BTS
5310
BTS
5312
BSN 5330
CP
5340
Network
(e.g., Internet)
5350

Fig. 56

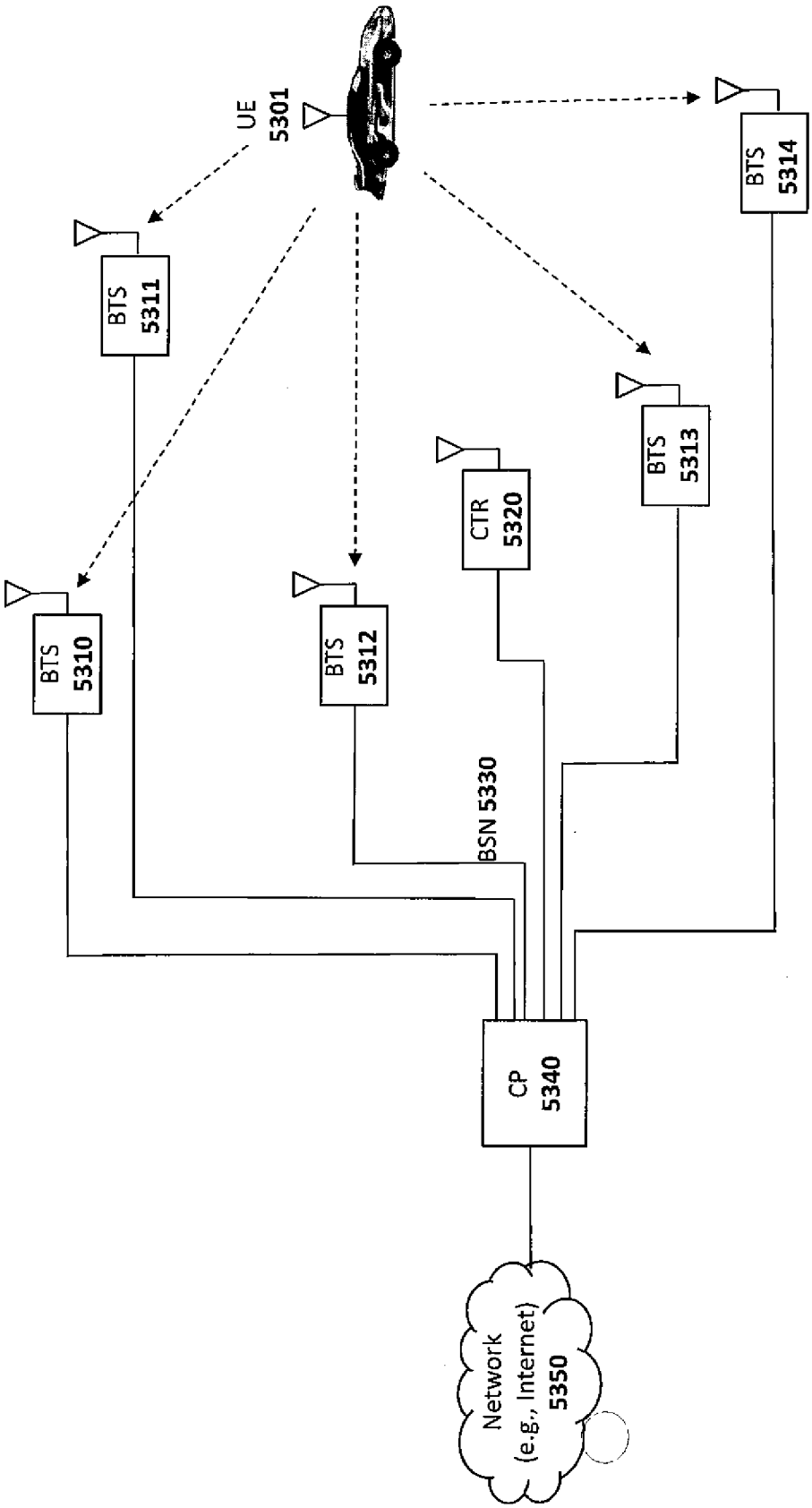
UE
5301
BTS
5310
BTS
5311
BTS
5312
CTR
5320
BTS
5313
BTS
5314
BSN 5330
CP
5340
Network
(e.g., Internet)
5350

Fig. 57

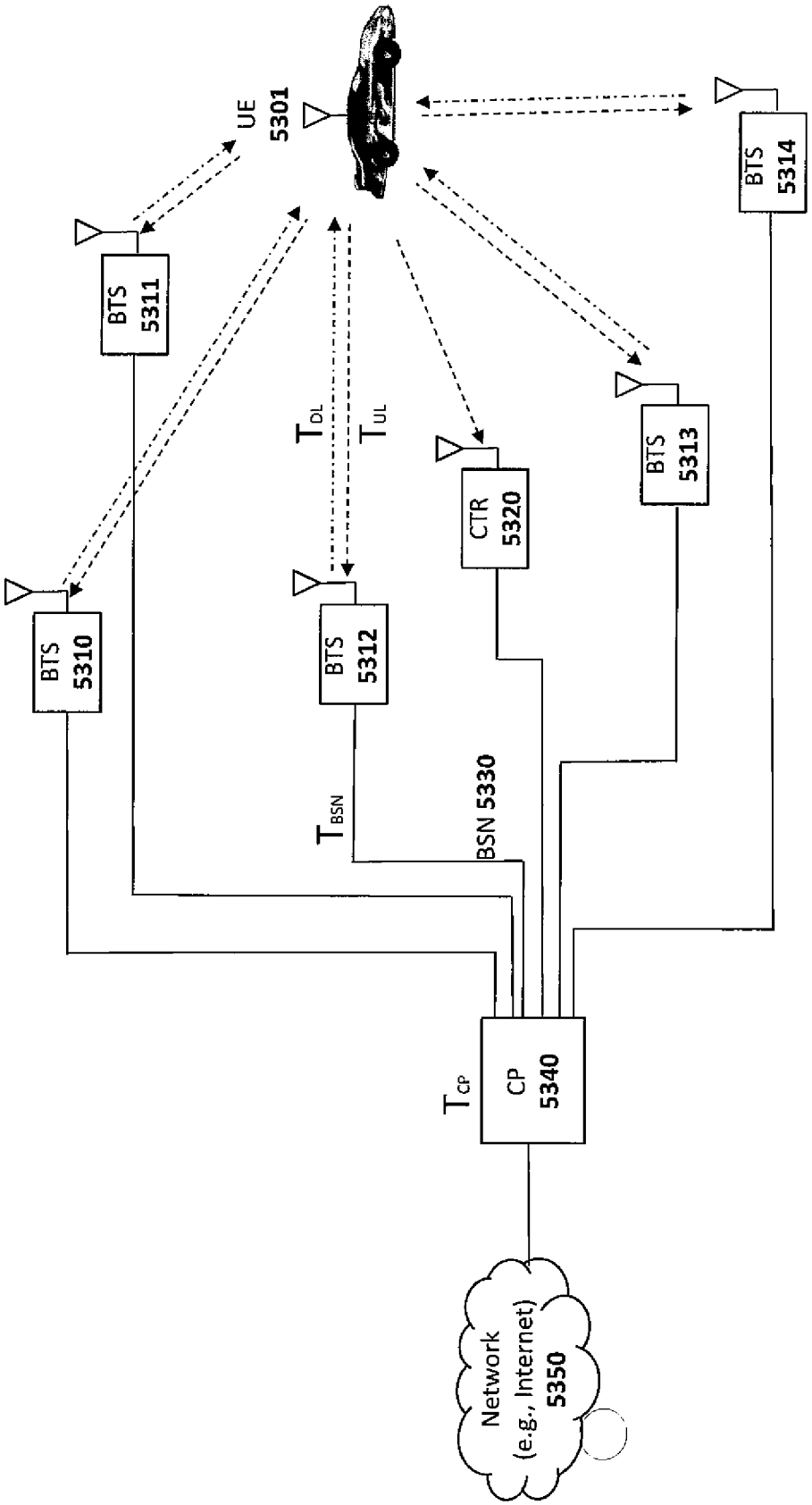
UE 5301
BTS 5310
BTS 5311
BTS 5312
BTS 5313
BTS 5314
CTR 5320
T_{DL}
T_{UL}
T_{BSN}
BSN 5330
T_{CP}
CP 5340
Network (e.g., Internet) 5350

Fig. 58

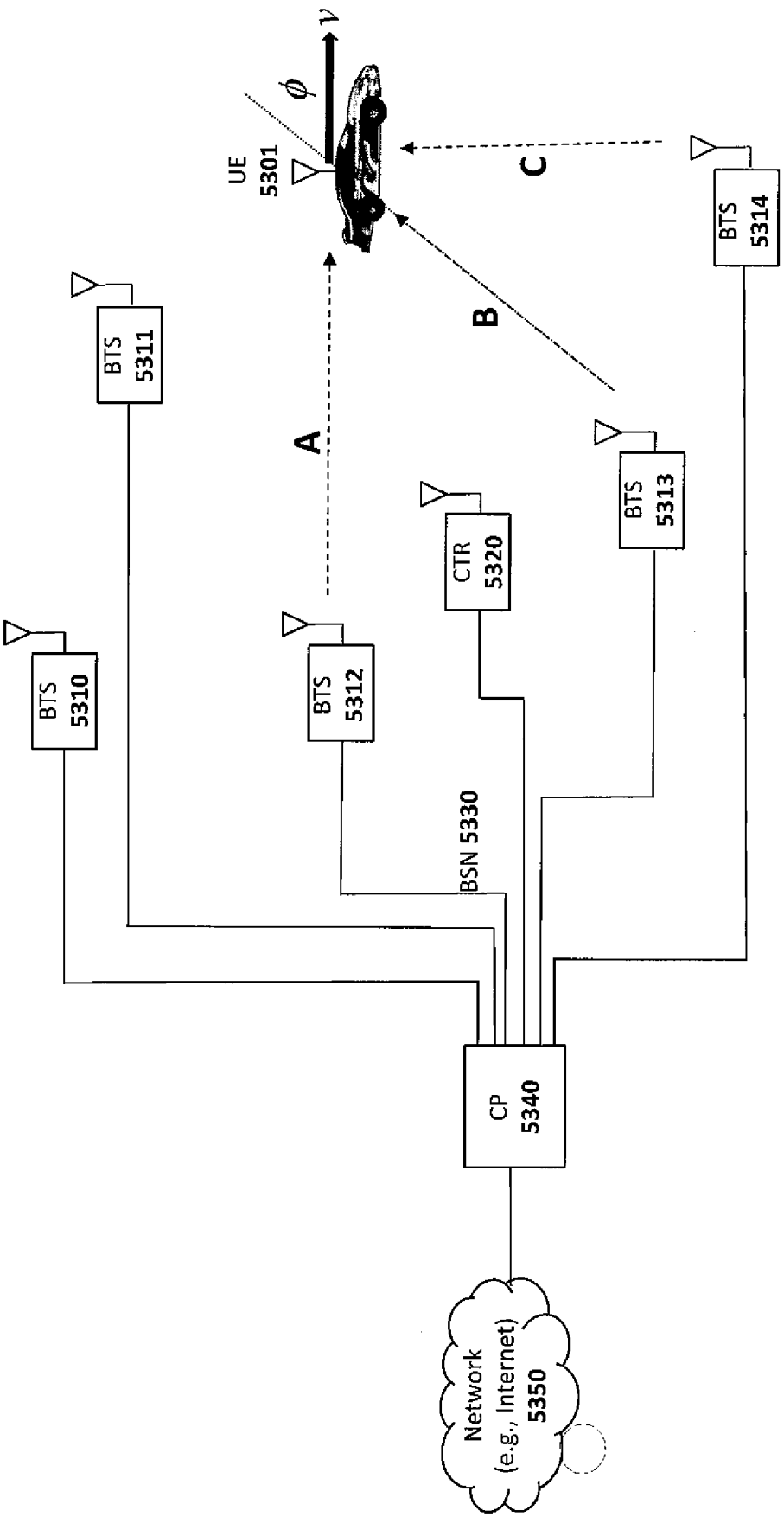
v
φ
UE
5301
A
B
C
BTS
5310
BTS
5311
BTS
5312
CTR
5320
BTS
5313
BTS
5314
BSN 5330
CP
5340
Network
(e.g., Internet)
5350

Fig. 59

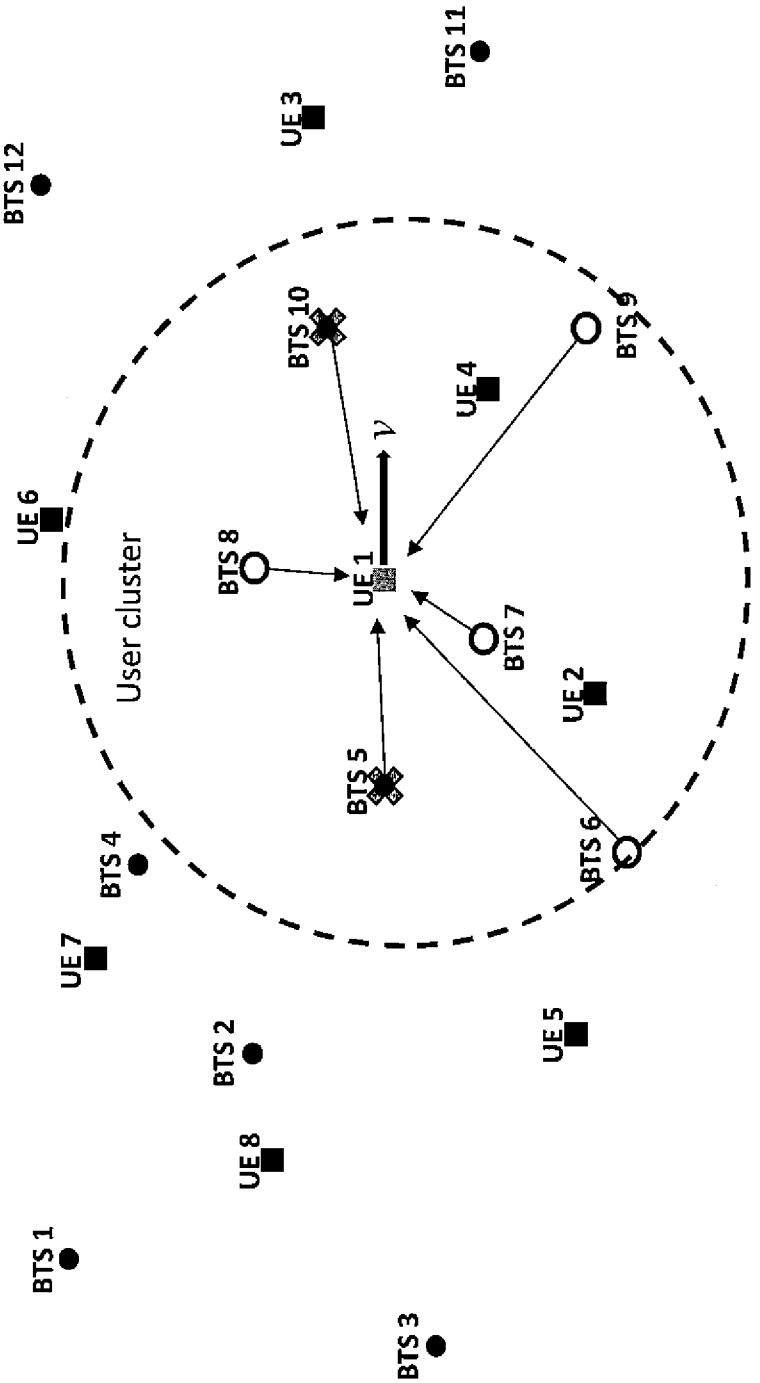
BTS 11
UE 3
BTS 12
BTS 10
BTS 9
UE 4
v
UE 6
BTS 8
UE 1
User cluster
BTS 7
UE 2
BTS 5
BTS 6
BTS 4
UE 7
UE 5
BTS 2
UE 8
BTS 1
BTS 3

Fig. 60

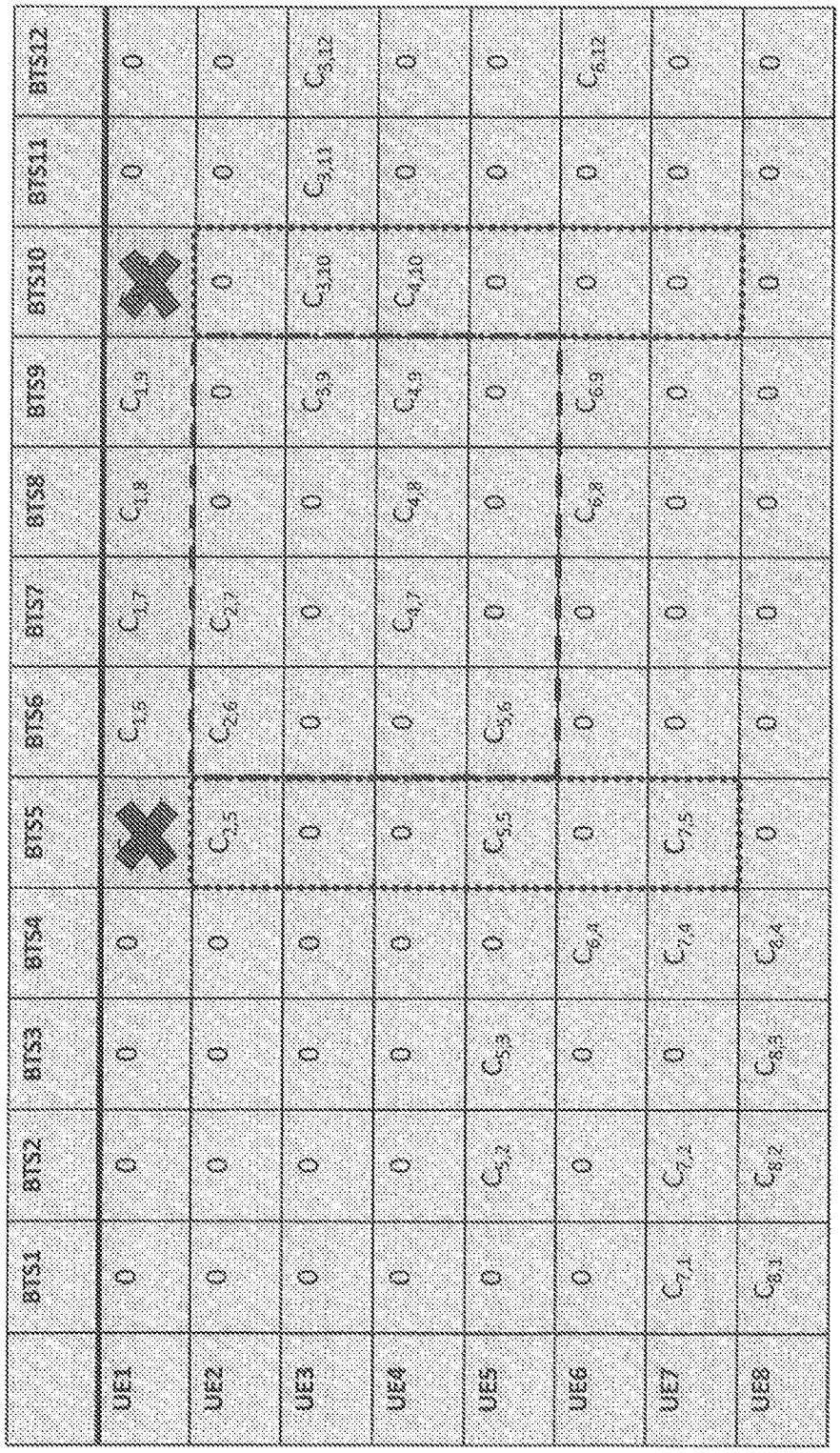

	BTS1	BTS2	BTS3	BTS4	BTS5	BTS6	BTS7	BTS8	BTS9	BTS10	BTS11	BTS12
UE1	0	0	0	0	X	$C_{1,6}$	$C_{1,7}$	$C_{1,8}$	$C_{1,9}$	X	0	0
UE2	0	0	0	0	$C_{2,5}$	$C_{2,6}$	$C_{2,7}$	0	0	0	0	0
UE3	0	0	0	0	0	0	0	0	$C_{3,9}$	$C_{3,10}$	$C_{3,11}$	$C_{3,12}$
UE4	0	0	0	0	0	0	$C_{4,7}$	$C_{4,8}$	$C_{4,9}$	$C_{4,10}$	0	0
UE5	0	$C_{5,2}$	$C_{5,3}$	0	$C_{5,5}$	$C_{5,6}$	0	0	0	0	0	0
UE6	0	0	0	$C_{6,4}$	0	0	0	0	$C_{6,9}$	0	0	$C_{6,12}$
UE7	$C_{7,1}$	$C_{7,2}$	0	$C_{7,4}$	$C_{7,5}$	0	0	0	0	0	0	0
UE8	$C_{8,1}$	$C_{8,2}$	$C_{8,3}$	$C_{8,4}$	0	0	0	0	0	0	0	0

Fig. 61

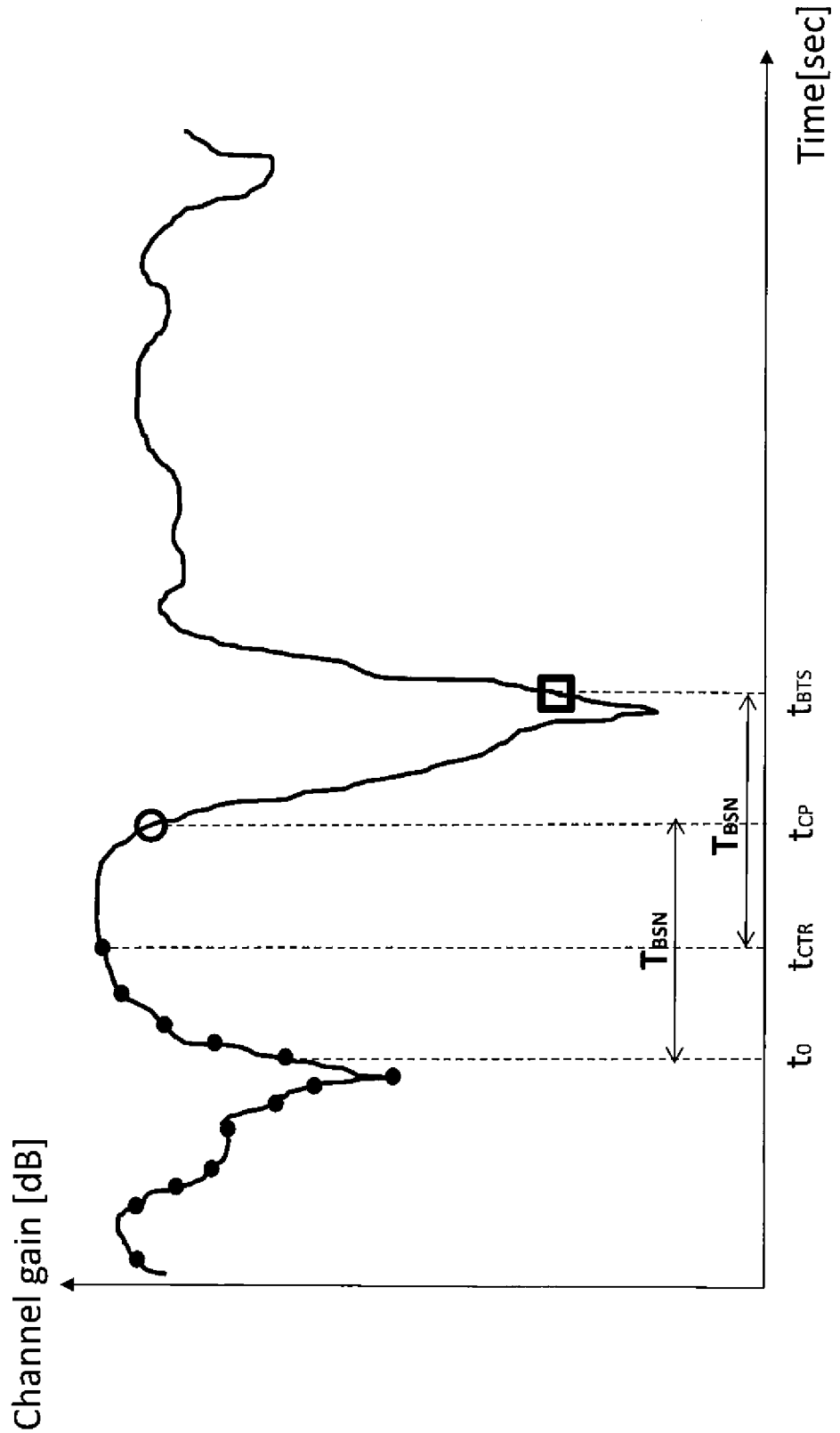

Fig. 62

INTERNATIONAL SEARCH REPORT

International application No.
PCT/US13/39580

A. CLASSIFICATION OF SUBJECT MATTER
IPC(8) - G08B 13/18 (2013.01)
USPC - 340/554
According to International Patent Classification (IPC) or to both national classification and IPC

B. FIELDS SEARCHED

Minimum documentation searched (classification system followed by classification symbols)
IPC(8): G04B 1/04, 1/18; G08B 13/18 (2013.01)
USPC: 340/554; 455/103, 151.4

Documentation searched other than minimum documentation to the extent that such documents are included in the fields searched

Electronic data base consulted during the international search (name of data base and, where practicable, search terms used)
MicroPatent (US-G, US-A, EP-A, EP-B, WO, JP-bib, DE-C,B, DE-A, DE-T, DE-U, GB-A, FR-A); Google/Google Scholar; IEEE; DialogPRO; Doppler, effect, mobility, change, propagation, environment, conditions, mobile, devices, user, equipments, wireless, multiuser, UEs, antennas, MIMO, BTS, CP, BSN, encoders, base, station, network, backhaul, MU-MAS, velocity

C. DOCUMENTS CONSIDERED TO BE RELEVANT

Category*	Citation of document, with indication, where appropriate, of the relevant passages	Relevant to claim No.
X --- Y	US 2012/0093078 A1 (PERLMAN S et al.) April 19, 2012, paagraphs [0185], [0190], [0268], [0304], [0307], [0327], [0330]	1-7 and 9-35 --- 8
Y	US 2009/0195355 A1 (MITCHELL C) August 6, 2009, paragraphs [0017], [0020]	8
A	US 6,061,021 A (ZIBELL L) May 9, 2000, column 2, line 55-column 3, line 55	1-35

☐ Further documents are listed in the continuation of Box C. ☐

* Special categories of cited documents:
"A" document defining the general state of the art which is not considered to be of particular relevance
"E" earlier application or patent but published on or after the international filing date
"L" document which may throw doubts on priority claim(s) or which is cited to establish the publication date of another citation or other special reason (as specified)
"O" document referring to an oral disclosure, use, exhibition or other means
"P" document published prior to the international filing date but later than the priority date claimed
"T" later document published after the international filing date or priority date and not in conflict with the application but cited to understand the principle or theory underlying the invention
"X" document of particular relevance; the claimed invention cannot be considered novel or cannot be considered to involve an inventive step when the document is taken alone
"Y" document of particular relevance; the claimed invention cannot be considered to involve an inventive step when the document is combined with one or more other such documents, such combination being obvious to a person skilled in the art
"&" document member of the same patent family

Date of the actual completion of the international search	Date of mailing of the international search report
13 August 2013 (13.08.2013)	20 AUG 2013
Name and mailing address of the ISA/US Mail Stop PCT, Attn: ISA/US, Commissioner for Patents P.O. Box 1450, Alexandria, Virginia 22313-1450 Facsimile No. 571-273-3201	Authorized officer: Shane Thomas PCT Helpdesk: 571-272-4300 PCT OSP: 571-272-7774

Form PCT/ISA/210 (second sheet) (July 2009)

INTERNATIONAL SEARCH REPORT

International application No.
PCT/US13/39580

Box No. II Observations where certain claims were found unsearchable (Continuation of item 2 of first sheet)

This international search report has not been established in respect of certain claims under Article 17(2)(a) for the following reasons:

1. ☐ Claims Nos.:
because they relate to subject matter not required to be searched by this Authority, namely:

2. ☐ Claims Nos.:
because they relate to parts of the international application that do not comply with the prescribed requirements to such an extent that no meaningful international search can be carried out, specifically:

3. ☐ Claims Nos.:
because they are dependent claims and are not drafted in accordance with the second and third sentences of Rule 6.4(a).

Box No. III Observations where unity of invention is lacking (Continuation of item 3 of first sheet)

This International Searching Authority found multiple inventions in this international application, as follows:
Group I: Claims 1-13; Group II: Claims 14-35

This application contains the following inventions or groups of inventions which are not so linked as to form a single general inventive concept under PCT Rule 13.1. In order for all inventions to be examined, the appropriate additional examination fee must be paid.

Group I: Claims 1-13 are directed toward a multiuser (MU) multiple antenna system (MAS) adaptively reconfiguring to compensate for Doppler effects due to user mobility or changes in the propagation environment.

Group II: Claims 14-35 are directed toward a method implemented within a multiuser (MU) multiple antenna system (MAS) to compensate for Doppler effect including mensuring Doppler velocity and assigning the first mobile user to a first BTS or to a first set of BTSs based on the measured Doppler velocity.

-***-Continued Within the Extra Page-***-

1. ☒ As all required additional search fees were timely paid by the applicant, this international search report covers all searchable claims.

2. ☐ As all searchable claims could be searched without effort justifying additional fees, this Authority did not invite payment of additional fees.

3. ☐ As only some of the required additional search fees were timely paid by the applicant, this international search report covers only those claims for which fees were paid, specifically claims Nos.:

4. ☐ No required additional search fees were timely paid by the applicant. Consequently, this international search report is restricted to the invention first mentioned in the claims; it is covered by claims Nos.:

Remark on Protest

☐ The additional search fees were accompanied by the applicant's protest and, where applicable, the payment of a protest fee.

☐ The additional search fees were accompanied by the applicant's protest but the applicable protest fee was not paid within the time limit specified in the invitation.

☐ No protest accompanied the payment of additional search fees.

INTERNATIONAL SEARCH REPORT

International application No.
PCT/US13/39580

-Continued from Box No. III: Observations where unity of invention is lacking-

The inventions listed as Groups I-II do not relate to a single general inventive concept under PCT Rule 13.1 because, under PCT Rule 13.2, they lack the same or corresponding special technical features for the following reasons:

The special technical feature of group I is a multiuser (MU) multiple antenna system (MAS) adaptively reconfiguring to compensate for Doppler effects due to user mobility or changes in the propagation environment. The special technical feature of group II is mensuring Doppler velocity and assigning the first mobile user to a first BTS or to a first set of BTSs based on the measured Doppler velocity.

The common technical feature shared by Groups I and II are a multiuser (MU) multiple antenna system (MAS) adaptively reconfiguring to compensate for Doppler effects. However, this common feature is previously disclosed by US 2012/0087430 A1 (Forenza). Forenza discloses a multiuser (MU) multiple antenna system (MAS) adaptively reconfiguring to compensate for Doppler effects (a MU-MAS system that changes the precoding as the wireless channel changes due to Doppler effect, abstract).

Since the common technical feature is previously disclosed by the Forenza reference, this common feature is not special and so Groups I and II lack unity.